Proceedings

of the 6-th International Conference on

STABILITY OF SHIPS

AND OCEAN VEHICLES

Volume II

Peter A. Bogdanov, Editor

22 - 27 September 1997
Varna, Bulgaria

P. Bogdanov, Editor
Proceedings of the 6-th International Conference on
Stability of Ships and Ocean Vehicles (STAB '97),
held 22 - 27 September 1997 at Sunny Day Complex, St. St. Konstantine and Helena Resort,
Varna, Bulgaria

ORGANIZERS:

Bulgarian Society of Naval Architects and Marine Engineers
National Committee of Theoretical and Applied Mechanics
National Marine Union
Union of Bulgarian Scientists - Varna branch

CO-ORGANIZERS:

International Maritime Association of the Mediterranean (IMAM)
Varna Free University (VFU)
Varna Technical University (VTU)

In order to make this volume available as economically and rapidly as possible, the autors' papers have been reproduced and printed without any reduction, correction, etc., in a standard way for all papers submitted. The autors are fully responsible for all the information contained in their papers.

PREFACE

STAB'97 is a follow-up Conference which continues the trend set by previous Conferences held in Glasgow (1975), Tokyo (1982), Gdansk (1986), Naples (1990) and Melbourne, Florida (1994). Being traditionally engaged with the most contemporary and important problems of stability and safety of ships and ocean vehicles, the STAB Conference is acknowledged as one of the most prestigious international events in the field of Marine Science, recognized not only by scientists, naval architects, shipbuilders and designers but also by officers of all branches of marine administration and control organizations, regulatory agencies, ship owners, marine consultants and operators, etc

The topics of the Conference can be classified as follows
- Theoretical and Experimental Studies on Stability of Ships and Floating Marine Structures
- Advances in Experimental Technique for Investigations on Stability
- Stability criteria: Philosophy and Research; Realistic Stability Criteria
- Operational Stability - the Influence of Environment
- Damage Stability
- Stability of Fishing Vessels
- Upgrading of Stability Qualities of Ro-Ro Ships
- Stability of Nonconventional Ship Types and Special Crafts
- Risk and Reliability Analysis in Stability and Capsizing
- Application of Expert Systems and On-board Computers Stability Monitoring and Control

The technical papers on these topics are distributed in two volumes of the Conference Proceedings The second volume includes also State-of-the-Art Review Reports as well as written contributions subject of two Panel Discussions
1 Damage Stability and Safety of Ro-Ro Vessels
2. Capsizing in Beam Seas - Chaos and Bifurcations

The Conference is organized by a local STAB'97 Secretariat with wide international participation. We are especially grateful to the members of the International Programme Committee and the International Advisory Board of STAB'97 as well as to the members of the ITTC Specialists Committee on Ship Stability for their considerable support and valuable contribution.
I would like to take this opportunity on behalf of the Organizers to thank the authors from about 30 countries having prepared interesting papers and written contributions in full accord with the objectives of the STAB'97 Conference

We look forward to the continuing success of STAB Conferences in Australia and other countries in the future

Peter A. Bogdanov
President of the STAB'97 Conference.
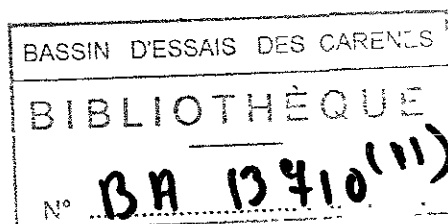
INTERNATIONAL PROGRAMME COMMITTEE

Prof. Bruce Adee	University of Washington, Seattle, USA
Prof. R. Bhattacharyya	US Naval Academy, Anapolis, Maryland, USA
Prof. Dr P. Bogdanov	Varna Free University, Varna, Bulgaria
Prof. P. Cassella	University of Naples, Naples, Italy
Prof W A. Cleary	Florida Institute of Technology, Melbourne, USA
Dr. E.A. Dahle	Det Norske Veritas, Høvik, Norway
Dr. A.V. Efimov	RUBIN Central Design Bureau, St Petersburg, Russia
Prof. A Francescutto	University of Trieste, Trieste, Italy
Prof. M. Fujino	University of Tokyo, Tokyo, Japan
Dr. S. Grochowalski	National Research Council, Ottawa, Canada
Prof. G. Hearn	University of Newcastle upon Tyne, United Kingdom
Dr. H. Hormann	Germanisher Lloyd, Hamburg, Germany
Prof. A. Incecik	University of Glasgow, Glasgow, United Kingdom
Prof. Dr. S. Kastner	Bremen Polytechic University, Bremen, Germany
Dr. R. Kishev	BSHC, Varna, Bulgaria
Prof. L Kobylinski	SNEP Foundation, Gdansk, Poland
Prof. V.B. Lipis	CNIIMF, St. Petersburg, Russia
Prof. V.A. Nekrasov	State Maritime Technical University, Nikolaev, The Ukraine
Prof. Dr. M. A. S. Neves	State University of Rio de Janeiro, Brasil
Prof. A. Jucel Odabasi	Istanbul Technical University, Istanbul, Turkey
Prof. A. Papanicolau	National Technical University of Athens, Greece
Prof. N.M. Perez	University of Chile, Valdivia, Chile
Dr N.N. Rakhmanin	Krylov Shipbuilding Institute, St. Petersburg, Russia
Prof. M.R Renilson	Australian Maritime Research Centre, Australia
Prof. L Perez-Rojas	Politecnical University Madrid, Spain
Prof. C. Sanguinetti	University of Chile, Valdivia, Chile
Prof. C. Guedes-Soares	Institute Superior Tecnico, Lisboa, Portugal
Prof. Dr. J. Sukselainen	VTT Manufacturing Laboratory, Espoo, Finland
Dr. S G Tan	MARIN, Wageningen, The Netherlands
Dr. N. Umeda	National Research Institute of Fisheries Eng., Ibaraki, Japan
Dr. D. Vassalos	University of Strathclyde, Glasgow, United Kingdom
Mr. H. Vermeer	Directorate of Shipping and Maritime Affairs, Rjiswik, The Netherland
Prof. Xiu-Heng Wu	Wuhan Transportation University, Wuhan, China
Dr Deuk-Joon Yum	Hyundai Maritime Research Institute, Ulsan, Korea

INTERNATIONAL ADVISORY BOARD

TABLE OF CONTENTS
Volume I

Page

ADVANCES IN EXPERIMENTAL TECHNIQUE
FOR INVESTIGATIONS ON STABILITY

OPERATIONAL STABILITY -
THE INFLUENCE OF ENVIRONMENT

DAMAGE STABILITY

STABILITY OF FISHING VESSELS

RISK AND RELIABILITY ANALYSIS
IN STABILITY AND CAPSIZING

APPLICATION OF EXPERT SYSTEMS AND ON-BOARD COMPUTERS FOR STABILITY MONITORING AND CONTROL

TABLE OF CONTENTS
Volume II

Page

THEORETICAL AND EXPERIMENTAL STUDIES
ON STABILITY OF SHIPS
AND FLOATING MARINE STRUCTURES

STABILITY CRITERIA: PHILOSOPHY AND RESEARCH.
REALISTIC STABILITY CRITERIA

UPGRADING OF STABILITY QUALITIES
OF RO-RO SHIPS

OPERATIONAL STABILITY -
THE INFLUENCE OF ENVIRONMENT

STABILITY OF FISHING VESSELS

STABILITY OF NONCONVENTIONAL SHIP TYPES
AND SPECIAL CRAFTS

RISK AND RELIABILITY ANALYSIS
IN STABILITY AND CAPSIZING

APPLICATION OF EXPERT SYSTEMS
AND ON-BOARD COMPUTERS
FOR STABILITY MONITORING AND CONTROL

State-ot-the-art Review Report to the Panel Discussions on
DAMAGE STABILITY AND SAFETY OF RO-RO VESSELS

Written contributions to the panel discussions on
DAMAGE STABILITY AND SAFETY OF RO-RO VESSELS

State-of-the-art Review Report to the Panel Discussions on

CAPSIZING IN BEAM SEAS - CHAOS AND BIFURCATIONS

Written contributions to the panel discussions on

CAPSIZING IN BEAM SEAS - CHAOS AND BIFURCATIONS

THEORETICAL AND EXPERIMENTAL STUDIES ON STABILITY OF SHIPS AND FLOATING MARINE STRUCTURES

3

A TIME-DOMAIN SIMULATION METHOD FOR STABILISER FIN EVALUATION AND DESIGN

Allan Magee, Jean-François LeGuen, Xavier Dupouy[1]

ABSTRACT

A time-domain simulation method for large-amplitude ship motions is presented. This method includes further developments to that used by [10]. (See [12].) It has the advantage of being rapid, while taking into account the most important non-linearities due to finite angle rotations, hydrostatics, the incident waves, and lifting surface forces. Here, particular emphasis is placed on the effects of stabiliser fins and rudders on ship motions in oblique seas. The effects of fluid velocities due to incident, diffracted and radiated waves on fin performance are studied. The verification phase now completed and numerical results are presently available for fixed and moving fins.

Consideration is given to the derivation of the auto pilot control laws. The codes MATLAB and SIMULINK are used to design and simulate optimal auto pilot control laws, based on the classic LQR formulation. These commands are refined by taking into account the wave exciting force (perturbation) and eventually including low-frequency offset (integral) corrections. The performance of these control laws is assessed using time-domain seakeeping calculations as a numerical testing tank. The performance of the newly derived commands are compared with the existing control laws derived from simplified hydrodynamic calculations (SMP) and improved after at-sea identification of the real ship/stabiliser system. It is shown that the numerical predictions provided by the time-domain calculations combined with the simple procedure to derive command laws provides good predictions in a short time, and thus can reduce expensive at-sea recalibration time and cost.

INTRODUCTION

Given the necessity of absolute security and reliability, the design of stabiliser systems for ships is a very costly and time-consuming procedure. External design constraints usually fix the configuration parameters: surface area, aspect ratio, section shape, location, orientation, maximum angle, motorisation and number of fins. Naval vessels may have additional requirements on radiated noise levels. On the other hand, the designer has more freedom in choosing the auto pilot controls laws within the limits of response speed and power of the actuators.

Prototype systems are usually verified by at-sea tests which can be long and particularly expensive if the command laws must be significantly modified. Since re-configuration is almost always too costly, ship owners must accept flaws in the system which can be expensive if the system performance does not meet contractual requirements.

Due to uncertainties in available numerical methods for calculating ship motions in oblique seas and the forces on stabilisers, the only feasible means of verifying the system are model and full-scale tests.

[1] Bassin d'Essais des Carènes, Chaussée du Vexin, 27100 Val-de-Reuil, FRANCE
e-mail· magee@becvdr.dga.fr

DESCRIPTION OF THE METHOD

To try to improve this situation, a time-domain simulation method for large-amplitude ship motions is presented. As opposed to existing frequency-domain methods, the time-domain approach has the advantage of be able to directly account for non-linear phenomena such as saturation of the control system, separation, etc. It provides a method to accurately and rapidly test proposed designs under widely varying conditions of oblique seas with forward speed, not available in usual narrow towing tanks.

General Description of the Code

The code is named RATANA. Its goal is to perform nonlinear simulations with the best approximations currently available, while maintaining sufficient rapidity to allow validation and comparison with realistic data. In this way, further improvements can be incorporated as they become available.

Basically, the method is similar to that used by [13], in which the incident wave and hydrostatic forces are calculated using the instantaneous immersed hull surface, while the radiation and diffraction forces, are linearised. Here we use a three-dimensional frequency domain code named DIODORE to calculate the hydrodynamic coefficients. External nonlinear forces are also included. The exact kinematic and dynamic models of the ship motions are used.

The internal code structure consists of a driver to integrate the equations of motion and subroutines to calculate the forces. Parameters are passed by commons. Modularity is maintained to ease the job of adding new contributions to the forces. The general functioning of the code is schematically described in figure 1. For the purpose of verification, RATANA posesses a small amplitude time- domain formulation.
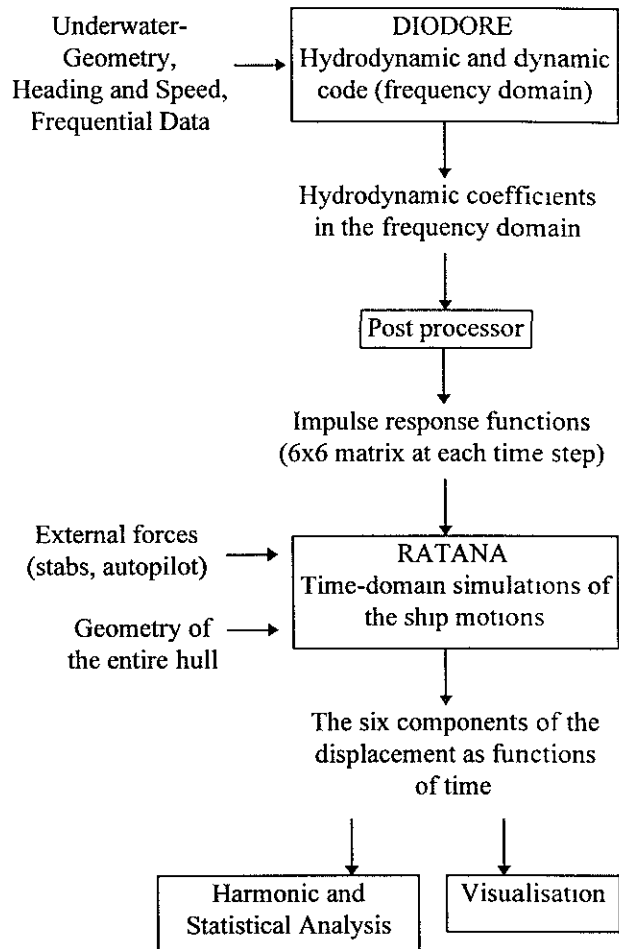
Figure 1. Schematic diagram of the functioning of the simulation method.

Kinematic Relations

As described in [10], three coordinates systems are used. See figure 2. The first system (x, y, z) has its origin fixed at the calm free surface level with the z-axis positive upwards. The second coordinate system (x', y', z') moves in steady translation with respect to the fixed system at the ship's forward speed, U_0 . Thus,

$$x' = x + U_0 t$$
$$y' = y \qquad\qquad (1)$$
$$z' = z$$

The third coordinate system (x'', y'', z'') is fixed at the center of gravity of the ship. Its

origin is given by the vector (x_1, x_2, x_3). The rotation of the ship is given by (x_4, x_5, x_6). These 6 generalised displacements are three translations surge, sway and heave and three rotations roll, pitch and yaw respectively.
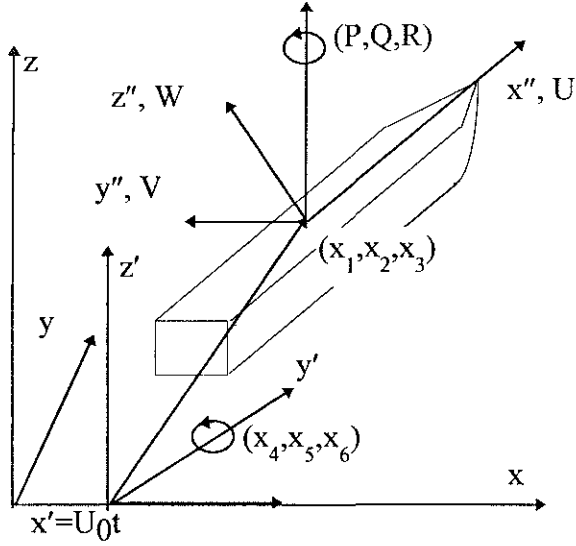
Figure 2. Coordinate systems.

The transformation of a point in the center of gravity system to the fixed system is given by

$$\begin{Bmatrix} x \\ y \\ z \end{Bmatrix} = \begin{Bmatrix} x_1 + U_0 t \\ x_2 \\ x_3 \end{Bmatrix} + [T] \begin{Bmatrix} x'' \\ y'' \\ z'' \end{Bmatrix} \qquad (2)$$

where,

$$[T] = \begin{bmatrix} c_5 c_6 & s_4 s_5 c_6 - c_4 s_6 & c_4 s_5 c_6 + s_4 s_6 \\ c_5 s_6 & s_4 s_5 s_6 + c_4 c_6 & c_4 s_5 s_6 - s_4 c_6 \\ -s_5 & s_4 c_5 & c_4 c_5 \end{bmatrix}$$

and,

$$c_n \equiv \cos(x_n) \qquad s_n \equiv \sin(x_n)$$

The velocities in the steadily translating system are related to the the velocity vectors $\vec{V}$ and $\vec{\omega}$ by the relations

$$\begin{Bmatrix} \dot{x}_1 \\ \dot{x}_2 \\ \dot{x}_3 \end{Bmatrix} = [T] \begin{Bmatrix} U \\ V \\ W \end{Bmatrix} \qquad (3)$$

$$\begin{Bmatrix} \dot{x}_4 \\ \dot{x}_5 \\ \dot{x}_6 \end{Bmatrix} = [S] \begin{Bmatrix} P \\ Q \\ R \end{Bmatrix}$$

$$[S] = \begin{bmatrix} 1 & s_4 \tan x_5 & c_4 \tan x_5 \\ 0 & c_4 & -s_4 \\ 0 & \dfrac{s_4}{c_5} & \dfrac{c_4}{c_5} \end{bmatrix}$$

where, $\vec{V} = \{U, V, W\}$ is the ship's velocity in the instantaneous ship-fixed system, and $\vec{\omega} = \{P, Q, R\}$ is the angular velocity in this same frame.

The velocity of a point in the ship's frame is given by:

$$\vec{V}_P = \begin{Bmatrix} U \\ V \\ W \end{Bmatrix} + \{P, Q, R\}^T \wedge \{x'', y'', z''\} \qquad (4)$$

Nonlinear Dynamics

Euler's equation of motion is written in the ship-fixed system as:

$$\begin{Bmatrix} \vec{F} - m\vec{\omega} \wedge \vec{V} \\ \vec{\Gamma} - \vec{\omega} \wedge \vec{h} \end{Bmatrix} = [[M] + [\mu]] \begin{Bmatrix} \dot{U} \\ \dot{V} \\ \dot{W} \\ \dot{P} \\ \dot{Q} \\ \dot{R} \end{Bmatrix} \qquad (5)$$

21

$$[M] = \begin{bmatrix} m & 0 & 0 & 0 & 0 & 0 \\ 0 & m & 0 & 0 & 0 & 0 \\ 0 & 0 & m & 0 & 0 & 0 \\ 0 & 0 & 0 & I_{xx} & 0 & -I_{xz} \\ 0 & 0 & 0 & 0 & I_{yy} & 0 \\ 0 & 0 & 0 & -I_{xz} & 0 & I_{zz} \end{bmatrix}$$

where, [M] is the generalised mass matrix, m is the mass of the ship, [μ] is the generalised instantaneous or infinite-frequency added mass (discussed below), and $\vec{h} = [I]\{P,Q,R\}$ is the angular momentum. The advantage of writing the equations of motion in the ship-fixed frame is that the mass matrix is independent of the motions. The forces and moments $\vec{F}$ and $\vec{\Gamma}$ include all the forces acting on the ship, with the exception of the instantaneous added mass. The calculation of the forces is discussed below.

A set of 12 coupled differential equations for the unknowns $\{\dot{x}_1,...\dot{x}_6\}, \{x_1,...x_6\}$ is established and solved according to the method described in [10].

Incident Wave and Hydrostatic Forces

The force due to the incident waves in the body-fixed coordinate system is written:

$$F_i = \iint_{S(t)} p_I n_i dS \qquad (6)$$

where,

n_i = generalised normal
$S(t)$ = instantaneous wetted surface
p_I = incident wave pressure

$$= -\rho \frac{\partial \varphi_I}{\partial t} - \rho g z \qquad (7)$$

$$\varphi_I = ig\sum_n \frac{\eta_n}{\omega_n} e^{k_n z} e^{i\omega_n t} e^{-ik_n(x\cos(\beta)+y\sin(\beta))}$$

The incident wave elevation is given by

$$\eta_I = -\frac{1}{g} \frac{\partial \varphi_I(x,y,0,t)}{\partial t} \qquad (8)$$

It is understood that the real parts of φ_I, p_I and η_I are to be taken. The case $\beta = \pi$ corresponds to head seas and $\beta = \pi/2$ corresponds to waves from the port side.

Assuming plane panels, the normal n_i for i = 1,2,3 is constant, but the normals 4, 5, and 6 vary linearly over the panels. The pressure is assumed to vary linearly over each panel. Thus, for each panel a linear function is integrated for the force and a quadratic function for the moment. The the sum is taken over all the panels. For flat panels we note that it is possible to integrate these terms analytically, but the resulting expressions are too time-consuming to evaluate.

At each time step, a fixed grid covering the whole surface of the body is cut at the intersection with the free surface. The pressure integration can be carried out up to z = 0 or z = η_I. In the latter case, a stretching is used (see [14]) by substituting (z-η_I) in place of z in (7). This approximation has the advantage that it satisfies $p_I = 0$ on z = η_I and approaches the linear pressure as z → −∞. In the large-amplitude results presented here, we have taken this approximation. Thus, we are able to at least partially take into account the upper part of the body which is ignored in a purely linear formulation.

Diffraction Forces

The diffraction forces are calculated using input from the frequency-domain pre-processor. In the time-domain simulations, these forces become

$$\vec{F}_d = \sum_n \eta_n \vec{X}_n e^{i\omega_{e_n}t} e^{-ik_n(x_1'\cos(\beta)+x_2'\sin(\beta))} \qquad (9)$$

where,

ω_{e_n} = encounter frequency of wave component n

X_n = complex amplitude of the nth component of the diffraction force

k_n = wave number ($= \omega_n^2 / g$)

$e^{-ik_n(x_1' \cos(\beta) + x_2' \sin(\beta))}$ = Phase angle to account for the horizontal displacement of the center of gravity. This term is taken equal to zero in the small amplitude formulation.

Linearized Time-Domain Radiation Forces

The forces due to radiated waves are calculated using the same time-domain method as in [10], but with a few important improvements. The radiation force is written:

$$\bar{F}_j = -\mu_{jk}\ddot{x}_k - b_{jk}\dot{x}_k - \int_0^t K_{jk}(t-\tau)\dot{x}_k(\tau)d\tau \quad (10)$$

where,

μ_{jk} = added mass at infinite frequency

b_{jk} = damping at infinite frequency

K_{jk} = impulse response function for the force in mode j due to a velocity in mode k

$\ddot{x}_k$ = generalised acceleration in mode k

$\dot{x}_k$ = generalised velocity in mode k

The impulse response function can be calculated knowing the damping at all frequencies by the relation:

$$K_{jk}(t) = \int_0^\infty (B_{jk}(\omega) - b_{jk})\cos(\omega t)d\omega \quad (11)$$

In practice, we only know the value of the damping up to a certain maximum frequency, ω_{max}. Above this value, the damping is approximated using an assumed asymptotic decay:

$$B_{jk}(\omega) \approx B_{jk}(\omega_{max})\left(\frac{\omega}{\omega_{max}}\right)^n + b_{jk}$$

Note that [2] has shown that in the formulation with forward speed, the terms b_{jk} are not all equal to zero, but satisfy the relation $b_{jk} + b_{kj} = 0$. However, in the slow-speed formulation, such as used in the frequency domain code DIODORE, we have $b_{jk} = 0$ for $k \neq 5,6$. The important point is to subtract off the high frequency limit so that the integral (11) can be performed.

The terms μ_{jk} are of primary importance for the accuracy of the time-domain calculations. Here, they are not calculated by the integral relation of [8] which is unreliable in the presence of irregular frequencies. The values of μ_{jk} can be obtained using a frequency-domain code, by choosing a very large value of the frequency. However, since the added mass approaches its infinite-frequency value very slowly (approximately logarithmically) one must choose a very large frequency, or calculate a series of values and extrapolate the result. Since the behaviour of the results may be affected by the irregular frequencies, this method may not be robust enough to assure sufficient accuracy.

A simple and effective alternative is to solve the boundary value problem at infinite frequency directly. The Green function for this problem is:

$$G = \frac{1}{r} - \frac{1}{r'} \quad (12)$$

All the terms necessary to solve this problem are already contained in typical frequency domain codes because the Rankine source terms are calculated to obtain the frequency domain Green function

$$G = \frac{1}{r} + \frac{1}{r'} + G_{wave} \quad (13)$$

where G_{wave} includes the terms dependent on the frequency. All that is needed is to change the sign of the image terms ($1/r'$) and apply the no-penetration boundary condition. The integral equation obtained is not subject to the influences of irregular frequencies. Its solution converges rapidly with mesh

23

refinement, and gives the exact solution required without any extrapolation or arbitrary choice of frequency. It is surprising that such a simple and useful solution is not already part of most frequency domain codes.

Viscous Roll Damping

Because the radiated wave damping is small, a formulation based purely on potential theory is not applicable for transverse wave calculations. The potential based terms must be augmented by real fluid corrections. See [5]. In a linearized formulation, such as SMP, the viscous, bilge keel, and eddy damping terms are calculated based on empirical formulas found in [9]. The resulting linear equivalent damping is a function of the roll amplitude, and this leaves some inconsistencies in the case of irregular seas because we cannot choose a single amplitude which is representative for all the frequency components. In addition, the roll damping depends on the chosen amplitude, and the amplitude depends on the chosen damping. Thus, iterations are needed to assure the convergence of such an approximation.

However, using a time-domain simulation, we are not constrained to a linear damping term. Here, the viscous roll damping contribution is written using linear up to third-order terms:

$$F_{4visc} = -B_{lin}\dot{x}_4 - B_{quad}\dot{x}_4|\dot{x}_4| - B_{cub}\dot{x}_4^3 \quad (14)$$

The linear, quadratic and cubic terms are determined by a least squares fit such that the total energy dissipated over one cycle at the resonant roll period, whatever the roll amplitude, is nearly the same as that dissipated by an equivalent linear term obtained from SMP. We have

$$Energy = \int_0^T M(t)\dot{x}_4(t)dt \quad (15)$$

where,

$$M(t) = \begin{cases} B_{equiv} & SMP \\ B_{lin} + B_{quad}|\dot{x}_4| + B_{cub}x_4^2 & RATANA \end{cases}$$

Thus, we are not obliged to specify any particular amplitude, nor to carry out iterations, because the time-domain formulation is valid for arbitrary amplitude. Figure 3 shows the equivalent energy fit for the roll damping.

In addition, by calculating a drag coefficient over the wetted surface, we can estimate at least a linear viscous damping term for surge and sway motions.
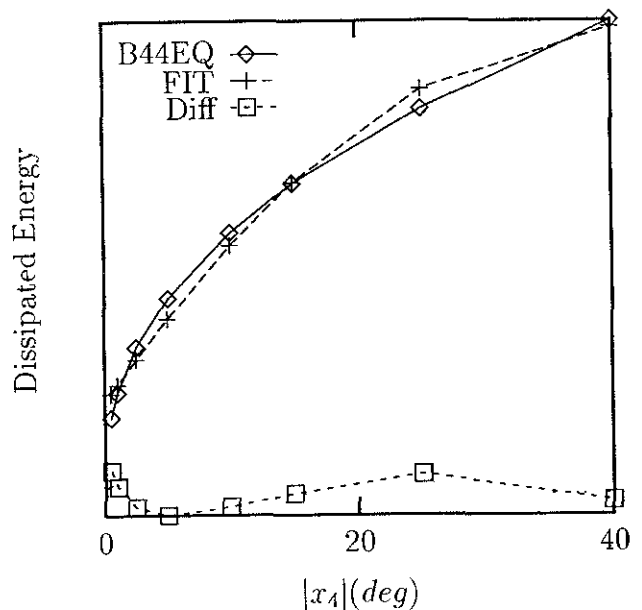
Figure 3. Equivalent energy method for the damping coefficient versus roll amplitude.

LIFTING SURFACES

We call lifting surface, a relatively high aspect ratio appendage which can be actively controlled (in particular anti-roll stabilisers and rudders). Fixed bilge keels and other low aspect foils are not considered here. The force on each lifting surface or foil is calculated at each time step. It is composed of lift and drag components. The following quantities are defined:

24

P = coordinates (x,y,z) in the body-fixed system representing the position of the surface. It is the point where the velocities are calculated and where the forces are applied.

S_f = projected surface

$\vec{V}_p$ = velocity of the point P in the instantaneous body-fixed system equation (4).
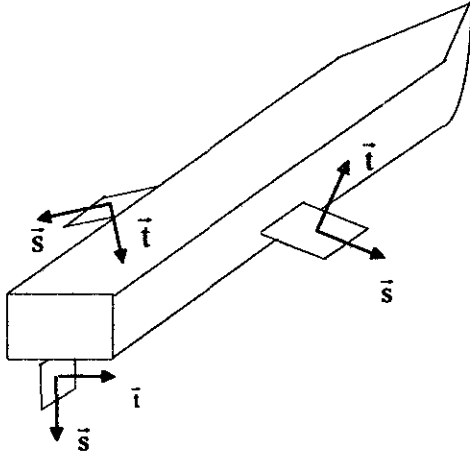
Figure 4. Coordinates for the lifting surface calculations.

The vectors $\vec{s}$ and $\vec{t}$ are unitary, specifying the orientation of the lifting surfaces. The angles δ_0 and α_0 are defined as

δ_0 = the angle between the vector $\vec{s}$ and $\vec{k}$

α_0 = the angle between the vector $\vec{t}$ and $\vec{s} \wedge \vec{V}_\infty$

$\vec{V}_\infty$ = the velocity in calm water at the point P

$\vec{u}$ = $\vec{s} \wedge \vec{V}_\infty$

The lift force is defined perpendicular to the flow which is assumed uniform with upstream velocity equal to the instantaneous fluid velocity in the ship-fixed coordinates. The velocity includes that due to the ship's own movements, as well as the velocities due to the incident and diffracted and radiated wave fields. The force, in the same referential is given by:

$$\vec{F}_p(t) = \frac{1}{2}\rho S_f \frac{\partial C_z}{\partial \alpha}\alpha u \vec{u} \qquad (16)$$

with:

C_z, the lift coefficient (dependent on the instantaneous value of α),

α, instantaneous foil incidence, defined by

$$\alpha = \frac{(\vec{t} \wedge \vec{u}) \cdot \vec{s}}{u}$$

The force can thus be expressed in the form:

$$\vec{F}_p(t) = \frac{1}{2}\rho S_f \frac{\partial C_z}{\partial \alpha}\alpha((\vec{t} \wedge \vec{u}) \cdot \vec{s})\vec{u} \qquad (17)$$

The lift coefficient is calculated using diverse formulas principally those developed in [6]. An option will be provided to use externally calculated lift and drag coefficients tabulated as a function of incidence and stored in an input file. A method for calculating these terms is described in [11].

For the moment, we use corrections to the 2-D lift curve slope (2π) for the thickness, 3-D aspect ratio effects, for the mean immersion, for the bilge radius, boundary layer, the precense of a propeller, separation, and for viscous drag.

In order to calculate the drag force (as in the case of the lift force) we consider that the velocity calculated at the point P is the velocity at upstream infinity of a uniform flow. The drag force is decomposed into a viscous drag term which acts in the direction of the foil and the induced drag which acts in the direction of the velocity. The viscous drag force is represented in the form:

$$\vec{F}_{tv}(t) = -\frac{1}{2}\rho S_f C_{xv}\vec{s} \wedge \vec{t} \qquad (18)$$

The induced drag is given by

$$\bar{F}ti(t) = \frac{1}{2}\rho S_f \frac{\partial C_{xi}}{\partial \alpha}\alpha \bar{V} \qquad (19)$$

with

$$C_{xi} = \frac{2C_z^2}{\pi A}$$

Fluid Velocity

To determine the forces, it is necessary to calculate $\bar{V}$. At each time step, the code Ratana determines the ship's velocity, including the forward speed in the instantaneous ship-fixed frame using the relation (4). The fluid velocity due to the incident, diffracted and radiated waves is projected into the ship-fixed frame to determine the relative velocity. For the moment, the radiated wave velocity is approximated by its value at infinite frequency. The incident wave velocities are calculated based on the instantaneous position of the point P.

AUTOPILOT COMMAND LAWS

At each time step, the upstream velocity is calculated and the incidence angle α deduced for each foil. To this incidence, we add an angle δ due to the autopilot law. The command law takes the form

$$\delta_c = \sum_{i=1}^{6}(k_{1i}x_i'' + k_{2i}\dot{x}_i'' + k_{3i}\ddot{x}_i'') \qquad (20)$$

where x_i'', $\dot{x}_i''$ and $\ddot{x}_i''$ are the movements, velocities and accelerations in the ship-fixed frame. The total incidence is thus $\alpha + \delta$.

Delays

It may be important to consider the difference between the commanded angle and the actual angle achieved by the foil. Delays could result from mechanical or hydraulic transmission,

inertial effects or calculation time of the stabiliser system software for example. The modelisation used is a second-order spring-mass-damper with a constant delay. The achieved angle $\delta(t)$ is a solution of:

$$a_1\delta + a_2\dot{\delta} + a_3\ddot{\delta} = \delta_c(t - t_c) \qquad (21)$$

where t_c is the delay to be accounted for, and (a_1 a_2 and a_3) represent the characteristics of the stabiliser system. This equation is solved by a fourth-order Runge-Kutta method.

Saturations

The calculation of the foil angles at each time step allows us to consider the possibility of saturation of the actuators. If the commanded angle or angular speed exceed the specified limits, then the following relations come into play:

$$\text{If } |\delta_c| > \delta_{max} \text{ then } \delta = (\pm)\delta_{max} \qquad (22)$$
$$\text{If } |\dot{\delta}_c| > \dot{\delta}_{max} \text{ then } \dot{\delta} = (\pm)\dot{\delta}_{max}$$

Derivation of an Optimal Command Law

Our goal is to stabilise the ship in the presence of regular waves at the resonant roll response period. We use the programs MATLAB and SIMULINK. The system of equations considered is:

$$\dot{X} = AX + BU + B_w W$$
$$Y = CX + DU + D_w W \qquad (23)$$

where, the vectors are defined as follows:

$X = \{\dot{y}, \dot{\phi}, \dot{\psi}, y, \phi, \psi\}$ is the state vector consisting of the horizontal mode displacements and velocities.

$W = \{\dot{\eta}, \eta\}$ is the so-called perturbation, consisting of the wave elevation and its time derivative.

$U = \{\delta\}$ is the vector of command coefficients for each stabiliser.

The matrix A contains the generalised added mass and damping coefficients and the coupling terms. The matrix B contains the forces due to stabiliser displacements. B_W contains the exciting forces, C is the identity matrix, D and D_W are zero in the present case. These equations are simply the coupled linear equations of motion for the horizontal modes.

The problem consists of finding the command U which minimises the following quadratic function:

$$J(U) = \int_0^\infty X^T(t)QX(t) + U^T(t)RU(t)dt \qquad (24)$$

with $Q \geq 0$ and $R > 0$. These matrices are the weights placed respectively on the movements of the ship and action of the stabilisers. Their relative values allow us to avoid the cases in which the actuators work too hard when there is little movement, or the movements get too large and the stabilisers don't work hard enough. The condition R strictly positive expresses the fact that any control action costs something, while some elements of Q may be zero, if we do not wish to control all the elements of the state vector.

One must also choose the absolute values for the weights. If large amplifications are used, the system stabilises well, but there is a risk of saturating the servo-actuators. If small amplifications are used, there is little effect on stability, but no saturation. Ideally, the amplification should be determined adaptively as a function of the estimated wave amplitude.

The command U(t) which minimises the above criteria is obtained by the LQR method [7]. It is a static feedback of the form

$$U = -KX \qquad (25)$$

where $K = R^{-1}B^TP$ and P is the unique positive symetric solution of the algebraic Riccati equation

$$A^TP + PA - PBR^{-1}B^TP + Q = 0 \qquad (26)$$

If we augment the state vector X with W, resulting in 8 components, the LQR method is not strictly applicable, because the vector W, representing the wave perturbation is not controllable. We add a feed forward of the type

$$U = -K_pW \qquad (27)$$

where K_p is obtained by applying a method derived from LQR known as the Linear Quadratic Estimator. A Kalman filter must be applied to estimate the vector W. The block diagram used by SIMULINK to simulate the system is given in figure 5. The resulting simulations of the roll, sway and yaw, motions are not shown here for lack of space, but will be presented at the conference.

Stability is assured by requiring the eigenvalues of (23) to have negative real parts. Stability margins should be specified. In the case of irregular seas, we should add integral feedback terms to overcome the steady offset, or responses with low-frequencies compared to the ship's natural frequencies. This step is left for a future study.

NUMERICAL RESULTS

Effects of Incident, Diffracted and Radiated Waves on Stabiliser Performance

The first effect of stabilisers fins, even in the fixed position, is to increase the roll damping. Figure 6 shows the effects on the roll transfer function for a ship in beam seas at 15 knots forward speed due to the different velocity contributions. Because the calculations are given for a Naval vessel, the scales have not been shown. Only relative comparisons can be given, for reasons of confidentiality.
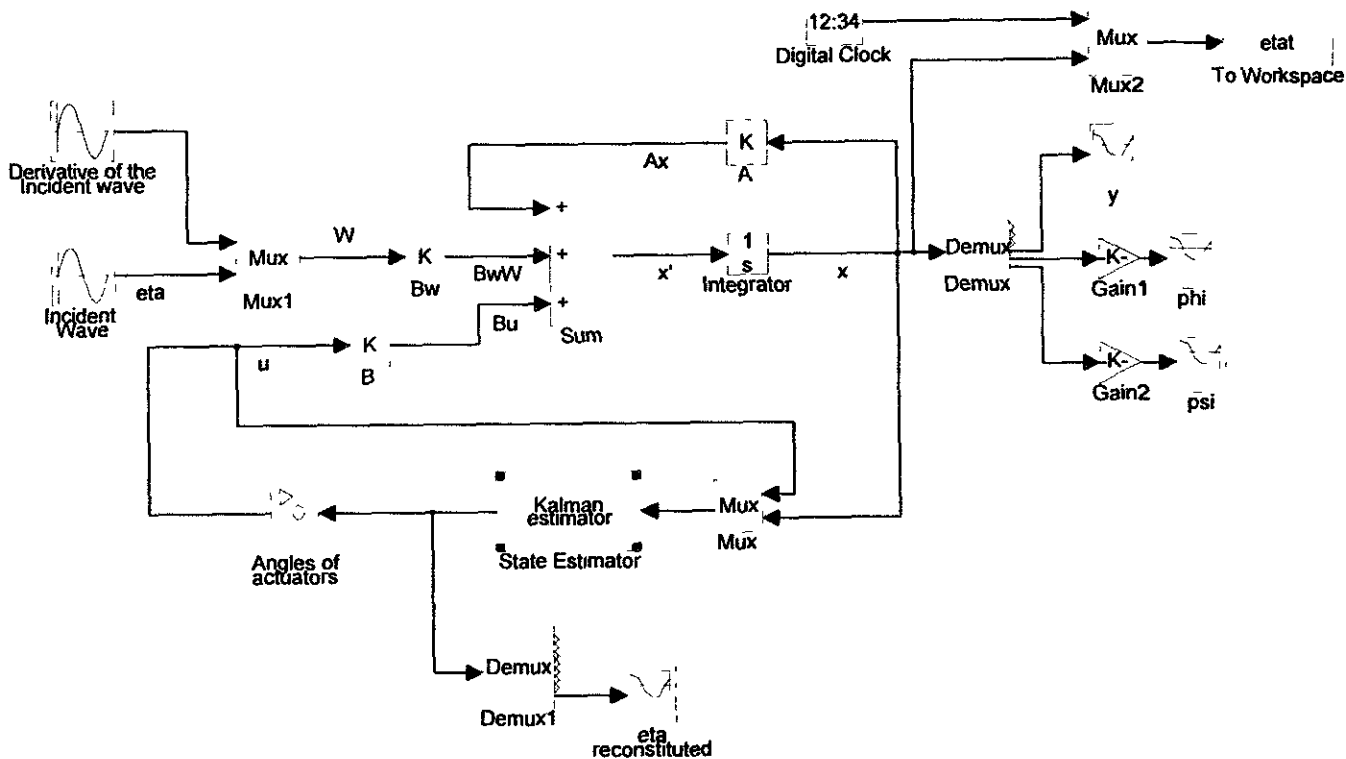
Figure 5. SIMULINK diagram for simulating the ship motion and stabiliser system.

The ship without stabiliser fins, but with fixed rudders (No Stabs, No Excit) is compared to the ship with fixed fins, but taking into account only the additional roll damping and excluding the velocities due to incident and diffracted waves (Fixed Stabs, No Excit). The velocity seen by the foils is thus the combination of the ship's forward speed, and the movement. The lift created resists the motion, and the roll response is reduced compared to the same ship without the fins.

On the other hand, the incident and diffracted waves induce velocities which affect the incidence on the foils. Including the velocities due to incident and diffracted waves (Fixed Stabs, Excit) the roll response is decreased near the resonant frequency and increased at higher frequencies. Finally, adding a command law (Mobile Stabs, Excit) reduces the roll response near resonance but increases it very slightly at higher frequencies. The peak frequency is also reduced compared to the fixed stabiliser case.
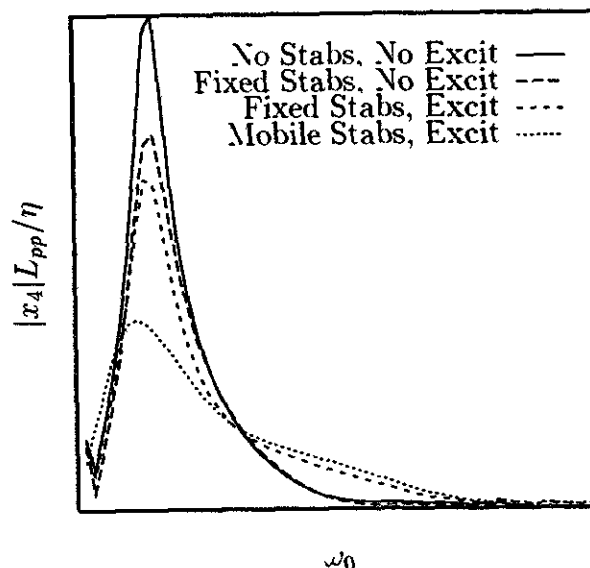
Figure 6. Effects of the different velocity contributions to stabiliser incidence on the roll transfer function in beam seas, $U_0 = 15$ knots.

28

Verification for Regular Waves

The functioning of the code RATANA has been fully verified using the small amplitude option. In this mode, the equations of motion are linearized, the small angle assumption is taken for the matrices S and T in equations (2) and (3), and the Froude-Krylov, hydrostatic and diffraction forces are calculated using the fixed mean position of the hull surface. However, the non-linear roll damping is included, and stabiliser forces are calculated using the full formulation given above. The stabiliser forces cannot all be entered into a linearised formulation. Low-frequency and mean forces are still present, even in the case of vanishing wave amplitude. Especially in the case of irregular seas, these should be accounted for in the linearized formulation, but this has not yet been done.

This small amplitude time-domain formulation is nearly equivalent to that used by DIODORE in the frequency domain. This option is extremely useful for verification, because it runs very rapidly and can be used to test the large-amplitude solution in the limit of small amplitude waves.

Figure 7 compares three sets of calculations for the transfer functions versus encounter frequency (rad/sec) for a ship at 25 knots forward speed in regular oblique seas of varying wavelength from astern (β=45 degrees). The ship is equipped with a pair of symmetric active stabiliser fins, here used only to control the roll. The rudders are used to control the yaw, but the sway is left free. This mode is controlled externally using an artificial spring which limits the drift, in the same way that tender lines are used in experiments.

The results labeled RATANA SA, for small amplitude, have been obtained by simulating the motions in the time domain in regular waves. The wave amplitude is augmented gradually at the beginning of the simulation using a ramp function ($1 - e^{-at}$) to avoid abrupt jumps in the solution due to transient effects. A post-processor for harmonic analysis has been applied to the resulting movements near the end of each simulation, after a steady harmonic motion has been achieved, in order to determine their respective amplitudes and phases.

As seen in the figure, the results from the small amplitude simulation agree well with the frequency domain solution. In this case, with relatively high forward speed in following waves, we note the well known effect that as the wave frequency increases, the encounter frequency first increases, reaches a maximum, then decreases and even becomes negative for short waves which the ship overtakes. The time domain method has no particular difficulties because the relations used to derive the impulse response functions guarantee the proper solution for negative encounter frequencies. However, an onboard measurement would not be able to distinguish, for a given absolute value of the encounter frequency, the contributions of the three possible waves.

To verify the functioning of the large-amplitude option, similar results from a second set of regular wave calculations have also been plotted on the figure 7 (using the large-amplitude formulation, but with very small waves, of 0.1m amplitude). The results, labeled RATANA LA, are virtually indistinguishable from the linearised results, thus confirming the small amplitude limit of the large-amplitude formulation.

Another test is to examine the behavior of the large and small amplitude results for a given frequency and for varying wave amplitudes. Figure 8 shows the first-order transfer functions versus wave amplitude for regular waves corresponding to the peak frequency of the roll response in figure 7. The results are
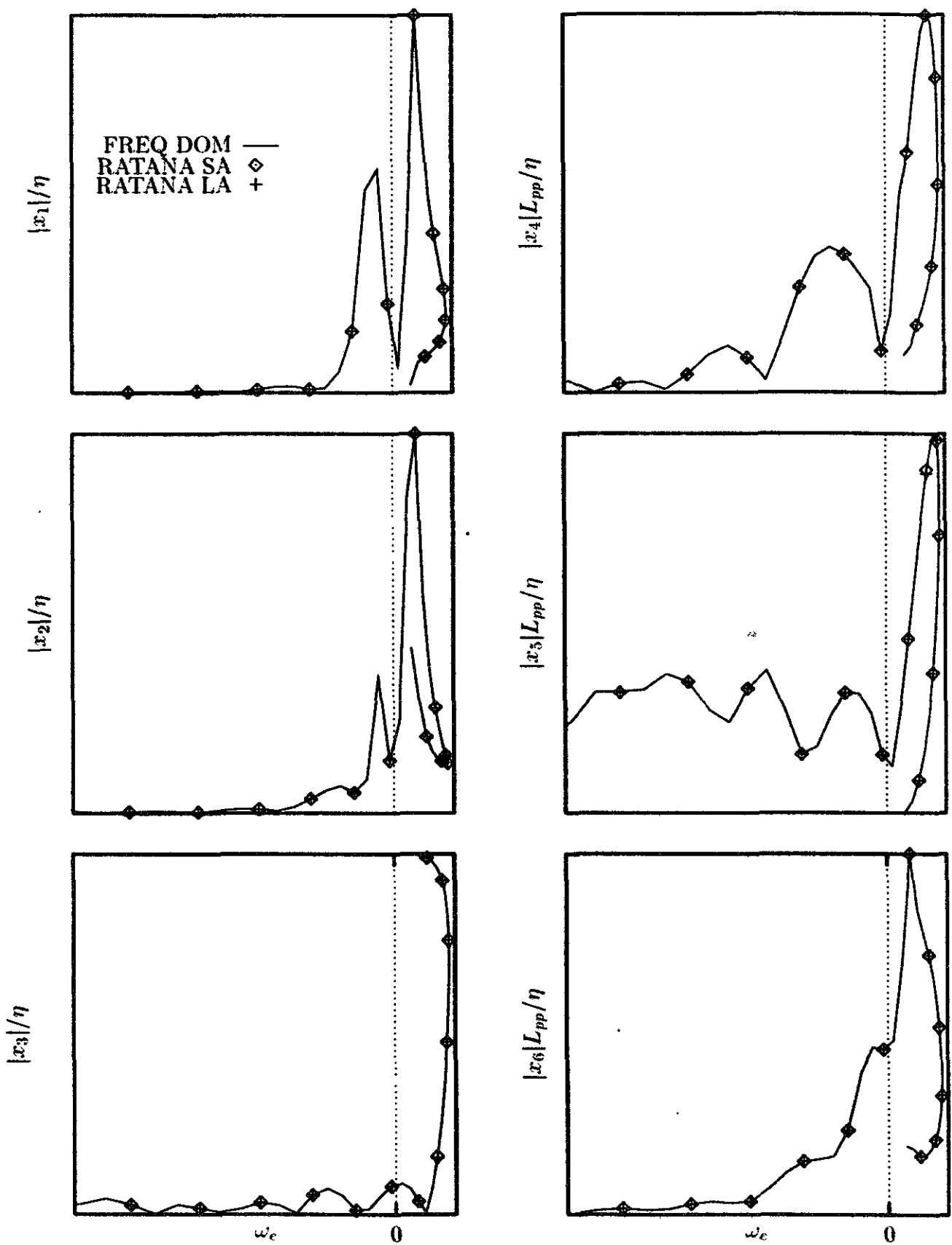
Figure 7. Transfer functions versus encounter frequency, $U_0 = 25$ knots, regular oblique seas ($\beta = 45$ degrees).
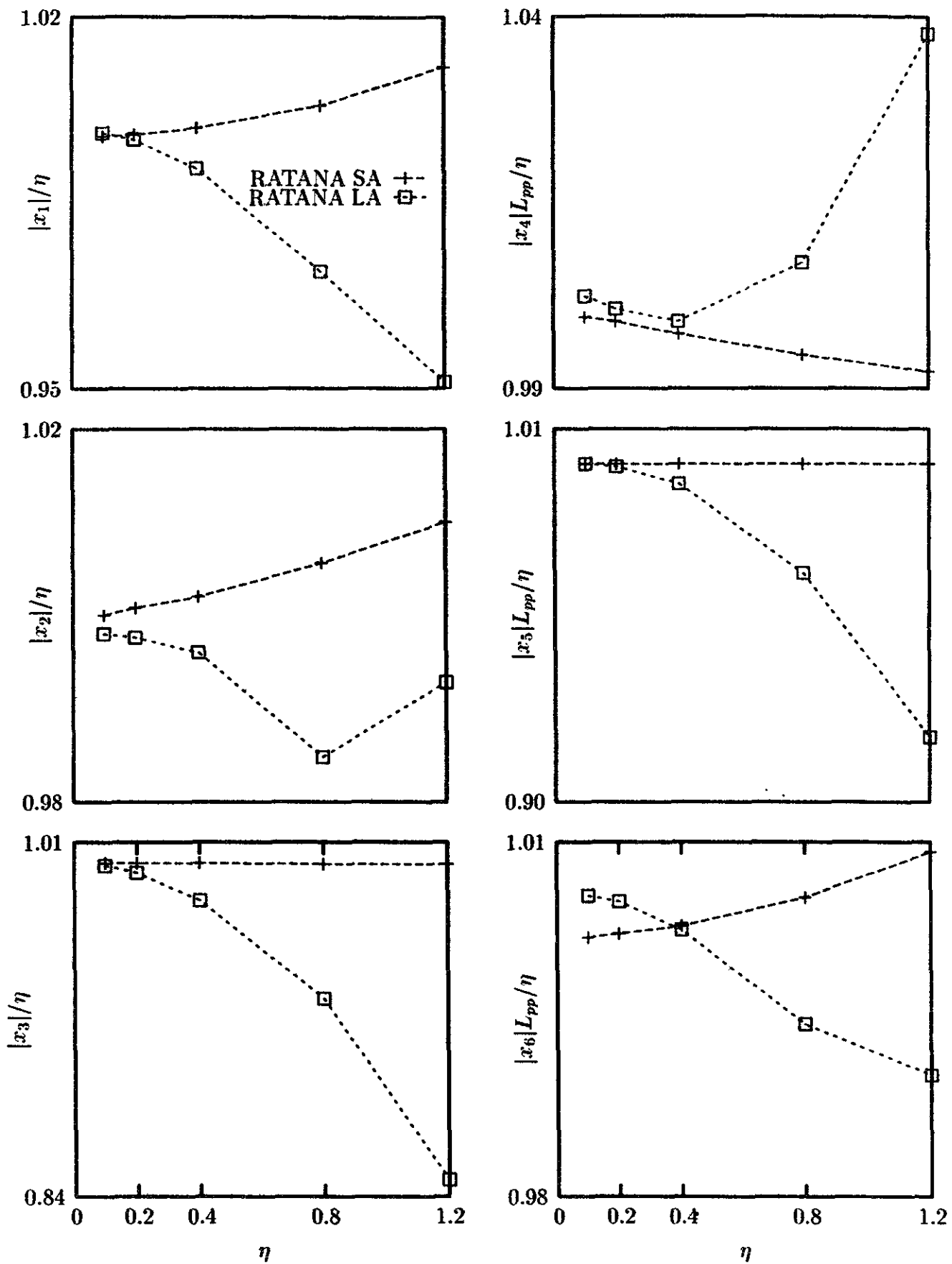
Figure 8. First-order transfer functions versus wave amplitude for regular waves corresponding to the peak frequency of the roll response (U_0 = 25 knots, β=45 degrees).

given relative to the small amplitude result at 0.1m wave amplitude. Satisfactory agreement is obtained, except for the sway motion at the largest amplitude, which does not follow the rest of the curve. For the yaw motion, the curves do not tens towards the same limit as $\eta \rightarrow 0$, but one should remark the greatly exaggerated vertical scale.

Irregular Waves

The next verification has been done in irregular beam seas at 15 knots forward speed. Figure 9 shows a part of the wave elevation time history as seen by an observer in the steadily moving reference frame, and the roll response of the ship. The chosen wave is a Pierson-Moskovitz spectrum for a Beaufort force 4-5 monodirectional seastate (Hs=2.3m, Tpic=9.0 sec).

The spectrum has been discretized according to the method of [4]. In this approach, the frequency range is divided into N equal intervals. Within each interval, a frequency is chosen in a random fashion. The amplitude of each component is chosen according to

$A(\omega) = \sqrt{2S(\omega)\Delta\omega}$. As opposed to choosing the mean frequency in each interval, this method has the advantage that the temporal history has a very long return period, (it almost never repeats) and very long simulations can be carried out. In addition, fewer frequencies are required to obtain good randomness of the wave signal. To be on the safe side, we have chosen 250 frequency components, which should be amply sufficient. The maximum frequency is chosen to be at least 2.5 time the peak frequency of the response. The phase of each component is chosen randomly in the interval $[0,2\pi]$.

According to [3] in the case of a zero mean, stationary, ergodic process with a Gaussian

distribution of the elevations, one can estimate the duration necessary to obtain the standard deviation within a precision ϵ (within a 95% confidence interval). The duration necessary is given by

$$T_h \approx \frac{1}{\epsilon^2} \frac{C'^2}{\sigma_z^4}$$

with,

$$\sigma_z^2 = rms^2 = (\int_0^\infty S_z(\omega_e)d\omega_e)$$

$$C'^2 = 2\pi \int_0^\infty S_z^2(\omega_e)d\omega_e$$

A one hour simulation time has been chosen here. For the wave elevation process, this assures a precision of approximately ±4% for the standard deviation. The time step is chosen to have approximately 50 time steps at the period of the peak response.

Compared with the theoretical spectrum (figure 10), the Fast Fourier Transform of the temporal signal using equal frequency steps does not give a very smooth spectrum, even for long time histories, because the input frequencies are not equally spaced, and hence fall, in a random fashion between the equally spaced values. What is done here is to average over the four nearest frequency values, reducing the frequency resolution but smoothing the spectrum somewhat.

Figure 9 also shows the angular displacement of the fins, and the angular velocity of the rudders of the ship calculated by RATANA using both the small and large-amplitude options. Figure 10 shows the roll response spectrum, compared with the theoretical result obtained from linear theory. It is clear that the real system performance is degraded with respect to linear theory because of saturation. Separation may also play a roll in the case of moderate or low forward speed.

Effects of Saturation on the Control Laws

As discussed above, the amplification setting of the stabiliser command laws are a compromise between good perfomance in moderate seas, and avoidance of saturation in high sea states. When there is limited saturation, the system performance degrades gradually, and the response tends toward the non-stabilised results. In the case of the present system, the stabiliser fins are mainly limited by the maximum angle and the rudders mainly in angular velocity. When saturation increases, the control system can become unstable, and even act in the wrong direction, producing undesired effects. In this case, the simulation based method is not a good means to evaluate system performance because of this unpredictable behaviour.

Figure 11 shows the roll motion, rudder angular velocity and acceleration at a point on the after deck for our ship in beam seas at 25 knots forward speed. The calculations are performed for a seastate 5, (H_S=2.7m, Tpic=9.0 secs). Two different autopilot command laws are compared: the existing law derived from SMP calculations and recalibrated after at-sea tests, and a new law, derived using the above-described procedure. The new command law does a better job reducing roll motion, because of increased rudder activity, despite the occasional saturation. The existing law is more effective in reducing acclerations, but does not saturate the rudder actuators. However, it is deceiving to compare the two laws based only on the relative performances, because the stability margins are not the same. Further improvements can be obtained in the new command laws with better refinement of the weights.

At-sea tests indicate that the roll response of this ship nearly doubled between sea states of H_S=2.3m and 2.7m in oblique quatering seas at 15 knots forward speed. It is suggestive and encouraging to note that the calculations for these cases indicate that saturation and separation come into play at the higher seastate, but not at the lower one. Of course, the calculations should be performed for multi-directional waves corresponding to the actual sea conditions.

CONCLUSIONS

It has been shown that the code RATANA is well adapted to the study of stabiliser fin and their command laws. Effects of incident, radiated, and diffracted waves are included. Nonlinear effects of saturation and separation can also be studied. Frequency-domain methods appear poorly adapted for studying these nonlinear phenomena. It has been shown that the linearised formulation is not conservative if saturation exists.

The extensions needed for simulating stabiliser fin systems in multi-directional sea states should not be too difficult, as the other parts of the code can already handle this case. A validation study to compare with at-sea identification of the ship/stabiliser system should be carried out. Well-adapted numerical methods for calculating the stabiliser forces should be used to verify the formulas used here.

Further refinement of the command laws obtained using MATLAB is needed. Addition of integral feedback terms and control of the stability margins should be performed in order to exploit its capacities to a maximum.

REFERENCES

[1] Adegeest, L.J.M. 1995. Nonlinear hull girder loads in ships. Ph.D. Diss. Technical University of Delft.

[2] Bingham, H.B., 1994. Simulating ship motions in the time-domain, Ph.D. Diss., Department of Ocean Engineering, MIT.

[3] Boudet, L, 1996. Recommandations concernant la qualité des simulations de la réponse d'un navire sur houle aléatoire, Etude no. 2520, Piece no. 7, Val-de-Reuil: Bassin d'Essais des Carènes.

[4] Boudet, L. and B. Molin, 1995. Analyse numérique et expérimentale du groupage des vagues, *Fifth Journées de l'Hydrodynamique* ROUEN, Val-de-Reuil: Bassin d'Essais des Carènes.

[5] Contento, G., A. Francescutto, and M. Piciullo, 1996. On the effectiveness of constant coefficients roll motion equation, *J. Ocean Engng*, Vol. 23:(597-618).

[6] Dallinga, R.P., and G. van Ballegoyen, 1995. CRS Motion Control: Physics of fin stabilisers, (confidential report).

[7] El Gaouhi, L. 1994. *Commande des Systèmes Linéaires*, Course notes from l'ENSTA.

[8] Greenhow, M., 1986. High- and low-frequency asymptotic consequences of the Kramers-Kronig relations, *Journal of Engineering Mathematics*, 293-306.

[9] Himineo, Y., 1981. Prediction of ship roll-damping - the state of the art, University of Michigan, Dept. of Naval Architecture and Marine Engineering, Report no. 239.

[10] King, B.K., 1990. A fast numerical solver for large amplitude ship motions simulations, *The Fourth International Conference on Stability of Ships and Ocean Vehicles*, 299-306, Naples.

[11] Laurens, J.-M. 1997. Simulation numérique de l'interaction hélice-gouverne, Etude no. 2528, Piece no. 4, Val-de-Reuil: Bassin d'Essais des Carènes.

[12] Magee, A.R. 1997. Appplications using a seakeeping simulation code, *Proceedings of the Twelfth International Workshop on Water Waves and Floating Bodies,*.Carry-le-Rouet, France.

[13] Oakley, O.H., J.R. Paulling, and P.D. Wood, 1974. Ship motions and capsizing in astern seas, *Proceeding of the Tenth Symposium on Naval Hydrodynamics*. Washington, DC : Office of Naval Research.

[14] Wheeler, J.D., 1970. Method for calculating forces produced by irregular waves, *Journal of Petroleum Technology*, 359-370.

ACKNOWLEDGEMENT
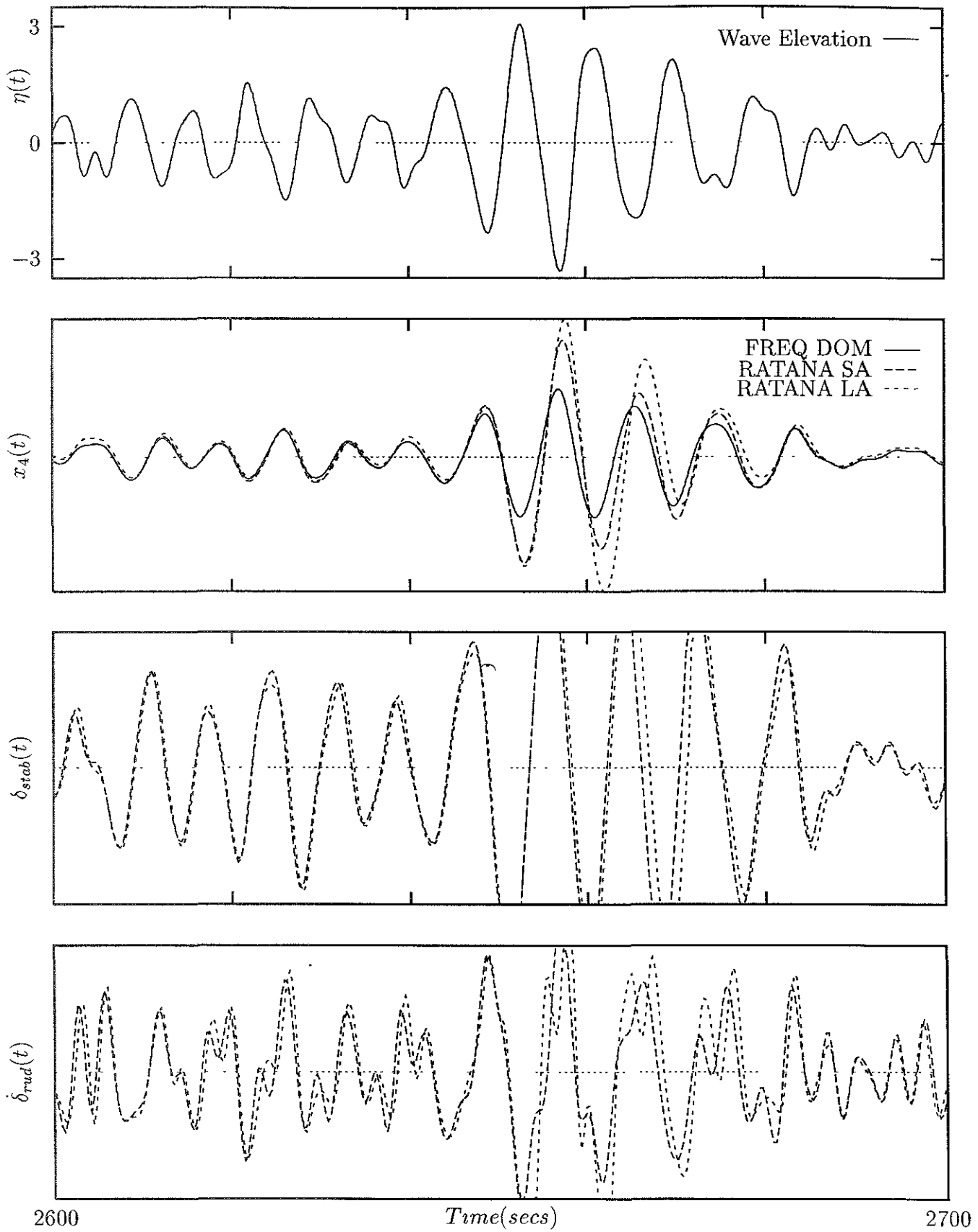
Figure 9. Wave elevation, roll response, angular displacement of the fins, and angular velocity of the rudders calculated using the small and large-amplitude options.
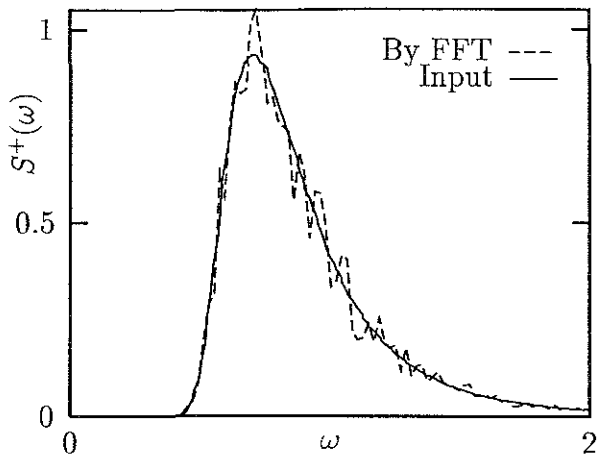
Figure 10a. Wave spectrum obtained by FFT compared with the input spectrum.
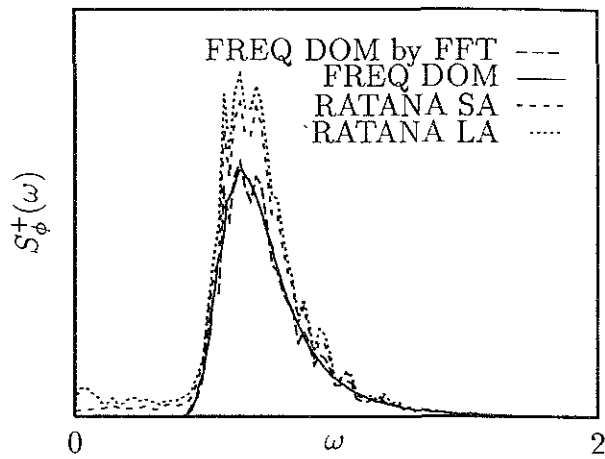
Figure 10b. The roll response spectra: frequency domain, small- and large-amplitude, $U_0 = 15$ knots, $\beta = 90$ degrees.
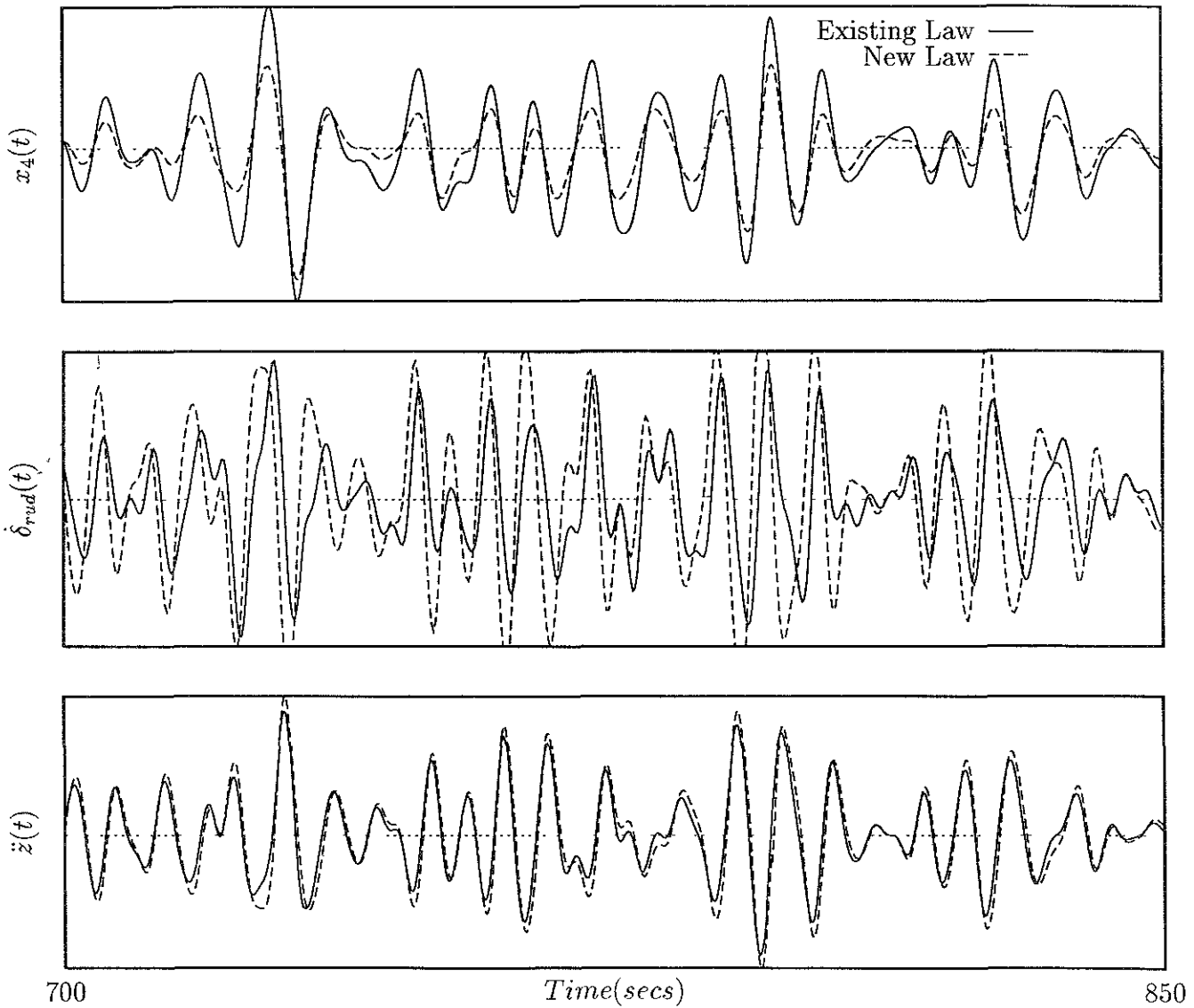
Figure 11. Roll motion, rudder angular velocity, and acceleration at a point on the after deck, $U_0 = 25$ knots, $\beta = 90$ degrees, using two different autopilot command laws.

36

STANDARTIZATION OF STABILITY: PROBLEMS AND PERSPECTIVES

Yu.I. Nechaev
State Marine Technical University,
State Enterprise «Admiralty Shipyard»,
Saint-Petersburg, Russia
E-mail: polestar@mail.wplus.net

INTRODUCTION

The theory of stability standardization is a conceptual basis providing the criteria relationships development of the basis of methods and models describing the dynamics of interaction of the ship and environment. The problem complexity, ·variety of physical pictures of heel and capsizing uncertainty and incompleteness of the initial information result in various approaches to stability requirements statement, variety of national systems standardization and the conditionally of the applied criteria. Although these approaches have much in common, points of views on the schematization problem of the interaction of the ship with the seas and wind are so different and the hydrodynamic factors have not yet been studied adequately, that the present standard application even to the same ship gives paradox conclusions and not permissible variability of criteria estimates. The problem condition of stability analysis and standardization influenced the practice of making international criteria system, where the IMO requirements are still supported, though they had been considered as for as in 60th and based on regulation of elements of the static and dynamic stability diagrams without considering the theory and experiment achievements in the discussed field and also without using fundamental results of mathematics and mechanics of the latest years.

In the present paper the peculiar features of the stability standardization system have been discussed and the approach to their construction has been stated on the basis of the criteria space information model using the fuzzy logic elements.

1. THE PECULIAR CHARACTERISTICS OF THE PROBLEM

The stability standardization is a complex problem. It exceeds the limits of the theory of ship and hydromechanics and includes such factors as law, economics, operation, construction, hydrometeorology and others. Considering all these factors in the whole standardization problem is a result of compromises and simplifications resulting in the conditionally of the standardization system.

In analyzing and standardizing stability a few characteristics must be taken into account:
- The qualified description of this phenomenon is of prime importance and very significant for practical applications where you cannot ignore the uncertainty and incompleteness of initial information.
- Making conclusions of the ship stability, in fact we mean not the dynamics of the interaction of the ship and environment, but the mathematical model of this phenomenon. The model ability to predict sharp jump-line changes in the ship behavior as a dynamic system influenced by random disturbances, depend on the model type and the set of parameters representing the system condition at the time moment under consideration. The general nature of these jump-line changes if so far not clear, though a lot of fundamental studies appeared on the topology of dynamic system phase space and the theory

of catastrophes. Any attempts to use these achievements in the applied stability problems where of no results that could be effective in practice

In estimating the adequacy of stability mathematical models we must consider the fact how real is received mathematical description in reflecting the interaction effect in the present situation and how successful is the trajectory. described mathematically, modeling evolution of the considered dynamic system. The adequacy level is determined by the confidence of the stability estimates by many of physical modeling methods. Taking into consideration that the measurement error in investigating stability on waves is 12-15 per cent. In the full-scale experiment is impossible, the confidence of the stability estimation by mathematical models methods cannot be higher than in the physical experiment.

The interaction dynamic investigation by integrating the non-linear determinated models in the long-time intervals resulted in appearing new peculiarities of the system behavior under various level of outer disturbances. These peculiarities are connected with appearing chaotic motions and forming such unusual structures as complex cycles, fractals and strange attractors [1-3]. Fig. 1 shows an evolution fragment of a phase trajectory of the studied dynamic system described by the non-linear deterministic model the ship rolling having the S-form diagram of stability ''and negative initial metacentric height. From the graph it follows that the system behavior is characterized by the phase trajectory wandering in different directions and describing the complex unwinding cycles in the rather long period of time.
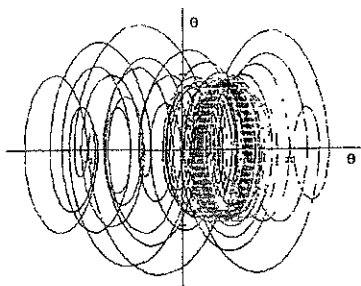
Fig. 1. The evolution of a phase trajectory of the dynamic system described by the non-linear deterministic model the ship rolling having the S-form diagram of

stability and negative initial metacentric height

Consideration of all these peculiarities in the ship behavior interpretation made this very complex interaction picture very obscure and difficult to state and choose the criteria relationships. Under the conditions the transition from determinated models to their probability analogue is quite natural The stochastic problem structure is often more simple to analyze than the structure of the determinated model derived from it. The semantic sense of the problem, possibility of accumulating and storing the information, its confidence evaluation, discussing and testing the consequences received from the analysis of different versions of the problem statement make it possible to solve the problem of the model information structure to be investigated.

Considering these peculiar characteristics the problem for improving the system of standardization and developing criterion ratios can be stated as follows. Suppose we have an information operator making transformation of the information about the interaction of the ship and environment. The structure of this operator must allow for two aspects, determining *principal requirements to the contents of the information streams*:

- In developing system of stability standardization, i.e. those operating with the uncertainty one must keep in mind that any negligible uncertainty in the input data in this problems results in a great uncertainty in solving, and this uncertainty must be accurately considered, because the solution is information about the most significant seakeeping capability of the ship. And here we must know which of the fuzzy calculation components and which of their combination are most suitable for solving the problem raised [6].
- The stability criteria choice and statement must consider the ship behavior peculiarities, as of a dynamic system, under the influence of external disturbances. The usual regime of operation in this case are stable states of equilibrium to which the stability fields correspond in the space of parameters. The system behavior on the boundary of fields and near them depends on the conditions of the problem. Small violations of the safe boundaries result in small changes of

the system, but small violations of dangerous boundaries result in a rather new state of the system, that cannot be permitted in operation practice Realization of this theoretical principles in the conditions of uncertainty and incompleteness of the initial information is connected with difficulties in stating and choosing threshold values of the criteria characteristics. The «fuzzy» calculation concept 'lows to avoid these difficulties and realize the main principle of this approach, i.e. tolerance of inaccuracy and practical truth for achieving interpretation, flexibility of solution.

The generalized model made on the base of this approach allows to construct models of formalized problems for the analysis and standardization of stability of ships and floating technical vehicles for the ocean exploration.

The investigation foresees the construction and consideration of direct and reverse problems models. The direct problem analysis solving is transition from the familiar structure and the system dynamics peculiarities to stability characteristics and criteria. The reverse problem (synthesis) is transition from the desired characteristics and criteria ratios to the system structure and its components properties. These models characteristics the formalized core of the stability standardization theory.

The interaction dynamics of the ship and environment can be expressed by the mathematical model:

$$dx/dt = f(X, Y, t), x(t_0) = X_0$$

$$F(X, t) \le 0, t \in [t_0, T],$$

where X-n is measuring vector of phase coordinates; Y-m is measuring vector of random disturbances; F(X,t) is region of changing the vector of phase coordinates, determining the safe operation conditions; $x(t_0) = X_0$ is incidental starting conditions.

Solution of this problem is a highly permissible value of the out parameters and on their base the stability criteria are formed

$$R_j \ge Q_j, j = \overline{1, J}.$$

$$Q_1 \in \Omega(z_1^* < z_G < z_1^{**}),$$

$$Q_1 \in \Omega(z_j^* < z_G < z_j^{**}),$$

$$Z_{cr} = (Z_G)_{nun}.$$

Here $\Omega_1 ... \Omega_j$ — are regions of changing the criteria ratios considering the initial information uncertainty and incompleteness. Using the notion about Z_{CR}, we can calculate the probability of capsizing as probability of increasing the highly permissible value by parameter Z_G

$$P(z_G > z_{cr}) = \int_{\Omega} P_1(c_1, ..., c_k) dc_1, ..., dc_k,$$

where Ω — is region of changing variables $C_1, ..., C_k$, where the inequality is performed

$$Z_G(c_1, ..., c_k) > Z_{cr}.$$

By the alternative problem statement, the value of the out parameter Z_{CR} is established, which may be increased with the stated probability P_0:

$$R(Z_G > Z_{cr}) = P_0.$$

So, the problem discussed is to synthesize the algorithm of analysis and stability standardization and also to determine the degree of validity in selecting the criteria ratios in the conditions of uncertainty and incompleteness of the initial information.

2. CONCEPTION AND APPROACH

Conception the developing the system of stability standardization, being the basis of the proposed approach, is founded on the principles of choosing the criteria values considering uncertainty and incompleteness of information. Under this conditions the information model of the criteria space is formed by using the fuzzy logic. The fuzzy calculations paradigm gives suitable solutions with inaccurate initial data about the object behavior and is widely used in investigating the non-linear dynamic systems, theory of chaos and fractal analysis. This new method of computational mathematics is supported by hardware (fuzzy processors) and software, and in some problem fields it is more effective then conventional methods, especially in the cases of developing intelligence systems of the analysis and prediction of dynamic objects behavior in extreme situations (Fig. 2).

The generalized information model (Fig. 3) may be taken as a model of knowledge processing in the analysis and standardization
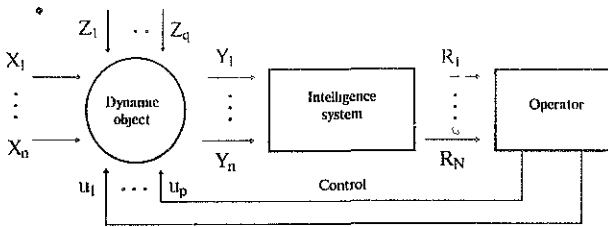
Fig. 2. Factors determining the model of interaction in the uncertain medium:

$X_1, \ldots ,X_n$ are controlled parameters of the outer disturbances;

$Y_1, \ldots ,Y_n$ are controlled parameters determining the results of interaction of the dynamic object and the environment;

$U_1, \ldots ,U_p$ are controlling parameters;

$Z_1, \ldots , Z_q$ are uncontrolled factors,

$R_1, \quad ,R_n$ are practical recommendation.

of the ship stability. The model formalizes the information processes (observations, computations and reasoning) aimed at developing the sound system of stability standardization on the basis of synthesis of the adequate mathematical model of the ship and environment interaction, the analysis of its behavior in various levels of outer disturbances, selection of critical situations and constructing the criteria equations system.
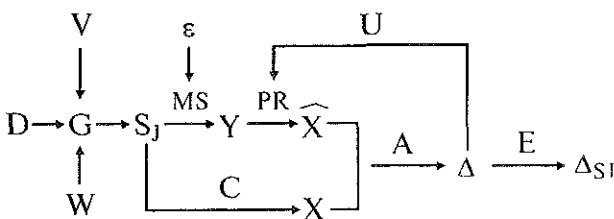
Fig. 3. Graph-scheme of the information model for studying the dynamics of interacting the ship and environment: D is the dynamic object (ship); V, W - environment (wind, seas); G is the model of situations generation; S_j - the concrete (J) situation; MS - measuring system, containing devices for observation and measurement of properties (kinematic and dynamic characteristics) of the investigate object in J-situation; ε is the measurement noise; Y - results of observations; PR - processor, processing the measurement results and a priori information by using the methods of mathematical and linguistical modeling; $\hat{X}$ is the result of the imitation modeling (new knowledge about the interaction dynamics), C - the interaction model (target operator) forming the true value of X (the result of physical modeling), A - adequator comparing $\hat{X}$ and X and given the estimate of the adequacy Δ of the received value X, U - control,

correcting the linguistic model or coefficients adjustment of the mathematical model, or where necessary the selection of other, more suitable models, E - operator, given the maximum permissible (achieved) the adequacy estimate Δ_{SJ}

One of the important problems arising in the algorithm realization, shown in Fig. 4, is forming the quality set of the acceptable solutions (alternatives), providing the choice of the criteria area $Kj(j = \overline{1,J})$. The minimum acceptable (threshold) value of the discussed standard is determined by each of the K_j criteria. Under real conditions the acceptability border (Fig. 3) is of fuzzy nature. Therefore, to define the linguistic variable «it is acceptable» more rigorous, it is reasonable to apply methods of fuzzy sets theory.
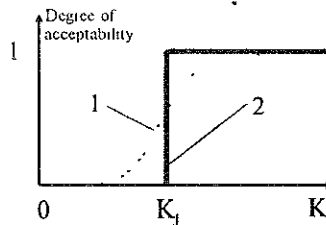
Fig 4. The degree of acceptability of the stability criterium value: 1 - the actual curve; 2 - the curve derived by, threshold value

Here you must keep in mind that excluding the good alternative (according to other criteria) is a more serious error then including the bad alternative into the set. Another problem is the lack of internal consistence of the threshold values of different criteria. Under consistency we understand such a set of threshold values all the selected criteria that if any of these values is not achieved, it is equally undesirable for the effective estimate of the standardization system. Applying the uncertain borders of the stability criteria is of great importance also because of the random nature of the input information on which the estimated scheme of the stability evaluation is constructed. In fact, the inclining experiment error, actual data inaccuracy about the ship loading and other factors result in the fact that the true value of the standardized parameter X actually is equal to $X_0+\varepsilon$ or $X_0-\varepsilon$ (Fig. 5).

Then according to requirements of standards the value $X=X_0$ (the criteria are followed without excess and deficiency), and in fact $X=X_0\pm\varepsilon$. The acceptability region of

the hypothesis $\bar{X} = X_0$, i.e. the interval $(X_{1-\alpha}, X_\alpha)$ is β (α is the significance level). This means that probability of making error of the second kind (the zero hypothesis is accepted though it is not correct) in finding the variation $\pm\varepsilon$ from the hypothetical value X_0 is β, and the $1-\beta$ value features «the criterium power». Decreasing α we reduce the probability of making error of the firs kind (the zero hypothesis when in reality it is correct). However, the probability β of making of error of the second kind is increased and the criterion power is decreased.
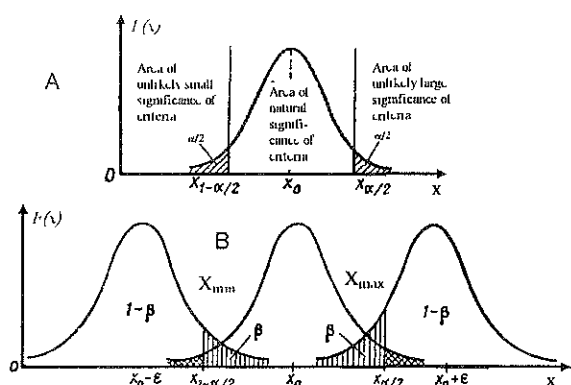
Fig. 5. Mistake for practical using of stability criteria: X_0 - area of standardized characteristics, (X_{min}, X_{max}) - area of actual changing in the exploitation conditions; A - area of null and alternative hypothesis; B - appropriate areas of second kind error

The problem of simultaneous decreasing α and β values under actual conditions of operation has not yet been solved because of very complex practical realization of the basic principle, resulting in the correct estimation of X.

3. PROBLEMS AND PARADOXES OF STANDARDIZATION

Complexity and chance are notions closely connected. In the problems of stability standardization simple criteria are often preferred to complex ones. But the deeper we try to understand the interaction mechanism of the ship and environment, the clearer it is that

the problem of criterial equations describing, these mechanisms is very sophisticated. Therefore in the course of solving this problem we come across unexpected results and paradoxes of standardization.

It is know that the safety guarantee of any, even very primitive standards, may be made as close to the unity as possible (ideal standards), if

$$\frac{1}{\sigma\sqrt{2\pi}} \int_\infty^0 \exp\left[-\frac{(\varphi - \bar{\varphi})^2}{2\sigma_x^2}\right] d\varphi = 0 \quad \text{and } \sigma \to 0,$$

$$\varphi_i = \left[(z_G - z_{CR})/z_G\right]100;$$

where $\sigma = \left[\sum(\varphi_i - \bar{\varphi})^2 / (N-1)\right]^{1/2}$;

$$\bar{\varphi} = \frac{1}{N}\varphi_i;$$

z_G, z_{CR} — actual and critical Z-axes of the ship center of gravity.

However we can achieve this only by making middle standards more rigorous. The elementary calculations show that even more based physical stability standards are less ideal than discussed by IMO in the 60th the simplified criterion of the original metacentric height $h_0 \geq 0,50 + 0,035B/f$, where B is breadth of the ship, f - freeboard depth amidships [5].

The paradox is that the above result is achieved by a very ineffective means - by making middle standard more rigorous, even in these cases where it is not necessary.

The paradox of zero probability has direct relation to the problem of probable stability standardization. In fact, the probability of ship capsizing is practically equal to zero, * but this event is not impossible. There is the question, if it is possible to compare «chances» of events having the zero probability, and if it is correct to combine events, having zero probability resulting in the end to the probability almost equal to unity, i.e. adding many «nothing»

results in «something». In the probability analysis and the stability standardization we come across the notions of rare phenomena (combination of external conditions in choosing calculation situations, effect of resonance waves packets of various forms and intensity, extreme waves, etc.). Small probability of these events gives the wrong impression that for certain types of ships it is practically impossible to be in situations, connected with simultaneous combination of many unfavorable factors or with arising dangerous after oscillations of large amplitude (main and parametric resonance).

Many surprises and paradoxes is connected with the application of the distribution laws. One of the peculiar features is due to asymptotic properties of these laws and consists in insensitivity of the probability criterion to large changes of the ship center of gravity Z-axes in the region of $P_0 \rightarrow 1$. Other features are connected with the transformation of the distribution laws on the output of the dynamic system depending on non-linear character and the acting disturbances level.

It is known that for normal distribution the arithmetical mean $\bar{\theta} = \frac{1}{N} \sum \theta_i$ as the parameter estimate θ is not displaced $E(\bar{\theta}) = 0$ and well-grounded $\lim p(|\bar{\theta} - \theta| < \varepsilon) = 1 \ \forall \theta$ with large values of N.

However if the distribution law is not known beforehand it may appear that θ is a displaced value of the mathematical expectancy with the least - dispersion, and in the case of multivariate distributions this estimate is not acceptable for the quadratic function of losses $\sum (\theta - \bar{\theta})^2$. If this checking in the static analysis of the original selection was not made, then standard values of criteria ratios in the system are not statically proved.

A lot of paradoxes is connected with the computer realization of the problems of stability standardization. Any statistical solution which can be made on computer is now available for investigators. As a result «stable» multivariate methods with a great number of operations are used in everyday practice not having sufficient theoretical base. Meanwhile, many empirical collisions, used in the statistical practice, can be proved by the theory of robast statistics but this is not always used in the standardization practice.

Striking examples of surprises and paradoxes are IMO criteria based on statistic standard of J.Rahola [4], proposed as far as 1939 on the basis of comparison of stability diagrams of emergency and safely operating ships. No consistent statistical analysis (as we understand it now) was not carried out at that time, and chosen for the analysis ship types (in general small steam launches) have nothing in common with modern sea transport and fishing ships for which they try to apply these criteria.

Investigation of the IMO criteria made by the author of the report shows that these criteria have statistical nature with reference to modern sea ship types, and comparison with other criteria as to contribution into the dispersion of the input characteristics (dispersion analysis) is not in their favor. What is the secret of such a great attention to this approach? The detail analysis shows that if physical criteria (e.g. weather criterion) is not decisive then the rest of national standard criteria, as well as IMO criteria, are essentially statistically and contain requirements to elements stability diagrams in various modifications. At the same time the minimum diagrams themselves accepted in standardization do not ensure against capsizing. In fact, if we use geometrical interpretation of J.Rahola determining the minimum stability diagram in various ship positions about the climbing waves then it is clear that the approach to the diagram elements standardization can be defined with some assumption only for the ship beam to the sea. Under this conditions we receive a comparatively narrow region separating the diagram ordinates of the sailing and emergency ship. In sailing with different heading angles on following waves this region is so wide, that there is no distinct safe border at all [3].

It is difficult to agree with the formal interpretation of the statistical approach as that excluding the direct consideration of external

heeling and restoring forces on waves, and also such factors as oscillation, heel damping, speed rating, etc. In the correct statistical analysis containing all its components - from selecting the essential factors to the construction and analysis of the mathematical models of interaction and developing the well-grounded system of statistical standardization - it is possible to achieve a result not yielding to conventional approaches accepted in developing physical criteria in scientific interpretation and practical significance.

Unfortunately, the experts' views at statistical and physical basis of stability standardization are so different so far, that a long-term and intensive research of experts of various countries by the coordinated program will be necessary before the international standardization problem of stability requirements is practically solved.

CONCLUSION

The problem of stability analysis and standardization is one of the most important directions connected with safe navigation. Uncertainty and incompleteness of the initial information are components belonging to statement and solving complex problems of the interaction dynamics of the ship and environment. To take this factors into consideration in developing stability standardization system it is necessary to use computers operating on fuzzy mathematics rules.

The described approach is based on applying mathematical apparatus of fuzzy sets in realization of the fuzzy algorithm of controlling the system of criterial space formation in the problem of stability analysis and standardization of sea ship. The disused technology can be realized on the basis of specially developed software ad hardware. This technology will by no means influence to final form of the criterial rations and characteristics of te stability standardization system as a applied formal apparatus contributes even more «flexible» analysis in forming the information model.

Thus, before we «take away the scaffolding around the building», which we call the stability standardization problem, it is necessary to decrease the problem complexity at the expense of peculiar features of its development and practical realization. And also we should prove methodically and describe mathematically the processes of the interaction of the ship and environment considering variety of physical pictures of heel and capsizing (from dynamic situations corresponding to the first and following inclinations of the ship on waves up to statical situations, when dynamics is of no significant role, and the dangerous inclination arises in the process of the steady drift), we should state stability criteria and realize the developed standardization system considering the uncertainty and incompleteness of the initial information.

REFERENCES

1 Kan M., Taguchi H Chaos and Fractals in Non-Linear Roll and Capsize Transaction. JSNA. Vol.169 1991

2. Nechaev Yu.I. Modeling the stability on seaway. Modern tendencies.- Leningrad, Sudostroyenie, 1989.

3. Nechaev Yu.I. The determinated chaos in the phase portraits of ship dynamics on seaway // In collected works: Non-linear problems of the mathematical physics and their application. Kiev, the Ukrainian Academy of Sciences. 1993, p.p 103-107.

4. Rahola J. The Judging of the Stability of Ship and the Determination of the Minimum Amount of Stability. Helsingfors. 1939

5 Sevastyanov N B. Stability of fishing vessrls - Leningrad, Sudostroyenie, 1970.

6 Zadeh L. Fuzzy sets as a basis for a theory of probability // Fuzzy Sets and Systems. 1978 Vol.1,pp 3-28

INTACT AND DAMAGE STABILITY CRITERIA AND EFFECTIVENESS OF THE VESSELS

P.N.KOLEV,   P.G.GEORGIEV
Technical University - Varna, Bulgaria
Shipbuilding Faculty

G. P. PETROV
Navigation Maritime Bulgare, Varna, Bulgaria
Safety and Quality Department

ABSTRACT

In the present paper are investigated the intact and damage stability requirements on the effectiveness of the small chemical tankers.·It is shown that the damage stability requirements are dominated comparing with intact stability ones. Optimal loading plans with damage stability constrains could be worked out using the proposed software for computer on-board system. In case of implementation of such approved software the exploatation of the vessels could be more flexible and time saving.

NOMENCLATURE

d	- ship's draft ;
GZ_{max}	- maximal righting lever;
Ix,Iy,Ixy	- second moments of S around main axis;
Ix_F, Iy_F, Ixy_F	- second moment of S around the axises which passes through the centre of flotation;
i_x, i_y, i_{xy}	- second moments of s about the central axis;
S	- projection of waterplane area;
s	- projection of area in damaged tanks;
SG	- specific gravity of cargo;
V	- underwater volume;
Vo	- constant volume;
(X_F, Y_F)	- centre of flotation;
(X_G, Y_G, Z_G)	- centre of gravity;
(X_B, Y_B, Z_B)	- centre of buoyancy;
(x_p, y_p, z_p)	- centre of gravity of seawater in damaged tanks;
(x_s, y_s)	- centre of area in damaged tanks;
ψ	- trim;
θ	- heel;

Subscripts:

l	- for parameters after flooding;

INTRODUCTION

At last several years a new damage stability requirements for most of the ship types have been come into the marine practice and for some types of ship they are revising. All of them are directed to increase the safety in navigation with respect to the environment protection and life saving at sea. Steadily increasing damage stability requirements begin dominate over that for the intact stability and determine the approaches in ship design as well as the effectiveness of ship operating [1]. The case in point are following requirements to intact and damage stability:

- **IMO Resolution A.749 (18)** - *Code on Intact Stability for All Types of Ships covered by IMO Instruments* ;

- **SOLAS Ch. II, Part B -1** - the regulations on subdivision and damage stability based on the probabilistic concept which takes the probability of survival after collision as a measure of ship's safety in the damaged condition

- IBC Code (*International Code for the Construction and Equipment of Ships Carrying Dangerous Chemicals in Bulk*).

- MARPOL 73/78.

At present paper the influence of two groups requirements over effectiveness of ship operating and possibilities of its increasing is discussed by way of example of 3200 tDW chemical carrier type 2.

INTACT STABILITY INVESTIGATION

The main particulars of the ship (Fig.1.) are:

Length Over All	L_{oa}	= 88.600 m
Length b/w perpendiculars	L_{pp}	= 82.000 m
Breadth	B	= 13.600 m
Depth	D	= 6.500 m
Draft (summer)	d	= 5.504 m
Displacement	Δ	= 4574.4 t
Deadweight	DW	= 3223.3 t

Cargo Tank Capacity:

Center cargo tanks	2090.27 m³
Wing cargo tanks	1328.70 m³
Slop tanks	145.56 m³
TOTAL	3564.53 m³
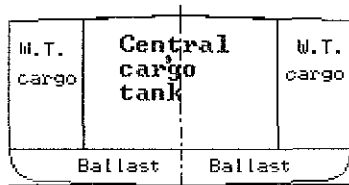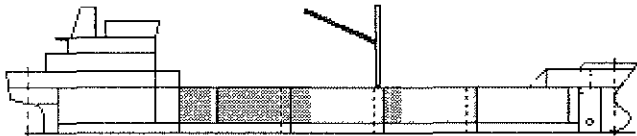
Fig.1. 3200 tDW chemical carrier.

At examination of intact stability and effectiveness of the ship the following circumstances are given an account of actual ship:
• For the ship permissible tank filling levels should be confirmed by Table 1 with respect to the scantling including sloshing pressure;

Table 1.

PERMISSIBLE TANK FILLING LEVELS			
Cargo SG	1 00 < S G <= 1 50	S.G. <= 1.00	
No 1,2 & 3 centre tanks	UPPER FILLS ≥ 65 %	UPPER FILLS	NO RESTRIC-TIONS
	LOWER FILLS ≤ 45 %	LOWER FILLS	
No 4 centre tank	UPPER FILLS ≥ 85 %	UPPER FILLS	≥ 85 %
	LOWER FILLS ≤ 25 %	LOWER FILLS	≤ 30 %
Wing tanks	NO RESTRICTIONS (S G <=1.20)		
GM <= 1.70 m in all loading conditio			

• In the *Stability Manual*, loss in GM due to free surface effects have been calculated by using the maximum free surface moment of each tank irrespective of the loaded level in tank except when tank are completely filled and empty;

• When carrying of heavy chemicals (SG > 1.4 t/m³) in central cargo tanks only, to satisfy the intact stability requirements about 120 t ballast must be taken.

Adopted approach for correction for free surface effects gives considerable reserve but concretely make worse the effectiveness of the ship. Formally it is not well-founded. The maximum effect of free surfaces is at 50% filling of tanks which is prohibited for cargoes with SG>1.0 t/m³. That's way using a precise approach for correction for free surface is advisable. Such approach is recommended by IBC too. [5]

On Fig.2. the free surface moments for cargo tank No 4 C depend on the angle of heel for approximate - 1 and exact approach - 2 (at different level of filling) are compared.
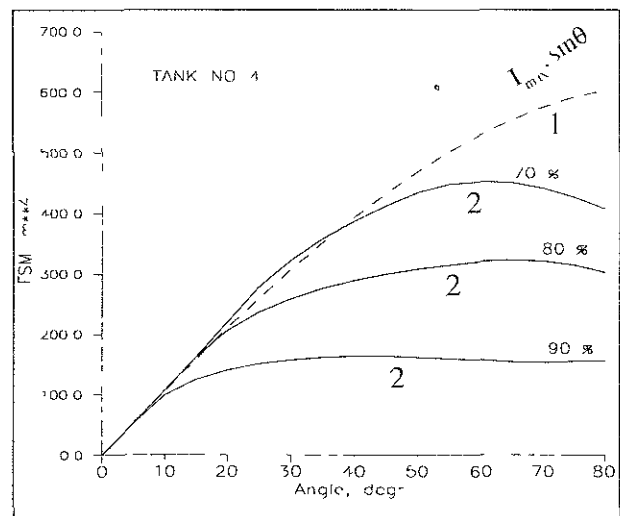
Fig.2. Free surface moment acc. aproximate - 1 and exact - 2 approach.

In Table 2 the obtained results for intact stability at carrying of heavy chemicals in central cargo tanks only are compared. Fig. 3. shows two stability diagrams.

Table 2.

ITEM	APPROACH 1	APPROACH 2
CARGO ,t	2844.4	2961.8
BALLAST,t	122.9	0
GZmax, m	0.227	0.416
$\theta 1°$	35	40
A30,mrad	0.039	>>0 03

θ_1 is angle of GZmax and A_{30} is area under righting lever curve up to 30° angle of heel.
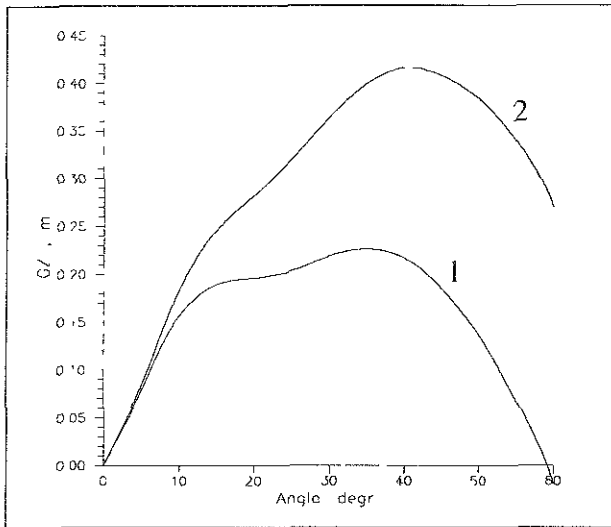
Fig.3. Intact stability diagram with different approaches for free surface correction calculation.

The results in the table show that is is possible to increase effectiveness of the ship by using exact approach for free surface corrections.

DAMAGE STABILITY INVESTIGATION

According to IBC [5] a type ship of 150 m in length or less should be assumed to sustain damage anywhere in its length except involving either of the bulkheads bounding a machinery space located aft.

There are two alternative methods of calculation and presentation of ship survival capability:

• A complete analysis of the limiting survival characteristics over the full range of intended loading conditions.

This systematic investigation of damage-survival characteristics should be undertaken by making calculations to obtain the minimum required GM or maximum allowable KG at a sufficient number of draughts within the operating range to permit the construction of series of curves of "required GM" or "allowable KG" in relation to draught and cargo-tank content in way of the damage;

• By approval of calculations based on service conditions proposed by the builder or owner, in which case the certificate of fitness should be endorsed in respect of the conditions accepted.

In case of the examinating ship in design documentation the second method is used. In *Stability Manual* 54 conditions for chemicals with SG in range (0.699 ÷ 1.499 t/m^3) for central tanks and SG in range (0.699 ÷ 1.199 t/m^3) for wing tanks are worked out (Table 3). For each condition the utilization in percent of the total volume of central tanks (first row) and wing tanks is presented in the table. The analysis of the conditions shows:

• at 24 conditions - 48% from the total number of conditions, tank No 3 C is empty (marked cells);

• there is not condition with cargo only in central tanks among all conditions. At the same time only these tanks are adapted to carry chemicals type 2 and all possible weight of the cargo (with

Table 3.

C.C.T SG t/m3		A	B	C	D	E	F	G	H	I
W.C T SG t/m3		0.699	0.799	0.899	0.999	1.099	1 199	1.299	1.399	1.499
A	0.699	98	98	98	92.5	84.1	77.1	69.8	66.5	61.7
		98	98	98	92.4	92.4	92.4	95.8	91.1	97.5
B	0.799	98	98	94.2	90.8	81.7	72.8	69.8	64.8	61.5
		98	98	94.7	83.9	85 4	90	84	84	92.8
C	0.899	98	98	90	87.8	81.3	72.8	67.6	64.3	59.1
		98	94.1	90	79.2	76 8	80	79.1	75.8	77.9
D	0.999	98	98	89.5	87.8	72.8	72.8	67.6	64 3	59.1
		93.9	84 7	81.6	71.3	82.3	72	71.2	68.2	70.1
E	1.099	98	98	89.5	87.8	72.8	72.8	67.6	64.3	59.1
		89.6	77	74.2	64.8	74.8	65.5	64.7	62	63.7
F	1.199	98	92.7	89.5	87.8	72.8	72.8	67.6	64.3	59 1
		82 2	75.6	68	59.4	68.6	60	59.3	56.8	58.4

SG = 1.416 t/m³) can be arranged there;
• the maximal amount of cargo at present conditions is 2884.4 t and only 1895.3 t is in central tanks.

It is obvious that compulsory using of wing tanks reduces effectiveness of the ship. In the same time they are designed for chemicals type 3 with SG < 1.2 t/m³ only.

In practice the chamicals carryed out with those ships are with SG > 1.2 t/m³ and type 2.

If chemicals will be carried at different condition from the standards, the Master must carry out the damaged stability calculation or on the base of a large number of pre-programmed damage stability scenarios to demonstrate compliance of new loading conditions with the damage stability criteria. It should be noted that this function should only be used by the Master to obtain a level of confidence that the new condition (not shown in the approved damage stability manual) will satisfy the requirements. However, it still be necessary for the actual condition to be approved by the flag Administration and added as an addendum to the approved manual, prior to the ship loading to that condition

On board of the ships (4 sister ships) has not possibilities for calculation and control of the damage stability requirements for conditions not included in the *Manual*.

For solving the problem, the program module **DSTAB** for *ALCOS* (*Auto Loading Computer On-board System*) [3],[4] has been developed.

MAIN PRINCIPLES OF THE MODULE *DSTAB*

The main principles of the computer program module are [2]:
• Three dimensional numerical model of the ship and compartment geometry;
• The metacentric height (GM), stability levers (GZ) and centre of gravity positions (KG) for judging the final survival conditions is calculated by the constant-displacement (lost-buoyancy) method;
• The calculations are done for the ship freely trimming;
• Free surface corrections for consumable liquids are constant (the maximal ones) and the approximate approach is used.
• For undamaged cargo tanks the program calculates actual position of centre of gravity of the liquid cargo depends on trim and heel angle;
• For damaged tanks containing cargo is assumed that the contents are completely lost from that compartment and replaced by salt water up

to the level of the final plane of equilibrium.
• There are two main categories of damaged tanks: I category - tanks fully immersed with salt water and II - tanks partly immersed and connected with sea water.

After damage the ship should be capable of surviving in a condition of stable equilibrium and should satisfy the following criteria [5]:
•The waterline, taking into account sinkage, heel and trim, should be bellow the lower edge of any opening through which progressive flooding or downflooding may take place;
•The maximum angle of heel due to unsymmetrical flooding should not exceed 25°, except that this angle may be increased to 30 ° if no deck immersion occurs;
•The righting-lever curve should have a minimum range of 20° beyond the position of equilibrium in association with a maximum residual righting lever of at least 0.1 m within the 20° range; the area under the curve within this range should not be less than 0.0175 mrad.

After damage the parameters of underwater volume and waterplane are:

$$V_1 = V - v$$
$$V_1.X_{B1} = V.X_B - v.x_p$$
$$V_1.Y_{B1} = V.Y_B - v.y_p$$
$$V_1.Z_{B1} = V.Z_B - v.z_p$$
$$S_1 = S - s$$

(1)

$$S_1.X_{F1} = S.X_1 - s.x_s$$
$$S_1.Y_{F1} = S.Y_1 - s.y_s$$
$$Ix_{11} = Ix - i_x - s.y_s^2 - S_1.Y_{F1}^2$$
$$Iy_{r1} = Iy - i_y - s.x_s^2 - S_1.X_{F1}^2$$
$$Ixy_{F1} = Ixy - i_{xy} - s.x_s.y_s - S_1.X_{F1}.Y_{r1}$$

At condition of equilibrium the following equations are valid:

$$V_1 - V_0 = 0$$
$$Myz + Mxy.tg\psi = 0$$ (2)
$$Mxz + Mxy.tg\theta = 0$$

where: $Myz = V_1.X_{B1} - V_0.X_G$
$Mxz = V_1.Y_{B1} - V_0.Y_G$
$Mxy = V_1.Z_{B1} - V_0.Z_G$

The characteristics of equilibrium - d_e, θ_e, ψ_e are solution of the system of 3 nonlinear equations (2). At present module θ = const (0,5,10,... degr) and d(θ) and $\psi(\theta)$ are solution of the system of first two equations of (2). The solution is finding by *Newton Method*. The iterations are stopped when corrections at n iteration are:

$$|\delta tg\psi| < 0.0005 ; |\delta d| < 0.01 \text{ m}$$ (3)

Table 4.

Item	SG=1.30	SG=1.40	SG=1.50
CARGO,t	2552	2552	2552
%	93.9	87.2	81.4
BALLAST,t	408	408	408
θ_0 (°)	23.4	20.3	22.7
GZmax,m	0.229	0.236	0.203
Range (°)	>20°	>20°	>20°

The righting levers are calculated like distance from actual position of centre of gravity G todisplacement force vector.

For reliable and successful operation of the *ALCOS* , IBM compatible PC with 486 processor and 4 mb RAM and VGA or SVGA colour monitor is necessary. The damage stability calculations take about 15 seconds on a IBM personal computer 6x86/133 MHz .

Numerical examples

The module **DSTAB** incorporated in *ALCOS* system has been used to calculate damage stability for conditions with cargo in central tanks only. Analysis of damage stability shows that the most severe flooding is at the middle, when the bulkhead between cargo tanks No 2 and No 3 is damaged. The obtained results for cargo with SG = 1.30 ; 1.40 and 1.50 t/m³ are presented in Table 4. In the table (%) means utilization of the total volume of the central tanks. The maximum one can be 98 %. The angle of equilibrium is θ_0. The amount of cargo is 2552 t (increase with 25 % in relation to this in Table 3) but still 408 t ballast in double bottom tank No 2 PS&SB and 3 PS&SB is needed.

POSSIBILITIES TO INCREASE THE EFFECTIVENESS

According to IBC [5] Reg. 2.8.2 in the case of small type 2 and type 3 ships which do not comply in all respects with the appropriate requirements, special dispensation may only be considered by the Administration provided that alternative measures can be taken which maintain the same degree of safety. The nature of the alternative measures should be approved and clearly stated and be available to the port Administration.

One possible measure is counter-flooding - a distinct corrective measure taken by the ship's personel to add, remove or transfer fluids in an attempt to improve a particular condition of the ship whether it is damaged.

For examinating ship counter-flooding is possible in two ways:

• counter-flooding of opposite double bottom ballast tank through ballast system;
• counter-flooding of oposite cargo wing tank from damaged one through cargo system.

This possibilities are investigated and obtained results for cargo (SG = 1.30;1.40 and 1.50 t/m³) are presented in Table 5 and Table 6.

Counter-flooding of DB ballast tank

Table 5.

Item		SG=1.30	SG=1.40	SG=1.50
CARGO, t		2611	2586	2640
%		96	88.4	84.2
BALLAST t		348	319	319
θ_0(°)	w/o	27.8	27.3	28.4
	50% 53 t	26	25.6	26.5
	100% 106 t	24.4	22.9	24.8

Counter-flooding of wing cargo tank

Table 6.

Item		SG=1.30	SG=1.40	SG=1.50
CARGO, t		2663	2763	2763
%		98	94.4	88.1
BALLAST t		211	197	197
θ_0(°)	w/o	30.8	32.3	29.9
	25% 47 t	27.1	28.8	25.8
	50% 95 t	23.7	25.2	22.3
	75 % 142 t	20.6	22.2	19.1

In the tables the angle of equilibrium- θ_0 without alternative measures and for different percents of counter-flooding is presented. For cargo with SG = 1.30 t/m³ after counter-flooding of opposite wing tank is possible to utilize the total volume of central tanks. The damage stability diagrams

51

for this condition are shown on Fig.4.
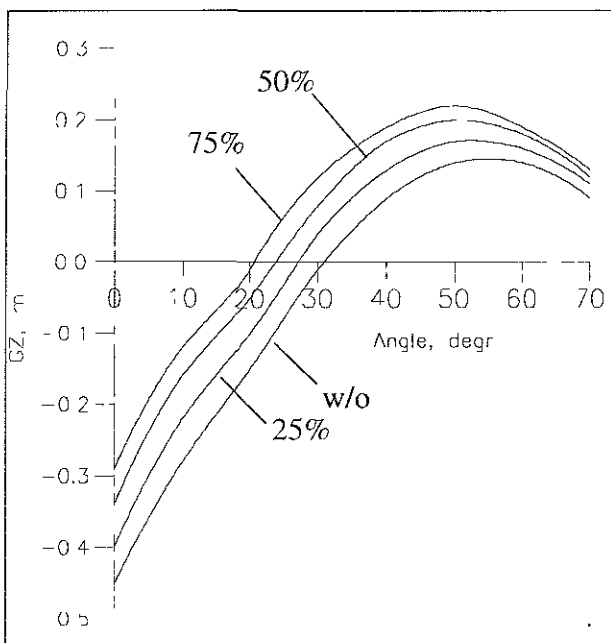
Fig.4. Damage stability diagram for different level of counter-flooding in opposite wing tank.

CONCLUSIONS

Based on the comparative investigation of the intact and damage stability criteria for 3200 tDW chemical carrier the following conclusion remarks can be provided:

1. The damage stability requirements directed to increase the safety at sea could be determinative for effectiveness of the ship;

2. The using the maximum free surface moment for cargo tanks free surface effects gives considerable reserve but makes worse the effectiveness of the ship

3. The control on damage stability requirements have to be solved by suitable software for computer on board of the ships;

4.It is necessary the Classification Societies to develop requirements for general approval of such computer programs. By this way the time consuming procedure for approval of new loading conditions not included in *Stability Manual* could be drop out.

REFERENCES

1.   Georgiev, P.,Probabilistic damage criteria of SOLAS and effectiveness of the ship,Scientific and Applied Shipbuilding Conference, Varna,1996, pp. 53-62.

2.   Georgiev, P., Calculation of damage draft and stability by personal computer. Anniversary Scientific Conference,"30 Years Shipbuilding Institute - Varna",vol. I, 28 May, 1992, pp. 47-57.

3.   Kolev, P.N.,Pctrowa, C.M., Georgiev, P.G.,Kolev. N.P., Tomov, I.G.,Simulation control and analysis by an auto loading system,CABS '95, International Conference on "Computer applacation on board ships", 26-28 September, 1995, pp.1.3-1, 1.3-8.

4.   Kolev, P.,Petrowa, Z., Gcorgiev, P., Pentchew P.,Auto Loading Computer Onboard System ALCOS,*Shiffbauforschung* , No 1, 1995. pp. 23 - 28.

5.   *International Code for the Construction and Equipment of Ships carrying dangerous Chemicals in Bulk* (IBC Code). IMO, London, 1994.

ACKNOWLEDGEMENTS

ON APPLICATION OF THE IMO CODE AS AN ALTERNATIVE TO NATIONAL STABILITY REQUIREMENTS OF THE RUSSIAN MARITIME REGISTER RULES

V.N.Golenshin[1], M.A.Kouteinikov[2], V.B.Lipis[3]

SUMMARY

IMO Code of Intact Stability for All Types of Ships Covered by IMO Instruments was adopted by Res. A. 749 (18) in September 1993. It incorporates recommendations of different previous IMO resolutions concerning intact stability and includes some new additional recommendations. As the minimum stability standard stated by IMO provides the most favourable economic conditions for ship owners the Code seems to be a basis for possible development of less onerous national requirements ensuring acceptable level of safety. At the same time Russian national stability requirements (Russian Maritime Register of Shipping Rules for Classification and Construction of Seagoing Ships, Part IV) differ from IMO Code recommendations in form, principal propositions and in general are more onerous.

IMO recommendations are based on wide classic statistics which takes into account ships with the length less then 100 m but there is now empirical basis for extrapolation of this recommendations to cover large new ships of different types. Taking into account this fact It seems that simple replacement of proved by long experience national requirements by IMO recommendations is not reasonable.

The idea of harmonisation of the national requirements with recommendations contained in IMO instruments is not new. Differences between Register's Rules and Draft IMO Stability Code were under consideration since 1985. But criteria were mostly compared from the strictness point of view. The results obtained gave sufficient grounds for provisional palliative measure: to include IMO Code recommendations as separate chapter in the Russian Maritime Register Rules.

The chapter is considered to be an alternative to the previous Rules stability requirements.

If the intent is to save principal propositions and scientific basis of Russian national stability requirements the complex harmonisation task is more difficult. This task has two principal parts:
- reconsideration of well known IMO instruments which are not used in national Rules;
- analyses of new IMO recommendations of general nature and for ships of different types.

In this address consideration is given to the aspects of requirements' general structure and specific criteria harmonisation.

[1]V.N Golenshin - Head of Section, Russian Maritime Register of Shipping (RS), Head Office, St Petersburg, Russia
[2]M A Kouteinikov - Principal surveyor, RS, Head Office, St. Petersburg, Russia
[3]V.B.Lipis - Prof., Ph. Dr., Head of Department, Central Marine Research and Design Institute (CNIIMF), St Petersburg, Russia

THE FIRST STEP IN RS RULES
AND IMO CODE HARMONIZATION

During the last 15 years investigations in the field of intact stability and seaworthiness of seagoing merchant ships were undertaken by the CNIIMF and RS in the following main directions [5] − [9]:

- the analyze of comparison stability calculations for 55 types of cargo and passenger ships (the main part of Russian fleet in 1982 − 85 years) on the basis of RS Requirements and IMO Recommendations;
- proposals on stability requirements on the based on probabilistic estimation of the environmental influence and ship's reactions on it;
- calculation — experimental analyze (including model and natural tests) and proposals on physical stability criteria perfection: taking into account the effect of following waves, gusty wind and more accurate regard for irregular waves;
- calculation — experimental analyze and proposals on requirements concerning intact stability of ships carrying deck cargoes (containers and timber cargo) including requirements to the values of metacentric height, angle of heel due to circulation and steady wind pressure made on the basis of 11 types of container ships and 16 types of timber carriers data (covering the main part of Russian fleet of this types of ships);
- on board investigations and calculation basis for developing the new requirements to novel automatic means of stability and seaworthiness control;

These works were performed in cooperation with different Russian scientific and design firms and also with Bulgarian Ship Hydrodynamics Center.

The results of these works were laid down to the basis of corrections made in Part IV of RS Rules (including 1995 edition) and of the active participation of Russian delegation in elaboration of new IMO IS Code [11].

The main direction of these investigations is harmonization of IMO Recommendations and RS Rules requirements including the intention to use the advantages of Russian science, practice and many years experience in use of stability requirements and safe operation of ships.

The main new feature of the Part IV of RS Rules 1995 edition is inclusion of the basic recommendations of IS Code as a separate Chapter 5 with the status of alternative requirements to the ships of unrestricted navigation. It is characteristic that the concept of new proposals to RS Rules and IS Code is common - the safety standard of new ships should be not less than the safety standard of existing ships.

There is intention to give new ships more reserves of stability but practically it is not so, especially regarding ships carrying deck cargo, Ro-Ro and ships of novel features. The classic IMO Recommendations are based on wide statistics taking into account ships with length less than 100 m, but there is not enough empirical basis for extrapolation of this recommendations to cover large new ships of different types. It is clear that the new recommendations are prepared taking into account all possible grounding but the distance to the border of the dangerous zone is still more relative for new especially large ships where casualties are always dealt with cargo shifting and the initial cause in 70% of cases is error in ship operation (so called "human element").

Therefore, IS Code reflects the general position of IMO regarding the increasing of safety standards of ships and environment protection at sea - the equal account of technical, operational and "human" elements. RS Rules on one side mostly give the safety standards to ensure constructional stability, and IS Code on the other side is recommending stability criteria and "other means for ensuring the safe operation of ships" [10]. In IS Code more consideration is given to recommendations heaving operational character and the questions of design technology are not so prevailing as in RS Rules.

The structure of criteria which are common for all types of ships in RS Rules and in IS Code are different from the priorities point of view. In Rules the first place is given to "weather criterion" and the requirements to static stability arms curve

are on the second place. In IS Code on the contrary the requirements to static stability arms curve which are reflecting the safe navigation statistics at all weather conditions are on the first place. The "severe wind and rolling (weather) criterion supplements the stability criteria based on the requirements to static stability arms curve. The comparison of main stability requirements is given in Table 1. The main stability criteria of RS Rules, Is Code and those used in alternative Chapter 5 of RS Rules Part IV 1995 edition are shown. The areas a, b and form factor c are determined according to IMO methods [10].

It should be mentioned that weather criteria K in the Code and RS Rules have some principal differences in physical meaning and give different numeric results. IMO weather criterion includes in fact 2 requirements - the required ratio of inclining and restoring moments' works in case of ship rolling from the angle of equilibrium due to a steady wind pressure Q_0 and the requirement regarding this angle Q_0 itself (see Table 1). There are also differences in wind load and angle of roll Q_r determination. The formulae for Q_r determination according to RS Rules and IMO Recommendations can be brought to the common form:

$$Q_r = 24° k \left(\frac{A_k}{LB}\right) X_1 \left(\frac{B}{d}\right) X_2 (C_B) X_3 \left(\frac{\sqrt{GM_0}}{B}\right); \quad (1)$$

were dementionless coefficients k, X_1, X_2, X_3 may be determined according to RS Rules Part IV Tables 2.1.2.1 − 1,2,3; 2.1.2.2 [4].

The coefficients k, X_1, X_2 in RS Rules and IS Code are the same and only X_3 ,

<div align="right">Table 1</div>

Comparison of IS Code, RS Rules and Alternative stability criteria

Stability criteria	Merchant seagoing ships of unrestricted navigation								
	all passenger and cargo ships			container ships with length $L>100$ m			timber carriers		
	RS	IMO	Alt	RS	IMO	Alt	RS	IMO	Alt
GM, m	>0	0,15	0,15	0,15 (0,20)	0,15	0,15	0,1 0,05 0,15	0,1 >0	0,1 0,05 0,15
GZ_{max}, m $L>100$ m $L<80$ m	0,2 0,25	0,2	0,2	0,2	0,042/c	0,2	0,2 0,25	0,2	0,2
Q_{max}, deg. $\frac{B}{D}>2$	$\geqslant 30$ up to 25	$\geqslant 25$ (30)	$\geqslant 30$ (25)	$\geqslant 30$ up to 25	$\geqslant 25$ (30)	$\geqslant 30$ (25)	$\geqslant 30$ up to 25	$\geqslant 25$ (30)	$\geqslant 30$ (25)
Q_v, deg. with icing, $\frac{B}{D}>2$	60 55 up to 50	— — —	60 — up to 50	60 — up to 50	— — —	60 — up to 50	60 — up to 50	— — —	60 — up to 50
Q_f, deg.	>60	—	>60	>60	—	>60	>60	—	>60
S_{30}, m·rad	—	0,055	0,055	—	0.009/c	0,055	—	—	—
S_{40/Q_f}, m·rad	—	0,090	0,090	—	0.016/c	0,090	—	0,080	0,080
S_{30-40}, m·rad	—	0,030	0,030	—	0.006/c	0,030	—	—	—
S_{Q_v/Q_f}, m·rad	—	—	—	—	0.029/c	—	—	—	—
Z_w, m	Z	$Z+\frac{d}{2}$	$Z+\frac{d}{2}$	Z	$Z+\frac{d}{2}$	$Z+\frac{d}{2}$	Z	$Z+\frac{d}{2}$	$Z+\frac{d}{2}$
P_{ws}, Pa	—	504	504	$0,6P_v(z)$	504	504	—	504	—
P_{wg}, Pa	$P_v(z)$ 706−1216	756	756	$P_v(z)$ 706−1216	756	756	$P_v(z)$ 706−1216	756	756
Q_0, deg	—	$16/0,8Q_{fb}$	$15/0,8Q_{fb}$	$15/0,5Q_{fb}$	$16/0,8Q_{fb}$	$16/0,8Q_{fb}$	—	$16/0,8Q_{fb}$	—
Q_r, deg	Q_r^r	Q_r^J	Q_r^J	Q_r^r	Q_r^J	Q_r^J	Q_r^r	Q_r^J	Q_r^J
$K \geqslant 1$	M_c/M_v	b/a	b/a	M_c/M_v	b/a	b/a	M_c/M_v	b/a	b/a

which in IMO Recommendations is also function of $\frac{KG}{d}$ (see Fig. 1), is different.

It can be seen on Fig. 1 that Q_r^I and Q_r^I values can become equal if $KG > d$ and $Q_r^I < Q_r^I$ if $KG < d$; and as coefficients in (1) k, X_1, $X_2 \leqslant 1$ the Q_r^I max is not greater than Q_r^Imax $= 36°$.

Fig. 1
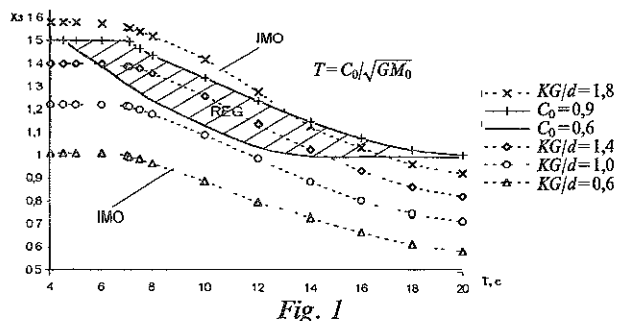
In practical meaning the ratio of weather criteria according to RS Rules and IMO Recommendations values is important. On the basis of large amount of calculations it is shown in work [9] that the K value according to RS Rules as a rule is less than according to IS Code. In common the difference is about 30% with variation coefficient 0.36. Proposals on harmonization of K calculation schemes are given in this work. As a result the K values according to different methods can be brought together with the common ratio 0.85 and variation coefficient 0.28.

At least it should be mentioned that on the contrary to RS Rules the classification according to the regions of navigation is not specified in IS Code and there are no general requirements regarding weather restrictions based on the results of K calculations.

So the idea of harmonization of stability requirements of RS Rules and IS Code recommendations is more complex and difficult than it is shown in Chapter 5 of Part IV of RS Rules 1995 edition which is included as a first step to provide a possibility of design approbation. The investigations in this direction are continuing and giving output for RS Rules and IS Code improvement.

LITERATURE

1. Blagoveschensky S.N. The principles, laid down into basis of sea-going vessels stability standardization. In vol.: Stability standards of sea-going ships. S.-P., Morskoy transport 1963, p. 105−140. (in Russian).

2. Lugovsky V.V. Theoretical basis of sea-going vessels stability standardization. S.-P., Sudostroenie, 1971, 264 p. (in Russian).

3. The Rules for Classification and Construction of Sea-going Ships, Part IV "Stability", Russian Maritime Register of Shipping, vol. 1, 1995, 464 p. (in Russian).

4. Consolidated text of the 1974 SOLAS Convention, IMO, 1993.

5. Orlov D.A., Shesterikov O.V., Kamenskaya E.N. Comparative analyze of sea-going vessels stability due to different criteria. CNIIMF Proceedings, S.- P., Transport, No 295, p. 68−80. (in Russian).

6. Kondrikov D.V. Probability criterion of ship's stability in storm conditions. S.-P., Sudostroenie, 1980, No 4, p. 12−13. (in Russian).

7. Kondrikov D.A., Volosenko E.E., Ozimova O.V. Ships stability as to weather criterion considering gusty wind. CNIIMF Proceedings, S.-P., Transport, 1985, p. 90−97 (in Russian).

8. Bogdanov A.I. Stability criterion. Safe speed and wave-to-course angle diagrams for a ship sailing in storm following sea. 18 SMSSH, v. 3, p. 81-1−81-9, BSHC, Varna, 1989.

9. Lipis V. Correlation of IMO and Russian Register Weather Criteria for Ship Stability Requirements. Proceedings of International Workshop "OTRADNOE-93", v. 2, Kaliningrad, 1993.

10. Code of intact stability for all types of ships. IMO, Res. A. 749(18), 1993.

11. Documents of IMO SLF Sub-committee, submitted by the Russian Federation. SLF 15/Add.1, 1983; SLF 33/inf.6, 1988; SLF 33/inf.7, 1988; SLF 33/inf.4, 1988; SLF 34/W.P.4/Add.1, 1989; SLF 36/3/9, 1991; SLF 37/3/6, 1992; SLF 37/inf.1, 1992; SLF 37/3/7, 1993; SLF 38/3, 1994; SLF 37/15, SLF 37/3/5, SLF 37/3/5/Add. 1,2,3, 1992; SLF 39/18, 1995.

12. Gavrilov A.Yu., Lipis V.B. Basic statements of new IMO Code on intact stability for all types of ships. The theses of Conference "Krylov readings" S.- P., 1993. (in Russian).

ON APPLICATION OF THE TERM "LARGE WINDAGE AREA"
TO EVALUATION OF WEATHER CRITERION FOR FISHING VESSELS

A.R.Togunjac, E.N.Troitskaya[1], V.N.Golenshin[2].

ABSTRACT

In practical application of IMO methods for weather criterion calculation (IMO Resolution A.749(18) using of weather criterion for fishing vessels with length over 45 m is recommended only in case they have large windage area. In order to determine possibility of making expression "large windage area" concretely defined stability criterion calculations according IMO recommendations were made for 12 fishing vessels. The analysis was carried out for load conditions having been taken in the process of designing the vessels. Thus actual and not hypothetical windage areas were considered. In the study a measure of correlation to weather criterion or a margin to critical situation is introduced. Results of the calculation are presented in form of tables and in graphical form.

Results obtained evidence that for real vessels it seems impossible to determine the range of values of small windage area for which weather criterion is realized with large margin as well as the area of values of large windage area at which reaching the critical situation is most probable. It is suggested that expression "large windage area" should be reckoned as vague and it should be recommended no to use this expression in methods for determination of weather criterion for fishing vessels as well as that weather criterion evaluation should be carried out for fishing vessels with length over 45 m with any windage area.

NOMENCLATURE

A_v — windage area of the vessel (projected area)
L_{pp} — length between perpendiculars
T — mean draught for the load considered

Weather criterion characterises the ability of a ship to withstand the combined effect of beam wind and rolling without losing its stability. In the framework of International Maritime Organization (IMO) recommendations on determining the weather criterion have been worked out for all types of ships, among them for fishing vessels. At present such recommendations for fishing vessels can be found in the following IMO documents now in force:

- Weather criterion for fishing vessels of 24 m in length and over (Resolution A.685(17) [1]
- Code on intact stability for all types of ships covered by IMO instruments (Resolution A.749(18) [2]

But assumptions of the above mentioned documents are not identical. The difference is that Resolution A.685(17) prescribes to control stability by weather criterion for ships of 45 m in length and over in all cases while Resolution A.749(18) orders to carry out such control only for vessels with large windage area (See paragraph 4.2.4.1. "having large windage area").

Thus according to the recommendations of document [2] necessity of control over the

8

vessel's stability by weather criterion depends on the fact if the vessel has large or small windage area, but definition of "large windage area" is not given.

This work is carried out in order to determine the possibility of making expression "large windage area" concretely defined.

Weather criterion is determined in IMO documents [1] and [2] in the following way:

"The ability of a ship to withstand the combined effect of beam wind and rolling should be demonstrated for each standard condition of loading, with reference to the figure Fig. 1, as follows:
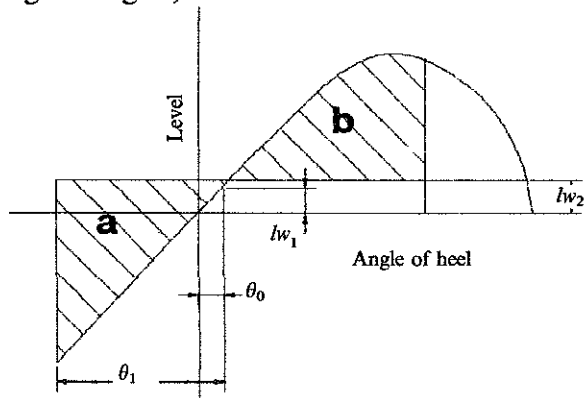
Fig.1 Weather criterion

- the ship is subjected to a steady wind pressure acting perpendicular to a ship's centerline which results in a steady wind heeling lever (l_{w_1});
- from the resulting angle of equilibrium (Θ_0) the ship is assumed to roll owing to wave action to an angle of roll (Θ_1) to windward. Attention should be paid to the effect of steady wind so that excessive resultant angles of heel are avoided;
- the ship is then subject to a gust wind pressure which results in a gust wind heeling lever (l_{w_2});
- under these circumstances, area "b" should be equal to or greater than area "a" (See Fig. 1);
- free surfaces effects should be accounted for in the standard conditions of loading."

IMO recommendations do not directly give the parameter which could be considered as measure of correlation to weather criterion or as a margin to critical situation (i.e. for cases of equality of areas "a" and "b"). But without a parameter of such kind it is impossible to make an analysis of interconnection between windage area and weather criterion. While making the calculations and analysing them heeling lever l_{w_0} at which $a = b$ to dynamic heeling lever l_{w_2} (see paragraph 3.2.2.1.3) ratio, i.e. $l_{w_0}/l_{w_2} = K$, was used as such quantitative estimate. In Russian practice of estimation of sea-going ability of a ship there is a quantitative check point for $l_{w_0}/l_{w_2} = K$, which is used by the Register of Shipping as a recommendation: "For ships, constructed specially for operation in extreme storm conditions, ... it is recommended that this value should be no less than 1.5" [3]. Thus, according to this recommendation ships having $K \geqslant 1.5$ were considered as most safe from the point of withstanding combined action of wind and rolling.

In this work results of weather criterion calculation according IMO recommendations for 12 fishing vessels of 45 m in length and over are presented. The calculations were carried out for the following load conditions:

- load line mark
- 100 % of catch and 10 % of stocks
- 0 % of catch and 10 % of stocks, or 20 % of catch and 10 % of stocks;
- 0 % of catch and 10 % of stocks, or 20 % of catch and 10 % of stocks with ice accretion.

When making the calculations relative windage area $\bar{A}_v = A_v/L_{pp}T$ was used, where

A_v — windage area of the vessel (projected lateral area)

L_{pp} — length between perpendiculars

T — mean draught for the load considered

In defining the task it was supposed that if interconnection of windage area $\bar{A}_v$ and parameter K is expressed obviously enough

than in the result of analysis of the carried out calculations it is possible to determine the area of values of small windage area A for which parameter $K \geqslant 1.5$ (margin is large), certain transitional area of values of $\overline{A}_v (1 < K < 1.5)$ as well as sought for area of values of $\overline{A}_v$ at which achievement of critical value $K = l_{w_0}/l_{w_2} = b/a = 1$ is most possible. Numerical value of the lower limit of this searched for area of values of $\overline{A}_v$ could define the expression "large windage area" concretely.

Let us have a look at the results of the calculations. In Fig. 2 characteristic dependence of parameter K on $\overline{A}_v$ is shown (ship project 503).
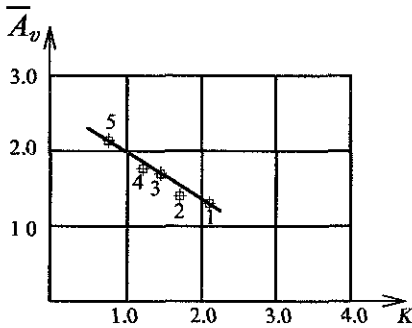
Fig. 2 Interconnection of windage area $\overline{A}_v$ and parameter K for ship pr. 503,
1 — load line mark; 2 — 100% of catch and 10% of stocks;
3 — 0% of catch and 10% of stocks;
4 — 0% of catch and 10% of stocks with ice accretion;
5 — 0% of catch and 10% of stocks with increased $\overline{A}_v$ by 30%.

The smallest values of parameter K for all vessels were the ones for minimal load conditions. Interestingly enough, at minimal load conditions ships from the studied selection with length less than 65 m have much smaller relative windage area than ships of 65 m in length and over (Fig. 3).
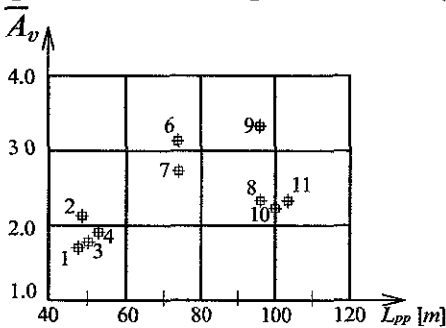
Fig. 3 Interconnection of windage area $\overline{A}_v$ and length L_{pp} for ships with 0% of catch and 10% of stocks (1,2...11 — Vessel No., Table 2).

It was also noted that for large vessels ($L > 65$ m) all values of parameter K are in the most safe area ($K > 1.5$) and exceed values of K for smaller vessels ($L < 65$ m) though windage area $\overline{A}_v$ of vessels with $L > 65$ m is much bigger than that of vessels with $L < 65$ m (See Table 1).

Table 1
Range of values of windage area $\overline{A}_v$ and parameter K
(load conditions : 0 % of catch and 10 % of stocks,
or 20 % of catch and 10 % of stocks)

L	Range for $\overline{A}_v$	Range for K
$L < 65$ m	1.65÷2.09	1.41÷1.83
$L > 65$ m	2.30÷3.36	1.82÷3.20

In order to estimate effect of windage area on value of parameter K as applied to a particular ship calculations with windage area increase by convention were made for ship project 503 ($L = 46.2$ m, load conditions: 0 % of catch and 10 % of stocks, or 20 % of catch and 10 % of stocks, icing). The calculations demonstrated that in conditions of windage area increase by 30% (from value $\overline{A}_v = 1.67$ to $\overline{A}_v = 2.18$) weather criterion in not complied with (area "b" is less than area "a", $K = 0.91$). At the same time windage area $\overline{A}_v$ is rather small and does not even reach the lower limit of windage area range for ships with $L > 65$ m (See Table 1), which comply with weather criterion in the same loading condition with large margin. From these examples it follows that windage area cannot be taken as independent criteria for determining advisability of control over fishing vessels by weather criterion. Only combined consideration of characteristics of righting level curve and windage area give possibility for proficient evaluation of results of combined effect of strong beam wind and rolling.

In conclusion we shall study interconnection of windage area $\overline{A}_v$ and parameter K for load conditions at which metacentre height GM is close to the value of 0.35 m (minimal value according IMO requirements) or reaches its lowest value (See Table 2).

Table 2

**Interconnection of parameter $K=l_{w0}/l_{w2}$
and windage area $\overline{A}_v$**

Vessel No.	Project Number (See [4])	L_{pp}, m	GM, m	$\overline{A}_v$	$K=l_{w0}/l_{w2}$
1	503	46.2	0.31	1.65	1.58
2	05026	48.0	0.34	2.09	1.41
3	1348	49.2	0.54	1.68	1.42
4	1332	52.0	0.39	1.94	1.83
5	1375	64.8	0.34	2.04	1.94
6	12913	76.8	0.34	3.05	2.49
7	12911	76.8	0.33	2.35	2.83
8	1376	94.0	0.33	1.67	2.45
9	1288	97.2	0.36	3.42	1.68
10	1386	100	0.35	2.30	3.06
11	1608	102.5	0.34	2.32	3.20
12	13490	118.0	0.46	2.90	2.42

Fig. 4 is a pictorial rendition of information contained in table 2. It turned out that vessels with close values of relative windage area have significantly different values of parameter K (cf. vessels No.2, 4, 5, 8, 10, 11) whereas vessels with close values of parameter K have significantly different values of relative windage area (cf. vessels No. 4 and 9; 8 and 6).
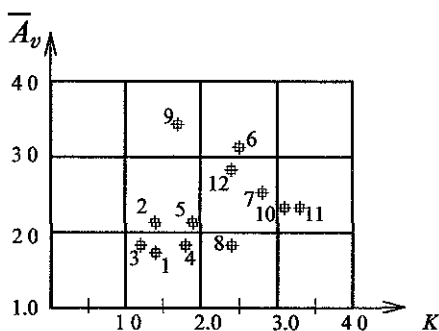
Fig.4 Interconnection of windage area $\overline{A}_v$
and parameter K for ships with $GM > 0.35$
or $GM = GM_{min}$ (1,2....12 — Vessel No., Table 2).

Thus, results obtained evidence that for real vessels it seems impossible to determine the area of values of small windage area $\overline{A}_v$ for which weather criterion is realized with large margin as well as the area of values of large windage area at which reaching the critical value of parameter $K = l_{w0}/l_{w2} = b/a = 1$ is most probable. Consequently, it does not seem possible to make expression "large windage area" concretely defined, so this expression should be reckoned as vague and it should be recommended to exclude expression "large windage area" form the text of the Code on intact stability for all types of ships covered by IMO instruments [2].

REFERENCES

1. Weather criterion for fishing vessels of 24 m in length and over — IMO Resolution A.685(17)

2. Code on intact stability for all types of ships covered by IMO instruments — IMO Resolution A.749(18)

3. Rules for classification and construction of seagoing vessels — Russian Maritime Register of Shipping — 1995 — p.318, paragraph 2.1.1.1.

4. Fleet of fishing industry — Reference book of type ships. — Moscow/Transport, 1990

UPGRADING OF STABILITY QUALITIES OF RO-RO SHIPS

Critical Review and Practical Implications
Of the SOLAS 95 Regulations
For the Damage Stability of Ro-Ro Passenger Ships

Apostolos D. Papanikolaou[1]

Ship Design Laboratory, Nat. Tech. Univ. of Athens
Heroon Polytechniou, 9, 15 773 Zografou, Athens, GREECE

Abstract

The present paper concerns the practical implications of the new SOLAS regulations pertaining to the damage stability of existing and new Ro-Ro passenger ships and attempts a critical review of the recent amendments to SOLAS Chapter II (intact and damage stability of Ro-Ro passenger ships). The paper summarizes results of a detailed study of the Ship Design Laboratory of NTUA, to determine the practical implications of the new SOLAS regulations to the Greek Passenger Ferry Fleet, and the Passenger Ferry ships in general, and to identify possible weaknesses of the new SOLAS regulatory framework, to be improved in the following years.

Introduction

Following the tragic loss of the *Estonia* in September 1994 and the public outcry, especially in Northwest Europe, the International Maritime Organization (IMO) appointed (following an unprecedented procedure) a Panel of Experts (POE) to identify weaknesses in the existing regulations and to propose within a five (5) months period a framework of amendments for improving the insufficient state of the art in the field of damage stability of Ro-Ro Passenger Ships.

The appointed Panel prepared, in the short time available, an extensive document addressing a large variety of amendments to the existing regulations (see, *Funder, 1995*, and *POE, 1995*[2]). The POE submitted its proposal through the MSC committee of IMO to the SOLAS 1995 conference for approval. The impressive work of the POE of IMO was enabled by the provision of technical information deduced from previous or parallel work of the participating experts and their supporting staff. It has been greatly influenced by results of parallel work of a large consortium of Northwest European companies, consisting of members of the maritime industry, research institutions and administrations (so-called: Joint R&D NORDIC Project, see, *Svensen*, 1995).

The proposals of the Panel of Experts of IMO have been only partly approved by the general assembly of the IMO conference in November 1995. In particular, the introduction of the "water on deck" penalty concept has been rejected as a worldwide

---

[1] Professor, Head of Ship Design Laboratory, NTUA and President of the Hellenic Institute of Marine Technology (HIMT)

[2] The proposal consists of 33 ANNEXES with specific regulatory amendments referring to both design, outfitting and operational measures

standard, due to insufficient scientific reasoning and the severe practical impact, especially on existing vessels. However, owing to the strong public pressure in Northwest Europe, the IMO convention accepted a resolution allowing interested states to increase the requirements of the generally accepted SOLAS 90 damage stability standard through bilateral agreements (Res. 14, Reg. 8-1). Following Res. 14 seven signatory states[3] from Northwest Europe came in February 1996 to the so-called "Stockholm Agreement", revising the original "water on deck" concept introduced earlier by the IMO Panel of Experts, but keeping the original "penalty idea" unchanged.

The present paper is based on a detailed study of the Ship Design Laboratory (SDL) of NTUA, performed at the stage of preparation of the Greek delegation for the SOLAS conference in November 1995. In addition, the present paper considers developments thereafter and until today.

Aims of the SDL-NTUA Study

The aims of the SDL-NTUA study performed in 1995 on behalf of the Greek Passenger Shipping Industry (see, *A. Papanikolaou et al. 1995d*), were specifically:

- firstly, to determine the extent to which existing ferries operating within the Greek coastal shipping, including the international routes between Greece and Italy, would be capable of meeting the substantially increased standards of residual stability after damage for Ro-Ro passenger ferries, including the assumed flooding of the car deck,

- secondly, to consider the practical and economic implications on design and operation for a sample of ships of the Greek Ro-Ro passenger ferry fleet, and

to consider, in addition, possible changes in the pattern of the world-wide Ro-Ro passenger ferry fleet,

- finally, to critically review the changes of the new SOLAS regulations, considering both general, scientific aspects as well as the specific conditions of operation of the Greek ferry fleet and the fleet of the Mediterranean countries in general.

Most recent research work of SDL-NTUA refers to the development of a mathematical model for the simulation of capsize of intact and damaged ships in waves (see, *A. Papanikolaou*, 1995a). Preliminary results of this work are presented at another session of the present conference (see, *A. Papanikolaou et al*, 1997).

Discussion of Results

The principal findings from the initial (1995) NTUA investigation into 6 (six)[4] Greek Ro-Ro passenger ferries, operating today in international and national trade, considering the new SOLAS regulations of IMO for "unlimited service"[5], as they were formulated in their original form[6] (see, *Funder, IMO "Panel of Experts", 1995)*, were the following:

---

[3] Denmark, Finland, United Kingdom, Germany, Ireland, Norway, Sweden

[4]The study is including in its final form 13 (thirteen) vessels

[5]"unlimited service" herein understood in the regulatory sense, for the ship to have the permission to trade world-wide (therefore, also, in Northwest Europe), without limitation as to the stability-safety standard. It is, also, understood, that the European Commission is currently reviewing the enforcement of a Pan-European stability-safety standard, bridging the existing gap between North and South Europe.

[6] The final formulation of the "water-on-deck penalty" stability concept, introduced by the POE of IMO and later modified by a Regional Agreement in Northwest Europe ("Stockholm Agreement"), differs significantly from the original one, but does not change the conclusions for the practical implications on existing ships *not complying with* the SOLAS 90 standard, though it weakens the severity of the practical impact.

1. In view of the age structure of the Greek Ro-Ro passenger ferry fleet[7] and the particular characteristics of a sample of ships, investigated in more details, it seems that a *significant number* of ships, especially those operating in the Greek national trade, with an age over abt 20 years, will be forced to withdraw from service, because the required cost for modifications to achieve the new word-wide stability standard, namely SOLAS 1990 two compartment standard, will exceed or reach a significant percentage of the market value of the vessel or the required modifications will technically lead to practically impossible solutions. An estimated 92 ships (82% of the total Greek fleet) with a total capacity of 450.000 GRT[8] fall in this category and will be severely affected by this procedure Considering the age and technology structure of the world-wide Ro-Ro passenger ferry fleet, it can be concluded, that the above implications are not unique to Greece, but a serious regulatory and techno-economic problem of world-wide significance

2. Considering those ships of the Greek Ro-Ro passenger ferry fleet, and ships in general, that with a "limited extent"[9] of modifications can reach SOLAS 1990 two compartment stability standard, especially those operating in international waters (route to Italy) and having today at least the SOLAS 1992 standard, they might be further modified to comply with the new SOLAS 1995 standard for "unlimited service". However these modifications will have the following practical impact:

2.1 In all cases, the required modifications will add structural weight and

will lead to a reduction of payload (also to a reduction of the available vehicle deck area), an increase of "turn round" time and of the operating cost, combined with a reduction of speed in case of fitting of sponsons (possible exemptions from this rule possible). In addition, the possible fitting of sponsons will affect the sea kindliness of the ship and the comfort of the passengers onboard.

2.2 The cost for the required modifications for ships not having but easily passing the SOLAS 1990 stability standard has been estimated to vary between 1.000.000 US $ (for a (3) three transverse movable bulkheads arrangement) and 4.000 000 US $ (for manifold arrangement measures, including the fitting of sponsons). Considering the typical trade pattern of Greek Ro-Ro passenger ships, that is highly seasonal, it seems that the additional running cost and the reduced payload capacity can lead to significant changes in the required freight rates, for the vessel to keep operating under the same profit conditions.

An estimated number of 15 ships (13% of the total fleet) with a total capacity of abt. 90.000 GRT fall in this category and will be affected by the above suggested measures.

3. Considering the new generation of Greek ships introduced recently in the international route to Italy, and having at least SOLAS 1990 standard, it seems that in view of the reduced weather dependent regional requirements in the Mediterranean Sea the required modifications will be very little, and in few cases not necessary at all. An exemption, from this rule, might apply to fast ships, due to their unique hull and stability characteristics. In any case, for unlimited international service on other routes, all vessels of this category will need modifications too, as outlined before under 2.

---

[7]average age of the Greek Ro-Ro passenger ferry fleet is abt 24 years (stand' spring 1995, see Fig. 1)
[8]The tonnage statistics refer to Ro-Ro passenger vessels over 1000 GRT
[9]"limited extent" of modifications herein understood in relation to the incurred modification cost vs. the value of the vessel

9 \

Another 4 ships[10] (4% of the total fleet) with a total capacity of abt 80.000 GRT fall in this category.

4. Considering the new generation of *high speed* Ro-Ro passenger ships, especially those following the *monohull* concept, it seems that they will be severely affected by the proposed new stability standard, unless they accept substantial design and operational restrictions[11]. At this moment it is not clear, from the IMO side, whether the high-speed vessels will be exempt from full compliance with the new regulations. The *multihull* high-speed concepts (catamarans, SWATHs and hybrids etc.) seem less sensitive to the proposed changes and will come through, depending on the design, without significant modifications.

At this moment only few ships[12] currently under construction for Greek interests fall in this category and will be affected by the above procedure.

5. A critical review of the originally proposed amendments by the Panel of Experts of IMO, especially of those related to Reg. II-1/8-1, 8-2, 8-3, revealed *several significant weaknesses*, that led, finally, to the partial rejection of the original POE proposal by the IMO convention in November 1995. The essential drawbacks of the original POE proposal, pertaining to the damaged stability rules, was

● firstly, the lack of understanding for the validity of the SOLAS 90 damaged stability standard versus the operational seastate[13], therefore the lack for a properly defined "starting point", on the top of which the "water on deck" penalty is applied.

● secondly, the unjustified "penalty" for a heeling moment corresponding to 0.5m constant height "water on deck", valid for all heel angles and all thinkable car deck arrangements (clear deck, central and side casing design) and without caring for proper relation to the actual ship motion characteristics. The reformulation of the "water on deck" penalty concept through the Stockholm Agreement improved slightly the situation, especially as to the consideration of the heel angle, however the concept remains fundamentally insufficient, in view of the above deficiencies

It is important to state, that the POE was aware of the above two uncertainties (validity of the SOLAS 90 standard and of the "water on deck" penalty concept) and suggested as an alternative to the "water on deck" damage stability exercise the so-called "Equivalent Model Test Method". This procedure, embedded in Res. 14 and the Stockholm Agreement, allows the evaluation of the damaged stability of Ro-Ro Passenger Ships in waves in a *rational* way. Insofar, this procedure might be considered as a milestone in IMO's regulatory work, that has been based, until recently, exclusively on *semiempirical* reasoning.

---

[10]This number refer to the NTUA-SDL data, as of Spring 1995 (includes *Superfast I & II* and *Aretousa*).

[11] The capability of the shipbuilding industry to develop high-speed monohull Ro-Ro passenger ship designs, *formally* complying with the new damaged stability rules, is not questioned The open question concerns the *full compliance* with *all* relevant rules applying to conventional ships and the consideration, in addition, of the increased damage risk due to the high-speed of operation.

[12]An estimated number of 5-10 ships fall in this category of vessels

---

[13] The fundamental assumption, that a ship complying with the SOLAS 90 damage stability standard can withstand seastates only up to a significant wave height of 1.5m is scientifically not justified. International state of the art (based systematic theoretical and experimental studies by many scientists around the world) suggests, that the above limit is well over 2.5 to 3.0m. This confirms fully the position of the Greek delegation at IMO in November 1995.

The Way Ahead

The adopted new standards of SOLAS for Ro-Ro passenger ferries are expected to change significantly the overall picture of the Ro-Ro passenger ferry fleet world-wide, and especially in Europe. Taking into account the simultaneous lift of the so-called "cabotage" regulation in the year 2004 in Europe and the approved compliance scheme with the new regulations[14] we might expect in the next decade the following developments (the majority of which should be welcomed by the shipbuilding and suppliers industry):

1.   It can be expected, that a significant number of orders for Ro-Ro passenger ship *newbuildings* will be placed world-wide, and especially in Europe An estimate of 50-60 ships of the Greek Ro-Ro passenger ferry fleet should be replaced by newbuildings.

2.   The shipbuilding and suppliers industry is expected to deal with a significant number of conversions of existing ships for compliance with the SOLAS 90 standard (especially in the Mediterranean) or the enhanced SOLAS 95 standard (Res. 14, NW Europe). It is understood, that ships fitted to pass the SOLAS 90 standard will be capable to pass[15], without further modifications, the enhanced SOLAS 95 standard following the "Equivalent Model Test Method". procedure.

3.   A number of relatively new ships, currently operating in Northwest European waters and having at least SOLAS 90 standard, might be transferred for trade in the Mediterranean, either by sale to Mediterranean shipowners or by joint-

ventures or by the introduction of independent new services after the lift of "cabotage". However, due to the fact, that only few existing ships, from all over Europe, pass the SOLAS 90 standard, these transactions will be much less, than initially thought, in view of 2.

4.   The developments in the design of Ro-Ro passenger ship newbuildings are expected to go in the following direction:

- The damage freeboard and residual stability after damage will dominate the design of future Ro-Ro Passenger ships.

- Small Ro-Ro passenger ships, with a length below approximately 100m and a corresponding beam of below approximately 20m, are expected to disappear in the future from regular Ro-Ro passenger service, because of the requirements for compliance with the SOLAS 90, two compartment standard, besides the enhanced SOLAS 95 Res. 14 standard, will practically lead to technically and economically non-feasible solutions.

- Future Ro-Ro passenger ships will all follow the so-called "double-hull lifebelt" concept, with longitudinal bulkheads at B/5 below the main (bulkhead) car deck, and longitudinal bulkheads at B/10 or even less (depending on the clearance form the outside shell) on the car deck itself.

- The intact freeboard will substantially increase and should exceed, amidships, the value of 2% L, in absolute terms the value of 2.5m for the smaller vessels. For operation in NW Europe even higher freeboards might prove necessary. This will immediately call for significant investments in new docking facilities.

---

[14] starting on October 1, 1998 for A/Amax less than 85% and ending October 1, 2005 for A/Amax equal or more than 97.5%, see, Fig. 2 for the complexities of the implementation procedure

[15] The exception proves the rule

• The outfitting of future Ro-Ro passenger ships, related to safety in general, will substantially extended and should contribute to an increased safety standard for passengers and crew. The overall transport efficiency of the Ro-Ro passenger ship as a transportation mode will be decreasing, however at the provision of an increased safety standard. When the increased safety standard can be combined with an increased comfort for the passengers, Ro-Ro passenger ships might keep their market share, against other modes of transportation, unchanged.

• Twin-hull vessel designs will gain importance against the traditional monohull concept, in view of the inherent enhanced transverse stability and resistance against capsizing. This aspect will be of additional importance for fast Ro-Ro passenger vessels operating in harsh weather environment.

5. Regulatory developments at IMO might go in the following direction:

• The reasoning for the implementation of the enhanced SOLAS 95 Res. 14 standard, in view of the limited validity of the SOLAS 90 standard, should be reconsidered, in view of most recent experimental and theoretical-numerical state of the art in the field of damage stability of Ro-Ro passenger ships in waves.

• The development of a "harmonized" damage stability standard for all types of ships, considering existing and currently valid deterministic and/or probabilistic stability criteria, has a long way to go. However, the *rational* assessment of the damage stability and safety of ships through properly defined model experiments and/or validated numerical simulation algorithms, as partly outlined in Res. 14 of SOLAS 95, is a possible way to follow for improving the safety of all types of ships, independently of the fulfillment of whatever *semi-empirical* criteria.

Concluding, it seems essential to state, that although it is possible to design (theoretically and practically) "unsinkable" ships (what cannot be claimed for other modes of transport, e.g. airplanes) it is practically impossible to design "unsinkable" Ro-Ro passenger ships as a *competitive mode of shortsea shipping transportation*. Taking into account that most recent Ro-Ro ship capsizes are due to "human failure", it is wiser to address the problem of ship safety globally and not by individual measures leading to the possible "keeling" of the Ro-Ro passenger ferry concept. Besides long overdue systematic research in the area of damage stability, for establishing a scientific "state of the art" in the field, it remains for IMO to integrate all aspects of marine safety into a generally acceptable *safety code for Ro-Ro Passenger ships*, thus to include besides the aspects of ship design (concept and technology) also the ship's operation (technology and human factors) and the operating environment (area of operation and seasonal characteristics), in order to solve properly the problem affecting daily the safety of thousands of passengers as well as the passenger shipping industry and economy as a whole.

References

1. *Aldwinckle D. S. and Prentice, D. (1990)*, "The Safety Record and Risk Analysis of Ro-Ro Passenger Ferries", Proceedings of Int. Symposium on Safety of Ro-Ro Passenger Ships, Dep. of Transport of U.K. and The Royal Inst. of Naval Architects - RINA, April 1990, London.
2. *Allan, T. (1994)*, "The Practical Implication of SOLAS'90 on Existing Ro-Ro Passenger Ships", Proc. Ro-Ro '94 Conference, Gottenbourgh.
3. *Carlsson, J. O. (1995)*, "First Line of Defence - To Prevent Water from Entering the Vehicle Deck", Proc. THALASSA '95 - 3rd Int. Pass. Shipping Conf. & Exhibition, Piraeus, April 1995.
4. *Dand, I. (1991)*, "Experiments with a Floodable Model of a Ro-Ro Passenger Ferry", Proc. of the 2nd Henry Kummerman Foundation Int. Conference, Vol. I & II, London, April 1991.
5. *Funder, T. R. (1995)*, "The Present Work of IMO's Panel of Experts on Ro-Ro Ferry Safety", Proc. THALASSA '95 - 3rd Int. Pass. Shipping Conf. & Exhibition, Piraeus, April 1995.
6. *Hutchison, B. L. (1995)*, "Water-on-Deck Accumulation Studies by the SNAME ad hoc Ro-Ro Safety Panel", Pres. Int. Workshop on Numerical and Physical Simulation of Ship Capsize in Heavy Seas, July 24-25, 1995, Loch Lomond - Glasgow.
7. *Judd, P. H. (1990)*, "Ro-Ro Passenger Ferry Survivability Study - Hull Form and Superstructure", Proceedings of Int. Symposium on Safety of Ro-Ro Passenger Ships, Dep. of Transport of U.K. and The Royal Inst. of Naval Architects - RINA, April 1990, London.
8. *Little, P. E. and Hutchison, B. L.*, "Ro/Ro Safety after *Estonia* - A Report on the Activities of the Ad Hoc Panel on Ro/Ro Safety", Journal Marine Technology, Vol. 32, July 1995, pp. 159-163.
9. *Lloyd, C. J. (1990)*, "Research into Enhancing the Stability and Survivability Standards of Ro-Ro Passenger Ferries - Internal Arrangements and Overview Study", Proceedings of Int. Symposium on Safety of Ro-Ro Passenger Ships, Dep. of Transport of U.K. and The Royal Inst. of Naval Architects - RINA, April 1990, London.
10. *Marsano, R. (1995)*, "Information Paper on the *Italian Research* at the Hamburg Ship Model Basin (HSVA)", August 1995.
11. *Papanikolaou, A. (1995a)*, "Dynamic Stability Analysis of Ro-Ro Passenger Vessels and Investigation of the Probability of Capsizing in Heavy Seaways", ΠΕΝΕΔ 1995 Res. Project, Greek Secretariat General for Research and Technology, 1996-1998, Athens.
12. *Papanikolaou, A., Kouimanis, J. (1995b)*, "Safety Aspects of Future Passenger/Car Ferries", Proc. THALASSA '95 - 3rd Int. Pass. Shipping Conf. & Exhibition, Piraeus, April 1995.
13. *Papanikolaou, A., et al. (1995c)*, "Study on the Practical Implications of the Proposed New SOLAS Regulations on Existing Greek Ro-Ro Ships and Critical Review of the Proposed New Regulations", Vol. I - III, Final Report, SDL-NTUA Report, September 1995.
14. *Papanikolaou, A., Spanos, D., Zaraphonitis, G. (1997)*, "On a 3-D Mathematical Model of the Damage Stability of Ships in Waves", to be pres. at the 6th Int. Conf. On Stability of Ships and Ocean Structures, STAB'97, Varna.
15. *Payne, S. (1994)*, "Tightening the Grip on Passenger Ship Safety: The Evolution of SOLAS", Journal The

Naval Architect, pp. E482-E487, Oct. 1994

16 Pucill, F. and Velschou, S. (1990), "Ro-Ro Passenger Ferry Safety Studies -Model Test of a Typical Ferry", Proceedings of Int. Symposium on Safety of Ro-Ro Passenger Ships, Dep. of Transport of U.K. and The Royal Inst. of Naval Architects - RINA, April 1990, London

17. Rogan, A. J., White, J. N.. (1990), "A Study to Compare the Residual Standards of Stability After Damage of Existing Ro-Ro Passenger Ferries", Proc. Int. Symposium on Safety of Ro-Ro Passenger Ships, Dep. of Transport of UK and The Royal Inst. of Naval Architects - RINA, April 1990, London.

18. Shimizu, N., Roby, K., Ikeda, Y. (1995), "An Experimental Study on Flooding into the Car Deck of a Ro-Ro Ferry Through Damaged Bow Door", Pres. Int. Workshop on Numerical and Physical Simulation of Ship Capsize in Heavy Seas, July 24-25, 1995, Loch Lomond - Glasgow.

19. Spanos, D. (1995), "Theoretical-Numerical Modeling of Large Amplitude Ship Motions and of Capsizing in Heavy Seaways", Dr.-Eng. Thesis, NTUA-SDL, in progress.

20 Svensen, T. (1995), "A New Safety Standard for Passenger/Ro-Ro Vessels", Proc. THALASSA '95 - 3rd Int. Pass. Shipping Conf. & Exhibition, Piraeus, April 1995

21. The Florida Institute of Technology, "STAB'94: Proceedings of the 5th Int. Conference on Stability of Ships and Ocean Vehicles", November 1994, Melbourne - Florida.

22 The Joint Accident Investigation Commission of Estonia, Finland and Sweden (1995), "Part-Report on technical issues on the capsizing on 28 September 1994 in the Baltic Sea of the Ro-Ro Passenger Vessel MV Estonia",
April 1995, Tallinn-Helsinki-Stockholm.

23. The Marine Directorate, Dep. of Transport of United Kingdom (1990), "The Way Ahead ", Proceedings of Int. Symposium on Safety of Ro-Ro Passenger Ships, Dep. of Transport of U.K. and The Royal Inst of Naval Architects - RINA, April 1990, London.

24. The Panel of Experts of IMO (1995), "Report of the Panel of Experts on Ro-Ro Ferry Safety to the Steering Committee on Ro-Ro Ferry Safety" include. ANNEX 1 to 33, MSC 65/4/Rev. 1, April 21 1995, London.

25. The Royal Inst. of Naval Architects (1996), Proc Int. Conf. On the Safety of Passengers in Ro-Ro Vessels - Presenting the results of the Northwest European Research and Development Project at IMO, London, June 7.

26. The Royal Institution of Naval Architects (1986), "The Safeship Project: Ship Stability and Safety", Proc. of Int. Conference, Vol. I & II, London.

27. The Royal Institution of Naval Architects (1987), "Ro-Ro Safety and Vulnerability - The Way Ahead", Proc. of the 1st Henry Kummerman Foundation Int. Conference, Vol. I & II, London.

28. The Royal Institution of Naval Architects (1991), "Ro-Ro Safety and Vulnerability - The Way Ahead", Proc. of the 2nd Henry Kummerman Foundation Int. Conference, Vol. I & II, London.

29. The Russian Federation, "Comments on the proposed amendments to the SOLAS Chapter II-1 (Reg. 8-1, 8-2, 8-3), subm. July 1995, MSC-IMO, Circ August 3, 1995.

30. The University of Naples - Dep. of Naval Engineering, "STAB'90: Proceedings of the 4th Int Conference on Stability of Ships and Ocean Vehicles", September 1990, Naples.

31. *Vassalos, D. (1994)*, "Survivability of Passenger Vessels", Pres. at the Hellenic Institute of Marine Technology and the Joint Branch of RINA/IME, April 1994, Athens.

32. *Vassalos, D. (1995a)*, "Review of Recent R&D Work on the Damage Stability and Survivability of Passenger/Ro-Ro Vessels", The Stability Research Group of the Dep. Of Ship & Marine Technology, Univ. of Strathclyde, May 1995, Glasgow.

33. *Vassalos, D. (1995b)*, "Int. Workshop on Numerical and Physical Simulation of Ship Capsize in Heavy Seas", July 24-25, 1995, Loch Lomond - Glasgow.

34. *Vassalos, D., Turan, O. (1994a)*, "A Realistic Approach to Assessing Damage Survivability of Passenger Ships", Proc. SNAME Annual Conference Meeting, November 1994, New Orleans.

35. *Watanabe, I.*, "Comments on the Italian Research Study (R. Marsano [10]) and the effect of central casing on the damage stability of Ro-Ro ships", Ship Dynamics Division of the Ship Research Institute, Ministry of Transport of Japan, Tokyo, September 4, 1995.

36. *Wild, G. P. (1995)*, "Safety - Making a Virtue Out of Necessity", Proc. THALASSA '95 - 3rd Int. Pass. Shipping Conf. & Exhibition, Piraeus, April 1995.

37. *Zwart, B. (1995)*, "De 'Estonia', Slachtoffer van een Trogstorm", Journal Schip & Werf de Zee, January 1995, pp. 37-40.

Appendix A

Brief Historical Review of Recent European Ro-Ro Passenger Ship Capsizes

During the last two decades, the most striking examples of European Ro-Ro passenger ship losses, that triggered national and international regulatory changes, are:

1.   The U.K. ferry *European Gateway*, which collided with *Speedlink Vanguard* off *Harwich / Felixstone* in the English Channel with the loss of 6 lives in 1982. Due to the collision damage of the ferry, both above and below the car deck, and the resulting transient asymmetric flooding, first of the watertight part of the hull and then of the car deck itself, the vessel quickly heeled to abt 40 deg, and capsized. It should be noted, that, against operational rules, *several watertight doors of the ship below the bulkhead deck had been kept open during operation* (for easing the work of the crew).

2.   The U.K. ferry *Herald of Free Enterprise*, which capsized at the entrance of *Zeebrugge* Harbor in 1987 with the loss of 193 lives. Again, against operational rules, the vessel had left the pier with the *bow door open* for better ventilation of exhaust gases accumulated in the car deck during loading. Due to the rapid increase of the vessel's speed immediately after the clearance from the harbor and the simultaneous turn, the resulting bow down trim and bow wave caused a rapid ingress of water through the open bow door onto the vehicle deck. This increased further the bow down trim, diminished the vessel's stability and caused a sudden heel of at first 30 deg, rapidly increasing to 90 deg. The vessel grounded on its side at the harbor's entrance.

3.   The Estonian ferry *Estonia* (built in Germany, 1980, former *VIKING SALLY*), which capsized in the Baltic Sea shortly after midnight on September 28, 1994 with the loss of 852 lives. The *immediate* cause of the accident was *failure of the bow visor locking mechanism in stormy sea conditions* (see, *Zwart, 1995,* for weather conditions). In addition, the inner

watertight barrier behind the bow visor ("second line of defense") was placed too far forward and not structurally independent of the bow visor, *thus it was not according to the regulations, at the time of built* (see, *Preliminary Report of the Joint Accident Investigation Commission, 1995*). After the detachment of the bow visor due to heavy wave impact loading, the inner ramp opened allowing the gradual ingress of seawater onto vehicle deck. The shipmaster's attempt to change course so as to avoid bow seas and therefore decrease the ingress of water onto the vehicle deck introduced additional dynamic effects and the build up of heel up to the complete capsize. The time between the first indications of something abnormal with the bow visor (metallic noises) and the complete capsize of the vessel was estimated at abt 50 minutes. The time elapsed between the first TV monitor observation by an engineer in the engine control room, that water was flooding into the car deck through the sides of the forward ramp and the complete capsize of the vessel was estimated at abt 20 minutes. A total of 137 survivors and 94 victims were collected by helicopters and assisting ships during the night and the early morning hours under worst weather conditions (*Part Technical Report of the appointed Investigation Commission, 1995*, final report still pending).

4.   Two more, but in the Western World less publicized, accidents occurred in Europe in the last fifteen years, namely in 1986, the capsize of the former SU passenger ship *Admiral Nachimow*, that was hit by the cargo ship *Pjotr Wassjew* (loss of 398 lives), and in 1993 the capsize of the Polish ferry *Jan Heweliusz*, that sank in stormy seas 15 sm outside the island of *Ruegen* (East Germany) with the loss of 55 lives.

The above tragic accidents, and especially the *"Estonia"* disaster, seriously affected the public opinion worldwide, especially in all major shipbuilding and passenger shipping countries, particularly in Europe, namely the United Kingdom and the Scandinavian countries Sweden, Norway, Denmark and Finland. The international community was mobilized through IMO and various relevant national authorities and institutions with the aim to significantly improve the safety level of existing and future Ro-Ro passenger vessels. Although it has been clear, from the above tragic accidents, that *human failure was the most important factor in all above cited accident cases* (and *in most cases the only factor*) the way followed by the Panel of Experts of IMO was to technically improve the safety standard of Ro-Ro passenger ships assuming the presence of water on the car deck *as an inevitable fact*, therefore given human failure in the engineering (design and construction) and the operation of Ro-Ro vessels as *always possible*.

With reference to the recent accident history of *Greek* Ro-Ro passenger vessels, we note in the *last 30 years (and actually after WW II)* two major fatalities with significant losses of human lives:

1.   The ferry *Heraklion*, which capsized in the *Falkonera* waters (SW Aegean Sea) on the route from Crete to Piraeus with the loss of 256 lives in 1966. With the ship sailing in heavy seas, a *not properly closed side door* was opened due to the impact of a *transversely stowed* and *not properly secured heavy truck*. The progressive ingress of water through the side opening resulted in the flooding of Ro-Ro deck and the loss of ship's stability. The vessel quickly heeled, trimmed additionally by stern, and capsized. This particular accident led to significant changes in the national and international regulatory requirements concerning the stowage and lashing of vehicles on the Ro-Ro deck and to improvements in the

arrangements of door openings and the design of the door closing mechanism. In addition, as far as the Greek coastal passenger shipping is concerned, *operational restrictions* have been imposed on all passenger ships sailing within the Greek coastal shipping system. These requirements relate the size of the ship, namely her length (initially her tonnage capacity), to the allowable seastate (actually the allowable windforce). Despite some weaknesses of the above regulatory procedure, due to the assumed simplified relation between ship size, ship type and allowable seastate, the effect of the regulation in practice was remarkable, because no other similar accident happened again in Greece until today.

2.   The Ro-Ro ferry *Chrissi Avgi*, which capsized in the *Cavo Doro* waters (South of *Euboea* island) on the route from to the port of *Rafina (East Attica)* to the *Cycladic* islands with the loss of 25 lives in 1983. The vessel was employed in mixed Ro-Ro passenger and Ro-Ro cargo service. On the specific travel, that led to the ship's capsize, the 55m vessel sailed out *as Ro-Ro cargo ship*[16] carrying trucks with dangerous goods (fuel gasoline). In quite heavy seas (Bf 8), the small ship received initially a substantial heel in *intact* condition, because of the movement of the not properly lashed heavy vehicles on the Ro-Ro deck. The movement of the vehicles provoked, in addition, an explosion on the car deck, which damaged the side shell of the hull and allowed the subsequent flooding of the Ro-Ro space. The accident is considered to have been provoked by manifold human failure at various levels.

Except for the above two notable accidents, involving Greek flag Ro-Ro passenger ships operating in Greek or international waters, no other notable event of capsizing,

due to intact or damage stability, has been registered for a period of more than 30 years in Greece. Note an *annual* movement of more than 38.000.000 passengers (20.600.000 passengers of which concern the open type shuttle ferry traffic), 3.600.000 private cars (1.310.000 for open type shuttle service) and 2.430.000 other freight units (stand: 1994, source: Union of Greek Coastal Shipowners). According to the above numbers, the probability of loss of a human live due to the capsizing of a Greek Ro-Ro passenger ship has been estimated to be less than 1 passenger live lost per 3.0 Mio traveled passengers, compared to abt one passenger lost per 10.000 travelers by car in a typical industrialized country[17] (in Greece, very likely, today's ratio for car accident losses is significantly higher).

Appendix B

Brief Review of Developments of Residual Stability Standards
From the 19th Century until the SOLAS 95 Conference

It is simply true to state, that the ship's damage stability problem and the related residual stability standards after damage have not received much attention in the past because of the difficulty to approach the very complex hydrodynamic problem of the progressive flooding of a ship moving in a random, possibly high seaway. The approach to the problem has been following, to a great extent, the state of the art in naval architectural science and technology, thus it was, at first, very simplistic but it became gradually more and more complex, following the state of knowledge in science and technology and the gathered experience from ship accidents and capsizes due to insufficient floatation and stability.

---

[16] As *cargo ship*, the ship could sail-out without a formal permission for poor weather conditions by the Coast Guard

[17] Ref. , e.g., United Kingdom

Historically, at the end of the 19th century, several appointed committees of the House of Commons in the United Kingdom contributed to the formulation of the first recommendations on the watertight subdivision of passenger vessels. In 1890, the first recommendation on a two compartments standard for passenger vessels over 425 ft (129 m) in length was established in the UK, ensuring that a ship should be capable of floating with any two adjacent compartments flooded or open to the sea. Independently of the fact, that this recommendation referred (practically) to the possible damage of a ship in calm waters and did not ensure a stability margin, besides floatation, for the ship in question, the recommendation is very advanced, for the time of implementation, and quite far reaching. It should prove right in the decades to follow. Following the loss of *Titanic* in 1912, and related work of the second Bulkhead Committee of the UK House of Commons, the 1st International Convention for the Safety of Life at Sea (SOLAS) was called in London in 1913 and laid down an empirical regulatory system for the subdivision of passenger vessels in watertight compartments through watertight bulkheads. In the same Convention the concept of the "margin line" was introduced, located at 3 inches (or 76 mm) below the bulkhead deck, a notion that remained "untouched" until today (though it could have been significantly improved over the past decades). It is also interesting to note, that the UK 1890 Committee on Watertight subdivision, used as "margin line" a line determined as percentage to the side depth of the ship, instead of the 3 inches "absolute" concept, thus relating the margin line to the size of the ship, what is considered scientifically more justified. The above regulatory work of SOLAS 1913 was finalized and approved after the end of the WW I, at the SOLAS 1929 Convention, where also details on the extent of possible hull damage were laid down. For the first time

in shipbuilding history, there was a specific safety standard for passenger ships against sinking, considering the progressive ingress of water onto the ship's hull and the eventual loss of the ship due to insufficient buoyancy.

The SOLAS 1929 standard did not consider specific requirements for the damage stability characteristics of the ship. A supplement to the 1929 standard, approved in 1932, specified the extent of permissible heel after flooding, that should be not more than 7 deg, and thus imposed indirectly requirements on the stability characteristics of the ship after damage. The extent of damage and the damage stability criteria were considered more detailed in the 1948 SOLAS Convention, introducing also the requirement for a *positive* residual metacentric height GM. It was 12 years later, namely at the SOLAS 1960 Convention, when a specific quantifiable criterion on residual stability was introduced, namely the requirement for a minimum residual metacentric height GM of 0.05m. This requirement represented an attempt to introduce a margin to compensate for the upsetting environmental forces (mainly wind and waves). A particular statement in the SOLAS 1960 regulations, namely "*Additionally, in cases where the Administration considered the range of stability in damaged condition to be doubtful, it could request further investigation to their satisfaction*", shows a first vague attempt to legislate the range of stability after damage. Also, it is interesting to note, that an additional vague, but very important, new regulation on "Watertight integrity above the Margin Line" was introduced, reflecting the general desire to "*do all that was reasonably practical to ensure survival after severe collision damage, by taking all necessary measures to limit entry and spread of water above the bulkhead deck*" (*see comments, Vassalos, 1995*).

Commenting on the SOLAS 1960 provisions, regarding the design of future passenger vessels and their safety against sinking and capsizing, 35 years later, *it proved insufficient to account for the rapid development of Ro-Ro passenger vessel technology in the years that followed. The most important new issue*, after SOLAS 1960, introduced through IMO resolution A265(VIII) and the SOLAS 1974 Convention, was *the probabilistic approach* for assessing damage location and extent, based on statistical data of accidents with failure. This approach was actually introduced more than 15 years before SOLAS 1974, namely in the late fifties by *Professor Kurt Wendel* and his associates (Germany). It should be also mentioned, that the well known *Rahola criteria*, published in 1939, are, as far as the overall methodology is concerned, far beyond the approach of SOLAS 1974. However, *Rahola's criteria* have been lacking support by updated accident data for new types of ships. In any case, the SOLAS 1974 convention did not provide improvements on the deterministic part of the regulations, though the scientific state of the art in ship hydrodynamics, and especially in seakeeping prediction methods, was significantly improved in the seventies. The equivalent regulations of SOLAS 1974 raised new damage stability criteria addressing the equilibrium as well as recommending a minimum GZ of at least 0.05m to ensure sufficient residual stability during intermediate stages of flooding. Following SOLAS 1974, the 1980 Passenger Ship Construction Regulations introduced requirements *on the range of the residual stability curve and on the stability of the vessel in intermediate stages*.

The loss of the UK ferry *European Gateway* in the early eighties (1982), due to collision and water flooding, demonstrated spectacularly the insufficiency of the amended SOLAS 1974 rules to address the problem of Ro-Ro passenger vessel damage stability effectively. Already in the late seventies, UK authorities and relevant institutions formed a consortium for a systematic research leading to the formulation of realistic stability criteria, the so-called SAFESHIP project. Results of this research, (see, e.g. [28]), actually confirmed the complexity of the subject, especially when attempt is made to account for the dynamics of the ship stability problem. Based on the results experience of the SAFESHIP project and additional theoretical and experimental research, initiated primarily by the Department of Transport of the UK, IMO adopted three years after the loss of the *Herald of Free Enterprise* the SOLAS 1990 residual stability standards for passenger and Ro-Ro passenger vessels, applying, under specific conditions, for the first time, also to cargo ships. These new SOLAS 1990 stability standards (later on amended through SOLAS 1992 to better account for the retrofitting of existing ships) require significantly higher values of residual stability characteristics after damage, namely:

1. A minimum range of positive stability of 15 deg beyond the angle of equilibrium after flooding, which should not exceed 12 deg for two compartments flooding and 7 degrees for one compartment flooding.

2. A minimum area of 0.015 m-rad under the residual GZ curve.

3. A minimum residual GM of 0.05m, with a max. GZ of at least 0.10m, increased as necessary to account for heeling moments due to the action of wind, passenger crowding and lifeboat launching.

Independently of the adoption of the above criteria, the practical implications of which remain still to be assessed by many IMO member states, including Greece, the

Department of Transport of the UK set-up a new extensive research program on Ro-Ro passenger vessel safety, focusing on the damage stability of Ro-Ro ships in waves and including fundamental theoretical and model experimental studies. It should be noted, that according to a study on behalf of the UK Department of Transport, the required modifications for a sample of 15 existing UK ferries, to update their standard to SOLAS 1990 level, have been estimated to cost as an initial investment in the worst case (fitting of sponsons or watertight doors/barriers on the Ro-Ro deck) 2.610.000 £ and in the best case (one ship out of fifteen checked) practically zero, whereas the additional running costs/annum could vary between zero (seven ships out of fifteen) and 5.000.000 £ (fitting of sponsons), the latter most probably being a case requiring additional machinery and significantly more fuel for keeping the service speed (see, Allan, 1994).

The implementation of the SOLAS 1990/92 criteria to existing ships remained outstanding, according to a phase-in procedure that changed continuously until summer 1994 (MSC/Circ. 649). It is particularly of interest to note, that this phase-in procedure for existing ships was originally based on the so-called (A/R) criterion (ratio of attained to required subdivision index), but later changed to follow the so-called (A/Amax) criterion, to be calculated according to a "simplified" probabilistic approach procedure. Resolution MSC.26(60) (adopted on April 10, 1992) invites the contracting governments to enforce the SOLAS 90/92 criteria to existing ships, as of October 1, 1994, whereas per MSC/Circ. 649/8.6.1994 the resolutions MSC.26(60)/1992 and MSC/Circ. 574/1991 are re-interpreted, obviously due to the uncertainties in the formulated regulations.

The tragic sinking of Estonia in late September 1994 introduced additional complications and strains in an already very difficult scientific, technological and regulatory subject.
Responding to the public demand for immediate action IMO formed in December 1994 a Panel Of Experts (POE) to urgently review the Ro-Ro ferry safety issue. The POE was asked to look at all aspects of Ro-Ro passenger ferry safety, including human factors and crew training issues (see Funder, 1995). The Panel was empowered to receive input directly from interested parties and scheduled to complete their work in time for the Maritime Safety Committee in early May 1995, thus within a 5-6 months period. In view of the complexity and the practical implications of the subject, besides the past history of developments in this particular area of regulatory work, starting in 1929, this particular time schedule could be considered in all respects insufficient.

The POE regulatory proposals addressed several, if not all, aspects of Ro-Ro passenger ship safety, ranging from the intact and damage stability, operational and construction matters, communications, Search and Rescue, fire safety, life-saving appliances, evacuation matters, crisis management etc (see, The Panel of Experts Report, 1995, ANNEXES 1 to 33). The submitted proposals of POE to repeatedly amend the SOLAS 1990 intact and damage stability criteria (ANNEX 5) were considered the most crucial for the future of existing, as well as of new Ro-Ro passenger ships, since they called for significant modifications both for existing Ro-Ro ship designs and for new design concepts.

Parallel to the IMO efforts, several countries formed almost simultaneously, or even before the IMO initiative, research groups with the aim to address the same issue both from a national point of view, as

well for assisting (and, to a certain degree, for directing) the work of the POE of IMO considering the set, very tight, time schedule. The most significant initiatives have been the following:

1. The NORDIC Group initiative, representing a consortium of 11 Scandinavian Authorities, Associations, Agencies and Classification Societies and of an equal number of subcontractors (research establishments, universities, shipyards etc.), leading to the formulation of the so-called NORDIC "Safety of Passenger/Ro-Ro Vessels" R&D project. The first phase of this project was finished in September 1995 (see Svensen, 1995). The NORDIC project initiative seems to have significantly influenced the proposals of the IMO Panel of experts, especially as to the requirement for all Ro-Ro passenger vessels to satisfy SOLAS 90 criteria *when burdened with one-half meter* of water on the Ro-Ro deck (see, comment, Little and Hutchison, 1995). This part of the proposed new regulations *is practically the most crucial one*, as far as the practical implications to the design of existing and future Ro-Ro vessels are concerned.

2. The SNAME ad hoc Panel on Ro-Ro Safety initiative, representing US and Canadian Coast Guards, ABS, Ferry owners and operators, NTSB, MARAD, and various consulting naval architects, leading to the formulation of an individual research program to assess the stability and safety standards of the U.S. and Canadian Ro-Ro passenger fleet, to consider specific issues of seawater ingress onto the damaged Ro-Ro deck and to prepare suitable recommendations to the POE and the IMO. The SNAME ad hoc Panel initiative seems to have concentrated on suggestions, how to consider the influence of the water freeing ports in estimating the water density on the Ro-Ro deck. Earlier experimental work of the Canadian Institute of Marine Dynamics (1993-1994)

on the validity of SOLAS 90 damage criteria and the survivability of Ro-Ro passenger ferries after flooding of the Ro-Ro deck seemed to have supported the SNAME ad hoc Panel initiative

3. The UK Department of Transport initiative, that actually goes back to the year of adoption of the last SOLAS 90 criteria and indirectly even before that date. The lastly adopted SOLAS 90 criteria were, according to the UK delegation, insufficient to address the real problem of stability of a damaged Ro-Ro ship in waves: It proved, namely, through systematic model testing, that a SOLAS 90 Ro-Ro ship, with assumed water ingress onto the Ro-Ro deck, was likely to capsize in moderate seastates with a significant wave height of just over 1.5m (see, T. Allan, 1994).

4. The Italian Research initiative that was based on systematic damage stability model experiments, performed at the German Towing Tank HSVA with a large size ship model (length 5.73 m, scale 1:30) according to the suggested POE regulations. (see, Marsano, 1995). The results of this particular research suggested that the water density on the damaged Ro-Ro deck never reached the "0.5m level" suggested by the POE of IMO for waves of 4.0m significant wave height. Instead, it reached a mean level of merely 0.17m, being in excellent agreement with earlier published experimental results of the SNAME ad hoc Panel (when relative motion included, see, e.g., Hutchison, 1995). In addition and because of the above, it appeared, in contrast to the position expressed by the UK delegation, that a SOLAS 90 ship under the worst intact or damage conditions is able to survive seastates of 4.0m significant wave height. Both above findings questioned directly the validity of the proposed amendments of the POE of IMO, especially the specifications of Reg. 8-1 and 8-2.

5. The present Greek research initiative that, among other things, related specifically to the Greek Ro-Ro passenger vessels, included theoretical - numerical simulations of the relative ship motions of the intact and damage ship in waves and estimated the likelihood of Ro-Ro car deck wetting (and flooding) under the specific environmental conditions, resulting from the POE regulations. The results suggested that for a damage freeboard over abt. 40% of the significant wave height the amount of water accumulated on the damage Ro-Ro deck was practically negligible and the vessel never came into danger to capsize. On the other side, the strict application of the proposed POE regulations required, for the particular test vessel, extensive modifications and compartmentation of the car deck. The results are in line with published results of the SNAME ad hoc Panel initiative and the Italian research.

Besides the above mentioned research initiatives from the Nordic countries, the United Kingdom and the USA, no other systematic, large scale studies or research results are known to have contributed to.the regulatory work announced in April 1995 by the POE. In the wake of the circulated amendments by the POE of IMO the Italian and Greek studies have been launched with the aim to critically review the proposed changes and to assess their practical impact especially on existing ships. The position of the Russian delegation to IMO suggested, that a SOLAS 90 ship might survive, in case of damage, seastates up to a significant wave height of 3.0m. Also, specific comments by the Japanese delegation to IMO on the published Ro-Ro damage stability model experiments and own investigations led to the conclusion that the influence of a central casing on the Ro-Ro deck is very crucial for the survivability of a damaged Ro-Ro ferry in waves, but flooding of the car deck alone, even with an amount of water greater than

20% of the ship's displacement, does not lead to the capsize of a SOLAS 90 ship with "clear" car deck.

Summarizing the above review of historical developments in Ro-Ro stability safety research and the related stability criteria, it seems that the International Maritime Organization attempted in 1995 to correct its own past failures (in approaching properly and timely the Ro-Ro stability safety issue) by addressing the full range of open technical questions at once. The implementation of new regulations, developed under strong public pressure within a very short time period (within only abt 5 months) severely affects both all new ships, but also all the existing ones, the majority of which did not comply even with the lastly approved standard (SOLAS 90). The impact and the practicality of the enhanced SOLAS 95 regulations remain to be proven in practice.

Following the above procedure, IMO significantly increased the stability standards of Ro-Ro ships, but still left many open questions on the Ro-Ro passenger vessel safety problem. Several new type of ships, particularly high speed monohulls, might prove worthless for "unlimited" service. The philosophy of the enhanced new regulations, namely to prescribe, through stringent regulatory requirements, "totally stable and unsinkable ships", given human errors as a fact, is not correct. A comparison with other kind of transportation vehicles, that can all easily produce disastrous accidents by simple human failure, makes the above strategy actually questionable. However, it seems that pressure from the public and a clear new strategy of the shipbuilding industry for *new safety oriented product developments* will finally dictate the technological developments in Ro-Ro shipping in the immediate and far future (see, e.g., *Wild, 1995*).

Greek Passenger Ferry Fleet:
Fleet Age Breakdown
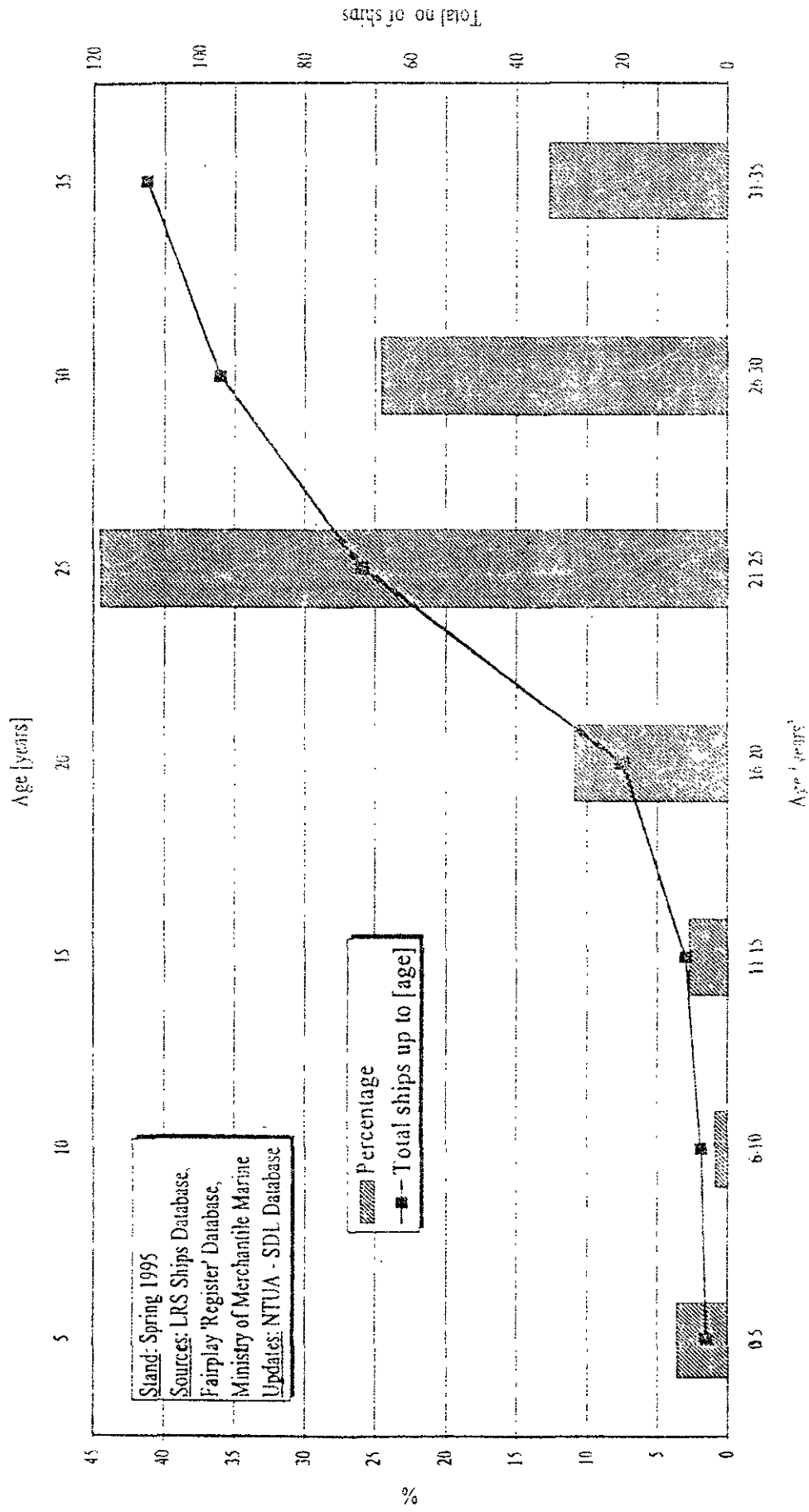
Fig. 1: Greek Ro-Ro Passenger Ferry Fleet - Age Breakdown

RO-RO SHIP DESIGN TECHNICAL DATA

Start

Design Specifications Trade Scenario

Initial Design Loading Scenarios

Calculate A/Amax

Damage Stability Software Module - A.265

Compliance with 2 compartment standard ?*

SOLAS 90 - Damage Stability Criteria for 2 compartment standard

Damage Stability Software Module - SOLAS 90

*) dates: 1.10.1998 - 1.10.2010

Compliance with SOLAS 90?**   No → **Sponsons Duck Tail Side casings Cross flooding Bulkheads Buoyancy Devices Reduce Draft**

**) dates: 1.10.1998 - 1.10.2005

Yes

Numerical Simulation of Capsizing of the Damaged Ship in the Seaway - *Capsizing Software Module*

SOLAS 90 + Stockholm A. Damage Stability Criteria for 2 compartment standard

Damage Stability Software Module - SOLAS 90+ WOD

Physical Simulation of Capsizing of the Damaged Ship in the Seaway - *Model Experiments at relevant Towing Tank*

Is Design Satisfactory ?   No → **Sponsons Duck Tail Side casings Cross flooding Bulkheads Buoyancy Devices Reduce Draft**

No

Final Decision

Fig. 2 : SOLAS 90 & SOLAS 90 + Water On Deck - Ro-Ro Ferry Control & Design - Decision Procedure

SYSTEMATIC MODEL EXPERIMENTS ON FLOODING OF TWO RO-RO VESSELS

J.M.J. Journée (DUT)
H. Vermeer (DGSM)
A.W. Vredeveldt (TNO)

SUMMARY

After the accident of the "Herald of Free Enterprise", research has been started in the Netherlands on the safety of Ro-Ro vessels.

One particular research project of the Ship Hydromechanics Laboratory of the Delft University of Technology concentrates on the ship's motion behaviour and the associated stability characteristics during the intermediate stages of flooding after a collision damage in still water. A mathematical model has been developed, describing the ship's motions due to flooding in the time domain. For validation purposes, a limited number of model experiments have been carried out in the past with two typical Ro-Ro ferries.

After these validations, recently a large number of additional model tests were held on a much more systematic basis. For the two vessels, the effect of the initial metacentric height, the ingress area, the initial angle of heel, the presence of longitudinal bulkheads and cross ducts, the reduction of permeabilities and down flooding on capsizing have been examined.

Results of these experiments are presented in this paper. Some important considerations with respect to the intermediate stages of flooding and the initial conditions are given.

1 INTRODUCTION

In close cooperation with the Directorate General of Shipping and Maritime Affairs in the Netherlands (DGSM), the Delft University of Technology (DUT) and the Netherlands Organization for Applied Scientific Research (TNO) are investigating the dynamic behaviour of ships during a sudden ingress of water after a collision in the side in still water at zero forward speed. During the model experiments on this sudden ingress of water, the roll motions of models of two typical Ro-Ro vessels were measured on time basis.

First, a series of model experiments has been carried out with a 1:50 model of a typical Ro-Ro vessel with a block coefficient of about 0.62, named here "Ferry-62". The transverse bulkhead between the fore and aft engine room was at half length of the collision gap. From the two midship engine rooms until aft, the ship is subdivided by transverse bulkheads only, over the full breadth of the vessel. Forward of the engine rooms, the ship is subdivided by two longitudinal bulkheads at one-fifth of the breadth from the hull, transverse bulkheads in the side at small mutual distances and no bulkheads in the centre part.

Then, similar experiments have been carried out with a 1:50 model of another typical Ro-Ro vessel with a block coefficient of

about 0.72, named here "Ferry-72". This ship has a quite different watertight division. Below the Ro-Ro deck, the ship is subdivided by two longitudinal bulkheads over the full length at one-fifth of the breadth from the hull. The length of the wing compartments is rather small, while the transverse bulkheads in the centre part are located at a much larger distance. To avoid large heeling angles in case of a lateral collision, cross ducts in the double bottom will transfer the incoming sea water to the other side of the vessel (equatizing arrangement).

For both models, the experiments were carried out at three different initial metacentric heights and four different collision gaps. The first preliminary results of this research project have been presented by Vredeveldt and Journée (1991) and Vermeer, Vredeveldt and Journée (1994). Within the framework of contract research of DUT for TNO, some experimental results were reported to TNO in limited distributed technical reports by Journée (1994) and Journée and Onnink (1996).

In the underlying paper, an overview of all experiments is given, while a selected number from this large amount of experimental results is presented and discussed. Also, some comparisons of experimental data with the results of theoretical approximations of the dynamic behaviour of the models during an ingress of water are given.

2 THEORETICAL APPROACH

Generally, ship motion calculations can be carried out easily with frequency domain programs. But, as a result of the formulation in the frequency domain, any system influencing the behaviour of the vessel should have a linear relation with the motions of the vessel. However, in a lot of cases there are several complications which perish this linear assumption, for instance the non-linear viscous damping, forces and

moments due currents, wind and anchoring, etc. Also, forces and moments due to a collision and the ingress of water afterwards may show a very strong non-linear behaviour.

To include these non-linear effects, it is necessary to formulate the equations of motion in the time domain, which relates instantaneous values of forces, moments and motions.

For this purpose, use has been made of work published by Cummins (1962) and Ogilvie (1964).

2.1 EQUATIONS OF MOTION

The floating vessel is considered to be a linear system with the translational and rotational velocities as input and the reaction forces and moments of the surrounding water as output. The object is supposed to be at rest at time $t = t_0$. Then, during a short time Δt, an impulsive displacement Δx with a constant velocity V is given to this object:

$$\Delta x = V \Delta t$$

During this impulsive displacement, the water particles will start to move. When assuming that the fluid is inviscid and free of rotation, a velocity potential Φ linear proportional to V, can be defined:

$$\Phi = V \Psi \quad \text{for: } t_0 < t < t_0 + \Delta t$$

in which Ψ is the normalised velocity potential.

After this impulsive displacement Δx, the water particles are still moving. Because the system is assumed to be linear, the motions of the fluid, described by the velocity potential Φ, are proportional to the impulsive displacement Δx:

$$\Phi = \chi \Delta x \quad \text{for: } t > t_0 + \Delta t$$

in which χ is the normalised velocity potential.

The impulsive displacement Δx during the period $(t_0, t_0 + \Delta t)$ does not influence the

motions of the fluid during this period only, but also further on in time. This holds that the motions during the period $(t_0, t_0 + \Delta t)$ are influenced by the motions before this period too. When the object performs an arbitrarily with time varying motion, this motion can be considered as a succession of small impulsive displacements. Then, the resulting total velocity potential $\Phi(t)$ during the period $(t_n, t_n + \Delta t)$ becomes:

$$\Phi(t) = \sum_{j=1}^{6} \left\{ V_{j,n} \Psi_j + \sum_{k=1}^{n} \left\{ \chi_j(t_{n-k}, t_{n-k} + \Delta t) V_{j,k} \Delta t \right\} \right\}$$

in which:
- n number of time steps
- t_n $t_0 + n\Delta t$
- t_{n-k} $t_0 + (n-k)\Delta t$
- $V_{j,n}$ j-th velocity component during period $(t_n, t_n + \Delta t)$
- $V_{j,k}$ j-th velocity component during period $(t_{n-k}, t_{n-k} + \Delta t)$
- Ψ_j normalised velocity potential caused by a displacement in direction j during period $(t_n, t_n + \Delta t)$
- χ_j normalised velocity potential caused by a displacement in direction j during period $(t_{n-k}, t_{n-k} + \Delta t)$

Letting Δt go to zero, yields:

$$\Phi(t) = \sum_{j=1}^{6} \left\{ \dot{x}_j(t) \Psi_j + \int_{-\infty}^{t} \chi_j(t - \tau) \dot{x}_j(\tau) d\tau \right\}$$

in which $\dot{x}_j(t)$ is the j-th velocity component at time t.

The pressure in the fluid follows from the linearised equation of Bernoulli:

$$p = -\rho \frac{\partial \Phi}{\partial t}$$

An integration of these pressures over the wetted surface S of the floating vessel gives the expression for the hydrodynamic reaction forces and moments F_i. With n_i for the generalised directional cosine, F_i becomes:

$$F_i = -\iint_S p n_i dS$$

$$= \sum_{j=1}^{6} \left\{ \left\{ \rho \iint_S \Psi_j n_i dS \right\} \ddot{x}_j + \int_{-\infty}^{t} \left\{ \rho \iint_S \frac{\partial \chi_j(t - \tau)}{\partial t} n_i dS \right\} \cdot \dot{x}_j(\tau) d\tau \right\}$$

When defining:

$$A_{i,j} = \rho \iint_S \Psi_j n_i dS$$

$$B_{i,j}(t) = \rho \iint_S \frac{\partial \chi_j(t - \tau)}{\partial t} n_i dS$$

the hydrodynamic forces and moments become:

$$F_i = \sum_{j=1}^{6} \left\{ A_{i,j} \ddot{x}_j(t) + \int_{-\infty}^{t} B_{i,j}(t - \tau) \dot{x}_j(\tau) d\tau \right\}$$

for i=1,..6

Together with linear restoring spring terms "$C_{i,j} x_j$" and linear external loads "$X_i(t)$", Newton's second law of dynamics gives the linear equations of motion in the time domain. When replacing in the damping term "τ" by "$t - \tau$", this term can be written in a more convenient form. Then, the linear equations of motion in the time domain are given by:

$$\sum_{j=1}^{6} \left\{ \left(M_{i,j} + A_{i,j} \right) \ddot{x}_j(t) + \int_{0}^{\infty} B_{i,j}(\tau) \dot{x}_j(t - \tau) d\tau + C_{i,j} x_j(t) = X_i(t) \right\} \quad \text{for i=1,..6}$$

in which:

$x_j(t)$ translational or rotational displacement in direction j at time t

$M_{i,j}$ solid mass or inertia coefficient

$A_{i,j}$ hydrodynamic mass or inertia coefficient

$B_{i,j}$ retardation function

$C_{i,j}$ spring coefficient

$X_i(t)$ external load in direction i at time t

Refering to the basic work on this subject by Cummins (1962), these equations of motion are called the Cummins Equations.

The linear restoring spring coefficients $C_{i,j}$ can be determined easily from the underwater geometry and the location of centre of gravity G of the vessel, but to determine $A_{i,j}$ and $B_{i,j}$, the velocity potentials Ψ_j and χ_j have to be found, which is very complex in the time domain. However, a much more simple method is given by Ogilvie (1964). He found these coefficients from the hydrodynamic mass and damping data, by using results of the linear 2-D or 3-D potential theory in the frequency domain. Relative simple relations are found between $A_{i,j}$ and $B_{i,j}$ and these frequency domain potential coefficients.

In Ogilvie's approach, te vessel is supposed to carry out an harmonic oscillation in the direction j with a normalized amplitude: $x_j = 1\cos(\omega t)$. After substitution of x_j, $\dot{x}_j$ and $\ddot{x}_j$ in the Cummins equations and comparing the time domain and the frequency domain equations, both with linear terms, he found:

$$A_{i,j} - \frac{1}{\omega} \int_0^\infty B_{i,j}(\tau)\sin(\omega\tau)d\tau = a_{i,j}(\omega)$$

$$\int_0^\infty B_{i,j}(\tau)\cos(\omega\tau)d\tau = b_{i,j}(\omega)$$

$$C_{i,j} = c_{i,j}$$

in which:

$a_{i,j}(\omega)$ frequency-dependent hydrodynamic mass or inertia coefficient

$b_{i,j}(\omega)$ frequency-dependent hydrodynamic damping coefficient

$c_{i,j}$ spring coefficient

The first expression with mass terms is valid for any value of ω, so also for $\omega = \infty$. Then the term with the integral, which will be divided by ω, vanishes. This gives for the potential mass coefficient:

$$A_{i,j} = a_{i,j}(\omega = \infty)$$

A Fourier re-transformation of the second expression, with the damping term, gives the retardation function:

$$B_{i,j}(\tau) = \frac{2}{\pi} \int_0^\infty b_{i,j}(\omega)\cos(\omega\tau)d\tau$$

It should be mentioned that, with this approach of Ogilvie, the coefficients on the left hand side of the Cummins equations are still linear. But, the external loads $X_i(t)$ in the right hand side of the equations may have a non-linear behaviour now. Also, non-linear roll damping terms can be added.

2.2 INGRESS OF WATER

The inclining moment is caused by the weight of the flood water present in the flooded compartments. Throughout the flooding process and the consequential heeling of the vessel both, the amount of water and its location of the centre of gravity, vary.

In general, the contribution of the weight of the flood water to the inclining moment in a particular compartment can be written as:

$$X_4 = \rho g v \left\{ y\cos\phi + z\sin\phi \right\}$$

with (see also figure 1):

X_4 inclining moment due to weight of water in a compartment

ρ density of flood water

g acceleration of gravity

v volume of water in considered compartment

y transverse distance between c.o.g. and centre line, measured parallel with the ship's base line

z vertical distance between c.o.g. and base line, measured parallel with the ship's centre line

ϕ heel angle

The total inclining moment equals the sum of the moments of each flooded compartment.
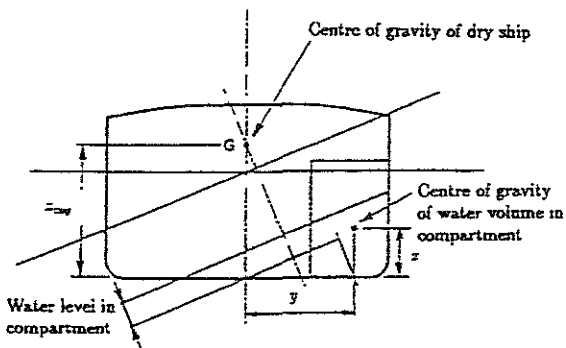
Figure 1: Definition of symbols

The inclining moment, as described above, refers to the intersection of the ship's centre plane and the base plane. The equations of motion of the ship refer to the ship's centre of gravity. Therefore, a correction must be applied on this moment:

$$X_{4_{cog}} = X_4 z_{cog} \cos \phi$$

with:

$X_{4_{cog}}$ inclining moment due to weight of water in a compartment with respect to ships c.o.g.

z_{cog} vertical distance between c.o.g. and base line, measured parallel with the ship's centre line

The amount of flood water in each compartment depends on the flow of water and

flow of air through the damage orifices and the cross flooding openings. In case of wing compartments, the effect of air vents have to be taken into account.

Water flow can be calculated by applying Bernoulli's law:

$$Q_{water} = A \sqrt{\frac{2 \, \Delta P}{\rho \, C}}$$

with:

Q_{water} flow rate between sea and damaged compartment or between adjacent flooded compartment

A flow area

ΔP pressure difference over ingress opening c.q. flooding connection between compartments

C coefficient accounting for flow resistance due to inlet-outlet effects, friction, etc.

For reference, it must be noted that the relation between the coefficient C and the pressure loss coefficient F, as applied in the explanatory notes issued by IMO, can be written as:

$$F = \frac{1}{\sqrt{C}}$$

The air flow can be calculated in a similar manner, however the formula is slightly more complicated due to the compressibility of the air:

$$Q_{air} = A \sqrt{\frac{2 \, R \, T \, \Delta P}{|P_f \div P_r| \, C}}$$

with:

Q_{air} flow rate of air through vents

A flow area

R specific gas constant of air

T temperature of air

ΔP pressure difference over air vent

P_f pressure at front of air vent

P_r pressure at rear of air vent

C coefficient accounting for flow resistance due to inlet-outlet effects, friction, etc.

In the case of the ingress openings and the cross flooding openings two complications occur. The pressure head varies along the height of the opening and the water levels may lie between the upper and lower edge of the opening. These complications can be catered for by dividing the opening vertically into a number of strips. Per strip, it can be decided whether water flow or air flow occurs.

Flow is assumed to stop when the pressure difference over an orifice, flow opening or air vent becomes zero. This happens when water levels in adjacent compartments are equal, which can only occur when these compartments extend vertically above the damaged water line.

In case of a compartment which is located fully below the damaged water line, it is assumed that some air (10 % of total compartment capacity) remains trapped inside the compartment. To calculate the air pressure in this trapped volume, the simple gas law is applied:

$$Q_{air} = \frac{R\,T}{V_{air}}$$

with:

P_{air} air pressure
V_{air} volume of trapped air

3 MODEL EXPERIMENTS

The experiments were carried out in Towing Tank No I of the Ship Hydromechanics Laboratory of the Delft University of Technology. This tank has a length of 142 metre, a breadth of 4.22 metre and a water depth of 2.50 metre.

De main dimensions of the full size vessels are given in table 1.

The scale of the two models was 1:50.

The models were positioned in a transverse manner in the tank at half the length of the tank. The distance between the models and the tank walls was about half a meter

		Ferry-62	Ferry-72
Length over all	m	161.00	179.30
Length L_{pp}	m	146.40	169.20
Moulded breadth	m	27.60	24.92
Depth Ro-Ro deck	m	8.10	7.85
Draught	m	6.22	6.08
Block coefficient		0.617	0.717
Volume	m^3	15,500	18,375
$1.20 * GM$	m	-	1.92
$1.00 * GM$	m	2.05	1.60
$0.80 * GM$	m	1.64	1.28
$0.60 * GM$	m	1.23	-

Table 1: Main dimensions of ships

and the roll damping waves could propagate over a long distance before they were, after reflection by the tank-ends, diffracted to the model.

3.1 EXPERIMENTAL SET-UP

During the experiments, the roll motions of the model were measured on time basis. The sign of these data corresponds to a right-handed orthogonal coordinate system with the origin in the centre of gravity G of the ship, the x-axis in the longitudinal forward direction, the y-axis to port side and the z-axis upwards. This means that heel or roll to starboard is positive and heel or roll to port side, so to the gap, is negative. The shape of the collision gaps is based on the result of a collision in the side by a ship with a bulbous bow, so a circular gap under the waterline and a triangular gap above the waterline.

The shape and the full scale dimensions (in mm) of the four collision gaps in the ship are presented in figure 2.

The reference line for the vertical measures in this figure is the ship's base line.

The projected areas of these gaps are given in table 2.

In the underlying paper, the time histories of the roll angles during the sudden ingress of water into the model are presented. A while before opening the gap the registra-
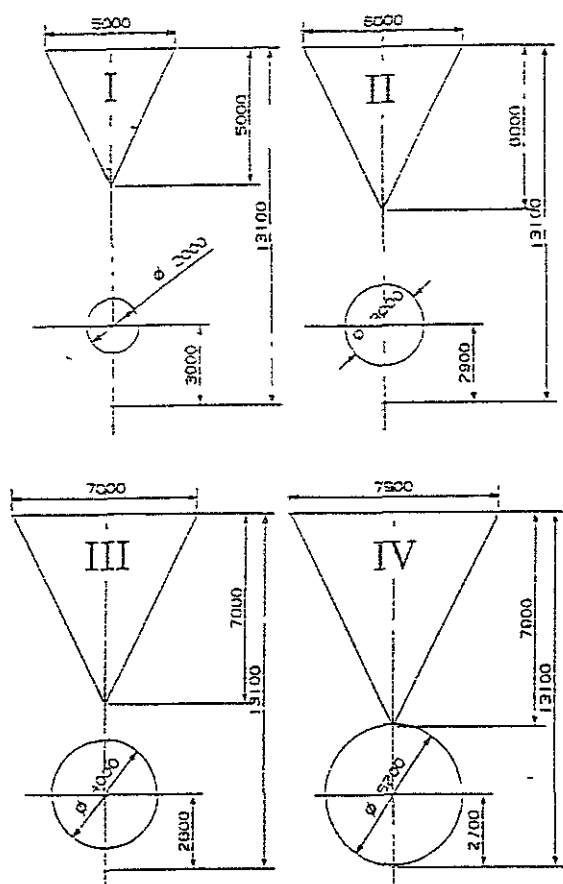
Figure 2: Collision gaps

tion was started and a time-reference signal was made available to obtain the instant of opening the gap, $t = 0$.

As soon as the port side gap is opened, water will flow into the model and the port side pressure on the model at the gap will drop down. Still, the effect of the inflooding water has to start. At the starboard side of the model the static water pressure on the model maintains. During a short time, this results in a total hydrostatic force to port

Gap	Projected gap area		
No	Circle (m^2)	Triangle (m^2)	Total (m^2)
I	3.14	12.50	15.64
II	7.07	18.00	25.07
III	12.57	24.50	37.07
IV	21.24	31.20	52.44

Table 2: Areas of collision gaps

side. Because the gap is below the centre of gravity, this force causes a small initial roll to starboard. After that, the effect of the flooding water will increase and the model starts to roll to port side.

The experiments were carried out in such a way that the effect of the growth of the gap after the collision with time on the ship motions could be neglected. So, the gap came into existence very sudden; it was nearly a step function. The gap in the hull of the model was closed by a flexible rubber flap, sticked with vaseline to the outside exterior of the hull around the gap. Without introducing a roll moment, the flap was catapulted away backwards by a spring construction on the model. The release of the sealed spring took place electrically, without touching the model. Experiments on catapulting away the flap from the model without a gap, showed that the discharge of the energy in the spring construction and the slight disturbance of the still water surface by the moving flap did not result in significant ship motions.

Each experiment has been started with a dry model. Water leaked between the flap and the hull via the gap into the model, if any, was pumped away just before starting the experiment. The discretised roll signals were stored in an ASCII-format on diskettes.

To examine the repeatability of the experimental results, a large number of experiments have been carried out twice or even three times.

3.2 EXPERIMENTS FERRY-62

The body lines of Ferry-62, the engine rooms with bulkheads and spaces and the location of the collision-gaps are shown in figure 13. The transverse bulkhead between the engine rooms was at half length of the gap. The engines were modelled by wooden blocks.

The experiments were carried out at three different values for the initial metacentric

height. The values of GM-ship were 2.05 meter (100 %), 1.64 meter (80 %) and 1.23 meter (60 %), respectively.

To obtain roll damping information, free rolling experiments were carried out with the intact model, so the model with a closed gap, and with the flooded model with gap I.

Then, capsize tests were carried out for the three metacentric heights and the four gaps. To examine the effect of a small initial heel angle, these experiments were repeated with an initial heel.

To examine the effect of the free surface of the flooded water on the Ro-Ro deck, the experiments which resulted into capsizing were repeated with a reduced deck width.

3.2.1 ROLL DECAY TESTS

For three metacentric heights of Ferry-62, free rolling experiments were carried out with the intact model, so the model with a closed gap, and for the flooded model with gap I.

The GM value of the intact ship, the heeling moments corresponding to the initial heel angles, the measured natural roll periods T_ϕ and the gyradii for roll of the ship $k_{\phi\phi}$, obtained from T_ϕ, are given in table 3.

Intact ship				Ship with gap I	
GM		T_ϕ	$k_{\phi\phi}/B$	T_ϕ	$k_{\phi\phi}/B$
(m)	(%)	(s)	(-)	(s)	(-)
2.05	100	15.3	0.395	15.3	0.395
1.64	80	17.0	0.395	19.3	0.445
1.23	60	19.2	0.385	20.4	0.410

Table 3: Still water test results of Ferry-62

The non-dimensional rolldamping coefficients $\kappa(\phi_a)$ are presented in figure 14.

The figure shows a very considerable increase of the roll damping during flooding of the engine rooms of the ship. This is mainly caused by the obstacles in the engine rooms, the simplified wooden models of the engines.

3.2.2 CAPSIZE TESTS

When not taking into account the sinkage during flooding, the Ro-Ro deck of Ferry-62 enters into the water at a heel angle of 7.8 degrees.

The capsize tests were carried out at the three metacentric heights of 1.23, 1.64 and 2.05 metre and the four gaps I, II, III and IV. To examine the effect of a small initial heel angle, these experiments were repeated with initial heel angles of the ship. For the smallest and the largest gap, the results are presented in figure 15.

Without an initial heel, the ship capsized for all gaps within 7 minutes at the lowest GM of 1.23 metre (60%) and survived at the other GM values.

But with an initial heel angle of about -3 degrees, the ship capsized in all examined cases. At a GM of 1.64 metre (80%), the ship capsized when the initial heel angle was about -1 degrees. At the actual GM of 2.05 metre, the ship capsized when the initial heel angle was about -3 degrees. The duration of capsizing is strongly depending on the size of the gap; at the largest GM, 7 minutes for gap I and 1 minute for gap IV.

To examine the effect of the free surface of the flooded water on the Ro-Ro deck, those experiments which resulted into capsizing were repeated at a reduced deck width. This was simulated by two beams of hard foam at the Ro-Ro deck at port side and at starboard, with a breadth of 2.50 metre. This modification did not result into an avoidance of capsizing. However, the time necessary for capsizing will be increased by about 50 per cent. An example is given in figure 3.

3.3 EXPERIMENTS FERRY-72

The body lines of Ferry-72, the engine rooms with cross ducts, bulkheads and spaces and the location of the collision-
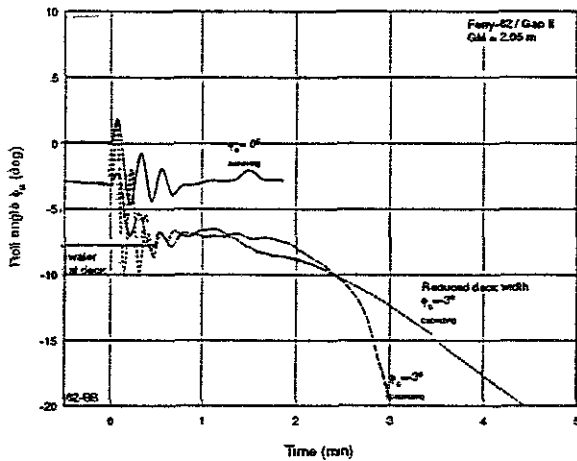
Figure 3: Example of the influence of a reduced deck width on capsizing of Ferry-62

gaps are shown in figure 16. The transverse bulkhead in the side at half the length of the engine room was in the middle of the gap. During the tests, the engine room was empty.

The experiments were carried out at three different values for the initial metacentric height. The values of GM-ship were 1.92 meter (120 %), 1.60 meter (100 %) and 1.28 meter (80 %), respectively.

To obtain roll damping information, free rolling experiments were carried out with the intact model, so the model with a closed gap, and with the flooded model with gap I.

Then, a series of capsize tests were carried out for the three metacentric heights and the four gaps. To examine the effect of a small initial heel angle, these experiments were repeated with an initial heel.

To examine the effect of the longitudinal bulkheads, also capsize tests were carried out with the model without these bulkheads, so with engine rooms over the full breadth of the ship.

To examine the effect of the cross duct in the double bottom, capsize tests were carried out with the model with a closed duct. To examine the effect of water on the Ro-Ro deck, some experiments which re-

sulted into capsizing were repeated with deck openings in the Ro-Ro deck.

A few experiments were carried out with the model without a cross duct but with 60 per cent of the volume hard foam in the two port side wing tanks.

Finally, some experiments were carried out in regular beam waves with an amplitude of 1.0 meter.

3.3.1 ROLL DECAY TESTS

For the metacentric heights of Ferry-72, free rolling experiments were carried out with the intact model, so the model with a closed gap, and for the flooded model with gap I.

The GM value of the intact ship, the heeling moments corresponding to the initial heel angles, the measured natural roll periods T_ϕ and the longitudinal gyradii for roll of the ship $k_{\phi\phi}$, obtained from T_ϕ, are given in table 4.

Intact ship				Ship with gap I	
GM		T_ϕ	$k_{\phi\phi}/B$	T_ϕ	$k_{\phi\phi}/B$
(m)	(%)	(s)	(-)	(s)	(-)
1.92	120	14.5	0.400	13.8	0.380
1.60	100	16.2	0.410	15.1	0.380
1.28	80	18.4	0.415	17.3	0.390

Table 4: Still water test results of Ferry-72

The non-dimensional rolldamping coefficients $\kappa(\phi_a)$ are presented in figure 17.

The figure shows an increase of the roll damping during flooding of water in the ship. The roll damping increases with the metacentric height.

3.3.2 CAPSIZE TESTS

When not taking into account the sinkage during flooding, the Ro-Ro deck of Ferry-72 enters into the water at a heel angle of 8.1 degrees.

The capsize tests were carried out at the three metacentric heights of 1.28, 1.60 and 1.92 metre and the four gaps I, II, III and IV. To examine the effect of a small initial heel angle, these experiments were repeated with an initial heel. For the smallest and the largest gap, the results are presented in figure 18.

Without an initial heel angle, the ship survived in all cases.

With an initial heel angle of -3 degrees and the smallest gap, the ship survived too. But with the largest gap, the ship capsized within 1.5 minutes for the lowest GM of 1.28 metre (80%) and it survived at the higher GM values.

With an initial heel angle between -4 and -5 degrees, the largest collision gap and the actual GM of 1.60 metre, the situation became critical. The ship hesitated to capsize or it capsized within 2.5 minutes.

To examine the effect of the longitudinal bulkheads in the engine room on the safety of the ship, also the time histories of the roll angles were measured during a flooding of the Ferry-72 model without these longitudinal bulkheads, see figure 4.
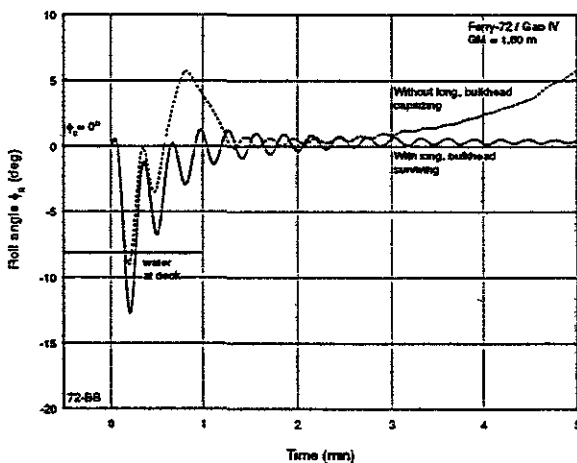
Figure 4: Example of the influence of
a longitudinal bulkhead on
capsizing of Ferry-72

After opening the gap with a zero initial heel angle of the ship, an extreme roll angle of -9 degrees was reached and some

water entered on the Ro-Ro deck. Then the ship returned oscillating to an upright position and it seemed to survived. But, due to the water flooding into the engine room, the ship sunk horizontally. As soon as the metacentric height became negative, the ship started to heel to starboard and finally it capsized after 7 minutes.

In these model experiments, the ship capsized to starboard because it had a small initial heel to starboard during the horizontal sinkage. This was caused by a small loss of port side mass of the rubber flap and the springs after catapulting away the flap.

To examine the effect of the cross duct in the double bottom, capsize tests were carried out with a closed cross duct. Some results are presented in figure 5 for the actual GM of 1.60 metre and the smallest collision gap.
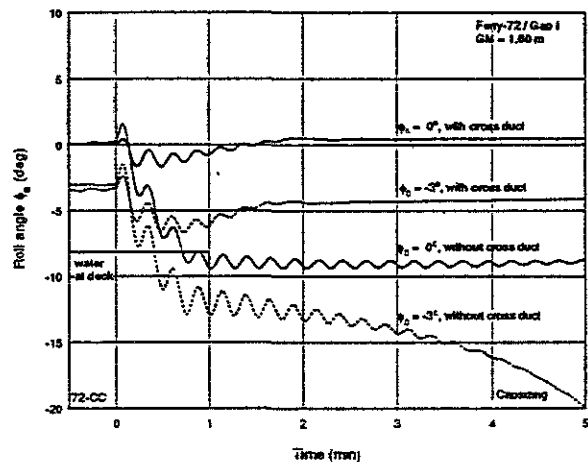
Figure 5: Example of the influence of
a cross duct on
capsizing of Ferry-72

With a cross duct and no initial heel, the ship remained safe. With an initial heel angle of -3 degrees, the ship survived with a final heel angle of -4 degeees, due to a negative initial metacentric height.

With a closed cross duct and no initial heel. the ship survived with a final heel angle of -9 degrees, due to a negative initial metacentric height and and the amount of water

in the port side wing tanks. Some water entered to the Ro-Ro deck, so this became a very dangerous condition.

With a closed cross duct and an initial heel angle of -3 degees, the ship capsized in 5 minutes.

A few experiments were carried out with the ship without a cross duct but with 60 per cent of the volume hard foam in the two port side wing tanks. The results are presented in figure 6 for the actual *GM* of 1.60 metre and the largest collision gap.
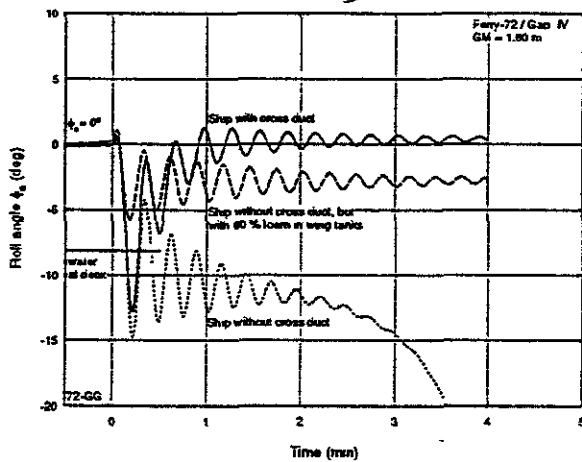
Figure 6: Example of the influence of permeability in a wing tank on capsizing of Ferry-72

As shown before, the ship remained safe with a cross duct.

Without a cross duct, the ship capsized after 3.5 minutes. But, with 60 volume per cent hard foam in the port side wing tanks, the ship remained safe with a final heel angle of -3 degrees.

To examine the effect of water on the Ro-Ro deck, some experiments which resulted into capsizing or nearly capsizing were repeated with deck openings in the Ro-Ro deck, through which water at deck could flow downwards. For the lowest metacentric height and collision gap III, an example of the results is given in figure 7.

Without deck openings and no initial heel, the ship remained safe.
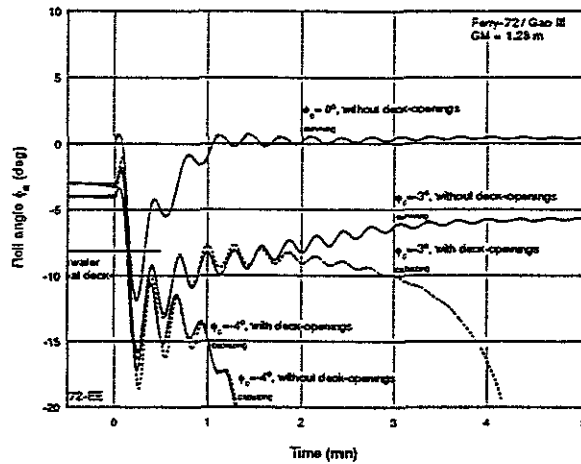
Figure 7: Example of the influence of deck openings on capsizing of Ferry-72

Without deck openings and with an initial heel angle of -3 degrees, the ship survived with a final heel angle of -6 degrees, due to a reduced metacentric height. With deck openings and with an initial heel angle of -3 degrees, the ship capsized after 4 minutes. Without and with deck openings and an initial heel angle of -4 degrees, the ship capsized within 1.5 minutes.

Finally, experiments were carried out in regular beam waves with an amplitude of 1.0 meter and a wide range of wave periods. Figure 8 presents some results for the actual *GM* of 1.60 metre, the largest collision gap and two regular wave periods.

In all wave conditions the ship remained safe.

4 VALIDATION OF THEORIES

The calculation method, as described in sections 2.1 and 2.2 and as implemented in the computer simulation program DYNING (DYNamic INGress of water), has been subjected to validation against model experiments. Unfortunately, no full scale test data could be obtained until now. As a consequence, any scaling effects are ignored.

91
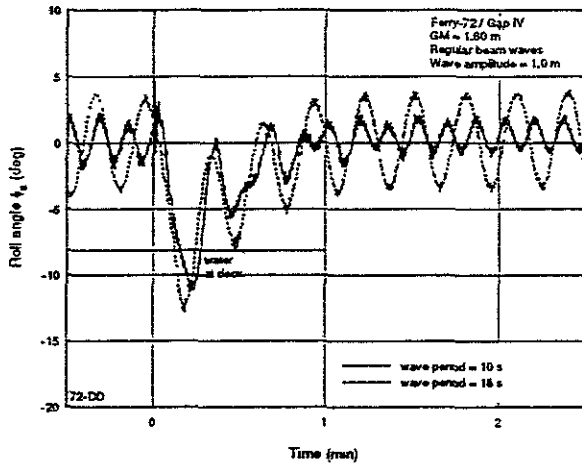
Figure 8: Example of the influence of regular beam waves on capsizing of Ferry-72

Figure 9: Measured and calculated roll due to sudden ingress of water of Ferry-62 for $GM = 1.64$ m
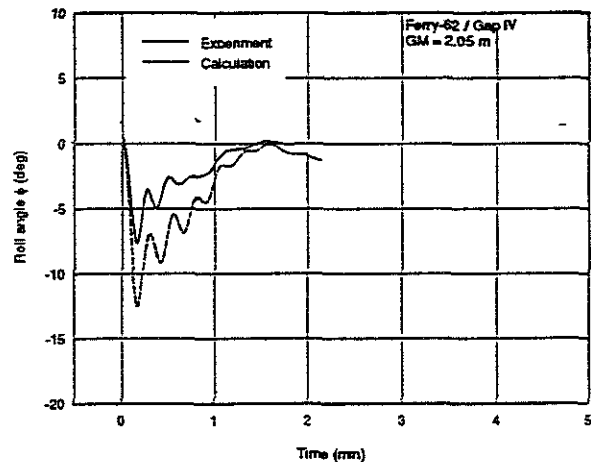
Figure 10: Measured and calculated roll due to sudden ingress of water of Ferry-62 for $GM = 2.05$ m

Prior to validation against some of the tests as presented in this paper, a preliminary validation has been carried out based on tests with a pontoon type model of 3.00 metre length, 2.10 metre width and a draught of 0.625 metre. The model was fitted with opposite wing tanks, connected with a cross duct. The results of this validation were satisfactory, as published in the past by Vredeveldt and Journée (1991).

Figures 9 and 10 show calculated and measured angles of roll for Ferry-62 due to sudden water ingress, obtained during a feasibility study of the tests described in this paper. These first model experiments on Ferry-62 are given in a limited distributed report by Journée (1994).

Figure 9 refers to a realistic GM-value of 2.05 metre. Figure 10 shows results for a GM of 1.64 metre, which would normally not be accepted during operation.

As can be seen, the calculated time span till maximum heel correlates well with the measured value. However, the calculated angle of heel is larger than the measured value. Moreover, in this case the calculated decay is much smaller than measured. The best suggestion for an explanation of both differences is that the sloshing effect of the floodwater is too large to be neglected.

However, it should be remarked that the chosen test case for the Ferry-62 does not take into account the presence of piping in the engine room, which is expected to have a large damping effect on the sloshing motions. Making any sensible remarks on this aspect seems impossible on the basis of theory and model experiments alone.

Figures 11 and 12 show calculated and measured roll motions for the Ferry-72 due to sudden water ingress as presented in this paper.

Figure 11 refers to a GM-value of 1.60 me-

92
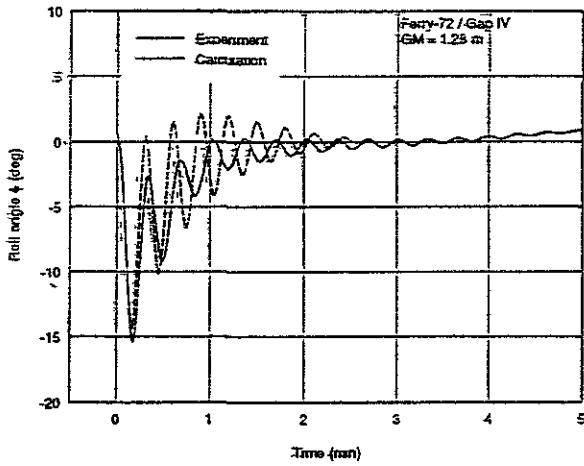
Figure 11: Measured and calculated roll due to sudden ingress of water of Ferry-72 for $GM = 1.28$ m
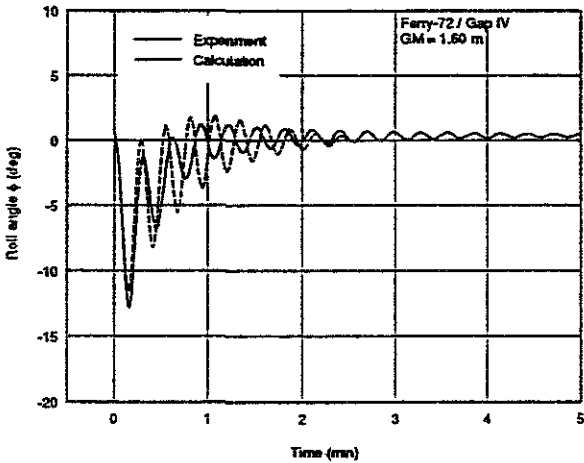
Figure 12: Measured and calculated roll due to sudden ingress of water of Ferry-72 for $GM = 1.60$ m

tre, which is realistic for this ship. Figure 12 refers to a GM of 1.28 metre, which is beyond operational limits.

In this case calculated and predicted angle of heel and time required till maximum heel show a reasonable resemblance with measured values. However, again calculated motion decay is smaller than measured, although the difference is much smaller than in case of the Ferry-62.

The results support the suggestion that sloshing plays a significant role. In the test case of the Ferry-72 the sloshing mo-

tions of the floodwater will be much smaller than in case of the Ferry-62 because of the limited tank width of the flooded compartment, 1/5 B instead of 3/5 B in case of the Ferry-62.

5 CONCLUSIONS

From the experiments with the Ferry-62 and the Ferry-72 some conclusions may be drawn:

1. The roll decay tests show that obstacles like engines will cause a considerable increase of the roll damping of a ship in a flooded condition.

2. The experiments described in this paper showed that certain combinations of the GM-value, the size of the collision gap and the magnitude of the initial heel angle can result in flooding of water on the Ro-Ro deck. As soon as this happens, a large probability on capsizing of the ship comes into existence.

3. It was found that the two longitudinal bulkheads in the engine room area of Ferry-72 was of paramount importance. Without these two bulkheads this ship will capsize, even at an upright initial condition. With an initial heel angle of -3 degrees, Ferry-72 with these bulkheads will survive while Ferry-62, not equipped with this type of subdivision. will capsize.

4. A cross duct has a very positive effect on the probability of survival of the ship. The restoring roll moment decreases, because water can flow in a short time from one side of the ship to the other side. Fitting obstacles in these ducts, like for instance pipes, should be avoided as far as possible.

5. The permeability of the wing tanks has a large effect on the probability of survival of the ship.

93

6. Deck openings in the Ro-Ro deck, through which water at deck can flow downwards, seemed to have a small negative effect on the safety of the ship. However, only one single case has been tested and the location of the deck openings is very important. So, this aspect needs further research.

For the Ferry-72 model the sloshing motions of the floodwater were much smaller than for the Ferry-62 model, because of the limited tank width of the flooded compartment of the first mentioned model. Sloshing was not included in the computer simulations in this paper. From the results of the simulations it appeared that a significant role of sloshing can be expected in the case of wide flooded compartments.

If the case of not too wide flooded compartments (Ferry-72), the roll motions predicted by the computer simulation program DYNING are in a satisfactory agreement with the experimental data. But in the case of wide flooded compartments (Ferry-62) the agreement was very poor. So, also this aspect needs further research.

6 REFERENCES

Cummins, W.E. (1962), The Impulse Response Function and Ship Motions, Symp. on Ship Theory, January 25-27, 1962, Hamburg, Germany, Schiffstechnik, Volume 9, Pages 101-109.

Ikeda, Y., Himeno, Y. and Tanaka, N. (1978), A Prediction Method for Ship Rolling, Report 00405, 1978, Department of Naval Architecture, University of Osaka Prefecture, Japan.

Journée, J.M.J. (1994), Experiments on the Dyamic Behaviour of Ferry-62 during a Sudden Ingress of Water, Report 1014-O (limited distribution), Ship Hydromechanics Laboratory, Delft University of Technology, The Netherlands.

Journée, J.M.J. and Onnink. R. (1996), Experiments on the Dyamic Behaviour of Ferry-72 during a Sudden Ingress of Water, Report 1034-O (limited distribution), Ship Hydromechanics Laboratory, Delft University of Technology, The Netherlands.

Ogilvie, T. (1964), Recent Progress Towards the Understanding and Prediction of Ship Motions, Proceedings of Fifth Symposium on Naval Hydrodynamics, Pages 3-128, September 10-12, 1964, Bergen, Norway.

Vermeer, H., Vredeveldt, A.W. and Journée, J.M.J. (1994), Mathematical Modelling of Motions and Damaged Stability of Ro-Ro Ships in the Intermediate Stages of Flooding, STAB'94 Conference, Melbourne, U.S.A.

Vredeveldt, A.W. and Journée, J.M.J. (1991), Roll Motions of Ships due to Sudden Water Ingress, Calculations and Experiments, International Conference on Ro-Ro Safety and Vulnerability the Way Ahead, April 17-19, 1991, London, U.K.

ACKNOWLEDGEMENT

CROSS SECTION A

CROSS SECTION B

HORIZONTAL SECTION
IN ENGINE ROOM
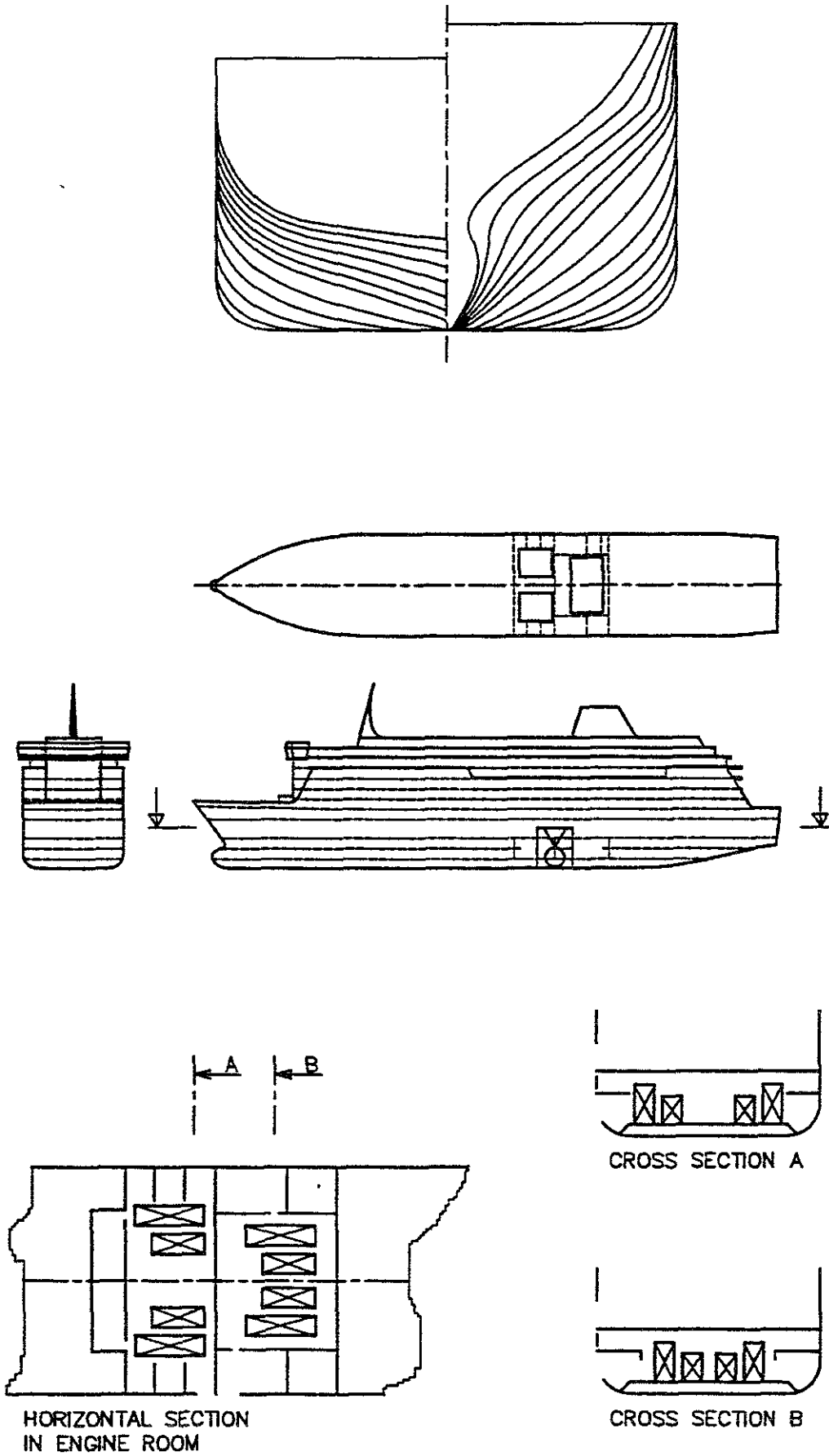
Figure 13: Lines plan and engine rooms of Ferry-62
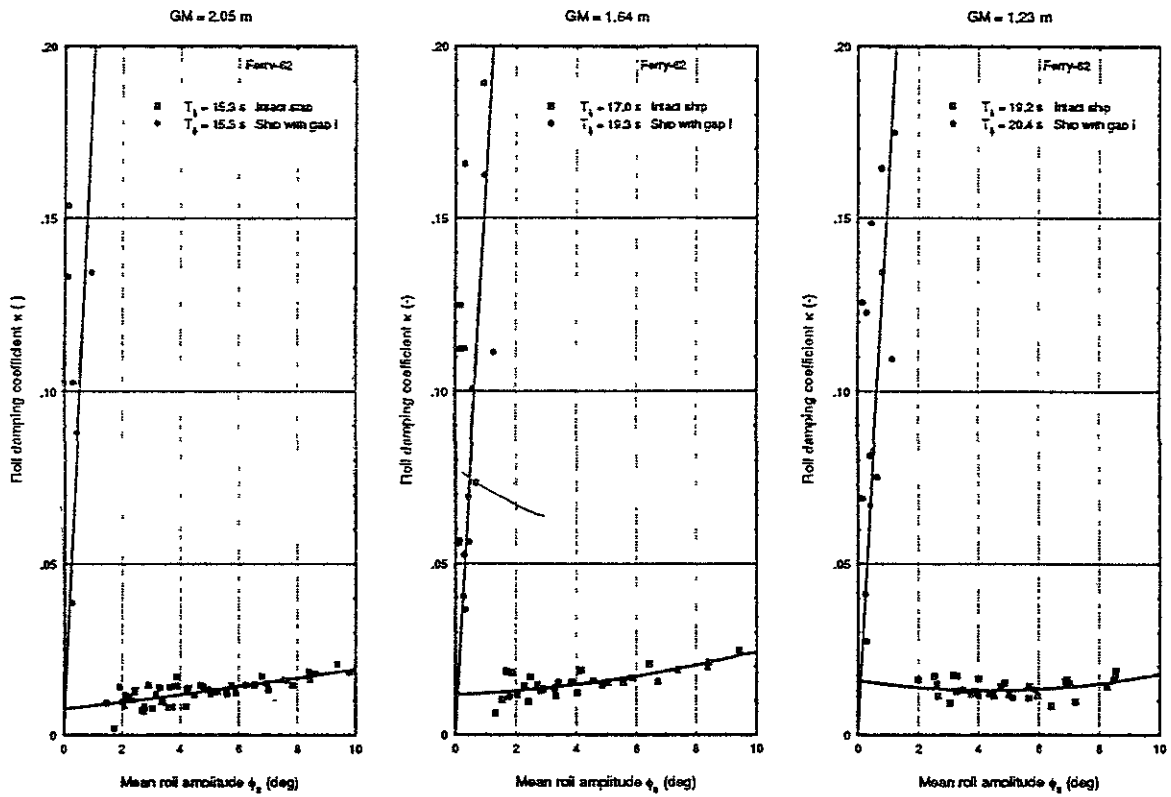
Figure 14: Non-dimensional roll damping coefficients of Ferry-62
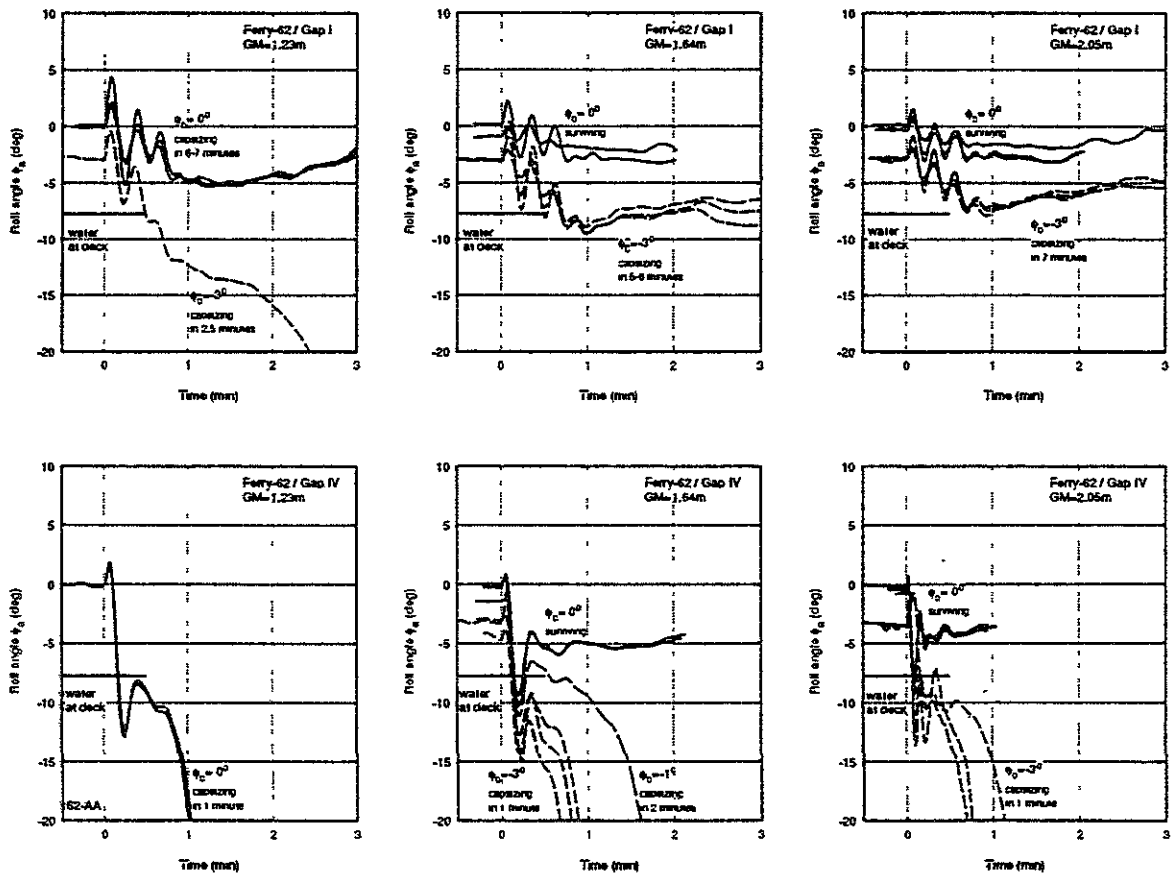
Figure 15: Some results of capsize experiments with Ferry-62

96
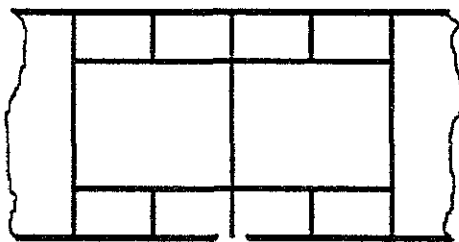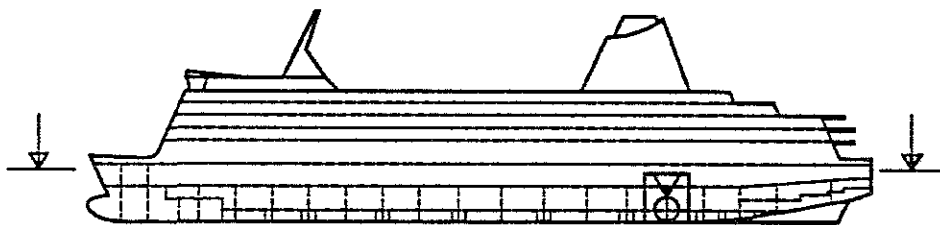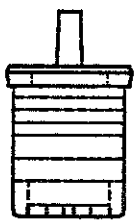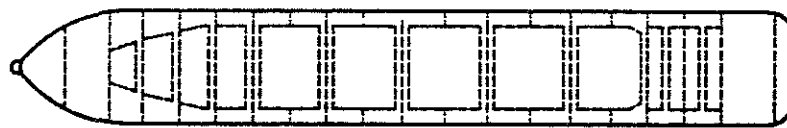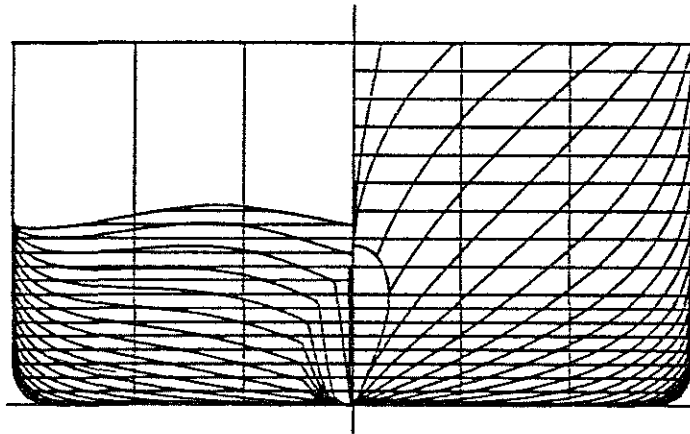
Horizontal section
in engine room
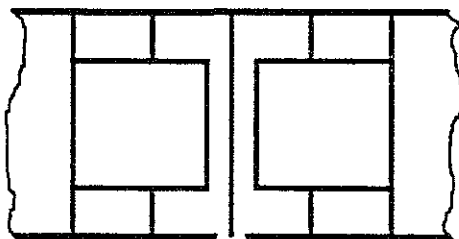
Horizontal section
in double bottom

Cross section

Figure 16: Lines plan and engine rooms of Ferry-72
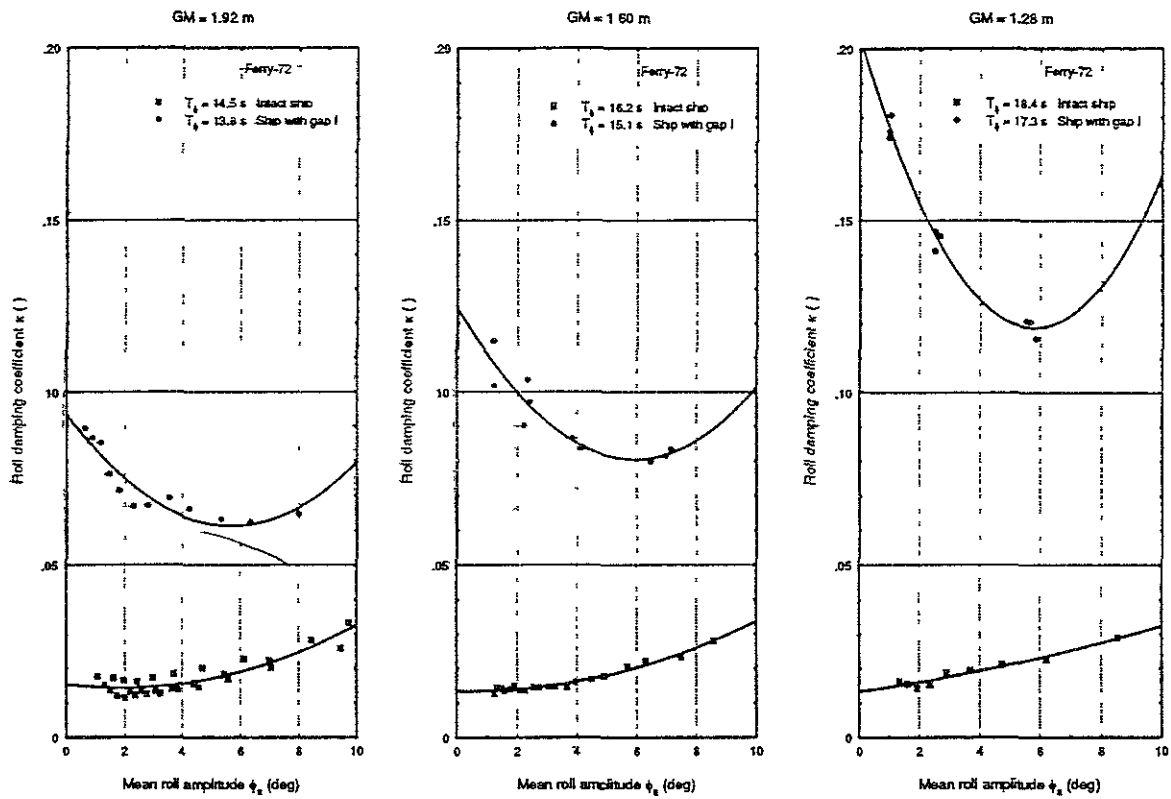
Figure 17: Non-dimensional roll damping coefficients of Ferry-72
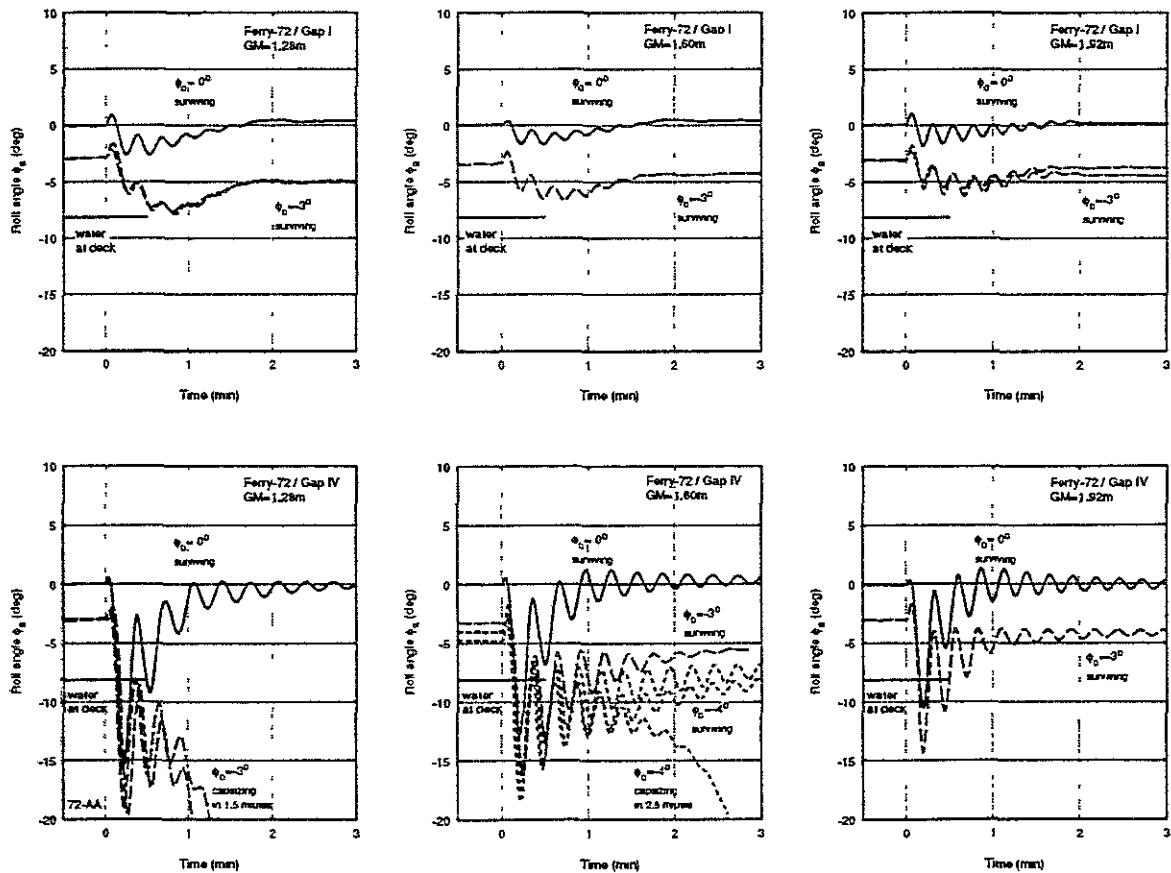
Figure 18: Some results of capsize experiments with Ferry-72

98

STABILITY OF A RO-RO PASSENGER SHIP WITH A DAMAGE OPENING IN BEAM SEAS

Shigesuke ISHIDA, Sunao MURASHIGE

SHIP RESEARCH INSTITUTE, Ministry of Transport
6-38-1, Shinkawa, Mitaka, Tokyo 181, Japan

SUMMARY

An experiment on the stability of a RO-RO passenger ship with a side damage was conducted in beam seas.   Capsize only occurred with a small GM value, in which SOLAS Regulation was not satisfied.   In non-capsize conditions the ship finally became in a stationary condition, with constant mean values of heel angle ϕ_0 and water volume on deck w_0.   The effect of experimental parameters on these values was discussed, making use of the supplementary data by a two-dimensional model test.   The capsize condition was also discussed by adopting those values just before capsize as ϕ_0 and w_0.

The mean height of water on deck above the calm sea surface H_d, which almost kept a certain plus value, was proposed as a key quantity.   It was concluded that the possibility of capsize can be evaluated by the static equilibrium curve which is calculated and drawn on the H_d-ϕ diagram without knowing the exact value of H_d.

1. INTRODUCTION

The safety standard of RO-RO passenger vessels was deliberated at IMO from 1994 to 1995 in order to prevent capsizing disaster like the one of Estonia in 1994.   The main topic of it was the stability standard in damaged condition because RO-RO passenger vessels have wide non-separated car decks.   Once free flooded water is piled up on them, the large heel moment could be the cause of capsize because of this feature.

There were several papers published on this problem like Bird et.al.[1], Vassalos[2], Velschou et.al.[3], Dand[4] and Shimizu et.al.[5] but flooding, accumulation of flooded water, and the interaction of ship motion and flooded water are so complicated that much more study is necessary for clarifying this phenomena.

In this study we conducted an experiment using a Japanese domestic car ferry model with a side damage in beam irregular and regular waves.   Analysis was carried out focusing on the mean heel angle and the mean water volume on deck, both in the stationary condition for non-capsize case, and just before capsize for capsized case. The mechanism of capsize was discussed making use of the stability curves and the height of water on deck above the calm sea surface.   A diagram was proposed which can roughly evaluate the risk of capsize by a fully static calculation.

2. EXPERIMENT

Model Ship and Damage Opening

Table 1 and Fig.1 show the model ship and the damage opening.   The damage

reached two compartments and followed the SOLAS Regulation 8.4. A vertically movable vehicle deck was provided. There was some space between the vehicle deck and the main hull, so this model simulated a ship with side casing. It should be noted that GM_d (GM in damaged condition) was far larger than the intact value because of the flare of bow and stern. Four wave gauges at the center of the damage and six water level meters were equipped in the deck.

Stability Curves

Measured and calculated gz curves are shown Fig.2. Water volume on deck w is drawn when it heels to damage side. Calculated gz curves with constant w are also shown Fig.3. $w/W=10\%$ is equivalent to the flooded water height of 39cm in upright condition. SOLAS Regulation 8.2.3 was satisfied except the condition of $GM_d=1.27m$.

We should keep it in our minds that ship does not roll along the curves in Fig.2 because the area of the damage opening over the vehicle deck is small compared to the volume of the deck, which means the flooding velocity is not high enough to make w equal to the one drawn in Fig.2. In a few cycles of rolling motion we should assume that w is almost constant and that the ship rolls along the stability curves in Fig.3.

Experimental Conditions

The experiment was conducted in irregular waves with JONSWAP spectrum and duration time of 30 minutes in ship scale. Basically significant wave height ($H_{1/3}$) was 4.0m and peak period (T_p) was 8.0sec., but varied keeping the equation of $T_p [sec] = 4\sqrt{H_{1/3}[m]}$. The test was also carried out in some regular waves. The main parameters were GM_d and wave height. Moreover the effect of center casing (CC), initial heel and the height of vehicle deck was investigated in some conditions. The damaged side of the ship was kept to weather side.

Experiment by Two-Dimensional Model

A supplementary experiment was also carried out in regular beam waves using a two-dimensional model which has the principal particulars listed in Table 2. It was a box-shaped model except round bilges. The damage of 20cm wide was opened only on the center of the vehicle deck. The ratio of (damage opening area)/(deck area) is larger than the 3D model. Moreover the main hull is intact, which means a smaller damping. So, the result of this experiment cannot be compared directly with the one of 3D model, but the experimental parameters, especially freeboard height, can be easily changed. The wave frequency and wave height were varied by 0.5 ~ 1.2Hz and 5.0 ~ 19.0cm respectively. The freeboard height was varied by 1.98 ~ 4.05cm.

3. RESULT IN IRREGULAR WAVES

Hereafter the test result of three-dimensional ship model is shown if not mentioned.

Figs.4 and 5 show the time history examples of roll angle ϕ and water volume on deck w. Positive roll angle means heeling to lee side. At the last stage of experiment ϕ and w had almost constant mean values, ϕ_0 and w_0 respectively, in the stationary condition. The effect of experimental parameters on ϕ_0, w_0 and water ingress rate at the beginning of experiment v was investigated as follows.

(1) Effect of GM_d (see Fig.6)

When GM_d gets smaller ϕ_0 becomes greater, but w_0 and v become smaller because small GM_d leads to a large heel angle to lee side in a short time, which makes the damage opening higher up the sea surface. The effect of wave height is small. The reason seems to be the constant wave slope.

(2) Effect of Center Casing (see Fig.7)

In Fig.7 (with CC) the tendency of ϕ_0 versus GM_d is the same as Fig.6 (without CC) but the opposite direction (to weather side)

100

because the flooded water stays mainly in the weather side compartment of the deck. The variation of w_0 is not so clear as Fig.6 because the movement of flooded water between two half-separated compartments is complicated. But in general, the tendency of w_0 is opposite to Fig.6 because heeling to weather side (lowering the damage opening) keeps flowing in and out of water. It can be seen that with the standard GM_d (3.12m) this ship almost keeps upright condition even if w/W gets as much as 40% and that it capsizes with the smallest GM_d.

(3) Effect of Initial Heel

When the ship has an initial heel angle of 4 degrees by a shift of weight to weather side, the time histories of ϕ and w are similar to the ones with CC (Fig.5) because heeling direction is the same. At the case of the smallest GM_d (1.27m) she capsized in about three minutes in model scale. So it can be concluded that heeling to weather side because of CC and/or cargo shift leads to a disastrous situation.

4. EFFECT OF ROLL RESONANCE

The results in regular waves with constant (wave height)/(wave length) ratio of 1/25 are shown in Fig.8, where ω_i is the angular frequency of incident wave. ω_r is the rolling natural period measured by free roll test which is carried out in damaged condition, but the vehicle deck is undamaged. ω_i / ω_r is called a tuning factor.

It can be seen that not only rolling amplitude and relative water amplitude but also water on deck w_0 have peaks around tuning factor = 1. The peaks are notable with CC because the motion of the flooded water is reduced by CC. Moreover heel angle ϕ_0 have some change around the same frequency. This result suggests that irregular waves for the stability test should include significant wave component of the roll resonance frequency and that the interaction of ship motion and water on deck should not be ignored.

Looking through the figures of roll amplitude in Fig.8, the peak frequency ω_{MAX} seems to shift to low frequency side with CC and to high frequency side without CC in some cases. The factors of shifting ω_{MAX}, characteristic to the damaged RO-RO passenger ships, are listed below.

(1) Large damping
(damping in damaged condition is 5 times as large as intact condition according to the free roll test)
(2) Static effect of the water on deck (including the sinkage of the ship)
(3) Dynamic effect of the water on deck.

All the effects of (1), (2) and the damping effect of (3) make ω_{MAX} shift to the low frequency side. But a calculation, modeling the ship and water on deck like a double pendulum, shows an opposite result[6], which could explain the tendency of the shift of ω_{MAX} without CC in Fig.8(a).

5. KEY FACTOR FOR THE BALANCE IN STATIONARY CONDITION

Balance in Stationary Condition

As mentioned in the previous sections the water ingress velocity from damage opening is not so high that in a few cycles of rolling motion the damaged ship moves along one of the stability curves shown in Fig.3, with constant volume of water on deck w. When w increases by flooding it transfers on to another stability curve with less stability. At last when the rolling energy overtake the dynamic stability the ship will capsize, but if this transference stops in a stationary condition under *a certain balance* she will survive. This *balance* will be discussed below.

The mean heel angle ϕ_0 and the mean water volume on deck w_0 in the stationary condition are shown in Fig.9. When the model capsized the values just before capsize are used. The solid lines show the equilibrium angles calculated from the

stability curves in Fig.3 for a given w. But if the stability curve is almost parallel to the horizontal axis near the equilibrium point like GM_d = 1.27m and w/W = 5%, some disturbance like wind moment can easily change the equilibrium angle from the exact one. So quasi-equilibrium angles, the crossing points of the stability curves with the lines of $gz=\pm0.0624$m (2% of GM_d of the standard condition), are also calculated and drawn by broken lines in Fig.9. The zone between these two broken lines will be called a equilibrium zone hereafter.

It can be seen from Fig.9 that the non-capsized experimental results are in or near the static equilibrium zones and that capsized results are away from them with surplus water on deck. According to Fig.3 gz is always negative with these combinations of GM_d and w/W, so it is a natural result that she capsized.

Height of Water Surface on Deck

It is necessary to know another key factor or key quantity which decides the balance in stationary conditions. As the key quantity we propose H_d, the mean height of the water surface on deck from the calm sea surface. If H_d has a large positive value at a moment the water on deck will flow out and vice versa, so H_d must be within a certain range. Fig.10 shows H_d which was calculated by experimental results of w_0 and ϕ_0. It can be seen that H_d is in the range of -0.26m ～ 0.78m in ship scale when the freeboard height is standard (f_d = 0.33m).

It should be necessary to investigate the variation of H_d as a function of ϕ and w before proceeding with the discussion on the experimental results. The calculated H_d in calm water is shows in Fig.11. As long as ϕ is small the water surface on deck is a little higher than the freeboard (0.33m) and is almost constant regardless of w because the flooded water spreads over the whole deck. On the other hand when ϕ_0 becomes large H_d tends to vary widely according to w because flooded water concentrates at the side corner

of deck. So, when H_d keeps a certain positive value in waves after the ship heels, that inevitably leads to a large value of w and to a less stable condition.

Returning back to Fig.10, the black and single marks show low H_d values when GM_d is small because the ship heels to lee side and the flooding stops in a short time. As long as wave height is small H_d is also small like the circles in Fig.10. But in other cases in which water is coming in and out of the deck, H_d keeps a high values in a small range between 0.4 and 0.8m.

In Fig.10 high H_d values can be seen when freeboard is raised to 1.5m. So, the effect of freeboard was investigated by the two-dimensional model test and the result is shown in Fig.12. It is natural that H_d is almost the same as f_d when w_0 and ϕ_0 are small because of the reason mentioned above. But when w_0 and ϕ_0 increase, in that condition the flow in and out of water easily occurs, the difference of H_d by f_d reduces drastically. So the effect of freeboard on H_d is small in dangerous conditions as long as wave is high enough to make flooding on deck. This means that increasing freeboard height improves the safety of ship because it reduces the amount of water on deck.

The effect of wave height on H_d was also investigated by the two-dimensional model test. Only the results in dangerous conditions ($w_0/W > 5\%$, $\phi_0 < 5°$) are shown in Fig.13. The linear correlation seems to be clear. The conclusion of Vassalos[2] is that H_d is proportional to $H_w^{1.3}$ (H_w : significant wave height). The strong dependence of H_d upon wave height is the same as that, but this figure suggests that the power of wave height can be less than 1.3 in swells.

It can be concluded that if GM_d is very small and the ship heels to weather side by the effect of CC or cargo shift in high waves, the ship will be capsized by much flooded water on deck because H_d is kept constant in waves. It should be noted that the stability curves of the damaged condition in Fig.2 is calculated

under the assumption that $H_d=0$. This ordinary calculation underestimates the amount of water on deck and the loss of stability in waves.

6. RISK ESTIMATION FOR CAPSIZE

The figure whose ordinate is changed to H_d from Fig.9 is shown in Fig.14. It can be seen that when GM_d becomes greater the tendency of the equilibrium zones change from right side down to right side up. From Figs.14 and the idea sketch in the right, we can see the process of the change of ship condition in waves and can estimate the risk for capsizing.

When flooding occurs by the first wave the ship condition locates on the point of (ϕ, H_d) = (ϕ_i, f_d), where ϕ_i is the initial heel angle. If the ship heels H_d becomes small, but that encourages flooding. So the chain of "flooding", "increase of H_d", "heel (flow out of some water at the same time)", "decrease of H_d" and "flooding" will be repeated. In the dangerous condition, i.e. the wave is high and the ship has a CC or ϕ_i <0 (weather side), the point moves almost parallel to the right side, keeping H_d constant and increasing w. Even if f_d is a little higher than the range in the figure the point moves into it soon. Finally if the point comes across the equilibrium zone like a figure of GM_d = 2.44m in Fig.14, the movement of the point stops and the ship starts to roll around the stable condition. But if the zone is right side down like the top figure in Fig.14, there is nothing to stop the movement of the point and the ship will capsize with much water on deck.

So the risk for capsizing can be roughly estimated from the tendency of the equilibrium zones without knowing exact H_d value. In order to make the ship capsize-resistant it seems crucial to make the gz at big heel angles large enough to make the zone right side up. It can be concluded for this ship that the minimum required GM_d is
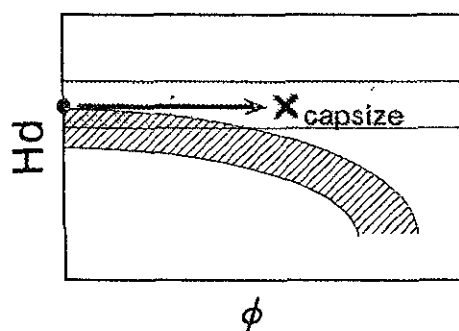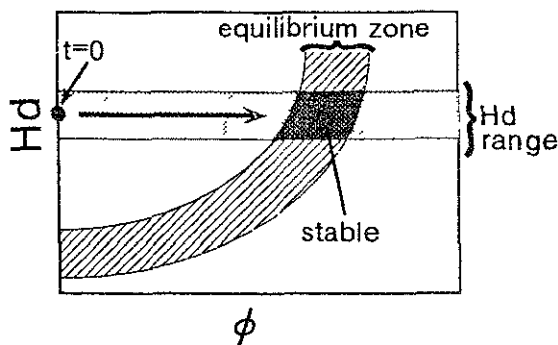
1.79m.

7. CONCLUSIONS

1) The effect of GM_d (GM in damaged condition) etc. on the mean heel angle and the mean water volume on deck in the stationary condition, ϕ_0 and w_0 respectively, is investigated. When GM_d gets larger w_0 also becomes larger, but the ship is stable with smaller ϕ_0 value. The tested ship did not capsize as long as SOLAS Regulation is satisfied.

2) When the ship heels to weather side she becomes unstable with much water on deck if GM_d is small. So cargo shift or existence of center casing might lead to a dangerous situation.

3) The test result in regular waves show that not only ship motion but also ϕ_0 and w_0 have some peaks near the resonant frequency of rolling, so the waves for stability test should include that wave component.

4) The water on deck keeps a higher mean

surface than sea surface as long as the damage opening of the deck is not made high by heeling to lee side. This difference of water surface, H_d, has a value in a small range in various conditions.

5) In dangerous conditions, i.e. the wave is not so low and the ship heels to weather side by CC and so on, H_d does not depend on freeboard height, but linearly depends on wave height.

6) In dangerous conditions, the ship transfers to less stable condition, repeating the chain of "flooding", "increase of H_d", "heel", "decrease of H_d" and "flooding". Finally if the rolling energy overtake the dynamic stability she capsizes.

7) By calculating the equilibrium zone and drawing it on H_d-ϕ diagram the risk of capsize can be roughly estimated without knowing the exact value of H_d.

8. REFERENCES

1) Bird,H., Browne,R.P. : Damage Stability Model Experiments, Trans. of R.I.N.A., 1973

2) Vassalos,D. : Capsizal Resistance Prediction of a Damaged Ship in a Random Sea, Symp. on RO-RO Ships' Survivability, 1994

3) Velschou,S., Schindler,M. : RO-RO Passenger Ferry Damage Stability Studies - A Continuation of Model Tests for a Typical Ferry, Symp. on RO-RO Ships' Survivability, 1994

4) Dand,I.W. : Factors Affecting the Capsize of Damaged RO-RO Vessels in Waves, Symp. on RO-RO Ships' Survivability, 1994

5) Shimizu,N., Roby,K., Ikeda,Y. : An Experimental Study on Flooding into the Car Deck of a RORO Ferry through Damaged Bow Door, Journal of the Kansai Society of Naval Architects, Vol.225, 1996

6) Murashige,S., Aihara,K., Yamada,T. : Nonlinear Roll Motion of a Ship with Water-on-Deck in Regular Waves, Second Workshop on Stability and Operational Safety of Ships, 1996

7) The Joint Accident Investigation Commission of Estonia, Finland and Sweden : Part-Report Covering Technical Issues on the Capsizing on 28 September 1994 in the Baltic Sea of the RO-RO Passenger Vessel MV ESTONIA, 1995

8) Dand,I.W. : Hydrodynamic Aspects of the Sinking of the Ferry 'Herald of Free Enterprise', Trans. of R.I.N.A., 1988

9) Some Results of Model Test , IMO RORO/ISWG/1/3/5, 1995

10) Ishida,S., Murashige,S., Watanabe,I., Ogawa,Y., Fujiwara,T. : Damage Stability with Water on Deck of a RO-RO Passenger Ship in Waves, Second Workshop on Stability and Operational Safety of Ships, 1996

11) Murashige,S., Ishida,S., Watanabe,I., Ogawa,Y. : A Model Experiment for a Relation between Flooding of a Ro-Ro Deck and Ambient Waves, 66th General Meeting of Ship Research Institute, 1995 (in Japanese)

12) Watanabe,I. : Disaster of Ro-Ro Passenger Ship "Estonia" and Safety Measure in IMO, 66th General Meeting of Ship Research Institute, 1995 (in Japanese)

Table 1　Principal Particulars of 3D Model

	Ship		Model	
	Intact	Damaged	Intact	Damaged
Lpp (m)	101.0		4.3	
B (m)	16.0		0.681	
D (m)	5.7		0.236	
d (m)	4.37	5.22	0.186	0.222
W	3821 t		272.7 kg	
$GM_{(o)}$(m)	1.62	3.12	0.069	0.133
Tr (sec.)	9.40	8.43	1.94	1.74
f (m)	1.17	0.33	0.050	0.014

f : freeboard
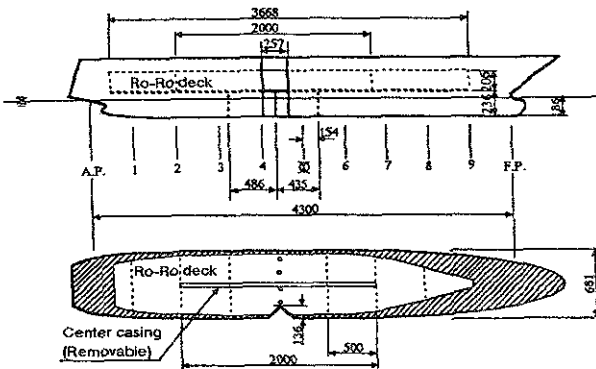
Fig.1　Model and Damage Opening (unit:mm, Broken lines and circles in the lower figure show water level meters and wave height gauges, respectively.)
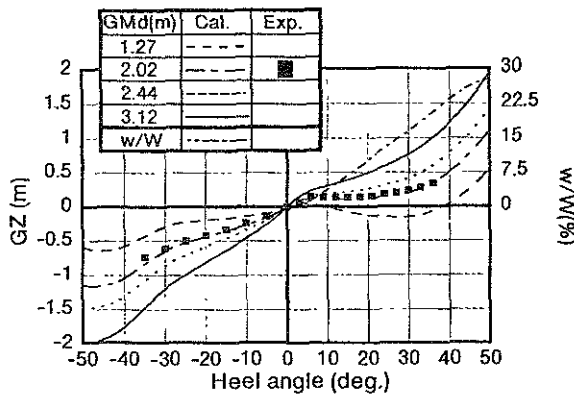
Fig.2　GZ Curves and Amount of Water on Deck in Damaged Condition
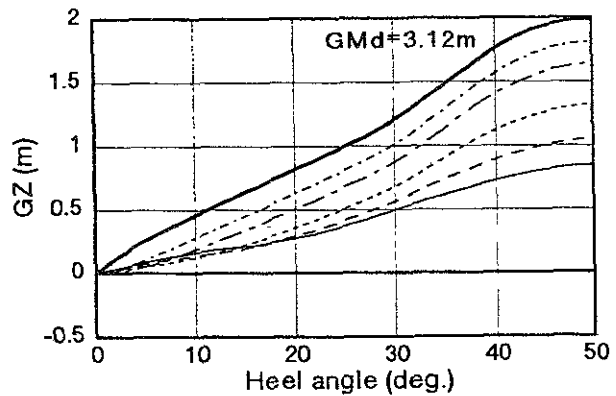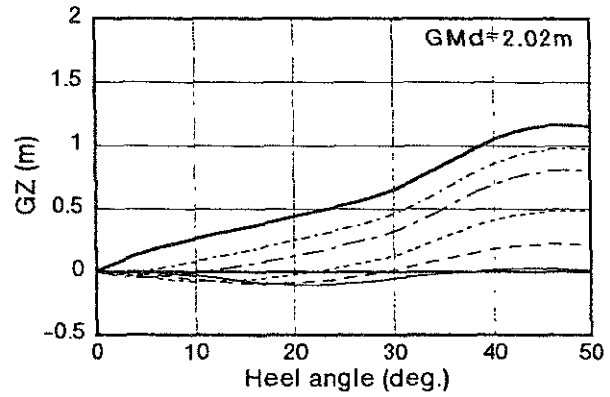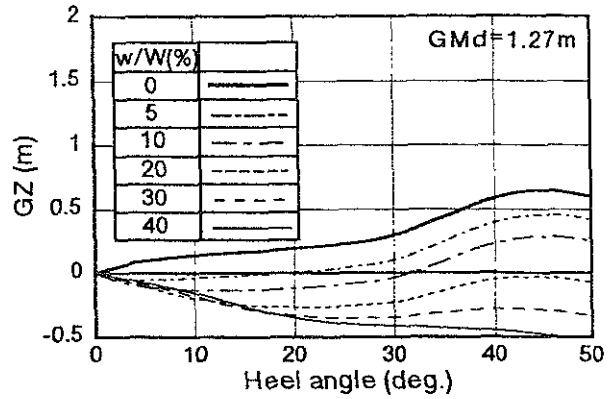
Fig.3　GZ Curves with Constant Amount of Water on Deck

14

Table 2　Principal Particulars of 2D Model

L (cm)	92.0
B (cm)	45.0
D (cm)	28.0
d (cm)	11.5
W (kg)	45.5
GM (cm)	4.7
Tr (sec)	1.54
f (cm)	2.5

f : freeboard
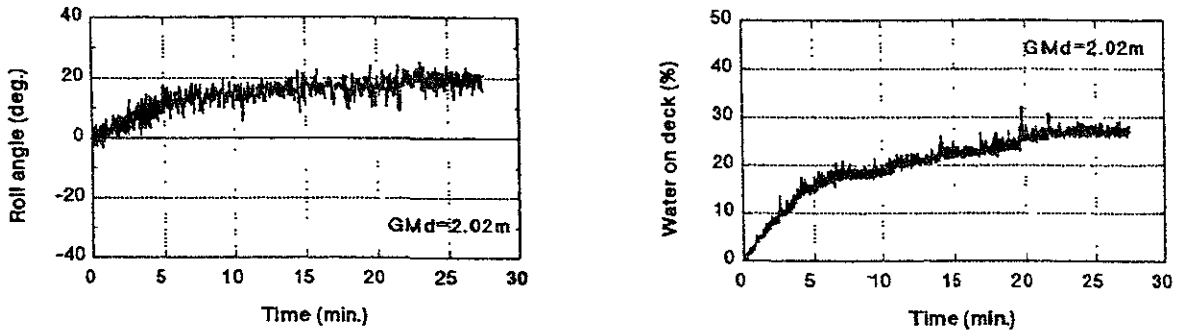
Fig.4　Time History of Roll Angle ϕ and Amount of Water on Deck w (No Center Casing)
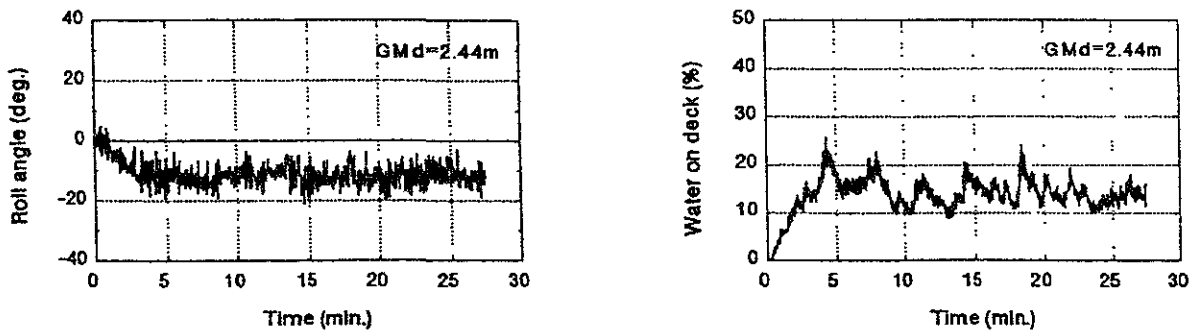
Fig.5　Time History of Roll Angle ϕ and Amount of Water on Deck w (With Center Casing)
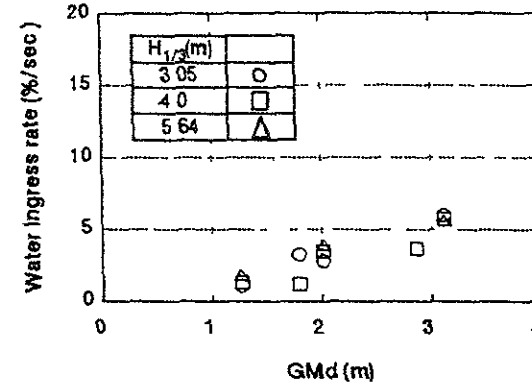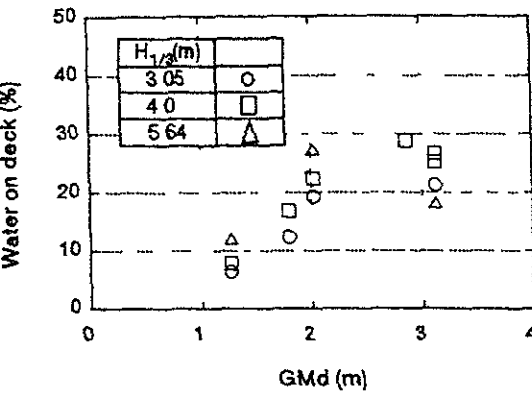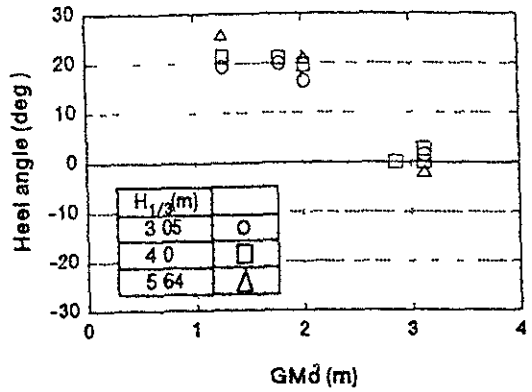
Fig.6 Experimental Results in Irregular Waves (No Center Casing)
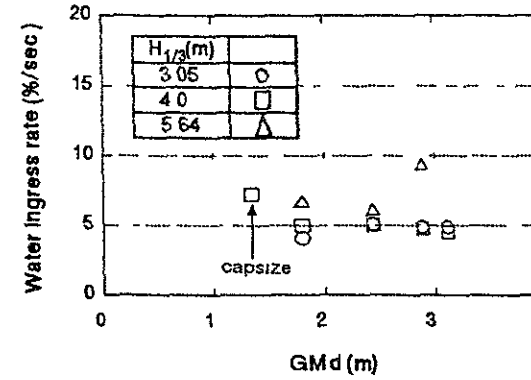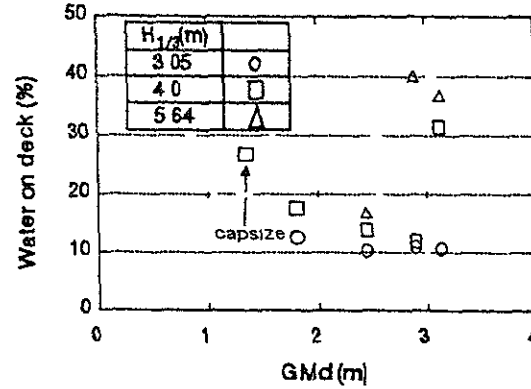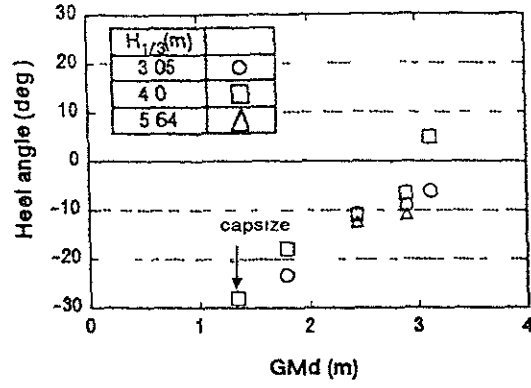
Fig.7 Experimental Results in Irregular Waves (With Center Casing)
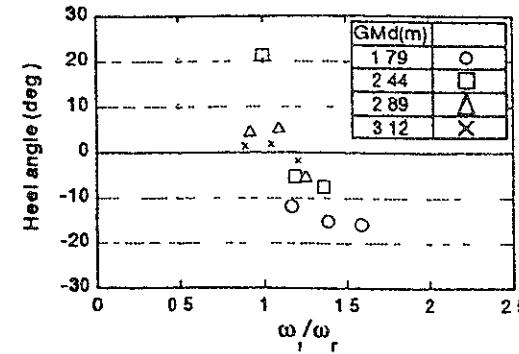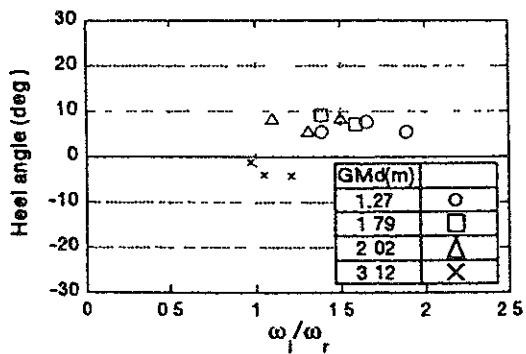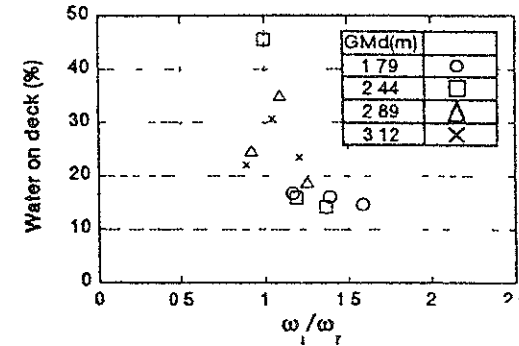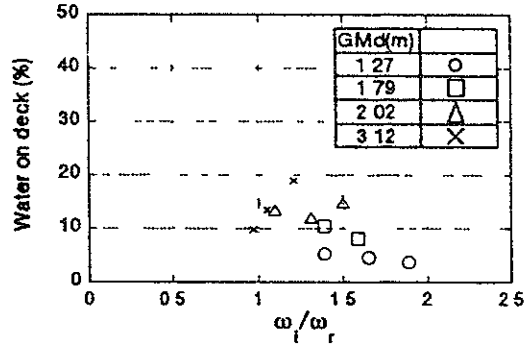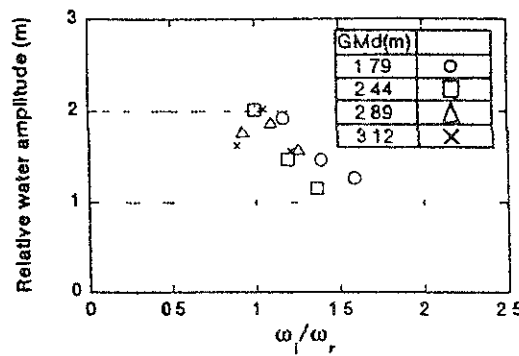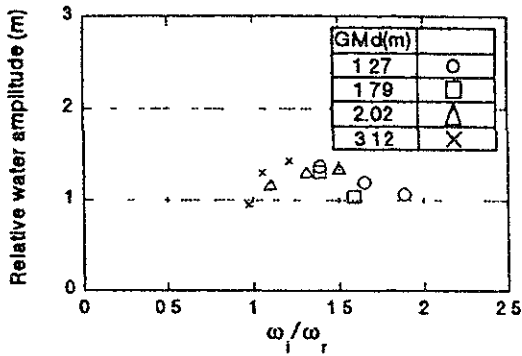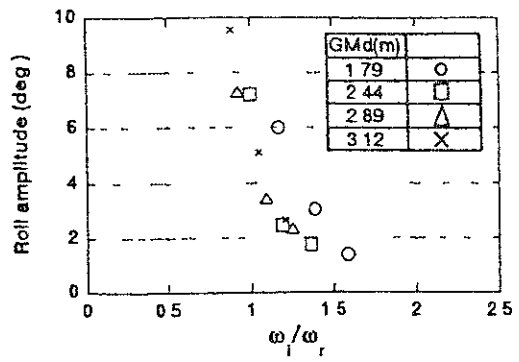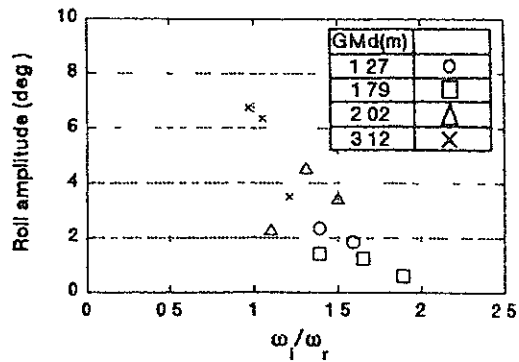
(a) No Center Casing

(b) With Center Casing

Fig.8 Frequency Responses in Regular Waves
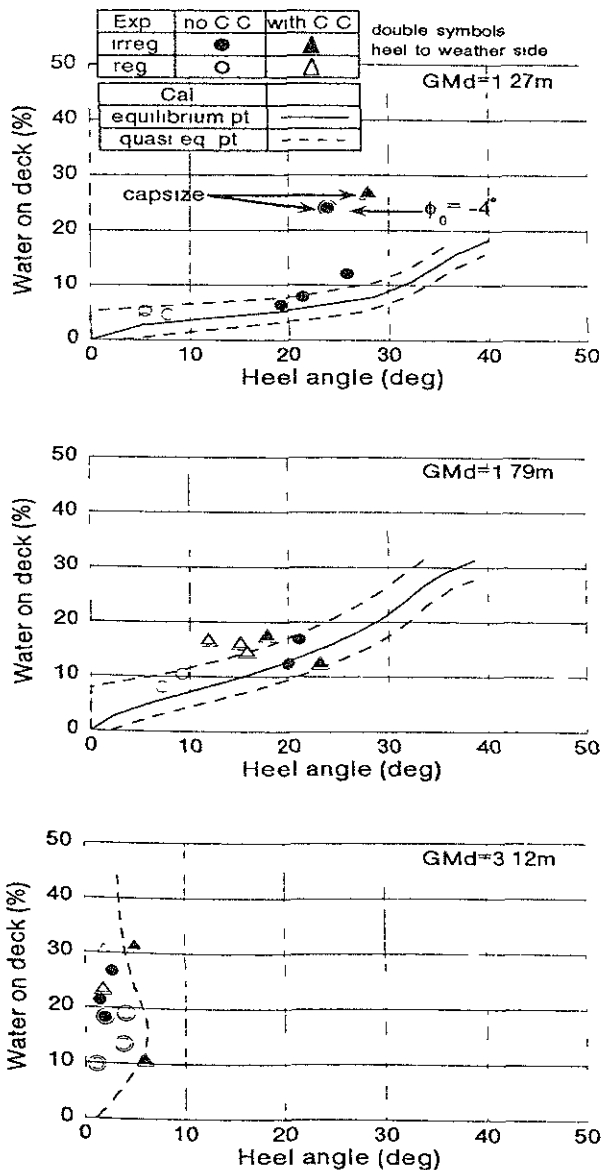
Fig.9 Amount of Water on Deck w_0 and Heel Angle ϕ_0 in Stationary Condition
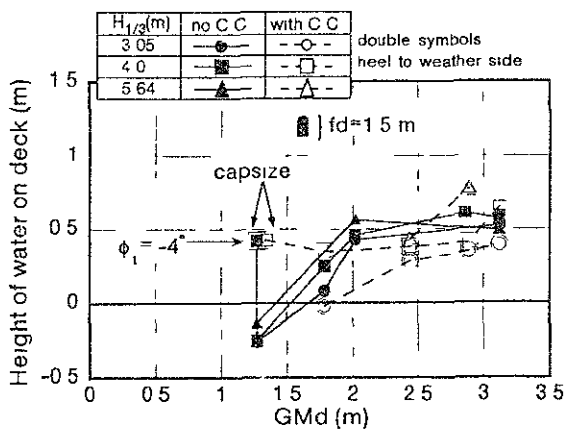
Fig.10 Height of Water on Deck H_d in Stationary Condition
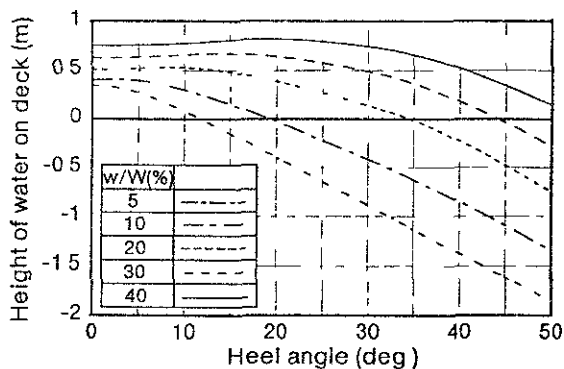
Fig.11 Height of Water on Deck H_d in Calm Water
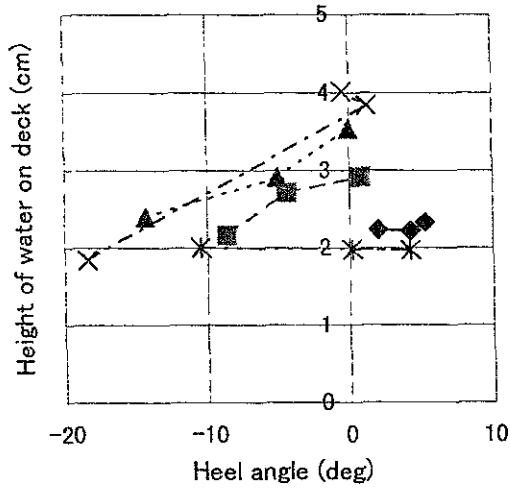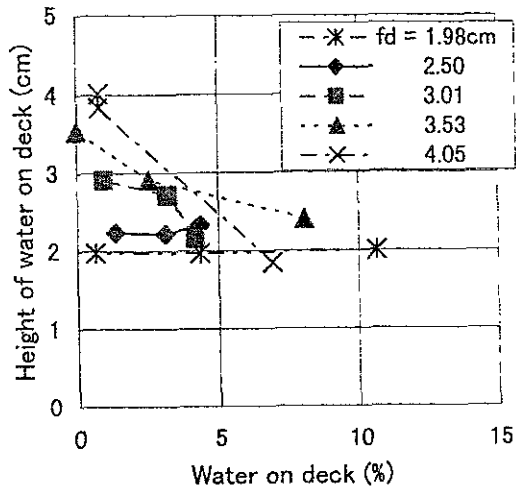
Fig.12 Effect of Freeboard on H_d
(2D Model, Model Scale)

Fig.13 Effect of Wave Height on H_d
(2D Model, Model Scale)
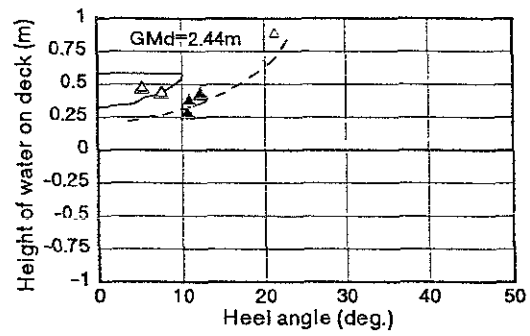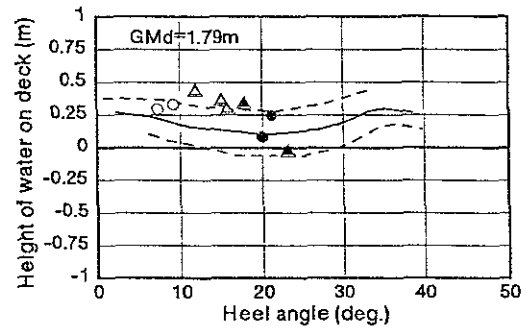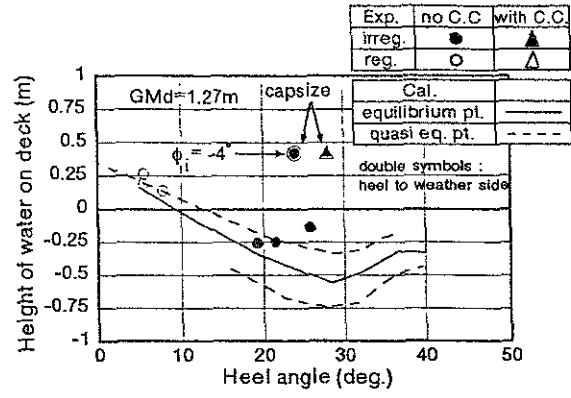
Fig.14 Height of Water on Deck H_d
and Heel Angle ϕ_0 in Stationary
Condition

110

OPERATIONAL STABILITY -
THE INFLUENCE
OF ENVIRONMENT

OPERATIONAL STABILITY PREDICTION AND ASSESSMENT FOR A SERIES OF 20000 TDW BULGARIAN BULKCARRIERS, BASED ON FULL SCALE TRIALS

V. Rakitin, R. Kishev, *Bulgarian Ship Hydrodynamics Centre*, Varna, **BULGARIA**

ABSTRACT

Inadequate operational stability and seakeeping behaviour was reported by the crews of the newly built series of 19000-20000 tdw bulk carriers. To check the situation and to draw measures for improving ship behaviour, full scale trials were undertaken along with accompanying calculations for alternative constructional decisions as well as loading schemes.

The ships operated along Black Sea - Mediterranean routes loaded one way only, thus ballast as well as full load conditions were thoroughly examined. Environmental conditions, ship motions and related effects, as well as main engine characteristics were measured continuously. In addition, ship stability and seakeeping had been calculated in details and permissible operational regimes were evaluated. Good coincidence was generally observed between calculated and measured reactions.

Recommendations were drawn for possible constructive measures to be undertaken in combination with changes in the loading scheme, to highten the natural roll period and to lessen the metacentric height, improving thus overal seakeeping performance.

NOMENCLATURE

B   Ship breadth
D   Weight displacement
g   Acceleration of gravity
GM   Metacentric height
H   Hull depth
h_W Observed wave height
H_S Significant wave height
L   Ship length

T_A Draft aft
T_F Draft fore
T_M Draft amidship
T_W Wave period
T_Φ Natural roll period
V_S Speed of advance
V_W Wind speed
Z_{max} Maximum heave amplitude
μ Heading angle
η Relative cargo density
λ_W Observed wave lenght
θ_{max} Maximum roll amplitude

1. INTRODUCTION

The series of four 19000-20000 TDW bulkcarriers feature a relatively shallow draft and large loading capacity, which results in too high initial stability. The ships can enter shallow water areas, which enlarges client interesses.

The ship's principal dimensions are as follows:
$$L = 159.0 \text{ m}$$
$$B = 25.0 \text{ m}$$
$$H = 11.5 \text{ m}$$
$$T = 8.0 - 8.2 \text{ m}$$
$$D = 25860 - 26650 \text{ t}$$

The general motives for launching wide full scale oservations were:

a) Sharp rolling with large amplitudes (up to 25-27 deg), observed on the leading (type) ship at BF 5 sea severity still at the acceptance trials in ballast condition;

b) Constantly observed large rolling amplitudes (up to 35-37 deg) in full load when anchored at still low sea states.

15

Continuous observations were implemented on the firs two ships of the series during their regular operation both in full load and ballast condition. After extensive type ship trials and on the basys of parallel numerical investigation, bilge keels were designed and mounted on next ships in the series, the second one being tested along the same route and following the same experimental program.

2. SEA TRIALS PROGRAM

The volume of full scale observations was compiled and further realized with an idea of collecting as much information about realistic ship behaviour as possible. It contained:

Loading - full load and ballast:

load	ship#	D	T_F	T_M	T_A
FL	1	26650	8.12	8.14	8.17
	2	26204	8.02	8.06	8.10
B	1	14258	3.50	4.55	5.60
	2	14845	3.08	4.64	6.20

Stability information according to the booklet:

load	ship #	GM	T_Φ
FL	1	4.10	9.30
	2	3.75	9.63
B	1	5.60	8.46
	2	5.36	9.23

Speed / revolutions:
Observations were accomplished both at anchorage or underway with a speed of:

load	ship #	V_S	RPM
FL	1	10.6-12.3	151
	2	9.0-12.5	140
B	1	7.5-12.2	150
	2	11.0	125

Headings - all headings encountered on route were distributed within 5 sectors, namely $\mu = 0$, 45, 90, 135, 180 deg;

Sea severity - Most measurements were performed in the water areas of Black Sea,

Ionian and Tyrrhenian Sea. The wave parameters were evaluated visually as well as by weather stations reports. Encountered waves were classified by Beaufort scale and ranged from Bf 3 to Bf 7, at corresponding wind speed of 3 -25 m/s;

Registration - successive 20 min portions at constant heading, speed and wave intensity;

Measured values:
    Roll motion;
    Pitch motion;
    Vertical motion;
    Vertical accelerations;
    RPM and speed of advance;
    Deck wetness and bottom slamming statistics (number per 20 min).

3. RESULTS OF OPERATIONAL STABILITY PREDICTIONS AND MEASUREMENTS

Major attention during the trials was paid to the reliable roll motions measurements and overal assessment of rolling as well as of the effectiveness of bilge keels mounted on the Ship #2. Natural roll period was repeatedly measured, as considerable difference was reported between the actual values and those calculated in the Stability Information Booklet. The measured natural roll periods ammounted to:

load	ship #	T_M [m]	T_Φ [sec]
FL	1	8.17	8.60
	2	8.06	9.14
B	1	4.55	8.80
	2	4.64	8.55

At full load condition, the difference between designed and actually measured periods causes an increase of 15% in initial stability and shifts roll resonance to lower sea states. At ballast, on the contrary, this discrepance acts positively, leading to slight lowering of GM, but the resonance remains still at low sea states, because of the high initial stability.

114

The ships become sensitive in roll mode after $H_s = 1.5$ m (Bf 3), but the roll motion amplitudes remain minor and do not depend considerably on heading angle Sharp increase in roll amplitudes was observed, although, in waves having average period close to the natural roll period, and those were waves most frequently encountered on the route, ranging in height from 2.5 to 5-6 m The maximum detected roll amplitudes were as follows:

load	ship #	θ_{MAX}
FL	1	27 5
	2	16 5
B	1	26.0
	2	14 0

Sample diagram of roll motion amplitudes observed during the trials is shown in Fig. 1.

The performed spectral analysis showed that the roll resonance zone (where spectral maximas of encountered waves and experienced roll overlap) is rather wide and covers practically all most frequent wave regimes To avoid this situation, speed and course changes have to be undertaken aiming at change of the wave encounter period

To help the officer in charge in making decisions when drawing ship route, polar operational diagrams were constructed and their applicability, usefulness and conformity to the practice were examined during the trials The diagrams covered·
   - Excess vertical accelerations,
   - Excess deck wetness;
   - Excess lateral accelerations at the bridge,
   - Excess rolling,
   - Rolling resonance boudaries
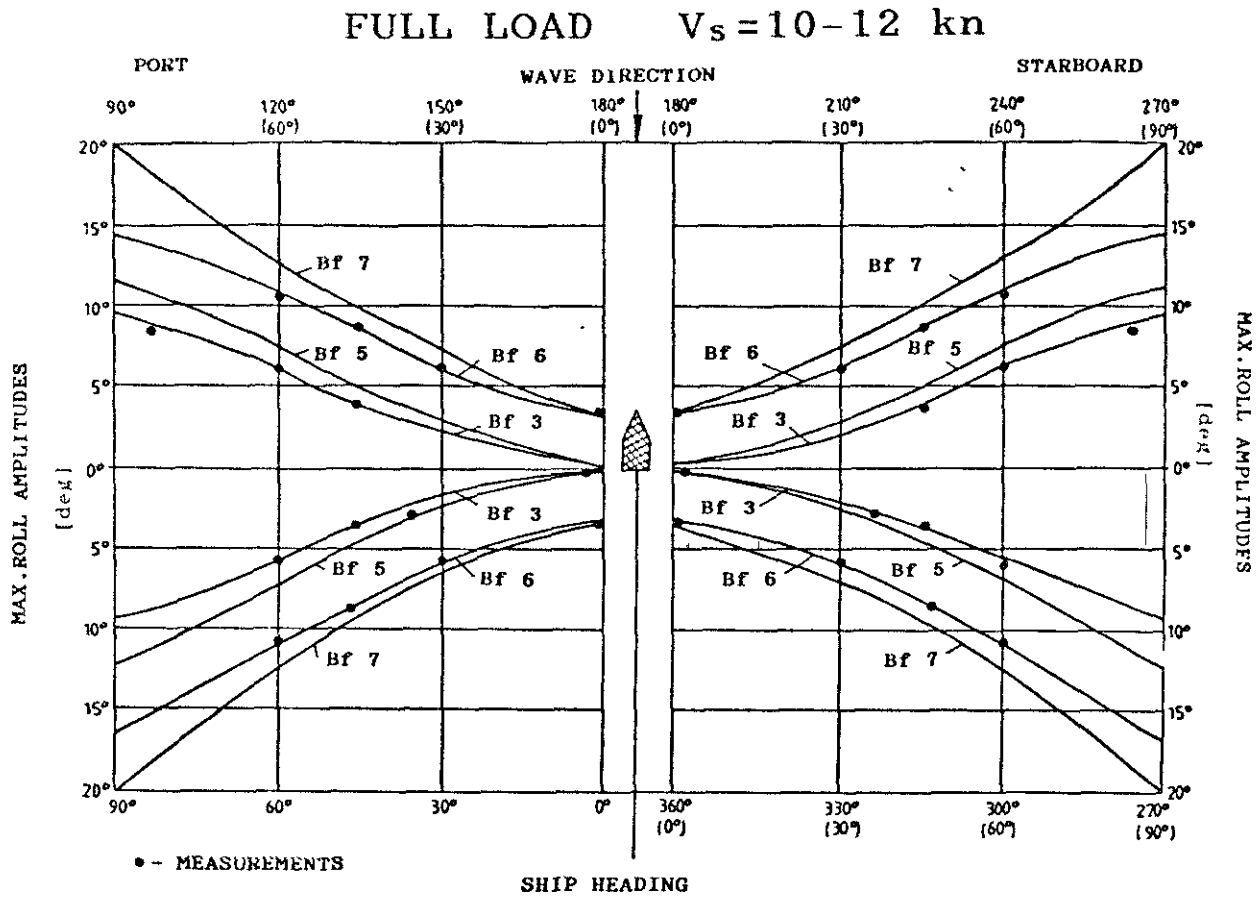
Fif. 1 Diagram of observed roll motion amplitudes for the type ship

Fig 2 Roll motions polar diagrams
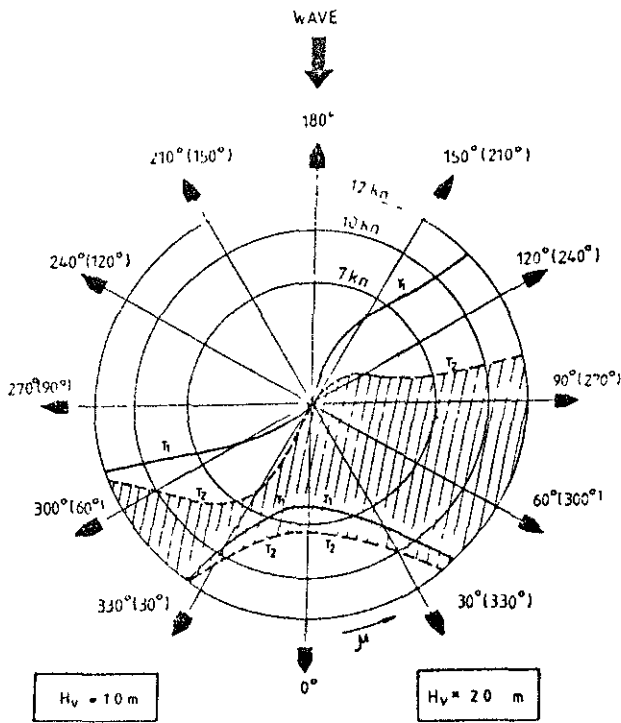
The practical utilization of the diagrams prooved the correctness of theoretical predictions concerning ship seakeeping and powering in waves, thus these were recommended to the personnel in command as a guide in selecting ship operational regimes. Similar diagrams were built to illustrate the influence of natural roll period on overal ship behaviour. As seen in Fig. 2, increasing the period T_1 by 1 sec to T_2 will lead to significant narrowing of the roll resonance zone.

4. ANALYSIS OF POSSIBLE APPROACHES FOR IMPROVING SHIP BEHAVIOUR

On the grounds of implemented full scale obser-vations and serial estimations of ship behaviour, following measures for improving her opera-tional stability were recommended and analysed:

4.1 Installation of bilge keels

Although not directly . influencing initial stability, installation of bilge keels is a common measure for lessening roll motion amplitudes and consequently improve operational stability. In practice, almost all ships having C_B < 0.79 have bilge keels. At larger fullness coeffic. nts, due to the great added mass moment of inertia, the bilge keels contribution becomes small, which makes its effectiveness low Increasing keel dimensions is of no big help, because of geometry restrictions and keel influence on resistance.

For ships under consideration, despite their fullness and large cylindrical part, bilge keels were designed by customer request and on the basis of model tests. The predicted decrease of roll amplitudes was estimated about 20%

Bilge keels effectiveness was evaluated during full scale trials by comarative analysis of roll motion characteristics of the two ships, as shown in Fig 3. The experimental results

116
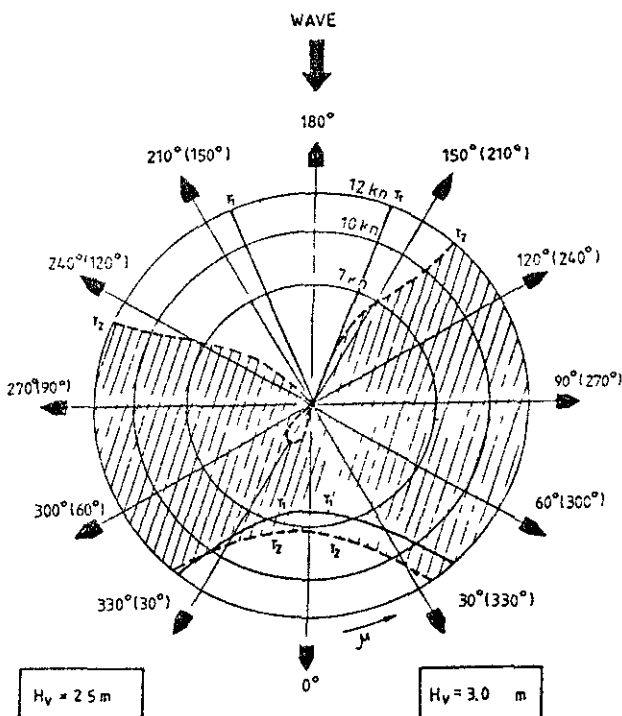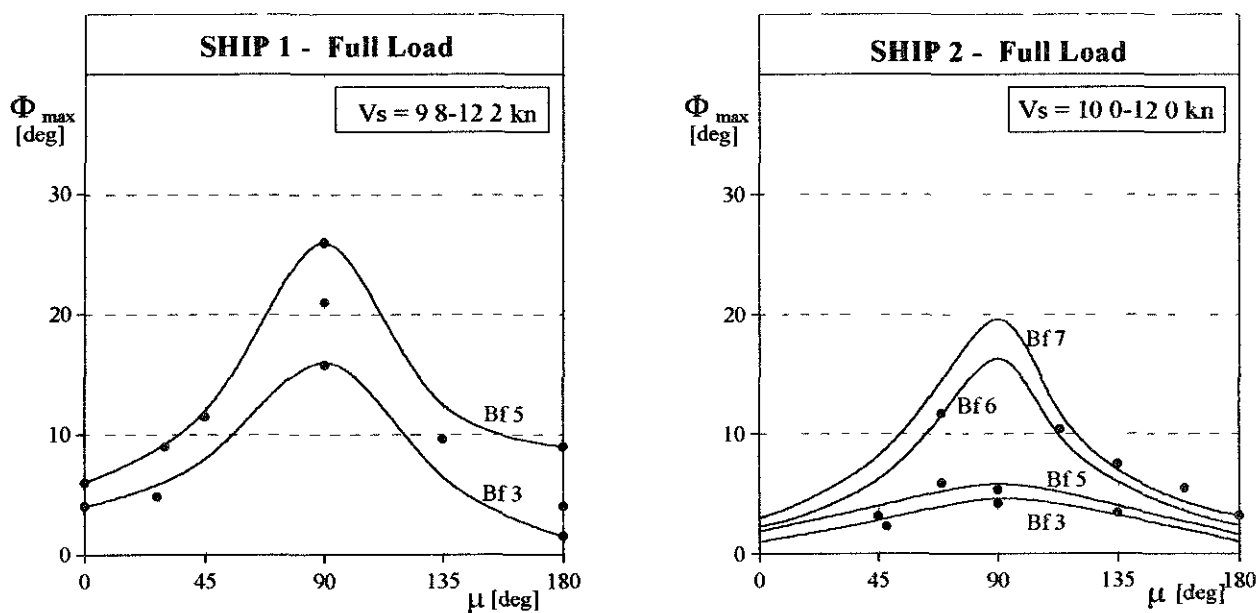
Fig. 3 Influence of bilge keels on roll motion magnitudes

confirmed preliminary estimations of approximately 30% decrease in resonance roll amplitudes of the second ship as compared to these of the first ship without keels, at similar sailing conditions. At the same time, natural roll period changed with 0.5 sec and resistance increase due to bilge keels causing speed loss of 0.1 kn was observed, which is quite acceptable.

4.2 Utilization of free surfaces

Free surfaces are in principle harmful for ship stability, but in this case they were considered as a mean for lessening the excessive metacentric height.

Control measurements were performed in ballast condition, letting free surfaces in different tanks. The resulting decrease in GM were, as follows:

- free surfaces in underdeck tanks (one port, one starboard) - Δ GM = 0.12 m;
- free surfaces in one of the bottom ballast tanks - Δ GM = 0.14 m.

The relatively small decrease in GM is due to the particular celular hull construction, which parts free surface area. Consequently, roll motion is only slightly affected.

Eventual application of this measure will be effective only at ballast condition, but will need a decrease of total quantity of ballast water up to 600 - 800 t, which will make trimming difficult. Accepting 800 t ballast when in full load will cause loss of loading capacity, at even smaller effect on initial stability.

4.3 Passive stabilizing tank

Strange as it might look on board a bulkcarrier, installation of small anti-rolling tanks was proved to be quite effective In case of arranging it around the deck height, a tank with 150 t mass total will highten the natural period up to 10.5 - 11.0 sec, thus shifting resonance zone consi-derably away. Two possible constructional decisions were suggested:

- Installation of rectangular FLUM type tank on the main deck, utilizing the free space between hatches;
- Transforming a couple of symmetrical underdeck tanks intended originally for washing water into a FRAM type passive tank.

Final decision has to be taken after detailed considerations as well as model tests.

117

4.4 Influence of relative density of cargo

Characteristic cases of loading as listed in Ship Stability Information Booklet include carrying bulk with different specific weight (relative density ranging from $\eta = 0.3$ to 1.43 m^3/t). The Booklet however was found to give sometimes misleading information about the relative density influence on GM and consequently on ship behaviour. On the ground of these observations, the characteristic loading cases were reanalysed using standard evaluation procedures. Natural roll periods were estimated by the formulae recommended by IMO Resolution A.562(14).
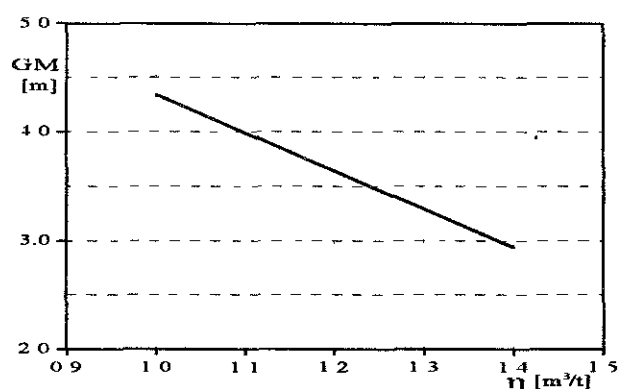
Fig. 4 Influence of specific weight of cargo on the metacentric height
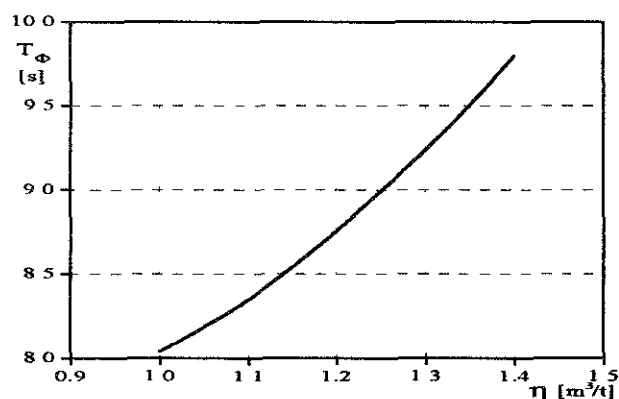
Fig. 5 Influence of specific weight of cargo on the natural roll period

In Figs. 4 and 5, the estimated influence of cargo relative density on GM and on the natural roll priod is illustrated. It is well seen, that actually this influence is quite signifficant and could be used as an instrument for improving ship behaviour, by switching the freight to light loads.

5. CONCLUSIONS AND RECOMMENDATIONS

The problems arising at the regular operation of the type ship of the series are mainly connected with the specificity of her geometry. The relatively short, rather wide and low-board hull predetermines the excess initial ship stability and consequently - the relatively low natural roll periods. At such conditions, even if the capsizing is practically impossible, the rolling is sharp, the ship gets easily into resonance and roll amplitudes increase rapidly even at moderate seas of Bf 5, which has negative influence on the crew and cargo.

Numerous constructive as well as operational measures could be recommended, aiming at improvement of the ship behaviour. Due to their economical indenture, their acceptance is a matter of client decision. As most relevant, following suggestions have to be considered, in order of practical realization ability:

a) Bilge keels installation on all ships of the series (this has been already accepted and realized by the customer);
b) Transformation of two side washing-water tanks into a passive anti-rolling tank;
c) Ship specialization for carrying light loads with a relative dencity over 1.0 m^3/t, to keep the CG high;

Selection of operational regimes has to be coordinated with the operational diagrams. Minding the intended installation of an onboard computer for navigational purposes, computerising of operational diagrams with further linking with bridge instrumentation to form an automated control system could be also recommended.

REFERENCES

Rakitin V., Kishev R. et al. - Full Scale Observations on Board Two 19000 - 20000 TDW Bulk-carrier Sisterships - IMAM'93, Varna, 1993

Explanation to a Large Roll Motion Phenomenon
in Irregular Waves

Jianbo Hua

Div. of Naval Architecture, Dept. of Vehicle Engineering
Royal Institute of Technology, S-100 44 Stockholm, Sweden

Abstract

A kind large roll motion problem is highlighted by showing the roll motion characteristics of a patrol ship in both regular and irregular waves calculated using a linear strip theory. This kind roll motion is a direct resonance problem and can take place only in irregular quartering to beam sea, i.e. the relative course angle (the ship course in relation to the wave direction) between about 50 to 80 degrees dependent upon the ship natural roll frequency.

A wave energy focusing mechanism is explained to cause this large magnitude roll motion. which can be dangerous to lead to capsizing. The necessary condition for the problem can be easily determined, which is related to the load condition in term of metacentre height, the ship speed, the wave condition and the relative course angle.

1. Introduction

Roll motion of a ship in waves is one of the most concerned seakeeping problems, since large roll motion will cause comfort problem, work interruption and cargo damage onboard, besides of capsizing. Obviously, this problem is an important factor in the evaluation of safety at sea and ship function efficiency. Great amount research works have up to now been devoted to study this kind problem with the aim to understand and reduce the problem and its consequence. A large numbers of reports are available, and the references from /1/ to /23/ is the result from a brief literature survey, covering basic roll motion mechanisms, experimental and theoretical determination of physical factors affecting the roll motion, mathematical modelling, probabilistic analysis and modern bifurcation chaotic description of strong nonlinear roll motion etc. Developments of anti-roll motion devices and capability analysis have also been an object of practical significance. Today, the ship roll motion theory is well established, and enable us make seakeeping analysis for different ship types so well qualitatively as quantitatively.

Since the beginning of this century, ships have become larger in size, higher in speed, and their hull form more unconventional. The consequence is that the roll motion characteristics becomes complex, and the risk increases for large roll motion. Unfortunately, a lot of capsize accidents have been reported, whereby loss of human life were often involved. Among others, large roll motion has been one of the most frequent factors behind these accidents. Thus, safety at sea has become an important issue for attention among the members in the ship building and sea transport branches.

For a naval architect, it is important to know the roll motion characteristics which the designed ship possesses. By using analysis tools it is possible to reduce the severity degree of roll problem by proper design modifications or by equipping anti-roll device, even though the resonance roll motion can never be eliminated. As known, the roll motion of a ship in waves is sensitive to its load condition, actual service speed, course angle and wave condition. The ship operator should therefore have good knowledge about the roll motion characteristics of his own ship, and could react by proper change of ship speed or/and course angle to manage his ship out of a dangerous situation.

In this paper, a large roll motion phenomenon will be highlighted from the result calculated based on a linear strip theory for patrol ship, and can be dangerous and lead to capsizing. Actually, this phenomenon was observed during a model measurement for a RoRo-ship according to /12/ and identified to be the most dangerous mode causing cargo shifting onboard. The phenomenon is here explained as the consequence of wave energy focusing. Later, the condition for this problem is discussed in terms of the relationship between the ship speed, load condition, ship course relatively to the wave propagating direction and wave conditions.

2. Presentation of the Large Roll motion Phenomenon

The extra-ordinary linear strip theory derived by Salvesen, Tuck and Faltinsen /19/ is applied here for the roll motion calculation. The modified P-M wave spectrum with significant wave height and zero-cross mean wave period as independent parameters is adopted for the description of long-crested irregular waves. The GZ-curve of the calculated ship is quite linearly proportional to the heel angle up to 40 degrees. That means that the linear approach for the calculation of restoring moment and the Froude-Krylov wave excitation moment is acceptable as far as the roll angle is below about 30 degrees. 10% of the critical roll damping is generally used in the calculation, which is a rough assumption. The roll damping can be here considered as an equivalent linear damping although the problem is nonlinear. Because the ship has a round hull form, the equivalent roll damping is fairly assumed for the roll angle up to 20 degrees. Since the hydrodynamic effect in term of radiation and diffraction wave is much less than the incident wave, the accuracy of the magnitude of roll motion at resonance is mainly governed by the accuracy of the roll damping and the Froude-Krylov wave excitation moment.

Actually, the roll motion of a ship in beam sea is most studied, because largest roll magnitude is expected in this situation. But it is not the case for all ships at all times. Here is an exceptional example. Fig.2.1 shows the significant roll angle of a ship in long-crested irregular waves of one meter wave height as function of relative

course angle for five zero-cross mean wave periods 3, 3.5, 4.0, 4.5 and 5 seconds. The main particulars of this example ship are shown in Tab.2.1.

Tab.2.1 Main particulars of the example ship

Length over all	50	m
Breath	7.2	m
Draught	2.1	m
Speed	16	knots
KG	3.3	m
GM	0.66	m

As seen in Fig.2.1, the maximal significant roll angle appears at the relative course angle of 70 degrees for all the zero-cross mean periods. Relative course angle of 90 degrees in the figure means beam sea, 60 degrees astern sea and 120 degrees bow sea. The maximal significant roll angle increases with decreasing zero-cross mean period, and can be up to about 22 degrees as the zero-cross mean period is 3 s. That is because shorter waves have greater wave slope. The roll motion magnitude decreases quickly down to between one third to the half of the maximum as the relative course angle changes with plus or minus 15 degrees.

Fig.2.2 gives the same result as in Fig.2.1 but in a contour plot, where contours of different significant roll angle levers viz. zero-cross and relative course angle are presented. The contour plot shows clearly that the high roll angles are very concentrated within the small variations of both relative course angle and zero-cross mean period.

As the load condition in term of KG-values (the vertical mass centre above the keel) changes from 3.3 m to 3.5 m, which means that the metacentre height GM decreases from 0.66 m to 0.46 m, the critical relative course angle moves down to about 67.5 degrees while the magnitude of the maximal significant roll angle increases for all the zero-cross mean periods, comparing Fig.2.3 with Fig.2.1. The critical relative course angle becomes 75 degrees for the KG of 3.0 m, see Fig.2.5 and Fig.2.6.

Fig.2.7 shows the significant roll angle as function of zero-cross mean period for different combination of GM-values and their corresponding critical course angle (CCA). As

seen, the problem is sensitive to the load condition in term of metacentre height. Large significant roll angles over 20 degrees for one significant wave height appear for different combinations of GM and Tz.

3. Explanation and Discussions

By considering the relationship between the encounter frequency and the natural roll frequency of the ship , it is not difficult to conclude that this kind large roll motion is a resonance problem. But the question remains why the roll motion magnitude is so large just at about the relative course angle of 70 degrees.

Fig.3.1 shows the roll transfer functions of the ship in regular waves for the different course angles of 60, 65, 70, 75 and 80 degrees. The ship speed is 16 knots and the metacentre height 0.66 m. The transfer function at 70 degrees course angle has very higher values over a wide frequency span in comparison with the others. Fig.3.2 shows the roll transfer function at the course angle of 70 degrees together with three wave energy spectra (scaled by a factor of 1000) for zero-cross mean periods 3, 3.5 and 4 s, and Fig.3.3 the roll transfer function together with the roll response operators for these three irregular waves. Fig.3.2 and Fig.3.3 show clearly that these three wave systems are effective to cause larger significant roll angle at the critical course angle.

It will be more convincing to explain the problem mechanism by showing the relationship between the encounter frequency ω_e and the wave frequencies ω for different relative course angle according to

$$\omega_e = \omega - \frac{\omega^2}{g} \cdot U \cdot \cos\beta \quad (3.1)$$

where U is forward speed and β relative course angle.

As seen in Fig.3.4, the wave frequencies between 1.5 to 2 rad/s have almost the same encounter frequency equal to the natural roll frequency 0.87 rad/s at the relative course angle of 70 degrees. The roll resonance will never tack place as the relative course angle is lower than 60-65 degrees. For the higher relative course angle, the number of waves in the wave

system causing roll resonance is limited. As shown in Fig.3.1, the roll transfer function at the relative course angle of 70 degrees has high values in the wave frequency interval between 1.5 to 2 rad/s. That means that all the waves within this frequency interval can cause roll resonance.

In addition, the wave excitation moments are much larger within the wave frequency interval between 1.5 to 2 rad/s than the ones at the lower wave frequencies. This is because that the wave lengths for the wave frequencies between 1.5 to 2 ad/s are 27.4 m to 15.4 , i.e. about 3.8 down to 2.1 time the ship breath. At a same wave amplitude, the wave slope across the beam becomes greater with shorter wave length, thereby the wave excitation moment on the roll motion increases with increasing wave frequency until the ratio of wave length to the ship beam approaches to about 2.6.

A condition to keep the wave excitation moment as great as possible is to have the unit-sign distribution of the wave excitation moment along the ship, i.e. $L_w \geq 2 \cdot L_{pp} \cdot \cos(CCA)$, where CCA is the critical course angle. For short waves, it requires CCA being closer to $\pi/2$.

As roll magnitude increases, the non-linear effects become larger. The roll damping increases with increases roll magnitude, which means that roll magnitude is overestimated when en roll magnitude exceeds more than 20 degrees at the roll damping of 10% of the critical roll damping. By considering the GZ-curve, the restoring moment decreases as the roll magnitude exceeds about 30 degrees. It is not possible to estimate the effect in a simply way. Therefore, further study should be carried out using time-domain simulation method in order to investigate the non-linear effects and risk for capsizing.

4. Conclusion

Conclusively, a large roll motion phenomenon is described and explained here as a consequence of wave energy focusing phenomenon. The problem can take place only as the load condition in term of metacentre height, ship speed, wave condition and relative course angle have a such relationship so that the most part of wave energy in an irregular wave

system becomes focused around the natural roll frequency of a ship. At the same time the corresponding wave components together have the maximal effect in term of wave excitation moment on the roll motion.

The linear strip theory applied here is not sufficiently to make satisfying quantitative estimation of the roll magnitude. 10% of the critical roll damping is generally used in the calculation, which is also a rough assumption. Despite of those, the previous presented result and analysis reveal an important roll motion phenomenon and the condition for this problem. In a severe sea the problem can lead to capsizing. If to predict the risk probability for capsizing, time domain simulation of nonlinear mathematical model describing the problem should be utilised.

As shows in Fig.2.7, it is possible to reduce the problem severity by increasing the value of the natural roll frequency, in an another word by increasing the metacentre height. For an example, an increase in metacentre height by 0.3 m will result in a reduction of the maximal significant roll angle with about 4-7 degrees in irregular waves of one meter significant wave height. But, work interruption and comfort ability onboard will at the same time become worse because the roll motion in beam and bow waves will generally increase.

If the problem is occurring to a ship in waves, a change in the ship course with about 10 degrees up or down will reduce the roll magnitude remarkable. Therefore, it is important to inform the ship operator about the problem and the possibility to avoid the problem. As a matter of fact, any ship with sufficiently high speed can be subjected to the problem with more or less probability, since a ship has various load conditions under her service life, and is subjected to various different wave conditions so that the early mentioned relationship can be fulfilled.

Reference

/1/ Blocki W. "Ship Safety in connection with Parametric Resonance of the Roll"
Intern. Shipbuilding Progress, Vol, 27, 1980.

/2/ Cardo A., et.al. "Ultraharmonics and Subharmonics in the Rolling Motion of a Ship: Steady-state Solution"
International Shipbuilding Progress, Vol 28, No.326, 1981

/3/ Féat G. and Jones D. "Parametric Excitation and the Stability of a Ship Subjected to a Steady Heeling Moment"
International Shipbuilding Progress, Vol 28, No.327, 1981

/4/ Féat G. et al. "Capsizing with Additional Heeling-Stochastic Criterion for Highly Nonlinear Roll Motion"
RINA 1984, Vol.126

/5/ Haddara M.R. "On the Parametric Excitation of Nonlinear Rolling Motion in Random Seas"
Intern. Shipbuilding Progress, Vol.27, No 315, Nov. 1980.

/6/ Himenon Y. "Prediction of Ship Roll Damping - state of the art"
The University of Michigan, College of Engineering, Rep. No. 239, September 1981.

/7/ Hua, J. " A Study of the Parametrically Excited Roll Motion of a RoRo-Ship in Following and Heading Waves "
International Shipbuilding Progress, 39, no.420 (1992) pp.345-366

/8/ Hua, J. and Rutgersson, O. "A Study of the Dynamic Stability of a RoRo-Ship in Waves"
STAB'94, Florida, 1994

/9/ Kan M., Saruta T. and Taguchi H., "Capsizing of a Ship in Quartering Waves"
J.S.N.A. Japan Vol.

/10/ Kan M., Saruta T. and Taguchi H. "Capsizing of a Ship in Quartering Waves"
(Part 5. Comparative Model Experiments on Machanism of Capsizing)
J.S.N.A. Japan Vol. 167, June 1990 and Vol.168. Dec. 1990

/11/ Kervin J.E. "Notes on Rolling in
Longitudinal Waves"
Intern. Shipbuilding Progress, Vol.2 No. 16,
1959.

/12/ Larsson, M. "Design Loads on Securing
Systems for Paper Reels"
Thesis for Master of Scince, Div. of Naval
Arch. Royal Institute of Technology,
Stockholm, 1997

/13/ Lindemann and Skomedal N. G.
"Parametric Excitation of Roll Motion and its
Influence on Stability"
Second International conference on Stability of
ships and Ocean Vechicles,Tokyo, Oct. 1982

/14/ NayfehA.H. et al. "Nonlinear Coupling
of Pitch and Roll Modes in Ship Motion"
Journal of Hydronautics, Vol. No. 4, 1973.

/15/ Nayfeh A.H. and Khdeir A.A., "Nonlinear
Rolling of Biased Ships in Regular Beam
Waves"
International Shipbuilding Progress, Vol 33,
No.381, 1986

/16/ Nayfeh A.H. and Khdeir A.A. "Nonlinear
Rolling of Biased Ships in Regular Beam
Waves"
International Shipbuilding Progress, Vol 33,
No.381, 1986

/17/ Nayfeh A.H. and Sanchez N.E.
"Stability and Complicated Rolling Responses
of Ships in Regular Beam Seas"
International Shipbuilding Progress, Vol.37,
No.410, 1990

/18/ Paulling J.R. and Rosenberg R.M.
"On Unstable Ship Motion Resulting from
Nonlinear Coupling"
Journal of Ship Research, Vol.3 No.1, 1959.

/19/ Salvsen N., Tuck E.O. andFaltinsen O.
"Ship Motions and Sea Loads "
Trans. Vol.78, SNAME, 1970

/20/ Sanchez N.E. and Nayfeh A.H.
"Nonlinear Rolling Motions of Ships in
Longitudinal Waves"
International Shipbuilding Progress, Vol.37,
No.411, 1990

/21/ STAB' 90 Fourth Internation Conference
on Stability of Ships and Ocean Vehicles
Sep. 24-28, 1990, Naples (Itaily)
/22/ Sjöholm U. and Kjellberg A.
"RoRo Ship Hull form:Stability and Seakeeping
Properties"
The Naval Architect, Jan. 1985.

/23/ Wright J.H. and Marshfield W.B.
"Ship Roll Response and Capsize Behaviour in
Beam Seas"
RINA 1980, Vol.122
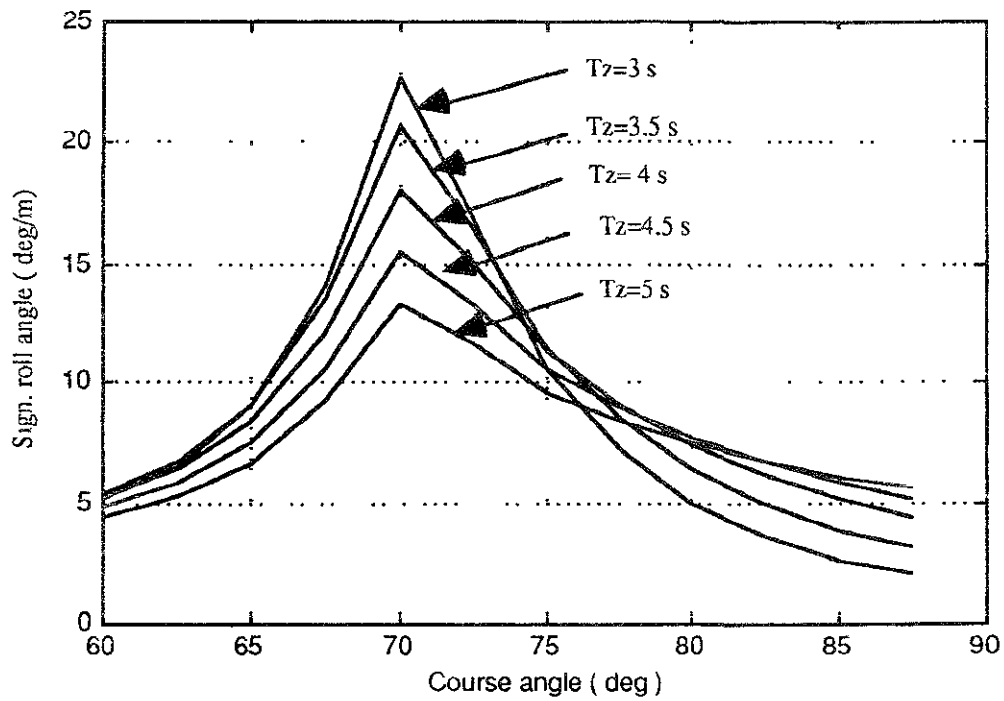
Fig.2.1   Significant roll angle per significant wave height as function
           of course angle for different zero-cross mean periods.
           KG is 3.3 m and speed 16 knots.
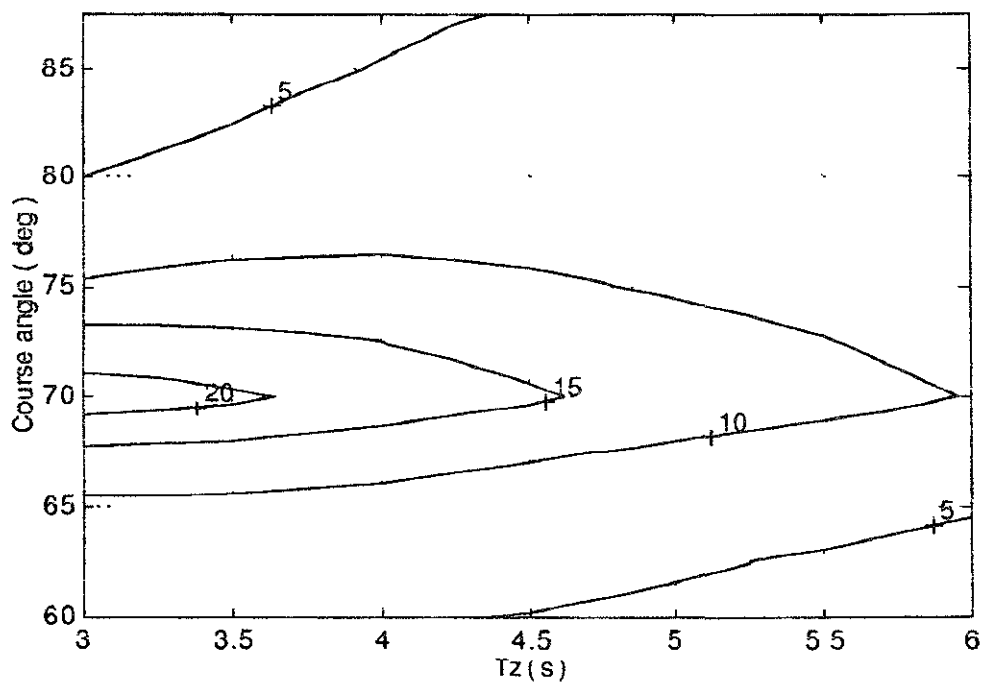
Fig.2.2   The contour plot of significant roll angle per significant
           wave height as function of course angle and zero-cross mean
           period. KG is 3.3 m and speed 16 knots.

124
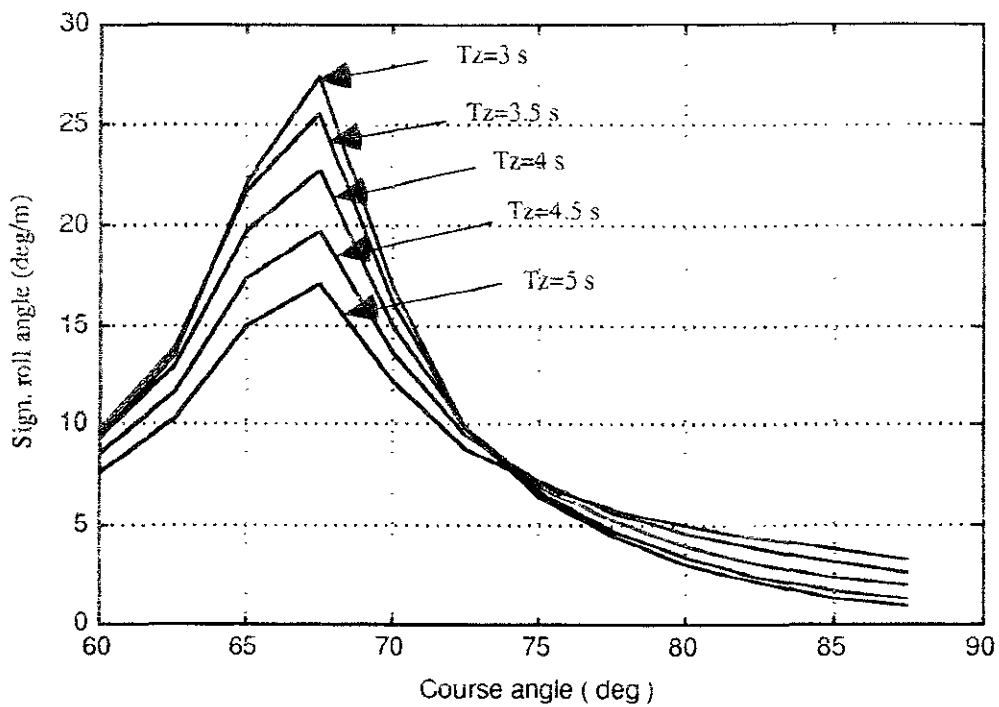
Fig.2.3   Significant roll angle per significant wave height as function
           of course angle for different zero-cross mean periods.
           KG is 3.5 m and speed 16 knots.
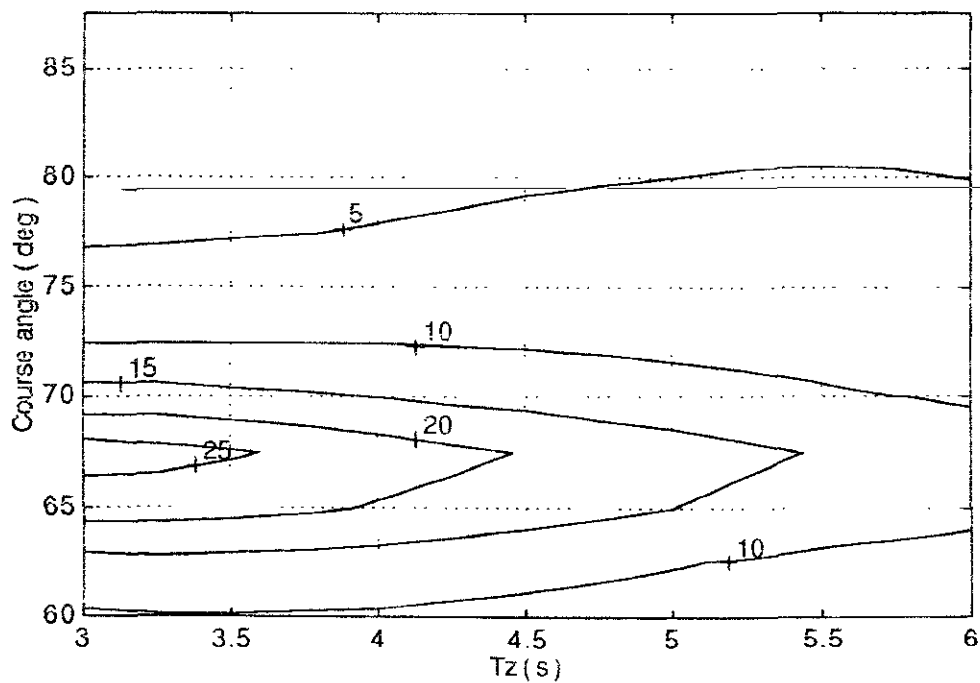
Fig.2.4   The contour plot of significant roll angle per significant
           wave height as function of course angle and zero-cross mean
           period. KG is 3.5 m and speed 16 knots.
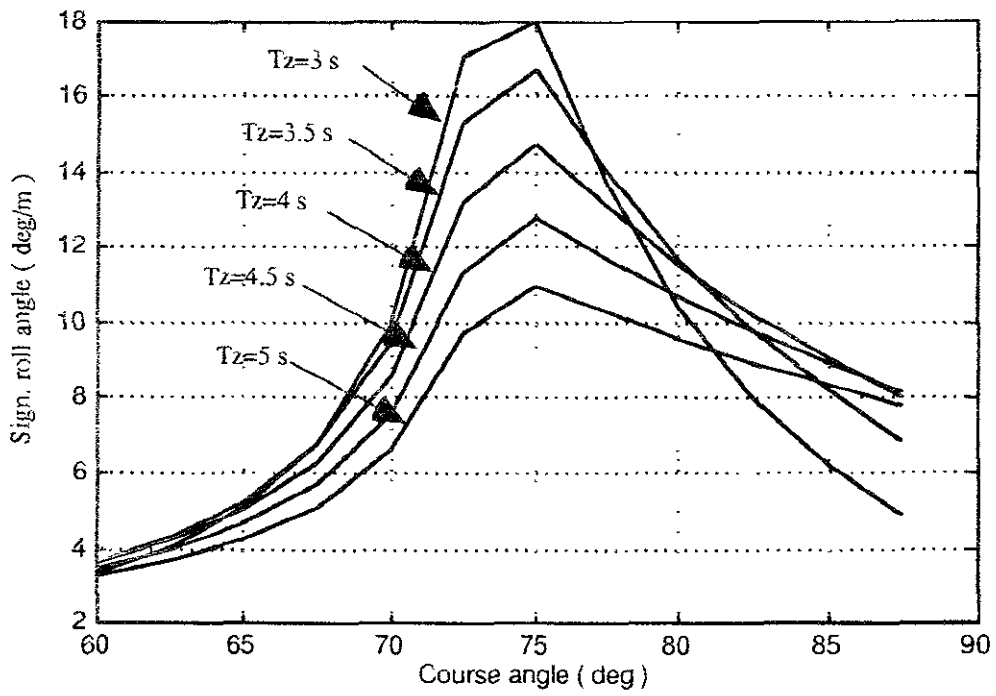
Fig.2.5   Significant roll angle per significant wave height as function
           of course angle for different zero-cross mean periods.
           KG is 3.0 m and speed 16 knots.
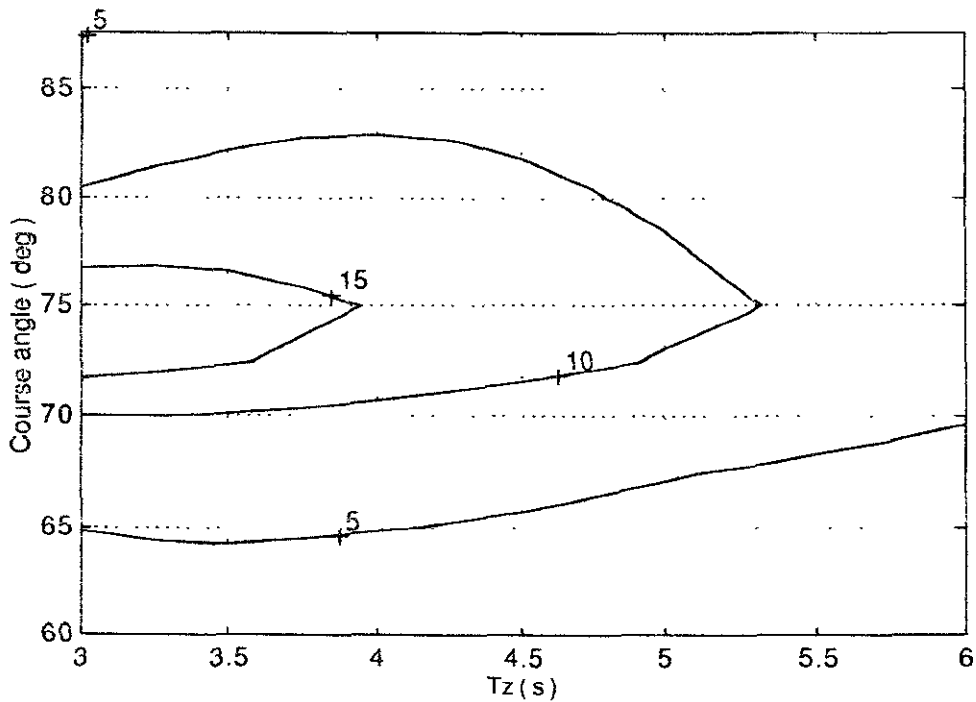
Fig.2.6   The contour plot of significant roll angle per significant
           wave height as function of course angle and zero-cross mean
           period. KG is 3.0 m and speed 16 knots.
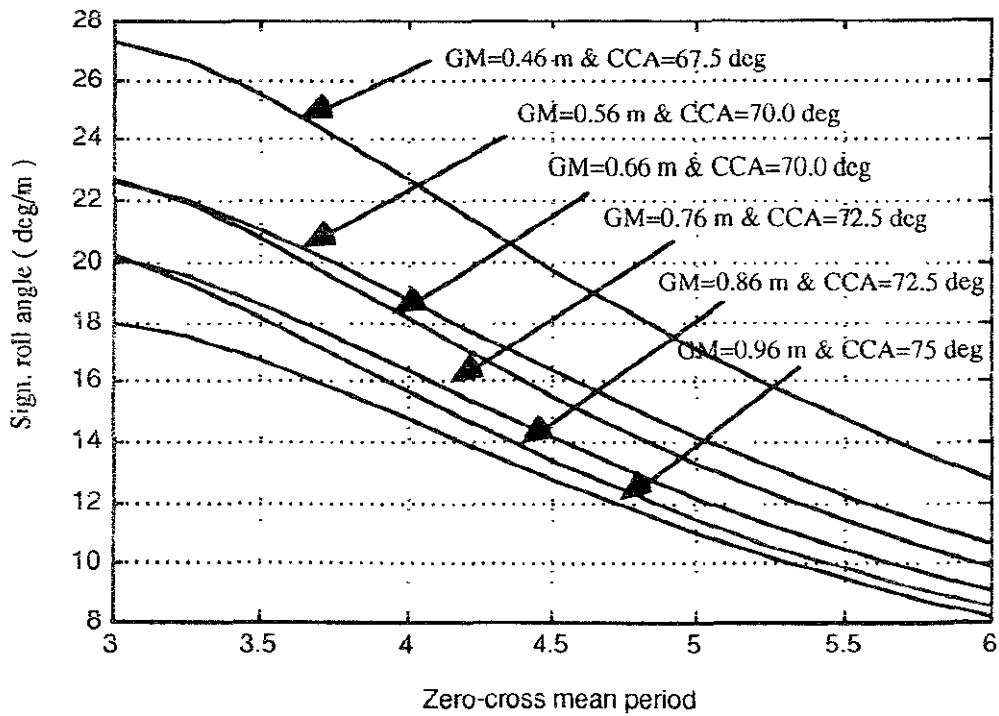
Fig.2.7   Significant roll angle as function of zero-cross mean period for different GM-values and their respective critical course angle (CCA).
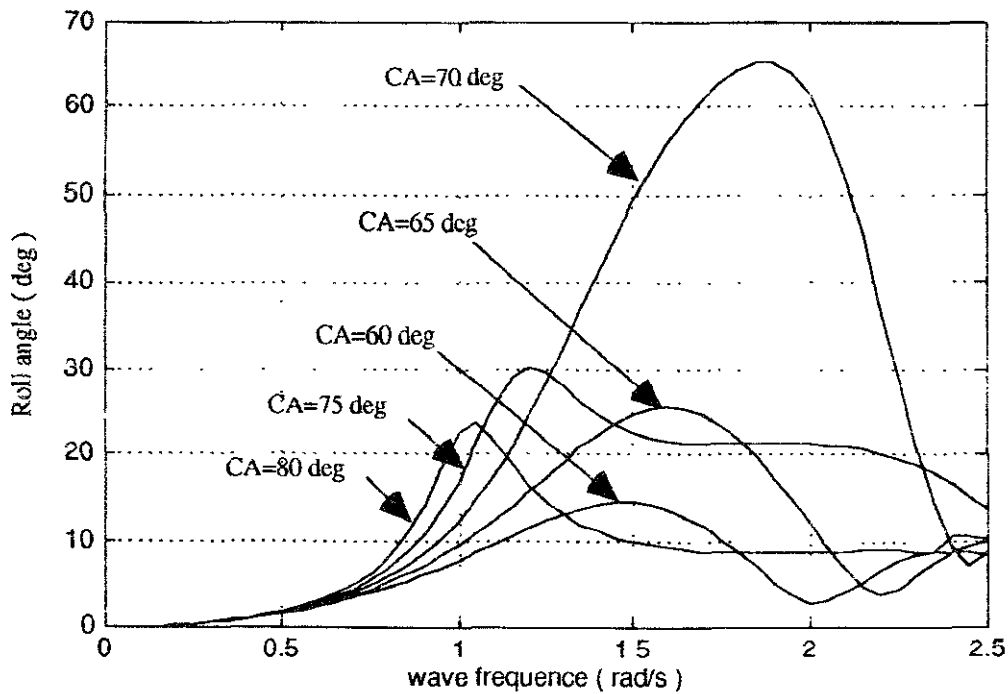
Fig.3.1   Roll transfer function at different course angles (CA). KG is 3.3 m and speed 16 knots.
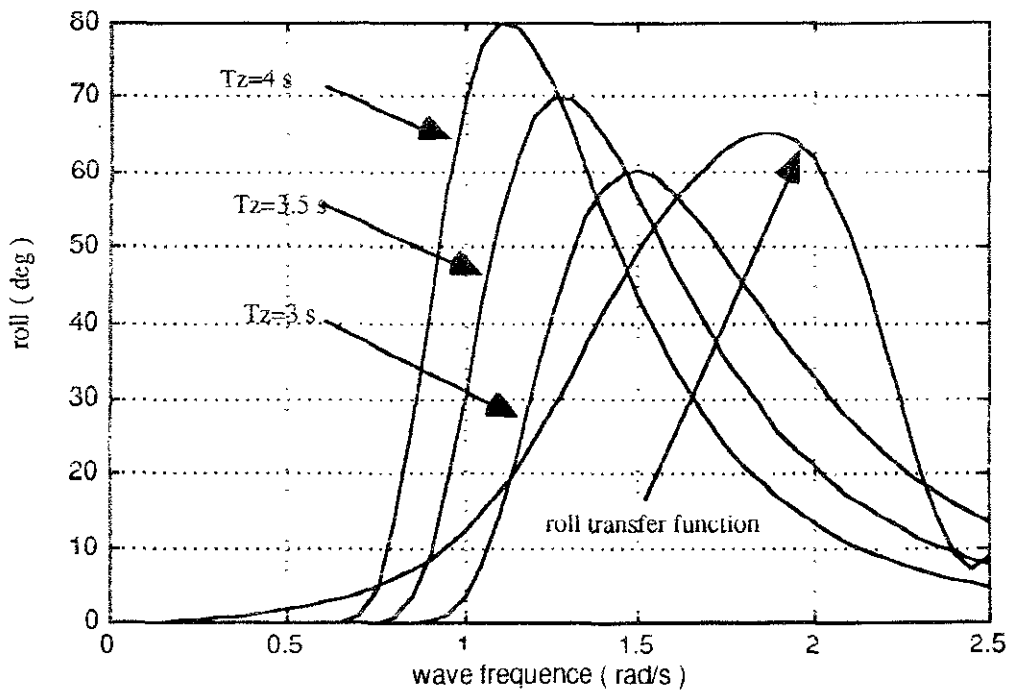
Fig.3.2 Roll transfer function at the course angle of 70 degrees in comparson with the three wave energy spectrum shapes with Tz 3, 3.5 and 4 s respectively. (the wave spectra are scaled by time 1000). The KG is 3.3 m and speed 16 knots.
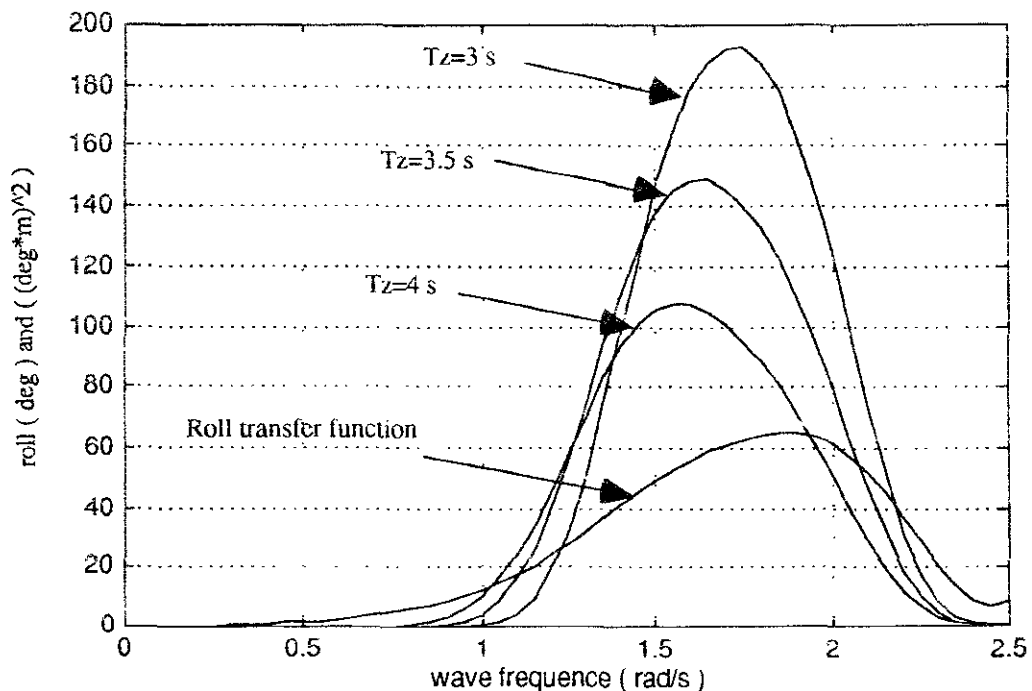
Fig.3.3 Roll transfer function at the course angle of 70 degrees in comparson with its response spetra with Tz 3, 3.5 and 4 s respectively. KG is 3.3 m and speed 16 knots.
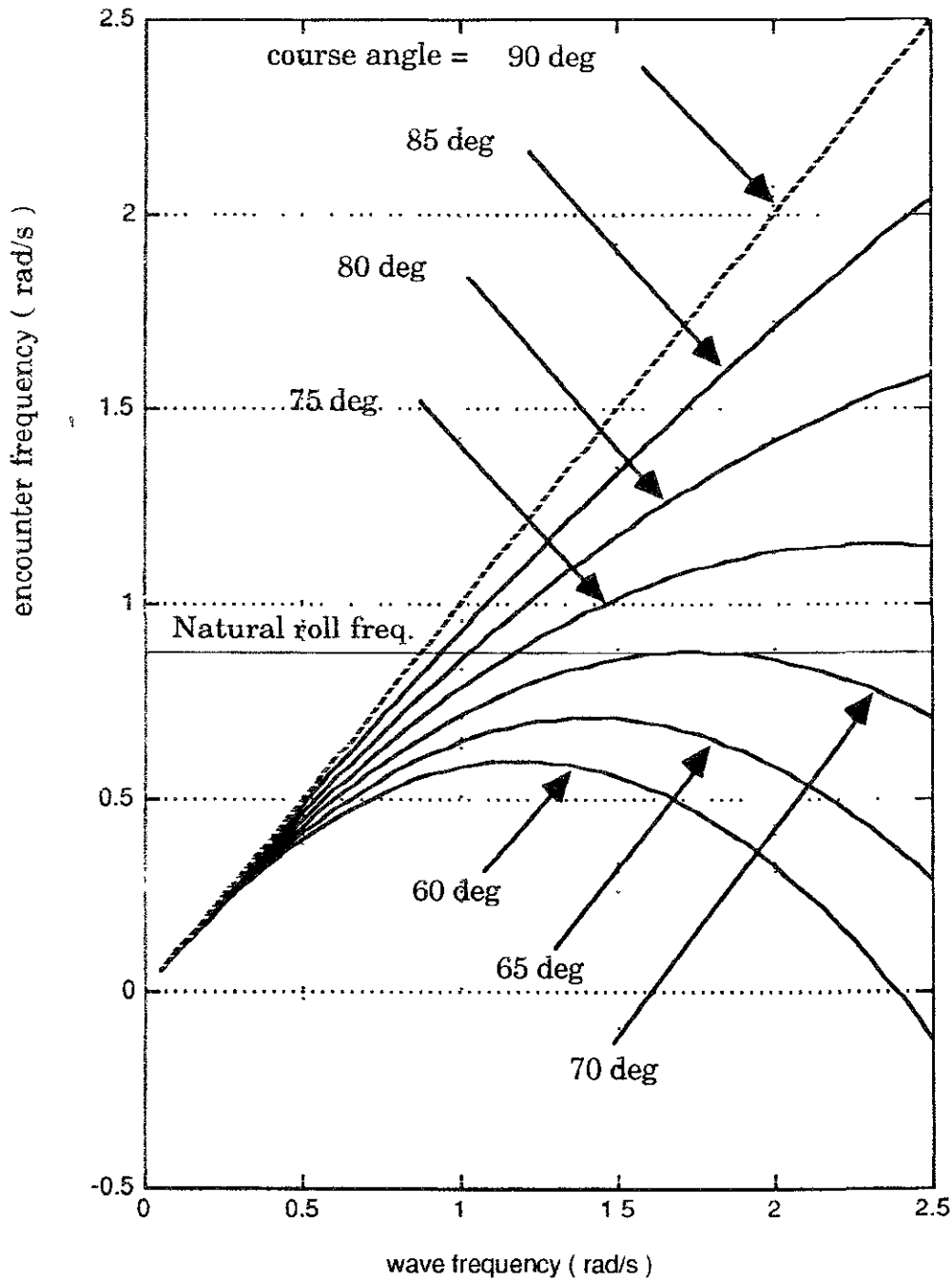
Fig.3.4   Encounter frequence as function of wave frquence for 16 knots ship speed and for different relative course angles.

OCCURRENCE OF WATER-ON-DECK FOR LARGE,

OPEN SHELTER-DECK FERRIES

S. Calisal [1] A Akinturk [1] G. Roddan [2], G. N. Stensgaard [2] ,

1 Dept. of Mech. Engineering, University of British Columbia Vancouver Canada
2 BCRI 3650 Wesbrook Mall Vancouver, B.C. Canada

NOMENCLATURE

f   : Freeboard
f_{mr} : Modified residual freeboard
$H_{1/3}$: Significant wave height
N_{dw} : Number of deck wetnessing observed
T_{ave} : Average wave period
$T_{1/3}$: Significant wave period
WL_{DB} : Dynamic waterline at bow

SUMMARY

The International Maritime Organization's (IMO) Panel of Experts (POE) suggested that all ferries fitted with bow doors should be designed to meet the SOLAS 90 stability requirements with a uniform one metre depth of water on deck. The proposed rule was an attempt to develop a regulation which will ensure that ro-ro vessels retain sufficient stability even in extreme incidents similar to the "Herald of Free Enterprise" and the "Estonia" accidents.

This design requirement was too severe for the design of local ferries operated in the Province of British Columbia   in sheltered waters. To provide some scientific data to the POE,   a model experimental study, to investigate the potential for bow-scooping on a typical Canadian west coast ferry, was done . The model study was backed up by parallel numerical studies.

The model of "Queen of New Westminster", a single-ended ferry with a bulbous bow was used for testing. The results for model tests and numerical   investigations   show   a   clear relationship between the occurrence of water on deck and the ratio of initial freeboard to significant wave height. In the range of sea conditions tested , no water on deck is observed when the bow freeboard is more than approximately two times the significant wave height.

The numerical calculations for this model suggests that for a given wave conditions and ship speed a minimum free board can be calculated and that this could be used as a design rule for ro-ro ships. Two design rules that can be used at an early preliminary design, using standard   ship motion programs, are proposed.

INTRODUCTION

During the development of proposed new rules for passenger ro-ro ships, the International Maritime Organization (IMO) Panel of Experts (POE) suggested that all ferries fitted with bow doors should be designed to meet the SOLAS 90 stability requirements when one cubic metre of water per square metre of deck area is scooped onto the deck through the bow door

131

opening. Such water on deck would have to be allowed for, from the bow to the first transverse bulkhead on the vehicle deck aft of the inner bow doors (collision bulkhead position). This proposed rule is an attempt to develop a regulation which will ensure that ro-ro vessels will remain safe even if damaged and in sea conditions similar to those which resulted in the capsizing/sinking of the "Herald of Free Enterprise" and the "Estonia".

will While it is conceded that this approach may well be valid for European-style ro-ro passenger ferries operating in exposed waters, it is seen by many Canadian operators and Coast Guard officials as too severe for typical Canadian west coast ferries. West coast ferries are fitted with bow doors, but they are "closed shelter deck" vessels with non-watertight enclosures around their vehicle decks. By contrast, European ferries typically have watertight enclosures around their car decks. B.C. ferries also differ from their European counterparts in that they sail in sheltered waters in which sea state is fetch limited.

Under the proposed regulations, the stability penalty for west-coast-style Canadian ferries will be even more severe than for the European-style ferries due to the fact that Canadian ships operating in less severe conditions will not be fitted with subdivision within the car deck (flood control doors), while subdivision will be required on the European ferries. The lack of flood control doors means that the bow-scooping water, 1 meter in depth, would theoretically extend from bow to stern of Canadian-style ships.

Thirty years of operating experience has not given any indication that bow-scooping is a potential hazard for Canadian west coast ferries. However, in order to provide some scientific data to the IMO-POE it was decided to undertake a model experimental program to investigate the potential for bow scooping on a typical Canadian west coast ferry. These tests were carried out at BCRI Ocean Engineering

Centre for the British Columbia Ferry Corporation and Canadian Coast Guard, Ship Safety.

DESCRIPTION OF EXPERIMENTAL STUDY

A 1:30 scale model of the "Queen of New Westminster" was used in this preliminary research program. The choice of model for the tests was based on a number of considerations. the model already existed, it was modified to suit the needs of the present series of tests, and it was a good example of a large, open shelter deck ferry. A photograph of the model is given in Figure 1.

To accurately reproduce the dynamics of water on deck the existing open model was decked over and fitted with main car-deck sides and with representations of the centreline casings. The car deck sides were modeled complete with accurately-scaled freeing ports located according to as-fitted drawings of the "Queen of New Westminster". As it is believed that parked vehicles may be a significant factor affecting the flow of water on the deck of a ferry, a number of hobby-type model cars and trucks (1:32 scale) were mounted on the forward end of the car deck. The bow doors were left off for all test runs.

Table 1 : Table of Configurations

Config.	Displ. (Tonnes)	Draft (m)	Trim (deg)	Freeboard at Bow (m)	Condition
A1	5,950	4.25	0.00	2.50	Max load level trim
A2	5,940	4.25	0.21 by bow	2.40	Min Bow Freeboard
B1	5,450	4 00	0.00	2 75	Light load

The model was tested in three configurations as described in Table 1 above.

WAVE ENVIRONMENT

The choice of the wave environment to test the model, was based on sea-states which could be encountered by an open shelter-deck ferry in the Straits of Georgia. A good source of information was found in the unpublished manuscript by D. A. Faulkner [2]. The data suggest that the 90 percent wave height probability level is about a 0.7 metre significant wave height; that is 90 percent of the time, sea states in Georgia Strait have a significant wave height of 0.70 metres or less. Based on this figure, it was decided to test the model in sea states with significant wave heights of 0.75 m, 1.0 and 2.0 m. While the probability of occurrence of the 2.0 m. wave is relatively low, it is the most likely wave height to result in significant water on deck. In order to cover the range of observed average wave periods, 4, 6 and 8 seconds average wave periods were used in the experiments.

The 8 second wave is uncommon, but not unheard of in the Strait of Georgia. This wave is considered important because at that period, the wavelength is 100.0 m, which approaches the 123.0 m waterline length of the "Queen of New Westminster". This makes the 8 second waves most likely to induce a significant pitch motion in head sea conditions.

It is also known that the highest seas occurred during the winter months. These waves run in a northwesterly or southeasterly direction, consistent with the prevailing wind directions and with maximum fetch up and down the Strait. These wave directions result in head or following seas for the ferries. This experimental study concentrated only on the head sea test condition, although a few exploratory runs in following seas were performed.

The following test matrix of sea conditions was developed to provide a representative sampling of significant conditions in which the ferry might be expected to operate:

Table 2 : Test Sea Conditions

$H_{1/3}$ (m)	$T_{1/3}$ (sec)
0.75	4, 6, 8
1.00	4, 6, 8
2.00	6, 8

Each irregular sea state was generated in the model basin by a paddle-type computer controlled wave-maker. The target wave spectra were developed from the two-parameter Pierson-Moscowitz spectrum based on significant wave height and period.

INSTRUMENTATION and TEST PROCEDURES

The incident waves were measured using a stationary capacitance-type wave probe. A capacitance wave probe was also mounted on the bow of the model to measure relative wave height. A sonic wave probe was used to monitor depth of water on-deck just abaft the bow doors. All speeds were monitored using an optical encoder transducer mounted to the towing carriage. Data was acquired by means of the "ASYSTANT" data acquisition software system, using a "Data Translation" I/O board. All data were sampled at 25 samples per second per data channel. This sample rate provides adequate time resolution of the incoming waves.

The model was towed free-to-trim and free-to-heave, but was restrained in roll, yaw and surge. The towing force was applied horizontally through a pivot located amidships. Speed, relative wave height, and water on deck were recorded for each run. Video of the model

motion and the occurrence of water on deck were also taken of each run.

Before beginning each experimental run, the wave-maker was allowed to run for a period of time sufficient for waves to travel the full length of the tank. This ensured that all major components of the wave spectrum were present in the tank during each test run. In this way, a fully-developed wave spectrum could be assured. At this time, the data acquisition process was started and the carriage was then accelerated up to speed. At the end of the run, data acquisition was terminated prior to carriage deceleration. Video was taken of the bow region for each run. This process was repeated for the entire wave matrix at speeds of 12, 15 and 18 knots.

EXPERIMENTAL RESULTS AND ANALYSIS

ANALYSIS OF DATA

A general review of the data revealed that significant deck-wetting occurred mostly when the full scale speed is about 18 knots . For this reason, the data was analyzed in detail for the 18 knot speed only. From the plot of depth of water on deck from the sonic probe, ten to twelve occurrences of waves coming over the bow were measured (Figure 2). The time period for each run at 18 knots is about two minutes full scale.

MRF = (Static Freeboard) - (Dynamic Waterline @ Bow + 0.5 Significant Wave Height)

<div align="right">Eqn 1</div>

Through the study of time-based plots of relative wave height and depth of water on deck, it was deduced that as the wave crests increases to the level of the deck, water on deck can be expected This result was formalized by defining a quantity which was

termed "modified residual freeboard" or "MRF" (Eqn 1, see also Figure 3).

Dynamic water line is obtained as the average of the measured wave height. With this definition the modified residual freeboard is positive if the significant wave crests are below the deck level, and negative if they are above deck level.

Tables 3, 4 and 5 present the results of an analysis of selected runs, reduced to the non-dimensionalized ratio "Modified Residual Freeboard/ Sig. Wave Ht." for the three configurations all tested at 18 knots. In addition the tables contain the visually observed number of occurrences of deck wetting events over the length of the run, which can be used as an index or rating of the degree of water-on-deck problem.

Figure 4 is a plot of the modified residual freeboard versus static freeboard, both ·non-dimensionalized by the significant wave height for the ferry running in head seas at 18 knots .The data from Tables 3, 4 and 5 indicate that substantial amounts of water can be expected on deck when the MRF is small or negative. A linear regression through the data indicates that a nominal freeboard at bow/ significant wave height ratio of 2.0 consistently yields a positive value for the MRF. Thus, based on the limited data available, it appears that the nondimensional ratio of (freeboard at the bow/ significant wave height) may be used as an easily-applied predictor of when waves are likely to come over the bow, and hence whether bow-scooping potential is present.

It was also observed that when water begins to come over the bow, it has a tendency to collect in the forward car deck area where there are only small deck scuppers, and no freeing ports Water thus accumulates on deck, the residual freeboard at the bow is reduced due to weight of water, and deck wetness increases. If this process continues unchecked, it may ultimately lead to disaster. While no detailed experimental measurements of depth of water on deck were

<div align="center">134</div>

made, the bow-scooping events, when they did occur, appeared to result in significant quantities of water-on-deck (perhaps more than 1 metre). Initially, water accumulation was localized to the foreward end of the car deck, resulting in trim by-the head. Trim-by-the-head aggravates bow-scooping tendencies, resulting in a potentially catastrophic feed-back loop once the dynamic bow-scooping process begins. These effects were observed despite the freeing port arrangement of the ship being accurately represented in the model. Indeed, once dynamic bow-scooping is initiated, the rate of flow onto the deck is far in excess of the freeing ports' discharge capacity, and deck flooding progresses rapidly

Based on the results from the Phase 1 "Queen of New Westminster" model experiments results of the 120-meter double-ended ferry, the provisional safe ratio of static Freeboard/Significant Wave Height remains at 2.5.

NUMERICAL STUDY

The experimental work as observed the researchers permits the following summary of the events leading to water accumulation on deck. As the model pitches and heaves in irregular head seas and when the average wave profile is below the deck level, the formation of a spray like water column was observed. In some cases larger amounts of water on deck were observed, resulting from a "scooping" action of the bow of the model. A picture of wave and spray formation around a bow in immersion is given in Figure 5 for another ship model (S175) tested in this tank [3]. This event had random characteristics, similar to the random characteristics of the sea state. A quasi-static analysis therefore can not predict the spray like formation or bow scooping. While the exact occurrence of the bow scooping is rather difficult the calculation of a minimum freeboard as a threshold value based on

statistical data seemed manageable. For the threshold of water on deck, one can expect to have the local relative motion of the wave and the model should be of the same order of magnitude as the freeboard at the bow Some experimental results could then be used to obtain this threshold value.

The observed dynamic and random characteristics of the water on deck formation suggest that.

a) The event is non-linear, ship motion and wave environment (significant wave height. significant period)

b) The event may have a threshold below which the deck water accumulation is insignificant.

c) The event is hull-form (flare, bow form) and wave-form (breaking wave) dependent

In this first series of tests, the researchers decided to attempt to identify the important physical variables responsible for the formation of water on deck, and search for a possible water-on-deck "threshold". If a threshold seemed to exist, then investigations could experimentally measure and establish such a limit. This parameter then could be tested extensively and might be identified as the major variable responsible for the accumulation of water on deck.

PROCEDURE

As all of the kinematic quantities were not measured during the initial experimental program, the following numerical procedure was adopted. A ship motion package (SHIPMO [4]) used was based on standard linear, strip-theory. Such programs are now easily available form various sources. The ship geometry was based on the body plan of the "Queen of New Westminster" Analytical predictions were run at three speeds, (12, 15, and 18 knots) corresponding to the model test speeds. The absolute motion (displacement, velocity, and

135

acceleration) in root-mean square (RMS) and relative motion characteristics in RMS for two stations (station zero and station one) were calculated for the test spectra. The experimentally-observed number of occurrences of water column and water on deck, which is termed 'deck wettings", were plotted against the calculated kinematic quantities.

RESULTS AND CONCLUSIONS OF THE NUMERICAL STUDY

As one would suspect, the formation of water build-up in the bow region and water column formation with resulting water on deck must depend on the combined relative motion between the wave and the ship. For this reason, the relative motion characteristics were examined by plotting them together with the appropriate experimental deck wettings. The plots of deck wettings versus absolute kinematic quantities in RMS for all speeds did not show any identifiable threshold for deck wetting. While the acceleration data suggested a threshold acceleration at 0.01g, the absolute displacement and velocity data did not show any significant trend.

Figure 6 to Figure 9 show the deck wettings versus the relative kinematic quantities. One can observe that a definite threshold exists for relative motion and relative speed. Figure 6 shows the number of deck wettings versus relative motion and relative speed at station zero for all tests speeds. For this ferry, running at the speeds considered, it seems that almost no water on deck is observable when the relative motion is less than 0.35 m RMS, and the relative speed is less than 0.6 meter/sec. RMS at station 0. At station 1 (Figure 7), the numbers are 0.4 m RMS for relative motion and 0.7 m/sec RMS for relative speed, which is somewhat higher than those for station 0. Study of Figure 8 and Figure 9 shows that as the speed increases the threshold relative motion

and relative speed decreases. That is, at a ship speed of 12 knots, the threshold relative motion is about 0.4 m RMS while at a ship speed of 18 knots this threshold is about 0.3 m RMS Similarly, at a speed of 12 knots, the threshold relative velocity is about 0.9 m/sec RMS, but at a ship speed of 18 knots it is less than 0.75 m/sec RMS

The second set of curves (Figure 10 and Figure 11) show the plot of deck wetness verses nondimensional Linear Dynamic Freeboard (LDF) and deck wetness verses Linear Relative Velocity. The term Linear implies that the calculations are done by a linear free surface formulation, the term Dynamic Freeboard refers to the variation of the freeboard during the motion of the ship and wave. As the number of full model motion cycles observed during the tank experiments were about 20 cycles LDF can only be calculated as a most probable smallest value. For this reason LDF is defined as.

LDF=(Static Free Board)-$\sqrt{2\ln n}$ (RMS of relative motion)   Eqn. 2

The plot of deck wetness versus the LDF nondimensionalyzed by the significant wave height (Figure 10) shows that if the non dimensional LDF for this hull remains above 3.5 statistically there will be no deck wetness. This result however is not by itself sufficient to explain all of the observed deck wetnesses mainly because of spray formation. For this purpose we studied the occurrence of deck wetness and the associated nondimensionalysed relative velocity. This is normally done for slamming predictions [1] Nondimensionalized relative velocity (NRV) is defined as:

NRV = (Relative Velocity)$_{RMS}$T$_{ave}$ / H$_{1/3}$ Eqn. 3

Figure 11 shows that the value of NRV is larger than 9.0 for the occurrence of deck wetness

136

Based on these two results we were able to deduce that for the formation of deck wetness two parameters should be checked during the early design stage and they should be kept above the suggested values to avoid deck wetness for the design sea-condition and ship speed. Namely the nondimensionalized LDF should be larger than 3.5 and NRV should be less than 9.0.

The set of these two rules can be possibly used during the ship design to establish the open deck level to minimize the risk of bow scooping for the open deck ro-ro ferries, for the expected environmental conditions.

The first series of experiments and subsequent numerical study established that the important kinematic quantities for the build-up of water on deck are the relative motion and the relative velocity at the bow. In addition, the numerical analysis showed that there is a relative threshold value which these variables must exceed for the formation of water on deck. The observed threshold is a decreasing function of ship speed. This result is important for operational decisions. Future tests should be carefully designed to address the non-linear nature of the problem and the existence of thresholds. As a result of the first series of testing the following recommendations may be made:

a) In future tests, relative motion should be directly measured at various points along the model.

b) To establish a correlation between the occurrence of water on deck and the amount of water on deck, the complete bow wave form should be measured. This is necessary as the relative motion is a function of the wave form and not of a local point wave height.

c) Non-linear, time-domain numerical computational methods could be used with benefit to calculate wave build-up and the motion of water on deck. This type of calculation could help the design of optimized bow forms which would reduce

the amount of water on deck. As these calculations include the complete hull geometry, very beneficial results for design and operation of ferries can be obtained.

d) The design method and rules suggested above could be used to set the level of the car deck for the Ro-Ro open deck ferries

CONCLUSIONS AND RECOMMENDATIONS

A detailed numerical analysis, combining both experimental and numerical results, showed, not unexpectedly, that relative wave height and relative wave velocity are important parameters to consider when studying the water-on-deck problem. Again, the relative wave height variable was identified during the experimental study as a key factor in deck wetting prediction, so the numerical findings are in general agreement with the experimental results.

The results from the "Queen of New Westminster" preliminary study of water-on-deck issues show a clear relationship between the occurrence of water on deck and the ratio of initial freeboard to significant wave height in the operating environment. In general, no water on deck is observed when the bow freeboard is more than twice the significant wave height

The experimental and analytical programs did show that if the vessel, with the bow doors open, were to be sailed at full speed (18 knots) directly into the most extreme seas found in the Straits (about 2 metres significant wave height by 8 second period), bow-scooping is possible.

A procedure to establish a minimum level for open decks is proposed. This design procedure based on easily available ship motion calculation methods. The procedure establishes a relation ship between the relative motion at the bow and the static freeboard. The second rule is based on the relative velocity at the bow. This procedure then permits for the establishment of a minimum free board

necessary to minimize the risk of bow scooping for a given design speed and wave condition. The procedure includes only the underwater geometry of the hull form. This could be insufficient for bow profiles with large flare.

REFERENCES

1. Bhattachayya R., 1978. "Dynamics of marine Vehicles". John Wiley and Sons.
2. Faulkner, D.A., 1982, "A Wind and Wave Climatology of the Strait of Georgia", Unpublished Manuscript.
3. Howard J. D. Calisal S. M. " Comparative Evaluation of the S-175 Hull Form "Second Canadian Marine Dynamics Conference Vancouver BC August 9-11 1993.
4. "SHIPMO-PC - Software for Seakeeping Predictions, User Manual". Fleet Technology Limited, Kanata, Ontario, Canada.
5. Roddan, G., Stensgaard., G. N., Noble, P., Molyneux, D. and Calisal, S. M. "Preliminary Experimental and Analytical Studies of Water-On-Deck Issues for Large, Open Shelter-Deck Ferries". Report No: 6-02-616-1 Advanced Systems Engineering Ocean Engineering Centre, BCRI, 3650 Wesbrook Mall, Vancouver, B.C. CANADA, V6S 2L2, July 1995.
6. Roddan, G., Stensgaard, G. N., Noble, P., Molyneux, D. and Calisal, S. M. "Experimental Studies of Water-on-Deck Issues for Large, Open Shelter-Deck Ferries, Phase II". Report No.: 6-02-616-2. Advanced Systems Engineering Ocean Engineering Centre, BCRI, 3650 Wesbrook Mall, Vancouver, BC, CANADA, V6S 2L2, Feb., 1996.

TABLES

Table 3: Head Seas, 18 (kn), (Configuration A1, Level Trim).

$T_{1/3}$ (sec)	$H_{1/3}$ (m)	WL_{DB} (m)	$f/H_{1/3}$	$f_{mr}/H_{1/3}$	N_{dw}
6	0.75	0.86	3.33	1.69	0
8	0.75	0.93	3.33	1.59	1-2
4	0.75	0.95	3.33	1.57	0
6	1.00	1.04	2.50	0.96	2
8	1.00	1.26	2.50	0.74	6-8
8	1.94	2.57	1.29	-0.53	15-20
6	1.67	1.29	0.40	0.23	15-20
4	1.74	1.74	1.44	-0.06	3-4

Table 4: Head Seas, 18 (kn), (Configuration A2, 0.21 deg trim by bow).

$T_{1/3}$ (sec)	$H_{1/3}$ (m)	WL_{DB} (m)	$f/H_{1/3}$	$f_{mr}/H_{1/3}$	N_{dw}
4	0.75	1.13	3.20	1.19	2
4	1.00	1.08	2.40	0.82	8
6	0.75	1.00	3.20	1.37	1
6	1.00	1.68	2.40	0.22	6-8
8	0.75	1.10	3.20	1.23	8-9
8	1.00	1.41	2.40	0.49	12-15
6	2.00	3.68	1.20	-1.14	20-25

Table 5: Head Seas, 18 (kn), (Configuration B1 - Displacement of 5,450 Tonnes, Level Trim)

$T_{1/3}$ (sec)	$H_{1/3}$ (m)	WL_{DB} (m)	$f/H_{1/3}$	$f_{mr}/H_{1/3}$	N_{dw}
6	0.75	0.87	3.67	2.00	0
6	1.00	0.88	2.75	1.37	0
8	0.75	0.89	3.67	1.98	0
8	1.00	0.83	2.75	1.42	3

FIGURES

Figure 1: General View of Model
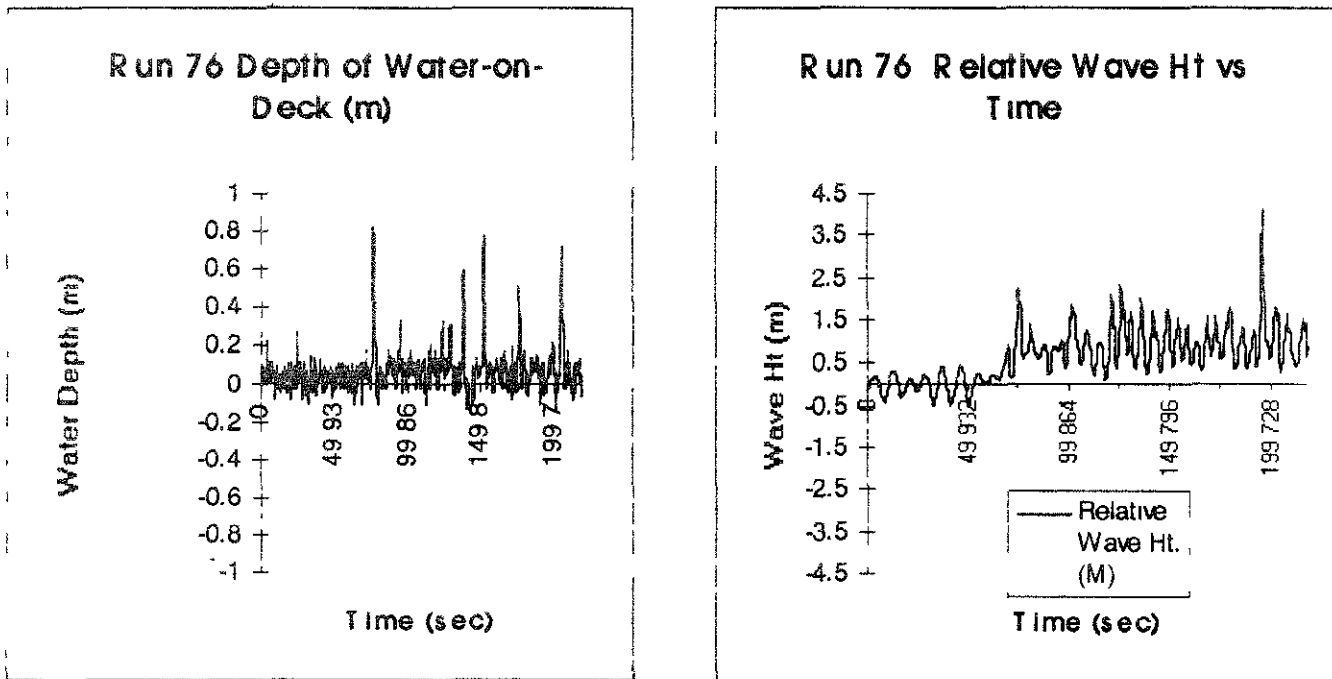
Figure 2: Run 76 — Relative Ht. vs. Time and Depth of Water on Deck (m)
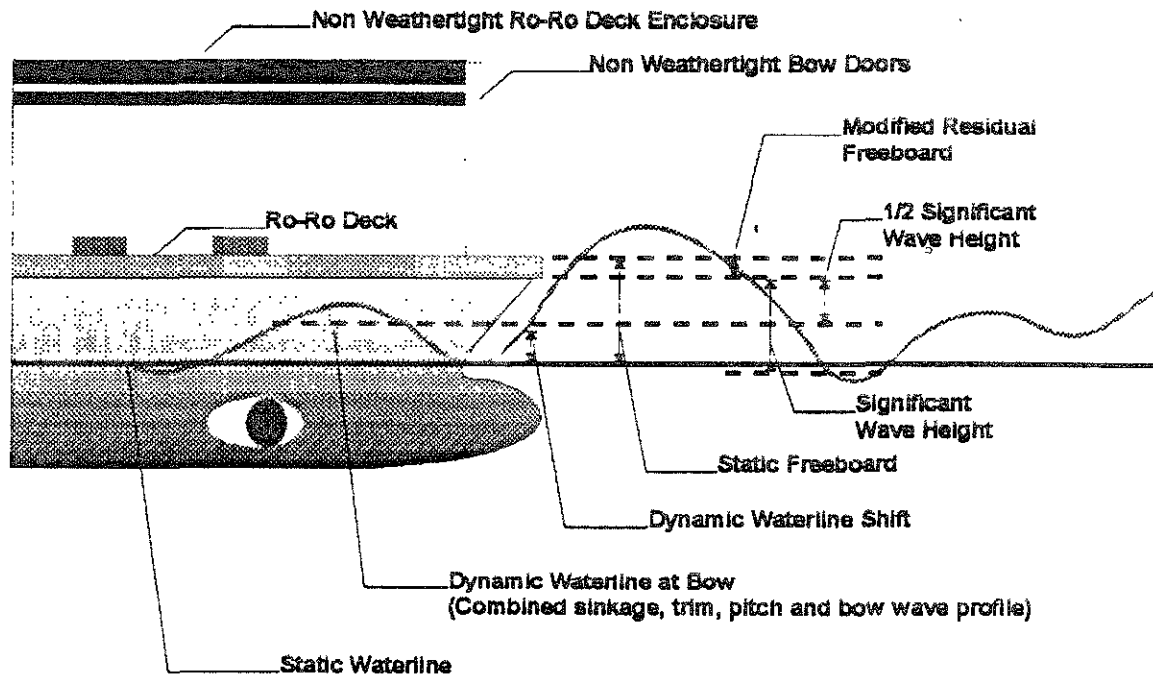
Modified Residual Freeboard =
(Static Freeboard - (Dynamic Waterline Shift + 1/2 Significant Wave Height))

If modified freeboard is positive no significant water comes on deck.
If modified residual freeboard is negative then significant water comes on deck.

Figure 3: Key to Terms Associated with Water-on-Deck Model Testing Results
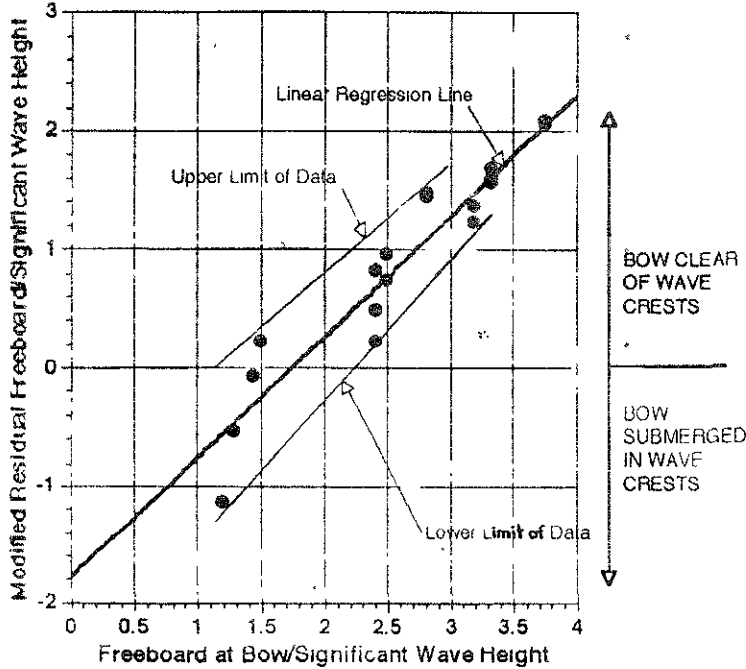
Figure 4: Bow Immersion/Emersion vs. Static Freeboard at Bow for Ro-Ro Ferry at 18 Knots in Head Seas
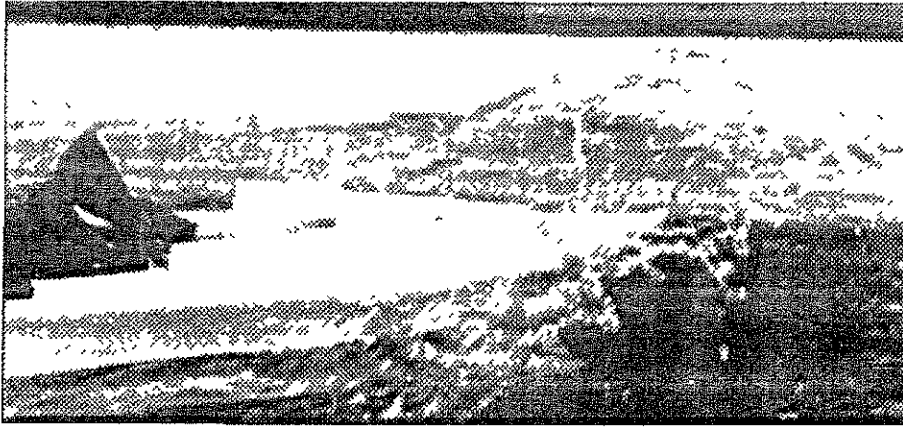
Figure 5: A picture showing an example of bow scooping during the model testing of S175.
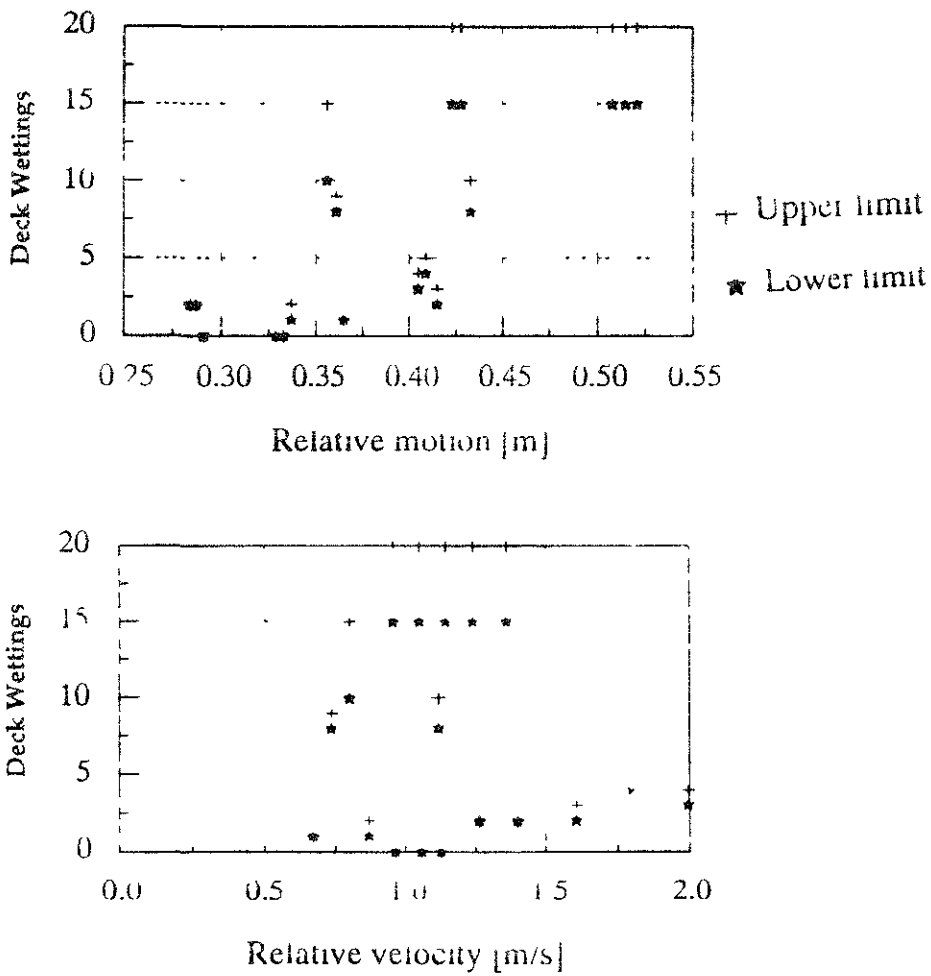
Figure 6: Relative Motion Characteristics at Station #0 from F.P. (All Speeds Combined)
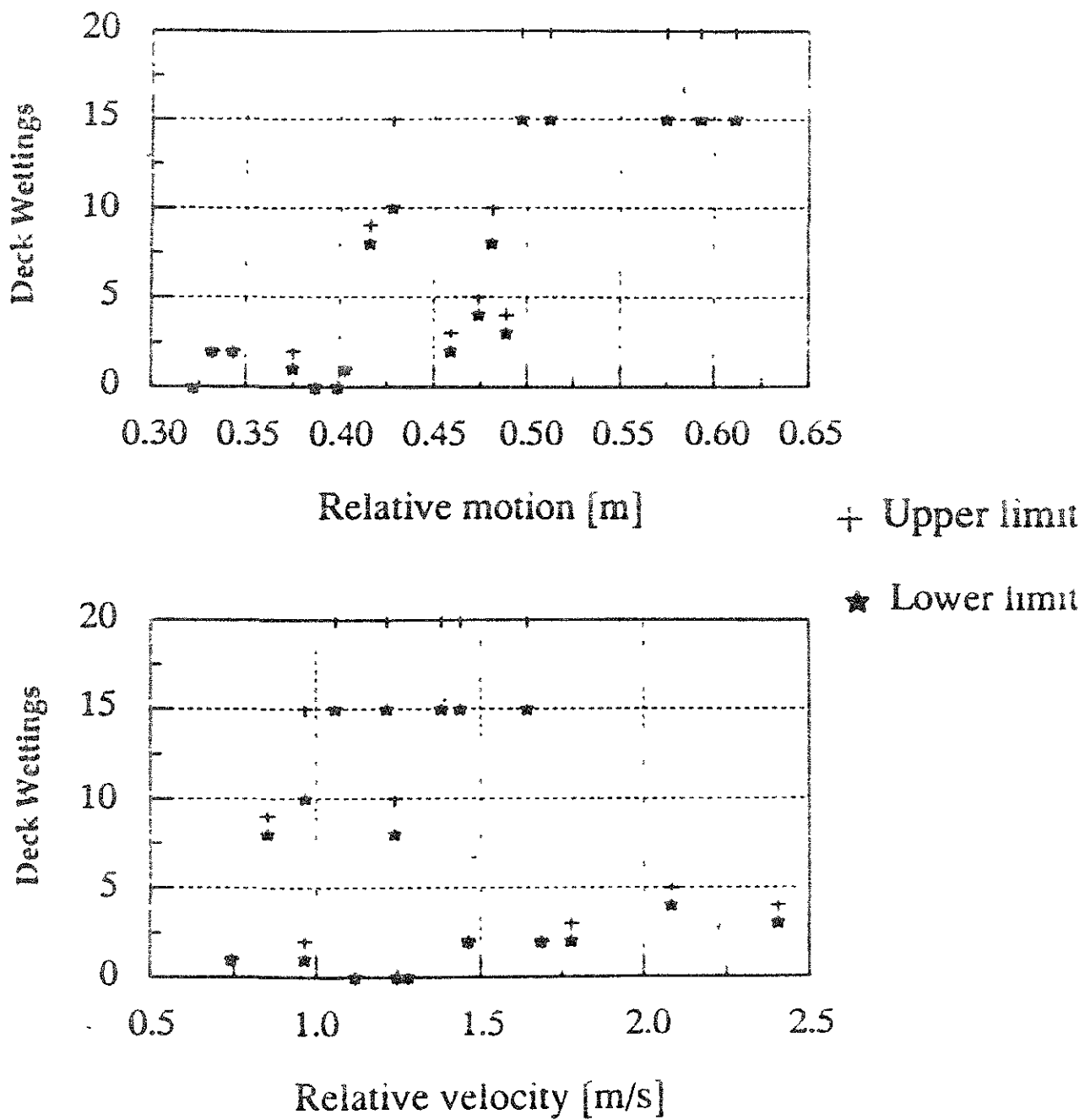
Figure 7: Relative Motion Characteristics at Station #1 from F.P. (All Speeds Combined)

142
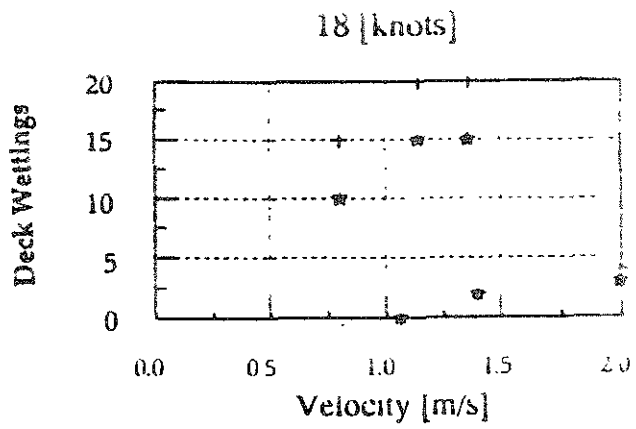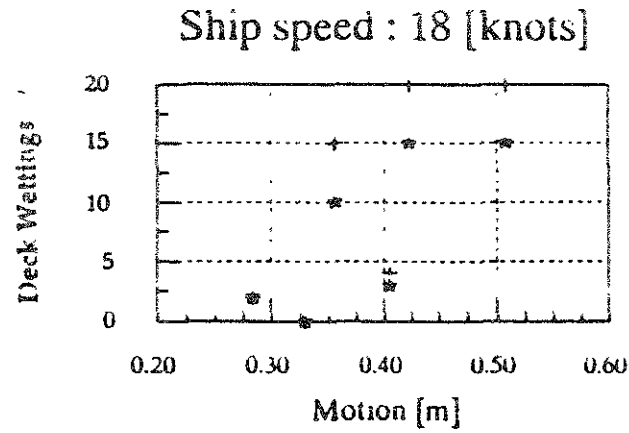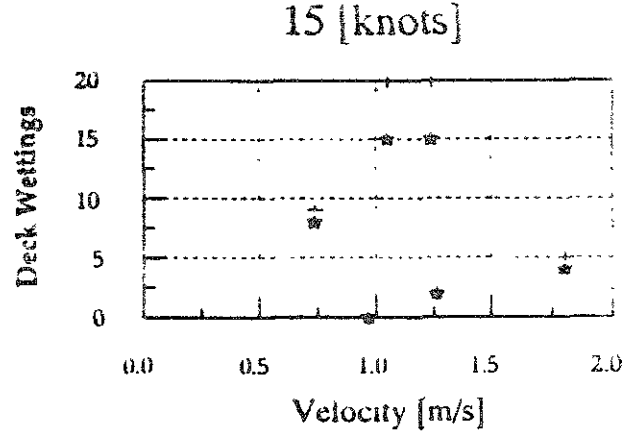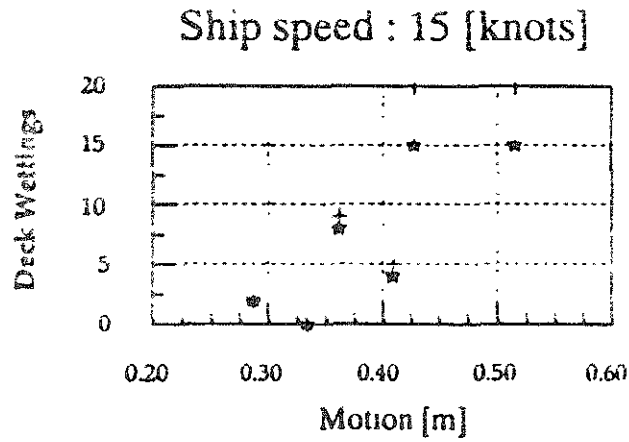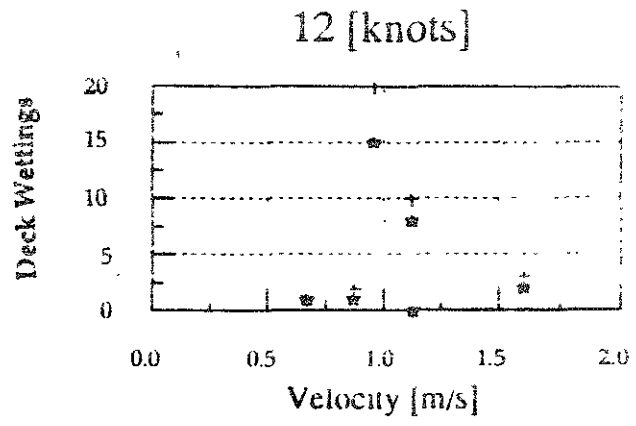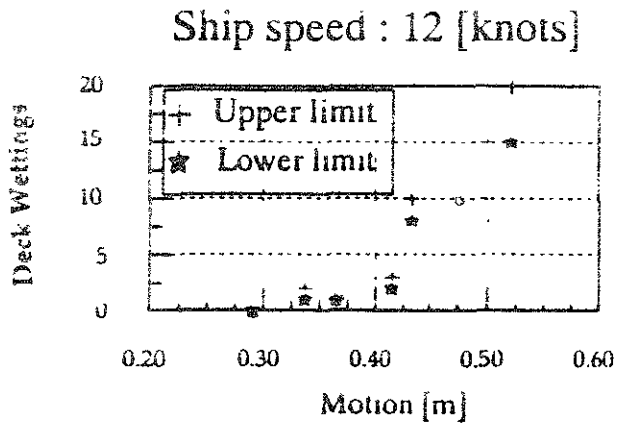
Figure 8: Relative Motion Characteristics at Station #0 from F.P.

143
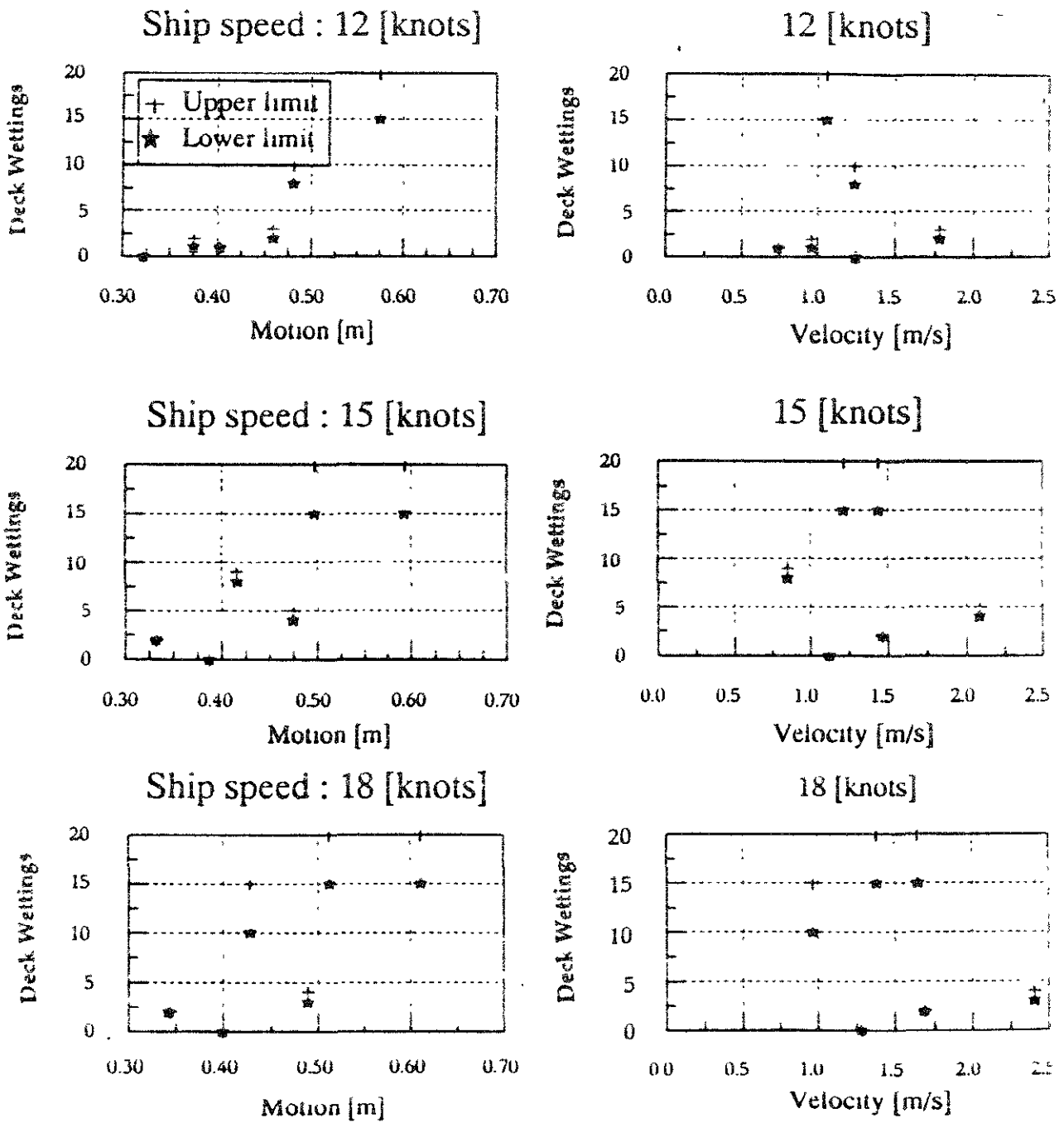
Figure 9: Relative Motion Characteristics at Station #1 from F.P.
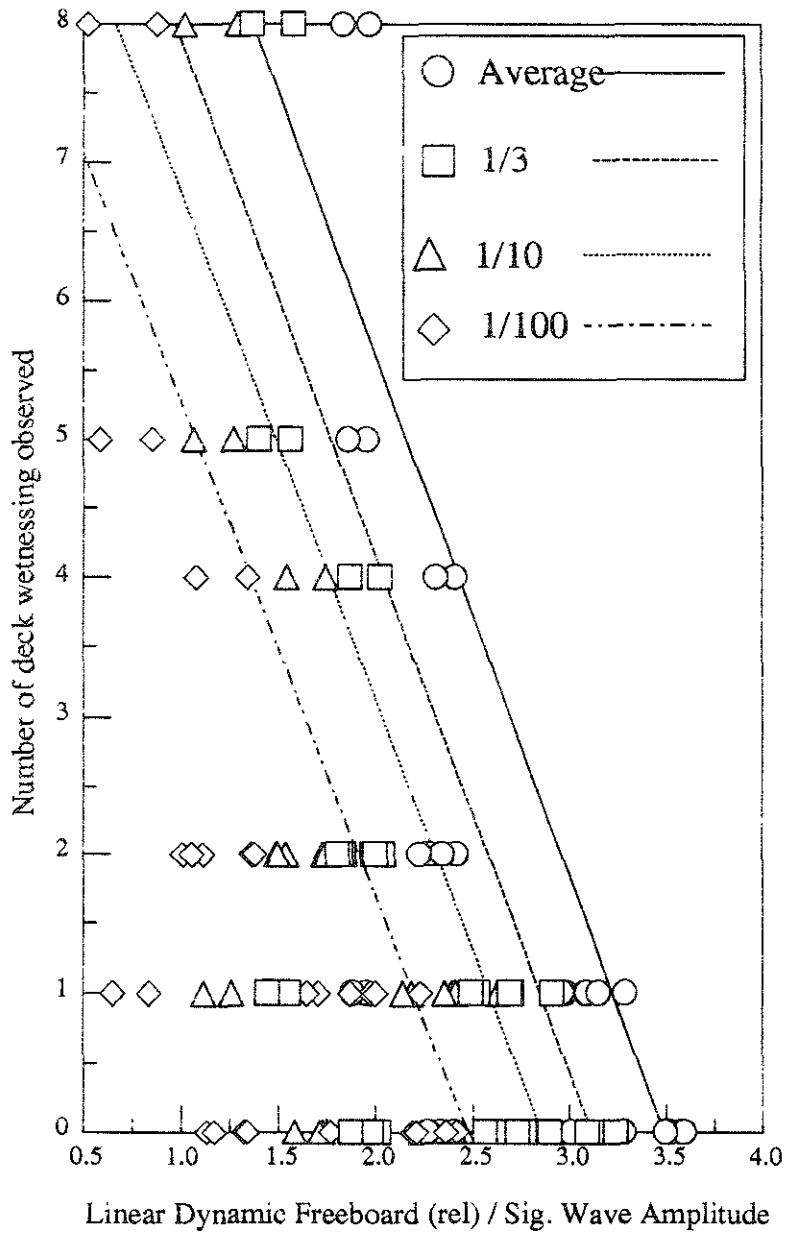
Figure 10: Based on the relative RMS motion characteristics at Station #0 from F.P. (all speeds combined)
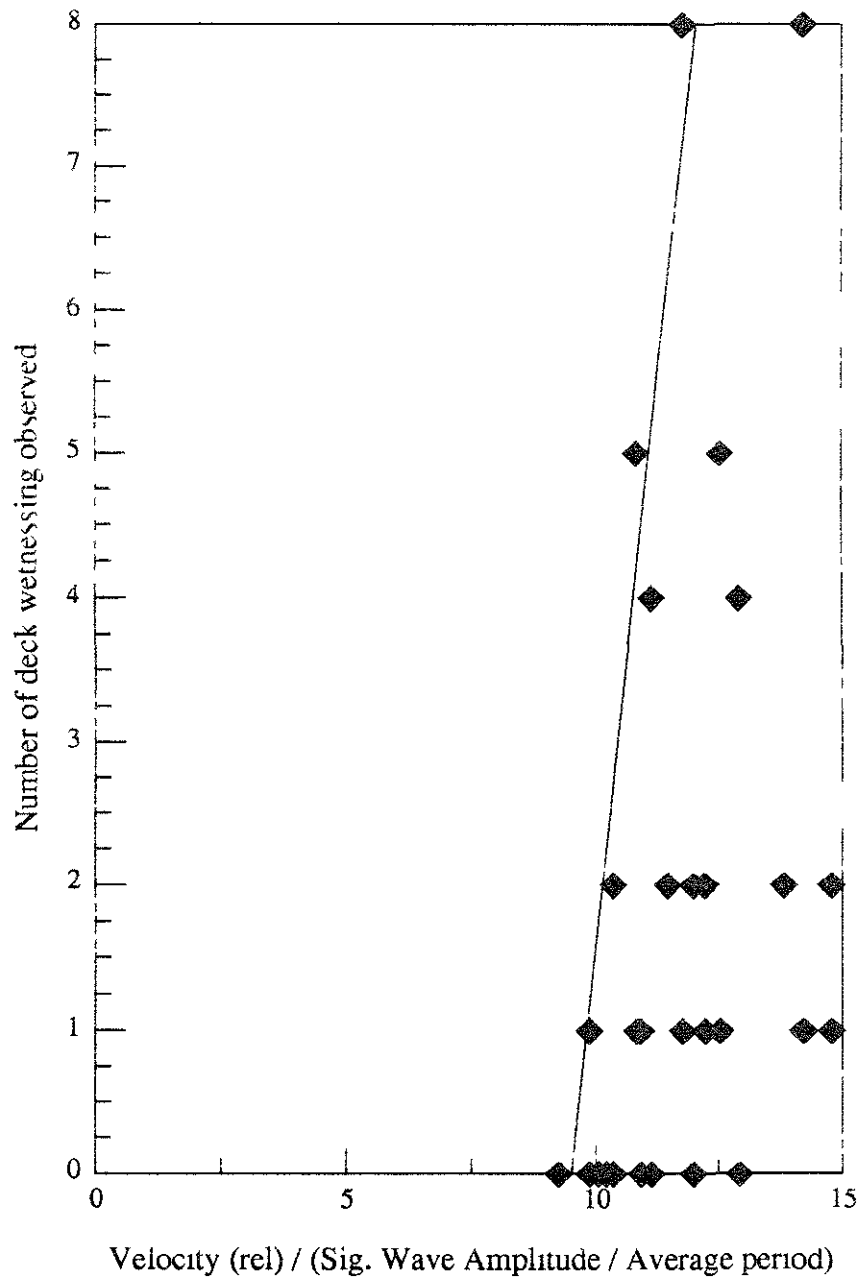
Figure 11: Based on the relative RMS motion characteristics at Station #0 from F.P. (all speeds combined)

The effect of GM on broaching and capsizing of small fishing vessels in following seas

By

Martin Renilson[*] and Andrew Tuite

Australian Maritime Engineering CRC Ltd

ABSTRACT

It is well known that the most dangerous condition for a small vessel operating in severe seas is when it is travelling in following or quartering waves.

A six-degree-of-freedom nonlinear mathematical model is developed to investigate the behaviour of vessels in following seas. The effect of the position of the vessel in the wave on the manoeuvring characteristics, the wave forces, the rudder effectiveness and the transverse stability is taken into account.

The mathematical model and proposed analysis method is used to determine the influence of GM and likelihood of broaching and capsizing on a typical Australian fishing trawler.

[*]Martin Renilson is on part secondment from the Australian Maritime College

1.0 INTRODUCTION

The question of ship safety in following seas has been discussed for many years. Despite an extensive amount of research into the complexities of broaching and capsizing, no acceptable solution for the problem has been achieved. The reason for this is that in a broach/capsize a ship is in a very extreme nonlinear condition which makes studies of the physics, either theoretical or experimental, difficult. (Vassalos and Maimun, 1994)

Many authors have tackled the difficult problem of modelling a vessel broaching. Pioneers such as Du Cane and Goodrich (1962) gave a comprehensive summary of the factors involved in broaching and presented a number of accounts of full scale incidents. Wahab and Swaan (1964) carried out linear stability analysis of lateral motions and showed that a ship which is directionally stable in calm water could be unstable in waves. Grim (1965) and Bose (1970) identified the dangers of a ship travelling at the same speed as the wave and identified that condition as a pre-requisite for a broach to occur. Renilson and Driscoll (1982) undertook a broaching analysis using a mathematical model based on calm water manoeuvring equations with additional wave force terms. Hamamoto and Nomoto (1982) performed experiments and theoretical analysis to ascertain whether wave orbital velocity had any effect on a vessel poised on a following wave crest. de Kat and Pauling (1989) extended a simulation program initiated by pioneering work carried out by Pauling and Wood (1974) to include diffraction and memory effects. Umeda and Renilson (1993 and 1994) and Umeda et al. (1995) carried out a global investigations using nonlinear dynamical system analysis which allowed the identification of critical conditions for broaching. Spyrou (1995 and 1996) adopted a dynamical analysis to investigate the steady state and transient behaviour of a vessel operating in a following sea using a multi dimensional state-space.

Over the past 35 years there has been a number of methods used to identify unfavourable combinations of ship and wave conditions. Experience has shown an extensive matrix of experiments, both free running and constrained, to be time consuming and rather expensive. A pure analytical approach using mathematical functions becomes too difficult as the complexity increases. The statistical approach is not suitable for taking into account the dynamic effects of broaching. The nonlinear dynamical systems approach becomes complicated with the increasing degrees of freedom of the model.

For these reasons an analysis method is used based on phase plane and time domain plots. Both phase trajectory plots and time domain plots are presented, highlighting the benefits of each method.

The proposed analysis method is then used to investigate the influence of GM for a typical Australian fishing trawler.

2.0 Mathematical Model

The motion of the vessel is analysed using two coordinate systems as seen in figure 1

1   Wave fixed, x_0, y_0 and z_0 with the origin at a wave crest, with the wave travelling in the direction of the x_0 axis

2   Body fixed, x, y and z with the origin at the vessel's LCG, with the x-axis pointing towards the bow, the y-axis to starboard and the z-axis downwards
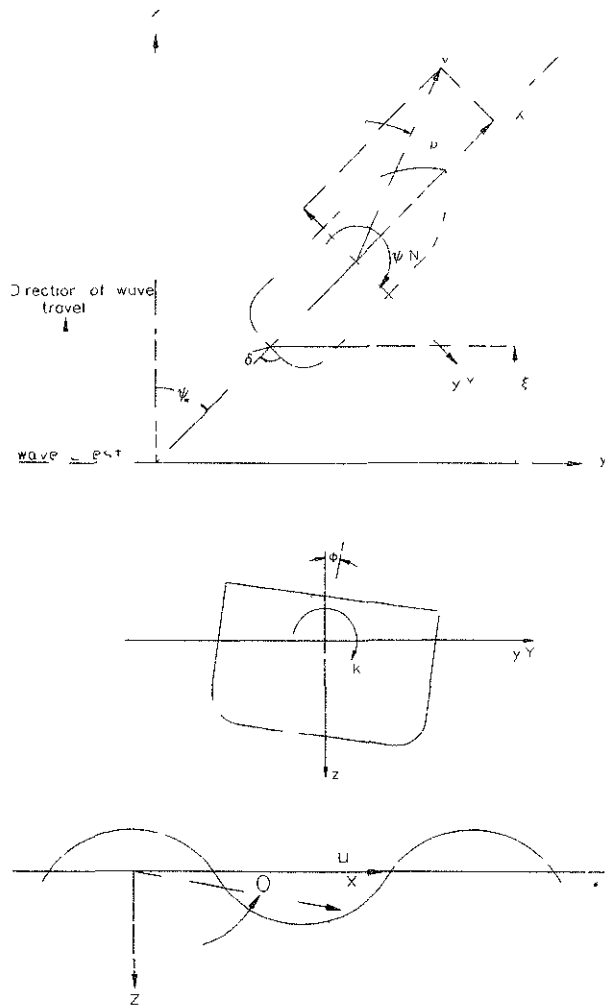
Figure 1: Coordinate system

A complete simulation of a vessel operating in a following sea is a very complex problem in comparison to a vessel operating in calm water   The vessel is subjected to two different hydrodynamic forces simultaneously, namely lifting forces in the horizontal plane acting on the vessel due to plane manoeuvring motion and the forces acting on the vessel arising from the incident wave

In addition, all these forces and moments, as well as the vessel's transverse stability and rudder effectiveness, are functions of the vessel's position in the wave

Using the quasi-static assumption the vessel's heave and pitch (z and θ) can be obtained as a function of the longitudinal position in the wave. Hence the dynamic part of the model reduces to the following four degrees of freedom:

$$X \quad = m(\dot{u} - v\psi) \quad = X_{wave} + X_{hull} + X_{rudder} + X_{propeller} + X_{wind} \tag{1}$$

$$Y \quad = m(\dot{v} + u\psi) \quad = Y_{wave} + Y_{hull} + Y_{rudder} + Y_{propeller} + Y_{wind} \tag{2}$$

$$N \quad = I_{zz}\dot{\psi} \quad = N_{wave} + N_{hull} + N_{rudder} + N_{propeller} + N_{wind} \tag{3}$$

$$K \quad = I_{xx}\dot{\phi} \quad = K_{wave} + K_{hull} + K_{rudder} + K_{wind} \tag{4}$$

The dynamic equations are based on Newton's 2nd law of motion. The notation is outlined in Section 7. X_{hull}, Y_{hull}, N_{hull} and K_{hull} are the hull hydrodynamic manoeuvring forces and moments defined as follows:

$$
\left.
\begin{aligned}
X_{hull} &= m(1 + X''_{v\psi})v\psi + \frac{m}{L}X''_{uu}u|u| + \frac{m}{gL^2}X''_{uuuu}u^3|u| + \frac{m}{gL^2}X''_{uvvv}uv^2|v| + X''_z \cdot \frac{u_{th} - |u|}{u_{th}} \cdot \frac{u}{u_{th}} \\
Y_{hull} &= m(Y''_{u\psi} - 1)u\psi + \frac{m}{L}Y''_{uv}|u|v + Y''_{|u|\phi}|u|\phi\frac{mu}{L} + Y_{nonlinear} \\
N_{hull} &= mLN''_{u\psi}|u|\psi + mN''_{uv}uv + N''_{u\phi}u\phi mu + N_{nonlinear} \\
K_{hull} &= K''_{|u|v}|u|vm + K''_{|u|\psi}|u|\psi m + K''_{u\phi}u\phi mL + K''_{\phi|\phi|}\phi|\phi|mL^2 + K''_{\phi}(\phi,\xi)mLg
\end{aligned}
\right\}
\tag{5}
$$

Empirical, theoretical and experimental methods are employed to determine the hull force manoeuvring coefficients used in the mathematical model.

The wave induced force and moment coefficients, X_{wave}, Y_{wave}, N_{wave} and K_{wave} are based on slender body theory with some simplifications. The wave induced surge force, X_{wave}, is calculated using the Froude-Krylov component of the force. The wave induced sway force, Y_{wave}, yaw moment, N_{wave}, and roll moment, K_{wave}, are calculated using both the Froude-Krylov and diffraction components. The wave forces and moments can be calculated as follows (Umeda and Renilson, 1995):

$$X_{wave} = X_{waveF-K} \tag{6}$$

$$Y_{wave} = Y_{waveF-K} + Y_{wavediffraction} \tag{7}$$

$$N_{wave} = N_{waveF-K} + N_{wavediffraction} \tag{8}$$

$$K_{wave} = K_{waveF-K} + K_{wavediffraction} \tag{9}$$

The Froude-Krylov components are defined by:

$$X_{wave\,F-K} = -\rho g \zeta k \cos\psi_w \int_{x(fp)}^{x(ap)} S(x) e^{-\frac{kz(x)}{2}} \sin(k\xi + kx_w \cos\psi_w) dx \qquad (10)$$

$$Y_{wave\,F-K} = \rho g \zeta k \sin\psi_w \int_{x(fp)}^{x(ap)} S(x) e^{-\frac{kz(x)}{2}} \sin(k\xi + kx_w \cos\psi_w) dx \qquad (11)$$

$$N_{wave\,F-K} = \rho g \zeta k \sin\psi_w \int_{x(fp)}^{x(ap)} S(x) e^{-\frac{kz(x)}{2}} x_{lcg} \sin(k\xi + kx_w \cos\psi_w) dx \qquad (12)$$

$$K_{wave\,F-K} = \rho g \zeta k \sin\psi_w \int_{x(fp)}^{x(ap)} S(x) \left(\frac{y(x)}{2}\right) e^{-\frac{kz(x)}{2}} z(x) \sin(k\xi + kx_w \cos\psi_w) dx$$

$$- \rho g \zeta k^2 \sin\psi_w \int_{x(fp)}^{x(ap)} c_2(x) \left(\frac{y(x)}{2}\right)^3 e^{-\frac{kz(x)}{2}} \sin(k\xi + kx_w \cos\psi_w) dx \qquad (13)$$

The diffraction components are defined by:

$$Y_{wave\,diffraction} = \int_{x(fp)}^{x(ap)} \left((\ddot{y}_{wave}\, AVM) + \left(\dot{y}_{wave}\, \frac{dAVM}{dx}\, v \right) \right) dx \qquad (14)$$

$$N_{wave\,diffraction} = \int_{x(fp)}^{x(ap)} \left((\ddot{y}_{wave}\, AVM) + \left(y_{wave}\, \frac{dAVM}{dx}\, v \right) \right) x_w\, dx \qquad (15)$$

$$K_{wave\,diffraction} = \int_{x(fp)}^{x(ap)} \left((\ddot{y}_{wave}\, AVM) + \left(\dot{y}_{wave}\, \frac{dAVM}{dx}\, v \right) \right) z(x)\, dx \qquad (16)$$

The moment induced by the rudder is a large component of the moment counteracting a vessel broaching. The modelling of this large component requires considerable detail. The rudder forces and moments, X_{rudder}, Y_{rudder}, N_{rudder} and K_{rudder}, are calculated from modelling the actual velocity of water flow acting over the surface of the rudder. The forces within the model are modified to take into account the change in fluid flow over the surface of the rudder due to the presence of the propeller and the wave. The vessel's auto pilot system is expressed as follows.

$$\delta_d = \delta + T_E' \left(\frac{L}{U}\right) \dot{\delta} = -K_p (\psi - \psi_d) - K_p T_d' \left(\frac{L}{U}\right) \psi \qquad (17)$$

The expression is based on work proposed by Eda (1971). The coefficients ($T_E' = 0.1$ and T_d' = 1.0) are considered normal for conventional ships.

The rudder effectiveness, heave and trim calculations were validated by a series of model experiments (Mak,1995). The forces and moments induced by the propeller and wind are based on theories proposed by Krupp Atlas (1986).

The mathematical model also takes into account the change in transverse stability relative to the longitudinal position in the wave.
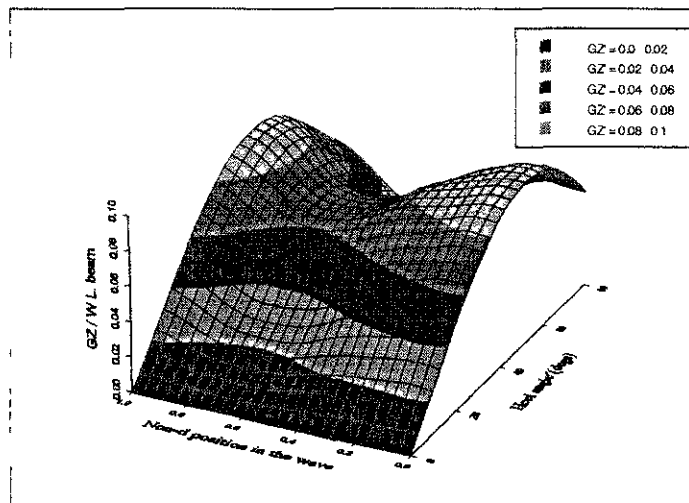
Figure 2: Hydrostatic roll restoring arm (Theoretical prediction)

$$(\frac{\lambda}{L} = 1.1, \ \frac{H}{\lambda} = \frac{1}{15} \text{ and } \psi_w = 0°)$$

Figure 2 illustrates the variation in roll restoring arm with heel angle and non-dimensional position in the wave for a single wave condition.

3.0 SIMULATION RESULTS - INFLUENCE OF GM

The mathematical model given in section 2 was used to determine the influence of GM on the behaviour of a sample vessel operating in a severe following sea. The sample vessel selected for the investigation is the Australian 25m Success Class trawler, which is outlined in Appendix A.

The roll motion of a vessel operating in a severe following seaway is dictated by the stability of the vessel which is a function of the vessel's metacentric height (GM). Roll has a strong influence on the yaw behaviour of the vessel. The coupling between yaw-roll and sway-roll influences the relative motion (yaw and sway) which in turn effects the vessel's position in the wave and hence its behaviour in following seas Thus, during following sea simulations, the vessel's metacentric height has to be analysed carefully.

154
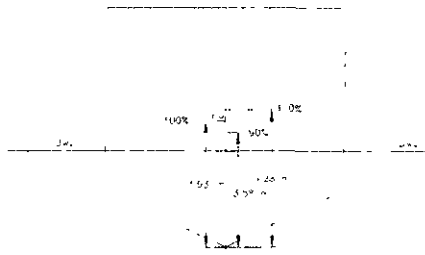
Figure 3: Systematic KG variation

The ship and wave conditions used for the simulation are given in table 2:

Wave encounter angle	15°
Wavelength / ship length	1.0 - 2.0
Wave steepness	1/8 - 1/20
Vessel Fn	0.39

Table 2: Conditions used for the investigation
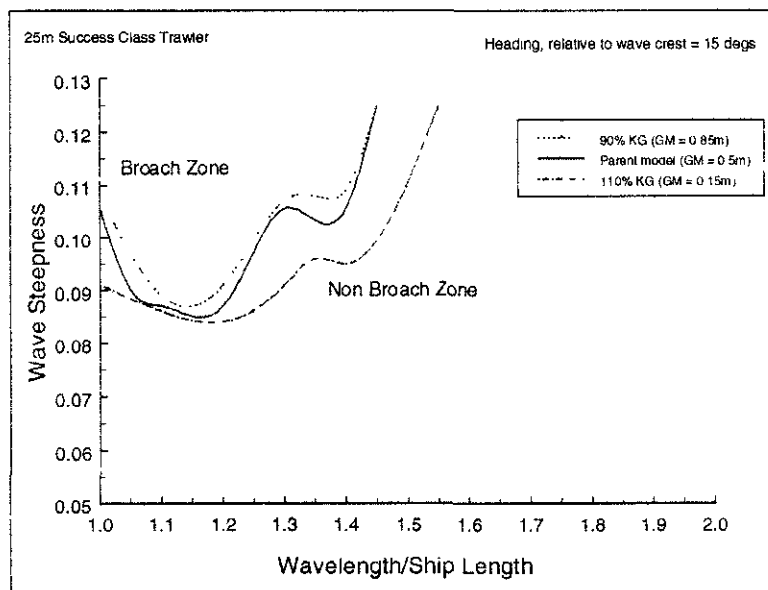
Figure 4: Broaching zones as a function of KG/GM

It can be seen in figure 4, by systematically increasing the transverse position of the centre of gravity (KG), the region where the vessel experienced a broach increased.

The wave induced forces and moments acting on the vessel remained constant with the systematic variation of KG. The increased likelihood of broaching with an increase in KG is a function of the reduction in directional stability with increasing KG.

156

3.1 Broaching simulation

Broaching-to occurs when the vessel's rudder restoring moment cannot counteract the large yawing moment induced by the wave for long enough for it to deviate rapidly from its initial heading to a new heading sufficiently different from the initial heading to cause concern. Often this is associated with a large heel angle. Unlike a capsize, there is no strict mathematical definition of a broach which is widely accepted.

The broaching phenomenon is easily described physically but quite difficult to describe mathematically. Many authors in the past have used a variety of different mathematical definitions but to date most have tended to be conservative, resulting in a different interpretation to what a mariner would consider a broach. Renilson and Driscoll (1982) defined a broach as:

$$\psi > \psi_{desired} + 40^{\circ} \qquad (18)$$

Bandyopadhyay and Hsiung (1994) concluded a broach was a function of the following three salient features:

I.   Sudden loss of ship manoeuvrability in waves;
II   Large heading deviation as a result of broaching-to; and
III. Occurrence of broaching-to in a short span of time

Although Bandyopadhyay and Hsiung (1994) highlighted these features they simply defined a broach as:

$$\psi > \psi_{desired} + 45^{\circ} \qquad (19)$$

To date, most investigations neglect the yaw acceleration ($\ddot{\psi} > 0$) component in their broaching definition. A vessel which deviates from it desired course and continues to yaw into the wave with full counteracting rudder applied ($\delta = \pm\delta_{max}$, $\dot{\psi} > 0$ and $\psi > \psi_{desired} + 20^{\circ}$) may not technically be experiencing a broach. Most descriptions of different vessel's broaching (Du Cane and Goodrich, 1962), explain in vivid terms a rapid yaw motion experienced. Such a rapid motion can only be defined as a positive yaw acceleration ($\ddot{\psi} > 0$) into the wave

Taking this into account the periodic attractors associated with a number of different conditions were studied, and the following definition of a broach derived.

Rudder angle	$\delta = \delta_{max}$
Yaw velocity	$\dot{\psi} > 0$
Yaw acceleration	$\ddot{\psi} > 0$
Heading angle	$\psi > \psi_{desired} + 20^{\circ}$

Table 1: Definition of a broach

Using the above definition, a matrix of simulations were undertaken to derive the broaching boundaries for the 25m Success class trawler. Three different metacentric heights were modelled (0 85m, 0.5m and 0 15m).

3.2 Capsizing simulation

Using the mathematical model incorporating the full nonlinear roll restoring moment, capsize simulations for the 25m Success class were conducted. For this investigation a capsize has been defined when the angle of heel (ϕ) exceeds 80 degrees. 80 degrees was chosen as it was the average value of the angle of vanishing stability, depending on the wave condition and the GM under investigation.

The simulations were conducted for three different metacentric heights, 0.25, 0.35 and 0.45m. 0.35m was chosen as it is the minimum requirement for fishing vessel's specified by the Uniform Shipping Law Code (1993). The effect of heading angle was also investigated to two heading angles, 5 and 30 degrees. Regions of capsize predicted from the simulations for heading angles of 5 degrees and 30 degrees are shown in figures 5 and 6 below.
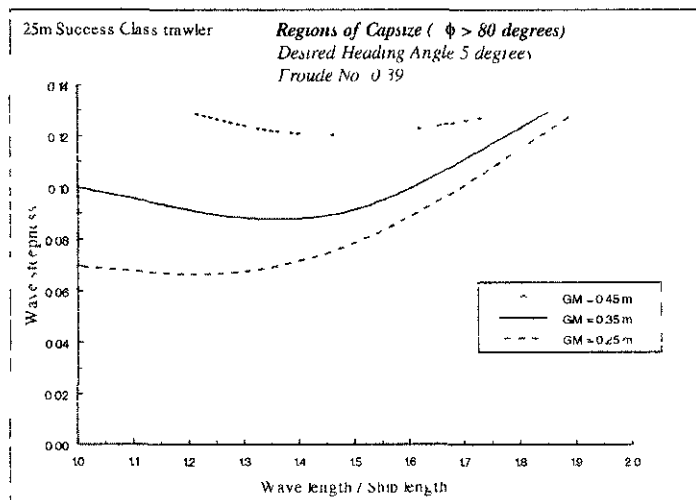
Figure 5: Capsize boundaries, $\psi_w = 5$ degrees
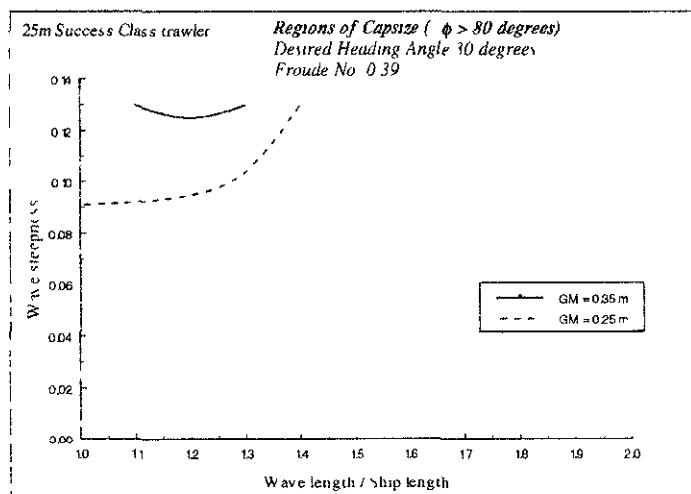
Figure 6: Capsize boundaries, $\psi_w = 30$ degrees

157

4.0 CONCLUDING REMARKS

A nonlinear six degrees of freedom mathematical model has been developed to investigate the behaviour of small vessels in following seas. This incorporated roll/yaw coupling, together with the effect of the wave on the nonlinear roll restoring moment, and the rudder effectiveness.

When applied to a 25m fishing vessel it was shown that raising the vertical centre of gravity increased both the likelihood of broaching-to and of capsizing.

5.0 ACKNOWLEDGMENT

6.0 NOMENCLATURE

ap	aft perpendicular of vessel
AVM	2-d sectional added mass (horizontal)
b	beam
Fn	Froude number
fp	forward perpendicular of vessel
	gravity
GM	metacentric height
H	wave height
I	moment of inertia
k	wave number
K	roll moment
KG	distance from the keel to the centre of gravity
K_{hull}	roll moment induced by the hull
$K_{propeller}$	roll moment induced by the propeller
k_r	gain of rudder autopilot
K_{rudder}	roll moment induced by the rudder
K_{total}	total roll moment acting on vessel
K_{wind}	roll moment induced by the wind
K_{wave}	roll moment induced by the waves
$K_{wave\,FK}$	roll moment induced by the waves - Froude-Krylov component
$K_{wave\,diffraction}$	roll moment induced by the waves - diffraction component
$K_{v\,u\,u\psi\,u\phi\,\phi\,\phi\,\phi}$	roll moment hull manoeuvring coefficients
L	length of ship
m	mass of ship (physical mass + added mass)
M	moment to heel vessel to measure change in GM

N	yaw moment
N_{hull}	yaw moment induced by hull
$N_{nonlinear}$	nonlinear yaw moment component induced by hull
$N_{propeller}$	yaw moment induced by propeller
N_{rudder}	yaw moment induced by rudder
N_{total}	total yaw moment acting on vessel
N_{wave}	yaw moment induced by waves
$N_{wave\ diffraction}$	yaw moment induced by waves - diffraction component
$N_{wave\ F\ K}$	yaw moment induced by waves - Froude-Krylov component
N_{wind}	yaw moment induced by wind
$N_{r\ u\psi\ u\ \phi\ u\ vv\ \psi\psi}$	yaw moment hull manoeuvring coefficients
T	draft of vessel
u	velocity in the x-direction
$\dot{u}$	acceleration in the x-direction
v	velocity in the y-direction
$\dot{v}$	acceleration in the y-direction
X	surge force
λ_c	x-distance from the centre of the strip to the wave crest
X_{hull}	surge force induced by the hull
$X_{propeller}$	surge force induced by the propeller
X_{rudder}	surge force induced by the rudder
X_{total}	total surge force acting on vessel
X_{wave}	surge force induced by waves
$X_{wave\ F-K}$	surge force induced by waves - Froude-Krylov component
X_{wind}	surge force induced by the wind
$X_{u\ u\psi\ uu\ uuuu\ uvvv}$	surge force hull manoeuvring coefficients
x_0	x-velocity in wave fixed coordinate system
$\ddot{x}_0$	x-acceleration in wave fixed coordinate system
y	mean wave orbital velocity
$\dot{y}$	mean wave orbital acceleration
Y	sway force
Y_{hull}	sway force induced by hull
$Y_{nonlinear}$	nonlinear sway force component induced by hull
$Y_{propeller}$	sway force induced by propeller
Y_{rudder}	sway force induced by rudder
Y_{total}	total sway force acting on vessel
Y_{wave}	sway force induced by waves
$Y_{wave\ F-K}$	sway force induced by waves - Froude-Krylov component
$Y_{wave\ diffraction}$	sway force induced by waves - diffraction component
Y_{wind}	sway force induced by wind
$Y_{v\ vr\ uv\ \phi\ u_c}$	sway force hull manoeuvring coefficients
y_0	y-displacement in wave fixed coordinate system
y_v	y-velocity in wave fixed coordinate system
y_a	y acceleration in wave fixed coordinate system
z	heave displacement of vessel
β	drift angle
δ	rudder angle
$\dot{\delta}$	rudder angle rate

δ_d	desired rudder angle
λ	wavelength
ϕ	heel angle
$\dot{\phi}$	roll velocity
$\ddot{\phi}$	roll acceleration
θ	pitch angle
ρ	density of water
ξ	distance from the wave crest to the transom of the vessel
ψ	heading angle, yaw angle
$\dot{\psi}$	yaw rate
$\ddot{\psi}$	yaw acceleration
ψ_d	vessel heading desired
ψ_w	vessel heading relative to wave crest
ς	wave amplitude

7.0 REFERENCES

Boese, P.(1970), *Steering a ship in a heavy following seaway.* Institut fur Schiffbau, Hamburg University March.

Du Cane, P. and Goodrich, G.J.(1962), *The following sea, broaching and surging.* Trans. RINA Vol. 104, April.

Eda, H.(1972), *Directional stability and control of ships in waves.* Journal of Ship Research, September

Grim, O.K. (1965), *The ship in a following sea*, DTMB translation 313, Feb.

Grochowalski, S., Archibald, J. B., Connally, F.J. and Lee C.K.(1994), *Operational factors in stability safety of ships in heavy seas.* Fifth International Conference on Stability of Ships and Ocean Vehicles. Melbourne.

Hamamoto, M. and Nomoto, K.(1982), *Transverse stability of ships in a following sea.* Proceedings of the 2nd International Conference on Stability of Ships and Ocean Vehicles, Tokyo.

de Kat, J.O. and Paulling, J.R.(1989), *The simulation of ship motions and capsizing in severe seas.* SNAME Annual Meeting, held New York.

Paulling, J.R., and Wood, P.D.(1974), *Numerical simulation of large amplitude ship motion in astern seas* Seakeeping 1953-1973, SNAME Publication.

Renilson, M.R. and Driscoll, A.(1982) *Broaching - An investigation into the loss of directional control in severe following seas.* Trans. Royal Institution of Naval Architects, Vol. 124.

Renilson M.R. and Thomas G.A.(1990), *A note on surging and loss of control of small fishing vessels in severe following seas.* 4th International Conference on Stability of ships and Ocean Vechicles, September Naples.

Renilson, M.R. and Tuite, A.J.(1995) *Broaching simulation of small vessels in severe following seas.* Proceedings International Symposium Ship Safety in a Seaway, Kaliningrad, Russia, May.

Renilson, M.R.(1997) *A note on the capsizing of vessels in following and quartering seas.* Ocean Engineering International, Vol 1 No 1, 1997.

Spyrou, K.J.(1995), *Surf-riding and oscillations of a ship in quartering waves.* J Mar Sci Technol, 24 - 36.

Spyrou, K.J.(1996), *Dynamic instability in quartering seas: The behaviour of a ship during broaching* Journal of Ship research, Vol. 40. No. 1, March, pp 46-59.

Tuite, A.J. and Renilson, M.R. (1995), *The effect of GM on the manoeuvring of a high speed container ship* Eleventh International Maritime and Shipping Symposium, Sydney.

Umeda, N. and Renilson, M. R.(1994), *Broaching of a fishing vessel in following and quartering seas nonlinear dynamical system approach.* Fifth International Conference on Stability of Ships and Ocean Vehicles, Melbourne.

Umeda, N and Renilson, M.R.(1993), *Broaching in following seas - a comparison of Australian trawlers and Japanese trawlers.* Bulletin of National Research Institute of Fisheries Engineering, No.14, March.

Umeda, N., Yamakoshi, Y. and Suzuki, S.(1995) *Experimental study for wave forces on a ship running in quartering seas with very low encounter frequency.* Proceedings International Symposium Ship Safety in a Seaway, Kaliningrad, Russia, May.

Vassalos, D. and Maimun, A.(1994), *Broaching-To thirty years on* Fifth International Conference on Stability of Ships and Ocean Vehicles, Melbourne

Wahab, R. and Swaan W.A.(1964), *Coursekeeping and broaching of ships in following seas*, Journal of Ship Research, April

USL Code (1993), *Uniform Shipping Law code.* As Ammended Oct 1993, Australian Maritime Safety Authority (Australia)

APPENDIX

A 25m Success class stern trawler was the sample vessel used for the investigation. This trawler was designed and built by the Australian Shipbuilding Industry Pty Ltd. in Western Australia These vessels are engaged in prawn trawling in the tropical waters off Northern Australia and during off season operate in regions around India, the Persian Gulf or South East Asia
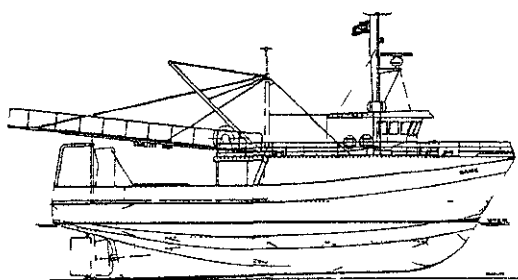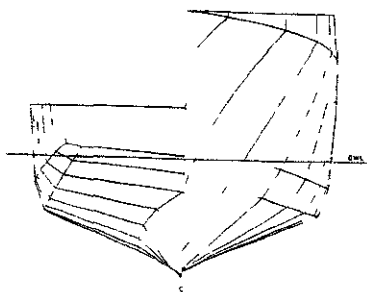
Figure A1. Hull Body plan   **Figure A2. Profile of 25m Success Class Trawler**

	Full scale
Length B.P.	22.05m
Beam W.L.	7.3m
Draught	3.0m
Displacement	203 7t
L.C.B.	3.1% aft
Cm	0.687
Cb	0.375

Table A1: Vessel particulars

STUDY OF THE NONLINEAR ROLL MOTIONS OF FISHING VESSELS IN REGULAR SEAS

by

T.A. Santos, N. Fonseca and C. Guedes Soares
Unit of Marine Technology and Engineering, Technical University of Lisbon
Instituto Superior Técnico, Av. Rovisco Pais, 1096 Lisboa, Portugal

ABSTRACT

The nonlinear rolling motion of ships in regular seas is studied. The nonlinear differential equation is analysed using the phase plane analysis and the Runge-Kutta fourth-order method of numerical solution. The damping moment coefficient is determined by the method of component analysis, leading to an equivalent linear damping coefficient. These methods were implemented in a computer program, which was used to analyse the behaviour of three fishing vessels and one fishery research vessel

INTRODUCTION

A vast number of ship dynamics problems can be solved using linear theory, obtaining good results from the practical standpoint, while avoiding mathematical complexities. When the motion reaches large amplitudes some nonlinear phenomena becomes apparent and linear theory approximations fail to describe them.

The most interesting motion in the context of ship safety from capsizing is the roll motion. The underlying reason for nonlinear models in the study of the roll motion of ships is to avoid a design which may lead to capsizing of the ship due to resonance or other nonlinear phenomena, which may cause the vessel to roll to a very high angle.

Much progress has been made in the last decades in understanding linear or small-amplitude motions, both for regular and irregular seas The roll motion of a ship exhibits well-known nonlinear features even for moderate sea excitations and thus to predict the maximum roll amplitudes that may lead to capsize, nonlinear theories are required. However, the understanding of large-amplitude nonlinear ship motions is limited. The two main obstacles are determining the hydrodynamic forces and obtaining general solutions to the nonlinear equations of rigid-body motion.

The solution of the nonlinear hydrodynamic problem in the time domain related with the nonlinear ship dynamics, is progressing, but it still resorts to empirical approximations, for example to estimate the viscous fluid force. This

means that the fully nonlinear simulation of the six-degree-of-freedom ship dynamics is not yet feasible. However, some attempts have been made to use different time simulation methods to solve the problem for sinusoidal excitation.

Due to these difficulties, a roll model is generally assumed which decouples the six degrees of freedom. The behaviour of a ship at sea is described by a system of six coupled second order differential equations, each representing one of the six degrees of freedom. However, the coupling coefficients are not all of the same order of importance. In each specific case some of these coefficients may become negligible with regard to others.

A number of assumptions may be made in order to decouple the six degrees of freedom. Thus, in beam seas, one can assume rolling to be an almost independent motion and neglect the pitch/heave influence due to bow/stern asymmetry. Therefore, a one degree of freedom roll model may be considered. Unfortunately, a general solution of this equation is unknown.

The research efforts in this field have been concentrated on the determination of approximate solutions for the one degree of freedom roll equation. First, the deterministic approaches to this problem will be considered (regular beam waves). Wright & Marshfield presented, back in 1979 [15], three methods of solution for the case of sinusoidal excitation, with and without bias: the harmonic balance method, a regular perturbation method and the method of averaging. Nayfeh & Kheider [8] introduced the multiple scale method, which is an extension of the perturbation method. They applied this method both to biased and unbiased ships in regular beam waves. The perturbation method has a major disadvantage, which is the fact that it is limited to weakly nonlinear systems, while capsizing of ships is a fully nonlinear phenomenon.

Other approaches to the problem of nonlinear rolling, still considering regular seas, exist. Among them there are the results of Virgin [13] who used the local analysis and numerical study of the associated Poincaré map, describing the chaotic dynamics involved in ship rolling. In this work a static bias term was incorporated in the equation to simulate a shift in cargo, a steady wind or the build-up of ice on one side of the deck. It is shown that this asymmetry in the statical equilibrium of the system has striking importance for dynamic stability including the growth of subharmonic resonance and chaotic motions leading to capsize. This result was subsequently confirmed in model experiments.

Thompson [10,11], investigated the phenomenon of ship capsizing in regular seas using numerical simulation and emphasising the transient behaviour. He introduced the concepts of basin erosion and integrity curve to predict ship capsizing, while illustrating the effect of initial conditions on motions leading to capsize. This is an advance in relation to the steady-state analysis of the previous methods.

A major shortcoming of the deterministic methods is their inability to describe rolling in a probabilistic sense. Back in 1982 Roberts [9] studied the one degree of freedom rolling motion under random excitation using the stochastic averaging method. The results seem to be best suited for wide-banded excitations and moderate amplitude motions.

Francescutto[2], introduced the stochastic nature of the sea in the perturbation analysis for very narrow-banded seas leading to near synchronous and first subharmonic motions. In recent years, the time to capsize has been determined by treating the total system energy as a Markov process.

Recently, geometric methods have been applied to the study of nonlinear dynamics, especially when chaos is present. These methods emphasise the analysis of the qualitative differences in the behaviour of solutions. According with these methods such concepts as Melnikov function, phase space flux and chaotic transport

phenomenon were introduced, both to deterministic excitation and random excitation. The works of Thompson [10] and Falzarano, Shaw and Troesch [1] illustrate these concepts. Resulting from these works is the concept of safe basin as the space of initial conditions which lead to bounded motion.

The criterion for the initial conditions to be transported across the safety boundary was established for unbiased ships in regular beam waves, for unbiased ships randomly excited, [5] and for biased ships under a random excitation [7].

In this work a numerical solution of the one degree of freedom differential equation of roll will be attempted. First, the damping moment coefficient is estimated for the case in which nonlinear effects become significative. Then the nonlinear differential equation of roll motion is solved.

ESTIMATING THE NONLINEAR ROLL DAMPING

General

Damping is a complex mechanism of energy dissipation, which causes a variable decrease in the amplitude of motion of a body immersed in a fluid. In the specific case of the rolling motion of a ship caused by waves, large amplitudes may be reached, resulting in dangerous conditions for the ship operation. That is the reason why the correct estimation of the large amplitude rolling motions in a given sea state is very important.

In order to correctly analyse this problem there is a need to consider several intervening factors such as: nonlinearities in damping, in righting moment and the stochastic nature of the wave exciting moment.

Using the strip theory it has been possible to obtain all the hydrodynamic coefficients necessary to the solving of the second order differential equation of motion describing the roll motion of a ship. The exception is the damping coefficient in roll denoted as B_{44}.

The difficulties in obtaining this coefficient for large amplitude motion arise from three sources: the effect of the fluid viscosity, the effect of the bilge keels and the strong dependence of this coefficient on the velocity of the ship. These effects contribute to the total damping coefficient in approximately equal quantities, further complicating the problem. As a consequence, for large amplitude roll motion, the differential equation describing the rolling motion becomes nonlinear and has to be solved using some iterative method.

Linear and Nonlinear Representations of Damping

The behaviour of a floating ship is represented by a system of six differential equations. In general the equations are coupled but some coefficients may not be considered because of their small value. In beam seas the roll motion may be assumed as uncoupled by ignoring the coupling between heave and pitch due to bow-stern asymmetry. In arbitrary waves the above mentioned couplings have to be considered.

The differential equation is:

$$A_\phi \ddot{\phi} + B_\phi \dot{\phi} + C_\phi \phi = E_\phi (\omega t) \qquad (1)$$

where $A_\phi \ddot{\phi}$ represents the mass moment, $B_\phi \dot{\phi}$ the damping moment, $C_\phi \phi$ the righting moment and $E_\phi (\omega t)$ the heeling moment. Several characteristics of the nonlinear equations are:

- the characteristics of the response depend on the amplitude of the exciting term and of the initial conditions,

- a quasi-stochastic behaviour of the response in time may be observed in spite of the deterministic nature of the excitation.

- the steady-state response of the system is periodic but not sinusoidal and may contain harmonics and sub-harmonics.

- the jump phenomena due to the nonlinearity of the righting moment causes the response curve to distort towards one side causing an enlarged synchronism interval.

When the damping is considered to be linear the respective coefficient is independent of the roll amplitude and may be obtained easily using the logarithmic decrement obtained with the roll extinction test. When the oscillations become large or the model contains appendices the fluid separation and the viscosity become significative. In these conditions, the dissipative term cannot be represented in the simple form $B_\phi \dot{\phi}$ because it depends of the amplitude and velocity of the motion. There are several ways to represent the dissipative term as a third or fourth power of velocity, especially if the bilge keel is present. The power series is yet another way to represent the dissipative term:

$$B_n(\dot{\phi}) = B_1\dot{\phi} + B_2\dot{\phi}|\dot{\phi}| + B_3\dot{\phi}^3 + ... \qquad (2)$$

where the B_i coefficients are considered constant during the specific motion considered. Nevertheless, these coefficients depend on the amplitude of motion, frequency and mode of oscillation.

As the above mentioned differential equation is difficult to analyse there is the necessity of substituting the non-linear damping by a linearized term:

$$B_n(\dot{\phi}) = B_e\dot{\phi} \qquad (3)$$

where B_e represents the equivalent linear damping coefficient. This coefficient presents a dependence on the amplitude ϕ_A, wave encountering frequency ω_e and advance velocity. During an infinitesimal movement this coefficient is considered constant.

There are several forms to express the coefficient B_e in terms of the nonlinear coefficients B_1 and B_2. The most usual procedure is to assume the energy dissipation Δw during half cycle of roll to be the same whether one uses linear or nonlinear damping. Considering $B_\phi(\dot{\phi})$ approximated to the third power it can be demonstrated that:

$$B_e = B_1 + \frac{8}{2\pi}B_2\omega\phi_A + \frac{3}{4}B_3\omega^2\phi_A^2 \qquad (4)$$

This formula has been used in some simple methods to estimate the coefficient B_e for several hull types and desired advance velocities. To get more reliable values of B_e another method such as the component analysis method is required.

The Component Analysis Method

In this method the damping of a monohull of conventional forms in its service condition, with one shaft and one rudder, is divided into seven components. The main components are due to viscous effects, lift, vortex, wave radiation and bilge keel. The bilge keel component is further subdivided into three subcomponents: normal pressure in the hull, normal pressure in the bilge keels and wave.

Therefore:

$$B_e = B_f + B_L + B_E + B_w + B_{BKN} + B_{BKH} + B_{BKW} \qquad (5)$$

The interactions between the different components exist and either are taken into account in the formulas used to calculate the various components or are neglected if they can be considered very small.

The viscous component is caused by the shear tension in the surface of the hull. For its estimate the wave influence is neglected and the ship is considered as an axisymmetric body.

The lift component is caused by the lift acting over the ship hull when it advances at a velocity U and rolls simultaneously. An adequate calculation of this component is very difficult, even for a hull of conventional forms. Yumuro et al [17] introduced a simple formula, based on manoeuvrability tests, which calculates the damping moment M_L. More recently, Ykeda et al [16] developed a formula based upon the Yumuro formula. This formula fails for several types of ships, for low draft/beam (d/B) ratio hulls and for ships in a low displacement condition.

The vortex component for a bare hull is caused essentially by the vortices generated by the separation of the fluid in the bidimensional flow. The total component is obtained by integrating the sectional components along the length of the

ship. The separation occurs essentially in the bottom of the hull near the bow and stern and in the bilge along the parallel mid body. In the works by Inoue and Watanabe [14] the vortex damping component takes a nonlinear form $M_{RI} = B_2|\dot\phi|\phi$ where B_2 may be considered constant depending on the geometry of the hull and amplitude of oscillation. When the hull advances with a certain velocity the nonlinearity diminishes with the consequence that the damping due to this component becomes negligible for Fn>0.2.

The component due to wave radiation can be obtained for Froude number equal to zero, using the strip theory. In this method the component is evaluated for each section of the hull using the bidimensional solution of the problem. In case the ship is moving with non-zero velocity a hydrodynamic approximation which models the flow is used. Ikeda [6] estimated the radiation component for the three-dimensional forms of conventional ships advancing with non-zero velocity. This formula can be used to estimate the ratio B_W/B_{W0} and B_{W0} can be calculated using the strip theory. The method just described is not very precise for ships of full forms or which have low d/B ratios.

The bilge keel damping component is divided in three parts, namely: normal pressure in the hull, normal pressure in the bilge keels and wave. The wave component will be neglected since this is thought to be very small. The bilge keel component does not vary too much with velocity but one can note an approximation to linearity of this component as velocity increases. The normal pressure in the bilge keel subcomponent can be estimated using as a basis the experimental results obtained for plane shells oscillating in water (without velocity). Among the works in this field the one by Ikeda et al is most important [16].

Ikeda has also done research in the other subcomponent, i.e., the normal pressure in the hull, which is caused by the changes in pressure in the hull because of the bilge keels. Ikeda et al made tests with models to measure those variations in pressure in the hull.

For zero advance velocity, with the exception of the lift component, which is zero, all the other components are calculated by integrating their sectional values along the length of the ship. One can obtain, therefore, the longitudinal distribution of the damping components. For an advance velocity different from zero the formulas used only give values of the components for the whole ship.

There are, yet, some other points worth being mentioned. The component B_F may be affected by the presence of bilge keels and waves, which effects can be neglected. The component B_F does not include the effect of appendices or waves and represents a nonlinear component of lift. The B_L component represents the linear part of B_F. In the B_W component the interaction between the waves and lift, and the waves and vortices, is included. The B_{BKH} term represents the interaction between the hull and bilge keel and the B_{BKW} represents the interaction between the bilge keels and the surface wave. The B_W, B_L and B_F terms are linear and the B_F and B_{BK} are nonlinear. The scale effect is only present in the case of the B_F term, which is very small in the case of the real ship, since this component is between 1/20 and 1/30 that of the model.

NONLINEAR ROLL MOTION OF SHIPS IN REGULAR SEAWAYS

Linear Rolling Motion of Ships

In order to describe the linear rolling of ships a one degree of freedom linear ordinary differential equation is used:

$$a\frac{d^2\phi}{dt^2}+b\frac{d\phi}{dt}+c\phi = M_0.\cos(\omega_e t+\varepsilon_1) \qquad (6)$$

The virtual mass moment of inertia for rolling is:

$$a = I_{xx} = I_{xx} + \delta I_{xx} \qquad (7)$$

The mass moment of inertia can be estimated according with:

$$I_{xx} = k_{xx}^2 \Delta \qquad (8)$$

where k_{xx}^2 is the roll radius of gyration (between 0.25 and 0.4 the beam) and Δ is the ship mass.

The damping coefficient b due to wave making may be calculated by the strip method. However, as the ship moves through the water and if roll is large, the calculations done using the strip method may not be very accurate.

The restoring moment of a ship in rolling motion is the righting moment (transverse) at any particular angle of inclination:

$$c\phi = \Delta \, GZ \qquad (9)$$

For small angles of inclination:

$$c = \rho g \nabla \, GM \qquad (10)$$

This relationship may be taken as valid for small amplitudes of roll (up to 10°).

The exciting moment is calculated by integrating for each ship section the difference in buoyancy of the triangles resulting from the imerged and emerged edges. It may be demonstrated, for beam seas ($\mu=90°$), that:

$$M_\phi = M_0 . \cos(\omega_e t + \varepsilon_1) \qquad (11)$$

where:

$$\varepsilon_1 = -\frac{\pi}{2} \qquad (12)$$

and

$$M_0 = \rho g \nabla k \xi_a GM = \rho g \nabla \alpha_M GM \qquad (13)$$

Therefore, it may written:

$$M_0 = \Delta . GM . \alpha_M . \sin(\omega_e t)$$

$$(14)$$

The above expressions may now be substituted in the differential equation obtaining:

$$\phi + 2\nu\dot{\phi} + \omega_\phi^2 \phi = \alpha_M \omega_\phi^2 \sin(w_e t) \qquad (15)$$

where:

$$2\nu = \frac{bg}{\Delta_1 k_{xx}^2} \qquad (16)$$

$$\Delta_1 = \Delta + \Delta \qquad (17)$$

$$\omega_\phi^2 = \frac{\Delta . GM \, g}{\Delta_1 k_{xx}^2} \qquad (18)$$

α_M – maximum effective wave slope

Δ_1 - added weight

which is a linear second order differential equation. This is a good approximation up to 8° of roll

Nonlinear Roll Motion of Ships

General

The general equation for nonlinear rolling in a regular seaway can be:

$$a\ddot{\phi} + B(\phi, \dot{\phi}) + c(\phi.t) = M(\omega_e . t) \qquad (19)$$

Considering the mass moment of inertia constant, the different damping contributions separable, the restoring moment $c(\phi,t)$ which can be described by a polynomial of the suitable degree and the wave exciting moment as $M_0 \cos(\omega_e t)$:

$$I_{xx}'\ddot{\phi} + b_1\dot{\phi} + b_2|\dot{\phi}|\dot{\phi} + c_1(t)\phi + c_3(t)\phi^3 + c_5(t)\phi^5 + ... = M_0 \cos(\omega_e t)$$

$$(20)$$

where I_{xx}' is the coefficient of virtual mass moment of inertia, b_1 and b_2 are the damping coefficients, $c_1(t)$, $c_3(t)$, $c_5(t)$ are the restoring moment coefficients and $M_0 \cos(\omega_e t)$ is the wave exciting moment.

The coefficients of the restoring moment can be determined by fitting the stability curve with a polynomial containing only odd power terms. The dissipation term (damping moment) includes a linear damping term associated with waves produced by the hull and a quadratic damping term associated with frictional resistance and eddies behind bilge keels and hard bilge corners. The wave exciting moment is closely approximated by the cosine expression in the differential equation as long as the length of the wave is large compared to the ship breadth.

In order to solve this equation, a number of distinct cases. in what regards the linear or nonlinear coefficients. can be considered. These cases are:

- Linear equation of motion: $b_2 = c_3 = c_5 = 0$ c_1 constant.

- Linear damping, nonlinear restoring moment with constant coefficients: $b_2 = 0$; c_1, c_3, c_5 constant,

- Nonlinear damping, linear restoring moment: $c_3 = c_5 = 0$; c_1 constant,

- Linear damping, linear restoring moment: $b_2 = c_3 = c_5 = 0$; c_1 function of time

In this work a small variant from the second case will be considered. Therefore, the nonlinear roll motion of biased ships will be studied. considering a linearized damping coefficient, which takes into account some nonlinear effects and a nonlinear restoring moment.

Analytical Solution of the Nonlinear Differential Equation of Roll

Using the perturbation methods, an analytical solution of the rolling motion differential equation may be calculated.

Consider, first, that there is no damping:

$$\ddot{x} + \omega_0^2 (x + \varepsilon x^3) = f_0 \cos(\omega_e t) \qquad (21)$$

It may be assumed that the solution is of the following form:

$$x(t) = u \cos(\omega t) + v \sin(\omega t) \qquad (22)$$

For this differential equation it can be demonstrated that:

$$\omega = \pm \sqrt{\omega_0^2 (1 + \frac{3}{4}\varepsilon A^2) - \frac{f_0}{A}} \qquad (23)$$

If the damping term is considered then the differential equation will be:

$$\ddot{x} + h\dot{x} + \omega_0^2 (x + \varepsilon x^3) = f_0 \cos(\omega_e t) \qquad (24)$$

and there would be a somewhat more complicated expression:

$$\omega^2 = \frac{1}{2}\left[2\omega_0^2(1+\frac{3}{4}\varepsilon A^2)-h^2 \pm \sqrt{h^4 -4\omega_0^2 h^2(1+\frac{3}{4}\varepsilon A^2)+4\frac{f_0^2}{A^2}} \right] \quad (25)$$

Equations (23) and (25) define the so called response curves which plot $|A|$. the modulus of the amplitude of the nonlinear roll, as a function of ω_e, the encounter frequency Several remarks and conclusions may be drawn.

The quantity A is negative on the response curves to the right of the curve for $M_0 = 0$ and positive to the left of it.

The motion is in phase with the external moment or $180°$ out of phase with it, according to whether the frequency is greater or lesser than the frequency for free oscillation.

Provided the excitation is sufficiently strong, the response is multivalued in a certain frequency range. i.e., it has three values.

Where the response curve is multivalued, the intermediate value corresponds to an unstable motion, which therefore cannot be observed, because any infinitesimal disturbance will grow and will lead the amplitude towards one of the stable values.

The appearance of one or the other of the stable values in the steady-state oscillation is determined by the initial conditions of the motion.

The response curve will twist to the right if $\varepsilon > 0$ and the opposite side if $\varepsilon < 0$.

The presence of a nonlinearity in the righting moment introduces a new phenomenon in the response called jump or hysteresis. The consequence of this is the already referred conclusion that the roll motions corresponding to points on the response curves between the vertical tangents are unstable.

The effect of the nonlinear restoring moment is that the natural period $2\pi/\omega_\phi$ for the linear equation is not constant but varies with the roll angle.

As already mentioned. the steady-state solution for which the vessel is attracted depends on the

initial conditions. This allows a partition of the phase plane into different regions, each corresponding to a particular steady-state solution. In general, it can be drawn a curve in the phase plane which separates the two regions. The points inside the curve attract the system to the greater amplitude steady-state solution while the points outside the curve attract the system towards the lesser amplitude steady-state solution.

A perturbation (a gust of wind) can bring the system for an even small instant of time to the external domain. Once there the system will remain there and evolve to the larger solution. From the dimension of the domains of attraction one can have an idea about the probability of occurrence of the two amplitudes, which are very different.

While for roll motion with linear restoring moment the frequencies of forced motion are always equal to the encounter frequencies, with nonlinear restoring moment the forced oscillation may have a frequency lower than the encounter frequency. There are several resonance conditions in addition to the synchronism. Among the predominant resonances there is an ultraharmonic for $\omega = \omega_0 / 3$ and a subharmonic for $\omega = 3\omega_0$. In these frequency regions the rolling oscillation consists of two terms, one which has the frequency of the excitation and other which has a frequency close to the fraction or multiple of the natural frequency in consideration.

The ultraharmonic and subharmonic resonances are generated by an appropriate coupling between the natural and forced oscillation, due to the nonlinearity of the righting moment. The ultraharmonic resonance corresponds to the coupling between the forced oscillation and itself, while the subharmonic resonance is generated by a coupling between the forced oscillation and the natural one. The corresponding tuning factors may fall in the energetic zone of the sea spectrum, so the practical occurrence of this resonances cannot be neglected.

Nevertheless, the ultraharmonic resonance will, most probably, not constitute a serious danger for the stability of the ship. The subharmonic resonance can have a relevant amplitude, as has been observed in model experiments, and may constitute a serious danger for the ship stability

Numerical Solution of the Nonlinear Differential Equation of Roll

The basic equation for the one degree of freedom nonlinear roll motion of a biased ship, is·

$$I_{xx}(w_e)\ddot{\phi} + b_1\dot{\phi} + \Delta GZ = M_i + M_0\cos(\omega t) \qquad (26)$$

where ϕ is the roll angle, I_{xx} is the virtual mass moment of inertia (including the added mass moment), ΔGZ is the restoring moment. M_i is the static heeling moment acting in the ship and $M_0 \cos(\omega_e t)$ is the wave induced external heeling moment acting on the ship.

Substituting equation (13) in equation (26) and multiplying and dividing the restoring term by GM, dividing all terms by I_{xx} and using (18), leads to:

$$\ddot{\phi} + b\dot{\phi} + \omega_\phi^2\left(\frac{c_1}{GM}\phi + \frac{c_3}{GM}\phi^3\right) = m_i + f_0\cos(\omega t) \qquad (27)$$

where:

$$b = \frac{b_1}{I_{xx}} \qquad (28)$$

$$\omega_\phi = \left(\frac{\Delta . GM}{I_{xx}}\right)^{1/2} \qquad (29)$$

$$m_0 = \frac{M_i}{I_{xx}} \qquad (30)$$

$$f_0 = \alpha_e . \omega_\phi^2 \qquad (31)$$

$$\alpha_e = \frac{2.\pi\xi_a}{\lambda} = k\xi_a \qquad (32)$$

APPLICATION TO THE STUDY OF FISHING VESSELS

The theoretical background above mentioned was implemented in a computer program

The method of component analysis needs as input the main particulars of the ship, the geometry of the hull and the nondimensional wave radiation coefficients B_{WO} as a function of the nondimensional wave encounter frequency. The results consist of the nondimensional coefficient B_E in function of the Froude number, nondimensional wave encounter frequency and amplitude of rolling; longitudinal distribution of the C_R (nondimensional coefficient of the damping moment of separation) and B_{BK} (nondimensional bilge keel damping coefficient) coefficients

Using this program, three models of fishing vessels, whose main particulars are listed in table 1, were studied. All three ships were considered in nearly full displacement service condition.

Table 1 - Test ships main particulars

S 1	V (t)	L_{pp} (m)	B (m)	T (m)	ω_n(rad/s)	C_B	Fn	b_{bk}/B	l_{bk}/L
Large Trawler	2833.2	70.00	13.20	5.20	0.866	1.50	0.274	0.015	0.25
Small Trawler	23.7	1.0	1.15	3.00	1.417	0.51	0.356	0.015	0.25
Long liner	1.33	4.4	8.0	3.41	5.54	0.52	0.370	0.015	0.25

The results obtained for these three models are presented in figures 1, 2 and 3. These graphics represent the adimensionalized Be coefficient in function of the Froude Number, wave encouter frequency and amplitude of the rolling motion.
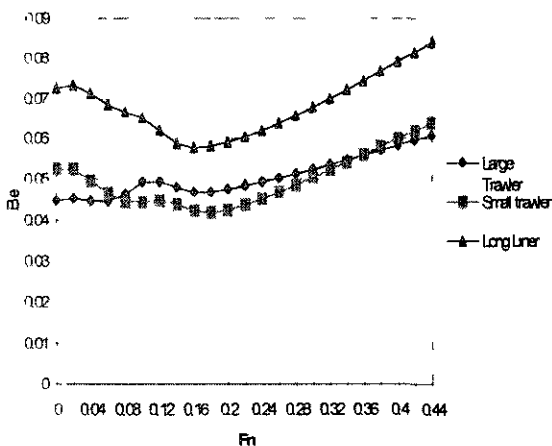
Figure 1 - Linear Equivalent Damping Coefficient versus Froude Number
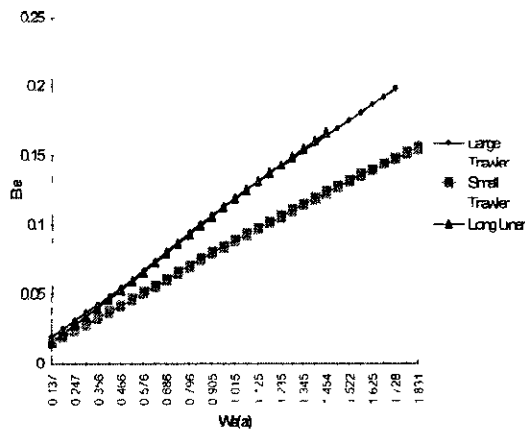
Figure 2 - Linear equivalent damping coefficient versus nondimensional wave encouterfrequency

The adimensionalized Be coefficient of the graphics multiplied by $\rho\nabla B^2\sqrt{\dfrac{2g}{B}}$ will give the equivalent linear damping coefficient The Froude Number is given by the well known expression $F_n = \dfrac{v}{\sqrt{gL}}$. The graphic in figure 2 was obtained considering a Froude Number of zero.
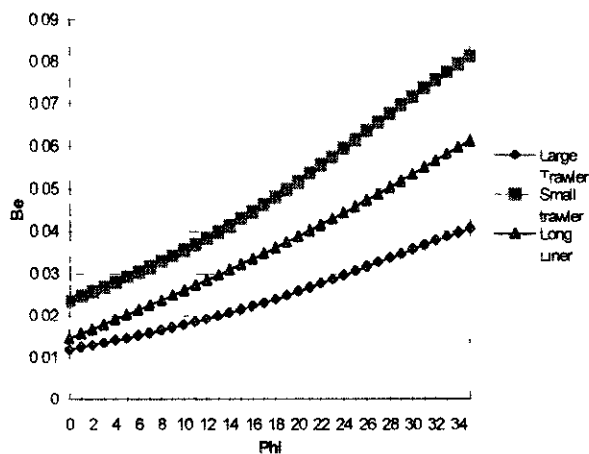
Figure 3 - Linear equivalent damping coefficient versus roll motion amplitude

This program can calculate the time response by a Runge-Kutta 4th Order Method while searching for the steady-state solution, as well as the response curves and attraction domains. It also calculates an analytical solution for the response curves using equation (25) and calculates

171

numerically a linear solution of the differential equation

Numerical calculations were carried out with the same models used for the linear equivalent damping calculations. The coefficients used in equation (27) were.

1 The linearized damping coefficients were obtained from figure 2, considering a maximum amplitude of 35°, an excitation frequency equal to the natural frequency and no velocity,

2 The virtual mass moments of inertia were taken as about $1.2 \times I_{xx}$, that is, considering an added moment of inertia of 20% (a standard procedure), where I_{xx} was calculated according with formula (8) taking k_{xx} approximately as 25% of the beam.

3 The natural frequencies, ω_0, were calculated according with (29),

4 The polynomials used to approximate the GZ curve were not odd power polynomials but rather a best-fit polynomial approximation of the static stability curve,

5 The amplitude of the wave excitation moment was calculated according with expressions (31) and (32),

6 The static bias term was not considered.

The results for the large trawler are summarised in figures 4, 5 and table 3

Figure 4 shows one example of the type of time domain simulations of the roll motion obtained for the large trawler In that figure, the transient phase of the movement may be observed and then the steady-state phase corresponding to the stabilisation of the movement.

Figure 5 shows the response curves for several wave excitation coefficients. In that figure it may be seen that as the wave excitation coefficient increases, the amplitude of the response also increases, as could be expected.
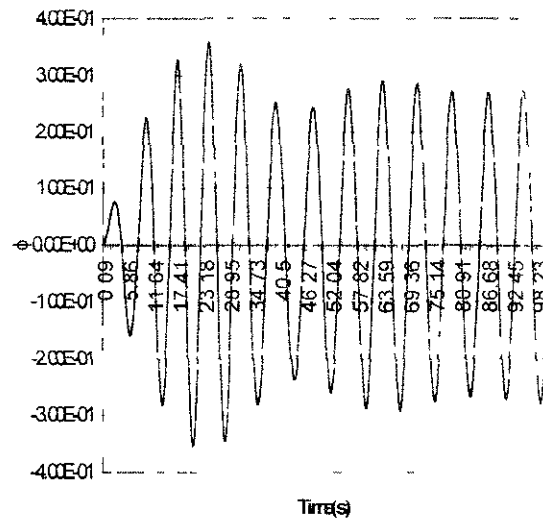
Figure 4 - Time history of the nonlinear ship rolling for the large trawler
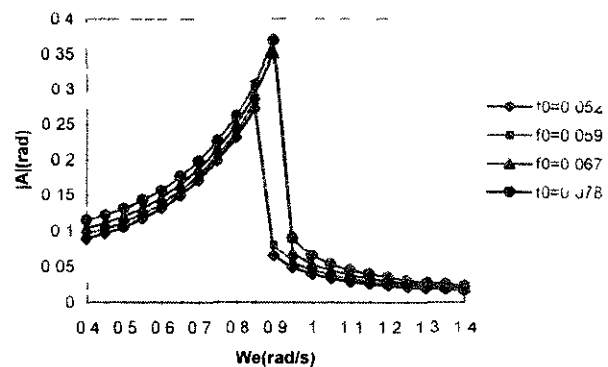
Figure 5 - Response curves amplitude versus wave encounter frequency for the large trawler

Table 3 (in Appendix) shows the steady-state amplitude of motion for systematical variations of the initial conditions. In that table it may be seen yet another interesting feature of the nonlinear roll motion, which is the dependence of the steady-state response on the initial conditions of the simulation The table represents in each column an initial displacement from the upright position and in each line an initial velocity. The values in the table represent the amplitude of the response in radians The initial displacements represented are comprised between -0.5 and +0.5 rad (-28° and +28°) and the initial velocities are comprised between -0.5 and +0.5 rad.s^{-1}, which are perhaps a little too extreme values of velocity. The instability of the

obtained responses can also be observed in the lower part of the table. In that region, a wide range of intermediate responses is shown. From table 3 and from figure 5 we may also conclude that, provided the excitation is sufficiently strong, the response can have several different values leading to the jump phenomena.

Figure 6 represents the response curves for the small trawler. In that figure the amplitude of the response of the small trawler increases a little as the wave excitation coefficient increases.
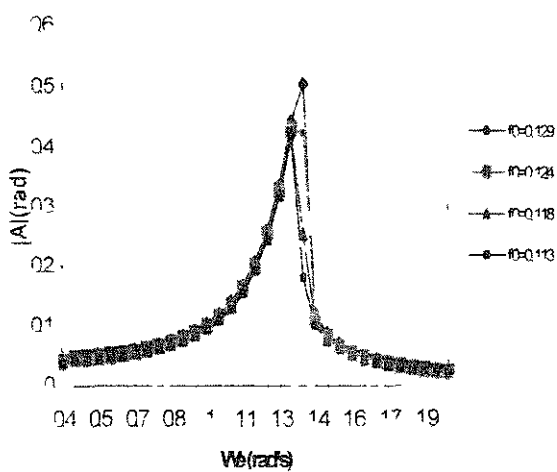
Figure 6 - Response curves for the small trawler
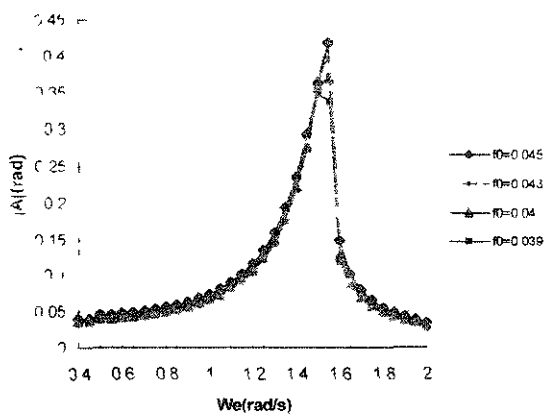
Figure 7 - Response curves for the long liner

Figure 7 represents the response curves for the long liner. For the long liner it may be seen that, as the wave excitation coefficient increases, the response of the long liner also increases.

It may be concluded that, for the two small fishing vessels studied, their response to nearly similar beam seas will have the same order of magnitude. The differences in the peak region are not very significant as this area is very dependent of the initial conditions.

APPLICATION TO THE STUDY OF A FISHERY RESEARCH VESSEL

Some studies were undertaken with an ocean research vessel, whose main particulars are listed in the following table.

Table 2 - Fishery research vessel main particulars

S.D.	L	Lpp (m)	b	B	(1ad s		D, B	S, t
Fishery Research	4.7	40.5	9.1	6.2	8.5	3.5	26.4	5

For this ship several odd power approximations of the stability curve were used. Once again, a near full service condition was selected. A comparison between two polynomials describing the righting arm curve was made to see any differences, which might occur in the response curves. The two polynomials are of the third and ninth degree. Comparisons between the results were made for the upright and 8° heeled ship.

b = 0.172 wo = 0.785 e = -1.56 fo = 0.06
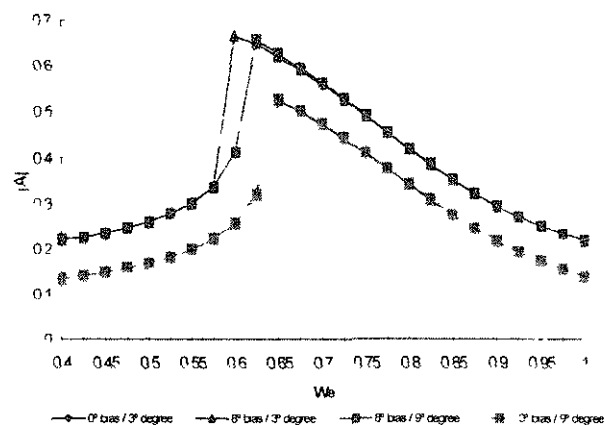
Figure 8 - Comparison of the third and ninth degree polynomials when the nondimensional excitation amplitude is 0.06 and the ship is upright and 8° heeled

The conclusion which may be drawn from figure 8 is that the two polynomials give almost equal response curves both when the ship is upright

173

ind biased (8° in this case), so the third degree polynomial is well suited for this study. The difference shown in the 8° biased position in the resonance domain is natural because that zone is heavily dependent on the initial conditions.

h = 0.172 wo = 0.785 e = -1.56 mo = 0.0 xo = 0.0 vo = 0.0
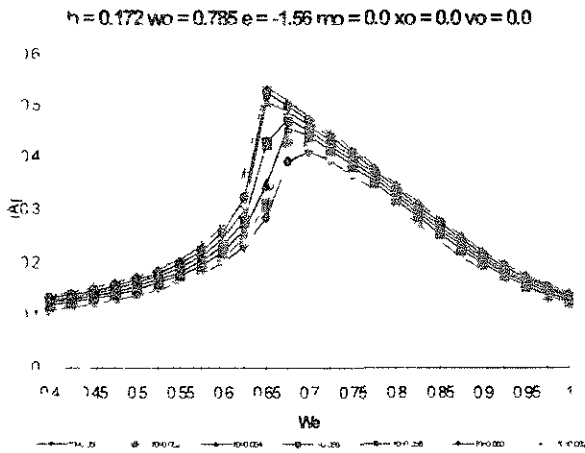
Figure 9 - Comparison of the response curves for several excitation amplitudes
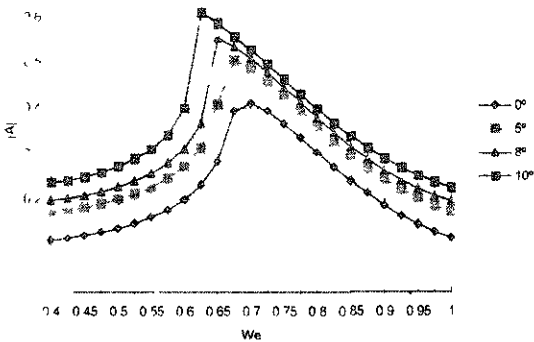
Figure 10 - Comparison of the response curves for several static bias angles and excitation amplitude (fo) of 0 05

In figure 9 response curves for several excitation amplitudes are shown As could be expected, and was previously noted for the large trawler, the amplitude of response increases as the excitation amplitude increases. In figure 9 it may be seen that for the case of the ocean research vessel this effect is somewhat clearer than for the fishing vessels previously studied.

In figure 10 response curves for several static bias angles are shown. It may be seen that as bias angles are shown. It may be seen that as

the static bias increases the amplitude of the response also increases

In figure 11 the time domain simulation of the response of the fishery research vessel may be seen when it is initially heeled to 8° One can note that the steady state response will develop around a medium value of 0 14 rad. which corresponds to the 8° bias

Figure 11 - Time domain simulation of the heeled ship motion

Finally, a systematic series of runs was made varying the initial bias and the wave excitation coefficient f_0. For each combination of these two factors and for a wave encounter frequency of 0.62 rad.s^{-1} the attraction domains were calculated. For reasons of space only the conclusions drawn from this study are presented

It was observed that for small wave excitation moments there was no attraction to the large amplitude steady-state response. As the wave excitation was increased the attraction domain to the large amplitudes became apparent The number of combinations of initial conditions that lead to large amplitude responses increased steadily as the wave excitation was increased

When an initial static bias was considered, the attraction domain towards the large amplitude response clearly increased, for the same value of the wave excitation moment. The attraction for large amplitude responses also showed up earlier (for smaller values of the wave excitation) For example, the attraction domain for large amplitudes with $f_0 = 0.059$ and a static bias of 5° is nearly equal to that for $f_0 = 0.062$ and a static bias of 0°.

It was also observed a very clear boundary between those initial conditions that lead to one of the two possible steady-state responses and those who lead towards capsize. Clearly, high values of both initial displacement and initial velocity lead, quite probably, to capsize

CONCLUSIONS

A numerical solution procedure (Runge-Kutta Fourth Order Method) for the one degree of freedom rolling motion differential equation was implementeded. A linearized equivalent damping coefficient was used. In the analysis of some fishing vessels with these techniques a number of interesting features was observed.

As regards the simulation results, it was found that as the wave excitation increases the response also increases, as is well known. If no critical displacement from the equilibrium position is reached, after an initial transient phase, the movement stabilises in the so-called steady-state response.

The steady-state response is multivalued in the sense that in the synchronism region there can be two possible responses of different amplitudes.

The amplitude of the actual response depends on the initial conditions of the movement. In the systematic calculations carried on, the domains of attraction in the phase-plane were clearly identified.

The influence of a static bias in the response was found to be an increase in the domain of attraction for the large amplitude response. It was also observed that this response oscillates around the angle of the static bias, as might be expected.

ACKNOWLEDGEMENTS

REFERENCES

1. Falzarano, J. M., Shaw, S.W. and Troesch, A.W., 1992, Application of global methods for analysing dynamical systems to ship rolling motion and capsizing. International Journal of Bifurcation and Chaos, 2, 1, 101-115

2. Francescutto, A. 1990, On the nonlinear motions of ships and structures at narrow band seas. Proceedings, IUTAM Symposium on the Dynamics of Marine Vehicles and Structures in Waves, London, 291-304

3. Himeno, Y., Prediction of ship Roll Damping - State of Art, report n° 239, Sept. 1981. Univ. of Michigan

4. Hsieh, S.R., Troesch, A.W. and Shaw, S W., 1994, A nonlinear probabilistic method for predicting vessel capsizing in random beam seas. Proceedings of the Royal Society of London, Series A-446, 1-17

5. Ikeda, Y., Himeno, Y., Tanaka, N., A prediction method for ship Roll Damping, report n° 0045, Dec. 1978, Univ. of Osaka

6. Jiang, C., Troesch, A. W., Shaw, S.W., 1996, Highly Nonlinear Rolling Motion of Biased Ships in Random Beam Seas. Journal of Ship Research, Vol. 40, n° 2, pp. 125-135

7. Nayfeh, A.H. and Khdeir, A.A. 1986. Nonlinear rolling of biased ships in regular beam waves. International Shipbuilding Progress, 33, 381, 84-93.

8. Roberts, J. B., 1982. A stochastic theory for nonlinear ship rolling in irregular seas. Journal of Ship Research, 26, 4, 229-245

9. Thompson, J. M. T., 1989, Loss of engineering integrity due to the erosion of absolute and transient basin boundaries Proceedings IUTAM Symposium on the Nonlinear Dynamics in Engineering Systems

10.Thompson, J M T., 1990. Transient basins. a new tool for designing ships against capsize. *Proceedings, IUTAM Symposium on the Dynamics of Marine Vehicles and Structures in Waves*, London, 325-331

11.Thompson. J M T.. 1989. Chaotic phenomena triggering the escape from the potential well. *Proceedings of the Royal Society of London*. Series A-421, 195-225

12.Virgin L. N.. The Nonlinear Rolling Response of a Vessel Including Chaotic Motions Leading to Capsize in regular Seas. *Applied Ocean Research*, 1987, vol. 9, n°2

13 Watanabe, Y. and Inoue. S.. Calculation Method for N value of Ship Rolling, *Trans West-Japan SNA*. vol. 14. 1957

14.Wright. J.H and Marshfield. W.B 1979. Ship roll response and capsize behaviour in beam seas *Transactions of the Royal Institute of Naval Architects*. **122**, 129.

15 Ikeda. Y , Himeno. Y.. Tanaka. N , Components of Roll Damping of Ship at Forward Speed. *Journal of the society of Naval Architects of Japan*, vol 143 (1978), p. 113

16 Yumuro and Mitzutani. A study on Anti-rolling fins (2), I. *Harima Engineering Review*, vol. 10 n° 2, 1970

APPENDIX

Table 3 - Fishery research vessel attraction domains

				1	1	1	1	1	1	1	1	1	1	1	1		1		
				J 049	J 049	049	U 049	U 049	U 049	U 049	J 048	J 048	U 048	1		1		
			J 048	J 048	0 048	0 049	0 049	0 049	0 049	J 049	0 048	0 048	U 048	U 05	05	1		
		049	U 048	U 048	U 048	0 048	U 048	0 049	J 049	049	0 049	U 048	J 48	J 049	U 05	049	04		
	U 049	J 049	J 049	J 048	0 048	U 048	U 048	J 049	0 049	U 049	0 049	0 048	U 048	J 049	U 05	U 048	047	0 04	
	J 049	U 049	U 049	J 049	0 049	U 049	U 048	J 048	U 049	U 049	U 049	0 049	U 048	0 05	0 049	0 04	U 049	052	05
J 049	U 049	U 049	J 049	0 049	J 049	U 049	J 049	J 048	J 048	0 049	0 049	0 049	J 048	0 05	0 048	0 047	J 051	05	J 04
	J 049	J 049	U 049	J 049	U 049	0 049	0 049	J 049	J 049	J 049	U 048	U 049	0 049	U 048	U 049	0 048	U 049	05	U 044	04
J 049	J 049	J 049	J 049	U 049	0 049	0 049	0 049	0 049	0 049	0 049	0 049	0 048	0 049	0 049	0 049	0 047	J 051	0 045	0 048	0 056
U 049	J 049	U 049	U 049	U 049	0 049	0 049	0 049	0 049	J 049	U 049	U 049	J 049	J 048	U 049	J 049	J 047	U 051	U 046	U 05	05
048	049	U 049	J 049	U 049	J 049	0 049	0 049	0 049	0 049	0 049	0 049	0 049	0 049	U 049	J 049	J 047	0 046	J 056	U 046	03
J 04	J 049	J 049	J 049	J 049	U 049	U 049	J 049	J 049	U 049	J 049	J 049	0 049	J 049	049	05	0 047	J 047	0 04	06
049	U 048	U 049	J 049	J 049	J 049	U 049	U 049	J 049	U 049	0 049	0 049	0 048	049	05	U 05	0 056	U 043	U 067	062
049	049	J 049	U 049	U 049	0 049	J 049	U 049	J 049	U 049	U 049	J 049	J 049	U 048	0 049	0 051	0 039	J 067	04	04
J 04	J 048	U 049	U 048	U 049	J 049	J 049	U 049	J 049	U 049	U 048	J 049	U 048	J 04	J 044	0 038	U 065	045	0 04	06
05	J 049	J 049	J 049	J 049	J 048	U 049	U 049	U 049	048	049	U 048	J 05	J 049	U 046	J 038	U 06	U 034	J 073	09
U 04	04	0 049	U 048	U 049	J 048	U 049	U 049	J 048	U 049	0 049	U 05	0 044	0 054	0 062	J 043	0 071	0 097	0 09	0 09	1
	J 07	J 065	J 055	J 049	U 051	U 049	U 049	J 052	U 044	056	039	0 068	U 045	J 072	J 096	0 074	J 067	J 067	
	1	0 067	U 07	0 041	J 067	0 057	0 063	U 065	0 043	U 058	09	0 09	0 063	0 072	0 069	U 061	U 057	1	1	
	1		34	0 042	0 077	0 067	J 067	J 075	0 063	0 045	0 074	0 092	U 104	U 111	U 114	0 113	1	1	1	1
		1		U 214	J 199	0 188	0 184	U 185	U 187	J 189	U 187	0 184	U 18	J 175			1			
	1					0 234	J 231	0 229	0 226	0 222	1				1	1			
		1			1	1	1	1	1	1	1	1		1	1			1	1

177

A TWO-DIMENSIONAL MODEL FOR THE PREDICTION OF THE BEHAVIOUR
OF TOWED UNDERWATER VEHICLES IN MARINE RESEARCH

Mathias Paschen
Institute of Naval Architecture
and Ocean Engineering,
University of Rostock
Albert-Einstein-Str. 2
18051 Rostock
Germany

ABSTRACT

The present paper deals with the prediction of motions of steerable towed underwater vehicles which may serve as carrier for sensors, hydroacoustic transducers or photographic and video devices preferably used for research and surveying purposes.

Motions in towing direction are investigated and motions vertical to towing direction as well as rotations around the transverse axis. The restriction to three degrees of freedom is not critical and suitable for most practical applications without neglecting the main physical relations.

The solutions of linearized equations of motion are taken to assess the stability of positions of equilibrium of the towed vehicle. They form the basis for a reliable analysis of the quantitative influence of single physical parameters on the motion pattern. The temporal constants are required in order to dimension appropriate controllers. The solutions of the complete equations of motion by means of numerical integration are of minor importance in this paper and can be regarded as verification of the simplified linearized model.

1. INTRODUCTION

Highly different interests from various fields as maritime economy including tourism, marine research related to natural sciences, maritime environmental protection or underwater archeology are shown by a rising request for multimedia data of aquatic spheres.

Controllable towed underwater vehicles are often used as carrier systems for the required sensors, hydroacoustic transducers, photographic and video devices. The properties and characteristics of those vehicles as there are manoeuvrability, stability and so on are important not only for the reproducibility of measurements and for the quality of measuring results but also for the security of the valuable technical measuring and observation devices and systems.

Engineering methods for analysing the motion pattern of submerged measuring probes, shearing dragon gears and similar vehicles of the most various application and construction characteristics - free-running or towed with ropes and cables - have been known for several decades. Not to mention all, we'd like to refer to some remarkable publications by **Schmiechen** (1964), **Niemann** (1967), **Karpenko** (1973), **Kröpelin** (1978), **Egorov** (1981), **Klingbeil** (1983) and **Majohr and Korte** (1995).

The basis of these investigations are mostly extensive non-linear and partly partial systems of differential equations of higher order. Solutions can generally be given only by means of numerical methods.

Simple analytical setups for the solutions as they were given for example by **Horn** and **Reckling** (1953) and by **Schmitz** (1961) for steered motions of ships on a smooth water

surface are advantageous for sizing the main dimensions and for forming the control circuits required for steering the towed vehicles.

It is the objective of this paper to find a mathematically and physically simple setup fulfilling the requirements mentioned above at a satisfactory accuracy. Here the author also refers to own papers ((**Paschen** (1983), (1985) and (1990)).

2. MATHEMATICAL MODELLING

The motion of a towed device carrier can be characterized in only three degrees of freedom - in the vertical plane of a infinitesimal, homogeneous fluid being calm in infinity, as translation in the z_1 - z_3 - plane of the space-fixed coordinate system and as rotation around the transverse axis. The motions of the towing vehicle have supposed to be known in point P. The towing cable is considered as massless and of infinitesimal minimum thickness and is connected in a suitable way

with the towed vehicle having no moments (cf Fig. 1).

The body-fixed x_i - coordinate system with $i = 1...3$ is preferred. The coordinate axes coincide with the main axes of inertia. The origin lies in the common centre of gravity of body mass and hydrodynamic mass For flooded bodies the water mass inside the device must be regarded

Taking these assumptions into account the equations of motion (1) are obtained (next page).

m is the mass of the device carrier, m_{11} and m_{33} are the hydrodynamic masses during the motion in x_1 or x_3 direction. I_{22} and J_{22} are the mass moment and the hydrodynamic moment with respect to the x_2 axis. κ is the body's angle of attack. The pitching angle α is the angle forming between the body's longitudinal axis and the direction z_1. Its temporal derivatives $d\psi/dt$ and $d^2\psi/dt^2$ are angular velocity and angular acceleration, respectively, and they are defined to be positive in x_2 direction.
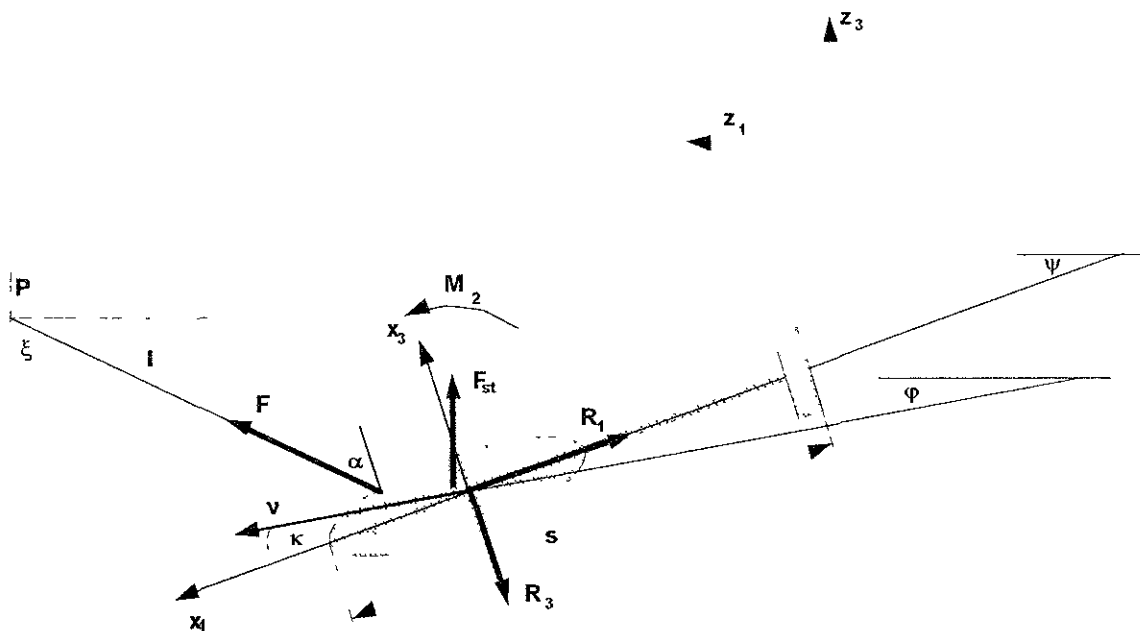
Fig.1:
Two-dimensional presentation of a submerged towed vehicle without flapped fins

182

$$\left(m + m_{11}\right)\left(\frac{dv}{dt}\cos\kappa - v\,\frac{d\kappa}{dt}\sin\kappa\right) + \left(m + m_{33}\right)v\,\frac{d\psi}{dt}\sin\kappa = F\sin\alpha - F_{st}\sin\psi - R_1$$

$$\left(m + m_{33}\right)\left(\frac{dv}{dt}\sin\kappa + v\,\frac{d\kappa}{dt}\cos\kappa\right) - \left(m + m_{11}\right)v\,\frac{d\psi}{dt}\cos\kappa = F\cos\alpha + F_{st}\cos\psi - R_3 \quad (1)$$

$$\left(I_{22} + J_{22}\right)\frac{d^2\psi}{dt^2} - \left(m_{33} - m_{11}\right)\sin\kappa\cos\kappa\,v^2 =$$

$$\left(-\zeta_1\cos\alpha + \zeta_3\sin\alpha\right)F - \left(\lambda_1\cos\psi + \lambda_3\sin\psi\right)F_{st} + M_2$$

The last term of inertia of the momentum equation is the so-called unstable momentum, occurring in real media only in half the amount.

In the following it will be combined with the momentum M_2 on the right side and not be mentioned separately.

On the right side of the equation there are the tensile force F of the towing cable and the static force F_{st} - resulting from the buoyancy and the weight of the device carrier. The corresponding leverarms are given by the coordinates ζ_1 and λ_1.

The forces and moments R_1, R_3 and M_2 resulting from the flow around the towed vehicle are determined by

$$R_i = \frac{1}{2}\,c_i(\kappa,\,k,\,\delta_j)\,\rho v^2 A$$

$$M_2 = \frac{1}{2}\,c_2(\kappa,\,k,\,\delta_j)\rho v^2 A\,s \quad (2)$$

The hydrodynamic coefficients c_i do not only depend on the body's shape and the Reynold's number but also on the inclination angle κ and the rudder angles δ_j. The damping is considered by the non-dimensional factor k

$$k = \frac{\dfrac{d\psi}{dt}\,s}{2\,v} \quad (3)$$

In the special literature this expression is explained in two different ways. With respect to flow induced vibrations of the body k is named as reduced frequency (**Mahrenholtz** (1986)). In papers on steered ship motions it is more common to have the term

'nondimensional curvature of path' Ω with Ω-2 k for expression (3) (**Schmitz** (1961)).

α is the angle of deviation of the towing cable related to the x_1 - x_3 coordinate system. ζ_1 and ζ_3 are the components of the point of application of the towing cable in the body-fixed coordinate system. The vertical distance between the buoyancy and the weight of the device carrier is given by λ_3. The horizontal distance of both to the origin of the coordinate system is λ_1.

The position of the centre of gravity of the towed vehicle is determined by the location of the leading point P knowing the length l and the deviation ξ of the towing cable

$$z_1^s = z_1^P - l\sin\xi - \zeta_1\cos\psi - \zeta_3\sin\psi$$

$$z_3^s = z_3^P - l\cos\xi + \zeta_1\sin\psi - \zeta_3\cos\psi \quad (4)$$

The relation between the motion of the leading point P and the motion of the towing vehicle's centre of gravity can be described in a simplified way

$$v_1^s = v\cos\varphi =$$

$$v_1^P - l\cos\xi\frac{d\xi}{dt} + \left(\zeta_1\sin\psi - \zeta_3\cos\psi\right)\frac{d\psi}{dt}$$

$$\quad (5)$$

$$v_3^s = -v\sin\varphi =$$

$$v_3^P + l\sin\xi\frac{d\xi}{dt} + \left(\zeta_1\cos\psi + \zeta_3\sin\psi\right)\frac{d\psi}{dt}.$$

A repeated differentiation to time t provides

$$\frac{dv}{dt}\cdot\cos\varphi - v\frac{d\varphi}{dt}\sin\varphi = \frac{dv_1}{dt} - l\cos\xi\,\frac{d^2\xi}{dt^2} + l\sin\xi\left(\frac{d\xi}{dt}\right)^2 +$$

$$+ \left(\zeta_1\sin\psi - \zeta_3\cos\psi\right)\frac{d^2\psi}{dt^2} + \left(\zeta_1\cos\psi + \zeta_3\sin\psi\right)\left(\frac{d\psi}{dt}\right)^2$$

$$-\frac{dv}{dt}\sin\varphi - v\frac{d\varphi}{dt}\cos\varphi = \frac{dv_3}{dt} + l\sin\xi\,\frac{d^2\xi}{dt^2} + l\cos\xi\left(\frac{d\xi}{dt}\right)^2 +$$

$$+ \left(\zeta_1\cos\psi + \zeta_3\sin\psi\right)\frac{d^2\psi}{dt^2} - \left(\zeta_1\sin\psi - \zeta_3\cos\psi\right)\left(\frac{d\psi}{dt}\right)^2$$

(6)

with the following geometric and kinematic interactions

$$\varphi = \psi - \kappa \qquad\qquad \xi = \psi + \alpha$$

$$\frac{d\varphi}{dt} = \frac{d\psi}{dt} - \frac{d\kappa}{dt} \qquad \frac{d\xi}{dt} = \frac{d\psi}{dt} + \frac{d\alpha}{dt} \qquad (7)$$

$$\frac{d^2\varphi}{dt^2} = \frac{d^2\psi}{dt^2} - \frac{d^2\kappa}{dt^2} \qquad \frac{d^2\xi}{dt^2} = \frac{d^2\psi}{dt^2} + \frac{d^2\alpha}{dt^2}$$

The differential equations describing the body's motions are all non-linear. In general it is possible to solve them only by means of numerical methods. For this the differential equations must be generated to their highest temporal derivations.

Longing for a clear presentation matrices are applied

$$A\,y = B. \qquad\qquad (8)$$

where

$$y' = \left\{\frac{dv}{dt},\ \frac{d\kappa}{dt},\ F,\ \frac{d^2\psi}{dt^2},\ \frac{d^2\alpha}{dt^2}\right\} \qquad (9)$$

The highest temporal derivatives and the time-dependent tensile force in the towing cable are then

$$y = A^{-1}\,B \qquad\qquad (10)$$

They can be solved e.g. applying the **Runge-Kutta** method.

In detail we have the coefficients:

$$a_{11} = (m + m_{11})\cos\kappa$$
$$a_{12} = -(m + m_{11})\,v\sin\kappa$$
$$a_{13} = -\sin\alpha$$
$$a_{21} = (m + m_{33})\sin\kappa$$
$$a_{22} = (m + m_{33})\,v\cos\kappa$$
$$a_{23} = -\cos\alpha$$
$$a_{33} = \zeta_1\cos\alpha - \zeta_3\sin\alpha$$
$$a_{34} = I_{22} + J_{22}$$
$$a_{41} = \cos(\psi - \kappa)$$
$$a_{42} = v\sin(\psi - \kappa)$$
$$a_{44} = l\cos(\psi + \alpha) -$$
$$\qquad -\left(\zeta_1\sin\psi - \zeta_3\cos\psi\right)$$
$$a_{45} = l\cos(\psi + \alpha)$$
$$a_{51} = -\sin(\psi - \kappa)$$
$$a_{52} = v\cos(\psi - \kappa)$$
$$a_{54} = -l\sin(\psi + \alpha) -$$
$$\qquad -\left(\zeta_1\cos\psi + \zeta_3\sin\psi\right)$$
$$a_{55} = -l\sin(\psi + \alpha)$$
$$a_{14} = a_{15} = a_{24} = a_{25} = a_{31} = 0$$
$$a_{32} = a_{35} = a_{43} = a_{53} = 0$$

(11)

and

$$b_1 = -(m + m_{33})\,v\,\frac{d\psi}{dt}\sin\kappa - F_{st}\sin\psi - R_1$$

$$b_2 = (m + m_{11})\,v\,\frac{d\psi}{dt}\cos\kappa + F_{st}\cos\psi - R_3$$

$$b_3 = -\left(\lambda_1\cos\psi + \lambda_3\sin\psi\right)F_{st} + M_2$$

184

3.1. The design task

The design task has the only objective to assure an equilibrium of forces and moments between the distribution of weights and buoyancy. the hydrodynamical forces and moments as well as the tensile force in the towing cable in order to realize a given angle of attack $\kappa = \psi$ at a known towing velocity v.

After a corresponding rearrangement of equation system (13) we obtain

$$\alpha = \arctan \frac{R_1 + F_{st} \sin\psi}{R_3 - F_{st} \cos\psi} \qquad (14)$$

$$F = R_1\sin\alpha + R_3\cos\alpha - F_{st}\cos(\alpha + \psi) \qquad (15)$$

$$-\zeta_1 \cos\alpha + \zeta_3 \sin\alpha = \frac{1}{F}\left[(\lambda_1 \cos\psi + \lambda_3 \sin\psi) F_{st} - M_2\right] \qquad (16)$$

If the resulting vertical force ($F_{st} \cos\psi - R_3$) has the value zero, then we have $\alpha = 1/2\, \pi$ according to equation (14). That means that exclusively for this case the coordinate ζ_1 is without any meaning

Because the tensile force of the cable F is always higher than zero for v > 0, due to $0 < \alpha\ \pi$ from equ. (16) we get

$$\zeta_3 = \frac{(\lambda_1 \cos\psi + \lambda_3 \sin\psi) F_{st}}{F\sin\alpha} + -\frac{M_2}{F\sin\alpha} + \zeta_1 \cot\alpha . \qquad (16a)$$

From this it is obvious, that many potential solutions exist for the fixation coordinates ζ_1 and ζ_3. If F and α are known these fixation coordinates are located on one straight line and they should allow the designer to take a reasonable decision for an appropriate handling.

After the equilibrium position is known the question must be raised about reactions of F, α and k to be expected due to suffieciently small changes of F_{st}, v, ζ_1, ζ_3, λ_1 and λ_3

Therfore equation (13) is transformed into

$$\left.\begin{array}{c} F\sin\alpha - F_{st} \sin\psi - R_1 \\ F\cos\alpha + F_{st} \cos\psi - R_3 \\ (-\zeta_1 \cos\alpha + \zeta_3 \sin\alpha) F + \\ -(\lambda_1 \cos\psi + \lambda_3 \sin\psi) F_{st} + M_2 \end{array}\right\} = d\Phi \quad (17)$$

Forming the total increment $d\Phi$ over all parameters for the unchanged position of equilibrium then with $\psi = \kappa$ we have

$$d\Phi = J\, d\Delta + M\, dP = 0 . \qquad (18)$$

The matrix J is type (3,3). the matrix M is type (3,6). The elements are defined as follows

$$J_{ij} = \frac{\partial\Phi_i}{\partial\Delta_j} \quad \text{with} \qquad (19)$$

$$d\Delta^1 = \{dF . d\alpha ; d\kappa\}$$

and

$$M_{ij} = \frac{\partial\Phi_i}{\partial P_j} \quad \text{with} \qquad (20)$$

$$dP^1 = \{dF_{st}; dv; d\zeta_1; d\zeta_3; d\lambda_1, d\lambda_3\}$$

After further mathematical operations the following equation is obtained

$$\frac{d\Delta_i}{dP_j} = -C_{ij} \qquad (21)$$

with $C = J^{-1} M$.

This equation allows to quantify the effect of changed parameters of the vector dP on $d\Delta$ immediately.

3.2. The task of recalculation

It aims at finding the solution vector Δ with

$$\Delta^1 = \{F ; \alpha ; \kappa\}$$

for the equation system (13) considering $\kappa = \psi$ The towing velocity v is supposed to be known for the given vehicle to be towed.

Due to the non-linear shares in α and k of this equation system algebraic solutions are not

$$b_4 = \frac{dv_1^p}{dt} + v\frac{d\psi}{dt}\sin(\psi - \kappa) +$$

$$+ l\sin(\psi + \alpha)\left[2\frac{d\psi}{dt}\frac{d\alpha}{dt} + \left(\frac{d\alpha}{dt}\right)^2\right] +$$

$$+ l\sin(\psi + \alpha)\left(\frac{d\psi}{dt}\right)^2 +$$

$$+ (\zeta_1\cos\psi + \zeta_3\sin\psi)\left(\frac{d\psi}{dt}\right)^2$$

$$b_5 = \frac{dv_3^p}{dt} + v\frac{d\psi}{dt}\cos(\psi - \kappa) +$$

$$+ l\cos(\psi + \alpha)\left[2\frac{d\psi}{dt}\frac{d\alpha}{dt} + \left(\frac{d\alpha}{dt}\right)^2\right] +$$

$$+ l\sin(\psi + \alpha)\left(\frac{d\psi}{dt}\right)^2 +$$

$$- (\zeta_1\sin\psi - \zeta_3\cos\psi)\left(\frac{d\psi}{dt}\right)^2 \qquad (12)$$

3. Investigations on the uniform straight-line motion

For simulating a non-steady motion pattern generally at first the steady condition of equilibrium must be determined for a special configuration of parameters. The mathematical formula required are resulting as special cases of dynamic relations in which all occurring derivatives of the variables to time t disappear except for a constant velocity v with $V^1 = \{v_1, 0, 0\}$.

The equilibration of steady behaviour of the body is given by the reduced formula

$$\begin{pmatrix} F\sin\alpha - F_{st}\sin\psi - R_1 \\ F\cos\alpha + F_{st}\cos\psi - R_3 \\ (-\zeta_1\cos\alpha + \zeta_3\sin\alpha)\,F + \\ -(\lambda_1\cos\psi + \lambda_3\sin\psi)\,F_{st} + M_2 \end{pmatrix} = 0 \qquad (13)$$

with $\kappa = \psi$.

This system of equations can be solved having two different objectives in mind.

One has to distinguish between the design task and the recalculation task.

It is the purpose of the design task to dimension and design the maximum number of three parameters of the towed vehicle.

In general with a given shape of the towed vehicle the static force F_{S1}, the coordinates λ_1 and λ_3 of the centre of gravity and the dependence of the hydrodynamic coefficients c_i on the angle of attack κ and on the rudder angles δ_j can be assumed as known.

As a rule the useful variation of the angle of attack κ and the heaving angle α of the cable could provide the fixation coordinates of the cable on the towed vehicle. The third magnitude to calculate is the tensile force F of the cable.

It is interesting to know α and κ in advance, because changing the heaving angle a of the cable (heaving or veering the cable) and changing the angle of attack allows to control the towing depth immediately.

However, the equations can also be used to design other elements of the gear than those mentioned above, e.g. to dimension the hydrodynamical steering facilities in order to assure the hydrodynamical vertical force R_3 required.

The recalculation allows the designer of the gear to analyse the effects of the variation of body parameters on the stationary motion pattern of the towed vehicle already in the design stage.

The recalculation offers the advantage to give the concrete performance parameters of the project by means of appropriate calculations of variants already in the project stage.

Expensive large-scale tests at sea can be reduced or fault designs can be corrected right in time. The prior task is to quantify the angles α and κ resulting from given parameters of the towed vehicle and to determine the cable tensile force F to be expected.

If required the design can again be specified.

186

applicable in general. As a rule they can be found by iteration only.

Therefore equation (13) is again transferred into the formula (17).

The solutions can be considered as being found if the condition

$$0 \leq |d\Phi| \leq \delta \qquad (22)$$

is fulfilled and δ is a suitably small error.

The most important problem in the application of iteration methods for the solution is to determine the initial approximation $\Delta_{(0)}$ and to investigate whether the series of approximations $\Delta_{(K)}$ to be calculated is converging against the seeked solution $\Delta_{(k+1)}$

Because $d\Phi$ is small, this function can be developed by a Taylor series neglecting terms of second or higher power. Then we have

$$d\Phi_i = \frac{\partial \Phi_i}{\partial F} \, dF + \frac{\partial \Phi_i}{\partial \alpha} \, d\alpha + \frac{\partial \Phi_i}{\partial \kappa} \, d\kappa \qquad (23)$$

Introducing matrices again in the interest of expediency, we obtain

$$d\Phi = J \, d\Delta$$

The expression is the same as the 1st part of equation (18). There the task has been to investigate the interaction between the vectors $d\Delta$ and dP with known position of equilibrium $d\Phi = 0$, which should remain unchanged.

Now it is up to simply find the position of equilibrium.

For solving the actual task the method by Newton-Raphson is suitable in the known form

$$\Delta_{(k+1)} = \Delta_{(k)} - d\Delta_{(k+1)} \qquad (24)$$

with

$$d\Delta_{(k+1)} = J_{(k)}^{-1} \, d\Phi_{(k)} \qquad (25)$$

J is the Jacobi matrix. Its elements are defined in the following way:

$$J_{11} = \sin \alpha \qquad J_{12} = F\cos \alpha$$

$$J_{21} = \cos \alpha \qquad J_{22} = -F\sin \alpha$$

$$J_{13} = -F_{s1} \cos \kappa - \frac{1}{2}\rho v^2 A \left(\frac{\partial c_1}{\partial \kappa} \right)$$

$$J_{23} = -F_{s1} \sin \kappa - \frac{1}{2}\rho v^2 A \left(\frac{\partial c_3}{\partial \kappa} \right)$$

$$J_{31} = -\zeta_1 \cos \alpha + \zeta_3 \sin \alpha \qquad (26)$$

$$J_{32} = \left(\zeta_1 \sin \alpha + \zeta_3 \cos \alpha \right) F$$

$$J_{33} = \left(\lambda_1 \sin \kappa - \lambda_3 \cos \kappa \right) F_{s1} +$$

$$+ \frac{1}{2}\rho v^2 A s \left(\frac{\partial c_2}{\partial \kappa} \right)$$

4. Setups for assessing the stability of the equilibrium position

From the previous passage it is obvious, that the position of equilibrium of the towed vehicle is determined by the selected design and operational parameters.

The theoretical assessment of the stability of this position of equilibrium after a short-time disturbance of finite extent is of very high practical importance. On the one hand this disturbance can occur in the location, i.e. the body is displaced from its position of equilibrium. It can on the other hand be a disturbance of the velocity. In this case a certain velocity value is given to the body with respect to the surrounding fluid, which differs from the value the body had so far.

In the special literature there is made a distinction between static and dynamic stability of the position of equilibrium.

The position of equilibrium can be analysed with repsect to its static stability by eliminating all terms of inertia in the equations of motion. It allows to make statements about the existence - or the lack, respectively - of forces and moments bringing the body into its original position after the action of flow at a certain location.

Although it is desirable to have a sufficient stability, it is however not enough to know it with respect to steering and control of such a body.

The time constants of the motion pattern we are interested in can only be quantified resulting from the analysis of the dynamic stability.

Regarding the definition of the 'dynamic stability' we agree with **Felix Klein** saying: "A position of equilibrium is supposed to be stable if disturbances remain arbitrarily small, if the initial disturbance is chosen to be sufficiently small (cf. **Hamel** (1949))".

If sufficiently small measurable disturbances do not diminish , then disturbances with great amplitudes can not die out as well.

Therefore the dynamic stability can be investigated by means of a linearized system of equations.

Here only small changes in the time-dependent parameters of the steady position of equilibrium are considered according to the preconditions $\alpha = \alpha_0 + d\alpha$, etc. and small terms of second or higher order are neglected.

If in case of smaller disturbances only a linear dependence of the hydrodynamic coefficients c_i on the angle of attack κ and on the angular velocity k is regarded as follows

$$c_i = c_{i0} + \frac{\partial c_i}{\partial \kappa} \Delta\kappa + \frac{\partial c_i}{\partial k} \Delta k \qquad (27)$$

we obtain the linearized equations of motion (28) with

$$\Delta k = \frac{\dfrac{d(\Delta\psi)}{dt} \cdot s}{2 \cdot v_0}$$

The term $(\varsigma_1 \cos \alpha_0 - \varsigma_3 \sin \varsigma_0)(\Delta\psi)^2$ is as a rule neglectable in comparison to the other terms because of the mostly small dimensions of the towed vehicle in ζ_1 and ζ_3 and because of the small angular velocity $\Delta\dot\psi$.

If one further takes into consideration that the deviations from the position of equilibrium , i.e. disturbances , occur with negligibly small changes of velocity, after rearrangement of

$$
\left(
\begin{array}{c}
\Delta v \cos(\psi_0 - \kappa_0) - v_0(\Delta\psi - \Delta\kappa)\sin(\psi_0 - \kappa_0) \\[4pt]
-\Delta v \sin(\psi_0 - \kappa_0) - v_0(\Delta\psi - \Delta\kappa)\cos(\psi_0 - \kappa_0) \\[4pt]
\Delta v \cos(\alpha_0 + \kappa_0) + v_0\left(\Delta\dot\psi - \Delta\dot\kappa\right)\sin(\alpha_0 + \kappa_0)
\end{array}
\right) =
$$

$$
\left(
\begin{array}{c}
(\varsigma_1 \sin \psi_0 - \varsigma_3 \cos \psi_0)\Delta\dot\psi - l\left(\Delta\ddot\psi + \Delta\ddot\alpha\right)\cos(\psi_0 + \alpha_0) \\[4pt]
(\varsigma_1 \cos \psi_0 + \varsigma_3 \sin \psi_0)\Delta\dot\psi + l\left(\Delta\ddot\psi + \Delta\ddot\alpha\right)\sin(\psi_0 + \alpha_0) \\[4pt]
-(\varsigma_1 \sin \alpha_0 + \varsigma_3 \cos\alpha_0)\Delta\dot\psi - l\left(\Delta\ddot\psi + \Delta\ddot\alpha\right) + \\[4pt]
+(\varsigma_1 \cos\alpha_0 - \varsigma_3 \sin\alpha_0)\left(\Delta\dot\psi\right)^2
\end{array}
\right)
$$

$$(28)$$

the two linearized vector equations we get the following linear system of differential equations

$$A \cdot y^* = B \cdot y \qquad (29)$$

with

$$y^{*T} = \left\{\Delta\ddot\alpha, \Delta\dot\alpha, \Delta\alpha, \Delta\dot\kappa, \Delta\kappa, \Delta F\right\} \qquad (30)$$

and

$$y^T = \left\{\Delta\ddot\psi, \Delta\dot\psi, \Delta\psi\right\} \qquad (31)$$

After left-hand multiplication of the matrices **A** and **B** with A^{-1} in equ. (29) finally we obtain

$$y^* = A^{-1} B \; y = C \; y \qquad (32)$$

It must be considered that the determinant of matrix **A** with

188

$$\det(A) = F^2 \sqrt{_0^2} F_0 \cos(\alpha_0 + \kappa_0) \cdot$$
$$[(m + m_{33})\varsigma_1 \cos\kappa_0 + (m + m_{11})\varsigma_3 \sin\kappa_0]$$

can become singular. Particularly the following conditions must be guaranteed.

$$\alpha_0 + \kappa_0 \neq \frac{\pi}{2}$$

$$\kappa_0 \neq \arctan\left(-\frac{(m + m_{33})\varsigma_1}{(m + m_{11})\varsigma_3}\right) \tag{33}$$

The following steps of the stability analysis are simple considering that with

$$y_1' = \sum_{i=1}^{3} c_{1i}y_i = \frac{d}{dt}\left(\sum_{i=1}^{3} c_{2i}y_i\right)$$

$$y_2' = \sum_{i=1}^{3} c_{2i}y_i = \frac{d}{dt}\left(\sum_{i=1}^{3} c_{3i}y_i\right) \tag{34}$$

$$y_4' = \sum_{i=1}^{3} c_{4i}y_i = \frac{d}{dt}\left(\sum_{i=1}^{3} c_{5i}y_i\right)$$

three setups are available for determining $\Delta\psi$ which are all equivalent.
In the following the upper expression is inserted into equ. (34), providing

$$c_{11}\ddot{\Delta\psi} + c_{12}\dot{\Delta\psi} + c_{13}\Delta\psi = \tag{35}$$
$$c_{21}\dddot{\Delta\psi} + c_{22}\ddot{\Delta\psi} + c_{23}\dot{\Delta\psi}$$

Because the coefficients c_{21} and c_{23} are equal to zero, the differential equation (35) can be simplified

$$(c_{11} - c_{22})\ddot{\Delta\psi} + c_{12}\dot{\Delta\psi} + c_{13}\Delta\psi = 0 \tag{36}$$

with the characteristic radices

$$r_{1,2} = -\frac{c_{12}}{2(c_{11} - c_{22})}$$
$$\pm \frac{1}{2(c_{11} - c_{22})}\sqrt{c_{12}^2 - 4c_{13}(c_{11} - c_{22})} \tag{37}$$

According to the definition the position of equilibrium is dynamically stable, if oscilations

remain small for a long period of time As a precondition the real part of the characteristic equation Real $(r_{1,2}) \cdot 0$. This condition is fulfilled, if

$$-\frac{c_{12}}{(c_{11} - c_{22})} > 0$$

$$c_{12}^2 - 4c_{13}(c_{11} - c_{22}) < 0 \tag{38}$$

Taking into consideration, that for the damping coefficients of slender bodies as a rule we have $\frac{\partial c_2}{\partial k} < 0$ and $\frac{\partial c_3}{\partial k} > 0$ the difference

$$c_{11} - c_{22} = \frac{(I_{22} + J_{22})\sin(\alpha_0 + \kappa_0)}{1[(m + m_{33})\varsigma_1 \cos\kappa_0 + (m + m_{11})\varsigma_3 \sin\kappa_0]} \cdot$$
$$+ \left(\frac{\varsigma_1}{1}\cos\alpha_0 - \frac{\varsigma_3}{1}\sin\alpha_0\right)\tan(\alpha_0 + \kappa_0)$$

$$\tag{39}$$

is always positive, if the conditions

$$\frac{\varsigma_1}{1} \ll 1$$
$$\alpha_0 + \kappa_0 \neq \tfrac{1}{2}\pi$$

are given, then the requirement can according to equ. (38a) be fulfilled in general But in case of $\alpha_0 + \kappa_0 \to \tfrac{1}{2}\pi$ the two characteristic radices will converge to zero The dynamic stability would not be given anymore.

5. Summary
In the given paper a two-dimensional model for the analysis of the motion pattern of towed submerged bodies is presented. which has already been used with success in the development and in the application of those devices at the Institute of the author for several times.
Here it was not the aim to obtain high accuracies with a rather sophisticated mathematical model, but to develop a tool which is practicable and allows to understand the complex interactions of the system.

6. References

Egorov, V.I. (1981)
Podvodnye buksiruemye. - Leningrad, Verlag Sudostroenie, 1981)

Hamel, G. (1949)
Theoretische Mechanik. - Springer-Verlag Berlin / Göttingen / Heidelberg, 1949, p. 268

Horn, F., Reckling, K.A.
Beitrag zur Theorie des Schleppens. - In: Forschungshefte für Schiffstechnik, Schiffbau, Schiffsmaschinenbau, No.4, November 1953, p 128 - 133

Karpenko, V.P. (1973)
Untersuchungen zur statischen und dynamischen Stabilität von Scherbrettern. - In: Fischerei-Forschung, Rostock, 11 (1973) 2

Klingbeil, K. (1983)
Untersuchungen zur Stabilität freifliegender Körper. - In: Schiffbauforschung, Rostock, 22 (1983) 4, p. 252

Mahrenholtz, O.
Fluidelastische Schwingungen. - In : Zeitschrift für Angewandte Mathematik und Mechanik, Berlin, 66 (1986) 1, p. 1 - 22

Majohr, J.; Korte, H. (1995)
Präzise Positionsbestimmung und automatische Bahnführung von geschleppten Unterwassergeräteträgern. - In: Proceedings Workshop "Methods for Development and Evaluation of Maritime Technologies", 11.-13. May 1995, University of Rostock

Niemann, U. (1967)
Die Berechnung von Querkräften und Momenten an manövrierenden Schiffen. Thesis at the Faculty of Engineering of TU Berlin, 1967, in: Mitteilungen der Versuchsanstalt für Wasserbau und Schiffbau Berlin, No. 49, 1967

Paschen, M. (1983)
Untersuchungen zur gezielten Fischerei. - In. Schiffbauforschung 22 (1983) No. 1

Paschen, M. (1985)
Untersuchungen zur Stabilität pelagischer Scherbretter.
in: Fischerei-Forschung 23 (1985) No. 3

Paschen, M. (1990)
Prediction of the trawl door position in pelagic trawls.
Report, in Documents of International Council for the Exploration of the Sea (ICES), Rostock in March 1990

Schmiechen, M. (1964)
Eine allgemeine Gleichung für Bewegungen starrer Körper in Flüssigkeiten und ihre Anwendung auf ebene Bewegungen von Doppelkörpern.
Thesis at the Faculty of Engineering of TU Berlin, 1964, in: Mitteilungen der Versuchsanstalt für Wasserbau und Schiffbau Berlin, No. 48, 1964

Schmitz, G. (1961)
Anwendung der Theorie des schlanken Körpers auf die dynamische Gierstabilität und Steuerbarkeit von Schiffen. - In: Wissenschaftliche Zeitschrift der Universität Rostock, 10 (1961) Mathematisch-Naturwissenschaftliche Reihe, No. 2/3, p. 175 - 190.

LOWERING A PLANING BOAT'S MAXIMUM TRIM ANGLE CHANGE

Y. Yoshida
International Boat Research
1-2-1-104, Fukuei, Ichikawa City, Chiba Prefecture, 272-01 Japan

ABSTRACT

This paper is concerned about a planing boat's maximum trim angle change. For stability, sight and work, pilots and crew want their boat's low trim angle change. While the lower change requires the higher resistance in high speed range. The mean value of total resistance coefficient's increment becomes 0.00454 / deg. against the maximum trim angle change control. Under the condition of controlling the maximum trim angle change successively, each hull form obtained the minimum resistance in high speed range. The improved hull forms become smaller in displacement volume, longer in total length, higher in cross point of chine line with keel line at bow, and higher in chine line. The empirical formulae for presuming resistance and floating position have been tested by not only new towing tests using models but also trial tests using a torpedo boat.

NOMENCLATURE

b_1 — half width at stern.

C_t — total resistance coefficient.

$\qquad C_t = R / 0.5\rho V^2 \nabla^{2/3}$.

$C_{t\,3.5}$ — C_t at $F_\nabla = 3.5$.

F_∇ — Froude number.

$\qquad F_\nabla = V / \sqrt{g \cdot \nabla^{1/3}}$.

$F_\nabla = 3.5$ means about 46 kt by a ship having 100 m³ in displacement volume.

g — gravity acceleration.

$\odot$ — model number i or its cluster number i.

R — total resistance.

S — wetted surface area.

V — speed.

$\triangle D$ — nondimensional draft change at stern. The draft change divided by b_1 or $\nabla^{1/3}$ takes positive for decreasing draft.

$\triangle\theta$ — trim angle change.

$\triangle\theta_{3.5}$ — $\triangle\theta$ at $F_\nabla = 3.5$.

θ — initial trim angle, which is the angle between water line at rest and the straight line between the points on keel line at Ord. 10 (stern) and 5 (midship), taking positive when bow up.

ρ — density.

∇ — displacement volume.

1. FLOATING POSITION

The change of floating positions of PT – 11 [1] is shown in Fig. 1. This torpedo boat has 35 m in overall-length, 1304.28445 kN (133 tonf) in displacement and about 221.8 m² in
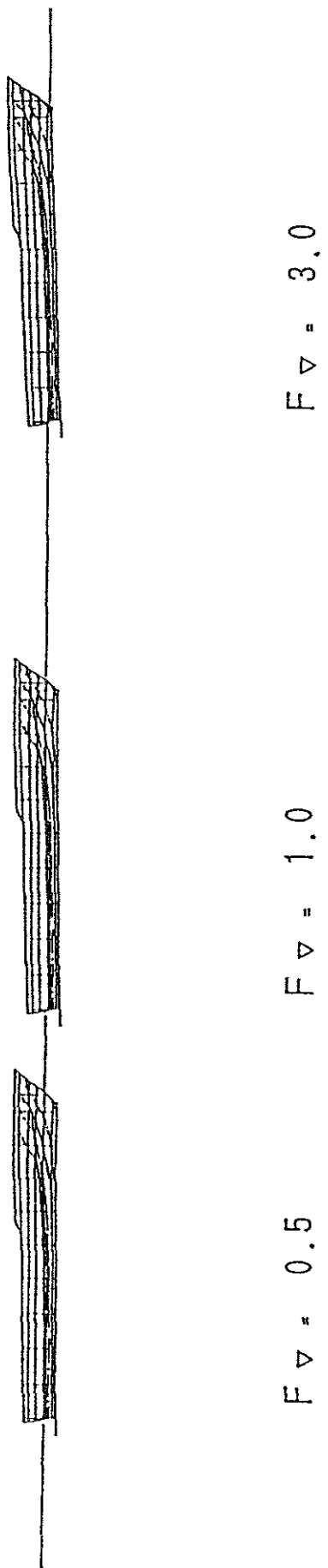
Fig. 1 Floating Position

wetted surface area at rest. If S = 221.8 m^2 at $F_\nabla = 0$ is set as 100 % in ratio, the area's ratio changes for 105 % at $F_\nabla = 1.0$ and 72 % at $F_\nabla = 3.0$. Speedincreasing causes the boat's stern to sink up to $F_\nabla = 1.5$, and then the stern rises gradually with higher speed. $\triangle\theta$ increases up to $F_\nabla = 3.0$. The change of stern ($\triangle D$) together with trim angle change ($\triangle\theta$) causes the boat to get the floating position as Fig. 1.

The present method to presume floating positions is as follows. The initial floating position at rest is set against the water line at rest. The base line is set as the straight line between the points on keel line at Ord.10 (stern) and 5 (midship). The angle of intersection between water line and base line is θ. At the first step the boat's draft is changed by using $\triangle D$ under keeping θ constant. At the second step the base line with the hull is turned by $\triangle\theta$ about the point on keel at Ord.10. The floating position as Fig. 1 is obtained by these steps. Then $\triangle\theta$ and $\triangle D$ is indispensable to presume the floating position. S is boat's surface area under water line. This is the base for calculating the frictional resistance of the boat. The S's changes with the boat's speed have been shown on the reference [2].

Also the boat's R changes with the floating position and is transformed into the nondimensional form by dynamic pressure C_t.

A set of C_t, $\triangle\theta$ and $\triangle D$ at a Froude number is called as resistance performance at the speed, which shows three conditions depending on speed range.

2. THREE CONDITIONS

Thirteen models of about 2.5 m length with wave-shaped bottom were used for the towing tests changing six kinds of displacements and center of gravities for each model, which means 78 models. [3] At F_∇ = 0.5, 1.0, ..., 3.5, 78 sets of C_t, $\triangle\theta$ and $\triangle D$ were obtained by the measurements.

The summary of the results is shown below.

2.1 Displacement condition

The stern sinks gradually to the lowest point from F_∇ = 1.0 to 1.5, and increasing $\triangle\theta$ from about 100 minutes to about 200 mimutes. There are few cases the bow sinks at low speed up to about F_∇ = 0.5, but then the bow gets upward. Under these conditions, C_t increases undulatingly, and makes the last hump on the total resistance coecoefficient at about F_∇ = 1.0, at which the wave making resistance will become the maximum. The larger $\triangle\theta$, the lager becomes C_t.

2.2 Semi-planing condition

The stern continues to rise from the lowest position after the last hump from F_∇ = 2.0 up to 2.5. As the hull will get greater $\triangle\theta$ reaching about 300 minutes, the wetted surface area and C_t decrease. In this condition small quantity of dynamic lift appears.

2.3 Planing condition

The dynamic lift appears remarkably beyond about F_∇ = 2.5. As increase in F_∇ from about 2.5 up to 3.5, the stern rises back to the point of initial draft at rest and goes further up. Its $\triangle\theta$ decreases than that of semiplaning condition and keeps ups and downs about 300 minutes and 150 minutes. This causes both wetted surface area and C_t to become small. R consists of frictional resistance, wave making resistance and so on. C_t decreases as $\triangle\theta$ increases, showing

reverse compared with that of the previous displacement condition.

The planing condition is the typical characteristic of planing boats.

3. LOWERING MAXIMUM $\triangle\theta$

The optimum hull forms under the condition of $\triangle\theta$ free were obtained about thirteen kinds of models. The optimum hull form means the hull form that gives C_{t35} the minimum value. Then the maximum $\triangle\theta$ levels were taken into the condition for each optimization. $\triangle\theta_{2.5}$ level is taken at intervals of 30 minutes such as 270, 240, 210 minutes and so on. Thirteen kinds of relations between $\triangle\theta_{25}$ and C_{t35} of each obtained hull form were plotted in Fig. 2. The reason why $\triangle\theta_{2.5}$ is on abscissa is that there is the strongest relation between $\triangle\theta_{25}$ and C_{t35}. The correlation coefficients among C_{t35} and $\triangle\theta_{2.5}$, $\triangle\theta_{3.0}$ and $\triangle\theta_{3.5}$ equal to -0.76, -0.71 and -0.60 respectively. $\triangle\theta_{25}$ has not only the strongest relation with C_{t35} but also shows the maximum $\triangle\theta$ on F_∇ and $\triangle\theta$ curve. Then F_∇ = 2.5 is selected for controlling the maximum $\triangle\theta$ level.

The number in the "◯" is the number of the model or its cluster. The six data which correspond six kinds of displacements and center of gravities for each model come near each other in the principal component coordinates Z_1, Z_2 and Z_3. This coordinates system is obtained by applying principal component analysis to the models' data. [3], [4], [5] The largest hexahedron formed by the six points of the data is called as cluster. A cluster keeps the model's characteristics.

The good examples showing hull

Fig. 2　△θ － Ct

194
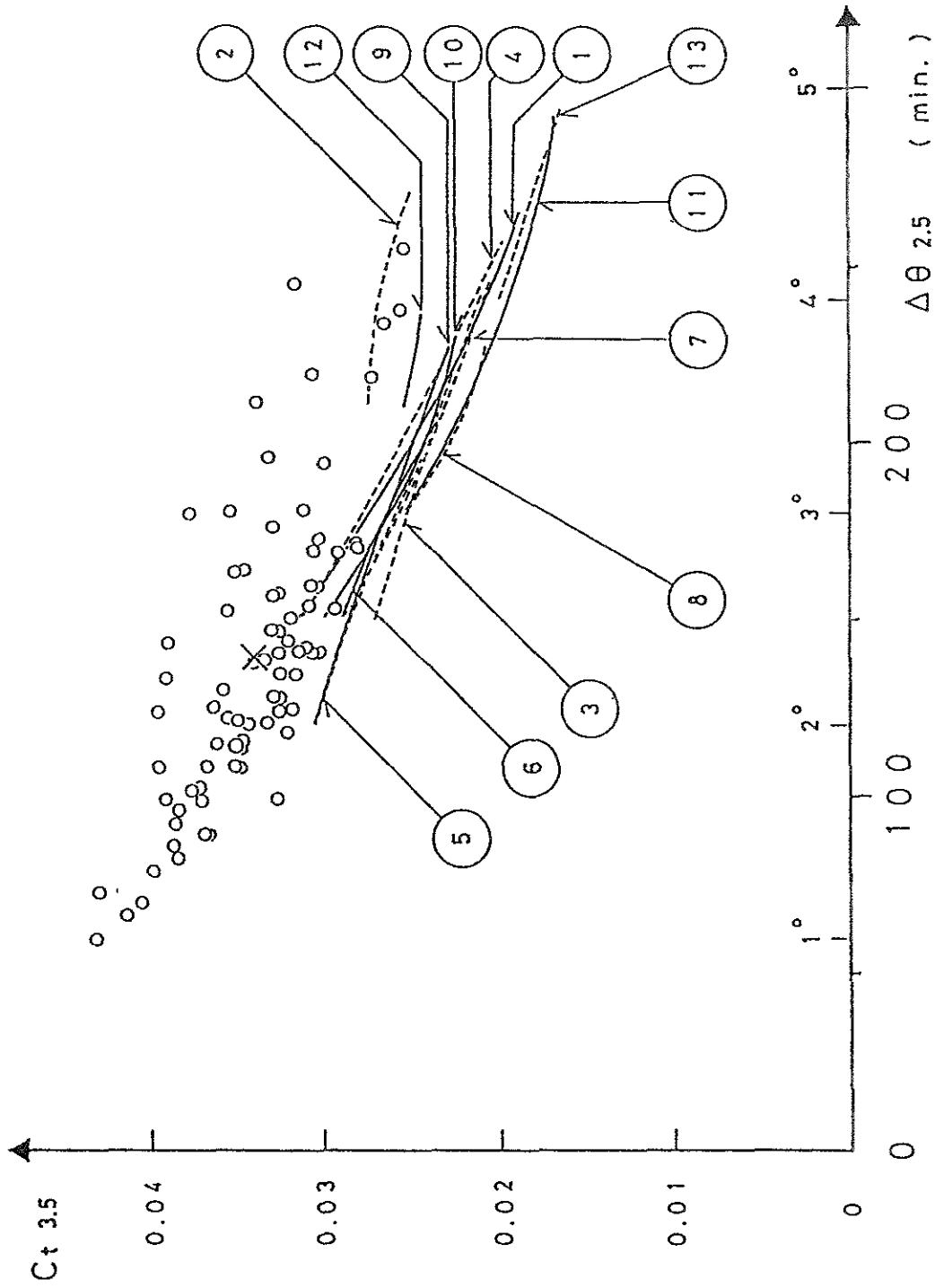
form's characteristics are ⑥ 6th cluster containing hull forms having smaller transom or longer hull, ⑫ 12th cluster containing hull forms having larger transom or shorter hull, ① 1st cluster containing hull forms having lager initial trim, ⑩ 10th cluster containing hull forms having smaller initial trim, ⑨ 9th cluster containing hull forms having higher chine hight, and ⑪ 11th cluster containing hull forms having lower chine height.

The idea of the calculation about the optimum hull forms are as follows. $C_{t\ 3.5}$ is selected as the objective function. This $C_{t\ 3.5}$ is the empirical formula made from the data of the towing tests, which is composed of hull form parameters etc.. The following four conditions from (1) to (4) are expressed by positive and e-ual sign.

(1) Hull form parameters etc. exist within the experimental data's range

(2) Hull form parameters etc. keep each mean value's approximate values

(3) Hull form parameters etc. keep inside a cluster

(4) $\triangle \theta_{2.5}$

Applying S U M T method [6] the minimum $C_{t\ 3.5}$ under these conditions is searched. The conditions from (1) to (3) correspond to $\triangle \theta$ free and all conditions from (1) to (4) $\triangle \theta_{2.5}$ controlled. After presuming the resistance performances of the obtained hull forms, quadratic interpolations by the method of least squares to the points of ($\triangle \theta_{2.5}$, $C_{t\ 3.5}$) were done. The obtained curves have decreasing tendency. [see F i g. 2]

$C_{t\ 3.5}$ values from 1st through 78th test model are plotted by "○" marks. "×" mark shows the mean value of them. They have the general trend of higher values than the curves' values

through the optimization technique.

The right edges of the curves are $\triangle \theta$ free. Curves show that stronger controlled $\triangle \theta_{2.5}$ causes a model's $C_{t\ 3.5}$ to increase. The mean value of $C_{t\ 3.5}$'s increment becomes 0.0045 4 /deg. through the linear interpolation to each curve's points.

With lowering the maximum trim angle changes such as 270, 240, 210 minutes and so on, the minimum resistance hull forms become smaller in displacement volumes, longer in total length, higher in cross point, of chine line with keel line at bow, and higher in chine line.

Let us take an example of resistance performance of them in the next chapter.

4. RESISTANCE PER-FORMANCE

Under controlling the maximum trim angle change $\triangle \theta_{2.5}$, two resistance performances of the optimum hull forms from ⑥ 6th cluster are obtained as shown in F i g. 3.

The resistance performance for controlled $\triangle \theta_{2.5}$ less than 180 minutes is expressed by solid line, while one less than 150 minutes by dotted line. By F_v and $\triangle \theta$ curves in F i g. 3 the maximum trim angle changes show their own values for $F_v \geqq 2.5$. The former initial trim angle $\theta = -52$ minutes compared with the later one -58 minutes.

With the stronger limitation of the maximum trim angle change $\triangle \theta_{2.5}$, the hump of C_t and F_v curve shows lower value and $C_{t\ 3.5}$ value of the curve higher value.

Finally the preciseness of the empirical formulae should be discussed.

5. EMPIRICAL FORMU-LAE

Note :
ΔΘ $_{2.5}$ ≦ 180 min.
ΔΘ $_{2.5}$ ≦ 150 min.

Fig. 3   Ct, Δθ and ΔD

196
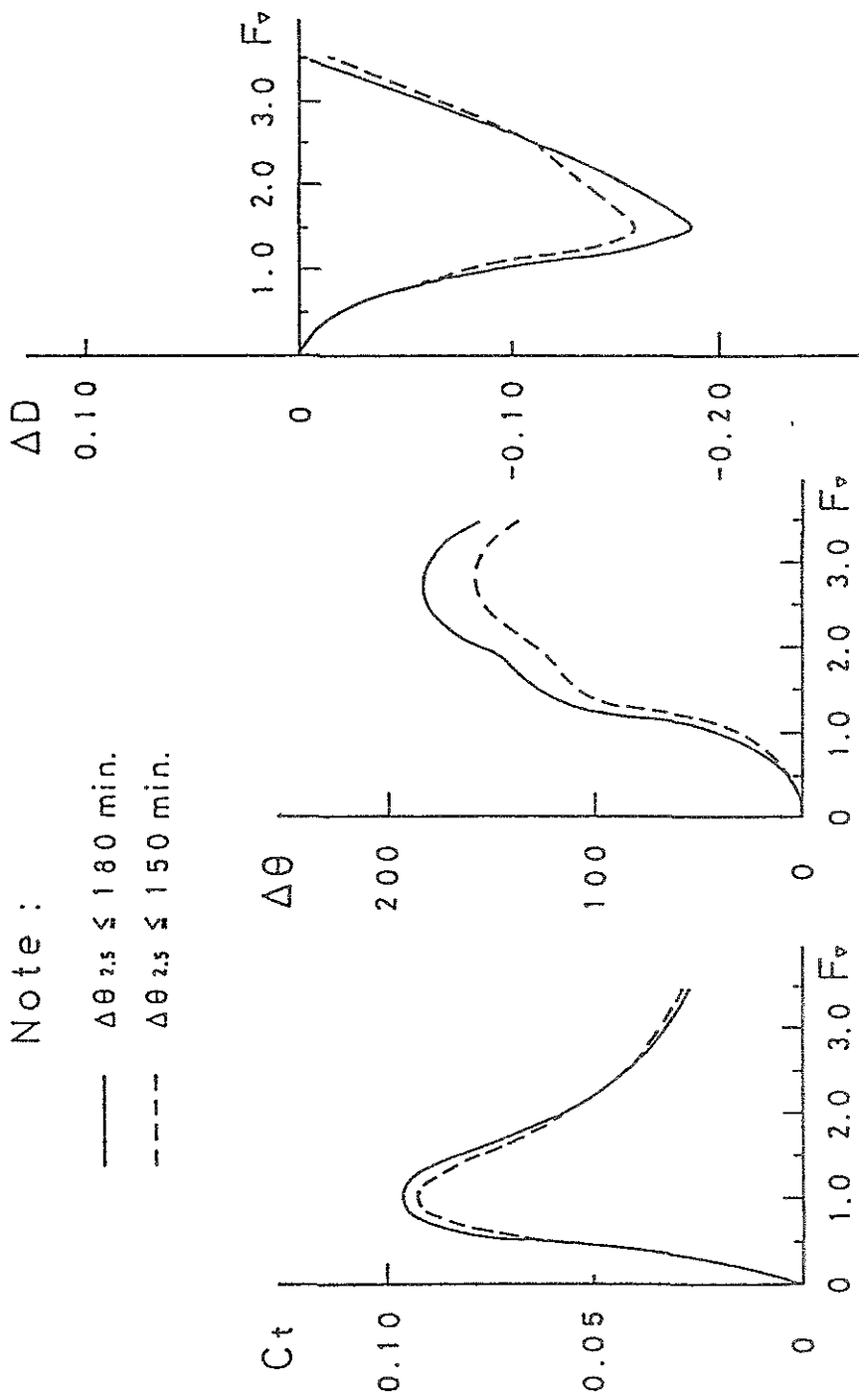
The C_{L35} and $\triangle\theta_{25}$ in the calculation of SUMT are taken from empirical formulae by the 78 sets of towing test data. The former works for the objective function and the later the restrictive conditions for the maximum trim angle change level.

All formulae are used to presume the resistance performance of each optimum hull form obtained.

In order to test empirical formulae for presuming C_L, $\triangle\theta$ and $\triangle D$, not only the towing tests by new five models [3], but also the trial tests by the torpedo boat [1] are executed.

As the effective horse power by the formulae shows about 50 % of the measured shaft horse power of the boat, one of the validities about the formulae is shown. [4], [7]

As shown in Fig. 4 $\triangle\theta$ was underestimated here, but the dependence on speed is quite similar.

The balance between resistance and thrust of the boat in high speed range is also obtained. [7]

The difference of $\triangle\theta$ between prediction and trial test is due to scale effect.

6. SCALE EFFECT

Sottorf measured R and $\triangle\theta$ about the flat plate which has 2.4 m in width and 9 tonf in displacement, defined as scale ratio $\lambda_F = 1$. Also against successive scale ratios of the models such as $\lambda_F = 2, 4, 8$ ......, the measurements have been done. [8]

The data up to $\lambda_F = 8$ are valid to presume R. Similar models having scale ratio less than $\lambda_F = 16$ are not valid to presume their R because of the surface tension's predominant influence to models not estimated.

Although $\triangle\theta$ for the minimum R is 4 deg. for $\lambda_F = 1$ by calculation,

while the experimental data containing the actual size's ones show from 2.5 to 5.5 deg.

6. CONCLUSIONS

For stability, sight and work, pilots and crew want their boats' low trim angle change. Trough the analysis of test data from models and a boat the conclusions are obtained as follows.

(1) The lower trim angle change requires the higher resistance in high speed range. The mean value of total resistance's increment becomes 0.00454/ deg. at $F_\nabla = 3.5$ (displacement volume basis) against the maximum trim angle control.

(2) Under controlling the maximum trim angle change, successively, each hull form has the minimum resistance in high speed range through the optimization.

(3) As stronger lowering the maximum trim angle change, the optimum hull forms become smaller in displacement, longer in total length, higher in cross point of chine line with keel line at bow, and higher in chine line.

(4) The validity of the empirical formulae were discussed by the data of trial tests of a torpedo boat.

(5) The difference of trim angle change between prediction and trial test data is due to scale effect.

7. REFERENCES

1. Raymond, V. and Blackman, B. (ed.) – Jane's Fighting Ships – London, 1975-1976, p.213.
2. Yoshida, Y. – Estimation of Resistance of Planing Craft by Principal Component Analysis – Transaction of the second International Conference in Commemoration of the 300-th Aniversary of Creating
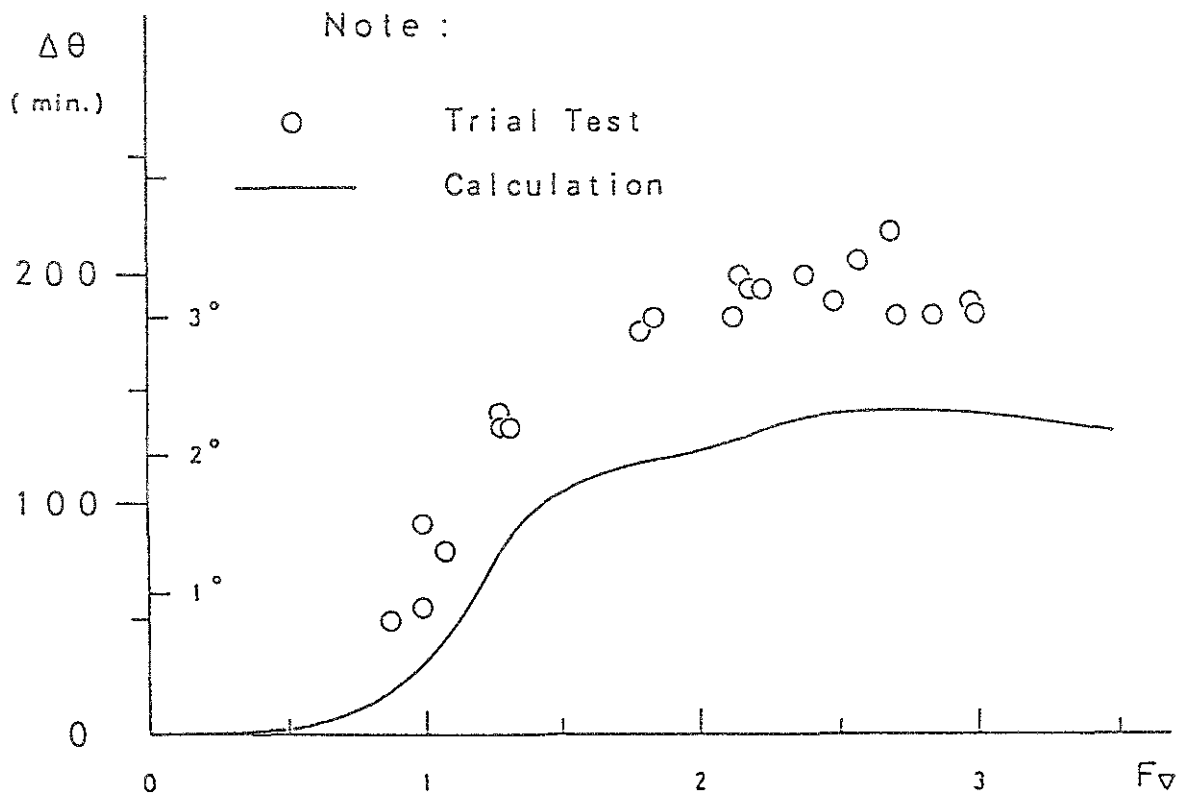
Fig. 4 $\triangle\theta$ of   Torpedo   Boat

Russian Fleet by Peter the Great and 290 years of Admiralty ship yards, St. Petersburg State Marine Tecnical University, Vol. 2, 5-12 Jun. 1994. pp. 65-72.

3. Yoshida, Y. and Nagai, T. - Applied Reliability Analysis of the Resistance Performance of High Speed Craft Models - Proceedings of HADMAR'91, Vol. 1, Varna, Bulgaria, 28 Oct. - 1 Nov. 1991, pp. 10⁻1-10⁻8.

4. Nagai, T. and Yoshida, Y. - Estimation of Resistance, Trim and Draft of Planing Craft - Ship Technology Research / Schiffstechnik, Vol. 40, No. 3, Aug. 1993, pp. 133-137.

5. Yoshida, Y. and Nagai, T. - Principal Component Analysis and Factor Analysis referring to Model Test Results in Still Water of

High Speed Craft - Journal of the Society of Naval Architects of Japan, Vol. 140, Dec. 1976, pp. 58-66.

6. Nagai, T. and Yoshida, Y. - Minimum Resistance Hull Form of Planing Craft with Controlled Trim Angle - Proceedings of the Sixth International Offshore and Polar Engineering Conference (ISOPE-96), Los Angeles, USA, 26-31 May 1996, pp. 263-270.

7. Yoshida, Y. - The method of Estimating a Planing Craft's Resistance and Floating Position at the Initial Design Stage - Doctorate Dissertation of Yokohama National University, 1995.

8. Sottorf, W. - - Versuche mit Gleitflächen, IV Teil, Analyse - Werft Reederei Hafen, 19 Jahrgang, Heft 6, pp. 65-70.

CAPSIZE RISK OF A TYPICAL FISHING VESSEL IN THE BLACK SEA

E. Aa. Dahle[1] and D. Myrhaug[2]

[1] Governmental Fishing Vessel Accident Commission, Norwegian Ministry of Justice, Oslo, Norway

[2] Department of Marine Hydrodynamics, Norwegian University of Science and Technology, N-7034 Trondheim, Norway

ABSTRACT

The purpose of risk analysis is to make a model of the system of interest that can be used for risk management of the system.

When applied to capsize, the model can consist of a fault tree for cause analysis, and an event tree for consequence analysis.

In the paper, it is stated that the primary goal of risk management is to eliminate capsize altogether. This can only be obtained by improved design of smaller vessels by extending the angle of vanishing stability.

For vessels of inferior design, i.e., vessels that can capsize, a method for calculation of frequency of capsize per year is presented in the paper. The calculation contains three steps. First, the capabilities of the vessel must be found in terms of the maximum wave height and steepness that the vessel can withstand without capsizing. Secondly, the frequency of occurrence of the demand, i.e., of waves exceeding the capability of the vessel, must be calculated.

Thirdly, the fraction of time that the vessel is in an exposed, beam on situation must be found. This fraction can be influenced upon, and can serve as an important tool in risk management. A practical illustrative example of this, with wave data from the Black Sea, is presented. Comparisons are made with a similar study which utilized wave data from Icelandic and Norwegian waters.

1. INTRODUCTION

Risk analysis has been used in the offshore industry of Norway since 1981. In 1992, application of risk analysis was made mandatory, and regulations were issued. These are built upon modern safety management principles, including internal company control, monitored by the government.

First, the field operator shall state his safety goals regarding human, environmental and asset safety. These goals are long term and ideal. From these, the operator shall derive risk acceptance criteria. These are short term goals that are to be moved closer to the safety goals when e.g. new technology becomes available, or when cost-benefit relations change.

In risk analysis, risk is normally considered as a combination of;
- probability of occurrence within one year (frequency)
- consequence

Therefore, risk can be reduced to acceptance level by reduction in frequency, consequence or both.

Measures that reduce the frequency of accident occurrence have first priority. Second priority is given to design measures that reduce the accident consequences.

2. CAPSIZE IN BREAKING WAVES FROM THE SIDE

Capsize in breaking waves from the side is a credible accident for smaller vessels. When applying risk analysis to capsize in breaking waves, the consequence of the accident is often total loss of the vessel, and often a considerable fraction of the crew perish. This is illustrated by the fact that while accidents in bad weather account for only 25% of the total vessel losses in the Norwegian fishing fleet, they account for 65% of the human losses, which proves that the probability of survival in capsize accidents is low, compared with other accident types. The reasons are that traditional lifesaving appliances are ineffective, and that the crew may be trapped inside the vessel when sudden capsize occurs.

2.1 Frequency reduction, preventing capsize to occur by good vessel design

The term capsize is strongly connected to the static stability curve of a vessel. As shown in Fig. 1, there are 3 typical shapes of the GZ-curve. For an intact vessel with a curve as shown in Fig. 1a, the vessel will turn back to an upright position after being hit by a wave, and capsize is not possible.

Obviously, the primary objective in risk analysis, to avoid the occurrence of an accident altogether, can be achieved by ensuring that the vessel has a stability curve as shown in Fig. 1a.

This approach was chosen by the Norwegian government in 1981, when regulations for new fishing vessels were enforced in which a minimum angle of vanishing stability of 80 degrees was required for new vessels between 25 GRT and 45m in length. This has been achieved by providing deckhouses and super-structures with efficient closing appliances, including these volumes in the stability calculations. Also, divisions in the fish hold must be provided to prevent shifting.

For such vessels, there will be no further need for risk analysis. However, the safety depends entirely upon keeping the deck enclosures closed weathertight in bad weather. Unfortunately, some fishermen do not follow the instructions in this respect. As an example, the Norwegian fishing vessel "Bordanes" capsized in October 1993, with a loss of 9 lives, because the deck enclosures were not closed properly, Sæveraas et al. [1].

Based upon otherwise good Norwegian record with new fishing vessels, it is strongly recommended to lay the emphasis on avoidance of capsize altogether by well known design measures, rather than to become lost in meditation on marginal stability research.

2.2 Frequency reduction, preventing capsize to occur by operational means

For a vessel with a curve as shown in Fig. 1a, the crew may be injured because the vessel can turn over by 360 degrees. In the context of this paper, such an incident is not considered as a capsize.

In Fig. 1b the most dangerous type of stability curves is shown. When such a capsize occurs, the crew will be trapped inside the vessel, while for a vessel as shown in Fig. 1c, there will at least be a chance of escape.

Vessels with intact stability curves as shown in Fig. 1b should be prohibited. In this paper the discussion of frequency reduction by operational means will be restricted to vessels with a stability curve with the shape shown in Fig. 1c.

2.3 Calculation of mean expected frequency of capsize in waves from the side

The method of calculating the capsize risk can be outlined as follows:

1. Systematic model tests, with known stability characteristics, in order to select and characterize potentially dangerous waves.
2. Frequency calculation of the identified, dangerous waves for the sea area under consideration.

3. Calculation of the probability of the vessel to be exposed to capsize.

As an example, the results from systematic model tests of the Norwegian fishing vessel M/S Helland Hansen (Fig. 2) is shown in Fig. 3. For a normal loading condition (small amounts of cargo), and fulfilling the stability recommendations of IMO [2] (stability curve as shown in Fig. 1c), the critical wave height of a plunging breaking wave is about 4m.

The frequency of occurrence per time period under consideration of steep waves at a random location is based upon the following mathematical model.

$$F(W) = \underset{j\ k}{\Sigma\Sigma} P_{3jk} \cdot (P_{4jk} \cdot t/T_{zk})$$
$$= t \cdot \underset{j\ k}{\Sigma\Sigma} P_{3jk} \cdot P_{4jk}/T_{zk} \tag{1}$$

where

j = index of significant wave heights H_{sj}
k = index of zero-crossing periods T_{zk}
t = time period under consideration (sec)
P_{3jk} = Prob$[(\epsilon \geq \epsilon_c) \cap (H \geq H_c)|H_{sj}, T_{zk}]$
= the conditional probability of steep $(\epsilon \geq \epsilon_c)$ and high $(H \geq H_c)$ waves for a given seastate (H_{sj}, T_{zk}) (see Myrhaug and Kjeldsen [3] and Myrhaug and Dahle [4] for more details). Here H is the zero-downcross wave height, and ϵ is the crest front steepness defined by

$$\epsilon = \cfrac{\eta'}{\cfrac{g}{2\pi}T^2 \cdot \cfrac{T'}{T}} = \cfrac{\eta}{\cfrac{g}{2\pi}TT'}$$

The symbols are defined in Fig. 4, and g is the acceleration of gravity. ϵ represents the mean crest front inclination of a zero-downcross wave in the time domain, and the definition is obtained by transforming the length scale to a time scale by using the dispersion relationship for linear deep water waves, i.e., $L = gT^2/2\pi$. This is of course an approximation for the nonlinear wave form given in Fig. 4, and may therefore distort the results. The subscript c denotes threshold value of the parameter. Knowledge of the relation between capability (i.e., stability) and demand (i.e., critical breaking waves) is necessary. This relation can be found by systematic model experiments as described in Dahle and Kjærland [5], see Fig. 3. Knowing the area below the stability curve from zero to the vanishing angle of stability, a minimum height H_c of the critical breaking wave can be found from Fig. 3.

As an example, a typical steep wave in a given seastate is considered, defined by the following threshold values, $\epsilon_c = 0.25$ and $H_c = 4$ m. The probabilities of occurrence are given in Dahle and Myrhaug [6], Table 1. These results are valid for any class of H_{sj} and T_{zk} for which there are values given in Dahle and Myrhaug [6], Table 1, and for the associated threshold values $\epsilon_c = 0.25$ and $H_c = 4$ m. Further discussions are given in Dahle and Myrhaug [6]. The general method of calculating P_{3jk} for other threshold values ϵ_c and H_c than those given in this example is given in Myrhaug and Kjeldsen [3].

Table 1. Conditional probability of occurrence of steep $(\epsilon \geq \epsilon_c)$ and high $(H \geq H_c)$ waves for a given sea state (H_{sj}, T_{zk}), $P_{3jk}=P(\epsilon_c=0\ 25, H_c=4m|H_{sj}, T_{zk})$.

$T_z(s)$ $H_c(m)$	<5	5-7	7-9	9-11
3.0-4.5	$1.1\ 10^2$	$4.9 \cdot 10^4$	$2.8\ 10^5$	$2.7\ 10^{-6}$
1 5-3.0	$1\ 6\ 10^{-4}$	$1.1\ 10^6$	$<10^{-6}$	$<10^6$
<1.5	$<10^{-6}$	$<10^{-6}$	$<10^6$	$<10^{-6}$

The probabilities of occurrence of steep and high waves in the seastates

occurring in the Black Sea are given in Table 1, and are obtained from Dahle and Myrhaug [6] From Table 1 it appears that the conditional probability of typical steep waves (1) decreases as T_z increases for a given H_c value, and (2) increases as H_s increases for a given T_z value, corresponding to the expected behaviour that the probability of occurrence of typical steep waves increases with increasing steepness of the sea state

The wave data upon which this approach is based, are obtained by Waverider buoys at deep water on the Norwegian continental shelf, and thus the wave steepness statistics are on the non-conservative side (Myrhaug and Dahle [4]). Data from more precise measurements at sea are becoming available (Myrhaug and Dahle [4]), but until systematic analysis of such data have been made, the present approach should represent a useful tool in engineering applications, even in other ocean areas, such as in the assessment of capsize of smaller vessels at sea as illustrated herein.

P_{4jk} = the probability of occurrence of H_{sj}, T_{zk} in the time period under consideration. $N_c = P_{4jk} \cdot t/T_{zk}$ gives the total number of waves in the seastate (H_{sj}, T_{zk}) within the time period t under consideration. For one year, $t = 3.15 \cdot 10^7$ (sec), while for one season of 3 months, $t = 7.9 \cdot 10^6$ (sec). Then F(W) in Eq. (1) gives the total number of waves in the time period t for which H ≥ 4 m and $\varepsilon \geq 0.25$.

Joint frequency tables of H_s and T_z are generally available, for instance from Hogben et al. [6], giving wave data on a world-wide basis. For the Black Sea, however, data were prepared by Bogdanov [8], and are given in Table 2.

Table 2. Probability of sea states $P_{4jk}=P(H_{sj},T_{zk})$ for the Black Sea (from Bogdanov [8]).

Winter

T_z (s) / H_s(m)	<5	5-7	7-9	9-11
3.0-4.5	0.01	0.01	0.01	
1 5-3 0	0.14	0.09	0.02	0.01
<1.5	0.58	0.09	0.03	0.01

Spring

T_z(s) / H_s(m)	<5	5-7	7-9	9-11
3.0-4.5		0.01		
1.5-3.0	0.07	0.06	0.01	
<1.5	0.75	0.07	0.02	0.01

Summer

T_z (s) / H_s(m)	<5	5-7	7-9	9-11
3.0-4.5				
1.5-3.0	0 06			
<1.5	0.84	0.08	0.02	

Autumn

T_z(s) / H_s(m)	<5	5-7	7-9	9-11
3.0-4 5	0.01	0.01	0.01	
1.5-3.0	0 10	0.03	0.01	
<1.5	0.78	0.04	0.01	

Figure 5 shows F(W)/t according to Eq. (1), that is, the frequency of encountering steep waves at a random position at sea divided by the time of duration of season and year, respectively. As suggested by the data in Fig. 5, F(W)/t is the same for Area 3 and 4, while it is about one tenth of these values in the Black Sea. The seasonal values for Area 3 and 4 are also fairly similar, but it is noticed that there are significant seasonal variations in all areas. It is also noticed that the value for

the winter season in the Black Sea is significantly higher than the other seasonal values, and comparable with the winter season value in the Norwegian Sea.

The probability of the vessel to be exposed to capsize (C) for a steep breaking wave (W) is.

$$P(C|W) = P_5 \cdot P_6 \cdot \sum_j \sum_k P_{1jk} \cdot P_{2jk} \qquad (2)$$

where

P_{1jk} = probability of exposed wave direction (i.e., heading of vessel) in seastate jk.

P_{2jk} = yearly fraction of time of exposure in seastate jk.

P_5 = probability of being hit by a steep breaking wave during the period of rolling that the vessel is most exposed. In this analysis, $P_5 = 0.5$.

P_6 = conditional probability of capsize, given that the vessel is hit by a steep breaking wave. P_6 is 0 for the "safe" regions. For "unsafe" regions in Fig. 3, the conditional probability has to be assessed from historical data, e.g. from Dahle et al. [8], see Ch. 4 for details.

Then, the frequency of capsize is;

$$F(C) = F(W) \cdot P(C|W) \qquad (3)$$

3. FREQUENCY REDUCTION OF CAPSIZE BY OPERATIONAL RESTRICTIONS

Evidently, there are numerous ways of reducing the risk of capsize by reducing one or more of the factors contributing to $P(C|W)$. The possibilities are summed up in the following.

P_{1jk}, Heading of vessel in seastate jk
Heading is decided by the skipper, and heading against the waves is common practice in severe weather. However, with the available data for F(W), it is possible to specify for which observed wave heights heading against

waves is necessary over the year to restrict the capsize risk to an acceptable level.

P_{2jk}, Yearly fraction of time of exposure in seastate jk
By systematically eliminating large wave heights in the calculation of F(W), the reduction of capsize risk by specifying for the skipper always to avoid severe weather above a given limit can be found. The expected weather must be estimated by listening to local weather forecast. If, however, the distance to sheltered area is considerable, safe heading must be chosen. Several requirements exist for this way of reducing the capsize risk, e.g. in Norway and in UK.

P_5, Probability of being hit by a steep breaking wave during the period of rolling that the vessel is most exposed
A wave hitting the vessel from the side within a 90 degrees sector is considered dangerous, i.e., $P_5 = 0.5$.

P_6, Conditional probability of capsize, given that the vessel is hit by a steep breaking wave
Large, unprotected openings may easily transform a Fig. 1a-vessel to a Fig. 1b or a Fig. 1c-vessel, and the skipper can make an otherwise safe vessel unsafe by not closing openings in the superstructure or deckhouse. If information is available, also calculation for an otherwise safe vessel can be made.

By applying risk analysis as outlined above, safe operation will be defined as operation over one year that results in a frequency of capsize in breaking waves that is below the acceptance criteria.

P_6 is 0 for the "safe" regions.

4. PRACTICAL EXAMPLE

In this example, capsize risk for M/S Helland Hansen in Icelandic and in Norwegian seas, fishing without and with operational restrictions, will be illustrated. It should be noted that the vessel is always in ballast or

lightly loaded condition having a stability curve as shown in Fig. 2. F(W)/t according to Eq. (1), which is used in this example, is given in Fig. 5.

Without restrictions, the P(CIW) factors are:

P_{1jk}, Heading of vessel in seastate jk

Risk reduction by heading is not assumed to be undertaken in any seastate, i.e., $P_{1jk} = 0.5$.

P_{2jk}, Yearly fraction of time of exposure in seastate jk

All fishing vessels spend a fraction of the year in the port for unloading, repair etc. Here, fraction spent at sea is set to 80%, i.e., $P_{2jk} = 0.8$.

P_s, Probability of being hit by a steep breaking wave during the period of rolling that the vessel is most exposed
$P_5 = 0.5$

P_6, Conditional probability of capsize, given that the vessel is hit by a steep breaking wave

From laboratory experiments of Dahle and Kjærland [5], it has been shown that plunging breakers, with an almost vertical front of the wave crest, can cause capsize of a smaller vessel in ballast or lightly loaded condition even with stability characteristics as recommended by IMO, see Fig. 2. It is now necessary to assess the fraction P_6 of typical steep waves above the threshold $H_c = 4$ m, $\varepsilon_c = 0.25$ that actually cause capsize. From Dahle et al. [9] the historical capsize frequency for the open sea outside Norway was $F(C)_{historical} = 2.8 \cdot 10^{-4}$ per year. As a rough estimate, all vessels are considered to be identical to the vessel shown in Fig. 2, in ballast or lightly loaded condition, and with stability in accordance with the IMO criteria. Then, from Eqs. (2) and (3) and by using this value of $F(C)_{historical}$ and the same figures as in the practical example below, Dahle and Myrhaug [6] found $P_6 = 3.4 \cdot 10^{-7}$. Then

the risk of capsize per year (i.e., $t = 3.15 \cdot 10^7$ sec), with no operational restrictions, can be calculated by combining Eqs. (1) to (3). The results for the Black Sea as well as for Icelandic Waters and Norwegian Sea are given in Table 3, showing that the risk of capsize is 0.000073 in the Black Sea, while it is in the range 0.00021 to 0.00026 in Icelandic Waters and Norwegian Sea.

Table 3. Example of capsize risk for M/S Helland Hansen in ballast or lightly loaded condition having a stability curve as shown in Fig 2 in the Black Sea, Iceland Waters and Norwegian Sea with. $P_{1jk}=0.5$, $P_{2jk}=0.8$, $P_5=0.5$, $P_6=3.4 \cdot 10^{-7}$, values of P(W)/t taken from Fig. 5, $t=3.15 \cdot 10^7$ sec.

Area	No operational restrictions F(C) (per year)
Black Sea	$0.73 \cdot 10^{-4}$
Icelandic Waters (3)	$2.6 \cdot 10^{-4}$
Norwegian Sea (4)	$2.1 \cdot 10^{-4}$

This results is to be expected, taking into account the milder wave climate in the Black Sea. The result also indicates that a uniformly and generally applied stability criterion gives very different risk levels for different sea areas. With an acceptance criterion in the range of 10^{-4}, it is clear that in the Black Sea, operations can be undertaken without restrictions for the sample vessel exposed to the specified dangerous waves (i.e., $H \geq 4$ m and $\varepsilon \geq 0.25$).

In Icelandic and Norwegian waters, however, operational restrictions would be

required to obtain such a risk level for capsize. Such restrictions are basically

- remain in port above certain wave parameter limits, based upon weather forecast;
- correspondingly, if at sea, heading against the prevailing wave direction.

More details of these restrictions are given in Dahle and Myrhaug [6].

5. CONCLUSIONS

The risk of capsize in steep waves from the side is well known. The most important way of reducing the risk is to design smaller vessels with tight deckhouses and superstructures, and to require that the skipper keeps the vessel closed as specified.

A secondary way of risk reduction for vessels without such design features is to give specified, operational restrictions to the skipper. Such restrictions must be based upon knowledge of the vessel's response to dangerous waves, and knowledge of the frequency of occurrence of such waves in the operational area of the vessel under consideration.

6. REFERENCES

1. Sæveraas, N., Aleksandersen, A. and Dahle, E.Aa., Report from the Governmental Fishing Vessel Accident Commission on the investigation of the loss of M/S BORDANES 28th October 1993, Norwegian Ministry of Justice (in Norwegian), 1994.

2. IMO, IMO Res. A. 168 Recommendation on intact stability of fishing vessels, London, 1968.

3. Myrhaug, D. and Kjeldsen, S.P., Prediction of occurrences of steep and high waves in deep water, J. Waterway, Port, Coastal, and Ocean Engineering, Vol. 113, 1987, pp.122-138.

4. Myrhaug, D. and Dahle, E.Aa., Ship capsize in breaking waves, In: S.K. Chakrabarti (Editor), Fluid Structure

Interaction in Offshore Engineering, Advances in Fluid Mechanics, Vol. 1, Computational Mechanics Publications, Southampton, UK, 1994, pp. 43-84.

5. Dahle, E.Aa. and Kjærland, O., The capsizing of M/S Helland Hansen, Trans. Royal Inst. for Naval Architects, Vol. 122, 1980, pp. 51-70.

6. Dahle, E. Aa. and Myrhaug, D., Capsize risk of fishing vessels, Ship Technology Research (Schiffstechnik), Vol. 43, 1996, pp. 164-171.

7. Hogben, N., Duncan, N.M.C. and Olliver, G.F., Global Wave Statistics, Unwin Brothers, London, 1986.

8. Bogdanov, P., Personal Communication, 1996.

9. Dahle, E.Aa., Myrhaug, D. and Dahl, S.J., Probability of capsizing in steep and high waves from the side in open sea and coastal waters, Ocean Engineering, Vol. 15, 1988, pp. 139-151.
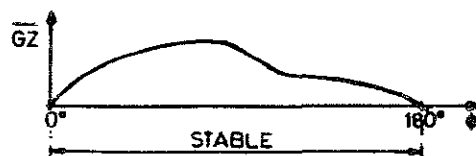
a. Self-righting.
Capsize not feasible
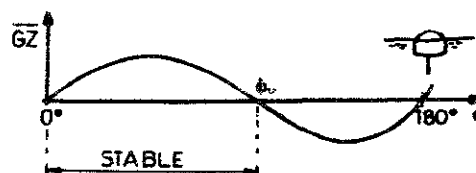
b. Capsize to 180°
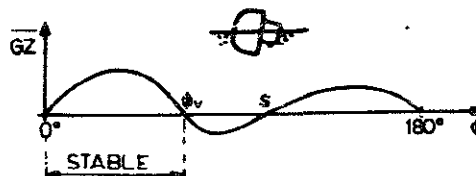
c. Capsize to stable side position (s)

Fig. 1 Definition of capsize
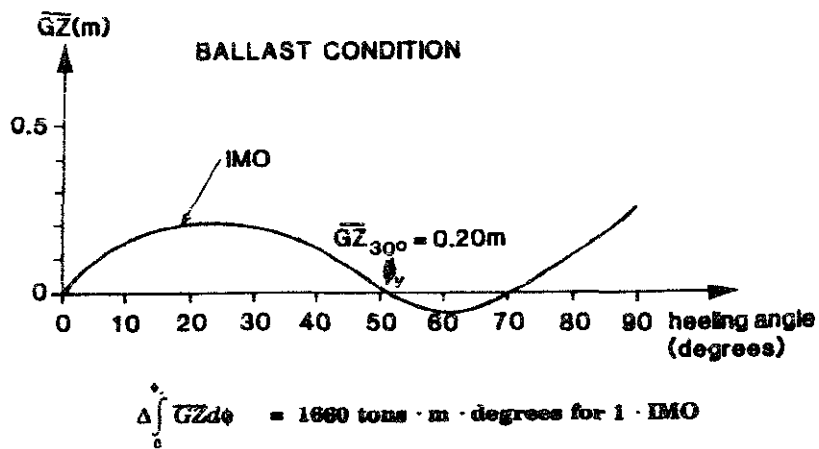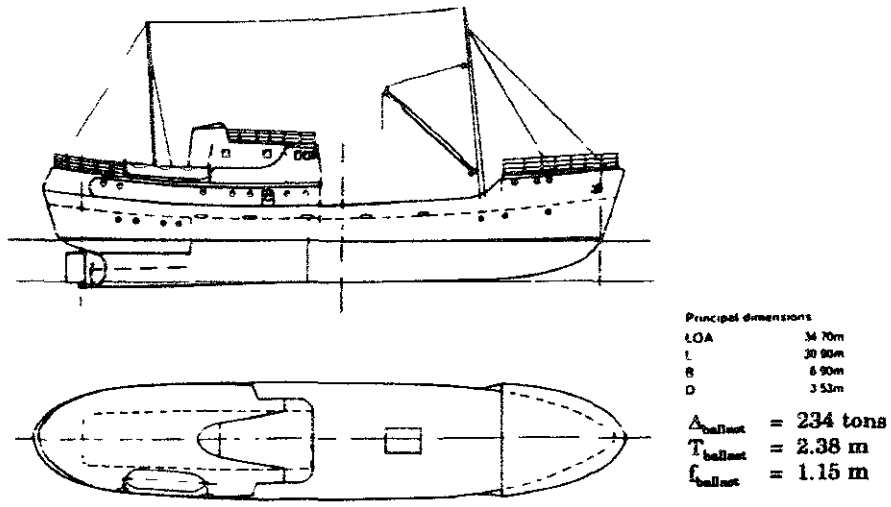
Fig. 2 Outline of the subject vessel M/S Helland Hansen
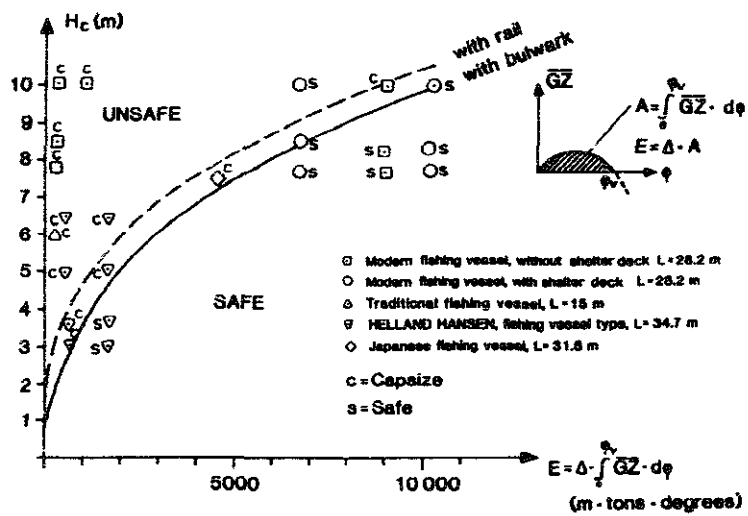
Fig. 3 Safe and unsafe regions as found from model tests of M/S Helland Hansen, Dahle and
Kjærland [5] (from Dahle et al. [9])

208
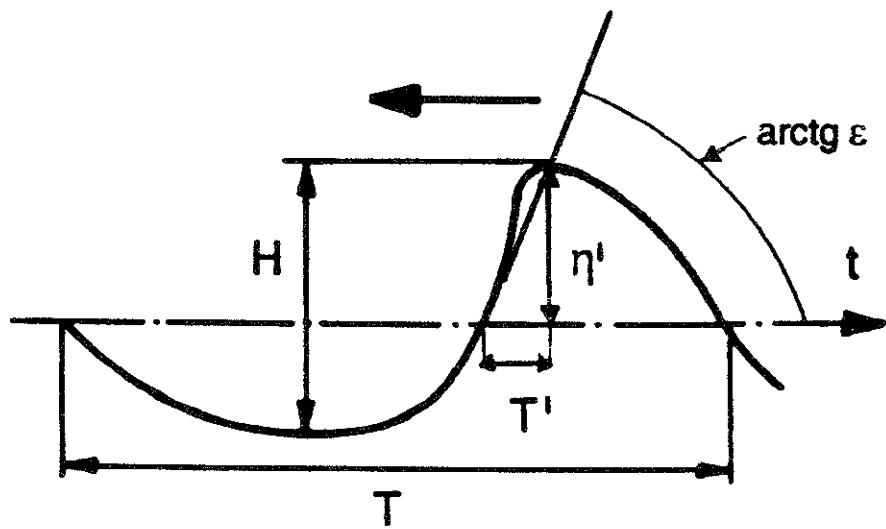
Fig. 4 Definition of zero-downcross waves
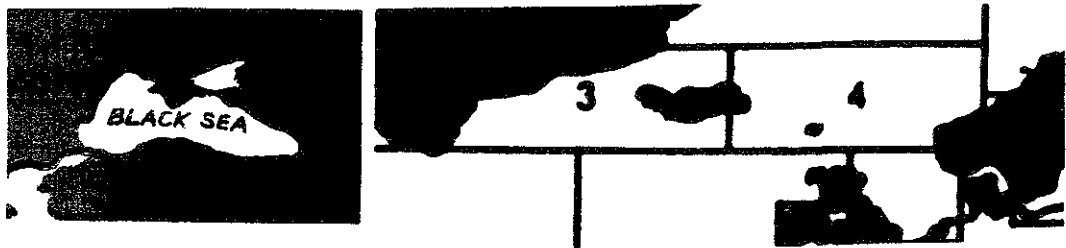
Black Sea	Spring 0.0000028	Summer 0.0000024	Autumn 0.000032	Winter 0.00010	Annual 0.000034
Icelandic Waters (3)	Feb-Apr 0.00015	May-Jul 0.000037	Aug-Oct 0.00013	Nov-Jan 0.00018	Annual 0.00012
Norwegian Sea (4)	Mar-May 0.00022	Jun-Aug 0.000055	Sep-Nov 0.00012	Dec-Feb 0.00012	Annual 0.00013

Fig. 5 F(W)/t according to Eq. (1) in the Black Sea, and for typical sea areas outside Iceland (Area 3) and Norway (Area 4)

PROBABILISTIC ASSESSMENT OF THE EXPECTED OIL OUTFLOW IN FOUR TANKERS

by

S. A. Ferreira and C. Guedes Soares

Unit of Marine Technology and Engineering, Technical University of Lisbon

Instituto Superior Técnico, Av. Rovisco Pais, 1096, Lisboa, Portugal

ABSTRACT

As a result of increased public concern over the marine transportation of oil, during the last decades, several authors have developed probabilistic theories for ship subdivision. The present paper outlines the results of a study applied to four different tankers. A software tool has been developed in a way to apply the probabilistic approach to the study of the subdivision of tankers. The main idea is the assessment of the effectiveness of various constructional features in reducing accidental oil spills following collision or grounding.

1 INTRODUCTION

An important purpose of the subdivision of ships is to preserve their floatability and stability, whenever a casualty occurs involving water ingress. The contingency effect is achieved by the limitation of the maximum amount of flooding associated with a hull penetration on a tank or compartment.

Collisions are common accidents among ships. They are random events and their consequences in terms of structural damage are also uncertain. The structural consequences of collisions can be described in terms of the dimensions and locations of the hull penetrations that cause flooding, parameters that can also be modelled by random variables.

In view of the uncertainties about the occurrence of collisions and their consequences, any decision about the location of watertight bulkheads (Figure 1) should be based on a probabilistic formulation.

In the case of tankers the main catastrophic consequence associated with hull penetration is the pollution induced by oil outflow, since the loss of stability for this type of ships is not frequent.

This study is aimed at the assessment of the probability of oil outflow resulting from collisions. For a fixed scenario of expected collision damage, the probability of oil outflow will be a function of the subdivision adopted.

The calculation of different measures of the probability of oil outflow has been implemented in a computer code that has been

used to study four tankers from two main types of designs. The study has shown that significant improvements in the performance of these ships could be attained if the probabilistic approach had been considered in the design of their subdivision.

2 PROBABILISTIC FORMULATION OF THE OUTFLOW FOLLOWING COLLISIONS

Wendel and his associates introduced the probabilistic approach for the assessment of ship subdivision, (Wendel et al, 1968), making possible the calculation of a numeric value that could be related to the achieved level of safety and to the residual risk of ship loss associated with a specific subdivision. Their principal concern was the increase of ship safety.

IMO only adopted the probabilistic concept in 1973 in Resolution A.265 (VIII), (IMO, 1974). The present IMO regulations on subdivision and damage stability are based on the probabilistic concept, which takes the probability of survival after collision as a measure of ship's safety in the damaged condition. This is quantified by the "attained subdivision index", A.

The probability of survival is determined as the probability that a compartment is flooded, multiplied by the probability that the ship will not capsize or sink with the considered space flooded.

During the last decades different authors have suggested improvements to the IMO formulation concerning the distribution of the longitudinal locations and the extent of ship collision damage. Examples of this effort are due to Abicht (1989, 1990), Jakic (1989, 1991, 1997) and Pawlowski (1996, 1997).

These proposals were introduced into the regulations very slowly. In fact, IMO did not introduce the new regulations on subdivision, based on the probabilistic approach for dry cargo ships, including the risky Ro-Ro ships, until 1st February 1992.

The present IMO regulations include the Pawlowski's approach for transversal subdivision and the "r-procedure" (IMO, 1974) for the combined, longitudinal and transversal, subdivision.

However, significant improvements to IMO regulations, have already proposed but they have not yet been implemented by IMO.
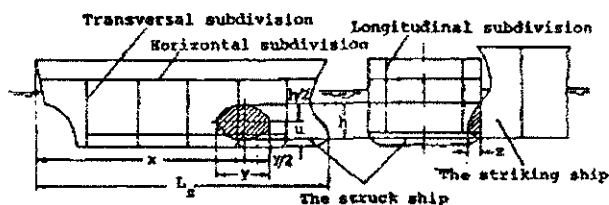

Figure 1- The collision causing flooding

The current regulations governing damage stability and oil outflow for tankers are based on the International Conference for the Prevention of Pollution from Ships, 1973, (IMO, 1986) and the Protocol of 1978 Relating to MARPOL '73 (IMO, 1978).

As mentioned before, the main problem with tankers is the damage that can be caused to the environment after a casualty. Since regulations in force are deterministic and prescriptive in nature, rather than goal setting, the environmental safety performance of existing tankers differs considerably.

In order to assess the risk of different tanker designs, Pawlowski (1996, 1997), proposed a probabilistic approach, that evaluates dissimilar configurations of this kind of ships based on merit functions. This procedure can be used as a tool to reduce the risk of oil pollution and damage to the environment.

Pawlowski presented four measures of merit for assessing the effectiveness of a tanker's subdivision from the stand point of protection of the environment: two global measures, describing the overall performance of the ship, and their local counterparts, related to a given part of the ship. These four measures are:

• the probability P_0 of avoiding the pollution of the sea by cargo, called also probability of zero outflow;

212

$$P - \sum P_k \qquad \text{for } i \in I_k \qquad (1)$$

- the local probability of zero outflow (from a given part of the ship) P.

$$P - \frac{\sum p_n}{\sum P} \qquad \text{for } i \in I, \qquad (2)$$

- the average probability O_m (global or overall mean outflow) in the case of collision involving the cargo tank area.

$$O_m = \sum p \cdot i \qquad \text{for } i \in I \qquad (3)$$

- and the local average outflow O_i (from a given part of the ship)

$$O = \frac{\sum p_i \cdot v}{\sum p} \qquad \text{for } i \in I, \qquad (4)$$

where

i - index representing each compartment or group of compartments under consideration.

p - probability of flooding a given compartment group.

p_{hi}- probability p_i of flooding a compartment group containing no oil.

v - volume of oil contained in the compartment group under consideration;

n - number of damage zones along the ship length

This study is aimed at quantifying the overall effectiveness of a particular tanker design in limiting the oil outflow and, therefore, the evaluation of the overall mean outflow is a very good indication to this performance. This parameter represents the sum of the products of each damage probability and the computed outflow for that damage case.

The significance of the probability of zero outflow is very large because this parameter represents the probability that no cargo will be released into the environment. This is the other measure evaluated for the tanker's study carried out

The probabilistic calculations of P_0 and O_m, can be performed in a more simplified way with the introduction of the notion of cumulative probability This simplification avoids the exhaustive calculations that would be needed to calculate the probabilities of each compartment and the combinations with the adjacent compartments Through the use of the cumulative probability, the calculation will be performed one compartment at a time which makes the procedure much simpler His use is due to the application of the additive property of the volume v, Then

$$O_m = \sum p \cdot v = \sum p_i \sum v_k = \sum_k v_k \sum_i p \qquad (5)$$

which results in

$$O_m = \sum_k c_k \cdot v_k \qquad (6)$$

where

v_k - is the volume of cargo contained in a certain tank:

c_k - is the cumulative probability for a certain tank, i e, the probability that at least this tank suffers a damage due to a casualty, alone or with other adjacent compartments.

The value of this parameter is easy to calculate if one assumes a rectangular damage that exceeds the distance b_k from the nearest longitudinal bulkhead (measured from the ship side), and that exceeds the longitudinal limits of the tank. In this case c_k is given by

$$c_k = 1 - r_i(b_k) - p_a \cdot [1 - r_a(b_k)] - p_f \cdot [1 - r_f(b_k)] \qquad (7)$$

where

p_a - is the probability of flooding, pi, calculated for the area that extends from the aft bulkhead of the considered compartment, to the aft end of the ship;

p_f - is the probability of flooding, pi, calculated for the area that extends from the forward bulkhead of the considered compartment, to the forward end of the ship;

r is the reduction factor due to the lateral compartments of width b_k, calculated for the total length of the ship;

r_a and r_f - these parameters have the same meaning of r_l, but in this case they are calculated for the areas described in p_a and p_f respectively.

With the introduction of this parameter, the calculation of the probability of zero outflow will be given by

$$P_i = 1 - c_0 \qquad (8)$$

where c_0 is calculated from (7), considering that the cargo area does not have any subdivision, being b_k the breadth of the wing ballast tanks.

As can be observed this value is only dependent from the transverse subdivision of cargo area, depending only from its limits and from the referred breadth.

Through a new mathematical arrangement of formula (6), the following relation for the calculation of O_m can be derived

$$O_m = \gamma . \sum_i c_i v \qquad (9)$$

where γ represents the reduction factor of O_m, due to the existence of longitudinal bulkheads in the cargo area. This factor is independent of the transverse subdivision, depending only of the number of longitudinal bulkheads in the cargo area and on their location.


Figure 2 – Nomenclature used

The γ factor, in the typical case of tankers with wing ballast tanks and two longitudinal bulkheads is given by

$$\gamma = \frac{1}{2}.(1 - v_2^*) + v_2^* . \frac{c_2}{c_1} \qquad (10)$$

where c_1 and c_2 are the cumulative probabilities calculated through formula (7), for the side tank and the central tank, respectively. Hence, in the referred formula b_k should take the values w_1 (for c_1) and w_2 (for c_2), that are the non-dimensional distances of that tanks to the ship side. The coefficient v_2^* gives the ratio between the volume of the central cargo tank and the total volume of that same compartment.

The following relations define the non-dimensional quantities:

$$w_1 = \frac{b_1}{B} ; w_2 = \frac{b_2}{B} ; w_c = \frac{b_c}{B_c} ; w_s = \frac{2.b_s}{B_c} \qquad (11)$$

The following relations can be easily derived

$$w_c = \frac{1 - 2.w_2}{1 - 2.w_1} = \frac{b_c}{B_c} \qquad (12)$$

$$w_s = 1 - w_c = \frac{2.b_s}{B_c} , \qquad (13)$$

from where one can derive the following important relation for the calculation of γ factor:

$$w_2 = w_1 + \frac{1}{2}.w_s.(1 - 2.w_1) \qquad (14)$$

This relation plays an important role, because in the calculation procedure only the characteristics w_j and w_s are input parameters.

The value of v_2^* is calculated through the following formula.

$$v_2^* = \frac{(1 + k_2)}{C_B} \cdot \frac{(1 - 2.w_2)}{(1 - 2.w_1)} \qquad (15)$$

where C_B is the ship block coefficient, and k_2 is a factor that gives the increase in volume due to ship camber. This factor, where H represents the height of the tank measured on the ship side, assuming that it can be approximated by a cosine of amplitude ΔH, would be given by:

$$k_- = \frac{\cos \pi w_2}{\pi.(0,5 - w_2)} \cdot \frac{\Delta H}{H} \qquad (16)$$

Introducing the mean cumulative probability value, the following formula for the value of the total mean outflow results:

$$O_m = \gamma.c_m.V_c , \qquad (17)$$

where $V_c = \sum_j v_j$ represents the total volume of cargo and c_m the mean cumulative probability (outflow risk) for all ship compartments:

$$c_m = \frac{1}{V_c} \cdot \sum_j c_j.v_j = \frac{1}{V_c^*} \cdot \sum_j c_j.v_j^* , \qquad (18)$$

where $V_c^* = \sum_j v_j^*$ is the total non-dimensional volume of cargo contained in the ship compartments:

$$v_j^* = \int_\Lambda \frac{S}{S_0} d\xi \approx \frac{S_j}{S_0}.\lambda_j , \qquad (19)$$

where $\frac{S}{S_0}$ is the transverse section of the cargo space, related to the midship area and λ_j is the non-dimensional length of a given segment.

The non-dimensional mean outflow is then given by.

$$O_m^* = \gamma.c_m \qquad (20)$$

This formula can be further developed in order to take into account other effects.

$$O_m^* = \gamma \cdot \frac{c_m}{c_0} \cdot \frac{c_0}{c_0^*} .c_0^* \qquad (21)$$

where γ is the reduction factor due to the existence of longitudinal bulkheads, $\frac{c_m}{c_0}$ due to the transversal compartimentation of the cargo space, $\frac{c_0}{c_0^*}$ due to the side tanks and double hull and c_0^* due to the spaces without cargo in the ends of the ship.

3   CALCULATION OF THE PROBABILITY OF OIL OUTFLOW

This section describes the calculation procedure that has been adopted in the software that has been developed and in the calculations reported here.

It is sufficient to derive the formula for the probability p of flooding a single compartment, since the probability p_i of flooding a group of adjacent compartments is expressed in terms of the probabilities of flooding the single compartments which make up that group

Figure 3 represents distribution function of ξ, adopted by Pawlowski (1996).
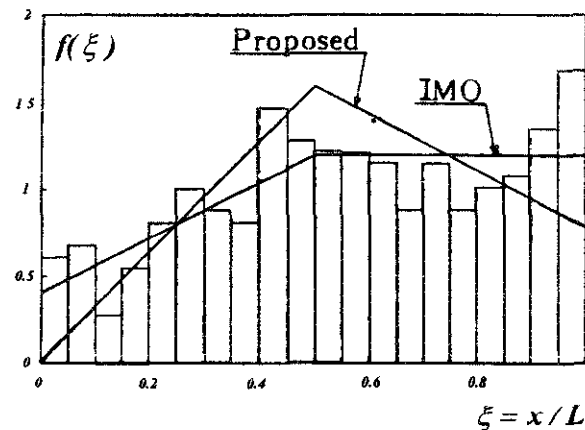
Figure 3 – Histogram of ξ adopted by IMO and proposed by Pawlowski.

which is approximated by the equation:

$$f(\xi) = 32\xi \quad \text{if } \xi \le 0.5$$
$$f(\xi) = 2.4 - 1.6\xi \quad \text{otherwise}$$

$$\tag{22}$$

$$F(\xi) = 0.4 + \frac{1}{4}(2\xi - 1)(1.6 + f)$$

Then the following is obtained for calculating p

$$p = \begin{cases} 1 & \text{if } J = 1 \\ F + \frac{1}{2}.a.g + 0.8q & \text{if } E_1 = 0 \\ 1 - F + \frac{1}{2}.a.g - 0.4g & \text{if } E_2 = 0 \\ a.g & \text{otherwise,} \end{cases} \tag{23}$$

where

$$F = F(\xi = E_{12})$$

$a - f_0$

g - first integral of the distribution function $F_c(\lambda)$

q - second integral of the distribution function $F_c(\lambda)$

$$F_c(\lambda) = 1 - (1 - y)^2$$

and for the last three cases, if J' is greater than 0, p is reduced by an amount 1.2.q, calculated with y taken as $\dfrac{J'}{\lambda_{max}}$., where

J – non-dimensional length of the compartment (by L_s),

J' – theoretical factor depending on the ship type and the length of the compartment;

λ_{max} - maximum non-dimensional length of the compartment;

y - normalised length of the compartment

Resorting to the use of the calculation of the reduction factor r, it is possible to represent the probability that the inboard space adjacent to a single wing compartment will not be flooded.

IMO has adopted an approximate formula, which was subsequently modified to produce slightly higher values of r, for very narrow tanks. In this work the formula proposed by Pawlowski was adopted for the calculation of this factor.

$$r = \begin{cases} 1 & J \le J_i \\ 1 - [1 - F_c(w)]\left[1 - \dfrac{F_c(v_0) + (1 - v_i)F(y_i)}{F_c(1)}\right] & \text{otherwise} \end{cases} \tag{24}$$

This expression proved to be simple and accurate for the two cases and is fairly accurate for other compartments.

The procedure described has been implemented in a program developed for personal computers under Windows 95 operating system. The tank arrangements in study are defined numerically and once this description has been done it is a relatively easy task for the computer to calculate the compartment groupings and the probabilities for every possible damage location and extent. The mathematical procedure used is completely explained the previous section.

The application is supplied with several features that enable a comprehensive working analysis tool. It also has a set of pull-down menus that gather all commands available in the program

It is also possible to view whenever needed, a powerful help-on-line, that exhibits full understanding explanations of the different application options All results can be displayed in table format or in graphical representation.

The effectiveness of a tanker design in reducing oil pollution can be related to the probability of oil outflow. Therefore this computer package can be used as a tool to decide on the location of the watertight bulkheads in order to minimise the probability of oil outflow.

3.1 Comparison With Other Approaches

As mentioned before, during the last decades many authors proposed several different

approaches for the probability of the appearance of longitudinal locations and extents of ship collision damage
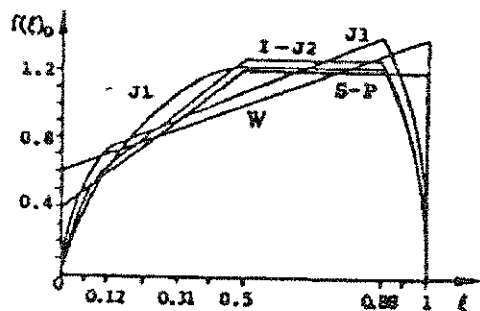

Figure 4 - The output" distribution densities of the Longitudinal Locations of Ship Collision Damages
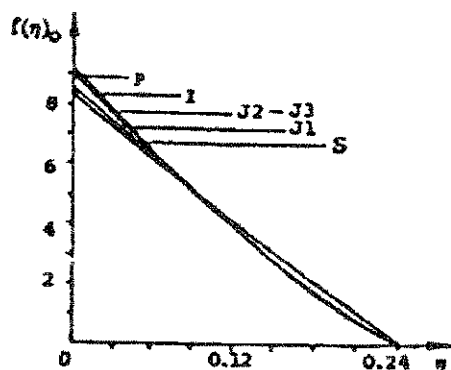
Figure 5 - The output' distribution densities of the Lengths of Ship Collision Damages

Figures 4 and 5 present the different approaches to the "output" distribution densities given by different authors They include the three Jakic's approaches [J1, J2, J3] Wendel's approach [W], the simplified distributions [S], IMCO s approach [I] and the first Pawlowski's approach [P]

The most important conclusion to take from these figures is that the work developed by Jakic removes the "impulses" from the distribution densities, preserving the good agreement with the statistical data from IMO This improvement was not included in the present calculation procedure because it has not been yet fully tested

Jakic and Pawlowski also proposed different approaches to substitute the inaccuracies of the r-procedure for the combined, transverse and

longitudinal subdivision However, IMO did not implement these improvements

4   EXAMPLE CALCULATIONS

The procedure described in the previous section has been applied to the study of four oil tankers, whose principal characteristics are shown in Table 1

Table 1 - Principal Particulars of the tankers studied

	Tanker A	Tanker B	Tanker C	Tanker D
	271 000	243 800	172 400	172 400
	260 000	236 000	163 000	63 000
	48 250	42 000	24 600	24 600
	24 100	19 200	14 300	4 300
	16 100	13 050	10 600	9 400
	17 200	13 050	10 600	9 400
	0 823	0 805	0 804	0 795
	1993	1984	1976	1975
	22945	16650	6938	6594
	145000	88950	28200	24192

4.1   Calculation of the Probability of Oil Outflow

Data regarding the compartmentation of the four ships are given in Table 2 TANKER A has eight central cargo tanks and eight ballast tanks Only cargo tanks 1, 7 and 8 have different capacities All the remaining cargo tanks are equal
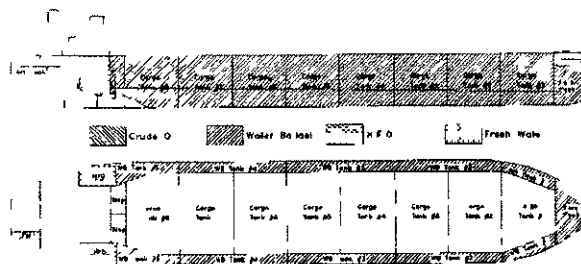

Figure 6 - Tanker A subdivision arrangement
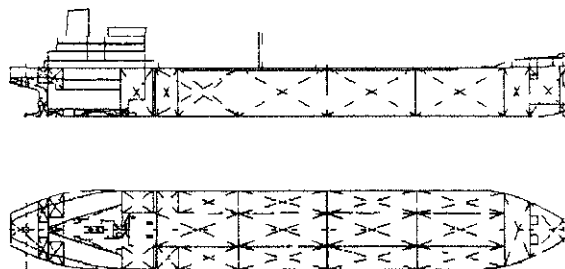
Figure 7 - Tanker C subdivision arrangement

TANKER B has its central cargo tank area subdivided into seven compartments, being only the two end compartments different from the others

Table 2 – Compartimentation of tankers investigated

Tanker A

Station	Cmpt	x(m)	x/Ls	length(m)
100	1	248 83	0 9570	25 02
93	2	223 81	0 8608	25 02
87	3	198 79	0 7646	25 02
81	4	173 77	0 6683	25 02
75	5	148 75	0 5721	25 02
69	6	123 73	0 4759	25 02
63	7	98 71	0 3797	25 02
57	8	73 69	0 2834	25 02
51		48 67	0 1872	

Tanker B

Station	Cmpt	x(m)	x/Ls	length(m)
91	1	194	0 7462	21 25
85	2	172 75	0 6644	21 25
79	3	151 5	0 5827	21 25
73	4	130 25	0 5010	21 25
67	5	109	0 4192	21 25
61	6	87 75	0 3375	21 25
55	7	66 5	0 2558	21 25
50		45 25	0 1740	

Tanker C

Station	Cmpt	x(m)	x/Ls	length(m)
76	1	145 1	0 5581	26 40
68	2	118 7	0 4565	26 40
60	3	92 3	0 3550	26 40
52	4	65 9	0 2535	26 40
44		39 5	0 1519	

Tanker D

Station	Cmpt	x(m)	x/Ls	length(m)
79	1	145 11	0 5581	26 40
68	2	118 71	0 4566	26 40
60	3	92 31	0 3550	26 40
52	4	65 91	0 2535	26 40
44		39 51	0 1520	

The last two ships are older than the previous ones. *Tanker C* has four central cargo tanks and four wing cargo tanks. In this ship only tanks two and three are equal in capacity.

The last tanker under investigation is similar to the former and has also four central and four wing cargo tangs, being the middle two equal between each other.

As can be seen in Table 2 all ships have all their compartments with the same length

The global outflow parameters for the four ships of three different types of subdivision are compiled in Table 3

Table 3 – Outflow parameters for the various types and location of subdivision

	Tanker A	Tanker B	Tanker C	Tanker D
O_M	0 0952	0.0852	0 0702	0 0692
P_0	0 5673	0 6738	0 2445	0 2444

From the results of the calculations performed, the following conclusions can be drawn·

- The larger tankers are safer to the environment (in relative terms). due to the smaller relative damage size,

- The tankers with wing ballast tanks are much safer than those with central and side cargo tanks.

4.2 Redesigning Tanker's Subdivision

For the design of tankers. a parametric study on the location of subdivision has a major interest from the point of view of minimisation of oil outflow, and for clarifying the influence of several parameters in the behaviour of the objective function, given by equation (21).

Pawlowski (1997) performed a sensitivity analysis over different tanker designs. aiming at the studying of the best location of longitudinal bulkheads This process was done through an iterative process, in which. for each ship length, w_l and w_s the γ factor is calculated At the same time, for each ship length and for each w_l, the minimum value of γ is calculated as a function of w_s. The minimum value of γ is then determined by the position between the two minimum values in a given vector

However, his analysis can be improved. One of the deficiencies was the fact that all calculations were made assuming that all tanks had the same length. The present formulation removes that restriction and the compartment lengths are now one of the inputs.

Another major improvement is the development of a procedure to perform also a sensitive analysis not only on the locations of longitudinal bulkheads, but also on the locations of the transverse bulkheads.

After evaluating the different performance indices of the various tankers. the subdivision of *Tanker A* and *Tanker C* is redesigned. i.e.. a new configuration of internal subdivision is analysed.

In order to perform such study the location of the longitudinal bulkhead of the wing ballast tank. w_l, is varied from $0.0B$ to $0.1B$ (B – breadth of the ship). For the location of the longitudinal bulkheads, w_s, the whole range of variation was considered, i.e., from 0.0 to 1.0 and for the number of transversal compartments the same was done from 1 to 24 transverse compartments.

The results for *Tanker A* and *Tanker C* are summarised in Figure 6, 7, 8 an 9, after the parametric study process.

Figure 7 is obtained with the calculated optimum value for w_s. From the figure 7 one can conclude that the number of compartments of this ship is adequate, because the effort that needs to be done to gain something in safety. is very high in this region of the curves.
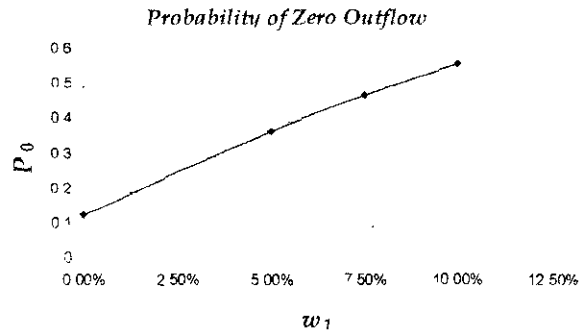

Figure 8 – Values of P_0 function of w_l for **Tanker A**

In what concerns the breadth of wing ballast tanks, it is visible from the figure that the mean outflow reduces with the increase of w_l. Since the value of w_l for *Tanker A* is approximately 10.0% of B (ship breadth) this value can be considered acceptable in terms of safety to the environment. Figure 8 confirms the above statements, where it is obvious the increase of the probability of zero outflow with the increase of w_l.
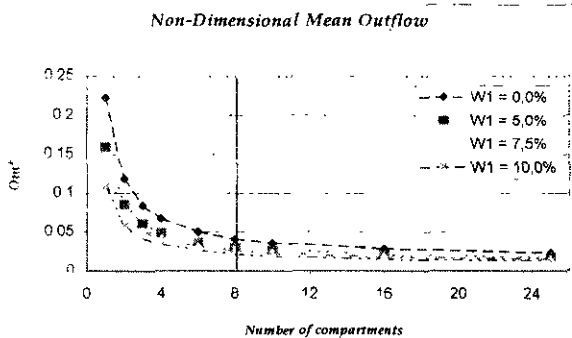
Figure 7 – Values of O_m* function of w_l for **Tanker A**

The parametric study performed indicated that *Tanker A* would be a safer design if $w_s = [0.500;0.510]$. This means that the ship should have a longitudinal bulkhead in order to improve its environmental safety.
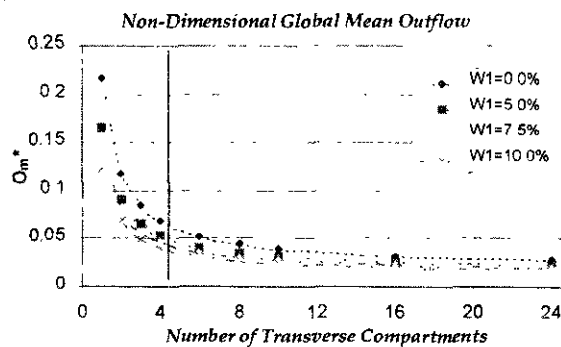

Figure 9 – Values of O_m* function of w_l for **Tanker C**

In case of *Tanker C* the parametric study performed indicated that this ship would be a safer design if $w_s = [0.540;0.550]$. However the value w_s for this ship was not far from these ones. Its value was 0.570.
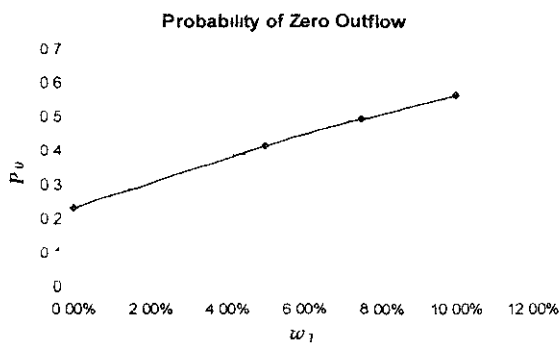
Figure 10 – Values of P_0 function of w_j for *Tanker C*

From Figure 9 it can be concluded that if the number of compartments of this ship were increased in one or two, the safety level with respect to the environment could have been increased by 15% to 25%.

In what concerns the breadth of wing ballast tanks, it is visible from the figure that the mean outflow reduces with the increase of w_j This confirms the observation for *Tanker A*.

Since *Tanker C* does not have wing ballast tanks, the inclusion of such tanks, would increase its safety in terms of environment protection. From Figure 10 this observation is obvious.

Comparing the values of the non-dimensional mean outflow for *Tanker A*, before and after the redesigning process, the performance index was improved by about 78%. This number is really high and this was accomplished, just with the introduction of longitudinal bulkheads, dividing the internal cargo space into an arrangement like the one shown in Figure 2

Table 4 – Global mean outflow of *Tanker A* and *Tanker C* before and after the redesigning process

	Before	After	%
TANKER A	0 0952	0 0213	-78
TANKER C	0 0702	0 0404	-43

For *Tanker C* the global mean outflow could be reduced in 43% with the introduction of wing ballast tanks. However, this new internal subdivision had the disadvantage that the cargo

area was reduced as well as the volume of cargo transported.

A parametric study of the location of transverse bulkheads was also performed However the improvements in ship safety were no significant, because the good location of the longitudinal bulkheads had already minimised the global mean outflow So it is of no interest to add any more information about this since the results obtained are more than sufficient to support the conclusion that even ships built not many years ago. could be greatly improved in what concerns their internal subdivision design. with minor efforts

It is important to emphasise that the location of the longitudinal bulkheads is dominant over the transverse bulkhead locations, which leads to the conclusion that only without previous redesign of the longitudinal bulkheads locations, can a redesign of the transverse bulkheads have any effect on the reduction of oil outflow. However, this effect is also negligible when compared to the redesign process of the longitudinal bulkhead locations. as can be observed in the table below

Table 5 - Global mean outflow of *Tanker A* and *Tanker C* before and after the redesigning process of the transverse bulkhead locations

	Before	After	%
TANKER A	0 0952	0 0945	-0 7
TANKER C	0 0702	0 0692	-1 5

5 CONCLUSIONS

The implementation of the MARPOL regulations has had a major effect on the reduction of operational oil pollution, but the same cannot be said for accidental oil pollution. There is a continued concern in minimising their consequences.

The probabilistic approach used here represents a more comprehensive method than the deterministic approach, in predicting the

220

effectiveness of various arrangements in mitigating oil spills

The method allows a value of expected outflow to be calculated in a similar manner to that used in calculating the "Subdivision Index"

The various arrangements presented here and analysed with the probabilistic approach led to the conclusion that some of them do not reduce the expected outflow which in some cases can be greater than that from segregated ballast tanker without protective location.

6 REFERENCES

1 Abicht, W., "New Formulas for Calculation the Probability of Compartment Flooding in the Case of Side Damage". *Schifftechnik*, Vol.36, No.2, 1989.

2 Abicht, W., "The Probability of Compartment and Wing Compartment Flooding in the Case of Side Damage - New Formulas for Practical Application", *Proc 4th Int. Conf STAB '90*, Napoli, 1990.

3. IMO, *Regulations on subdivision and stability of passenger ships* (as an equivalent to Part B of Chapter II of 1960 SOLAS Convention), London, 1974, 114 pp.

4. IMO, "Protocol of 1978 relating to the International Convention for the Prevention of Pollution from Ships, of 1973", in *International Conference on Tanker Safety and Pollution Prevention*, IMO, London, 1978. pp. 37-106.

5 IMO, *MARPOL 73/78, Regulations for the Prevention of Pollution by Oil-Annex I*, IMO, London, 1986, pp. 22-165.

6 IMO Resolution MSC 19(58) on the adoption of amendments to the 1974 SOLAS Convention, regarding subdivision and damage stability of cargo ships, *Report of the MSC on its 58th session*, IMO, London, MSC 58/25, annex 2, 1990, 13 pp.

7 IMO, "SOLAS, Consolidated Edition, 1992, Part B-1, Subdivision and damage stability of cargo ships" *Publication No. IMO-110-E*, 1992.

8. Jakic, K., "Suggestions for Improvements of the Probabilistic Approach, Adopted by IMO, to the Appearance of Longitudinal Locations an Extents of Ship Collision Damage", *Int. Shipbuild Progr.*, Vol 36, No 406, 1989, pp 157-192

9 Jakic, K., "Probability of the Appearance of Longitudinal Locations and Extents of Ship Collision Damage - Analysis of Recent IMO Efforts and New Proposals for Improvements", *Int. Shipbuild Progr.*, Vol. 38, No. 414, 1991, pp 157-192.

10 Pawlowsky, M., "Probabilistic Approach to Tankers Subdivision *Risk and Reliability in Marine Technology*. C. Guedes Soares, (Ed.), Balkema, 1997.

11. Jakic, K., "Probabilistic Concept of Ship Subdivision", *Risk and Reliability in Marine Technology*, C. Guedes Soares, (Ed.), Balkema, 1997

12. Wendel, K, "Subdivision of Ships", *Proc. Diamond Jubilee Int Meeting - 75th Anniversary*, SNAME, New York, paper No. 12, 1968, 27 pp.

WAVE LOADS TO THE GROUNDED VESSEL

Yuri L. Vorobyov (Odessa State Maritime University, Ukraine)
Alexander F. Nilva (Center of Salvage and Special Fleet of
the Black Sea and Azov Sea Region, Ukraine)

ABSTRACT

The paper describes the solution of the hydrodynamic problem concerning forces on a ship hull stranded in shallow water conditions under the action of incoming regular wave system. The approximate solution of the boundary value problem for diffraction potential is estimated, the formulae for exciting forces are derived. The results of calculations are compared with data of special model tests performed in model basin of the Odessa State Maritime University (OSMU).

NOMENCLATURE

$b(x)$, h - hull width at the station x and water depth, measured in streched coordinates;

$C(x)$ - coefficient of blockage at station x;

c - incident wave velocity of propagation ;

E - the layer $0 \leq z \leq H$ with a part bounded by hull wetted surface S excluded;

$E_0(a)$ - the strip $0 \leq Z \leq H/\varepsilon$ with a part bounded by frame contour $L(x)$ excluded;

F_2, F_3 - lateral, vertical diffraction force;

H - aquatorium depth;

$H_0^{(1)}(x)$ - Hankel function;

$I_0(x)$, $N_0(x)$ - Bessel and Newman functions;

L, B, T - ship length, beam and draft;

N - normal to hull surface;

n - outward normal to cross section line;

O, x, y, z - cartesian coordinate system;

r - incident wave amplitude;

S - wetted surface of ship hull;

S_w - waterline area;

$U_{c,s}(x)$ - cosine (sine) components of the stream velocity on the outer boundary of the inner zone;

Y_l, Z_l - streched coordinates;

α - angle between the velocity of wave propagation and positive Ox;

ε - small parameter;

Σ - free surface of ship hull;

Σ_0 - xy plane with the part $[-L/2, L/2]$ of x axis excluded;

σ - frequency of encounter;

Φ, Φ_0 - velocity potentials of incoming and diffracted waves;

$\Phi^{c(s)}$ - amplitude of cosine (sine) components of velocity potential Φ;

1. INTRODUCTION

When studying the possibilities of saving operation for a vessel stranded in shallow water conditions and working out the plan of such an operation one has to make several serious technical forecasts, namely:

- to evaluate the reserve of strength of a stranded vessel under real conditions of wave action;

- to evaluate the probability of ship removing under wave action (both for

incoming and ship passing by waves) and to check the possibility of afloating the ship

In /1/ the empirical formulae are given to estimate the action of surf and broken waves on the stranded vessel.

In /2/ the attempt is made to verify the above mentioned formulae. The problem of are devided into two parts: the Froude-Kriloff part and the hydrodynamic diffraction part.

The Froude-Kriloff part is calculated by integration of hydrodynamic pressure in wave over the hull wetted surface. The hydrodynamic part is caused by diffraction of incoming waves on the hull of the ship stranded. The theoretical problem of the diffraction force evaluation is one of the most complicated among the problems of hydrodynamic theory /3/, /4/. The matched asymptotic expansion method (MAEM) is the most effective tool for theoretical investigation of hydrodynamic problems in special shallow water conditions when the depth-to-draft ratio of a vessel is close to unity and the depth-to-wave length ratio is small enough. The method was successfully used in publications of E.O.Tuck /5/, Y.L Vorobyov /6/ and their co-authors In this paper MAEM is applied for special hydrodynamic problem connected with salvage operations.

Let us take a ship stranded in shallow water conditions. The cartesian coordinate system *Oxyz* is fixed on the hull. The origin placed at the cross point of the waterline, the diametral plane and the midplane, *X*-axis is pointed to the bow, *Y*-axis is pointed to starboard and *Z*-axis is pointed down. The fluid is ideal and incompressible, its perturbed motion is irrotational. The velocity potential $\Phi(x,y,z,t)$ is the sum of cosine and sine components

$$\Phi(x,y,z,t) = \Phi^c(x,y,z) \cos\sigma t + \\ +\Phi^s(x,y,z) \sin\sigma t. \quad (1)$$

The potentials Φ^c and Φ^s satisfy the differential systems

evaluating the exciting forces acting on a ship hull stranded in shallow water condition (the vertical clearance is small and even zero) under the regular incoming waves.

In accordance with the linear wave theory the exciting forces and moments (EF)

$$\left(\frac{\partial^2}{\partial x^2} + \frac{\partial^2}{\partial y^2} + \frac{\partial^2}{\partial z^2}\right)\Phi^{c,s}(x,y,z) = 0,$$

$$(x,y,z) \in E, \quad (2)$$

$$\left(\frac{\partial}{\partial z} + \frac{\sigma^2}{g}\right)\Phi^{c,s}(x,y,z) = 0,$$

$$(x,y) \in \Sigma; \quad (3)$$

$$\frac{\partial}{\partial N}\Phi^{c,s}(x,y,z) = 0, \quad (x,y,z) \in S; \quad (4)$$

$$\frac{\partial}{\partial z}\Phi^{c,s}(x,y,H) = 0, \quad -\infty < x,y < \infty; \quad (5)$$

$$\Phi^{c,s}(x,y,z) = \Phi_*^{c,s}(x,y,z),$$

$$r^2 = x^2 + y^2 \to \infty. \quad (6)$$

The incoming wave potential Φ_* is represented by sum

$$\Phi_*(x,y,z,t) = \Phi_*^c(x,y,z) \cos\sigma t + \\ + \Phi_*^s(x,y,z) \sin\sigma t. \quad (7)$$

Using (1) and (7) and taking

$$\Phi(x,y,z,t) = \Phi_0(x,y,z,t) + \\ + \Phi_*(x,y,z,t), \quad (8)$$

we have

$$\Phi_0(x,y,z,t) = \Phi_0^c(x,y,z) \cos\sigma t + \\ +\Phi_0^s(x,y,z) \sin\sigma t. \quad (9)$$

Potential Φ_* and its components Φ_*^c, Φ_*^s are known. The functions Φ_0^c Φ_0^s are to be determined.

2. THE BOUNDARY VALUE PROBLEMS FOR DIFFRACTION POTENTIAL IN OUTER AND INNER ZONES

Let us take a ship to be a slender body. It means that $B/L = O(\varepsilon)$, $T/L = O(\varepsilon)$ and the hull form varies slowly enough along the longitudinal axis. The incoming waves are long $H/\lambda = O(\varepsilon)$ and the aquatorium is shallow $H/T=O(1)$. The supposition that incoming waves are long is not very restrictable because short waves produce weak action on a vessel. According to MAEM procedure the flow field around the ship is devided into two zones: far field where $y/L = O(1)$ and near field where $y/L = O(\varepsilon)$

Two boundary value problems are formulated in both zones. The solutions of these problems are asymptotically matched on the boundary of zones.

From the far field point of view as $\varepsilon \to 0$ the hull degenerates into a cut $[-L/2 \le x \le L/2]$ of xy plane.

Let us expand functions $\Phi_0^{c,s}(x,y,z)$ into series by small parameter $(z-H) = O(\varepsilon)$. Taking the first terms of these expansions and using (2), (3), (6) we get the differential systems for sine and cosine components

$$\left(\frac{\partial^2}{\partial x^2} + \frac{\partial^2}{\partial y^2} + k^2 \right)\Phi^{c,s}(x,y) = 0, \tag{10}$$

$$(x,y) \in \Sigma_0;$$
$$\Phi^{c,s}(x,y) \to 0, \quad r^2 = x^2 + y^2 \to \infty \tag{11}$$

The dispersion relation for wave motion in shallow water conditions is as follows

$$k = \frac{\sigma}{\sqrt{gH}}. \tag{12}$$

The boundary conditions on the ship hull in the outer zone are not formulated as soon as the hull surface belongs to the inner zone. The only correlations that come from the physical considerations are

$$\Phi(x,+0) - \Phi(x,-0) = \begin{cases} \Delta(x), & |x| \le \dfrac{L}{2} \\ 0, & |x| > \dfrac{L}{2}, \end{cases} \tag{13}$$

$$\frac{\partial}{\partial y}\Phi(x,+0) - \frac{\partial}{\partial y}\Phi(x,-0) =$$

$$= \begin{cases} f(x), & |x| \le \dfrac{L}{2} \\ 0, & |x| > \dfrac{L}{2} \end{cases} \tag{14}$$

It is taken in (13) and (14)
$$\Phi(x,y) = \Phi^c(x,y) - i\Phi^s(x,y)$$
$$\Delta(x) = \Delta^c(x) - i\Delta^s(x),$$
$$f(x) = f^c(x) - if^s(x).$$

Using the Green theorem for Helmholtz equation (10), we find

$$\Phi(x,y) = \omega(x,y) + \frac{\partial}{\partial y}\psi(x,y) \tag{15}$$

$$\omega(x,y) = -\frac{i}{4}\int_{-L/2}^{L/2} f(\xi)\mathcal{H}_0^{(1)}\left(k[(x - \right.$$
$$\left. - \xi)^2 + y^2]^{1/2}\right)d\xi, \tag{16}$$

$$\psi(x,y) = -\frac{i}{4}\int_{-L/2}^{L/2} \Delta(\xi)\mathcal{H}_0^{(1)}\left(k[(x - \right.$$
$$\left. - \xi)^2 + y^2]^{1/2}\right)d\xi. \tag{17}$$

The Hunkel function $\mathcal{H}_0^{(1)}(u) = J_0(u) + iN_0(u)$. Both $\omega(x,y)$ and $\psi(x,y)$ are even functions in y. Let us expand $\Phi(x,y)$ in the Taylor series in y near $y = 0$

$$\Phi(x,y) = \omega(x,\pm0) + \frac{\partial}{\partial y}\Psi(x,\pm0) +$$
$$+ y\left[\frac{\partial}{\partial y}\omega(x,\pm0) + \frac{\partial^2}{\partial y^2}\Psi(x,\pm0)\right]. \tag{18}$$

As soon as ω and ψ are even functions in y from (13), (14) and (18) it comes

$$\Delta(x) = \pm 2\frac{\partial}{\partial y}\psi(x,\pm0);$$

$$f(x) = \pm 2\frac{\partial}{\partial y}\omega(x,\pm0). \tag{19}$$

Inserting (19) into (18) we find

$$\Phi(x,y) = \left[\omega(x,\pm 0) \pm \frac{1}{2}\Delta(x)\right] +$$

$$+y\left[\frac{\partial^2}{\partial y^2}\psi(x,\pm 0) \pm \frac{1}{2}f(x)\right] + O(\varepsilon^3) \qquad (20)$$

The functions $\Delta(x)$ and $f(x)$ are unknown and found by matching procedure.

In the near field y and z coordinates are stretched by the ratio ε ($Y = y/\varepsilon$, $Z = z/\varepsilon$). When $\varepsilon \to 0$ the flow in the inner zone becomes two dimensional (in planes $x = const$).

The two dimensional boundary value problems in $x = const$ planes are as follows

$$\left(\frac{\partial^2}{\partial Y^2} + \frac{\partial^2}{\partial Z^2}\right)\Phi^{c,s}(Y,Z;x) = 0,$$
$$(Y,Z) \in E_0(x); \qquad (21)$$

$$\frac{\partial}{\partial Z}\Phi^{c,s}(Y,0;x) = 0, \quad |Y| > b(x); \qquad (22)$$

$$\frac{\partial}{\partial Z}\Phi^{c,s}(Y,h;x) = 0, \quad -\infty < Y < \infty; \qquad (23)$$

$$\frac{\partial}{\partial n}\begin{Bmatrix}\Phi^c\\\Phi^s\end{Bmatrix}(Y,Z;x) = crk\cos(n,Y) \times$$

$$\times \begin{Bmatrix}\sin\alpha\,\cos(kx\,\cos\alpha)\\\sin\alpha\,\sin(kx\,\cos\alpha)\end{Bmatrix} + O(\varepsilon), \qquad (24)$$

$$(Y,Z) \in \mathcal{L}(x)$$

At the large distance from the hull frame $\mathcal{L}(x)$ it comes

$$\lim_{Y \to \pm\infty}\Phi^{c,s}(Y,Z;x) =$$
$$= U^{c,s}(x)[Y \pm C(\infty)] \qquad (25)$$

So the flow in the inner zone corresponds to the two dimensional flow round the hull frame $x = const$ with velocities $U^{c,s}(x)$ at the infinity. Thus the formula (20) presents the solution of the problem at the inner boundary $y = \pm 0$ of the outer zone and the formula (25) presents the solution of the problem at the outer boundary $Y = y/\varepsilon \to \pm\infty$ of the inner zone. Rewriting (25) in the outer variables we use the simplest matching principle: the inner limit of the outer solution

equals the outer limit of the inner solution As soon as for the cross flow of the fluid $\omega(x,\pm 0) = f(x,\pm 0) = 0$ we have

$$\Phi^{c,s}(x,y) = \pm\frac{1}{2}\Delta^{c,s}(x) +$$

$$+y\frac{\partial^2}{\partial y^2}\psi^{c,s}(x,\pm 0), \qquad (x,y) \in \Sigma_0 \qquad (26)$$

3. THE SOLUTION OF THE INTEGRO - DIFFERENTIAL EQUATION

The procedure of solving the integro-differential equation that comes for the radiation problem for swaying motion of ship hull in shallow water conditions when $H/L = O(\varepsilon)$ is given in /6/.

The named problem differs from the problem under investigation by the boundary condition at the frame $x = const$ That is the existing boundary condition (24) has to be changed to the following one

$$\frac{\partial}{\partial N}\Phi^c(Y,Z;x) = \cos(n,Y);$$
$$\frac{\partial}{\partial N}\Phi^s(Y,Z;x) = 0. \qquad (Y,Z) \in \mathcal{L}(x)$$
$$(27)$$

Comparing (27) with (24) we find out that the solution given in /6/ has to be multiplied by the constant in Y and Z quantity. Let us present the potential jamp $\Delta(x)$ as a sum $\Delta(x) = u(x) + iv(x)$. In /6/ the integro - differential equation for $\Delta(x)$ is turned to such a system

$$u(x) = \frac{1}{2\pi}\int_{-L/2}^{L/2}K(x,\xi)\left\{2 + \frac{u(\xi)}{C(\xi)} + \right.$$

$$+\frac{k^2}{2}\int_{-L/2}^{L/2}[v(\tau)\,I(k|\xi - \tau|) + \qquad (28)$$

$$\left. +u(\tau)Q(k|\xi - \tau|)\,\right]\,d\tau\right\}d\xi$$

$$v(x) = \frac{1}{2\pi} \int_{-l/2}^{l/2} K(x,\xi)\left\{\frac{u(\xi)}{C(\xi)} + \right.$$

$$+ \frac{k}{2} \int\left[v(\tau)I(k|\xi - \tau|) - \right. \qquad (29)$$

$$\left.\left. -u(\tau)Q(k|\xi - \tau|) \right] d\tau\right\}d\xi.$$

The Kernel $K(x, \xi)$ is a follows
$K(x, \xi) =$

$$= ln\left[\frac{(\frac{L}{2})^2 - \xi x + \sqrt{\left[(\frac{L}{2})^2 - \xi^2\right]\left[(\frac{L}{2})^2 - x^2\right]}}{(\frac{L}{2})^2 - \xi x - \sqrt{\left[(\frac{L}{2})^2 - \xi^2\right]\left[(\frac{L}{2})^2 - x^2\right]}}\right]$$

$$(30)$$

The other functions in (28), (29) are

$$I(x) = \frac{1}{x}J_1(x);$$

$$Q(x) = N_0(x) - S(x);$$

$$S(x) = \frac{\partial}{\partial u}E(u)\Big|_{u=x}, \qquad (31)$$

$$E(x) = N_1(x) - \frac{2}{\pi}\frac{1}{|x|};$$

$J_1(x)$ and $N_1(x)$ - Bessel and Newman functions

Let us expand $u(x)$ and $v(x)$ into the Fourier series at the cut $[-L/2; L/2]$. Taking finite number N of terms and using the condition at the ends a the cut $\Delta(\pm L/2) = 0$, we have

$$u(x) = \sum_{n=1}^{N}\left\{a_{2n}\,sin\left(\frac{2n\pi x}{L}\right) + \right.$$

$$\left. + b_{2n-1}\,cos\left[(2n-1)\frac{\pi x}{L}\right]\right\} \qquad (32)$$

$$u(x) = \sum_{n=1}^{N}\left\{c_{2n}\,sin\left(\frac{2n\pi x}{L}\right) + \right.$$

$$\left. + d_{2n-1}\,cos\left[(2n-1)\frac{\pi x}{L}\right]\right\} \qquad (33)$$

Inserting (32), (33) into the system (28), (29), using the expansion

$$= \sum_{n=1}^{N}\frac{1}{2n} \qquad (34)$$

and applying the orthogonality of $sin(2n\pi x/L)$ and $cos[(2n - 1)\pi x/L]$ on the cut $[-L/2, L/2]$, we receive the systems of linear equations for coefficients a_{2n}, b_{2n-1} and c_{2n}, d_{2n-1} The systems are not given here because they are cumbersome but easy for effective calculations. The calculations show that series (32) and (33) have very fast convergence and the sum of five terms provides the error smaller then 1%.

4. THE EXCITING FORCES AND MOMENTS

The exciting forces and moments acting on the ship from the incoming waves are determined by integration of hydrodynamic pressure of wave motion over the hull surface. The hydrodynamic pressure is determined separately for incoming and scattered wave motions. For example, the components of transverse hydrodynamic force are:
- the Froude-Kriloff part

$$\begin{Bmatrix}F_{*2}^c \\ F_{*2}^s\end{Bmatrix} = \frac{2\rho gr}{ch\,kH}\int_{-L/2}^{L/2}\begin{Bmatrix}cos \\ sin\end{Bmatrix}(kx\,cos\alpha)\times$$

$$\times \int_0^T ch\,k(z - H)\,sin(ky\,sin\alpha)\times \qquad (35)$$

$$\times cos(n, y)\,dzdx;$$

- the diffraction part

$$\begin{Bmatrix}F_2^c \\ F_2^s\end{Bmatrix} = -\frac{\rho grk}{ch\,kH}sin\,\alpha\int_{-L/2}^{L/2}v(x)\begin{Bmatrix}sin \\ cos\end{Bmatrix}\times$$

$$\times(kx\,cos\alpha)\int_0^T ch[k(z - H)]cos(ky\,sin\alpha)\times$$

$$\times cos(n, y)dzdx.$$

$$(36)$$

The function $v(x)$ is determined by the Fourier series. The procedure of equating the coefficients of this series is shown in the previous paragraph of the paper. The formulae of the analogous structure are derived for other components of exciting forces and moments.

5. THE RESULTS OF CALCULATIONS AND EXPERIMENTS

The formulae derived are used for systematical calculations of forces and moments acting on a stranded ship from the incoming regular waves under shallow water conditions. The results are compared with the experimental data obtained in testing pool of the Odessa State Maritime University. The exciting forces and moments were measured on fixed models, the stranding was emitated for different areas of hull to soil contact. The special measuring system makes it possible to record five components of exciting forces (transverse and vertical forces, rolling, pitching and yawing moments). On fig. 1 and fig. 2 the results of calculations (solid lines) and experiments (dots) are given for sway force $\overline{F_2} = \dfrac{F_2}{\rho g r L T}$ and heave force $\overline{F_3} = \dfrac{F_3}{\rho g r S_w}$ as functions of $\overline{\lambda} = \lambda/L$ for a bulker of "Zoja Kosmodemianskaya" type stranded in such a way that the contact of hull and soil extents on 90 % of ship length. The calculated and experimental data show satisfactory correspondence.

6. CONCLUSIONS

The results of the theoretical investigation of exciting forces and moments acting on a stranded ship hull from the incoming regular waves make it possible to find optimal ways of performing the rescue works. The obtained method provides a possibility for calculating of exciting forces and moments acting on a hull under shallow water conditions when the water depth to ship draft ratio is close to unity. The accuracy of the method is increasing while this ratio tends to unity.

REFERENCES

1. Dounayevski J.I. Raising of ships stranded. - Moscow, Transport, 1984, 168 p. (in Russian).

2. Methodics for ship static and dynamic calculations during saving operations and ship repair. - General instructions 31.72.04-85, Moscow, "Mortechinformreclama", 1986, 200 p. (in Russian).

3. Liapis N., Faltinsen O.M. Diffraction of Waves around a ship. JSR, 1980. Vol 24, N3, pp. 147-155.

4. Vorobyov Y.L., Ngo Kan Experimental investigation of exiting forces in oblique waves for shallow water condition. - Sudostroenie i sudoremont, Proceedings. Moscow, Reclaminformburo MMF, ed.10. 1978, pp.10-15 (in Russian).

5. Tuck E.O. Ship motions in shallow water. JSR, 1970, Vol 14, N4, pp. 317 - 328.

6. Vorobyov Y.L. On determination of hydrodynamic forces for a ship surging and yawing in shallow water. - Sudostroenie i sudoremont, Proceedings, Moscow, Reclaminformburo MMF, ed. 8, 1977, pp.18-24. (in Russian).
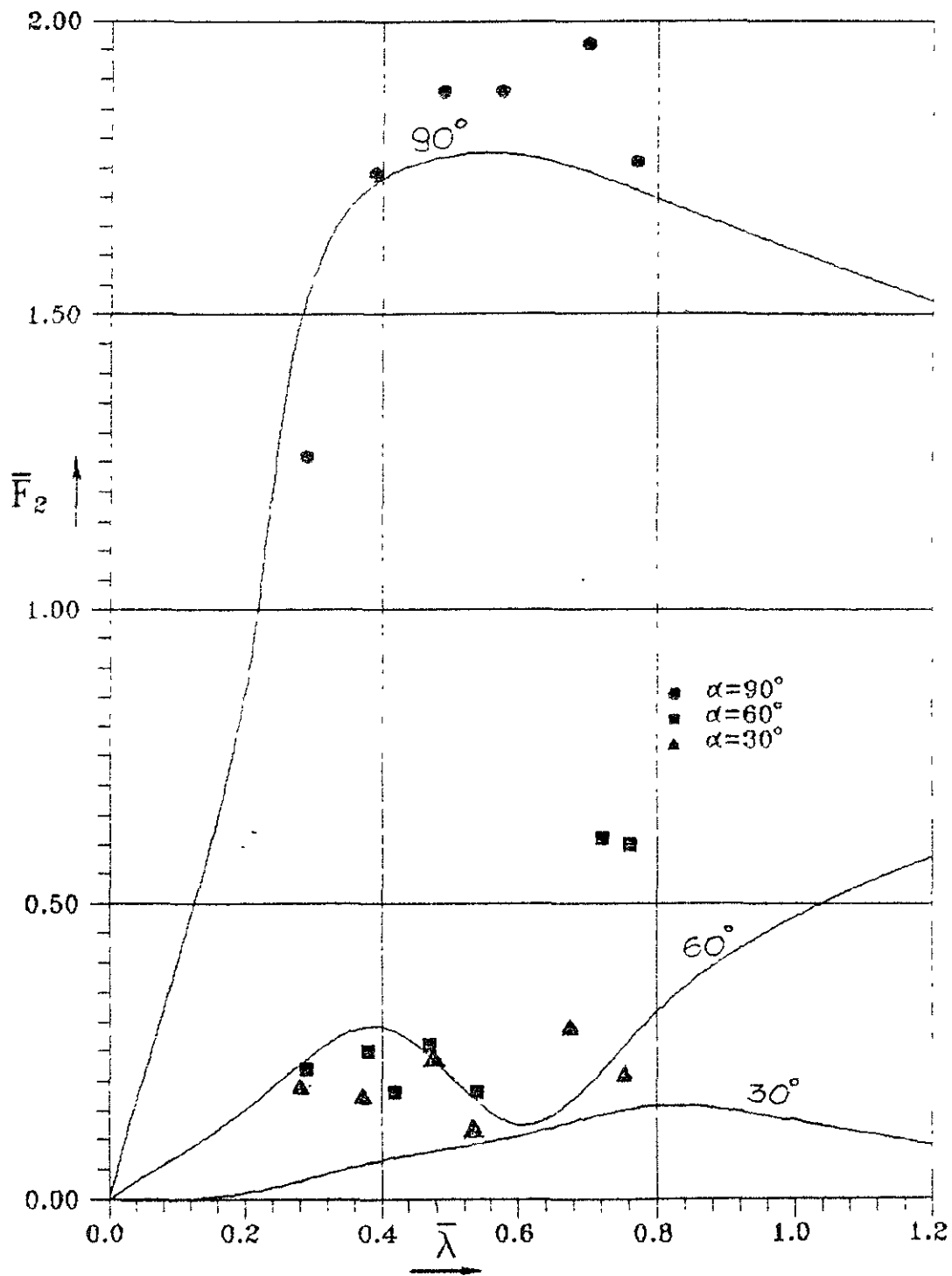
Fig. 1
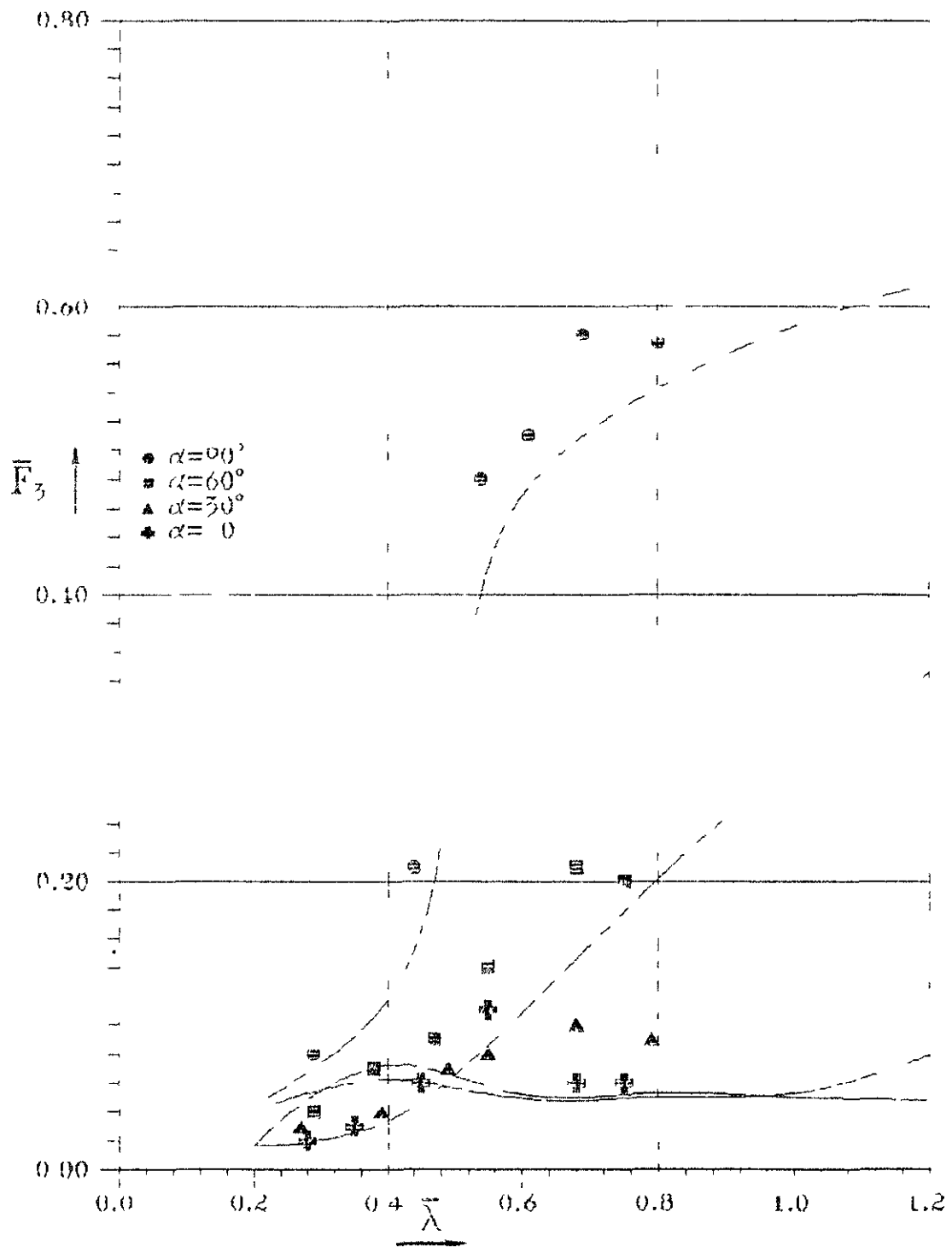
Fig. 5.2

APPLICATION
OF EXPERT SYSTEMS
AND ON-BOARD COMPUTERS
FOR STABILITY MONITORING
AND CONTROL

STABILITY PROOF OF THE COURSE ANGLE CONTROL SYSTEM OF THE UNDERWATER VEHICLE KRAB II

Andrzej Piegat

Maritime Technology Faculty, Technical University of Szczecin, Al.Piastów 41, PL - 71065 Szczecin Poland, fax (4891) 340946

ABSTRACT

To control ships and other floating marine structures such as underwater vehicles there are more and more neural controllers applied.

Technical regulations of many countries require stability proof for control systems. Because neural controllers realize usually nonlinear algorithms the stability proof is very difficult. This possibility is given by the hyperstability theory of Popov. The paper shows how the method can be applied for neural control system of underwater vehicles. Because the dynamics of the vehicles is qualitatively similar to ships one the method can be also used for ships.

Key words : stability, underwater vehicles, neuro-fuzzy control.

1. INTRODUCTION

In control systems of ships and other floating structures there are applied various devices with nonlinear characteristics such as steering engines, propellers with limited power etc. In these systems more and more intelligent, self-learning neuro-fuzzy controllers are applied [3]. Because technical regulations require stability proof of control systems, scientists are working now very intensively on stability of control systems with neural and fuzzy controllers as e.g. [1], [2], [6].

Also for digital control systems of the UV Krab II with neuro-fuzzy controller, described in [3] and [4] the stability checking was necessary.
It will be shown below how such checking can be realized.

2. DIGITAL CONTROL SYSTEM OF THE UNDERWATER VEHICLE KRAB II

The general scheme of the system is presented on Fig.1
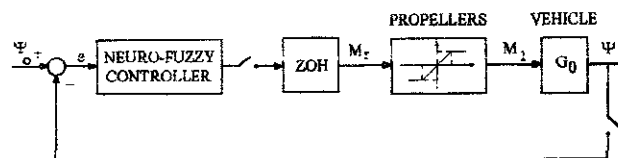
Fig.1.Control system of the underwater vehicle Krab II.

The UV-Krab II has a course transfer function given by (1) :

$$G_0(s) = \frac{\psi(s)}{M_1(s)} = \frac{0,021929}{s(1 + 0,30372s)} = \frac{b_0}{a_2 s^2 + s} \left[\frac{rad}{N \cdot m} \right] \tag{1}$$

The torque generated by the propellers is limited to the range shown on Fig.2.
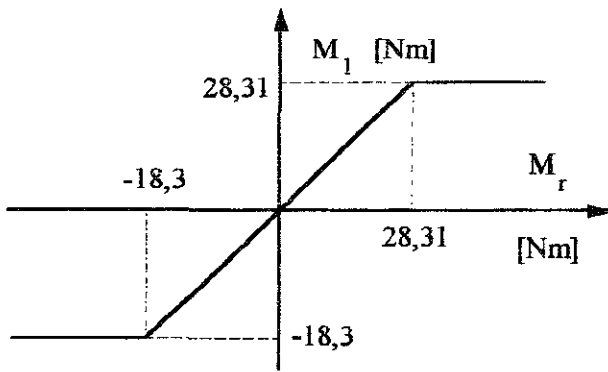
Fig.2. Static characteristic F of the vehicle pro-
pellers.

The UV is controlled by the neuro-fuzzy con-
troller (shortly n-f controller) shown on Fig.3
and described more precisely in [3].

The n-f controller was learned in the system
with reference model shown on Fig.4.
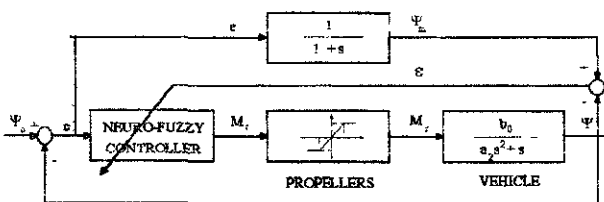
Fig.4. Learning system of the neuro-fuzzy con-
troller.

After learning with triangle reference signal Ψ_0
with amplitude +1 and -1 following parameters
of the n-f controller (Fig.3) were achieved :

$k_p = 13.002$ $k_d = 0,913906$ $k_i = 0$ $k_{1p} = 1$
$k_{2p} = 0,758144$ $k_{3p} = 0,807841$ $k_{4p} = 0,958144$
$k_{5p} = 0,041856$ $k_{6p} = 0,192159$ $k_{7p} = 0241856$
$k_{8p} = 0$ $k_{in} = 1-k_{ip}$, $i = 1 \div 8$.

Owing to special membership functions with
extrapolation truth [5], Fig.5 linearization of the
controller action was possible.
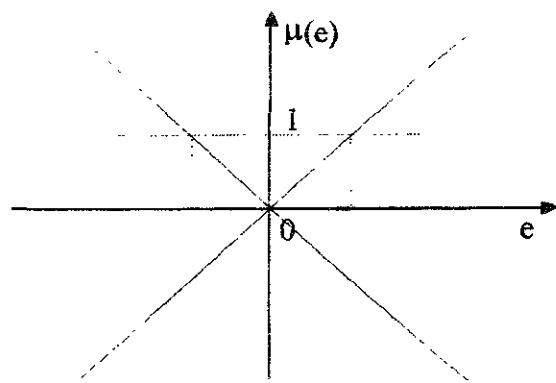
Fig.5. Membership functions used in the n-f
controller for defuzzification.

Basing on the controller scheme (Fig.3) its
gains can be calculated according to (2) :

$K_p = 0,66666k_p [1+(2k_{2p} -1) +(2k_{3p} -1) +$
$+(2k_{4p} -1)] = 26,42256$
$K_d = 0,66666k_d [1-(2k_{2p} -1) +(2k_{3p} -1) -$
$+(2k_{4p} -1)] = 0,111556$ (2)
$K_i = 0,66666k_i [1+(2k_{2p} -1) -(2k_{3p} -1) -$
$+(2k_{4p} -1)] = 0$

The n-f controller learned the action of a PD-
type controller and realizes the functions :
$$M_r(t) = K_p e(t) + K_d \dot{e}(t)$$

Because the controller is digital in the control
system a ZOH (zero-order hold) must be ap-
plied to hold the control signal between sam-
pling instants, Fig.6.
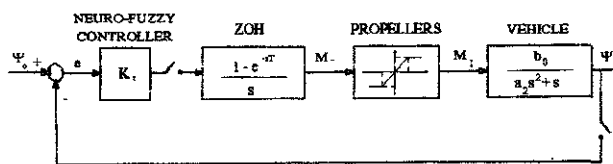
Fig.6. General scheme of the digital control
system of the UV Krab II.

3. STABILITY CHECKING OF THE NEURO-FUZZY CONTROL SYSTEM

Stability checking of nonlinear control systems
with the hyperstability method consists of fol-
lowing steps [2], [6]:
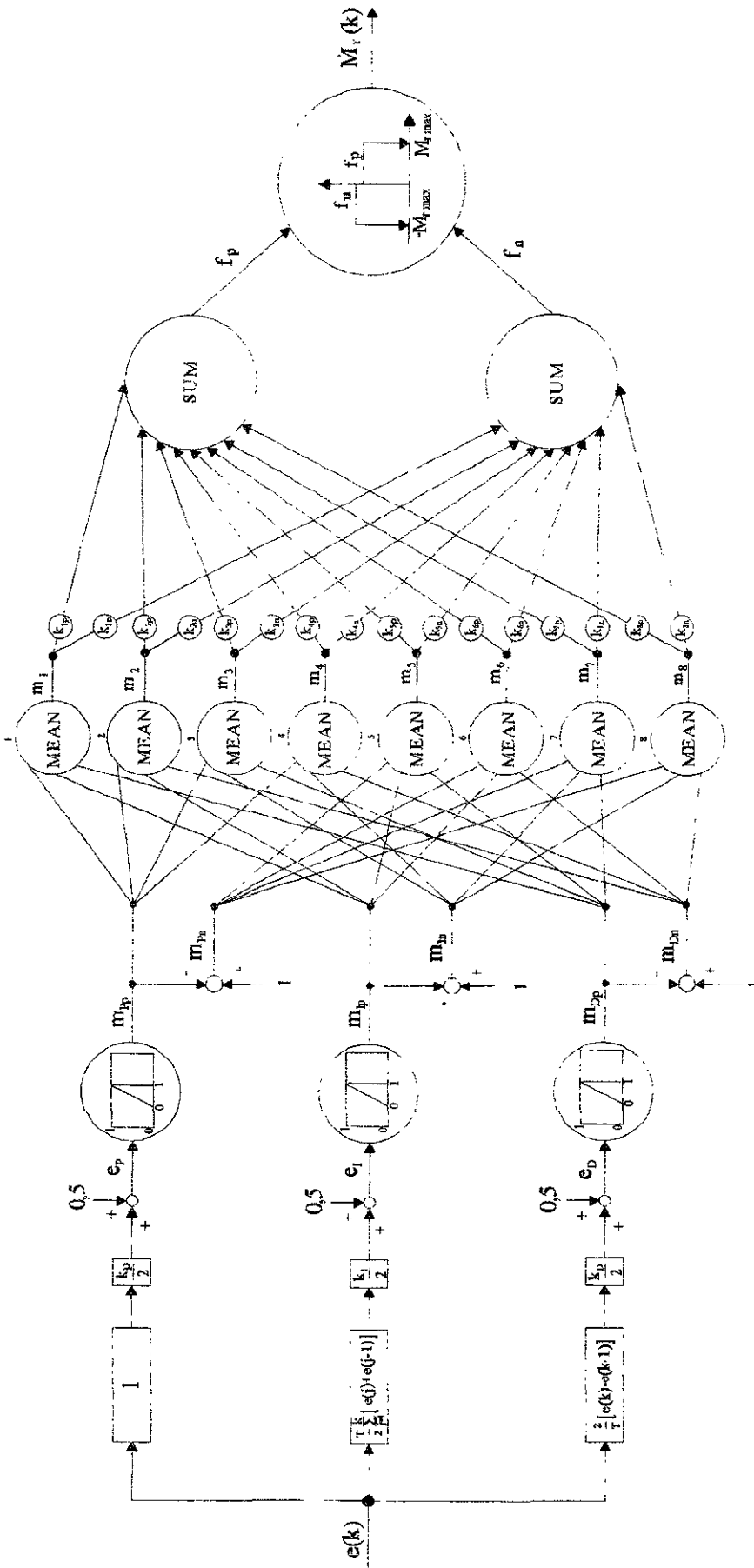
Fig.3. Neuro-fuzzy controller of the vehicle Krab II

235

I. transformation of the control system in special standard form,

II. discretization of the linear part of the standard system,

III. stability checking of poles of the linear part and their possible stabilization by adding of special degrees of freedom,

IV. checking if the linear part is positive definite and Hermitian one and possible satisfying of this condition by adding of special degrees of freedom.

V. controllability and observability checking of the linear par

VI. construction of Popov-hyperstability conditions for the nonlinear part of the control system

VII. simultaneous checking of the hyperstability conditions for the linear and nonlinear part.

Fig.7. shows the standard scheme of the UV-control system for stability checking in analog and digital version
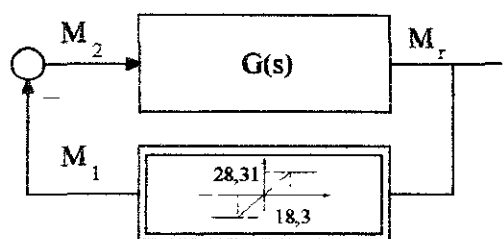
$$G(s) = \frac{(1-e^{-sT})b_0(K_p + K_i s)}{s(s + a_2 s^2)}$$
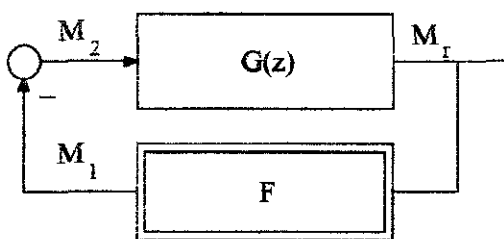
$$G(z) = \frac{b_0 T^2 (K_p T + K_d - K_p z^{-1})}{T + a^2 - (T + 2a_2)z^{-1} + a_2 z^{-2}}$$

Fig.7. Standard scheme of the neuro-fuzzy control system of the UV in analogue and digital version.

Poles checking of the linear part G(z) shows one pole to be on the border of the unit circle and its stabilization must be made by adding of the degree of freedom d_1, Fig.8.

Mathematical analysis of the transfer function G(z) shows also its non-positive definitivity. To make it positive definite a special degree of freedom d_2 (Fig.8) is added.
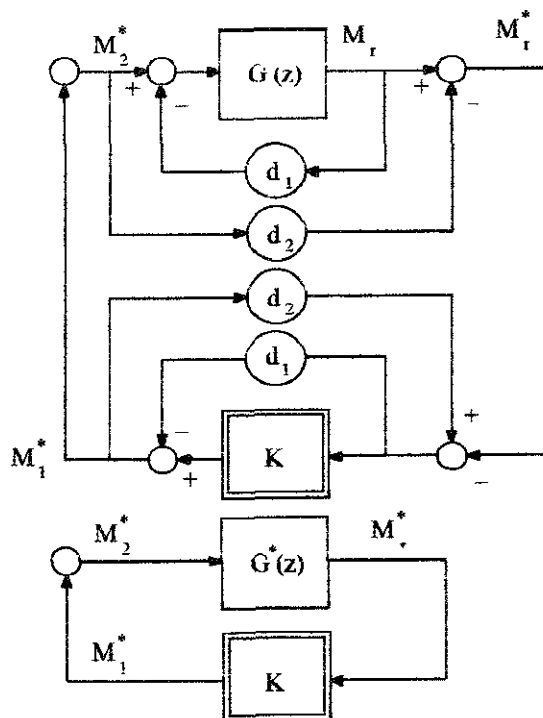
$$G^*(z) = \frac{G(z)}{1 + d_1 G(z)} + d_2 \qquad M_1^* = \frac{M_r^*(1 - d_1)}{1 + d_2(d_1 - 1)}$$

Fig.8. Standard scheme of the UV-control system with additional degrees of freedom d_1, d_2 and its simplified form.

Transfer function $G^*(z)$ of the linear part has form (3).

$$G^*(z) = \frac{num(z)}{den(z)} + d_2 \qquad (3)$$

$$num(z) = b_0 T^2 (K_p T + K_d - K_p z^{-1})$$

$$den(z) = T + a_2 + d_1 b_0 T^2 (K_p T + K_d) -$$
$$+(T + 2a_2 + d_1 b_0 K_p T^2)z^{-1} + a_2 z^{-2}$$

The transfer function $G^*(z)$ has stable poles when the condition (4) is satisfied

$$d_1 > 0 \qquad (4)$$

An analysis of the transfer function $G^*(z)$ shows it is Hermitian one i.e. it satisfies condition (5) [6].

$$H(\omega) = 0.5[G^T(e^{j\omega}) + G(e^{-j\omega})] \qquad (5)$$

is positive definite for all $\omega \geq 0$ when the following quantitative condition is satisfied

$$-0.001930188 - 0.000002317\, d_1 +$$
$$+d_2(-0.429819747 - 0.000009542\, d_1 + \qquad (6)$$
$$+ 0.000001876\, d_2) > 0$$

The hyperstability criterion requires also the Popov condition (7) for the nonlinear part of the system must be satisfied [2], [6]

$$\sum_{k=0}^{k_1} M_1^*(k)M_r^*(k) \geq -\beta_0^2, \quad \forall k_1 > 0 \qquad (7)$$

where. β_0 is a finite number

The condition (7) is satisfied when the inner function of the sum (7) will be nonnegative

$$M_1^*(k)M_r^*(k) \geq 0, \quad \forall k \qquad (8)$$

The relation $M_1^* = F^*(M_r^*)$ is shown on fig 9
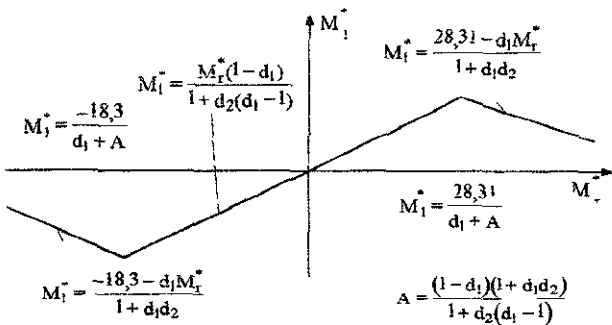
Fig.9.Function F^* realized by the nonlinear part of the control system with additional degrees of freedom d_1, d_2

The Popov-hyperstability condition (7) for the nonlinear part takes the form (8)

$$M_1^* M_r^* = \frac{(-18.3 - d_1 M_r^*)M_r^*}{1 + d_1 d_2} \geq 0 \qquad (9)$$

for the first sector $M_r^* \leq \dfrac{-18.3}{d_1 + A}$

For the second sector (Fig 9)

$$\frac{-18.3}{d_1 + A} < M_r^* \leq \frac{28.31}{d_1 + A}$$

the Popov-condition has the form (10)

$$M_1^* M_r^* = \frac{M_r^{*2}(1 - d_1)}{1 + d_2(d_1 - 1)} \geq 0 \qquad (10)$$

And the third sector (Fig 9)

$$M_r > \frac{28.31}{d_1 + A}$$

is has the form (11)

$$\frac{(28.31 - d_1 M_r^*)M_r^*}{1 + d_1 d_2} \geq 0 \qquad (11)$$

Mathematical analysis of the all Popov-conditions (9,10,11) shows they are satisfied when following conditions for the degrees of freedom d_1 and d_2 are satisfied

$$1 + d_1 d_2 > 0$$
$$\frac{1 - d_1}{1 + d_2(d_1 - 1)} > 0 \qquad (12)$$

To prove the control system hyperstability such values for the coefficients d_1 and d_2 must be found which will simultaneously satisfy the conditions (4) and (6) for the linear part $G^*(z)$ and (12) for the nonlinear part F^*
Such numbers were found as

$$d_1 = 10^6 \qquad d_2 > 1.234015 \cdot 10^{-6} \qquad (13)$$

Finding the numbers (13) ends the stability proof for the neuro-fuzzy control of the UV Krab II.

Experiments with the vehicle controlled by the n-f controller have confirmed the real control system stability

4. SUMMARY

Stability checking of control systems for ships and other floating structures with strongly nonlinear elements was hitherto very difficult or even practically impossible in the case of more complicated systems.

The intensively developed hyperstability theory allows systematic stability checking also for very complicated control systems with modern selflearning neuro-fuzzy controllers what was shown in the paper on example of the underwater vehicle Krab II.

5. REFERENCES

1 Franke D.. Fuzzy control with Lyapunov stability Proceedings of the International Conference ECC 93, 5-9.09 93, Duisburg, Germany, pp.493-496.

2 Opitz H.P. The theory of hyperstability a systematic method for the stability analysis and synthesis of nonlinear systems, Automatisierungstechnik 6/1986, pp.221-230.

3 Piegat A., Pluciński M.. Intelligent controller of the underwater vehicle Krab II, Proceedings of the First International Conference on Marine Industry MARIND'96 2-7 06.1996, Varna, Bulgaria, vol.I, pp.303-311

4 Piegat A., Pluciński M., Skórski W. Technical systems and control algorithms of the underwater vehicle Krab II, First Int.Conf MARINE TECHNOLOGY ODRA 95 Szczecin, Poland 20-22.09.1995, pp.579-588.

5 Piegat A.. Extrapolation truth, submitted for publication to IEEE TRANSACTIONS ON FUZZY SYSTEMS in May 1996.

6 Schmitt G., Günther S The Hyperstability Curves Criterion as a graphical frequency domain stability criterion for nonlinear multivariable feedback systems, Automatisierungstechnik 6/96, pp.281-288.

ONBOARD COMPUTER AIDED SYSTEM FOR MONITORING AND CONTROL OF STABILITY AND SAFETY AFFECTING PARAMETERS

Y.D. Zhukov, B.N. Gordeev, A.Y. Greshnov, E.O. Prischepov
Ukrainian State Maritime Technical University
9, Geroev Stalingrada Str., 327025 Nikolaev, Ukraine

ABSTRACT

The measuring information system for safety affecting parameters monitoring and control (SAPMAC) is described. Level measuring subsystem (LMS) has several basic functions: liquid and friable cargoes level (ullage) automated remote monitoring, determination of location of separation level of non-mixed liquids or solutions, evaluation of appearance and percentage of water in different liquids or solutions. Additional functions of the system: liquids' quantity and outlay monitoring, measuring of temperature of liquid and friable cargoes, liquids and solutions' density express-analysis. The system effectiveness for different types of ship's cargo (light petroleum products, spirit solutions, aggressive mediums, liquefied under high pressure gas, water solutions, etc.) is analyzed. LMS subsystem is based on the generally presented method of polymetric signals generating and processing.

1. FUNCTIONS OF SAPMAC

Sensitivity analysis of different known criteria allowed to determine the set of stability and safety affecting parameters which are to be controlled in real time domain onboard the ship to improve her operational safety.

Among various ship loads the basic place on influence to parameters of ship stability and her safety at sea is occupied by liquid cargoes, to which concern: fuel, oils, aggressive liquids, various kinds of water (drinking, washing, sea and other). In this connection on courts there is the sharp necessity of the online real time control of the levels of liquid cargoes, sizes of free surfaces and quantity of liquids in tanks and capacities.

Except information maintenance of the onboard stability monitoring system the constant quantitative and qualitative control of liquid loads and loose cargoes storage parameters allows to know, to an example:
- actual quantity of fuel and oils in a current moment of time for exact account of optimal speed, course and distance, which the vessel can safely cover;
- amount of fresh, drinking and washing water for correct dosage of consumption and betimes definition of operating time of distilling station;
- integrity control of tanks or other capacities - storehouses of liquids;
- necessity and time of start or switching-off of devices and systems, ensuring swapping and redistribution of liquid loads;
- condition of dry compartments and rooms, occurrence of a liquid in which is inadmissible and can be by the reason of any failure (infringement of integrity of pipelines, floatation compartments, tanks, etc.).

The duly detection of the named parameters enables to accept necessary measures.

2. THEORETICAL BACKGROUND

The principles of action of appropriate measuring computer aided systems are determined by character of controllable environments, conditions both purposes of the control and character of that information, which is necessary for receiving for the subsequent processing (measurement or signal system, simultaneous processing of a number of parameters, frequencies or sizes of time intervals of measurement, accuracy, etc.).

Unfortunately, by virtue of significant distinction in character and conditions of the control of liquid loads until recently a universal method of measurement of their level was not created.

The nomenclature, peculiarity of keeping and property of liquid loads, being subject to the control on board the ship are considered in details in [1-3]. The constructive, operational, economic and special requirements to ship level measuring instruments are systematized, domestic and foreign devices and systems of considered assignment was analysed from onboard the ship application point of view.

The drawbacks of known devices are impossibility of conducting simultaneous measurements of levels, temperature and density of controlled liquid or loose cargo, complexity of algorithm of work, complexity of manufacturing of a sensitive element and insufficient operativeness and accuracy of measurement.

That is why nontrivial principles and the methods of impulse reflectometrics (which were used on an extent of many years for failure detection in copper and optic fiber cables) were modified for the named problem solution [3-7].

The specified method is advanced for liquid or loose cargo level assessment by use of reflectometric measuring transformer with rough probing probe and patented computer aided hardware and software [4,5].

Perfect electronics and advanced probing probes configuration has allowed to develop up to present time precise, repeated and reliable devices for onboard computer aided measuring information system (MIS) for automated remote control of ullage, separation level, temperature and density of liquid and loose cargoes. The system includes special measuring channels for ship draft control [3,7].

As a special sensitive element of measuring transformer of the system a similar two-wire line of various designs is used, for each of which primary parameters, referred to unit of it's length, are known: r_0 - resistance of direct and return wires; L0 - inductance of a loop, formed by direct and return wires: g0 - conductivity between wires; C0 - working capacity between wires.

The long line can be simulated as set of indefinitely small elements connected in a chain of length dx, each of which has resistance $r_0 dx$ and inductance dx, conductivity $g0 dx$ and capacity $C0 dx$, and instant values of a voltage and current in the beginning of a chosen element being u and i respectively (fig. 1).
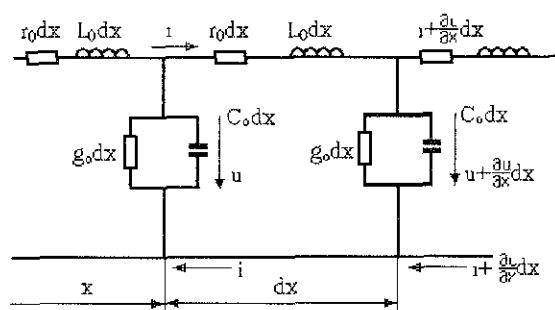

Fig. 1 Long line simulation model

Thus resistance $r_0 dx$ and inductance $L0 dx$ are considered as included in one of two wires. The simulation model of long electrical line, presented in Fig. 1 enables us, in general case,

predict values of it's parameters with the help of the following equation:

$$\frac{d\dot{I}}{dx} = (r_o + j\omega C_0)\dot{u} = \dot{Y_0}\dot{u}. \qquad (1)$$

We use following denotations in formula (1):

$\dot{z_0} = r_0 + j\omega L_0$ - complex resistance;

$\dot{Y_0} = g_0 + j\omega C_0$ - complex conductivity of the unit of length of a line.

The solution of appropriate linear differential equations of the second order with constant factors concerning a current I gives:

$$I = \frac{C_1 e^{-\gamma x} - C_2 e^{\gamma x}}{\sqrt{\dot{z_0}/\dot{Y_0}}}, \qquad (2)$$

where: C_1 and C_2 - integration constants.

The denominator of the formula (1), have dimension of resistance, refers to as by wave resistance Z_u of a line, dependent alongside with other parameters and from dielectric constant ε of liquid environment, in which two-wire line is placed. This dependence makes a basis of a principle of determination of level and separation level of environments with different value of dielectric constants ($\varepsilon_{air} = 1$, $\varepsilon_{water} = 81$, etc.).

As at arbitrary resistance of charge z_2 at the end of the line

$$(\dot{u}_2 - \dot{I_2} z_c) \neq 0, \qquad (3)$$

there is the return wave in the line.

This is taken into account by introduction of so-called complex factor of reflection of a wave r, by defining it in a general case as the relation of complexes of voltages or currents of return and direct waves in any point of a line:

$$r = \frac{z_2 - z_c}{z_2 + z_c} e^{\gamma x}. \qquad (4)$$

In narrower sense of a word factor of reflection is determined in points, where is any heterogeneity (the end, the beginning of a line, transition of a line through separation of environments with different dielectricity constant, for example, air - water or water - petroleum and etc.). Knowing, for example, direct wave of a voltage and factor of wave reflection, it is not difficult to calculate a return wave of voltage. So one can state:

if $\dot{u}_{np} = \dot{A} e^{\gamma x}$ then $\dot{u}_{o6p} = r\tilde{\dot{A_3}} e^{\gamma x}$. $\qquad (5)$

The similar correlation also is true in the case of a pulse entrance signal (for example, as delta function).

But as it was mentioned above SAPMAC is intended for the control of the following parameters in real rough sea conditions of operation of a vessel: loading of a vessel (mean draft, angles of trim and list), levels of liquid (liquefied under high pressure natural gas included) and loose cargoes, their density, humidity and temperature, and also current (in real time scale) parameters of dynamics of a vessel [4-7].

Thus the nomenclature of controllable parameters of various physical environments assumes use of large number of gauges of the primary information, working on various physical principles. Usually in such situation one can speak about construction of multichannel measuring information systems (MIS) of the third generation [8,9]. Systems of a kind are based on use of specific measuring transformers, and complex algorithms of information signals processing.

The attempts of practical construction of traditional MIS of the third generation for the decision of the specified problems have met difficulties both of technical, and economic character. From one side, the MIS of a kind have a plenty inputs of information from gauges of different physical nature. Besides, the

account of physical properties of entrance signals and their quantitative characteristics creates additional restrictions and complexities at creation and use of onboard MIS.

On the other hand, functional assignment of considered systems has determined them as systems, on an output of which turns out not only measuring information, but also quantitative and qualitative judgements about a condition of a vessel, including elements of identification of external influence, forecast and control.

For a vessel of the average size [1-3,7] the number of controllable parameters reaches $i=12$ in various points (cargo compartments and capacities, draft measuring units, etc.) $l= (100-120)$ with frequency of gauges debriefing from 10 up to 100 Hz. In result one should speak about necessity of development of MIS with about $N=1000$ measuring channels for all independent entries $X= \{[x1], [x2],..., [xN]\}$.

Necessity to install for each measuring channel energy supply and information transition cables (and for systems with variable speed of reception both distribution of the information and contours of return information) results in bulky and expensive structure of cable connections of MIS (each of $N=1000$ of measuring channels requires 4-6 wires cable each in length from 25 up to 100 meters).

Presence of input signals $G=G (q1, q2,..., qM)$, the direct separate measurement of which is impossible, on the first sight may even more complicate a described situation.

One of nontrivial solutions of the problem is to use optical fiber connecting cables, which are not so heavy and expensive. But fundamental way out lies through elimination the necessity of such a number of cable lines by itself. And this can be done with the help of polymetrical signals generating and processing.

The concept of a polymetric signal for the first time was introduced in [4-7].

The polymetric signal represents a function of time, which reflects change of a current or voltage at passage of the appropriate pulse in length of a similar two-wire line with given parameters, placed in controllable environment, in a given temporary interval.

The basic distinctive feature of such signal is the fact, that various its parameters or the combinations of these parameters carry in self the information on the physical characteristics of specified environment. So, the temporary intervals between characteristic peaks of a polymetric signal define distance between sections of various phases of controllable environment (gasified, liquid with low density, liquid with increased density, loose firm fraction, etc.). The relative amplitude of these peaks carries the information on temperature of environment. The relative duration of peaks and other ratio allow to determine density and other physical characteristics of environments.

The production of a described polymetric signal is rather complex and nontrivial problem, which includes following major problems:
- the development of mathematical models of polymetric signals with various information capacity;
- the development of methods for construction similar long two-wire lines (gauges) with given parameters;
- the development of the electronic circuits for generation and reception of pulses of the given form for sounding of environment with the help of such gauge;
- the development of mathematical methods and corresponding software of decomposition and processing of such signals. ensuring high metrological characteristics of the systems. and other.

242

Below some practical results, received on the basis of development of elementary soliton model of polymetric signal, are stated:

$$y(t,x) = y_o/ch[(x - vt)/l],$$ (6)

where: $v = v_0[1+(y_o/2h)]$, and l is defined by ratio

$$0.75(y_o l^2/h^3) = 1.$$ (7)

The basic achievement of the described approach is occurrence of a practical opportunity of construction universal MIS, in which the required amount of cable lines decreases minimum on ten times, and the majority of gauges is combined in one idle time structure with increased reliability and survivability.

3. FUNCTIONAL LAYUOTS AND STRUCTURES OF SAPMAC

The above mentioned MIS for automated remote control of ullage, separation level, temperature and density of liquid and loose cargoes is based on the described principles of indication of heterogeneity of arbitrary kind in measuring lines.

Two isolated from each other and from external environment electric conductors (the specific constructive designs are presented in [3,5]) are placed into the tank with nonmixed liquids on whole height. A high-frequency pulse of a voltage   is sent into these two-wire line. In places of change of wave resistance of the line Z_θ (which is determined by dielectricity constants of liquids ε_i) the pulse signal, as the special case of a wave, is reflected.

The reflected pulses, accepted on an entrance of the line, are allocated in time domain. Time of delay of a reflected signal in relation to the sent one is proportional to the distance up to each possible heterogeneity of wave resistance

in the measuring line (separation level of two liquid or loose environments, special marks installed in the line, etc.). Thus the corresponding formula is rather simple:

$$l = 0.5 \ V \ t,$$ (8)

where: l - distance from an exit of the pulse signal generator up to border of transition, V - speed of distribution of pulses in the measuring line, t - time of delay of a reflected signal in relation to sent one (fig. 2).
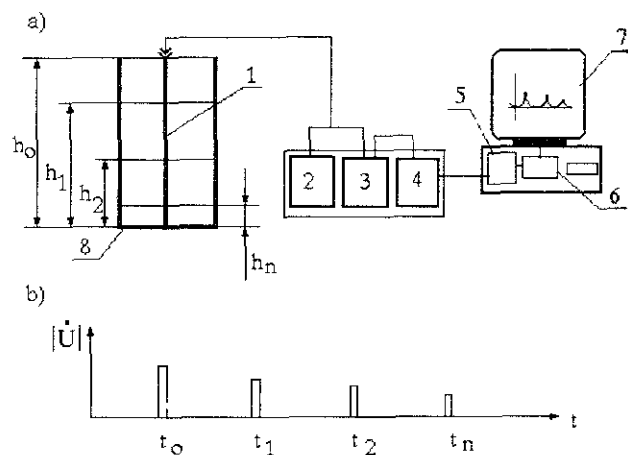

Fig. 2. A function chart of level measuring device (à) and typical time chart of sent and reflected signals (b): 1 - measuring two-wire line; 2 - pulse signals generator; 3 - receiver; 4 - amplifier; 5 - analog-digital converter; 6 - processor (device of processing of signals); 7 - indicator; 8 - capacity with nonmixed liquids.

Factor 0,5 takes into account a double way of a sent and reflected signal. The amount of reflected pulses is determined by the number of separation levels of nonmixed environments various dielectricity constants.

The computing device 6 calculates all needed parameters of liquids in each tank: volume, height, number of layers of nonmixed liquids, etc., using information on pulses U_1, U_2, U_3, ... , U_n or on the appropriate moments of time $t_0, t_1, t_2....t_n$ (fig. 3). The numerical analysis is held after analog-digital conversion of the initial polymetric signal and after solving some

complex problems, connected with stochastic instability of this signal in time, frequency and amplitude domains.
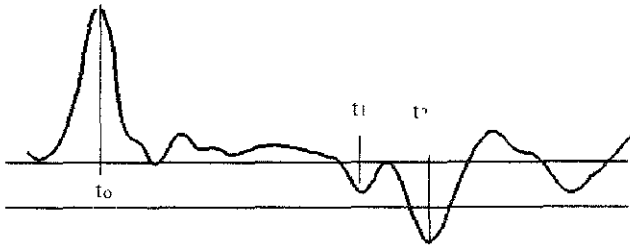

Fig. 3. Real time diagram of reflected signals for fuel tank (the level is determined by t_1) with uderproduct water (the level is determined by t_2).

The top level of each liquid in the tank or capacity is determined as:

$$h_i = 0.5 V (t_{i+1} - t_i), \ i = 1, N; \qquad (9)$$

and it's volume under the formula:

$$V_i = F(h_i; h_{i+1}) \qquad (10)$$

where: F - calibration function.

Total volume is determined as a sum

$$= \sum V_i, \ i = 1, N. \qquad (11)$$

Relative complexity of information processing of signals time reflectogramm, received in dynamical conditions is obvious. This kind of problem causes necessity of development of special software for monitoring system [7].

Modified circuits were developed for ship loading and stability affecting parameters control MIS (fig. 4 and 5).

In this design with the purpose of increase of accuracy of measurements at significant removal of several measuring lines from the central processor the high-frequency switchboard 9 is entered, and generators and the receivers for each measuring line are

incorporated in separate remote electronic blocks 10, placed directly on each measuring line.
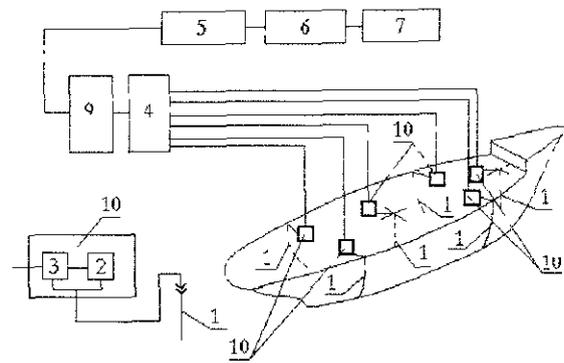
Fig. 4. Structure of modified MIS for ship loading and stability affecting parameters control: 1 - measuring lines; 2 - pulsing generator; 3 - receiver; 4 - amplifier; 5 - analog-digital converter; 6 - processor; 7 - indicator; 9 - switchboard; 10 - measuring head (remote electronic block).
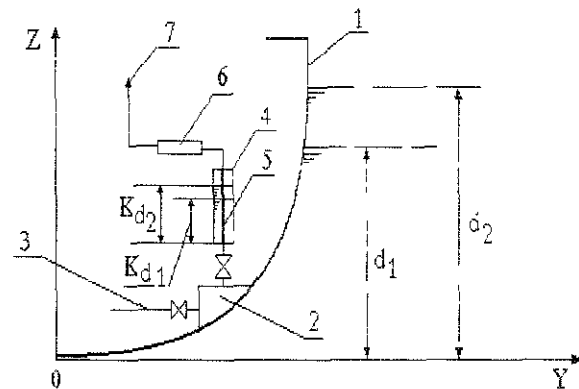
Fig. 5. Structure of functioning of tight draft measuring unit with a built-in two-wire measuring line: 1 - plating of the ship hull; 2 - kingstone box; 3 - pipeline of ship systems; 4 - tight draft measuring unit (pipe of height 0,5 m and diameter 100 mm); 5 - two-wire measuring line; 6 - remote generator - receiver; 7 - radio cable PK-50 (to the central processor); d_1, d_2 - two variants of ship draft; k - scale factor of draft measuring unit.

Research of serviceability and reliability of elements of a developed MIS for automated remote control of ullage, separation level, temperature and density of liquid and loose

244

cargoes was held onboard of small craft "Alfa", tanker safety boat "Redan", lighter carrier "Indira Gandi", tawing vessel of Nikolaev trade seaport "ПС-361" and research vessel "Delta".

During the testing coaxial, angular and strip gauges were used as measuring lines, showing reasonable operational and metrological characteristic, such as (in average): absolute instrumental error of level measuring - not more than 3 mm; length of probing probes - from 1 to 15 meters; distance from computer to measuring transformers - up to 500 m; number of measuring channels within one base block from 6 to 40; number of base blocks within one computer - up to 3; operation temperature from minus 36 to plus 60 degrees C; consuming power - 250 Wat; spark safety barrier, protection category 0ExiaIIBT3.

4. REFERENCES

1. Zhukov Y.D. - Instrumental Means for Ship Stability Accident Prediction - Proc.ISME Cobe'90. Vol.2./Cobe, Japan,1990. pp.4.7-4.12.

2. Zhukov Y.D. - Instrumental Ship Dynamic Stability Control - Proc. of 5 IMAEM/Athens. Greece,1990, pp.251-259.

3. Zhukov Yu.D. - Small Craft Rough Sea Safety Support in Design and Operation - Dr. of Sci. Dis./USMTU, Nikolaev, 1994, 287 p.

4. Zhukov Y., Gordeev B., Leontiev A., Logvinenko Y. Computer-aided Simulation of Polymeasuring of Parameters of Liquid Energy-carriers//Proc. of 1-st International Modelling School "Krym Autumn '96". - Rzeszov. RUT, 1996 - P.12.

5. Zhukov Y.D., Gordeev B.N. - Impulse polymetrics in onboard systems for ship ecological monitoring (in Rus.) - Proc. of 1-st Int. Conf. "Problemes of energy saving and ecology in shipbuilding", Nikolaev, Ukraine, 1996/USMTU, Nikolaev, 1996, p.81.

6. Gordeev B.N. - Problems and prospects of development of maritime impulse polymetrics (in Rus.) - Proc. of 1-st Int. Conf. "Problems of energy saving and ecology in shipbuilding", Nikolaev, Ukraine, 1996/USMTU, Nikolaev, 1996, p.82.

7. Zhukov Y.D. - Fuzzy algorithms of information processing in onboard systems for ship ecological monitoring (in Rus.) - Proc. of 1-st Int. Conf. "Problems of energy saving and ecology in shipbuilding", Nikolaev, Ukraine, 1996/USMTU, Nikolaev, 1996, p.83.

8. Tsapenko M.P. - Measuring information systems - Energoatomizdat, Moscow, 1985 - 440 p.

9. Karandeev L.B. - Measuring information systems and automatics/ Bulletin of USSR AS - Moscow, 1961, №10, pp. 15-18.

AKNOWLEDGEMENTS

State-of-the-art Review Report

to the Panel Discussions on

DAMAGE STABILITY AND SAFETY
OF RO-RO VESSELS

Panel Dicussion
Damage Stability and Safety of RoRo Passenger Ships
State of the Art Review
H. Hormann
GERMANISCHER LLOYD

Introduction

In September 1994 the "Estonia" went down. This tragic accident occurred at a time when the RoRo passenger ship operators and the designers of such ships were amidst the regulatory transformation triggered by the "Herald of Free Enterprize"-desaster.

The "Estonia" must be compared with the "Titanic". The latter was the cause for the first international safety convention. What was set into motion by the "Estonia"?

We are predominantly interested in the stability aspects, but we must not forget that this is only part of the comprehensive review of safety regulations, which took place within IMO and outside. The rule of the day was "turn every stone" of the safety provisions for such ships - as the chairman of the now almost legendary Panel of Experts put it, this unprecedented institute of IMO which was instrumental in the very quick regulatory response. - The SOLAS amendments were in place less than 14 months after the accident.

The Regulations

When weighing the damage stability requirements adopted at the SOLAS-Conference (and those superimposed on them by the Stockholm Conference), one must take into account the significant pressure exerted at the time on those discussing the amendments, which came from the communities having suffered the most and from the general public at large.

It is a phenomenon which can be observed frequently: the level of safety required by regulations is accepted by the general public up to the moment at which a high profile accident occurs. Then there is an imperative demand for a higher level of safety, even if an individual case, in particular its cause, may not have a measurable impact on the objective risk level (It is an interesting fact that the risk levels publicly accepted are very different for the different means of transport for people, and this acceptance level is almost immune towards rational arguments!)

Now that the emotions have gone, we can have a more neutral look at the regulations now existing:

The so-called SOLAS 90-standard, established after the "Herald of Free Enterprize" introduced for the first time retro-active requirements in the field of damage stability. It was very evident, when on this basis the discussion started after "Estonia" (on where do we go from here?), the emphasis was to in the first place cover existing ships. The rule-evolution process is normally to set new requirements for ships to be built in future and then consider, whether and how to extend them backwards. SOLAS 90 still went this old way: criteria for new ships were set and a somewhat reduced version applied to existing ones with a scale of target dates for compliance, depending on a "quality" parameter.

Now in 1995 the post-ESTONIA-conference dismissed the reduction for existing ships, deleted the exemptions and tightened the scale of target dates by several years. The effect is that _all_ RoRo passenger ships contracted before 1. July 1997 must comply latest by 1. October 2005 with full SOLAS'90-standard for new ship. That in essence is:
- a minimum range of residual righting lever curve of 15° beyond the angle of equilibrium

- an area under the residual righting lever curve of 0.015 m rad
- a residual righting lever within this range which exceeds the defined heeling moments by 4 cm and which is in no case less than 10 cm.

The values constitute quite a significant increase compared with the requirements which existed unchanged for a very long time before 1990, actually since 1960 and (for recapitulation) was just: 5 cm residual GM, 7° (15°) final heel due to unsymetrical flooding, no consideration of adverse moments due to passenger crowding, launching of lifeboats on one side, wind pressure.

Is the SOLAS 90 standard adequate?
The question, whether the SOLAS'90 criteria were sufficient, was discussed ever since their inception Final answers were not produced in 1990, so this key question popped up again naturally in 1994/1995.

Before reporting on the further development triggered by this question, I would reflect on the ramifications. To cater for the worst possible seastate for a ship in the worst damage condition is impossible; an objective judgement on the basis of probability assessments was too time demanding for the situation. So the establishment of a reasonable figure for the probability of survival could not be undertaken and if - it had to meet the challenge of public opinion, as explained earlier on.

This situation was unpleasant for the rule setters, because IMO was already - and still is - in the process of converting the deterministic subdivision regulations into mainly probabilistic ones, with complementary deterministic support. Despite of this one had to proceed purely deterministic - with the misgiving that objective judgement on the suitability of minimum values to be chosen was not achievable.

Consistently the key question was not replied to unisono, i.e. different opinions remained on what should a damaged ship be able to cope

with in terms of internal and environmental adverse effects. - This triggered the notorious Resolution 14 of the SOLAS' 95 Conference, which sets forth the option of requiring a higher standard (up to a defined upper limit) for a geographic region "having regard to the prevailing sea conditions and other local conditions".

History of this resolution is interesting and so are the legal aspects as well as questions of safety philosophy, but this is not ours at this time. We shall confine our attention to the technical contents of the first application of this option: the set of damage stability requirements known as the Stockholm-Agreement.

To put it in slightly provocative terms: there was the arbitrary level of safety represented by SOLAS' 90, now another arbitrary addition in safety was made - once again the actual provisions were driven by little technical substantiation, much more by subjective opinions and even emotions. I do certainly not say that this is not acceptable as a way to set standards of safety. But the question with us (and others) now is still, are the technical requirements adequate.

The Stockholm criteria
Stockholm superimposed on the worldwide standard in essence an additional layer of water on the roro deck, 0.5 m water, if the residual freeboard is less than 0.3 m, with a gradual reduction to 0, when 2 m freeboard remain. A further parameter to reduce the 0.50 m water on deck is the significant wave height in the area of service; the limiting values for the significant wave heights are 1.5 m on one end and 4.0 m on the other. In practical terms: if a ship trades in a geographically defined restricted area with a significant wave height of 1.5 m or less, water on deck need not be taken into account, even if it has a residual freeboard of 30 cm or less.
Is that now adequate? Who can say!

Admittedly there were a number of well-thought-through justification attempts for the figures finally chosen, but all together cannot

wipe out the taste of arbitrariness. - There is, however, a relief for the naval architect's uncomfort, when looking at this situation: The alternative, also laid down in the Stockholm Agreement, for the calculatory superimposition of water on deck is a model test. The individual ship is to be tested in a reasonably realistic testmethod (also given) and proof established that it will not capsize in the irregular seaway representing the ship's intended area of operation. - No question this judgement is objective, but regrettably directly only as far as the model is concerned. The transcription of the model results into true size is subject to uncertainties again. - Nevertheless, here is an approach which, at least theoretically, could produce results for individual ships, answers to the question: what is sufficient stability. It remains to be seen what the experience with such model tests has already and will bring about.

Safety in General

In accordance with the title of this panel discussion we should not loose sight of all the additional technical and operational requirements, which were adopted at the SOLAS'95 Conference to enhance RoRo passengers ship safety. Part of them deal with separate safety issues, e.g. life saving appliances. The overwhelming majority, however, is directly or indirectly linked to the stability requirements; to mention just a few

- rigorous requirements for the closing appliances in the roro deck, in particular the bow doors both concerning the hardware and operation. This indeed should reduce the likelyhood of water getting on the car deck;
- common working language, a very practical means to reduce operational mistakes, e.g. failure to meet closing routines;
- requirements concerning escape routes; also they are related to the survival capability.

All these provisions can be seen as supporting and complementing the central piece of the

enhancement of safety: the augmented damage survivability requirements.

Direct part of them, to complete the review, is the regulation phasing out the 1-compartment-ships. The theoretical thrust of this is obvious: how can we defend a safety concept which is dependent (in a black and white fashion) from the avoidance of certain "vertical lines" at the shell to be struck in a collision? A closer look reveals on the one side that there is very little, if any, known experience of a 1-compartment-ship foundering, because two compartments were opened by a collision; on the other side we have to realize that this new regulation

- is confined in its application to RoRo passenger ships; what is the difference to any other passenger ship?
- related only to such ships carrying 400 or more persons,

so up to 400 persons on a roro ship and much higher numbers on other ferries or cruise ships are subjected to this risk; - another proof for the arbitrariness prevailing in present day regulations.

Outlook and conclusions

The key question, what is the level of safety sufficient for RoRo passenger ships, remains open. The valid answer at the regulatory level is defined by the SOLAS' 95 and Stockholm Conferences. But, as we have seen, the answer was not derived by objective judgement on the basis of physical facts. So, can this answer survive the times?

What is clear, are the expectations of the industry (as formulated recently in an ICS publication):

"... the hope must now be for many years of safe and efficient ferry transport under a stable regulatory regime".

I think this hope qualifies for being called just.

As well reasoned as this certainly is, this must not drive naval architects at large, in particular designers and those professionally maintaining rules and regulations to lean back and wait. Evolution has to go on here as in other fields - and it does.

251

I mentioned already the ongoing work to make all the various sets of survivability regulations consistent be introducing the probabilistic approach with certain deterministic supplements; the model for this is the set of regulations now in force for dry cargo vessels.

Another, for our purposes much more interesting project is the Joint North West European Project for RoRo Ferry Safety (JNWERP). This research project has established a framework for new damage stability standards - which are, however, not right away introduced into the international regulations setting machinery; and they can't at the moment (let aside the justified call for a hold by the industry), because the studies so far did not tackle the question, what is achievable and - again - what level of requirement is recommendable. But, while sticking to the methodology of A265 and SOLAS dry cargo ship regulations culminating in the requirement A > R, the project took a fresh approach in identifying first the weaknesses inherent in the SOLAS' 90 regulations. This exercise revealed several risks which are not covered so far by regulatory means, e.g.

- damage beyond the deterministic assumptions
- bottom damage penetrating the inner bottom
- "raking" damages
- flooding or progressing flooding through accidentally open closing appliances or doors
- cargo shifting.
- water on the roro deck (which was then included in general terms through Resolutions 14 of the '95 Conference)

The main weakness was identified as the lack of a second line of defence in general. For this the probabilistic concept implemented as for cargo ships has to be augmented by a deterministic "minor damage" concept. But also combinations such as rapid water ingress after a collision and inner doors open at the time of collision were addressed.

The factor representing the probability of survival after a damage (s-factor) attracted special attention. The effects covered so far (in the cargo ship regulations) can be supplemented by including the effects of water on deck, cargo shift and progressive flooding.

Over and above the familiar subdivision index A, a capsize index is proposed, representing the control of the development of major damages including those, which the ship cannot survive. The attempt was driven by the fact that capsize is a fatally rapid process; a "controlled sinking" without capsize leaves much more chances. It is therefore of interest to categorize the mode of non-survival in a specific damage situation and weigh the sinking cases more favourably than capsizing ones.

As said, this project produced interesting proposals, in part just those of principle, but at any rate a valuable step in the strive for a level of safety of RoRo passenger ships constituting a balance between public demands and solutions which can be financed using yardsticks as objective as possible.

Written contributions to the panel discussions on

DAMAGE STABILITY AND SAFETY OF RO-RO VESSELS

Ro-Ro Passenger Ferry Water-On-Deck Requirements
Commentary for STAB '97
Varna, Bulgaria : September 22-27, 1997

by Mr. H Paul Cojeen and LCDR Patrick E. Little[1]

The inability of the International Maritime Organization (IMO) to adopt a water-on-deck based damage stability standard following the *Estonia* disaster underscores the need for a flexible approach for maritime safety issues. Casualty statistics show that water accumulation on the ro-ro deck and the ensuing loss of stability has been a major factor in the capsizing of 44 ro-ro cargo and passenger vessels in the last 15 years. The opportunity to correct this shortcoming in SOLAS may have been lost because of the failure of the participants to recognize the need for flexibility, propose a straightforward solution and follow through with effective consensus building.

Ro-ro passenger ferries are a vital transportation link around the globe. Yet, ro-ro passenger ferries cannot be grouped into neat categories based on size and/or operation. For example, tankers are easily described by the terms Suez-max, Cape-size or handy-size. Ro-ro passenger ferry designs are a function of route, with the routes being distinguished by location, length and wave climatology. At one end of the spectrum, there are cruise-ship type ferries crossing the Baltic Sea on overnight trips in weather that can be severe. The risks encountered by ro-ro passenger ferries operating in Northern Europe differ dramatically from those on inter-island services in the Mediterranean Sea and Far East. This fundamental difference in risk appeared to be lost during the debate leading up to and at the SOLAS Conference on ro-ro passenger ferry safety. The Northern Europeans, recognizing the potential severity of conditions on many of their routes, steadfastly argued for damage survivability in 4 m wave heights. The Southern Europeans, on the other hand, don't operate in those types of conditions and could not see the need for such a standard. We can understand both positions.

The differences in operations and risk was further compounded by the fact that many countries apply the provisions of SOLAS directly to their domestic fleets. Thus, domestic ro-ro ferries operating on inter-island transportation routes would have to pay the costs for the upgraded standards. Because of the difference in operational risks, many countries felt the stringent water-on-deck damage stability standards were irrational and financially too severe.

These factors highlight the need for a single standard for ro-ro passenger ferries that takes into account the difference in operating profile. Ultimately, the SOLAS Conference decided to go with a two-step approach. The first step required all existing ro-ro passenger ferries to upgrade to the SOLAS 90 damage stability standards on an accelerated timetable. This was an important first step. The second step was the optional higher standard outlined in the regional agreement of Conference Resolution 14. Unfortunately, the two step approach gets away from one of the fundamental premises of IMO: uniformity of standards. There are many needs for uniform standards, including a common level of safety, ease of transportation among countries and an improved market for used vessel sales. With the two-step approach, there is still no uniform damage stability

[1] Naval Architecture Division, U.S. Coast Guard Headquarters, Washington, D.C.
(The views expressed here are not necessarily those of the U.S. Coast Guard or the Department of Transportation.)

requirement that explicitly recognizes the water-on-deck hazard.

The solution to the paradox of a single standard for vessels with different operating profiles was available at the SOLAS Conference but not effectively used. The Society of Naval Architects and Marine Engineers (SNAME) convened an ad hoc panel to study ro-ro passenger ferry safety following the sinking of the *Estonia*. Tasks of the Ad Hoc Panel included conducting basic research on the accumulation of water on ro-ro decks and assessing the impact of the POE's work on the North American ro-ro passenger ferry fleet. The main recommendation of this group was a simple formula (shown in non-dimensional form in Figure 1) that rationally linked a water-on-deck requirement to the relevant variables of significant wave height and freeboard;

$$D = 0.15H_s - 0.30f$$

where: D = depth of water to be applied on deck;

H_S = significant wave height;

f = freeboard at the location of damage.

This formula was proposed to the Panel of Experts (POE) and they developed a similar proposal. We were disappointed that although the POE agreed with the main premise of a standard based on the relevant variables, the POE proposal was not as easy to understand and did not consistently reduce the water on deck burden at lower significant wave heights or higher freeboards. It's not meaningful to plot the POE criteria on the non-dimensional graph in Figure 1, but the f = 0.3 m and H_S = 4.0m point is noted for comparison. Although there has been additional research since the SOLAS Conference, the Ad Hoc Panel formula was the best information available at the time.

The lesson is that recognizing the need for a flexible approach is only part of the process: the packaging and implementation are equally important. Proposals at IMO should be as simple as possible so that their impact can be easily understood. Unfortunately, the POE proposal did not meet this test. For a given vessel, it is not easy to assess the impact because interpolations are required for sea state and freeboard. Even a graphical approach might have been more appropriate. As an example, the Ad Hoc Panel equation clearly shows that if the vessel's freeboard is half of the significant wave height, no depth of water is applied on deck. In connection with the simplicity of the formula, it's important to market the proposal to the affected parties so they clearly understand how it will affect them. There was never an attempt to build consensus among the affected parties. The POE proposal may have been adequate for all involved, but the complexity of the formula coupled with a lack of effort to convince countries of the impact significantly reduced the possibility of adoption. Alternatively, the final result may have been predetermined with the POE having little flexibility for change.

To underscore the difficulty of this issue, it's important to note that we have not been successful in implementing a standard based on operational risk at home either. Our hope in the United States was to apply a rational framework to our domestic vessels in partnership with our neighbors in Canada. Another offshoot from the SNAME study was the recognition of commonality between the Canadian and United States ro-ro passenger ferry fleets. Our vessels range from small river crossing vessels with no bulwarks or side structure to European-style vessels operating overnight in remote locations or severe weather conditions. We also hoped that the activity of the SNAME work provided the interaction between the vessel operators and regulators necessary to implement such a regional agreement. Unfortunately, the failure of IMO to implement the flexible standard outside of the regional agreement jeopardized this goal. We've made informal approaches on implementing the agreement, but the industry has been reluctant to implement a standard higher than that contained in SOLAS for a

operating environment that is more benign in general.

On an encouraging note, the Alaska Marine Highway Systems voluntarily designed their new Ocean Class ro-ro passenger ferry to meet the 0.5 m of water on deck requirement initially proposed by the POE. The design uses B/5 longitudinal bulkheads below the subdivision deck. The resulting wing voids are cross-connected port and starboard to minimize asymmetric flooding. With the introduction of

these design features a large residual freeboard and ample residual stability is maintained in the damaged condition without flood control doors on the car deck. The lesson from this newbuilding project is that a water on deck damaged stability standard does not impose an unreasonable challenge to new designs, and that the resulting designs do not have to compromise the efficient loading of the vehicle deck.
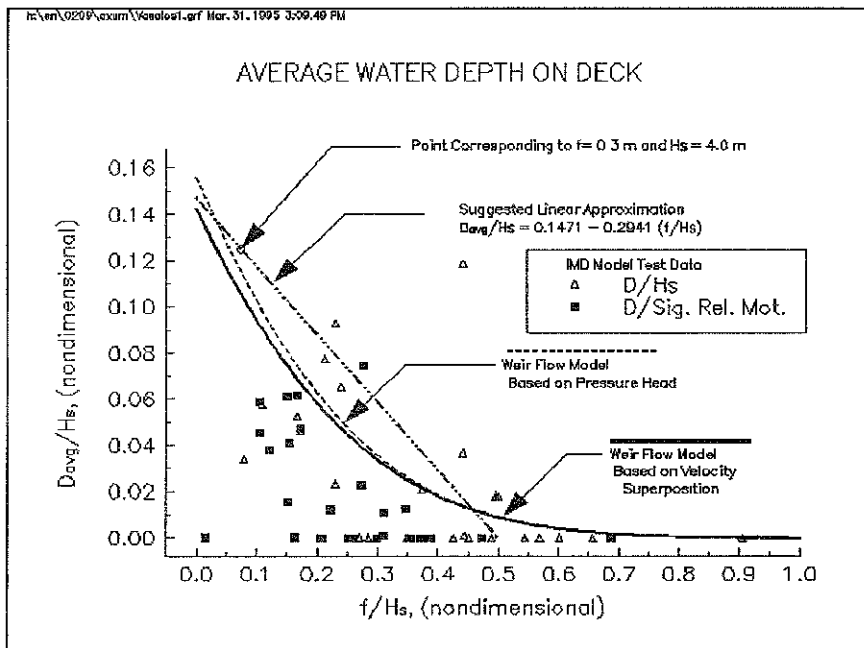

Figure 1

STABILITY OF RO-RO PASSENGER SHIPS

Ricardo Marsano
Genoa, Italy

Ro-Ro passenger ships of modern conception can be subdivided into three groups as follows:

First Group

The "Conventional" Ro-Ro Passenger Ships carrying passengers with cars, caravans, etc. and a limited number of freight vehicles.

These Ships have a passenger capacity ranging between 1000 and 3500 persons whereas their ro-ro deck capacity is often below 1200 linear meters.

Second Group

The "Mixed" Ro-Ro Passenger Ships carrying passengers with cars, caravans, etc. and a consistent number of freight vehicles.

These Ships have a passenger capacity ranging between 400 and 2500 persons with a ro-ro deck capacity between 1000 and 2000 linear meters.

Third Group

The "Trailer and Passenger" Ro-Ro Passenger Ships carrying a limited number of passengers, mainly drivers, a limited number of cars, caravans, etc. and mainly freight vehicles.

These Ships have a passenger capacity between 100 and 200 persons with a ro-ro deck capacity between 1000 and 2500 linear meters.

Ships belonging to this group are constantly increasing in their number and their size.

SOLAS'90 stability Standard has certainly met - with the exception of a limited number of mainly European Nordic Countries - the worldwide expectations in terms of safety adequacy, considering the consistent amount of new requirements and regulations which were developed and introduced in 1995 by the International Maritime Organization with a relatively narrow phasing-in on dates of compliance. SOLAS'90 Stability Standard is certainly standing at a severe level. It is not possible to formulate at this early stage a technical option on its adequacy in terms of enhanced safety criteria.

As I experienced in the period between 1995 and 1996 the study and the conversion of five existing ro-ro passenger ships - belonging to the Second Group hereabove - for the purpose of complying immediately with SOLAS'90 Stability Standard, I found out as I expected that such standard is undoubtedly a heavy burden for existing passenger ships. I had the interesting experience of the conversion in 1996 of two sisterships (Golfo degli Ulivi and Golfo dei Poeti), overall length over 150 m, with the adoption of extensive side sponsons of 1.5 m breadth. It may be interesting to mention that the sponsons were accurately studied and designed in an innovative way in order to avoid negative collateral effects: both ships have achieved an increase of their service speed of 0.2/0.4 knots at corresponding conditions of deadweight and propulsion power.

Bearing in mind the significantly high GM value pertaining to SOLAS'90 Stability Standard, Ro-Ro Passenger Ships belonging to the Second and Third group are particularly concerned with consistently high GM values when carrying a partial cargo of freight vehicles. Ballasting, which is often necessary when sea conditions

are adverse, is of course worsening the problem. This was the main concern with the conversion of "Golfo Degli Ulivi" and "Golfo dei Poeti" in 1995. It was possible to overcome the problem of excess high stability with reduced deadweight by the adoption of the free surface effect in specific double bottoms and side tanks, thus reducing in some conditions of load the GM value to bearable limits (about 2.0 m). This was possible with an innovative computerized system, combined with a fully monitorized system of ballasting and stripping.

It was in addition necessary on all five ships converted for compliance with SOLAS'90 Stability Standard to review and to improve the lashing equipment, in order to withstand high acceleration values affecting freight vehicles in . adverse sea conditions with the new GM values pertaining to SOLAS'90 Stability. It may be interesting to mention that new trailer horses of innovative design with a breaking load of 180t were adopted, replacing the existing ones of about 30t breaking load.

A considerable study has been done and no doubt that more research will be carried out in order to investigate the crucial concept of ro-ro passenger ships' stability.

I am confident that the outstanding problem of unbearably high GM values will be carefully considered and will be a matter of meditation.

We well know that in February 1996 the Stockholm Agreement introduced in specific West North European routes and/or areas a specific requirement in term of ro-ro passenger ships' stability, that is SOLAS'90 plus additional water-on-deck. This specific requirement was not scientifically and technologically supported and consistently less severe than the similar concept developed by the Panel of Exporters, resulting in Resolution 14 of SOLAS CONFERENCE'95.

We all know that the concept of SOLAS'90 plus water-on-the deck (0.5 m^3/m^2) introduced with Resolution 14 and in February 1996 with the Stockholm Agreement, although the latter in a consistently less severe way, followed the public opinion's demand for much stricter requirements; it must be remembered that after

the dramatic Estonia's tragedy the public opinion was nurished with the concept of 0.5 m water-on-deck.

It was certainly difficult to make the public opinion to understand and to accept that the SOLAS'90 Stability Standard was already a significant improvement of ro-ro passenger shops' stability. The unfortunate fact was that SOLAS'90 existed already, although pertaining to a limited number of newly built ro-ro passenger ships. Resolution 14 and later on the Stockholm Agreement were in fact political issues and not technical issues, following the Estonia's tragedy and the political need to develop and to introduce an innovative requirement in terms of damage stability.

If the main concern for scientists and naval architects is the survival of a damaged ro-ro ship shipping water on deck, no matter if this is basically a theoretical exercise as the risk of water entering from the bow should not exist considering the new regulation applying to the bow door and to the inner door; moreover the risk of water entering from the damaged ship's side is covered with SOLAS'90 Stability Standard, as reported by the significant number of ships' model basin tank tests and experiments which have been carried out from 1995 onwards. If however it should be considered necessary to develop a new generation of ro-ro passenger ships perfectly safe and capable to withstand an additional volume of water-on-deck, the only possible solution is in my opinion to increase to /1,0 m) the residual freeboard in damaged condition.

May I make the following considerations:

1. The well known requirement of Transverse Bulkheads on the main deck has a technical sense if their structural strength is adequate and properly designed against the impact of unlashed or improperly secured freight vehicles.

   Such Transverse Bulkheads should be watertight and always closed at sea (not occasionally, when the Master considers it may be proper).

   It must be however considered that ro-ro passenger ships fitted with Transverse

Bulkheads in the number of three or even more, are not commercially and economically operative.

This is the conclusion of accurate studies and investigations made already in 1996 by the so called "Moderate Countries".

2. It is not advisable, for the reasons already mentioned, to increase the stability over and above SOLAS'90 Stability Standard to cope with the considerable free surface effect resulting from a consistent additional volume of water-on-deck, such as the one of the Stockholm Agreement.

3. Ships' model basin tank tests and experiments have shown that when SOLAS'90 is complied with and when a consistent residual freeboard of 0.6/0.6 m is available, the damaged ship is perfectly able to survive and to withstand the incoming waves up to 4.0 h_s (significant wave height) or even more.

Although recognizing the concept that evolution has to go on and that new research projects on damage stability standards should certainly deserve the utmost attention and consideration, it should be followed by the principle that quite many accidents and catastrophic events can be prevented by introducing a new set of specific requirements in the design of ro-ro passenger ship instead of a new set of regulations on damage stability.

May I point out the following:

A. Bottom damage penetrating the inner bottom
A new requirement on double bottom height could be investigated.

B. Flooding or progressive flooding through accidentally open closing appliances or doors
Flooding or progressive flooding is unlikely to happen considering that watertight doors must be remotely operated, such very reliable and fail safe appliance should not cause accidental opening of doors. Moreover if existing regulations are properly complied with, piping failure should not produce any major flooding or progressive flooding.

C. Cargo shifting
From the reports on the loss of the ro-ro passenger ship "Herald of Free Enterprize" it stands out that when this ship was refloated the freight vehicles were duly lashed, standing in place at their loading position. It must be noted that the ship capsized before sinking and lay down on her side.

It is well known that according to regulations the lashing equipment must be entirely reviewed and significantly improved Shifting of cargo is actually not likely to happen.

As concerning the cargo load of the freight vehicles, same will not shift transversally - as it was claimed -but it will eventually fell down on ship's deck and will hardly move significantly towards the ship's side.

An additional consideration should be given to the existing new requirements that all freight vehicles must be properly lashed and secured prior to ship's departure.

The final conclusion is that cargo shifting should be not taken into consideration, following the implementation of the new · regulations.

Conclusions

It is in may opinion very difficult to identify in general and for all events a "second line of defence".

Some arbitrary concepts which by experience have proven to be consistently safe must necessarily be maintained although being in conflict with a new probabilistic approach in terms of damage stability standard.

It is important to remember and to bear in mind that when developing and formulating new sets of damage stability requirements, same must not jeopardize the basic concept of a ro-ro passenger ship.

This is, may I point out, the main outstanding problem that scientists and naval architects have to consider when approaching and developing revolutionary concepts and criteria on damage stability.

Carlos
A.E.S.A , M

NEW VESSELS

All shipowners in our ferry passenger vessels designs and contracts, want to fulfil the Stockholm Agreement. This shipowners come from the Nordic countries and other countries that have not signed the Stockholm Agreement

EXISTING VESSELS

Our fleet is going step by step. The vessels with a chance in the future are improving their safety and of course their stability, many of them even to implement the Stockholm Agreement. Other vessels that are very old and not prepared for the new future, are proceeding to improve their stability according to the previous A/Amax and SOLAS'92 Amend-ments.

Are the regulations technically feasible?

If a vessel comply with SOLAS'90 and has a freeboard after damage bigger than 1 m the North European set of regulations have been found feasible. The new required maximum KG to fulfil Stockholm Agreement with water on deck, is very similar and only a little higher than the required KG to fulfil SOLAS'90 without water on deck. The configuration of the vessel would be with slide casings and in few cases with B/5 longitudinal bulkhead for the 60% of the length of the garage. See fig. 1.

Dependency of the distribution density of water on deck, with the freeboard and significant wave height.

The first distribution of water on deck dealing with the freeboard and significant wave height, that we received from the Canadian Research in Hamburg and base for our discussions (POB) at the end of February of 1995, is according with my information very approximated to realty The distribution was confirmed in the research held in the Pardo model basin tank few months later. I understand this distribution as an "average of water on deck" during the time of the experiment.

This is for me the big difference with the hypothesis of the Stockholm Agreement, where the "amount of water on deck" changes with the heel, and only is constant the height of the water on side of the vessel over the main deck in all the time. This hypothesis produces a small influence in the theoretical calculation compared with the theoretical calculations for SOLAS'90.

Therefore our proposal of the POB was nearer of the real phenomena, but the problem is that the theoretical model to calculate the stability with water on the deck is not enough correct. The theoretical model is a static study and the real vessel is in a dynamic scenario.

The different model tests carried out in different countries have showed that the results of these

tests are more optimistic than the results done with the theoretical model. But why we do not find this difference? (See fig. 1, theoretical model for calculation in intact and damage condition.) The answer could be in the real configuration of these vessels above main deck. The buoyancy effect of the superstructure is evident if we analyze the dynamic balance of the vessel over the waves and sea.

If the heel angle position of the vessel is on the opposite side of the damage (see fig. 2), we have a consistent buoyancy that is missing in the theoretical calculation, because we only consider in the theoretical calculation the buoyancy bellow the main deck and without any effect of the superstructure.

If the heel angle position is on the side of the damage (see fig. 3) may be, the level of water inside (water on deck) is different of the level outside (wave height and sea level) and in many balances the effect of buoyancy will be positive, therefore another time we have a righting arm that is missing in the theoretical calculation model.

In some way this effect of buoyancy for open superstructures written in the International Convention of Load Lines 1930, and allowed a reduction of the freeboard under some conditions.

Also in the conclusions of the research made by UK after the Herald Free Enterprise sunk, is written that "is difficult to evaluate the superstructure buoyancy effect above of main deck in damage condition".

This conclusion was written in my opinion because there is a buoyancy effect that was not considered by the theoretical model.

Therefore we must propose to change the calculation theoretical model a little. One thing would be to come back to distribution of water proposed by OP (may be modified by the values coming from the different experiences coming from model basin tanks). On the other side I would propose certain value of permeability to the superstructure above main deck. This value would be to approximate the results of model test carried out to the theoretical model

calculation. The permeability value is function of the value of freeboard after damage, the size of the damage, the internal configuration of the garage and the GM of the vessel after damage.

Nordic research

The main conclusion of this research has been the proposal presented on the last SLF of IMO in September 96 about a new probabilistic method for the calculation of damage stability for passenger ferry vessels.

This proposal has two new concepts to be calculated:

- Water on deck (h critic)
- Function of Hs (significant wave height) versus h critic
- Shift of cargo

I would like to comment above some discrepancies that I have dealing with the water on deck, the function of the significant wave height and "h critic" concepts.

1. According to the definition expressed in the proposal "h critic" is the value of the height of water on deck that produced the loss of the vessel. This value is the height of the volume of the water on deck that makes the value 0 (zero) on the GZ curve (righting arm curve) at the angle of θ max. The GZ curve is the after damage righting arm curve of water on deck corresponding to damage case under consideration (see fig.4).

In my opinion this conclusion can be done without any experiment or research because is mathematical consequence of the theoretical concept of the curve. If you find a heeling moment that produce an angle of equilibrium corresponding to this θ max., and you will have the vessel without stability and therefore it would be expected the loss of the vessel. I have different values from model test, that don't demonstrate the loss of the vessel for the defined value of "h critic". (The explanation is

because this stability GZ curve doesn't have in account the buoyancy effect of the superstructure above main deck, as I have mentioned above) (You should also note that the freeboard after damage is not related in this definition)

You know the big influence of this concept for the new ro-ro passenger designs My feeling is that it would be necessary to study with other opinions this important "h critic" concept or define other parameter for to have in account the water on deck effect dealing with the real phenomena

2 The function of the significant wave height dealing with the "h critic" is defined according to the proposal based in Nordic Research as

$$Hs = (h \; critic/0 \; 085)^{1/1 \; 3}$$

This function is more or less our proposal (POB) for the amount of water on deck dealing with the significant wave height and in some way similar to the proposal of the US and Canadian Coast Guards made in their research, but this function has never been realised to the concept of 'h critic" as defined in the research of Nordic countries In this function is missing some influence of the freeboard after damage in the damage case

Model test

My conclusions coming from the model tests are the following

1 The model tests have always been more optimistic than the theoretical calculations made for the same damage case tested

2 A SOLAS'90 vessel never capsize for a freeboard after damage of 0 3 m and a sea state with a significant wave height of 4 m

3 A symmetrical side casing has a better behaviour then that of a central casing

4 An important buoyancy from the superstructure on main deck has been demonstrated with a considerable value of the righting arm over the value calculated from the theoretical model
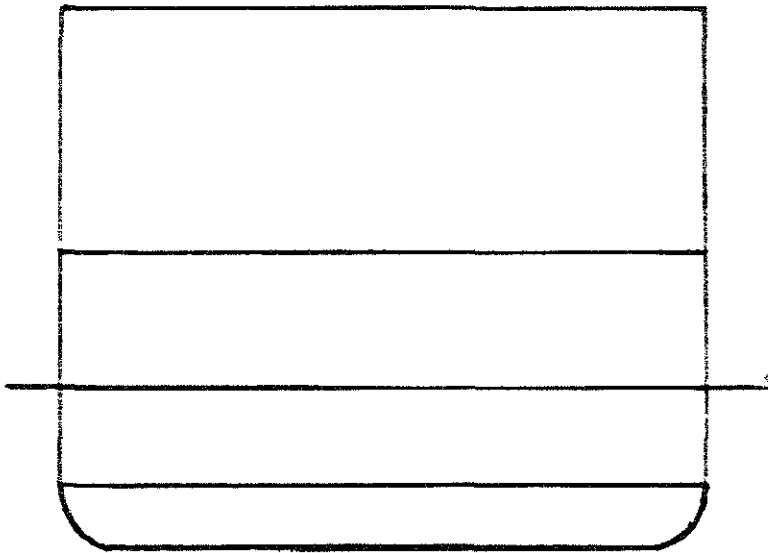
INTACT CONDITION
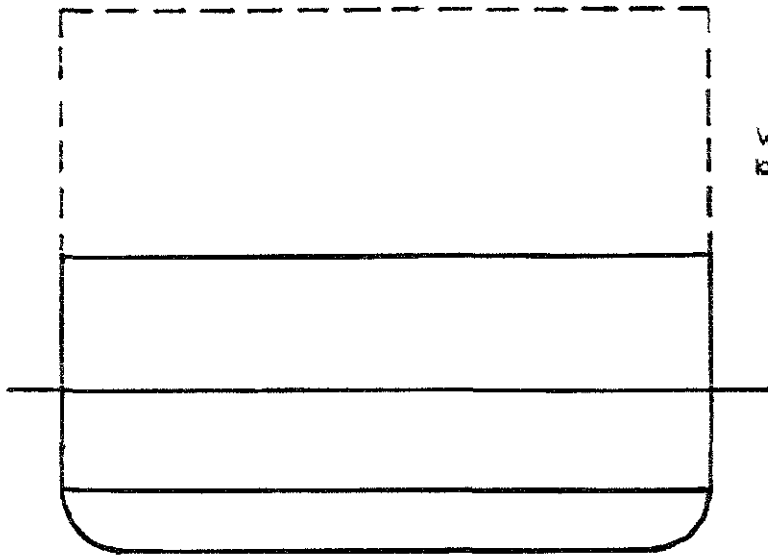
Without superstructure
buoyancy effect

DAMAGE CONDITION

FIG. 1

266
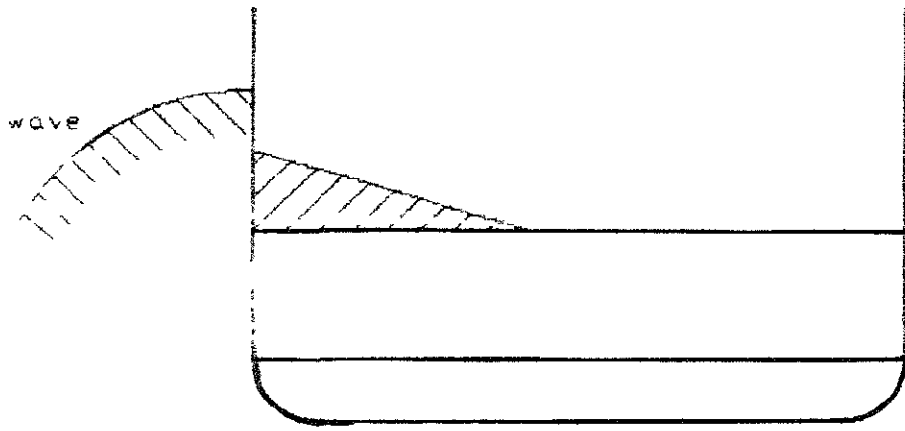
Opposite damage side

water on deck

wave

Damage side

FIG. 2 & 3

267
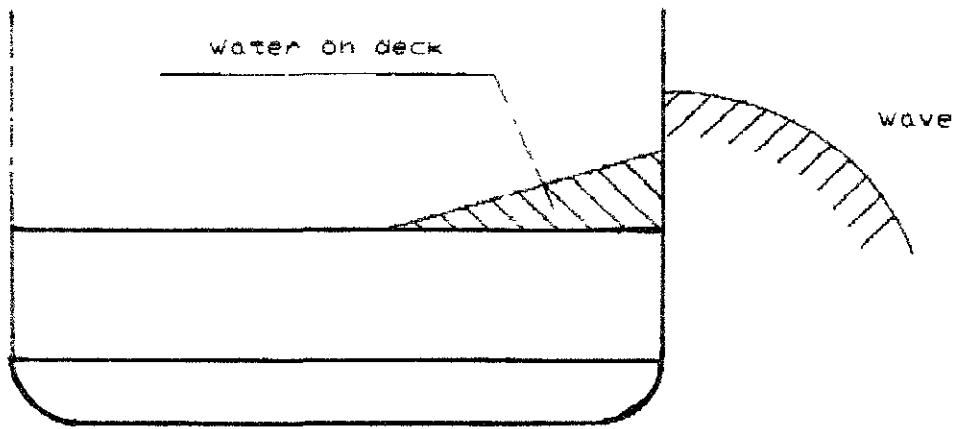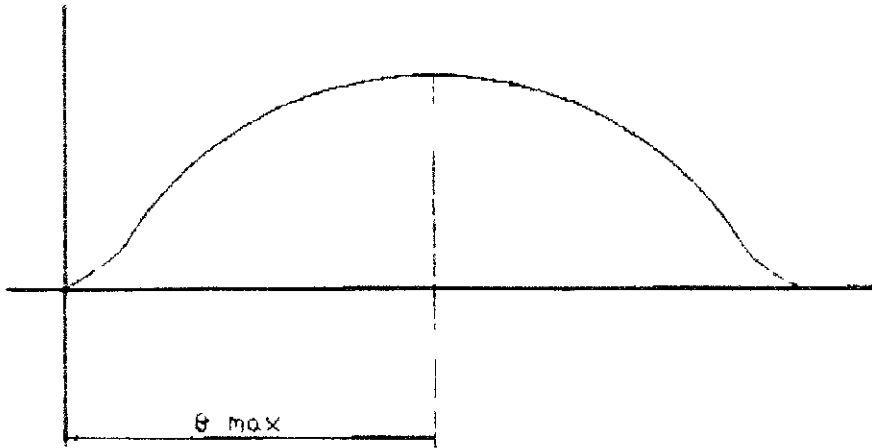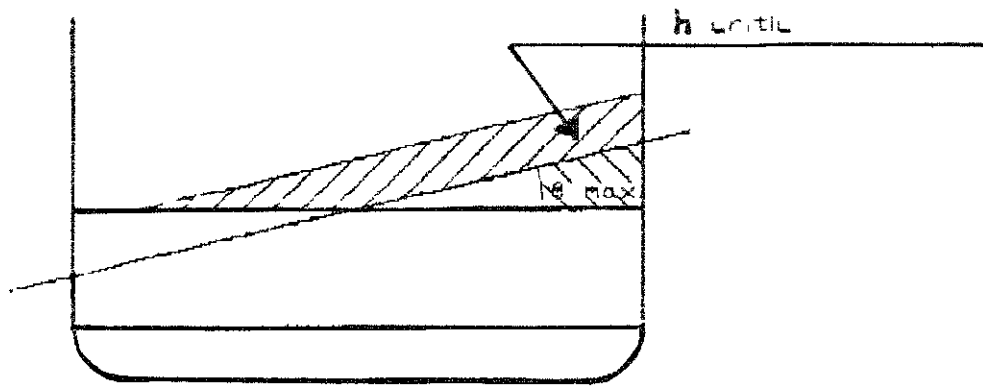
θ max. correspond to h critic
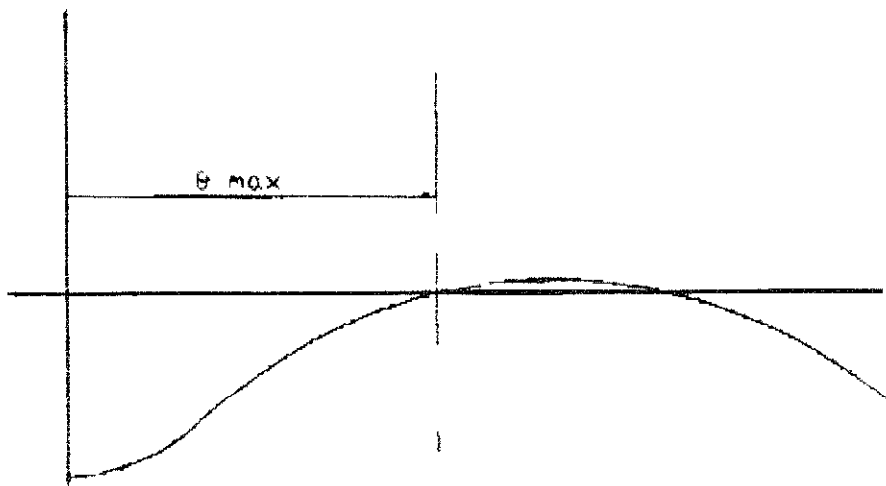
θ max. correspond to h critic

FIG. 4

RESULTS OF THE JOINT NORTH-WEST EUROPEAN RESEARCH AND DEVELOPMENT PROJECT ON SAFETY OF RO-RO VESSELS

Tor E. Svensen, Det Norske Veritas Pte Ltd, South-East Asia Region, Singapore

The results of the Joint North-West European Research and Development Project on Safety of Ro-Ro Vessels, can be summarised as follows.

•Despite the various "political" arguments about Ro-Ro safety, the research work carried out has demonstrated that Ro-Ro vessels with large open spaces are highly vulnerable to rapid capsize if flooding of the roro space occurs. Current SOLAS regulations are inadequate in that they do not address the real issues and do not encourage safer designs.

•The introduction of a probabilistic rule framework for all ship types should be encouraged Ro-Ro vessels will simply be a version of this framework where the risk of large scale flooding and corresponding probability of survival is included. The technical feasibility of these new rules have been demonstrated in the joint North-West European Research and Development Project.

The Joint North-West European Research programme brought about the following most important results.
•a better understanding of the physics relating to large scale flooding and the related dynamics of the ship.
•a realisation of the substantial differences in survivability between centre-casing vessels and side-casing vessels.
• a proposed new probabilistic stability framework that includes the special considerations of the Ro-Ro vessel design.
• a proven testing of the proposed new probabilistic stability framework showing clearly that it is possible to design new and much safer Ro-Ro vessels without incurring any substantial economic penalties.
• on the positive side, the safety assessment demonstrated that even with present rules, the risk to individual passengers is no higher than for other comparable means of transport. However, the risk of large scale accidents with 100+ casualties is higher than for other means of transport and close to the borderline of unacceptable ALARP region.

Finally I would like to comment that the joint North-West European Research programme demonstrated that it is possible for Marine Administrations, Shipowners Associations and Classification Societies from several countries to join forces on important safety issues and to produce results in a relatively short time. I was very encouraged by the high degree of positive co-operation in the project.

THE HAMBURG SHIP MODEL BASIN EXPERIENCE IN APPLICATION OF IMO TEST METHOD FOR INVESTIGATION OF DAMAGED RO-RO VESSELS

P. Blume, HSVA, Hamburg, Germany

To date HSVA has performed several investigations on damaged Ro-Ro vessels in accordance with the IMO test method. Most of them have been as a part of a current research project conducted in co-operation with Germanisher Lloyd and the TT-line. The first tests demonstrated the strong influence of the freeboard The beneficial effect of additional subdivision of the Ro-Ro deck decreases with increasing freeboard Limits between safe and unsafe conditions found by systematic KG-variation are in the same order of magnitude as the results of hydrodynamic calculations according to SOLAS 90 and show a similar trend. The test results will also be compared to theoretical calculations using simulation techniques. The first attempts show most promising results.

State-of-the-art Review Report

to the Panel Discussions on

CAPSIZING IN BEAM SEAS - CHAOS AND BIFURCATIONS

CAPSIZING IN BEAM SEAS - CHAOS AND BIFURCATIONS: HINTS FOR A PANEL DISCUSSION

Alberto FRANCESCUTTO

DINMA - University of Trieste, via A. Valerio, 10 - 34127 Trieste, Italy
e-mail: francesc@univ.trieste.it

ABSTRACT

This paper contains a short description of some recent issues, research results, open problems and practical needs, in the field of *nonlinear rolling dynamics in beam waves.*

INTRODUCTION

About twenty years ago the first papers [1-4] presenting analytical approaches to the dynamics of ship rolling in a regular beam sea, containing indications that the ship behaviour could be much more complicated than it was suspected before, appeared in the scientific literature. Of course, the origin of each branch of science is as a rule quite confuse, especially when it entails substantial transfer of knowledge from other branches of science. As a consequence, it is generally not possible to trace back with great precision to the first appearances of written evidence In the following, we will mainly refer to issues that will help *to warm-up* a panel discussion on the subject mentioned in the title of this paper more than writing a short history of developments in this subject.

Following these first approaches, a huge amount of papers developing further aspects of the complex dynamics of nonlinear rolling motion followed soon (see [5] and the references therein quoted). Chaos, symmetry breaking and their consequencies were discussed in detail as regards their application to *nonlinear rolling in a regular beam sea of a ship* with upright equilibrium or in biased conditions.

At the same time. the application of new analytical techniques allowed to obtain approximate solutions for the rolling motion in a stochastic beam sea (see [6] and the references therein quoted). The first papers on the possibility of bifurcations in a stochastic beam sea then appeared [7,8].

Many papers dealt with analytical/numerical approaches, most of them based on a very simplified mathematical modelling of the *system,* i.e. of the ship rolling in waves Due to the intrinsic difficulties of the analysis involved, the matching between Naval Architecture and System Dynamics was usually extremely poor, with issues concerning either:

- the extreme nonlinear dynamics of a ship described by a poor hydrodynamic modelling;

or
- the mild (i.e. the behaviour in the absence of bifurcations and chaos) nonlinear dynamics of a ship described by more adequate hydrodynamic modelling.

Recently, the existence of bifurcations and of the consequent jumps of amplitude in ship rolling was proved experimentally by means of experiments on scale models in a towing tank [9.10].

The new features connected with the complex dynamics of roll motion appear of great interest in the light of the new approaches to ship safety and in particular with the keywords *"designing, operating, training for safety"* [11,12]. This was the reason for the organization, in the frame of the 6th *International Conference on Stability of Ships and Ocean Vehicles,* of a Panel devoted to "Capsizing in Beam Seas - Chaos and Bifurcations". The Panel was organized by proposing to the discussers a series of papers [13-22], prepared by leading scientists,

containing written evidence on several aspects of the mentioned subjects

In the following of this paper, some open problems connected with the complex roll dynamics in beam waves are introduced in a synthetical way. To focus discussion, some *extreme* sentences are expressed These sentences are. of course. only partly true, or have to be taken with caution, or simply express an unsatisfactory state of the art. The first of these sentences and the most important for its theoretical and practical implications is.

"a properly designed, built and operated ship will never capsize in intact conditions in beam waves".

MATHEMATICAL MODELLING OF ROLLING MOTION IN BEAM WAVES

As explained in the introduction, the mathematical models adopted are usually too simplified and the coeffcients are often simply guessed on semiempirical basis

a) Large amplitude rolling

This is usually modelled as a single degree of freedom ordinary differential equation, i.e. through a concentrated parameters model. The effect of the other transversal motion, at least when the interaction with the sloshing of liquids on board is not taken into account, is generally considered to be negligible. The parameters of the differential equation are obtained from experiments on scale models or on full scale measurements by means of Parameter Identification Techniques [13,10, 23] The existence of the complex nonlinear dynamics is often tied to values of some relevant parameter lying in a narrow interval This aspect entails the importance of the evaluation of the *quality* [24] of the experimental data and particularly of the uncertainty of the estimated parameter values [25,26]

An alternative way consists in a fully hydrodynamic approach like the Numerical Wave Tank [14,15], at present two-dimensional but with great potentialities.

b) Extreme rolling and Capsizing

This also is usually modelled by means of single degrre of freedom mathematical models Due to the complexity of the analysis. the model is with concentrated parameters assumed to be constant indepently on the frequency and the amplitude attained by the roll motion

There is some experimental evidence that this approach is unsatisfactory inasmuch as it cannot explain the differences of roll amplitude in dependence on the sign of the bias for biased ships in beam waves Experiments [16,27] indicate that a ship exhibits an extreme saturation of the maximum roll amplitude versus excitation intensity that prevents the ship from capsizing (see introduction!) unless one or more of the following phenomena will happen·

- the ship has extremely poor roll damping (bare rounded hull);

- the metacentric height is very low;

- there is shift of cargo;

- the freeboard is low so that there is easy access and retention of water on deck

In the case of extreme rolling and capsizing the interaction between roll motion and vertical motions is important and has to be properly described. This coupling would be implicitly included in the fully hydrodynamic approach above mentioned, but its matching with a basin erosion analysis code is at present impracticable. The consideration of a multidegrre of freedom system obtained by coupling the ordinary differential equations of roll motion and of the vertical motions is possible The effect of coupling, regards at least the evaluation of the correct phase lag between roll and vertical position with respect to the wave and the evaluation of the righting moment that, as a consequence of heave and pitch. is something intermediate between the fixed trim and the free trim computation. We just remind that the correct evaluation of the righting arm, and of its polynomial

representation, is *crucial* in the dynamic analysis [17,18].

Here the problem of the values of the coefficients of the equations and of their uncertainty is even more important.

Finally, it has to be observed that, for an evaluation of the probability of capsizing, the effect of a rough sea should be considered [19].

COMPLEX DYNAMICS OF A SHIP IN BEAM WAVES

This is really very complicated. Even nowadays, in the presence of a quite diffuse knowledge of the basic mechanisms of nonlinear system dynamics, the appearance of bifurcations, chaos and symmetry breaking is regarded as strange and with suspect. In the past this peculiarity retarded the discovery of these phenomena in experimental tests (some mulfunction occurred!). This issue, in connection with the difficulty in reproducing these phenomena either in experimental, analytical or numerical approaches (due to the strong dependence on initial conditions and on the values of relevant parameters), can synthetically be expressed as:

"Nonlinear dynamics is the branch of science where you don't find what you don't know".

As stated in the Introduction, many papers appeared in the last ten years describing several aspects of ship roll dynamics in beam waves. It is worth noting that the research issues are (slowly) converging towards design indications for improved ship safety [5,21].

PRESENT REGULATIONS

Intact Ship
As discussed in previous papers [11,12], the existing "stability rules" don't take into account *explicitly* the above mentioned phenomena. The rules either:

a) under misleading name actually state boundedness requirements for rolling motion (Weather Criterion);

or

b) contain a set of requirements, expressed in terms of the stability curve and of the area under the stability curve (the so-called *dynamic stability*), that should guarantee a *reasonable* degree of safety to the ship.

Both approaches are given in terms of *mandatory prescriptions*. Nowadays, it is generally realized that some degree of inconsistency is hidden in both approaches, and particularly in the philosophy of the mandatory prescriptions. Reasoning in the more correct terms of *safety to be proved to the satisfaction of the Body appointed to the control*, means that the possible risk for the ship represented by the nonlinear rolling complex dynamics should be explicitly evaluated [20].

In this frame, the concept of "intact ship (rigid body)" should be disregarded. There are many important phenomena connected with roll motion dynamics which, without affecting the hull integrity, contribute to a degradation of the capability of the ship to resist the environmental action such as:

- shifting of cargo;

- water on deck;

- loss of operability.

These mechanism could onset a chain of events leading to the loss of the ship. Moreover, the actual stability conditions at sea are often partly unknown. Procedures as described in [13] could help to develop very helpfull "stability monitors".

Damaged Ship
There are many issues concerning the roll motion dynamics and the survival of the ship in non intact condition. In first place, a hull opening or flooding from doors or other usually safe openings can be the result of heavy cargo shift or loss of operability connected with excessive transversal motions or accelerations.

Furthermore, the motion of a damaged ship could entail a complex dynamics due to the roll/sloshing coupling [22,23].

CONCLUSIONS

Conclusions are left to the issues of the Panel, but some interim statement can be drawn. In particular, we agree completely with the conclusions of Vassalos et al [16] calling for additional improvements in this field:

"... work in this area has not advanced to the point where material of substance could be offered to the practising Naval Architect to enhance or ensure ship safety. Some innovative concepts, however, appear to hold promise for achieving further advances in the field of ship stability ...".

ACKNOWLEDGEMENTS

REFERENCES

1. Wellicome, J. F., "An Analytical Study of the Mechanism of Capsizing", Proc Int. Conf. STAB'75.

2. Cardo, A., Ceschia, M., Francescutto, A., Nabergoj, R., "Sugli effetti dello smorzamento nel moto di rollio di una nave soggetta ad azione sbandante periodica", Tecnica Italiana, Vol. 43, 1978, pp. 111-121.

3. Cardo, A., Ceschia, M., Francescutto, A., Nabergoj, R., "Effects of the Angle-dependent Damping on the Rolling Motion of Ships in Regular Beam Seas", Int. Shipb. Progress, Vol. 27, 1980, pp. 135-138.

4. Cardo, A., Francescutto, A., Nabergoj, R., "Ultraharmonics and Subharmonics in the Rolling Motion of a Ship: Steady-state Solution", Int. Shipb. Progress, Vol 28. 1981, pp. 234-251

5. Thompson, J. M. T. Designing Against Capsize in Beam Seas: Recent Advances and New Insights", Appl. Mech Rev., Vol. 50, 1997, pp. 307-325.

6 Roberts, J. B., Spanos, P. D., "Random Vibrations and Statistical Linearization", Wiley, Chichester, 1990.

7. Francescutto, A., "On the Nonlinear Motions of Ships and Structures in Narrow Band Sea", Proc. IUTAM Symp. on Dynamics of Marine Vehicles and Structures in Waves. London. 1990, Elsevier Publishing, pp. 291-304.

8. Francescutto, A., "Nonlinear Ship Rolling in the Presence of Narrow Band Excitation", In J.M. Falzarano and F Papoulis (eds.), Nonlinear Dynamics of Marine Vehicles, ASME, New Jersey, 1993, pp. 93-102.

9. Francescutto, A., Contento, G., Penna, R., "Experimental Evidence of Strongly Nonlinear Effects in the Rolling Motion of a Destroyer in Beam Sea", Proc Int. Conf. STAB'94.

10. Francescutto, A., Contento, G., "Bifurcations in Ship Rolling: Experimental Results and Parameter Identification Technique". To appear.

11. Francescutto, A., "Is it Really Impossible to Design Safe Ships?", Trans. RINA, Vol. 135, 1993, pp. 163-173.

12. Francescutto, A., "Towards a Reliability Based Approach to the Hydrodynamic Aspects of Seagoing Vessels Safety", Proc. OMAE'92, Calgary, 1992, Vol. 2, pp. 169-173.

13. Debonos, A. A, "Stochastic Identification of Rolling Motion Parameters: Towards an On-line Assessment of Ship Stability", Proc. this Conference.

14. Contento, G., "On the Direct Computation of Large Amplitude Motions of Floating Bodies

in Regular and Irregular Waves: The Numerical Wave Tank Approach. An Application to Subharmonic Oscillations in steep Waves", Proc this Conference.

15 Tanizawa, K . Naito. S , "An Application of Fully Nonlinear Numerical Wave Tank to the Study on Parametric and Chaotic Roll Motions". Proc. this Conference

16 Vassalos. D., Spyrou, K , Umeda. N . "Testing the Transient Capsize Diagram Concept". Proc. this Conference.

17. Scolan, Y. M., "Some Aspects of the Ship Rolling Motion Associated to the High Degree Polynomial Restoring Moment", Proc this Conference.

18. Zamora, R., Sánchez. J. M., Rojas, L. P., "Bifurcation Set of Rolling Equations in Beam Seas: Two Different Behaviours". Proc this Conference.

19. Senjanovic, I , Cipric, G., Parunov, J., "Probability of Ship Survival in Rough Sea". Proc. this Conference.

20 Spyrou, K. J , Cotton, B , Thompson, J. M. T., "Developing an Interface Between the Nonlinear Dynamics of Ship Rolling in Beam Seas and Ship Design". Proc. this Conference

21 Belenky, V. I., Umeda, N . "Contemporary

Remarks on Classic Weather Criteria". Proc this Conference

22. Nechaev. Yu I . Deglyarev. A. B , Bouchanovsky. A. V . "Chaotic Dynamics of Damaged Ship in Waves", Proc. this Conference.

23 Francescutto, A . Contento. G . "An Investigation on the Applicability of Simplified Mathematical Models to the Roll-Sloshing Problems", Proc. ISOPE'97, Honolulu, 1997. Vol 3. pp. 507-514

24 Masia, M . Penna. R., "Quality of Experimental Data in Hydrodynamic Research", Proc. Int Symp. on "Advanced Mathematical Tools in Metrology", Berlin, 1996.

25. Spouge. J. R , "A Technique for Estimating the Accuracy of Experimental Roll Damping Measurements". Int. Shipb. Progr , Vol. 39, 1992, pp. 247-265.

26. Penna. R., Contento, G Francescutto, A.. "Uncertainty Analysis Applied to the Parameter Estimation in Nonlinear Rolling", Proc this Conference.

27. Contento, G., Francescutto, A . Sebastiani, L., "Experimental Results of Nonlinear Rolling in Biased Conditions in Beam Waves". Proc This Conference.

Written contributions to the panel discussions on

CAPSIZING IN BEAM SEAS -
CHAOS AND BIFURCATIONS

CHAOTIC DYNAMICS OF DAMAGED SHIP IN WAVES

Yu.I.Nechaev[†], A.B.Degtyarev[††], A.V.Boukhanovsky[‡]

[†] — Professor, Dr.Sc., [††] — Associate Professor, Ph.D., [‡] — Research Fellow, Ph.D.
Marine Technical University, 3 Lotsmanskaya str., 190008 St.Petersburg, Russia
Institute of High-Performance Computing and Data Bases,
PO Box 71, 194291 St.Petersburg, Russia
deg@fn.csa.ru, nonlin@fn.csa.ru

Quality investigation of nonlinear deterministic model that describes damaged ship rolling under the regular excitations in different ship movements regimes indicates complicated evolution of phase trajectories that break phase space symmetry. Such violation results in attractor set appearance. The most complicated situation is damaged ship with negative initial metacentric height. Phase portrait at different stages of development reminds of self-organising systems behaviour. Self-organising process consists of system transition from one to other stable state. In this case phase trajectory is "drawn in" one or other attractor. "Limited cycle" attractor type appears in some system states, in other states equilibrium depends on time. Different motion types can result in chaotic oscillations and strange attractor appearance. The results of chaotic systems investigation allow to separate different scenarios of strange attractors organisation. Infinite duplication of limited cycle (strange attractor corresponds to limited cycle with infinite period) could be observed when all parameters at the system input are deterministic. Other quality peculiarities in nonlinear deterministic systems behaviour are noticed when merging of two or more equilibrium states (one part of them is stable and the other part is unstable) is occurs at some level of external excitations and system parameters. This phenomenon is connected with quality variations in system behaviour when it jumps from one motion regime to other. Jump (catastrophe) can have more complicated character in dependence of system parameters. In some cases limited cycle can disappear and the system can transit either in stable limited cycle or in more complicated attractor.

Fragments of phase trajectory evolution of investigated dynamic system with different configurations of multisign nonlinear function that describes restoring moment of damaged ship are shown in fig.1. Therefrom it follows that ship's behaviour is characterised by phase trajectory that wanders in different directions and draws complicated untwisted cycles at the large time interval. When we consider rolling in random sea there are two important problems

1. Calculation of probability of danger ship inclinations;

2. Classification of situation on the basis of irregular oscillations (inverse problem).

Nonlinear ship motion in real sea cannot be described in terms of classical theory of stationary processes. So the problem

becomes more complicated. The results of numerical modelling show that oscillations of damaged ship with negative initial metacentric height can have not settled attracting set, and trajectory randomly transits from focus to focus depending on external excitation intensity. Besides, oscillation regimes without stability solution set may arise even for nondamaged ship with nonlinear stability diagram. This phenomenon was named "practical non-ergodicy" [1]. Both these phenomena are shown in modulating of initial oscillation process $\vartheta(t)$ near current equilibrium position by processes of more global variance diapason.

Not only transit from focus to focus but also essential trajectory drift connected with system parameters variance during flooding characterise damaged ship. In this case nonstationarity is evolutionary.

Thus the simplest probability model of damaged ship oscillation in real sea could be presented as follows

$$\Theta(t) = \mu(\varepsilon t) + \nu(\varepsilon t)\ \vartheta(\varepsilon t, t) \qquad (1)$$

where

$\mu(x)$ is pulse random process of system transient between focuses.

$\nu(x)$ is pulse process of system transient between attraction sets in bifurcation zone (i.e. "practical non-ergodicy" imitation)

$$\vartheta(\varepsilon t, t) = \int_{-\infty}^{+\infty} A_{\varepsilon t}(\omega) \exp[i\omega t]\, d[q_\eta(\omega)] \quad \text{is}$$

parametric nonstationary process considering ship oscillations and trajectory drift during flooding.

ε is small parameter

It is clear that (1) transits into St.Denis and Pierson idea for undamaged ship with linear stability diagram.

In fig.2 general ship oscillation process and its decomposition on separate components are shown.

Since rolling process $\Theta(t)$ is correlated in time and essentially nonlinear (non gauss), probabilistic modelling is the most accurate method for problem solving [2]. In particular modulating pulse processes $\mu(x)$ and $\nu(x)$ have very wide spectrum and are well approximated by Markov chains. Evolutionary nonstationary process $\vartheta(\varepsilon t, t)$ is well approximated by autoregressive process with parametrically nonstationary coefficients. Parameters of the model could be determined with the help of different methods. However, such approach is essentially limited.

Estimation results show that in general statistical assessments both point and interval considerably differ from the same classical assessments. Model assessment of ship motion distribution density with stopped flooding process is shown in fig.3

On the other hand probabilistic model has to be used for multidimentional statistical analysis of random processes realisation (factor and discriminate analysis above all). Such approach permits to typify characteristic data of accident situations and to create ensemble of samples for real events discrimination. In particular, analysis of random process distribution histograms allowed to classify 4 basic accident situations but phase trajectories on halfperiods allowed classify only 2 situations (sign of initial metacentric height).

REFERENCES

1. V.Belenky, A.Degtyarev, A.Boukhanovsky On probabilistic Qualities of Severe Rolling. //*Proc. of* Inter.symp. Ship safety in seaway., Kaliningrad, 1995, v.1, paper 7
2. V.Rozhkov Methods of probabilistic analisis of oceanological processes. — L.: Hydromet. ed., 1973 (in Russian)
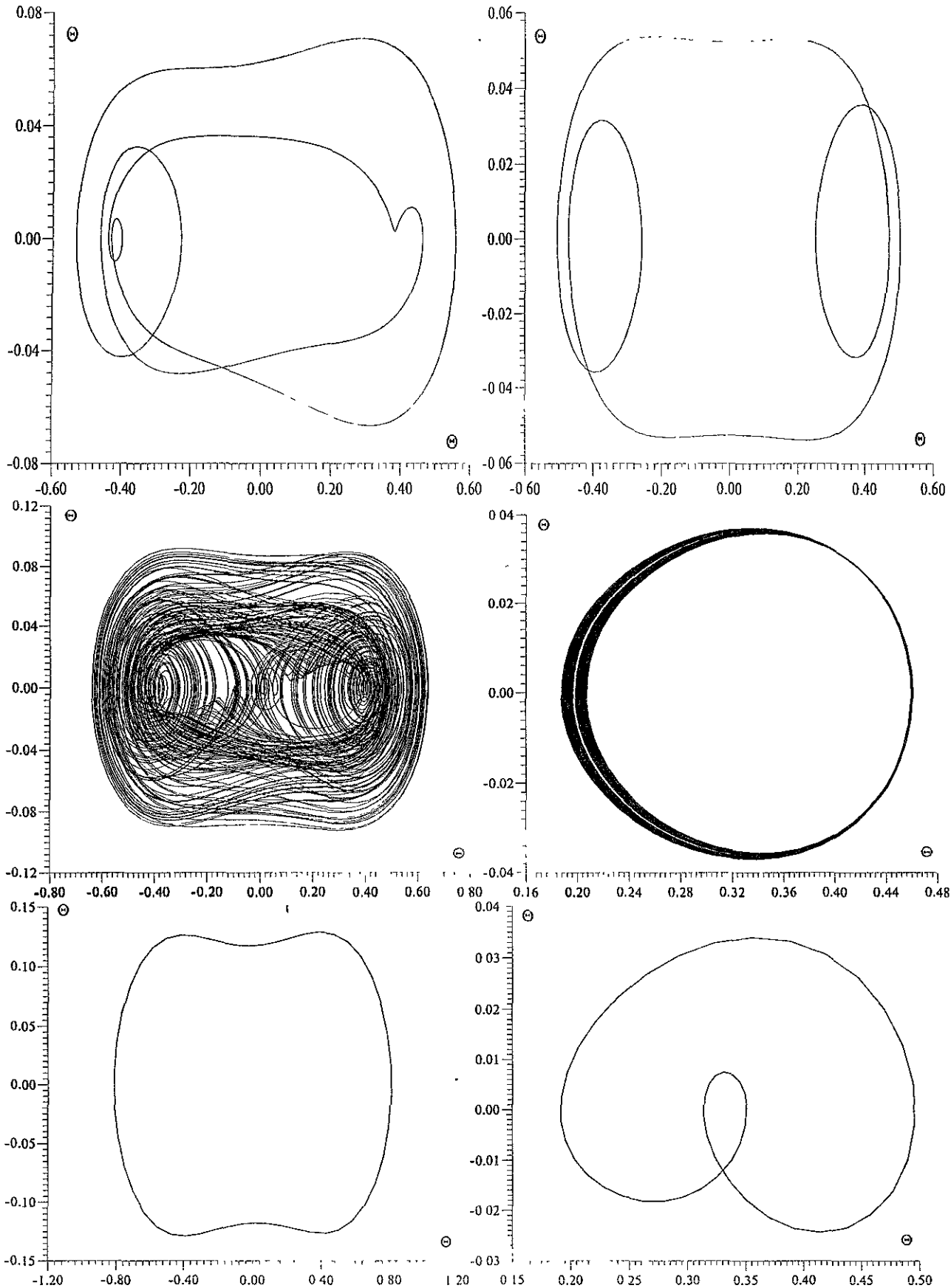
Fig.1 Phase trajectory evolution of ship with different nonlinear stability diagrams (with negative initial metacentric height) and initial conditions.
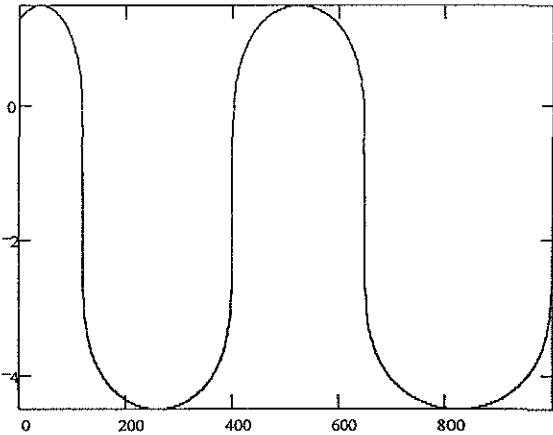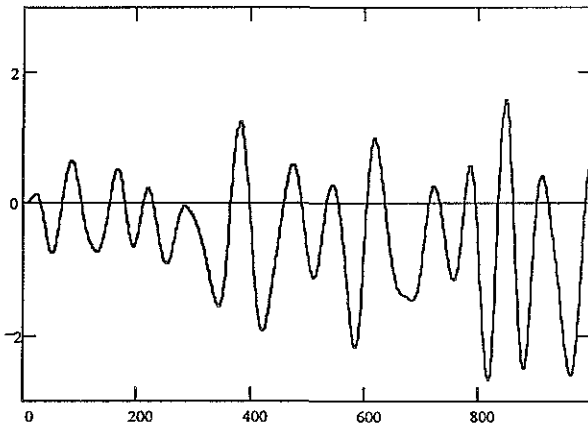
a)   b)
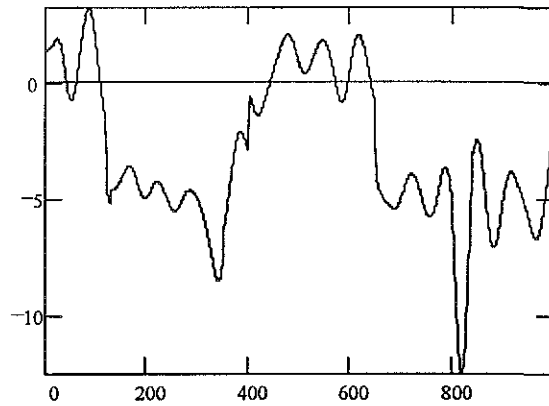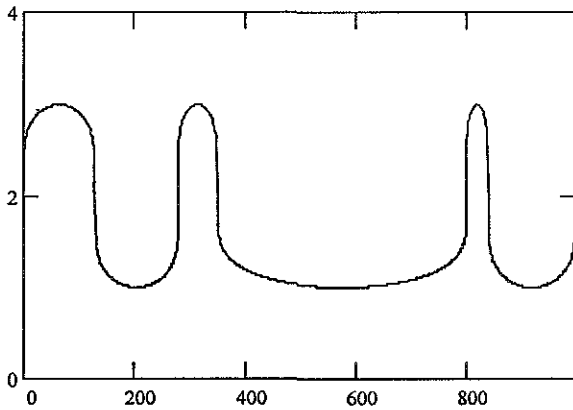
c)   d)

Fig.2 Ship rolling (a) and its decomposition (b,c - pulse processes, d - parametrically nonstationary process)
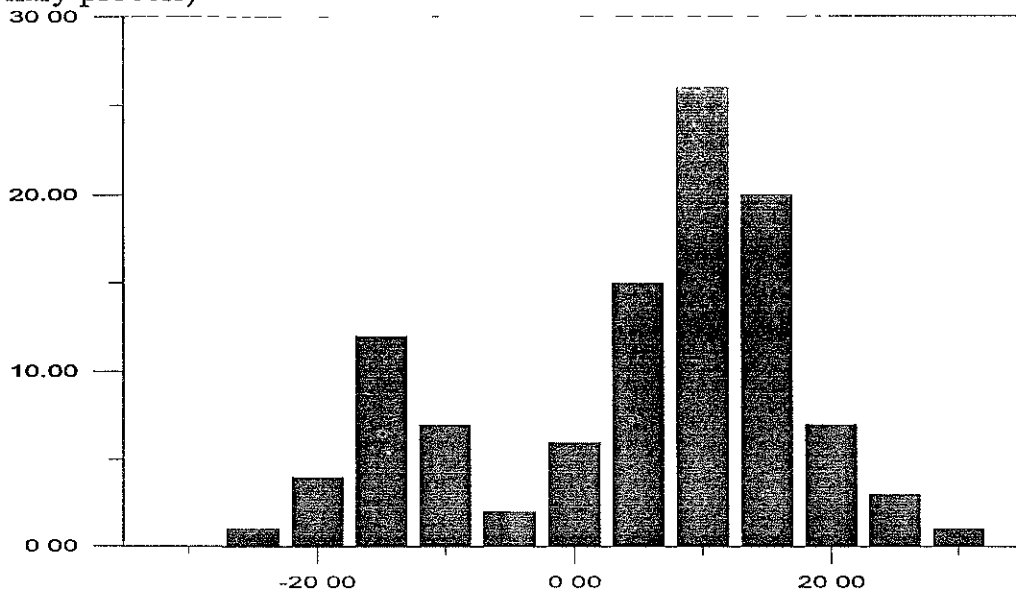

Fig.3 Model assessment of ship motion distribution density

AN APPLICATION OF FULLY NONLINEAR NUMERICAL WAVE TANK TO THE STUDY ON PARAMETRIC AND CHAOTIC ROLL MOTIONS

Katsuji Tanizawa [†] and *Shigeru Naito* [‡]

† Ship Research Institute, Tokyo, Japan

‡ Osaka University, Osaka, Japan

1 INTRODUCTION

Responses of floating bodies such as ships or ocean structures to incident waves are one of the main concern in ocean engineering. The responses are usually treated as harmonic assuming small amplitude wave and body motions. Under the assumption, the frequency responses have been investigated by linear or perturbation theories. But, the body motions are not always harmonic in real ocean. When amplitude of wave and body motions are large in rough seas, nonlinear effects become dominant. Capsizing in the plunging breaker is the extreme example. Even if the amplitudes are small, nonlinearity due to body shape, mooring force, free water on the deck etc. affect to the body motions and parametric or chaotic motions may be resulted.

For the analysis of such a nonlinear roll motions, time domain fully nonlinear simulation can be a powerful tool. Time domain fully nonlinear simulation methods are studied by Vinje [5], Cointe [7], Tanizawa [8, 13], Van Daalen [9], Sen [10], Cao [11], Francescutto [14] and others in the past decade and fully nonlinear numerical wave tanks have been developed. In this study, applicability of the fully nonlinear numerical wave tank [16] to parametric and chaotic roll motions with internal free water is examined.

In our previous study [18], we applied the numerical wave tank to the analysis of parametric roll motions of bow section body and showed the simulated harmonic and parametric motions, critical wave height of the parametric excitation, etc. are well agree with the experimental results. In this study, we apply the same numerical wave tank to the analysis of parametric and chaotic roll motions with internal free water. This study is still under going.

2 FULLY NONLINEAR NUMERICAL WAVE TANK

·2.1 Mathematical formulation

Motions of a floating body inside a two-dimensional wave basin is considered. As Fig.1 shows, fluid domain Ω_1 is bounded by free-surfaces S_{f1} , a piston wave maker S_p , bottom and rigid wall S_b and a floating body S_{s1} , and fluid domain Ω_2 is bounded by free-surface S_{f2} and internal surface of floating body S_{s2} . Here, gravitational acceleration g , density of outside fluid ρ_1 and width of floating body B are chosen as units to nondimensionalize the problem. An space-fixed Cartesian coordinate system $o - xz$ is used with x coincident with the calm free-surface and z positive upward. The fluid is assumed to be homogeneous, incompressible, inviscid and its motion irrotational. The fluid motion can be described by a velocity potential ϕ and its time derivative ϕ_t . In the fluid domain Ω_κ, $\kappa = 1, 2$, ϕ_κ and $\phi_{\kappa t}$ satisfies Laplace's equation

$$\nabla^2 \phi_\kappa = \nabla^2 \phi_{\kappa t} = 0 . \tag{1}$$

Green's second identity can be applied on both ϕ_κ and $\phi_{\kappa t}$

$$c(\mathcal{Q}) \left\{ \begin{array}{c} \phi_\kappa(\mathcal{Q}) \\ \phi_{\kappa t}(\mathcal{Q}) \end{array} \right\} = \int_{S_\kappa} \left\{ \begin{array}{c} \phi_\kappa(\mathcal{P}) \\ \phi_{\kappa t}(\mathcal{P}) \end{array} \right\} \frac{\partial}{\partial n} \ln r(\mathcal{P},\mathcal{Q})$$
$$- \ln r(\mathcal{P},\mathcal{Q}) \left\{ \begin{array}{c} \dfrac{\partial \phi_\kappa(\mathcal{P})}{\partial n} \\ \dfrac{\partial \phi_{\kappa t}(\mathcal{P})}{\partial n} \end{array} \right\} dS , \tag{2}$$

where $\mathcal{P}, \mathcal{Q}$ are points on the boundary, n is outward normal direction of the boundary, $r(\mathcal{P},\mathcal{Q})$ is distance between $\mathcal{P}$ and $\mathcal{Q}$, $c(\mathcal{Q})$ represents the angle subtended at $\mathcal{Q}$ by boundaries.

On the free-surface, kinematic boundary condition and dynamic boundary condition for zero atmospheric pressure are applied as

$$\frac{D\phi_\kappa}{Dt} = -z + \frac{1}{2}(\nabla \phi_\kappa)^2 \tag{3}$$

$$\frac{Dx}{Dt} = \nabla \phi_\kappa , \tag{4}$$

where $x = (x,z)$. On the body surface, impermeability condition with respect to ϕ_κ is expressed as

$$\frac{\partial \phi_\kappa}{\partial n} = V_n , \tag{5}$$

where V_n denotes the normal velocity of the body surface S_{s1} and S_{s2} . Denoting translating and angular velocities of the body as v_0 and ω respectively, V_n is written as

$$V_n = n \cdot (v_0 + \omega \times r) . \tag{6}$$

Impermeability condition on the body with respect to $\phi_{\kappa t}$ [13] can be written as

$$\frac{\partial \phi_{\kappa t}}{\partial n} = -k_n \left(\nabla \phi_\kappa - v_o - \omega \times r \right)^2 + n \cdot (\dot{v}_o + \dot{\omega} \times r)$$
$$+ n \cdot \omega \times (\omega \times r) + n \cdot 2\omega \times (\nabla \phi_\kappa - v_o - \omega \times r)$$
$$- \frac{\partial}{\partial n} \left(\frac{1}{2}(\nabla \phi_\kappa)^2 \right) , \tag{7}$$

where k_n is curvature of body, $\dot{v}_o, \dot{\omega}$ are translating and angular accelerations of the body respectively.

On the floating body surface, $\dot{v}_o, \dot{\omega}$ can not be specified explicitly and implicit boundary condition should be applied [15]. Denoting the inertia tensor of the floating body as $\mathcal{M}$ and generalized normal vector of body surface as $N = (n, n \times r)$, the implicit boundary condition is written as

$$\frac{\partial \phi_{\kappa t}}{\partial n} = N\mathcal{M}^{-1} \left\{ \sum_{\kappa=1}^{2} \gamma_\kappa \int_{S_{s\kappa}} -\phi_{\kappa t} N ds \right\}$$
$$+ N\mathcal{M}^{-1} \left\{ \sum_{\kappa=1}^{2} \gamma_\kappa \int_{S_{s\kappa}} \left(-z - \frac{1}{2}(\nabla \phi_\kappa)^2 \right) N ds + F_g \right\}$$
$$+ q_\kappa - \frac{\partial}{\partial n} \left(\frac{1}{2}(\nabla \phi_\kappa)^2 \right) , \tag{8}$$

where $\gamma_\kappa = \rho_\kappa/\rho_1$ is specific gravity of fulid with respect to external water, F_g is sum of gravity, mooring force and other external forces acts to the body and q_κ is the term which cab be explicitly evaluated from the solution of velocity field as

$$q_\kappa = -k_n \left(\nabla \phi_\kappa - v_o - \omega \times r \right)^2$$
$$+ n \cdot \omega \times (\omega \times r) + n \cdot 2\omega \times (\nabla \phi_\kappa - v_o - \omega \times r) . \tag{9}$$

With these boundary conditions and Green's second identity with respect to ϕ_κ and $\phi_{\kappa t}$, both velocity and acceleration fields can be solved numerically by BEM. The solutions are integrated with respect to time by 4th order Runge-Kutta method, then fluid and the body motions are simulated in time domain. The free-surface is traced by MEL [4].

2.2 Artificial damping zone

Following a preceding work of Cointe et al. [7], damping terms are added to dynamic and kinematic free-surface boundary conditions to give artificial damping effect to free-surface. The free-surface boundary conditions inside a damping zone are given as

$$\frac{D\phi}{Dt} = -z + \frac{1}{2}(\nabla\phi)^2 - \nu(x_e)(\phi - \phi_e) \tag{10}$$

$$\frac{D\boldsymbol{x}}{dt} = \nabla\phi - \nu(x_e)(\boldsymbol{x} - \boldsymbol{x}_e) . \tag{11}$$

where $\nu(x_e)$ is the damping coefficient

$$\nu(x) = \begin{cases} \alpha\omega(\dfrac{x - x_0}{\lambda})^2, & for \quad x_0 \le x \le x_1 = x_0 + \beta\lambda \\ 0, & for \quad x < x_0 \quad or \quad x > x_1 \end{cases} . \tag{12}$$

In the definition of $\nu(x)$, ω and λ are angular frequency and wave length of the incident wave respectively. The performance of this damping zone is controlled by two nondimensional parameter α and β. α is used to control the strength of damping and β is used to control the length of damping zone. $\phi_e, \boldsymbol{x}_e$ are reference values. This damping zone damps down differences $\phi - \phi_e$ and $\boldsymbol{x} - \boldsymbol{x}_e$. When the damping zone is applied in front of a rigid wall and works as a simple absorber, the reference values are set to $\phi_e = 0, \boldsymbol{x}_e = (x_e, 0)$. And when the damping zone is applied in front of a wave maker and works as an absorbing wave maker, the reference values are set to the solution of the wave generated by the wave maker. This solution can be computed by numerical simulation of the wave without bodies in the tank. For practical purpose, linear analytical solution can be a good substitution. Linear propagating wave generated by a piston wave maker is described as

$$\phi(x, z, t) = \frac{4s \tanh kh \sinh kh}{\omega(2kh + \sinh 2kh)} \cosh k(z + h) \cos(kx - \omega t) \tag{13}$$

$$\eta(x, t) = -\frac{\partial\phi}{\partial t}\bigg|_{z=0} = \frac{4s \sinh^2 kh}{2kh + \sinh 2kh} \sin(kx - \omega t) \tag{14}$$

where s is stroke of the wave maker and k is wave number of the generated wave. Wave reflection coefficient of this damping zone is less than 2%, when the tuning parameter is appropriately set to $\alpha = \beta = 1$ for a regular wave. [7, 16].

3 SIMULATION OF PARAMETRIC AND CHAOTIC ROLL MOTIONS

3.1 Floating body and the conditions of the simulation

As a model of flooded ship heeling in calm water, a triangular floating body is considered. Fig.2 shows the shape of the body, downward triangle with rounded vertex. The angle of the vertex is $\pi/2$. Inside of the body, free water exists. The density of both internal and external water is $1000 kg/m^3$. The weight of internal water is 25 kg that is half of the body weight. The natural rolling period of this body with internal water is about $1.7s$ and natural sloshing period of the lowest mode is about $0.81s$. Further detail of the principal dimensions are presented in Table 1.

As a trial, a regular wave, which length and height are $1.127m$ and $3cm$ respectively, is chosen for the following simulation. The period of this regular wave is $0.85s$. Since this period is half of natural roll period, parametric roll motion is easy to be excited. In addition, this period is near to the natural sloshing period of the internal water and the large sloshing motion can be expected.

3.2 Simulated body motions

In Fig.3, simulated motions are plotted. Two different body motions can be observed in this figure. In the first stage, harmonic motions are dominant. As time passed, in the second stage, the amplitude of parametric motion is getting larger gradually. Finally, in the third stage, the parametric motions become dominant and are converging to the limit cycle. In this simulation, these three stages are simulated seamlessly. In the parametric stage, the amplitude of sway and roll are much larger than that of in the harmonic stage and double period motions can be observed clearly. To the contrary, the amplitude of heave in parametric stage is smaller than that of harmonic stage. The energy of heave motion is considered to be transferred to the sway motion and mainly to roll motion.

Other two interesting phenomena are observed in the simulated motions. One is the difference of wave drift force between harmonic and parametric stages. In the plot of sway motion, the mean drift distance in parametric stage looks a little larger than that of in harmonic stage. Another is the difference of mean heave level between harmonic and parametric stages. In the harmonic stage, the mean level is identical to zero. But in parametric stage, the mean level is nearly 20% of wave amplitude. This suggests the existence of lifting force in parametric stage. The mechanism of these phenomena is considered to be highly nonlinear and still not clearly understood.

Fig.4 shows the phase plot of simulated motions. Limit cycle of harmonic and parametric stages are clearly observed and the transition stage between them also can be seen clearly. The aspect ratio of these phase plots are set so that the harmonic motions are plotted as a circle. Phase plot of sway motion looks chaotic but this is due to the slow drift motion and not due to chaotic motion.

To visualize the motion of water, simulated instantaneous profiles of the free-surface inside and outside of the body at $t/T_w = 84.75, 85.50, \ldots, 86.50$ are plotted in Fig.5, where T_w is the period of the incident wave. The wave motion outside of the body is not large, but the wave motion inside is quite large. The inside wave generated by internal wall of the body travels from one side and the wash up to the other side. In this simulation, this internal wave motion is also periodically stable and not chaotic.

To have a limit cycle in parametric oscillation, damping force proportional to $\dot{\theta}^2$ or higher is indispensable. But, in general, damping due to wave radiation is so weak that the parametric roll motions are diverging. In the above simulation, the internal wave motion interacts to the body and external wave motion and, as a results, acts as higher order damping to have the limit cycle. This is another interesting result for future study.

4 CONCLUSION

In this study, applicability of the fully nonlinear numerical wave tank to parametric and chaotic roll motions with internal free water is examined. This topic is still under investigation and following items are tentative conclusion.

1. In a small amplitude regular wave, a harmonic and parametric motion of triangular body with internal water can be simulated seamlessly.
2. In the parametric motions, shift of mean drift force and center of heave motion from the harmonic motions are simulated. The mechanism of these shifts are considered to be highly nonlinear.
3. The limit cycle of parametric motions are obtained. The motion of internal water acts important roll to have this limit cycle.
4. The simulated parametric motions are periodically stable and no sign of chaotic motions are obtained.

We are now trying to catch chaotic roll motions using the numerical wave tank, but have not succeeded yet. Some good indexes to find the condition of chaotic motions are required to avoid trial and error with various wave length, wave height, amount of internal water, Meta-center height and etc.

288

References

[1] Hsu,C.S. (1977), "On nonlinear parametric excitation problems", *Advances in Applied Mechanics, Vol.17*, pp245-298

[2] Skomedal,N.G. (1982), "Parametric excitation of roll motion and its influence on stability", *Proc. of 2nd Int. Conf. on Stability of Ships and Ocean Vihecles, Tokyo*, pp113-125

[3] Kyozuka,Y. (1977), "A study on the unstable roll motions of moored floating bodies in regular waves.", *Master thesis, Osaka Univ.*, pp1-82

[4] Longuet-Higgins,M.S. and Cokelet,E. (1976), "The deformation of steep surface waves on water ", *Proc. Roy. Soc. ser.A350*, pp1-26

[5] Vinje, T. and Brevig, P. (1981), "Nonlinear Ship Motions", *Proc. of the 3rd. Int. Conf. on Num. Ship Hydro.*, ppIV3-1-IV3-10

[6] Sen, D., Pawlowski, J.S., Lever, J. and Hinchey, M.J., (1989), "Two-dimensional numerical modeling of large motions of floating bodies in waves", *Proc. 5th Int. Conf. Num. Ship Hydro., part1*, pp257-277

[7] Cointe,R.,Geyer,P.,King,B.,Molin,B. and Tramoni,M. (1990), "Nonlinear and linear motions of a rectangular barge in perfect fluid", *Proc. of the 18th Symp. on Naval Hydro., AnnArbor, Michigan*, pp85-98

[8] Tanizawa, K. (1990), "A numerical method for nonlinear simulation of 2-D body motions in waves by means of B.E.M.", *Journal of SNAJ*, Vol.168, pp223-228

[9] Van Daalen, E.F.G. (1993), "Numerical and Theoretical Studies of Water Waves and Floating Bodies", *Ph.D. thesis, University of Twente, The Netherlands*

[10] Sen,D. (1993), "Numerical simulation of motions of two-dimensional floating bodies", *Journal of Ship Research, vol.37*, pp307-330

[11] Cao, Y., Beck, R. and Schultz, W.W. (1994), "Nonlinear motions of floating bodies in incident waves", *9th Workshop on Water Waves and Floating Bodies, Kuju,Oita*, pp33-37

[12] Tanizawa, K. (1995a) "A Nonlinear Simulation Method of 3-D body Motions in Waves", *10th Workshop on Water Waves and Floating Bodies, Oxford*, pp235-239

[13] Tanizawa, K. (1995b) "A Nonlinear Simulation Method of 3-D Body Motions in Waves", *Journal of SNAJ*, Vol.178, pp179-191

[14] Francescutto, A., Contento,G. and Armenio,V. (1996) " A fully hydrodynamic approach to the motion in waves of ships with free surface liquids on board." *11th Workshop on Water Waves and Floating Bodies, Humburg*

[15] Tanizawa, K. (1996a) "A Nonlinear Simulation Method of 3-D Body Motions in Waves, Extended Formulation for Multiple Fluid Domains", *11th Workshop on Water Waves and Floating Bodies, Humburg*

[16] Tanizawa,K. (1996.b) "Long time fully nonlinear simulation of floating body motions with artificial damping zone", *Journal of SNAJ*, Vol.180, pp311-319

[17] Murashige,S. and Aihara,K. (1997) "Chaotic Motion of a Flooded Ship in Waves", *Technical reports of Math. Eng. Sec., The univ. of Tokyo*, METR97-01

[18] Tanizawa, K. and Naito, S. (1997) " A study on parametric roll motions by fully nonlinear numerical wave tank", *Proc. of 11th ISOPE Conf., Honolulu, Hawaii*, vol.3, pp69-75

37

Table 1: Principal dimensions

Floating Body			
Breadth at W.L.	$B_{W.L.}$	0.81	m
Draft	d	0.3636	m
Weight	W	50.0	kg
Center of inertia	KG	0.3	m
Radius of inertia	R_I	0.25	m
Spring constant of mooring	k	51.07	N
Internal Free Water			
Density	ρ_2	1000	kg/m^3
Weight	w	25.0	kg
Natural Period of Sloshing	T_s	0.815	s
Hydro-static Property			
Meta-center height	GM	0.074	m
Natural period of heave	T_h	0.737	s
Natural period of roll	T_r	1.846	s
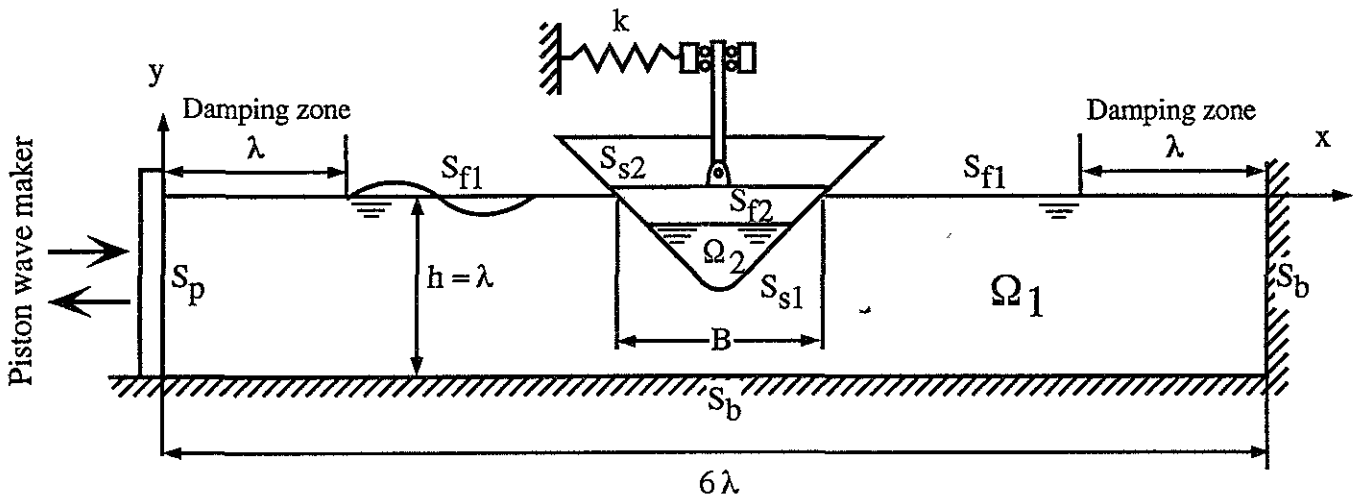
Figure 1: Numerical Wave Tank
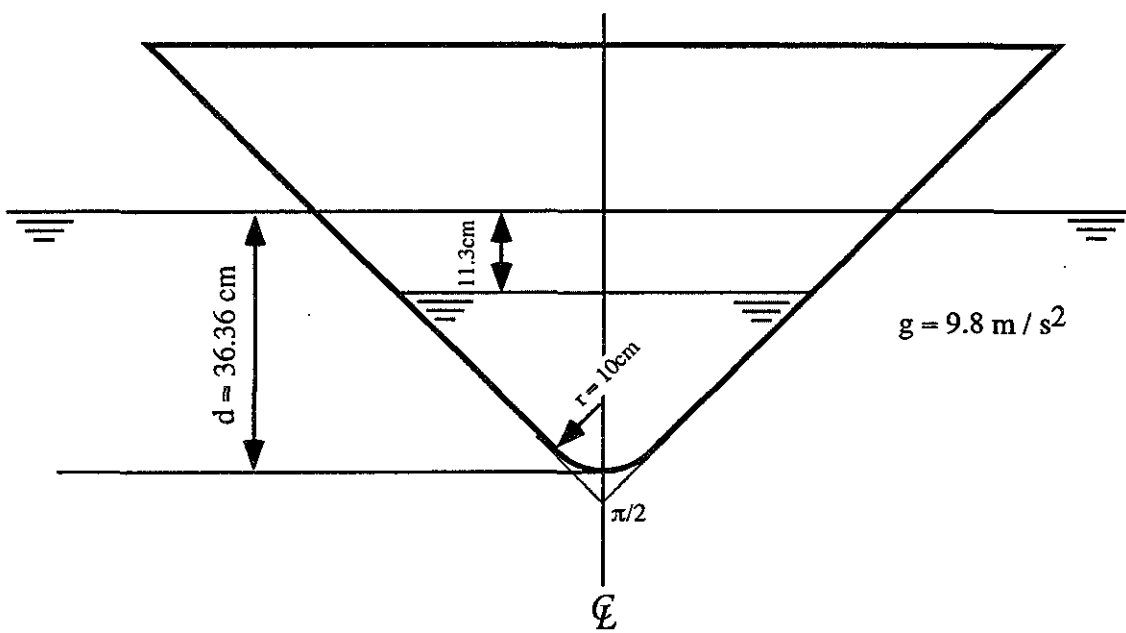
Figure 2: Shape of Floating Body
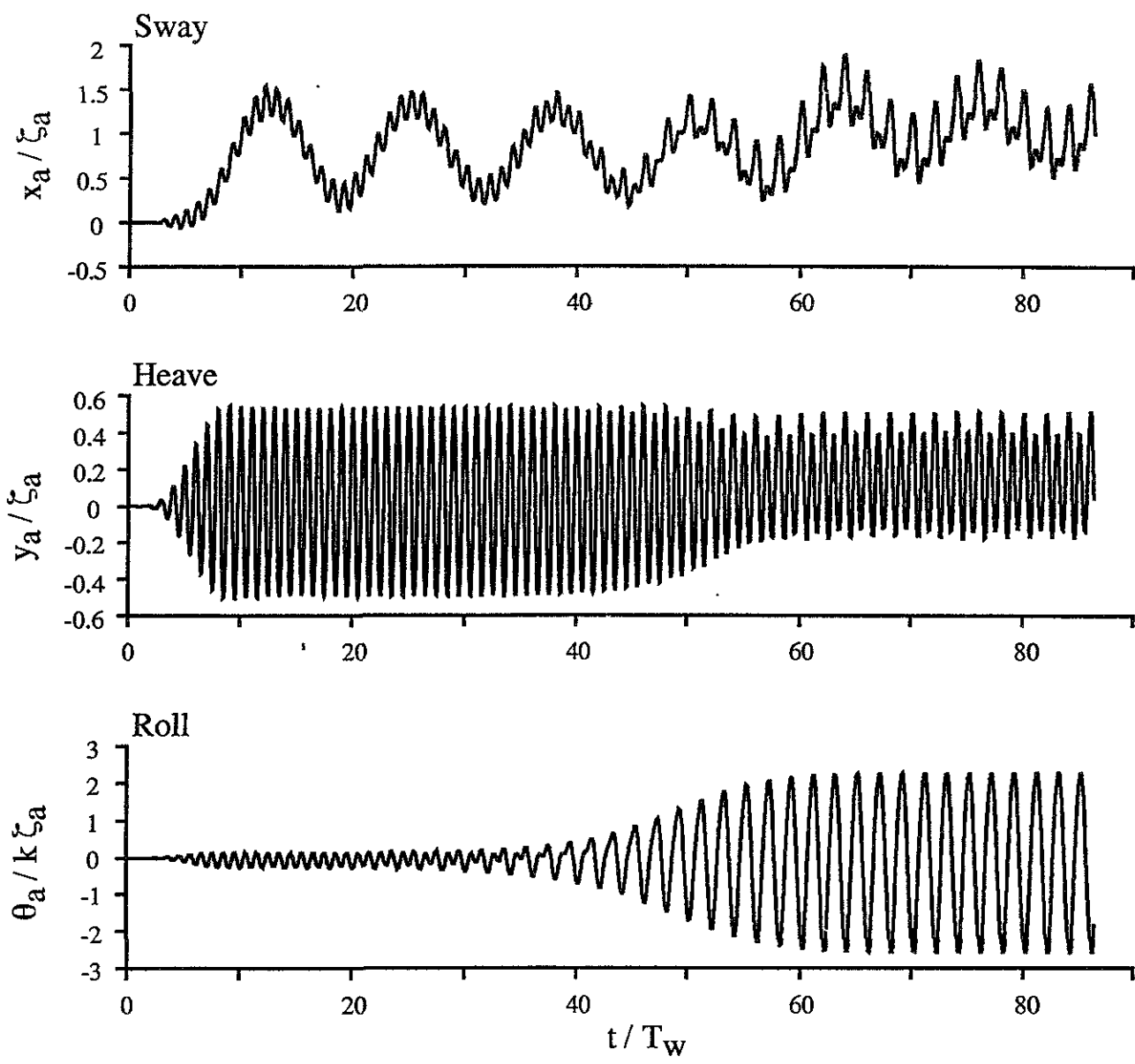
Figure 3: Simulated body motions
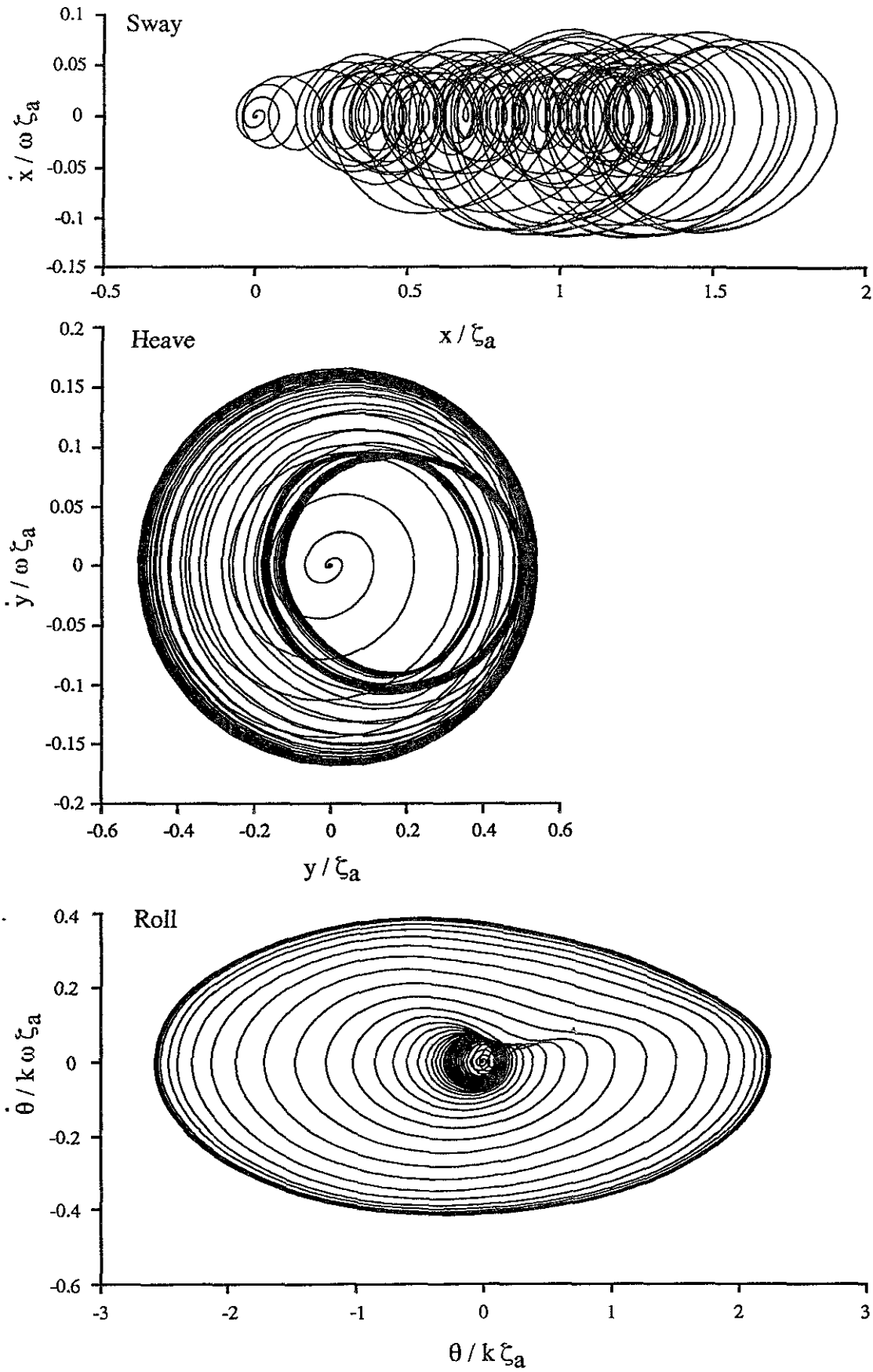
Figure 4: Phase plot of simulated motions

293
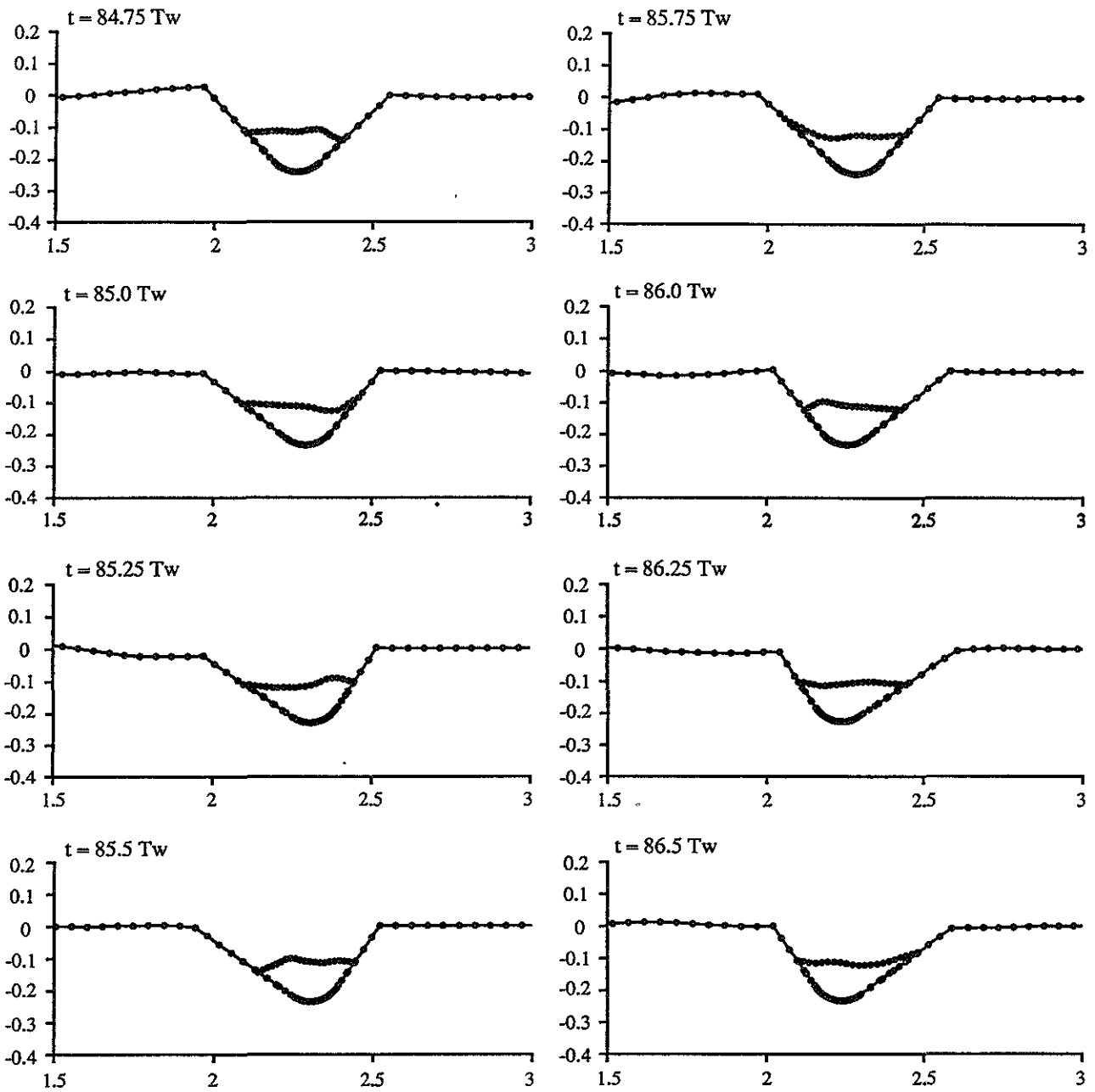
Figure 5: Instantaneous shape of free-surface inside and outside of body

BIFUCARTION SET OF ROLLING EQUATION IN BEAM SEAS: TWO DIFFERENT BEHAVIOURS

Prof. R. Zamora, Prof. J.M. Sánchez, Prof. L. P. Rojas
E.T.S.I. Navales - Universidad Politécnica de Madrid

ABSTRACT

In order to get a clearer insight in the qualitative behaviour of the rolling motion of a ship, we analyse in this paper the bifurcations, sudden jumps in the amplitude, of the weakly nonlinear multiparameter oscillator that we have chosen as the mathematical model for the rolling of a ship in regular beam seas. By applying to this oscillator the Krylov and Bogoliouvov method of averaging, we obtain a polynomial function relating the amplitude of the oscillations and the parameters. Assigning values to these parameters we get different families of polynomial functions, some of them closely related to canonical representatives of the elementary catastrophes, the independent mathematical models that we have used to get the qualitative conclusions of our analysis. In the case we have studied more thoroughly we have considered two different ships illustrating two different behaviours. We conclude discussing other non-linearities obtained when a higher number of nonzero parameters are considered.

NOMENCLATURE.

A	- Roll amplitude
a_i	- Damping moment coefficients
c_i	- Rolling moment coefficients
GM	- Metacentric Height
I	- Moment of inertia
M_0	- Amplitude of wave excitation
m	- Non dimensional amplitude of wave excitation
x	- Non dimensional roll angle
t	- Time
α_i	- Rolling moment coefficients
β	- Phase angle
δ	- 3rd order damping moment coefficient
ϕ	- Roll angle
μ	- 1st order damping moment coefficient
τ	- Scaled time
Ω	- Encounter frequency
Ω_0	- Proper frequency
ω	- Scaled encounter frequency
ω_0	- Scaled proper frequency

1.-INTRODUCTION.

It is well known that the linear models of an evolutionary process cannot be used to analyse or predict some of the observable phenomena, that are essentially non-linear. In the rolling motion of a ship a wide variety of these phenomena that escape the linear theory take place: bifurcations, jump discontinuities in the amplitude of the motion, "chaos" and others. Experimental evidences of some of these effects have been reported in (1)

This article will analyse the bifurcations of the non-linear rolling equation of a ship. The bifurcation set, the set of points in the

parameter space where changes occur in the structure of the solution orbits will be determined. In this particular case, when we refer to these changes of structure, we mean the sudden jumps in the amplitude of the rolling of the ship. To facilitate the analysis of the bifurcation set, we will project it over the plane in which we refer to the frequency of the wave versus a certain function of the slope of the wave, to be stated precisely later on. The influence of the third and fifth degree non-linear terms in the righting couple, as well as the one of the third degree in the damping force will be discussed separately.

The rolling equation to be used is the normal beam seas non-linear rolling equation. The approximated solution has been computed in the neighbourhood of resonance, using the Krylov and Bogoliouvov techniques.

2.-THE ROLLING EQUATION AND THE APPROXIMATED ANALYTIC RESOLUTION.

The non-linear oscillator

$$I\ddot{\phi} + a_1\dot{\phi} + a_3\dot{\phi}^3 + \Delta\sum_i c_i\phi^i = M_0\cos\Omega t$$

$$(i = 1,3,5,...) \qquad (1)$$

has been chosen as a suitable model of the rolling motion of a ship in a seaway. Equation (1) is considered a good representation of the rolling motion in regular beam seas. The reason for selecting a cubic approximation of the damping force is two fold, it facilitates the mathematical manipulation and it is a good approximation of the real process. We take $c_1 = GM$ (the metacentric height) and choose the other coefficients c_i ($i = 3,5,...$) that better fit the lever arm curve.

By introducing the variables

$$x = \frac{\phi}{\phi_0} \quad , \qquad \tau = \Omega_0 t$$

where ϕ_0 represents the heel angle relative to the maximum value in the static lever arm curve, we get the non-dimensional version of

equation (1). In this way, when $x < 1$, the ship will be oscillating with heel angles corresponding to the area where the ship behaves stable, while when $x > 1$, she is in the dangerous area where the lever arm of the righting couple decreases as the heel angle increases. We also scale the time in such a way that the new proper frequency ω_0 equals 1, although we will continue to denote it by ω_0, and the actual non-dimensional frequency ω, coincides with the old synchronisation factor $[\Omega / \Omega_0]$.

As a result, our rolling equation is

$$\ddot{x} + 2\mu\dot{x} + \delta\dot{x}^3 + \omega_0^2 x + \sum_i \alpha_i x^i = m\cos(\omega\tau) \quad (2)$$

($i = 3,5$) where a fifth degree approximation in the righting couple has been considered sufficient.

The presence of non-linearities prevents an exact analytic solution for equation (2) thus we build an approximated solution in the neighbourhood of the resonance frequency, where we expect the larger rolling amplitudes.

The resulting solution can be obtained using standard perturbation methods such as the averaging technique from Krylov and Bogoliouvov [2] or the method of multiple scales [3].

We test in both cases a solution of (2), that is a sinusoid function similar to the forcing function, with the same angular frequency ω, but out of phase by β.

$$x = A\cos(\omega\tau + \beta) \qquad (3)$$

the amplitude A of the resulting oscillations will satisfy

$$\left(\frac{25}{64}\right)\alpha_5^2 A^{10} + \left(\frac{15}{16}\right)\alpha_3\alpha_5 A^8 +$$

$$+\left[\left(\frac{9}{16}\right)\left(\alpha_3^2 + \delta^2\omega^2\right) + \left(\frac{5}{4}\right)\left(\omega_0^2 - \omega^2\right)\alpha_5\right]A^6 +$$

$$+\left[\left(\frac{3}{2}\right)\left(\omega_0^2 - \omega^2\right)\alpha_3 + 3\delta\mu\omega^4\right]A^4 +$$

$$+\left[\left(\omega_0^2 - \omega^2\right)^2 + 4\mu^2\omega^2\right]A^2 - m^2 = 0$$

$$(4)$$

3.-BIFURCATION SET.

To obtain the bifurcation set, we begin by taking as a first approximation, $\delta = 0$ and $\alpha_5 = 0$ in (4)

$$\left(\frac{9}{16}\right)\alpha_3^2 A^6 + \left(\frac{3}{2}\right)(\omega_0^2 - \omega^2)\alpha_3 A^4 +$$
$$+\left[(\omega_0^2 - \omega^2)^2 + 4\mu^2\omega^2\right]A^2 - m^2 = 0 \qquad (5)$$

The considered simplification is acceptable in the way that jump discontinuities in the amplitude will depend basically on α_3. [4] Further on we will take the parameters δ and α_5 into consideration.

The transformation

$$A = \left[B + 8\frac{\omega_0^2 - \omega^2}{9\alpha_3}\right]^2 \qquad (6)$$

will reduce, without loss of generalisation, equation (5) to equation

$$B^3 + pB + q = 0 \qquad (7)$$

where the second degree term in B has been eliminated and p, q are known functions of the current parameters.

Equation (7) also represents the equation of the equilibrium surface (the catastrophe manifold) of a cusp catastrophe [5,6]. The changes in the topological behaviour of the physical system are produced by the coalescence of two sheets in the equilibrium surface. Thus, we are bound to the existence of two distinct solutions for equation (7), one of them two-fold. By imposing this condition to equation (7) we get the following expression defining the bifurcation set.

$$243\alpha_3 m^4 + 48\alpha_3(\omega_0^2 - \omega^2)\left[(\omega_0^2 - \omega^2) + 36\mu^2\omega^2\right]m^2 +$$
$$+256\mu^2\omega^2\left[(\omega_0^2 - \omega^2)^2 + 4\mu^2\omega^2\right]^2 = 0 \qquad (8)$$

To analyse the bifurcations of this first approximation, we have considered two separate cases depending on the sign of α_3, sign that is essential in the analysis of the behaviour of the vessel.

To illustrate the first case $\alpha_3 > 0$, we have chosen a 60 meter long tuna ship with two different cargo loading conditions corresponding to the α_3 values of 1.045 and 3.4. The corresponding level arm curves are represented in figures 1 and 2. The lever arm curve near the origin lies above the line $GZ=GM\phi$, our cubic approximation can be considered adequate up to about 25 degrees.

The projection of the bifurcation sets of the two cargo loading conditions over the $\omega - m$ plane are illustrated in figures 3 and 4. We represent in figures 5,6 and 7, that are related to figure 3, the frequency response curves corresponding to three constant values of the amplitude of excitation. In the case with the greatest value of α_3, the bifurcation set has been displaced downward, favouring the appearance of jumps in the amplitude for a lower intensity of excitation.

The rolling amplitude versus excitation amplitude curve represented on figure 8 shows the possible rolling amplitude jumps consequence of small variations of the wave amplitude.

The lower branch of the two branched bifurcation set, defines the frequency of resonance for each value of the amplitude of excitation. As the slope decreases in this lower branch, the frequency of resonance moves to the right as α_3 increases; consequently, we should expect the most important motions, not for the values of the frequencies of excitation close to the proper values of the ship, but for values greater than these and increasing with α_3.

In the case for which $\alpha_3 < 0$ we have chosen two different cargo loading conditions in the 20 meter long fishing vessel associated to α_3 values of -0.3 and -0.43. The corresponding level arm curves are illustrated in figures 9 and 10. The lever arm curves lie beneath the line $GZ=GM\phi$. In this particular case, the cubic approximation is adequate up to about 50 degrees.

The bifurcation set of both cargo loading conditions are shown in figures 11 and 12. We notice that, though they are similar probably due to the small differences between the stability curves, as α_3 decreases the bifurcation set is displaced downward.

Holmes and Rand [6] predicted the existence of an unstable area of large amplitude of rolling in the frequency response curve for very low encounter frequency values. In our study, the amplitude values of this predicted area, are clearly out of the range of mathematical stability of equation (2) [6], as well as out of the area of resonance for which we propose this analytic solution.

In figures 13 and 14, corresponding to $\alpha_3 = 1.045$, we can see the influence of the damping linear term coefficient μ. In both cases as μ increases the bifurcation set is displaced upward; thus, increasing the threshold intensity value beyond which the bifurcations are produced and decreasing the gap between the resonance frequencies and the proper frequencies of the ship. The same conclusions hold when $\alpha_3 < 0$.

4.- OTHER NON-LINEARITIES.

If we consider now $\delta \neq 0$ and $\alpha_5 = 0$, we observe in equation (4) that the model of behaviour is the one of the cusp catastrophe, as a consequence, the equilibrium surface is again of the type of equation (7) and we will obtain, for the bifurcation set an equation similar to equation (8). We represent in figures 15 and 16 this bifurcation set for each of the conditions before studied. We can see that as δ increases, the possibility of multifold solutions decreases significantly, accompanied by a parallel increase of the threshold value of the excitation amplitude beyond which these solutions are expected.

The introduction of a fifth degree term in the righting couple $\alpha_5 \neq 0$, modifies completely the model of behaviour that will now be that of a butterfly catastrophe, introducing as a consequence a new intermediate equilibrium stable solution.

Writing $A^2 = B$, (4) is a fifth degree equation in B that through a process of elimination of the fourth degree coefficient can be identified with the equation defining the catastrophe manifold of a butterfly catastrophe. Conclusion predicted by Zeeman [7].

The standard study of this elementary catastrophe manifests the existence of five possible ship equilibrium solutions, three of them which are stable and two others unstable.

The new stable equilibrium position corresponds to intermediate values of the amplitude and is attained in the same way. So, for some values of the parameters, the behaviour is qualitatively similar to those already studied, for others the jumps have an intermediate step. ·

Nayfeh and Khdeir [8] studying the influence of α_5 in the frequency response curve of the rolling equation by comparing the analytical and numerical solutions, proved that there is an overestimation of the maximum values of the amplitude when the parameter is considered and also that α_5 has no significant influence in the amplitude jumps.

5.- CONCLUSIONS

1. The non-linearity of the righting couple motivates the presence of multifold solutions of the rolling equation for the same excitation frequency. The area within the parameters space where these solutions show up is limited by the bifurcation set, where the characteristic rolling amplitude jumps take place.

2. The projection of the bifurcation set on the frequency versus amplitude of excitation plane is the catastrophe set of a cusp catastrophe. This set is located in the areas of periods smaller than the proper period of the ship ($\omega > \omega_0$) when $\alpha_3 > 0$ and just the opposite ($\omega < \omega_0$) when $\alpha_3 < 0$.

3. The two branches of the bifurcation set define the eventual jumps between states corresponding to amplitudes which are not simultaneously resonant that can be produced by small changes in the values of the parameters ω and m as a consequence of a physical action (a rare wave, a change of drift etc.)

4. The lower branch of the bifurcation set represents the frequency response curve (frequency versus amplitude of excitation curve) where the maximum of the rolling amplitude (resonance) is attained. In the non-linear model this maximum value is not attained at ω_0, the maximum point is greater than ω_0 when $\alpha_3 > 0$ and smaller than ω_0 for $\alpha_3 < 0$.

5. As α_3 positive, increases the bifurcation set displaces downward so that the jumps in the amplitude will eventually happen for smaller values of the frequency of excitation. The contrary happens when α_3 negative, increases although due in part to the small difference in the values of α_3 considered in this study, this effect is not very evident. In none of the two cases have we appreciated any influence of α_3 in the cusp point frequency.

6. In the two cases considered an increment in the damping linear term coefficient μ produces an upward displacement of the bifurcation set that is beneficial in the sense that the jumps occur for large values of the intensity of excitation and also modifies the cusp point frequency.

7. The introduction of a cubic term in the damping does not change qualitatively the model of behaviour.

8. The dependence of the bifurcation set on δ, the coefficient of the third degree damping term, is very similar to the one already studied on μ. We can assert that an increment in the damping will limit the possibility of jumps to large values of the intensity of excitation.

9. The introduction of a fifth degree term in the righting couple modifies completely the model of behaviour that will now be that of a butterfly catastrophe.

6.- REFERENCES

1. Francescutto, A., Contento, G., and Penna, R. "Experimental evidence of strong nonlinear effects in the rolling motion of a destroyer in beam sea", Fith International Conference on Stability of Ships and Ocean Vehicles, Florida, 1994.

2. Mitropolski, Y.A., "Problèmes de la theorie asymptotique des oscillations non stationaires", Gautier-Villars, Paris, 1966.

3. Guckenheimer, J. Y Holmes, P., "Nonlinear oscillations, Dynamical Systems and Bifurcations of Vector Fields", Springer-Verlag, New York, 1983.

4. Cardo, A., Francescutto, A. and Nabergoj, R., "On the maximum amplitudes in nonlinear rolling", 2nd International Conference of Ships and Ocean Vehicles, Tokyo, 1982.

5. Thom, R., "Stabilité Structurelle et Morphogénèse", Inter Editions, Paris, 980.

6. Holmes P.J. and Rand D.A., " The bifurcations of Duffing's equation: An application of catastrophe theory", Journal of Sound and Vibration, Vol. 44, 1976.

7. Zeeman, E.C., "Catastrophe theory", Addison-Wesley, 1977.

8. Nayfeh, A.H., y Khdeir, A.A., "Nonlinear rolling of ships in regular beam seas", International Shipbuilding Progress, vol 23, 1986.

9. Zamora, R., "Bifurcaciones de la ecuación de balance no lineal del buque", Dr. Th. E.T.S.I.Navales, Universidad Politécnica de Madrid, Madrid, 1992
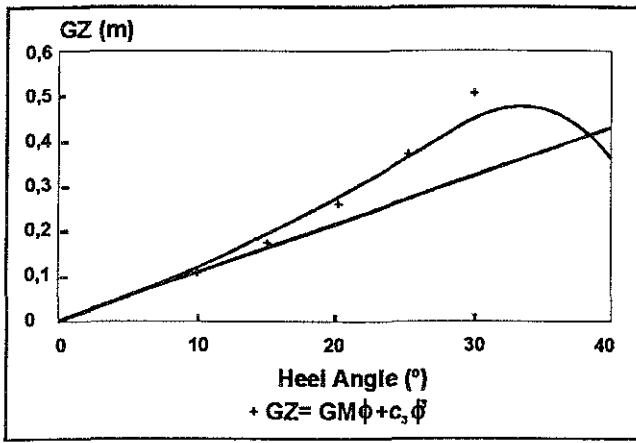
Figure 1
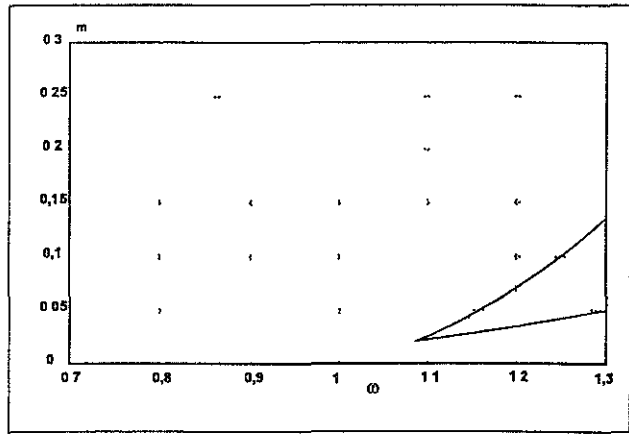


Figure 4.- Bifurcation Set-$\alpha_3 = 3.4$, $\mu = 0.04$
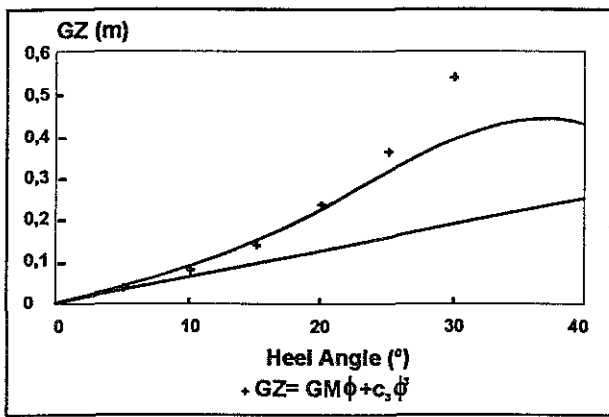
Figure 2
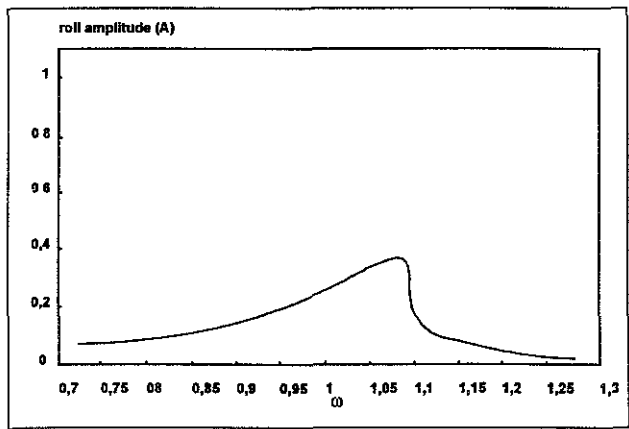
Figure 5.- Roll Amplitude $\alpha_3 = 1.045$, $\mu = 0.04$, m = 0.04
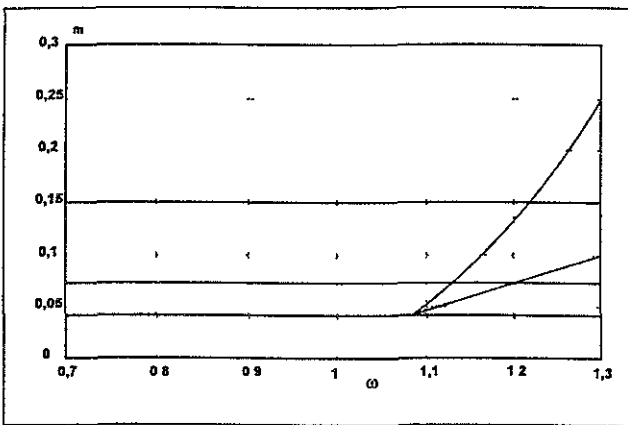
Figure 3.- Bifurcation Set-$\alpha_3 = 1.045$, $\mu = 0.04$
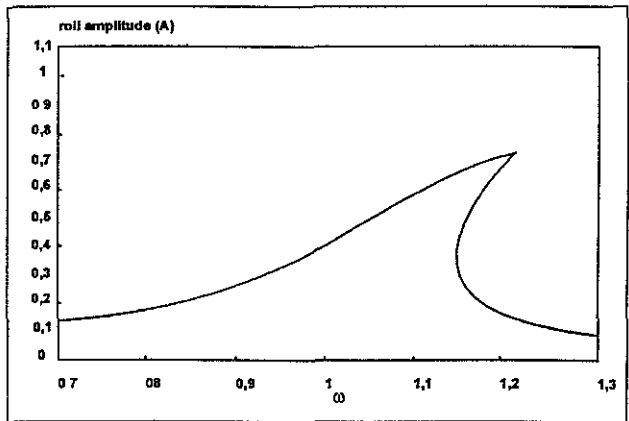

Figure 6.- Roll Amplitude-$\alpha_3 = 1.045$, $\mu = 0.04$, m = 0.07

300
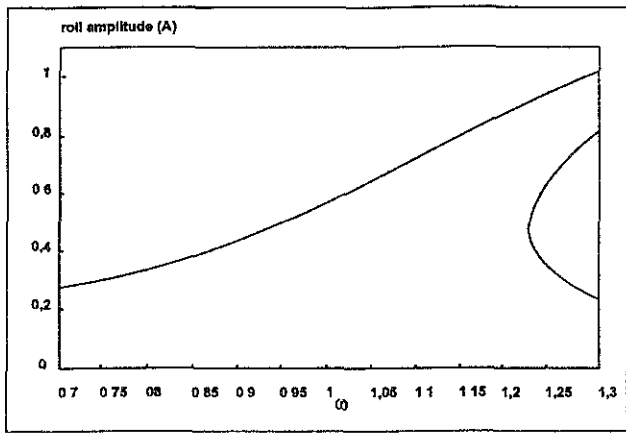
Figure 7.- Roll Amplitude-α_3 = 1.045, μ = 0.04, m = 0.15
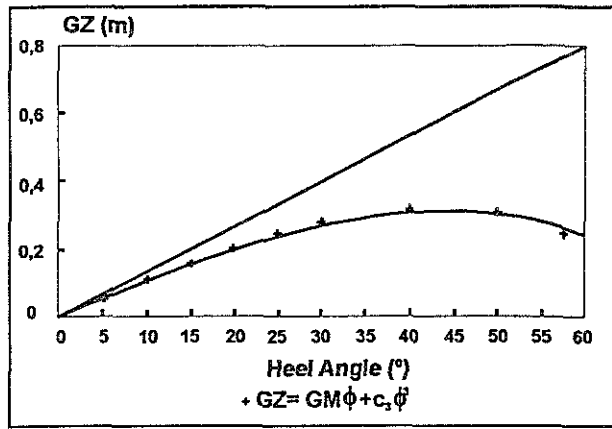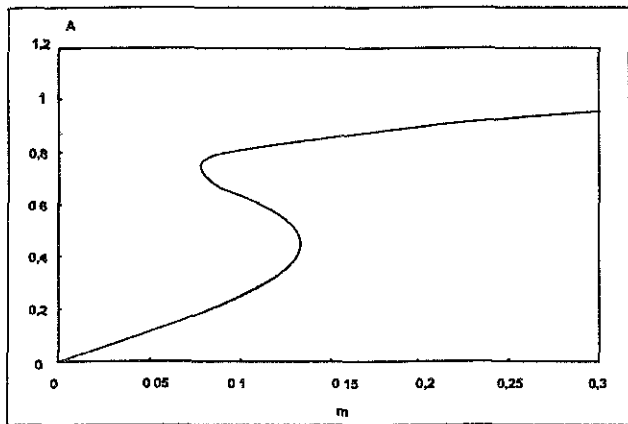
Figure 10

Figure 8.- Roll phase lag-α_3 = 1.045, μ = 0.04, ω = 1.2
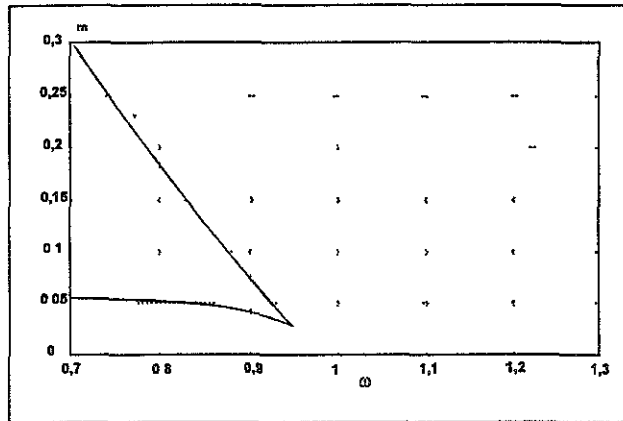
Figure 11.- Bifurcation Set-α_3 = 0.3, μ = 0.025
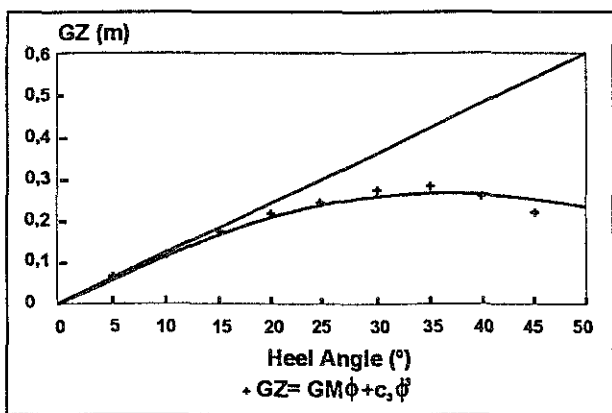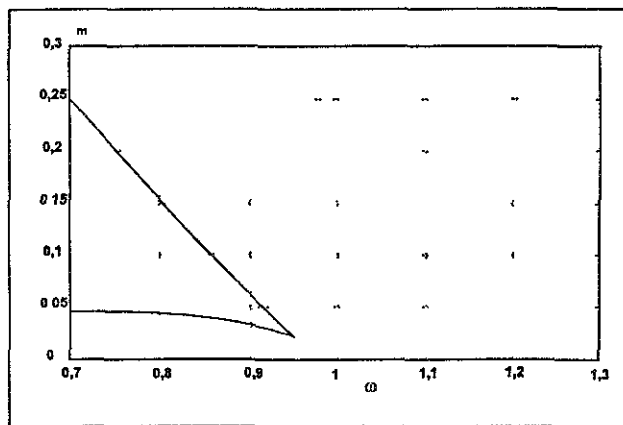
Figure 9

Figure 12.- Bifurcation Set-α_3 = 0.3, μ = 0.025

301
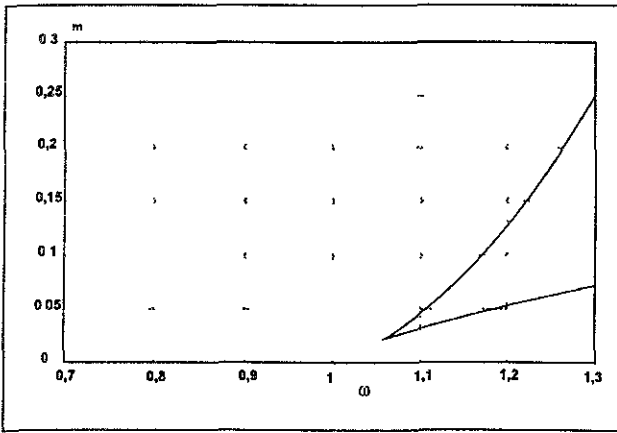
Figure 13.- Bifurcation Set-α_3 = 1.045,μ = 0.03
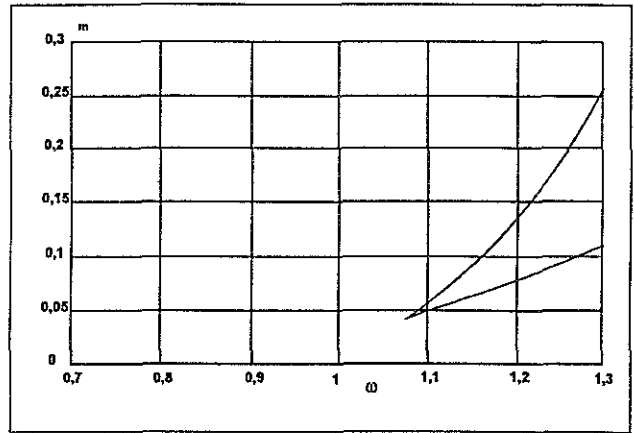

Figure 15.- Bifurcation Set-α_3 = 1.045,
μ = 0.04, δ = 0.01
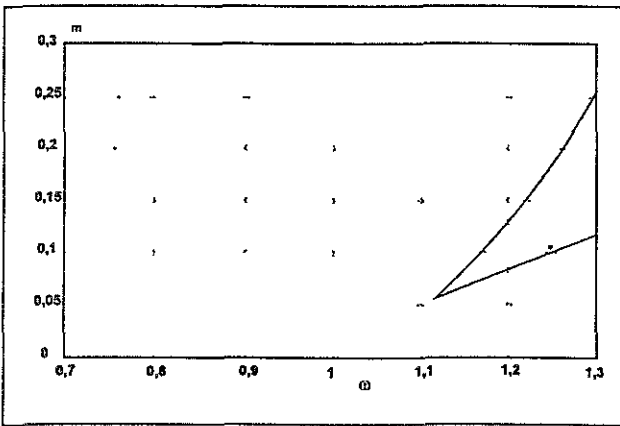
Figure 14.- Bifurcation Set α_3 = 1.045, μ = 0.05
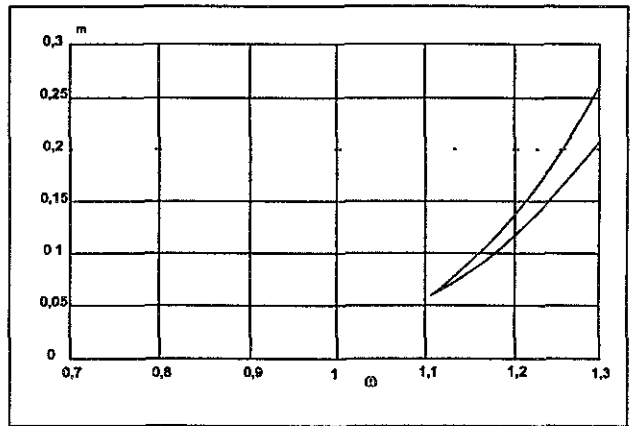
Figure 16.- Bifurcation Set-α_3 = 1.045,
μ = 0.04, δ = 0.1

Some aspects of the ship rolling motion associated to high degree polynomial restoring moment.

Y.M. Scolan

Ecole Supérieure d'Ingénieurs de Marseille

Technopôle Château Gombert

13451 Marseille Cedex 20

1 Introduction

We are concerned here with the ship rolling motion whose solution is calculated for an ordinary differential equation of type:

$$\ddot{x} + D(\dot{x}) + P(x) = E(t) \qquad (1)$$

where $\ddot{x}$ and $\dot{x}$ denotes the second and first derivatives of the motion x with respect to time t; the variables have been made nondimensional. Without $D(\dot{x})$ and $E(t)$, which denote the damping and the forcing respectively, the dynamical system is a hamiltonian one. The function $P(x)$ represent the restoring force: it is often a polynomial. Up to a quintic polynomial, the hamiltonian system has still analytical solutions which are provided here. These solutions are used in the frame of the Melnikov method. This provides a condition for the critical forcing amplitude in terms of the characteristics of the nonlinear dynamical system otherwise excited harmonically. It is shown there exist frequencies of excitation where unconditionnal stability is expected. This would suggest a limitation of the Melnikov method.

2 Analytical solutions for hamiltonian systems

The well known Duffing oscillator associates a third order polynomial to a second order derivative and analytical are easily obtainable. By increasing the degree of the polynomial that respresents the restoring moment, one can also exhibit analytical solutions. This is exposed in Scolan (1997) where all the physical solutions are provided. A distinction is to be done concerning the numbers of zeroes of the polynomial; here only odd polynomials with a single positive zero are considered.

The restoring moment: $P(x)$ aned the corresponding hamiltonian: $\dot{x}^2$ are given below:

vanishing stability P_5	
$P(x) =$	$-x(x^2 - x_v^2)(x^2 + b^2)$
$\dot{x}^2 =$	$\frac{1}{3}\left(x^2 - x_v^2\right)^2\left(x^2 + \frac{x_v^2 + 3b^2}{2}\right)$
vanishing stability P_3	
$P(x) =$	$-x(x^2 - x_v^2)$
$\dot{x}^2 =$	$\frac{1}{2}\left(x^2 - x_v^2\right)^2$

For higher degree of the polynomial, a numerical integration is performed to obtain a parametrization of x and its derivative $\dot{x}$. The Melnikov method follows from the calculation of the integral (see Guckenheimer and Holmes 1983):

$$M(\tau) = \int_{-\infty}^{+\infty} \dot{x}D(\dot{x})dt +$$

$$\int_{-\infty}^{+\infty} \dot{x}E(t + \tau)dt = M_D + M_E(\tau) \qquad (2)$$

where τ is a phase with same dimension than t. The zeroes of $M(\tau)$ indicate the intersection of stable and unstable manifolds defined in the phase space $(x, \dot{x})$. When the forcing $E(t)$ is a harmonic excitation evolving at circular frequency ω with amplitude A, a critical amplitude may be defined as follows:

$$A_{critical} \leq \frac{-M_D}{M_E(\omega)} \qquad (3)$$

where $M_E(\omega)$ is the amplitude of $M_E(\tau)$. The existence of zeroes of $M_E(\omega)$ is dicussed here as the degre of $P(x)$ increases.

The solution for a third order polynomial is given below:

$$M_E(\omega) = \int_{-\infty}^{+\infty} \dot{x}(t)\cos\omega t\, dt = \frac{\sqrt{2}\pi\omega}{\sinh\frac{\pi\omega}{\sqrt{2}x_v}} \quad (4)$$

It is worth noting that this is simply the Fourier transform of a gaussian function.
For the quintic polynomial the solution is not calculable easily.

$$M_E(\omega) = \int_{-\infty}^{+\infty} \dot{x}(t)\cos\omega t\, dt =$$

$$\frac{u}{w}\int_0^{+\infty}\frac{\cos\frac{\omega}{2w}t\,\cosh\frac{t}{2}}{(1+v\cosh t)^{3/2}}\,dt \quad (5)$$

with

$$\begin{cases} u &= 6x_v^2\sqrt{\frac{(x_v^2+3b^2)(x_v^2+b^2)^3}{(5x_v^2+3b^2)^3}} \\ v &= \frac{x_v^2+3b^2}{5x_v^2+3b^2} \\ w &= \sqrt{\frac{(x_v^2+b^2)x_v^2}{2}} \end{cases} \quad (6)$$

this is the Fourier transform of a certain function and tables provide the solution:

$$M_E(\omega) = \frac{u\pi\omega\sqrt{v}}{2\sqrt{2}w^2\sinh\frac{\pi\omega}{2w}}$$

$$\Re\left((1+\frac{i\omega}{2w})v^{\frac{i\omega}{2w}}F\left(\frac{3}{2}+\frac{i\omega}{4w},1+\frac{i\omega}{4w};2;1-v^2\right)\right) \quad (7)$$

where $\Re$ denotes the real part of a complex number and F is the Gauss hypergeometric function.

3 Analysis of the Melnikov criterion

Comparisons are made for different odd polynomial restoring moment as:

$$P(x) = x\,(x^2-x_v^2)\,(1+x^2+x^4+...) \quad (8)$$

This is illustrated in the left figure below where it should be noted that the area under each curve (in the interval $[0,x_v]$) is exactly the potential energy at $x = x_v$ (the area is also its maximum value).
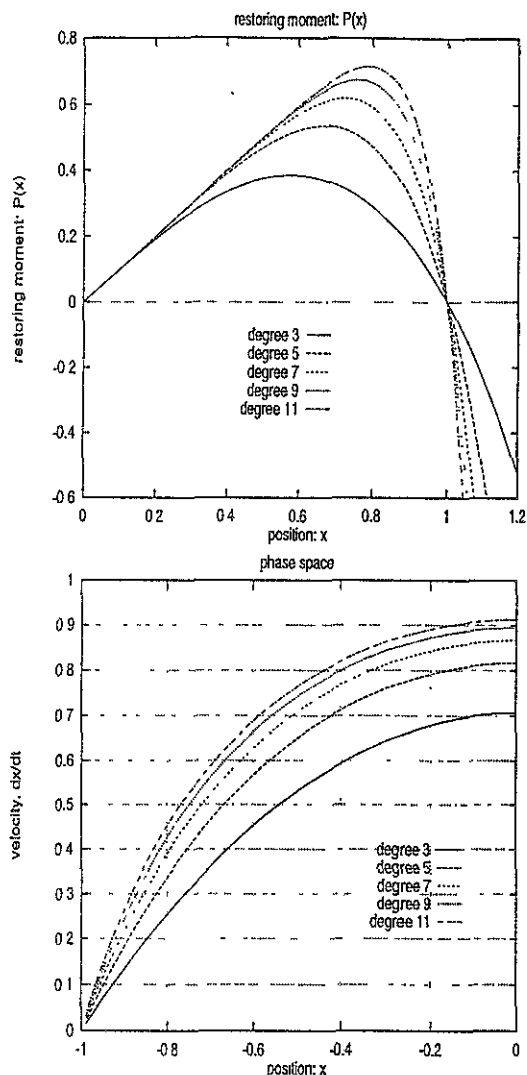
Figure 1: Restoring force and part of heteroclinic orbit for odd polynomial restoring force, the degree varies from 3 to 11 with $x_v = 1$.

Let us consider a linear damping component as $\dot{x}$ (the coefficient $\mu_1 = 1$), the numerator of equation (3) is simply $\int_{-\infty}^{+\infty}y^2(t)dt$ alternatively $\int_{-x_v}^{+x_v}y(x)dx$; that is actually twice the area under the curve of the right figure. This is so far quite consistent with the physics of the phenomenon: the larger the area under $P(x)$, the more stable the dynamic system and the larger the critical amplitude obtained from Melnikov analysis.

The following figures show how evolves the $M_E^2(\omega)$ with ω.

304
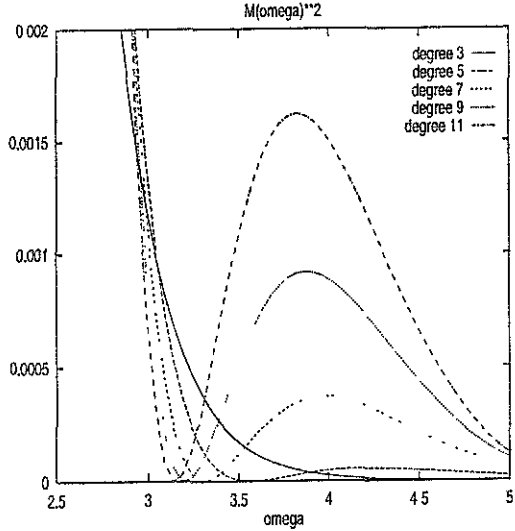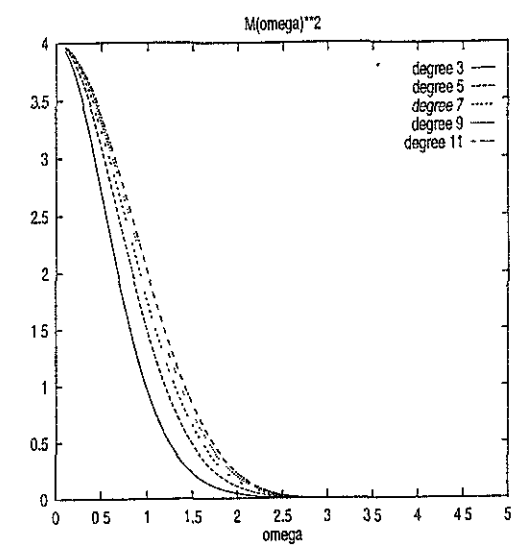
Figure 2: Variation of the fluctuating Melnikov function amplitude with circular frequency, the zero of $M_E^2(\omega)$ is zoomed on the right figure.

It is worth noting there exists one or more frequencies where $M_E(\omega) = 0$ as soon as the degree is more than 3 (let us note ω_m these frequencies). This means that for regular excitation at these frequencies, the Melnikov method predicts a critical amplitude of forcing which is infinite; this may have no physical meaning. These zeroes can be determined precisely by analysing the hypergeometric function in equation (7). Let us consider the dynamical system:

$$\ddot{x} - x(x^2 - 1)(x^2 + 1) = 0 \qquad (9)$$

The following figure illustrates the corresponding variation of $M_E(\omega)$ from which the exponentially decreasing term has been removed.
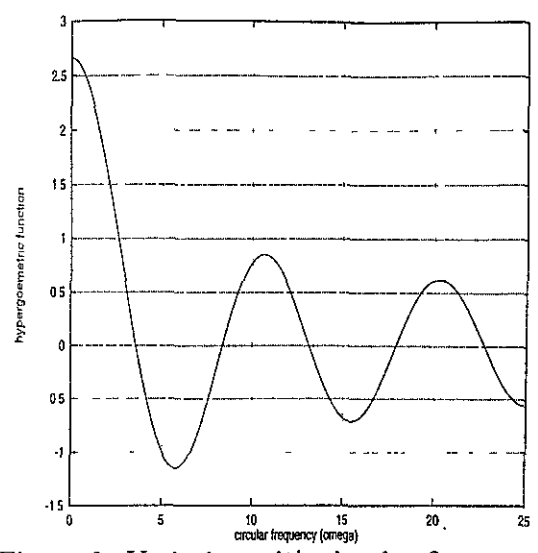

Figure 3: Variation with circular frequency of the term $M_E(\omega)$ expurgated of the exponential decreasing term in equation (7).

It should be noted these results follow from a study that separates each frequency and they should have therefore no meaning for an irregular excitation (see Hsieh et al. 1993) unless the spectrum of the forcing is narrow and centered about one of these frequencies. This is nevertheless a required condition to justify that the total inertia (including added mas) is not dependent on the frequency of excitation.

Another way to confirm the existence of such frequencies is to calculate the erosion of the attraction basin for the same but forced dynamical system. This erosion is defined here as the ratio of the numbers:

$$\text{erosion coefficient} = \frac{N^{bounded}}{N^{total}} \qquad (10)$$

where $N^{bounded}$ is the number of initial conditions for which $|x| + |\dot{x}| < \infty$, and N^{total} denotes the total number of studied initial conditions. Practically, the solution is calculated for $51 \times 51 = 2601$ initial conditions taken in the domain $(x, \dot{x})_{t=0} \in [-1., 1.] \times [-0.9, 0.9]$ and it is supposed to be unbounded as soon as $|x| + |\dot{x}| > 30$. The erosion coefficient is plotted below:

305
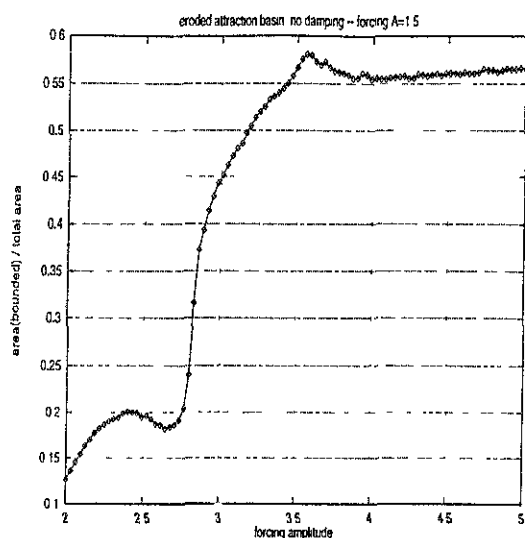
Figure 4: erosion of attraction basin for eq. $\ddot{x} + x - x^5 = A\cos\omega t$ with $A = 1.5$.

Here one notices that the first zero is about $\omega_m \approx 3.57$ which is precisely where the erosion reaches its minimum, alternatively the corresponding erosion coefficient (defined above in equation 10) has its maximum. This finally shows that the Melnikov analysis is probably questionnable when the dynamical system is excited about these frequencies ω_m.

4   Conclusion

The Melnikov function is calculated both analytically and numerically starting from a Hamiltonian system where the restoring term is a polynomial whose degree is odd and varies from 3 to 11. In the frame of the Melnikov method, this exhibits a critical excitation force amplitude that can be infinite at some frequencies of the one-harmonic forcing. This corresponds to zeroes of the fluctuating term of the Melnikov function and they only appear when the degree of the polynomial representing the restoring moment is quintic at least. The first zero only seems to be significative. The analysis of the erosion of attraction basin confirms the existence of these "cancellation" frequencies.

5   References

1. Guckenheimer J. & Holmes P., 1983, "Nonlinear oscillations, dynamical systems, and bifurcations of vector fields.", Applied Mathematical Sciences, N° 42, Springer–Verlag.

2. Hsieh S.-R., Shaw S.W. & Troesch A.W., 1993, "A nonlinear probalistic method for predicting vessel capsizing in random beam seas.", Proc. R. Soc. Lond. A 446, pp 195-211.

3. Scolan Y.-M., 1997, "Technical note on ship rolling associated to high degree polynomial restoring moment by using the Melnikov Method.",accepted for publication in Applied Ocean Research.

PROBABILITY OF SHIP SURVIVAL IN ROUGH SEA

Ivo Senjanović, Goran Ciprić, Joško Parunov
University of Zagreb, Faculty of Mechanical Engineering and Naval Architecture,
I. Lučića 5, 10000 Zagreb, CROATIA

ABSTRACT

Using the state-of-the-art in nonlinear dynamics, a new approach to predict possible ship capsizing in rough sea is described. Ship rolling is simulated by a single degree of freedom. The random wave excitation is a function of sea state and encounter frequency. The differential equation of motion is solved in the time domain by the harmonic acceleration method. The roll response of an intact and a damaged ship is analysed in the time and frequency domain, as well as in the initial value plane. The safe basin for calm sea and the eroded basin for rough sea are used to determine the probability of ship's survival.

NOMENCLATURE

D, d - absolute and relative damping moment
g - gravity constant
h - wave height
I - virtual moment of inertia (ship mass and added mass)
M, m - absolute and relative wave moment
n - index of harmonic wave
p - probability
R, r - absolute and relative restoring moment
S - energy spectrum
T - time period
t - time
U - ship speed
α_0 - effective wave slope coefficient
ε - random phase angle

λ - wave length
φ - roll angle
χ - heading angle
ω - wave frequency
$\tilde{\omega}$ - wave frequency step
ω_e - encounter frequency
ω_0 - natural roll frequency

1. INTRODUCTION

The ship stability criteria are rather conservative since they prescribe the form and the area under the righting arm curve /1/. Thus, a very important role of nonlinear dynamic phenomena is not taken into account /2/. This might be an explanation why many intact ships where lost in rough sea /3/. Therefore, the state-of-the-art in nonlinear dynamics should be used in the analysis of stability criteria, and accordingly new stability criteria should be established /4,5/.

The problem of ship rolling in regular beam seas has been quite well investigated. The nonlinear phenomena, like amplitude jumping, superharmonic and subharmonic response, symmetry breaking, period doubling, and transition to chaotic motion, as an indication of ship capsize, are the main subjects in /6,7,8/. However, the obtained results are far from practical usage since there is rolling of ships in rough sea. Unfortunately, the well known spectral analysis is not valid for large amplitude motion /9,10/.

Having in mind the above facts, it is preferable to analyse the nonlinear problem of

ship rolling in rough sea by numerical simulation in the time domain. In that way it is possible to construct a ship safe basin in the initial value plane for calm sea and an eroded basin for different sea states and values of encounter frequency. Finally, these results are used to determine the probability of ship survival. This is subject of the paper, which presents an outline of the results of recent investigation described in /11,12/.

2. OUTLINE OF THE THEORY

For the sake of simplicity, uncoupled ship rolling is considered. It is described by the differential equation of motion:

$$I\ddot{\varphi} + D(\dot{\varphi}) + R(\varphi) = M(t) \qquad (1)$$

or in the normalised form

$$\ddot{\varphi} + d(\dot{\varphi}) + r(\varphi) = m(t) \qquad (2)$$

where the relative damping moment is viscous

$$d(\dot{\varphi}) = D(\dot{\varphi})/I = d_0|\dot{\varphi}|\dot{\varphi} \qquad (3)$$

and the relative restoring moment may be approximated by the polynomial

$$r(\varphi) = R(\varphi)/I = \sum_i k_i \varphi^i \qquad (4)$$

The relative excitation of an irregular wave may be presented by a series of harmonic components /9, 10, 13, 14/, i.e.

$$m(t) = M(t)/I =$$
$$\alpha_0 \omega_0^2 \pi \sin \chi \sum_{n=1}^{N} \frac{h_n}{\lambda_n} \cos(\omega_{en} t + \varepsilon_n) \qquad (5)$$

The harmonic wave height is obtained from the corresponding wave energy spectrum $S(\omega)$

$$h_n = 2\sqrt{2\widetilde{\omega}S(\omega_n)} \qquad (6)$$

while the wave length is

$$\lambda_n = \frac{2\pi g}{\omega_n^2} \qquad (7)$$

and the encounter frequency

$$\omega_{en} = \omega_n - \frac{\omega_n^2 U}{g}\cos\chi \qquad (8)$$

For instance, for the Adriatic Sea Tabain's wave energy spectrum is valid /15/.

$$S(\omega) = 0.862\frac{0.0135g^2}{\omega^5}\exp\left[-\frac{5.186}{\omega^4 h_{1/3}^2}\right]1.63^p \qquad (9)$$

where

$$p = \exp\left[-\frac{(\omega - \omega_m)^2}{2\sigma^2 \omega_m^2}\right]$$

$$\omega_m = 0.32 + \frac{1.8}{h_{1/3} + 0.6}$$

$$\sigma = \begin{cases} 0.08 & if \ \omega < \omega_m \\ 0.10 & if \ \omega > \omega_m \end{cases} ; \qquad (10)$$

In the above formulae the units m, s, rad have to be used.

3. ILLUSTRATIVE EXAMPLE

A fishing vessel with the following particulars is considered /16/

length overall	L_{oa}	= 30.7 m
length between pp.	L_{pp}	= 25.00 m
breadth	B	= 6.90 m
depth	H	= 4.96 m
draught	T	= 2.67 m
displacement	Δ	= 195 t
natural roll freq.	ω_0	= 1.32 rad/s

The relative restoring moment for the intact and the damage vessel (for the case of engine room flooding with permeability coefficient 0.75), is shown in Fig. 1.

The energy spectrum of the relative excitation moment for the vessel rolling in the Adriatic Sea in the case of significant wave height $h_{1/3}$=2.5 m, vessel speed U=4 m/s and

heading angles $\chi=60^0$ and 90^0, is shown in Fig. 2.

The influence of the flooding is neglected. Energy concentration in the case of quartering sea, due to the grouping of harmonic component waves, is evident.
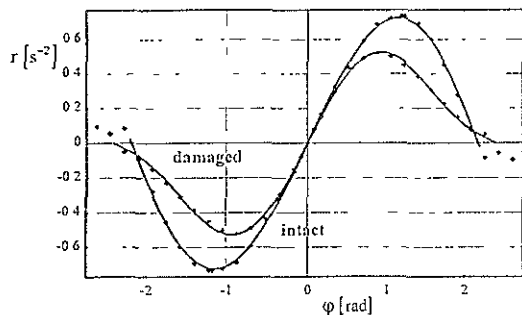

Fig. 1.   Relative restoring moment for intact and damaged vessel,
ᵒ ᵒ ᵒ real, —— approximate
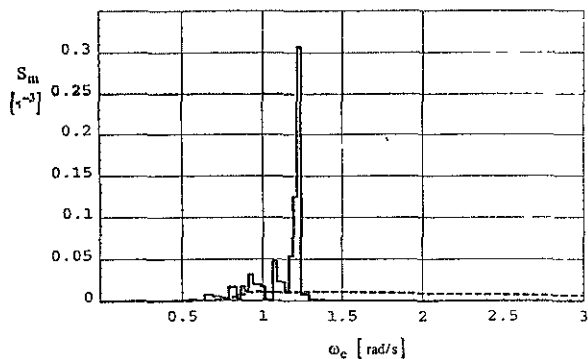
Fig. 2.   Energy spectrum of relative excitation moment, $h_{1/3} = 2.5$ m, $U = 4$ m/s,
—— $\chi = 60°$, ᵒ ᵒ ᵒ $\chi = 90°$

The differential equation of rolling motion (2) for the specified input data is integrated applying the harmonic acceleration method /17/. The roll energy spectrum of the intact and the damaged vessel are shown in Figs. 3 and 4 respectively. The vessel's response for the quartering sea is larger than that for the beam sea due to larger excitation in the former case. Also, the response energy presented by the zero statistical moment of the response spectrum is larger for the damaged vessel than for the intact one.
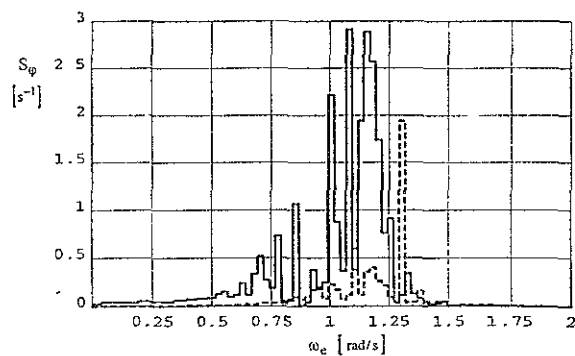
Fig. 3.   Roll energy spectrum of intact vessel, $h_{1/3}=2.5$ m, $U=4$ m/s,
—— $\chi=60°$, ᵒ ᵒ ᵒ $\chi=90°$
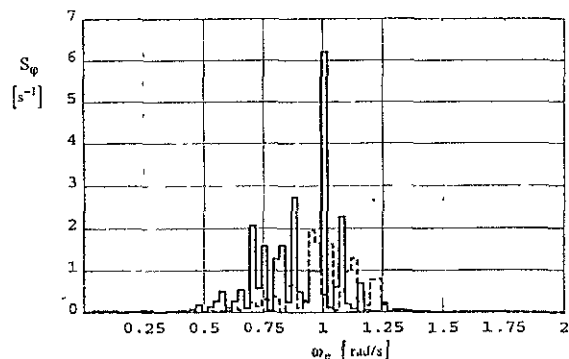
Fig. 4.   Roll energy spectrum of damaged vessel, $h_{1/3}=2.5$ m, $U=4$ m/s,
—— $\chi=56°$, ᵒ ᵒ ᵒ $\chi=90°$

The safety of the rolling vessel may be analysed in the initial value plane as a control space. For this purpose, rolling is determined for different combinations of initial conditions $\varphi(0) = \varphi_0$ and $\dot\varphi(0) = \dot\varphi_0$, two sea states given by the significant wave height $h_{1/3} = 0$ and 2.5 m, three vessel speeds $U = 0, 2$ and 4 m/s, and the whole domain of heading angle with a discrete step of $\Delta\chi = 10°$. Some interesting results for the intact and the damaged vessel are shown in Figs.6 to 9 with a resolution of 200x200 = 40000 grid points. Referring to the legend given in Fig.5, the black area is the safe basin, since the vessel survives within the whole period $\tilde{T} = 2\pi/\tilde\omega$. The bright area represents the capsize domain where the vessel capsizes at the very beginning of rolling motion, $0 < t/\tilde{T} < 1/5$. The remaining shades
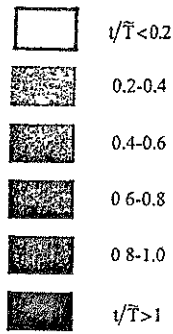
Fig. 5. Legend of time intervals to capsize
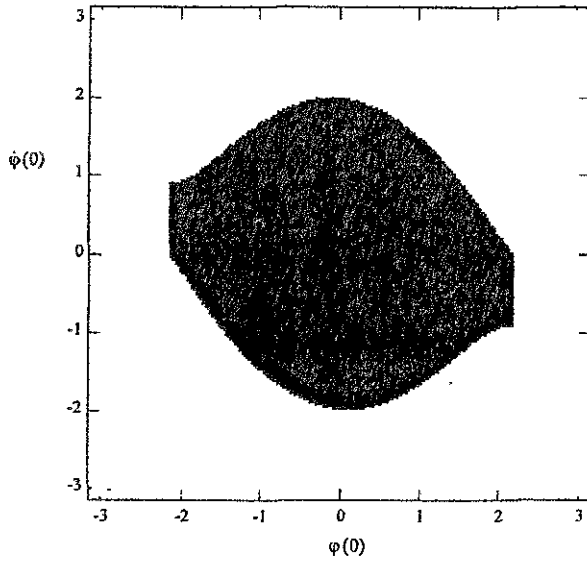
Fig. 6. Safe basin of intact vessel
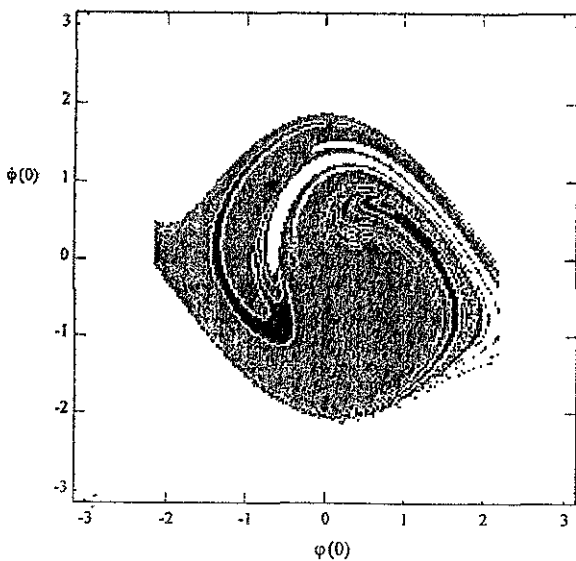
Fig. 7. Capsize boundary of intact vessel,
$h_{1/3}$=2.5 m, U=4 m/s, χ=60°

denote some transition time intervals to capsize. In the case of calm sea, $h_{1/3}$ = 0, the safe basin is compact with a smooth capsize boundary, Figs.6 and 8. The safe basin for the damaged vessel is reduced in the considered case for 17%. For rough sea the erosion of the safe basin is progressive with sea roughness. It also depends on the vessel speed and heading angle. The erosion of the safe basin is very large for the quartering sea. The maximum erosion for the intact and the damaged vessel is achieved at χ = 60° and 56° respectively, Figs.7 and 9.
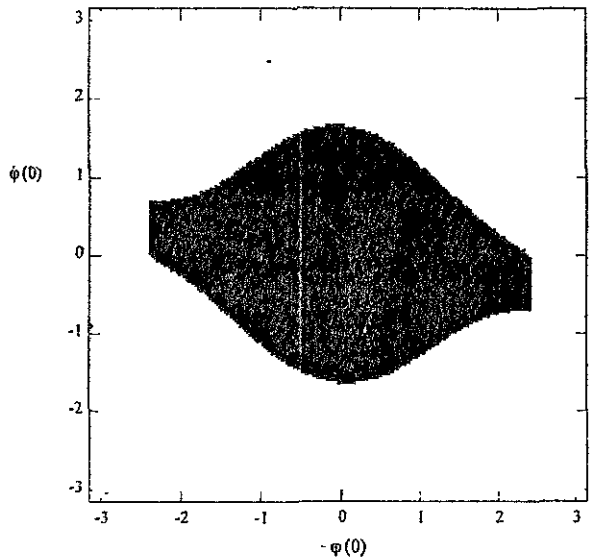
Fig. 8. Safe basin of damaged vessel,
$h_{1/3}$=2.5 m, U=4 m/s, χ=56°

The probability of the survival of the rolling in rough sea may be defined as the ratio between the areas of the safe basin obtained for the case with and without wave excitation. Such diagrams are constructed for both the intact and the damaged vessel, and for the considered sea state $h_{1/3}$ = 2.5 m, Figs.10 and 11. The vessel speed U = 0, 2 and 4 m/s is a parameter and the heading angle is a variable. The probability of survival of the floating vessel, U= 0 m/s, is minimum for beam seas, and it is larger for the intact than for the damage condition. Quartering seas are very dangerous for the stability of the voyaging vessel. The probability of survival for both the

310

intact and the damaged vessel is considerably reduced at high speed and $\chi = 60^0$ and 56^0 respectively, Figs.10 and 11. Therefore, the vessel in quartering seas has to reduce speed and/or change direction in order to avoid capsizing.

Fig. 9. Capsize boundary of damaged vessel, $h_{1/3}$=2.5 m, U=4 m/s, χ=56°
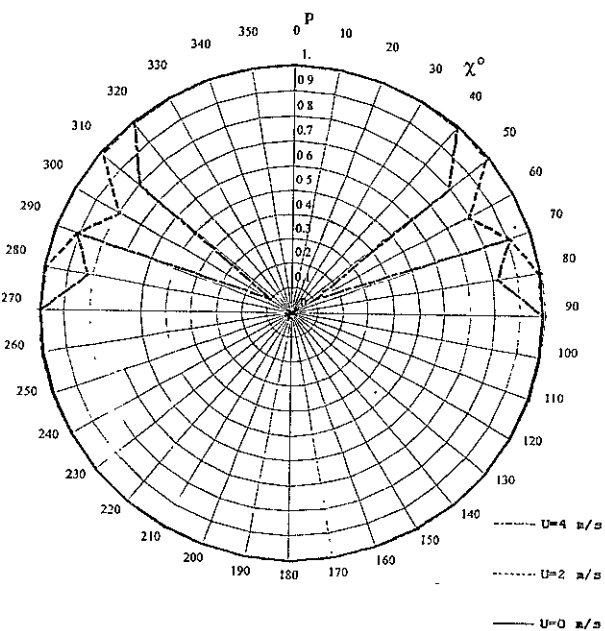
Fig.10 Probability of intact vessel's survival $h_{1/3}$ = 2.5 m

Fig.11 Probability of damaged vessel's survival $h_{1/3}$ = 2.5 m

4. CONCLUSION

The stability criteria which are based on ship hydrostatics are not sufficient to ensure ship dynamic stability. Therefore, ship stability has to be analysed within rolling and capsizing in rough sea as a nonlinear random process. The time integration of the governing differential equation of motion is preferable. The initial value plane as a control space is a very useful visual presentation of ship behaviour. This may be also used for the construction of the survival probability diagram.

In order to bring this new approach to practical use it is necessary to extend the investigation to coupled ship motion, better definition of hydrodynamic coefficients, more reliable wave excitation, sloshing effect for damaged ships, etc. /18/. Such a probabilistic definition of ship stability has to be verified experimentally /19/. In the meantime, the survival diagrams like those given in Figs.10 and 11 may be used onboard to avoid dangerous situations.

311

REFERENCES

1. *** Principles of Naval Architecture, Volume I - Stability and Strength - edited by E.V. Lewis, SNAME, Jersey City, NJ, 1988.

2. Cartmell M.- Introduction to Linear, Parametric and Nonlinear Vibrations-Chapman and Hall, London, 1990.

3. Dahle E.A., Nisja G.E.- Intact and damaged stability of small crafts with emphasis on design, International Conference on Design Considerations of Small Craft, RINA, London, 1984.

4. Thompson J.M.T.- Basic concepts of nonlinear dynamics- Proc. IUTAM Symp. Nonlinearity and Chaos in Engineering Dynamics, London, July 1993.

5. Senjanović I.- Harmonic analysis of nonlinear oscillations of cubic dynamical systems- Journal of Ship Research, Vol.38, No.3, Sept. 1994, pp.225-238,

6. Cardo A., Francescutto A., Nabergoj R.- Nonlinear rolling response in a regular sea, International Shipbuilding Progress, 31, 3, 1984.

7. Kan M., Taguchi H.- Chaos and fractals in capsizing of a ship- Proceedings of NADMAR'91, 1991.

8. Peyton J.C., Cankaya I.- Generalized harmonic analysis of nonlinear ship roll dynamics- Journal of Ship Research, Vol.40, No.4, 1996, pp.316-325.

9. Price W.G., Bishop R.E.D.- Probabi-listic Theory of Ship Dynamics- Chapman and Hall, London, 1974.

10. Lloyd A.R.J.M.- Seakeeping: Ship Behaviour in Rough Weather- Ellis Horwood Limited, Chichester, UK, 1989.

11. Senjanović I., Parunov J., Ciprić G.- Safety analysis of ship rolling in rough sea -Chaos, Solitons and Fractals, Vol. 8, No. 4,1997, pp.659-680.

12. Senjanović I., Ciprić G., Parunov J.- Survival analysis for fishing vessel rolling in rough sea- The 6th International Symposium "Technics and Technology in Fishing Vessel", Ancona, 1997.

13. *** Intact Stability Criteria for Passenger and Cargo Ship- IMO, 1987

14. *** Norme relative alla stabilità delle navi, Registro Italiano Navale- edicioni 1/1/91, 1991.

15. Tabain T.- Temporary navy standard for sea state at the Adriatic, Brodarski institut, Zagreb, 1977 (in Croatian).

16. Cardo A., Contento G., Francescutto A., Copola C., Penna R.- On the nonlinear ship roll damping components, NAV'94, Roma, 1994.

17. Senjanović I., Lozina Ž.- Application of the harmonic acceleration method for nonlinear dynamic analysis, Computers and Structures, 47, 6, 1993, pp.927-937.

18. Oh I., Nayfeh A. and Mook D.- Theoretical and experimental study of the nonlinear coupled heave, pitch and roll motions of a ship in longitudinal waves- 9th Symposium on Naval Hydrodynamics, Seoul, Korea, 1992.

19. Francescutto A., Contento G.- An experimental study of the coupling between roll motion and sloshing in a compartment- 4th International Offshore and Polar Engineering Conference, Osaka, Japan, 1994.

STOCHASTIC IDENTIFICATION OF ROLLING MOTION PARAMETERS: TOWARDS AN ON-LINE ASSESSMENT OF SHIP STABILITY

Dr. Andreas A. Debonos
Naval Architect and Marine Engineer
129 Lombardóu Str., 114 75 Athens, Greece

ABSTRACT

The persisting significant number of ship casualties due to capsize, involving even cases where the established stability criteria appear to be in principle satisfied, inaugurated efforts to develop methods for more realistic stability assessment, based on the dynamic behavior of the vessel in a seaway, taking also into account the probabilistic nature of the wave excitation.

As the rolling motion is closely associated to the phenomenon of capsizing, effective identification of rolling parameters is a safe start towards that dynamic assessment of ship stability. Some new techniques for parametric estimation of roll are outlined hereby, capable to handle a non-linear model for rolling, by processing solely roll histories, without need of the wave excitation record. This is suitable for on-line applications, since only the roll angles can be recorded using instrumentation on board, as the wave excitation cannot be readily measurable in the proximity of the ship.

1. STATEMENT OF THE PROBLEM

1.1 Ship Stability and Capsize

Ship stability, that is the situation of non-capsizing of the ship considered as a floating rigid body subject to perturbations about its equilibrium, without ambiguity about this state, is a special concern for the naval architect and the ship operator. Stability problem has been receiving attention for over a hundred years, and the particular difficult task of establishing rules for preventing ship capsizing has grown up from cumulative experience of failures. It must be noted, that despite the greater sophistication of both shipbuilding and navigational aids, capsizing caused by severe weather and/or from shifting cargo remains a paramount factor causing shipping casualties.

Given the intrinsic difficulty in translating the stability definition into the language of symbols, there is a need to decide on the measure of ship stability. That means that stability can only be practically defined with respect to certain disturbances, the measure of which compared to pre-set critical values provides the required stability assessment.

In this context, the approach which is currently in widespread use, is based entirely on static considerations. It involves simple and direct checks of the static righting lever curves (i.e., the vessel's roll restoring moment characteristics as a function of the roll angles in still water) to insure that they satisfy specific criteria derived from the casualty records of a large number of actual known losses. These criteria are closely related to the hull form geometry and the mass distribution of the ship, making no explicit use of external forces or motion characteristics. In this view, other significant factors affecting stability are ignored, such as the excitation process, the damping and the non-linearities in the ship motion model; the latter seems to play a significant role, particularly in cases involving high amplitude roll angles.

The rather crude static stability criteria, based on an entirely empirical approach, are in these days of questionable value in assessing safety. Recent developments in ship dynamics modelling and experimental techniques, and advances in computer technology have now made possible undertaking research on more realistic and effective stability criteria.

The development of stability criteria taking full account of vessel's dynamics in a realistic environment needs certainly serious difficulties to overcome, thus, it is widely recognized as long term process. Over the years, several proposals for modification to the still-water stability regulations have been made (example the IMO's proposal for the "weather criterion" on 1986), but doubts have been expressed about their suitability for wider application, principally because they are again based on a static or pseudo-dynamic treatment and the effect of waves is not explicitly modelled.

1.2 Ship Rolling Motion and Capsize Mechanism

The phenomenon of capsizing is strongly connected to the behavior of the ship in rolling, given that the former is always preceded by large amplitudes of rolling motion. In that context, capsize may be regarded as a departure of roll response trajectories from a stable to a globally unstable behavior.

The rolling motion of a ship may reach dangerously large amplitudes leading to capsize due to an adverse combination of factors, some external to the ship, including environmental conditions (i.e., winds, waves, currents, temperature changes etc.), or some internal, as the displacement, the metacentric height, or the shape of the righting moment lever curve as a function of the roll inclination. External factors have long been recognized and treated as probabilistic. The internal ones are also subject to variability, maybe not performing the same random character of the external factors, however their variations may be substantial and to some extent uncontrolled; for instance, both internal and external factors with interdependencies between them may affect the variability of

the restoring moment curves (see Caldwell and Yang, 1986).

The risk that a given ship with a given set of characteristics will capsize, which clearly represents a safety measure for ship stability, consequently is continuously affected by many varying parameters. An On-Line ship stability assessment, in form of analytical knowledge of the current conditions related to the rolling motion is, therefore, essential for the safe and financially efficient operation of the ship.

In this respect, and given that the rolling behavior is a matter for probabilistic (rather than deterministic) analysis, the ability to predict the probability of the roll amplitudes reaching a specific critical level in a specific sea state is a matter of considerable practical importance. It has been shown, that, at least in the case of beam wave excitation, a single-degree-of-freedom model can be used as a basis for prediction purposes, where the rolling motion is considered to be uncoupled from the other lateral motions (sway and yaw) experienced by the ship (see Roberts, 1982). A reasonably good agreement between theoretical predictions, obtained by the method of stochastic averaging and experimental results, has been demonstrated for a model ship rolling in beam waves in a wave tank (see Roberts and Dacunha, 1985). Furthermore, for an accurate prediction of large amplitude roll, it is necessary to include non-linearities in both the damping and the restoring moment terms of the equation of motion. Extensive experimental work has suggested that a simple linear-in-the-parameters representation is sufficient; but the problem of determining the parametric values for a specific ship remains, and it forms the main focus of my work.

1.3 Limitations of existing work to be surpassed

Since non-linearities exist in both the roll damping and the restoring moments, and both the wave input and the roll response are stochastic in nature, it is evident that the . development of identification techniques efficient in solving the rolling motion prediction problem is a complex and difficult task. Moreover, the estimation

314

approach must be applicable on-line.

Although restoring moment parameters can, in principle, be computed from hydrostatics and a knowledge of the mass distribution of the ship, it is not possible to predict the damping parameters from hydrodynamic theory. As an alternative to the theoretical prediction, based on fluid dynamic theory, one can attempt to estimate the appropriate ship roll parameters from experimental data. Recent work (see Countzeris et al., 1991) has shown that it is possible to estimate all the parameters from experiments on a ship rolling in irregular seas, if simultaneous records of the roll response and the wave height are available. Typical results have been found to agree with those obtained from either free-decay, or forced roll experiments. This approach is useful when studying the behavior of scale models in a wave tank. However, for full scale ships at sea, it is generally not possible to obtain time histories of the wave height in the vicinity of the ship. One is, therefore, forced to rely on estimates derived solely from measurements of the variation of the roll response with time.

In principle, it is possible to deduce all the required parameters in a single-degree-of-freedom ship roll model, if a stochastic model for the excitation is assumed. If a linear model is adopted, and the excitation is assumed to be a wide-band process, then one can estimate the roll natural frequency (and hence linear restoring moment parameter) by frequency domain (spectral analysis) or time domain methods (average zero-crossings). The linear damping coefficient may also be estimated from the spectrum of the response. Unfortunately, for large amplitude motion, which is of our special concern in terms of stability assessment, the effects of non-linearities are significant and application of linear methods yields insufficiently accurate estimates.

Established identification methods as the Invariant Imbedding (previously used to analyze simulated roll data derived from a lightly damped linear model, see Romelling and Jacobsen, 1982) and the Maximum Likelihood method may be applied in principle, but as it is shown they give seriously biased estimates. Discrete-time

ARMA estimation techniques appear also to be applicable, but transformation from continuous to discrete time tends to be ill-conditioned, and the problems associated with this approach are severely compounded when non-linearities are introduced into the continuous model.

In view of the inadequacy of the existing estimation methods as above to give acceptable estimates for the roll model (for an overview see Debonos, 1993), and also their inability to handle non-linearities and the problem of stochastic (practically unknown) excitation, development and testing of novel parametric identification methods has been attempted. These methods are capable of dealing (up to certain extent) with a non-linear roll model with stochastic excitation, using measurements of the roll amplitude only, as it is precisely required for a realistic assessment of stability on-line.

So, it is opened up the possibility of continuously monitoring all relevant ship roll parameters on board the vessel by using a PC and an appropriate inclinometer for measuring the roll angles, and displaying up-to-date information to the officer on watch. Decisions taken by the officer on watch on the basis of this information and of accumulative experience, during a storm for example, could optimize safety.

Furthermore, although these estimation techniques refer specifically to ships - and indeed to the rolling motion of ships - they have much wider applications to a variety of dynamic systems involving stochastic excitation. Examples include the response of structures to wind loading or seismic excitation and the monitoring of land vehicles transversing random surfaces.

2. ILLUSTRATION OF THE SPECIFIC IDENTIFICATION PROBLEM

As it happens in numerous previous studies, the non-linear rolling motion of a ship in irregular seas is modelled by the following equation of motion of a non-linear oscillator:

$$dx_2/dt + a_1 x_2 + n_1 x_2 |x_2| + a_2 x_1 + n_2 x_1^3 = f(t) \quad (1)$$
$$x_1 = x(t) \quad (2)$$
$$x_2 = dx_1/dt \quad (3)$$

where $x(t)$ the roll time history, a_1, n_1 and a_2, n_2 the linear and non-linear damping and stiffness factors respectively; $f(t)$ is assumed to be a stationary stochastic process with zero mean. If the bandwidth of this input process is significantly greater than that of the response, $f(t0$ may be approximated as an ideal white noise with a correlation function of the form of the Delta (Dirac) function with a scalar $D = 2 \pi S_0$, where S_0 is the constant spectral level of the white noise process which approximates $f(t)$.

It is also convenient to consider a partly linearized version of Eq. (1). This involves the replacement

$$a_1 x_2 + n_1 x_2 |x_2| \rightarrow a_{1eq} x \qquad (4)$$

where a_{1eq} is the equivalent linear damping parameter. Standard statistical linearization provides a relationship between linear, quadratic and equivalent linear damping, and the standard deviation of the velocity of x (see Roberts and Spanos, 1990).

The specific identification problem which is to be addressed is as follows: how can a sample function of the response $x(t)$, over a period $0 < t < T$, be processed to yield estimates of the system parameters a_1, a_2, n_1, n_2 and D?

3. SUMMARY OF THE DEVELOPED ESTIMATION METHOD

Given the inherent difficulty to estimate all the required parameters, particularly to separate the linear and the quadratic damping terms for the non-linear model, a combined estimation technique has been optimized, making use step by step of identification methods with non-uniform theoretical basis. These can be summarized as follows (for a review of all the possible methods from which the optimum estimation path is selected, see Debonos, 1996). It also needs mentioning, that though both stiffness parameters are obtained directly, the damping parameters can only be estimated in two successive identification steps:

1. *Moment method to estimate a_2 and n_2.*
From the stationary moment equations of 2nd and 4th order corresponding to the

system modelled by Eq.(1), one can easily formulate an algebraic system of equations 2 x 2 resulting in the following simple formulae for a_2 and n_2, $E()$ denoting expectation :

$$a_2 = [E(x_2^2)/E(x_1^4)-3E(x_1^2 x_2^2)/E(x_1^6)]$$
$$/[E(x_1^2)/E(x_1^2)-E(x_1^4)/(x_1^6)] \qquad (5)$$
$$n_2 = [E(x_2^2)-E(x_1^2)a_2]/E(x_1^4) \qquad (6)$$

2. *Spectral method to estimate a_{1eq}.*
A spectral relationship can be derived from Eq.(1) with the substitution from (4), by transcribing it into frequency domain. Using standard spectral relationships for the derivatives of processes, one obtains :

$$F(\omega) = (\omega^4 + a_{1eq}^2 \omega^2 - 2 a_2 \omega^2 + a_2^2) S_{xx} + n_2^2 S_{zz} + 2 (a_2 - \omega^2) n_2 S_{xzr} + 2 a_{1eq} \omega n_2 S_{xzi} = S_0 \qquad (7)$$

where $y = x_2 |x_2|$, $z = x_1^3$, S_{vu} (cross) spectra of the magnitudes v and u defined by the Fourier relationship; subscripts r and i denote, respectively, the real and imaginary parts of the cross spectra. All spectral quantities in Eq.(7) except S_0 can be estimated from the response sample function via the FFT algorithm. By minimizing the cost function J

$$J = \Sigma [S_0 - F(\omega)]^2 \qquad (8)$$

over a sufficient number N of discrete frequencies, using a standard optimization algorithm one can obtain estimates for the parameter a_{1eq}, the excitation level S_0 considered as one more unknown.

3. *Energy envelope method for separating linear and quadratic damping terms*
This method is based on the stationary solution of the Fokker-Planck-Kolmogorov (FPK) equation governing the probability density function of the energy process $E(t)$ of the system, which may be approximated as a one-dimensional continuous Markov process :

$$w(E) = k A(E)$$
$$e\{-2 [a_1/D_2 E + n_1/D_2 g(E)]\} \qquad (9)$$

where, $w(E)$ can be readily estimated as the energy density histogram of the roll record, $A(E)$ and $g(E)$ are known functions dependent on a_2, n_2 (the latter supposed

316

already estimated) and peak amplitude b, and k a normalization factor. Clearly estimates of $a_1/D^2 = e_1$ and $n_1/D^2 = e_2$ can be found by fitting Eq.(9) to estimates of w(E) derived from the histogram of the estimated energy levels.

4. *Statistical linearization equations to find* a_1, n_1 *and* D

If one has already estimated e_1 and e_2, the statistical linearization equation (see Roberts and Spanos, 1990)

$$a_{1eq} = a_1 + 2 n_1 D / (\pi a_{1eq})^{1/2} \qquad (10)$$

provides the third source of information to compute by using a conventional numerical method (ex. Newton-Raphson) the unknown terms a_1, n_1 and D.

4. METHOD VALIDATION THROUGH SIMULATION

To test the proposed method, simulated sample functions of the roll angles x(t) were generated by numerically integrating Eq.(1) for realistic values for the parameters, using a Runge-Kutta algorithm. Two types of Gaussian excitation processes were used in the study - white noise and correlated excitation. The simulation method is described by Roberts et al., 1994.

Four particular cases studied are summarized in the following tables:

Table 1

Stiffness estimation results for a system fully non-linear (four cases with overall damping ζ 7.4%, 3.1%, 7.4% and 3.1% respectively

Expected a2	Estimated a2	Expected n2	Estimated n2
White Noise Excitation			
0.504	0.499	3.0	2.988
0.504	0.501	3.0	2.992
Correlated Noise Excitation			
0.504	0.485	3.0	2.668
0.504	0.496	3.0	2.827

Table 2

Damping and excitation intensity estimation results for the same four cases presented in Table 1

Expected Values			Estimated Values		
a1	n1	D	a1	n1	D
White Noise Excitation					
0.012	0.350	0.132	0.027	0.331	0.135
0.006	0.140	0.090	0.008	0.113	0.078
Correlated Noise Excitation					
0.012	0.350	0.140	0.002	0.341	0.121
0.006	0.140	0.095	0.008	0.134	0.081

5. CONCLUSIONS

Based on the above and also on more results from a multitude of specific examples chosen for study, here follow the principal conclusions drawn:

1. All the parameters can be estimated from response measurement alone.

2. Separation of linear and non-linear damping contributions is more difficult than estimating their stiffness counterparts, and estimation can be achieved in two identification steps.

3. A white noise approximation is adequate for the cases studied, and the (equivalent for the case with correlated excitation) white noise intensity is correctly estimated.

6. REFERENCES

1. Caldwell J.B. and Yang Y.S., Risk and Reliability Analysis Applied to Ship Capsize: A Preliminary Study, Proc. Intern. Conf. on the Safeship Project: Ship Stability and Safety, RINA, 1986, Paper No.3.
2. Roberts J.B., A Stochastic Theory for Non-Linear Ship Rolling in Irregular Seas, Journ. of Ship Research, SNAME, Vol.26, 1982, pp. 229-245.
3. Roberts J.B. and Dacunha N.H.C., Roll Motion of a Ship in Random Beam Waves : Comparison between Theory and Experiment, Journal of Ship Research, SNAME, Vol.29 No.2, 1985, pp. 112-126.
4. Kountzeris A., Roberts J.B. and Gawthrop P.J., Estimation of Ship Roll Parameters from Motion in Irregular Seas, Trans.of the RINA, Vol.132, 1991, pp. 253-266.
5. Romelling J.U. and Jacobsen B.K., At Sea Measurements for Identification of Stability, Proc. of 14th OTC, Houston, Paper No.4389, 1982, pp. 173-176.
6. Debonos A.A., Estimation of Non-Linear Ship Roll Parameters Using Stochastic of Identification Techniques, PhD Thesis, Univ. Sussex U.K., 1993.
7. Roberts J.B. and Spanos P.D., Random

Vibration and Statistical Linearization, J.Wiley & Sons, Chichester, 1990.

8. Debonos A.A., Digital Computer Aided Assessment of Dynamic Ship Stability Parameters, Proc. Intern. Conf. Circuits, Systems and Computers, Hellenic Naval Academy, 1996, pp. 165-170.

9. Roberts J.B., Dunne J.F. and Debonos A., Stochastic Estimation Methods for Non-Linear Ship Roll Motion, Probabilistic Engineering Mechanics, Vol.9, 1994, pp. 83-93.

ON THE DIRECT COMPUTATION OF LARGE AMPLITUDE MOTIONS OF FLOATING BODIES IN REGULAR AND IRREGULAR WAVES: THE NUMERICAL WAVE TANK APPROACH. AN APPLICATION TO SUBHARMONIC OSCILLATIONS IN STEEP WAVES.

Written contribution by Giorgio CONTENTO

Department of Naval Architecture, Ocean and Environmental Engineering
University of Trieste
via A. Valerio, 10 - 34127 Trieste, Italy
e-mail: contento@univ.trieste.it

Wave loads on fixed structures and motions of floating bodies in waves have been studied since long ago. The human challenge to more and more difficult environmental conditions (floating production platforms installed in 1000 m depth and even more with 20-30 m height design waves) asks for reliable predictions both in the ocean/coastal engineering field and in the ship design.

In the past the complexity of the fully hydrodynamic approach has driven the researchers to some gross simplifications in the general mathematical formulations of the fluid-body interaction problem. In the case of fixed bodies, wave loads have been evaluated according to some simplified models, let us mention the *Morison* force *[1950]* for small bodies or the linear diffraction methods for large bodies *[Mac Camy-Fuchs, 1954]*. In the case of freely floating or partially restrained bodies, linear and non-linear dynamics (Ordinary Differential Equations) have often taken it upon themselves to substitute the complex hydrodynamics, charging some concentrated parameters with the hard task to represent the whole physical phenomenon (damping, excitation, ...). This method has been specifically applied to the simulation of the motions that feature a strongly nonlinear behaviour, like ship rolling in extreme conditions, whereas moderate amplitude heave and pitch motions have been successfully approached by the linear radiation-diffraction theory *[Salvesen et al., 1970]*.

Despite their approximation of the actual situation, ODE based methods are of fundamental help in disclosuring basic phenomena that characterise the behaviour of a nonlinear system (saturation, bifurcation, ultra-subharmonic oscillations, chaos,...) *[Thompson, 1997]*. In some cases they give all the needed answers about the behaviour of the body at sea *[Contento et al., 1996; Francescutto et al., 1997]* and can be a powerful basis for an improvement of rules towards ship safety.

Nowadays the possibility of direct hydrodynamic computations of fully nonlinear wave-body interactions is closer. Large steps have been and currently are done in the computational fluid dynamics field and in particular in the simulation of unsteady free surface flows.

In response to the ocean engineering call for nonlinear wave loads prediction to deal with some new platforms typologies (ringing and springing of TLP, slow drift oscillations, ...), several numerical tools dedicated to the higher order *[Chakrabarti, 1990; Kriebel, 1990]* or fully nonlinear *[Lalli et al., 1995]* diffraction problem have been developed and are currently and successfully applied to large structures design.

On the contrary, though wave loads on small structures (jacket type) have been dealt since the early beginning of the oil production era through the consolidated Morison's type methods, still the question on the incident wave kinematics in the presence of steep unsymmetric

waves remains (rigorously speaking) unanswered. Stretching methods *[Wheeler, 1970]* are generally used when no further informations are avilable.

Both the attempt to pursue the fully-nonlinear way in wave loads predictions on large fixed bodies and the call for accurate wave kinematics in the Morison method witness the practical need to extend the presently used linear hydrodynamic models to fully nonlinear ones.

In this context the so called 'Numerical Wave Tank - NWT' approch looks very promising. The way to deal with fully nonlinear waves has been drawn by the pioneering work of *Longuet-Higging et al. [1976]*. Since then many applications have appeared in literature. They refer to both the environmental description (a recent work by *Wang et al. [1995]* has shown the applicability of the NWT to the study of the instabilities of wave trains leading to wave grouping and ultimately breaking) and the wave-body interaction.

Some difficulties are still encountered in the simulations of freely floating body motions. The body exact approach applied to fully 3D computations still seems to be a privilege of few researchers *[Isaacson, 1982; Dommermuth et al., 1987; Lin et al., 1997]* whereas several papers and applications have appeared in the 2D case *[Cointe, 1990; Contento, 1995; Faltinsen, 1977; Sen et al., 1989; Sen, 1993; Vinje, 1981; Zhao, 1993]*.

Contento and Casole [1995] have presented some numerical results concerning the physical characteristics of the waves generated in a numerical wave tank by a flap wavemaker. The application of the procedure to the free floating body problem and some meaningful results have been presented too *[Contento, 1995; 1997]*.

A further application of the NWT method consists in the computation of the motions in waves of 2D shipsection-like bodies in the presence of free surface inviscid *[Tanizawa, 1996]* or viscid *[Francescutto et al., 1996]* liquids on board.

As an example, some results concerning an application of the NWT approach to nonlinear ship motions are here presented. For an exhaustive description of the mathematical model and numerical features, refer to *Contento and Casole [1995]*. The powerfulness of the method in capturing particular nonlinear phenomena of the roll motion is evidenced. A body with a square cross section, the draught corresponding to half side, is subjected to a train of steep regular waves. The dimensions and mechanical characteristics of the body are approximately those of a container in the intact condition: B=1.625 m, T=0.650 m, M=1057 kg, I_G=7530 kgm^2, KG=0.532 m, GM=0.132 m, natural roll frequency ω_0=0.486 rad/s. The amplitude of the wavemaker motion has been chosen in order to generate waves with a steepness approximately 1/16. In Figs. 1 to 3 the time records of the motions of the body in waves are shown for the wave frequencies ω=2ω_0, ω=2.5ω_0 and ω=3ω_0. A quasi steady state behaviour is obtained, mostly for the heave and sway superposed to a steady drift. The time records corresponding to ω=2ω_0 are unfortunately not long enough because in this situation the immersion of the "deck" of the body has occurred with a consequent code failure.

Despite the relatively small amplitude of the roll motion, a typical nonlinear behaviour is observed. From a preliminary visual analysis of the time record, it seems that after the wave front has reached the body, the roll exhibits some synchronous oscillations but subsequently it loses the synchronism with the excitation showing oscillations dominated by the natural roll period. This behaviour can be observed for all the frequencies used. To check this qualitative observations and obtain quantitative informations, a Fourier analysis with a moving time window has been applied to the time series of the roll. The results of this analysis in terms of components amplitude are reported in Fig. 4 for the case ω=2ω_0, in Fig. 5 for the case ω=2.5ω_0 and in Fig. 6 for the case ω=3ω_0. It can be seen from these plots, mostly in the cases ω_{wave}=2.5ω_0 and ω_{wave}=3ω_0, that, at least in the available time records, a quasi steady state amplitude of the subharmonic oscillation is obtained, i.e. the

amplitude of the Fourier components corresponding to the natural roll frequency ω_0 keeps a steady value. The cause of the presence of this subharmonic response could be attributed to the small roll damping obtained in the approximation of the inviscid flow and at the same time by the large amplitude excitation. To check the influence of the damping, a further run of the code has been performed in the case $\omega_{wave}=2\omega_0$ with an additional linear damping term $-b_{44}\dot{\phi}$ in the RHS of the roll equation, assuming

$$b_{44}\sqrt{B\Big/2g}\Big/MB^2 = 0.013.$$ The results of this computation are plotted in Fig. 1 (dashed line). Basically, the only distinguishable differences from the previous case (with wave damping only) are found in the amplitude of the roll motion, the values at peaks being obviously lower with the additional damping but the subharmonic behaviour being still present.

This comparison has to be considered in a qualitative sense, but the capability of a fully hydrodynamic approach to capture nonlinear phenomena is well evidenced. As a matter of fact, though the introduction of an additional damping term in the roll motion equation does not explicitly modify the fluid flow around the body and in particular does not introduce any viscous effect like vortex shedding, which would probably play an important role in extreme situations like these $H_{wave} / B = 1.9 \div 2.7$, some meaningful informations about the intrinsic nonlinear behaviour of the body in waves derive automatically from the fully hydrodynamic method.

This is nothing but one of the many possible applications of the NWT method to ship motions. The way is open.

References

Chakrabarti, S.K., 1990, 'Nonlinear Methods in Offshore Engineering', Elsevier.
Contento, G., 1995, A Numerical Wave Tank for the Free Floating Body Problem, *Proc. 10th Int.*
Workshop on Water Waves and Floating Bodies, Oxford.
Contento, G., Casole, S., 1995, On the Generation and Propagation of Waves in a Numerical Wave Tank, *Proc. 5th Int. Conference on Offshore and Polar Engineering ISOPE'95*, The Hague, Netherland, Vol. 3, pg. 10-18.
Contento, G., Francescutto, A. Piciullo, M., 1996, On the Effectiveness of Constant Coefficient Roll Motion Equation, *Ocean Engineering*, Vol. 23, 597-618.
Contento, G., 1997, Numerical Wave Tank Computations of Nonlinear Motions of 2D Arbitrarily Shaped Free Floating Bodies, to appear on *Ocean Engineering*.
Dommermuth, D.G., Yue, D.K.P., 1987, Numerical Simulation of Nonlinear Axisymmetric Flows with a Free Surface, *Jou. Fluid Mech.*, Vol. 178, 195-219.
Faltinsen, O.M., 1977, Numerical Solutions of Transient Nonlinear Free Surface Motions Outside or Inside Moving Bodies, *Proc. 2nd Int. Conf. Num. Ship Hydro.*, Berkeley, 347-357.
Francescutto, A., Contento, G., Armenio, V., 1996, A Fully Hydrodynamic Approach to the Motion in Waves of Ships with Free Surface Liquids on Board, *Proc. 11th Int. Workshop on Water Waves and Floating Bodies*, Hamburg.
Francescutto, A., Contento, G., 1997. Bifurcations in Ship Rolling: Experimental Results and Parameter Identification Technique, to appear.
Hogben, N., Standing, R.G., 1975, 'Experience in Computing Wave Loads on Large Bodies', *Proceedings, Offshore Technology Conference*, Dallas, Texas.
Kriebel, D.,L., 1990, 'Nonlinear Wave Interaction with a Vertical Circular Cylinder. Part I: Diffraction Theory', *Ocean Engineering*, Vol. 17, n° 4, pp. 345-377.
Isaacson, M.St. Q., 1982, Nonlinear-wave Effects on Fixed and Floating Bodies, *Jou. Fluid Mech.*, Vol. 120, 267-281.
Lalli, F., Di Mascio, A., Landrini, M., 1995, 'Nonlinear Diffraction Effects Around a Surface-Piercing Structure', *Proc. 5th Int. Conference on Offshore and Polar Engineering ISOPE'95*, The Hague, Netherland, Vol. 3, pg.314-323.
Lin, W.M., Weems, K., Zhang, S., Salvesen, N., 1997, LAMP (Large-Amplitude Motions Program) for Ship Motion Simulations and Wave Load Predictions, *ONR Workshop on "Computational Ship Hydrodynamics"*, David Taylor Model Basin.
Longuet-Higgins, M.S., Cokelet, E.D., 1976, The Deformation of Steep Surface Waves on Water. I A Numerical Method of Computation, *Proc. Royal Society of London*, A, Vol. 350, 1-26.
Mac Camy, R.C., Fuchs, R.A., 1954, 'Wave Forces on Piles: A diffraction Theory', U.S. Army Corps of

Engineering, Beach Erosion Board, Tech. Memo, No. 69, Washington D.C.

Morison, J.R., O'Brien, M.P., Johnson, J.W, Schaff, S.A., 1950, 'The Force Exerted by Surface Waves on Piles, Petroleum Trans., *AIME*, Vol. 189, pg. 149-157.

Salvesen, N., Tuck, E.O., Faltinsen, O.M., 1970, Ship Motions and Sea Loads, *Trans. SNAME* , Vol. 78, 250-287.

Sen, D., Pawlowsky, J.S., Lever, J., Hinchey, M.J., 1989, Two-Dimensional Numerical Modelling of Large Motions of Floating Bodies in Waves, *Proc. 5th Int. Conf. Num. Ship Hydro.*, Hiroshima, 257-277.

Sen, D., 1993, Numerical Simulation of Motions of Two-Dimensional Floating Bodies, *Jou. Ship Research*, Vol. 37, 307-330.

Tanizawa, K., 1996, A Nonlinear Simulation Method of 3-D Body Motions in Waves, Extended Formulation for Multiple Fluid Domains, *Proc. 11th Int. Workshop on Water Waves and Floating Bodies*, Hamburg.

Thompson, J.M.T., 1997, Designing Against Capsize in Beam Seas: Recent Advances and New Insights. *Appl. Mech Rev*, Vol 50, 307-325.

Vinje, T., Brevig, P., 1981, Nonlinear Ship Motions, *Proc. 3rd Int. Conf. Num. Ship Hydro.*, Paris, 257-268.

Wang, P., Yao, Y., Tulin, M., 1995, 'An Efficient Numerical Tank for Non-linear Water Waves, Based on the Multi-Subdomain Approach with BEM', *Int. Jou. Num. Meth. in Fluids*, Vol. 20, 1315-1336.

Wheeler, J.D., 1970, 'Method for Calculating Forces Produced by Irregular Waves', *Jou. of Petroleum Tech.*, 359-367.

Zhao, R., Faltinsen O.M., 1993, Water Entry of Two-Dimensional Bodies, *Jou. Fluid Mech.*, Vol. 246, 593-612.
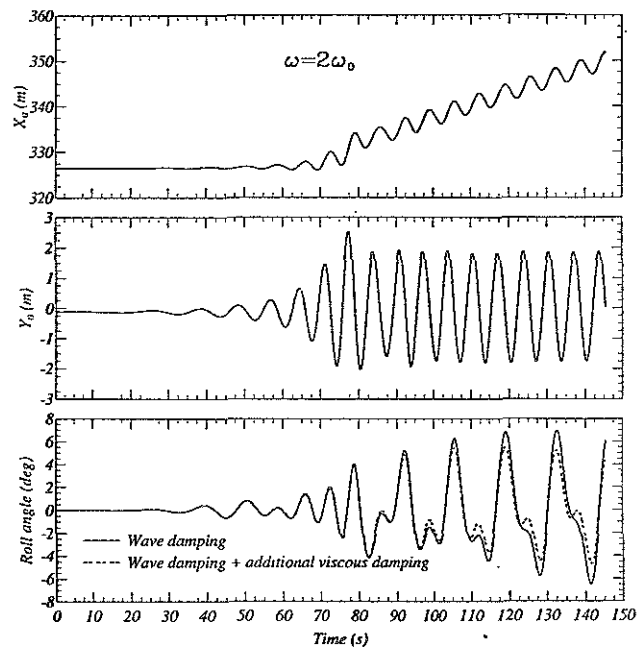
Fig. 1   Time records of the motions of the body when $\omega_{wave}=2\omega_0$. The dashed line corresponds to the simulation with an additional damping term in the roll equation. The roll motion exhibits a typical subharmonic behaviour.
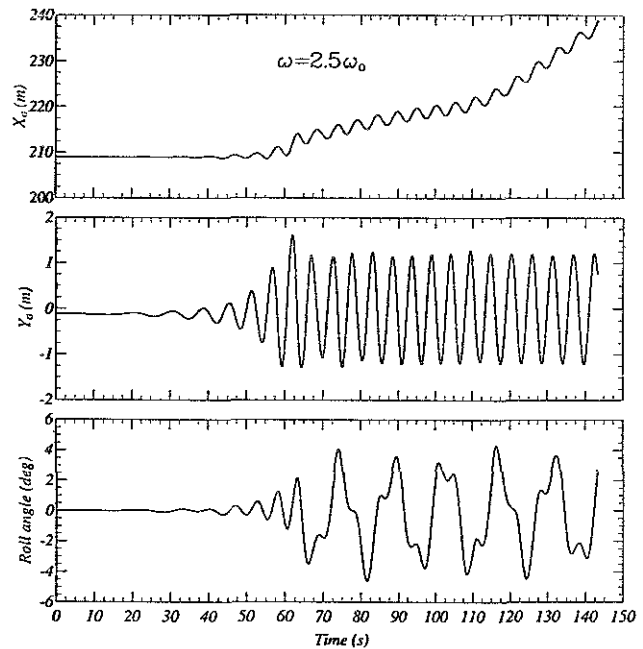

Fig. 2   Time records of the motions of the body when $\omega_{wave}=2.5\omega_0$. The roll motion exhibits a typical subharmonic behaviour.
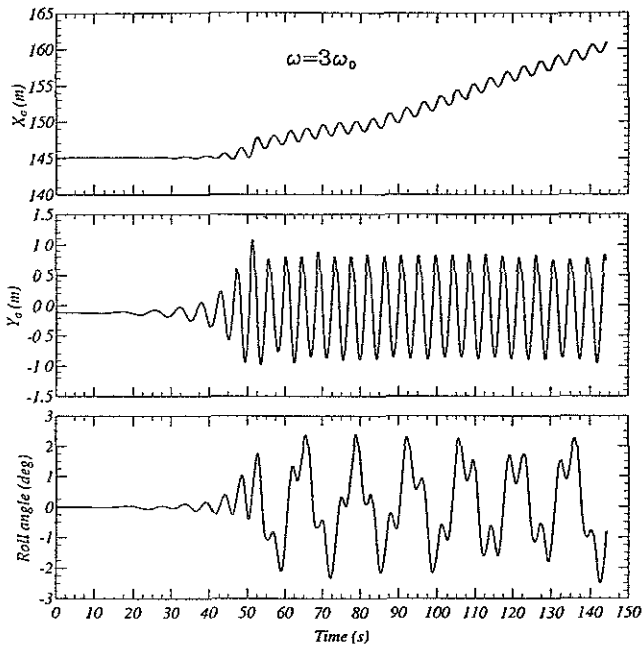
Fig. 3   Time records of the motions of the body when $\omega_{wave}=3\omega_0$. The roll motion exhibits a typical subharmonic behaviour.
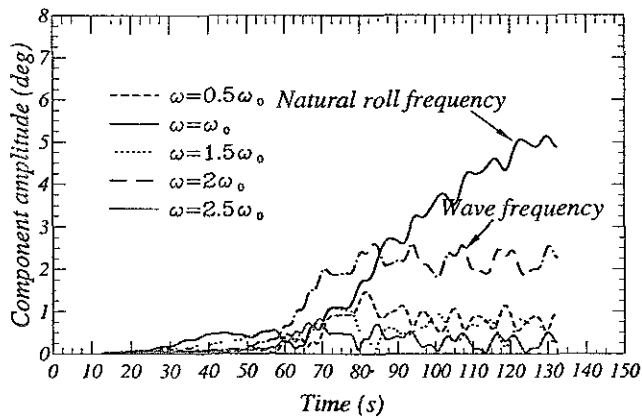
Fig. 4   Fourier analysis of the roll with moving time window when $\omega_{wave}=2\omega_0$. Each line corresponds to the amplitude of different Fourier components.
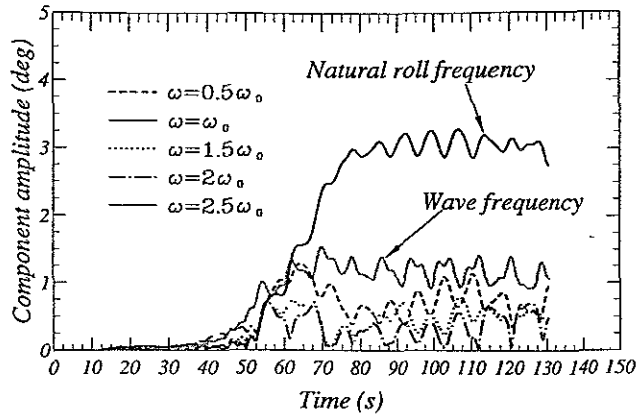
Fig. 5   Fourier analysis of the roll with moving time window when $\omega_{wave}=2.5\omega_0$. Each line corresponds to the amplitude of different Fourier components.
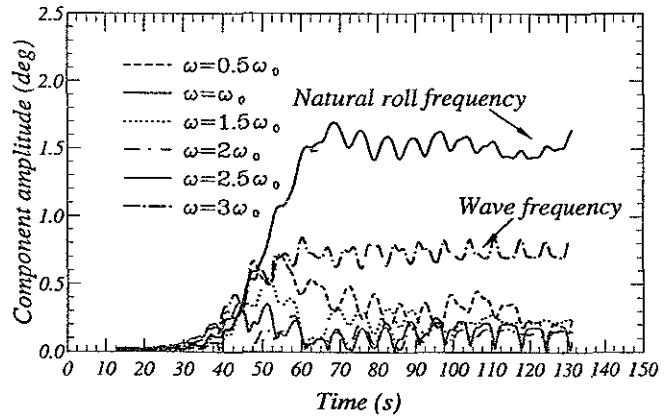
Fig. 6   Fourier analysis of the roll with moving time window when $\omega_{wave}=3\omega_0$. Each line corresponds to the amplitude of different Fourier components.

323

CONTEMPORARY REMARKS ON CLASSIC WEATHER CRITERIA

V.L. Belenky and N. Umeda
National Research Institute of Fisheries Engineering,
Ebidai, Hasaki, Kashima, Ibaraki, 314-04, Japan

ABSTRACT

This paper describes that classic weather criteria can be justified for capsizing with harmonic roll motion in beam seas. By focusing on roll motions in the vicinity of vanishing angle, effect of wave moment for a energy balance and relationship with chaos and bifurcation are remarked. Moreover, it is pointed out that weather criteria have some shortcomings for harmonic motion in quartering seas, subharmonic motion and so on.

1. INTRODUCTION

Capsizing is a transition to oscillation near a stable position that is dangerous from practical point of view (Sevastianov, 1979) Since capsizing is a great threat for a ship, crew and passengers, national and international stability criteria have been established to prevent capsizing. While most of them are almost empirical, weather criteria, such as IMO Res. A. 562, can be regarded as physics-oriented criteria, because they directly take wind and wave effect into account.

The IMO weather criteria were established by combining domestic criteria of Japan (Yamagata, 1959) and Soviet Union (Blagoveshchensky 1932). The main idea of these criteria is an energy balance concept, and can be found in literature in 1910's and 1920's. Therefore nowadays these criteria can be regarded as rather classic. That is, after these days ship dynamics has developed very much and now discuss even that chaos can be found in

ship roll motions. Thus some theoreticians often ignore the weather criteria without their effort to examine the significance of the criteria. Some practical people sometimes try to extend the weather criteria without reminding the theoretical background of the criteria. Both of these movements might disturb a proper progress in the field of ship stability. Thus this paper examines the weather criteria with contemporary ship dynamics and discusses a research direction in ship stability for future.

2. OUTLINE OF WEATHER CRITERIA

A ship is assumed to be in beam wind and waves without forward velocity as the most dangerous situation. As shown in Fig.1, the ship is inclined to an angle, ϕ_0, by a steady beam wind and roll owing to wave action to angle of roll ϕ_1. Then, adding a gust wind pressure, a balance of restoring energy and heeling energy is examined with the GZ curve and heeling lever. That is, if area 'a' is equal to or greater than area 'b', the ship is regarded as capsized. Because, once the roll angle exceed the unstable equilibrium, ϕ_c, the ship definitely capsizes as far as time-dependent external moment does not exist. The formula to calculate the roll angle, ϕ_1, was approximately obtained by assuming harmonic resonance with non-linear damping moment in irregular waves. Although some theoretical inconsistency is found, the obtained roll angle is assumed to correspond to the average of 1/200 highest.
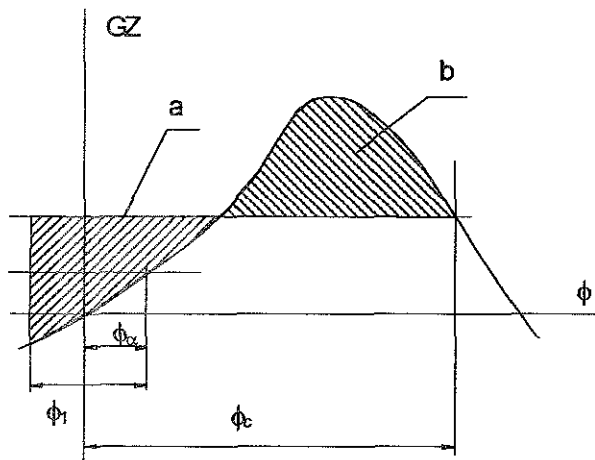
Fig 1 Energy balance stage of weather criterion

3. BACKGROUND OF WEATHER CRITERIA

From a contemporary view point, some questions can raise for the above weather criteria. Mechanic of solid body give us several methods to find out what are conditions of capsizing, and the method of energy balance is just one of them. These methods could be classified in three major groups by assumptions applied·

- Motion stability analysis (capsizing is a loss of motion stability)
- Phase plane methods (capsizing is a crossing of separatrix on phase plane)
- Piecewise linear methods (GZ curve is presented as a broken line in vicinity of angle of vanishing stability)

Development of these methods allows us to consider weather criterion wider than in 40s and 50s when it was originally implemented. So we shall understand weather criterion as an indicator of ship's ability to keep her stability in severe weather conditions, in particular, to withstand squall of wind during her rolling motion in beam seas.

However, a dynamic system describing capsizing of a ship has severe nonlinearity in righting term; it should include at least three positions of equilibria: two stable (upright and upside down) and unstable one between them (angle of vanishing stability). Due to absence of strict theoretical methods, approximate and indirect ones have to be applied. One of the

most popular of them is motion stability method. Its development started form simple determination whether rolling motion is stable or not (Wellicom 1975, Ananiev 1981) and then considered more general problem on nonlinear behaviour of ship.(Nayfeh 1986, Virgin 1987, Cardo and Francescutto 1981) and coupling with extensive numerical analysis led to safe basin and transient capsize diagram concepts (Rainey and Thompson 1990).

This analysis highlighted complexity of nonlinear phenomena involved in nonlinear behaviour study such as fold and flip bifurcations, deterministic chaos, high orders resonances and sensitivity to initial conditions. Dealing with these phenomena we should remember about adequacy mathematical models, trying to find out if they are qualities of nature or consequence of applying our assumptions. The most natural and evident (and expensive) way to do it is an experimental one (Marshfield and Wright 1980, Francescutto 1994). The other way (that is additional to the previous one) is to compare the above results with the ones yielded by another mentioned methods. At least, if the different assumptions lead to the same results, there is a serious possibility that qualities of the nature reflected more or less correctly.

The second mentioned above method (phase plane method) allows to utilise classic concept of separatrix (phase trajectory that divides area of attraction of different stable equilibria points). The event of capsizing is associated here with crossing of phase trajectory of forced motion with separatrix. Main assumption here is that the separatrix could be used for excited motion while, it is the border between two attraction areas for free motion by the definition.

Attempts to validate this approach numerically has been made in 70s by N.Sevastianov and Pham Ngock Hoe (Sevastianov 1977) and some strange behaviour was discovered. The system with one degree of freedom was modelled. Wave excitation was chosen asymptotically regular to avoid influence of initial condition:

326

$$\alpha = \alpha_0(1 - \exp(-p^2t^2))\sin \omega t \qquad (1)$$

where α_0 and w are amplitude and frequency of wave excitation and p is parameter of the speed of increasing waves. Some of phase trajectories contained small motions or 'loops' near angle of vanishing stability, see fig. 2
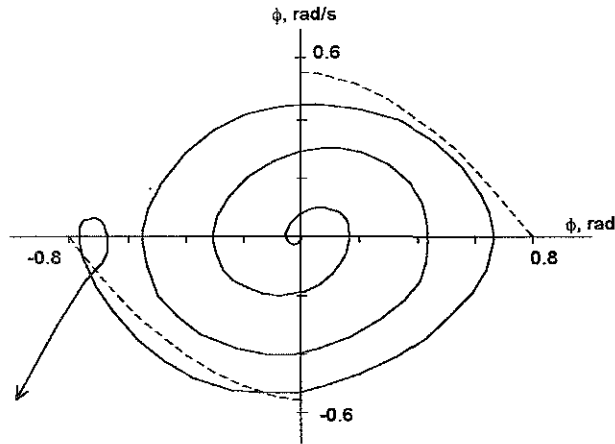

Fig. 2. Result of numerical simulation of ship roll and capsizing. Small motion around unstable equilibrium is present. Separatorices are shown be dashed lines

However the main methodological point of this approach is that it is reflects classical definition of stability (given by Euler and known in contemporary translation from Krylov 1958) in terms of theory of oscillation. The definition says: «we call stability the ability of a ship to float in an upright position and, if inclined under the action of an external cause, to return to the above said position after the external cause ceased acting». Physical meaning of this definition was questioned in (Sevastianov 1977): why external forces should disappear at the moment when we would like to learn about stability ? However, simulation showed that all crossings of separatorices were «punished» by capsizing that demonstrated practical value of classical definition.

Another merit of this approach is clear and simple transition to probabilistic capsizing: Separatorices yield safe basin where combine probability density should be integrated in order to receive probability of non-capsizing. Recent investigation by one of the authors allows to propose even more simple formula for this matter (Umeda 1992):

$$P(X) = \int_{-\infty}^{\phi_a} f_-(\phi)d\phi + \int_{\phi_b}^{\infty} f_+(\phi)d\phi \qquad (2)$$

This formula takes into account air pressure due to wind squall and time: the probability of capsizing during one period of roll oscillation is produced here. Here $f_-(\phi)$ is distribution density of roll amplitudes, see for detail (Umeda 92). Safe basin is shown in fig. 3.
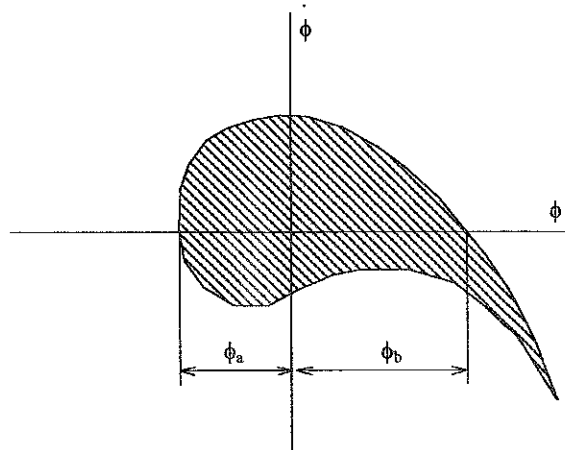
Fig. 3 Safe domain in case of asymmetrical rolling

However the question why we can «forget» about excitation in the moment of determination of stability still important for phase plane method, even if we know that we can do that for practical calculations. Analogous question arises for classic weather criteria why can we ignore wave exciting moment or time-dependent external moment at the stage of energy balance. One of the authors recently solved this question (Belenky, 1993) using piecewise linear approach.

Normally GZ curve has a non-linear nature shown on fig. 4. If we consider a capsizing as a transition process to another equilibrium, a general topology should be kept. Even the simplest piecewise linear presentation allows to do that, see fig.4.

If necessary the presentation on figure 4 can be easy generalised for multy range broken line coupling with true nonlinear curve before the maximum of the GZ curve, see fig.5.See (Belenky 1997) for details. We will proceed our consideration with the presentation on fig.4 for simplicity sake.
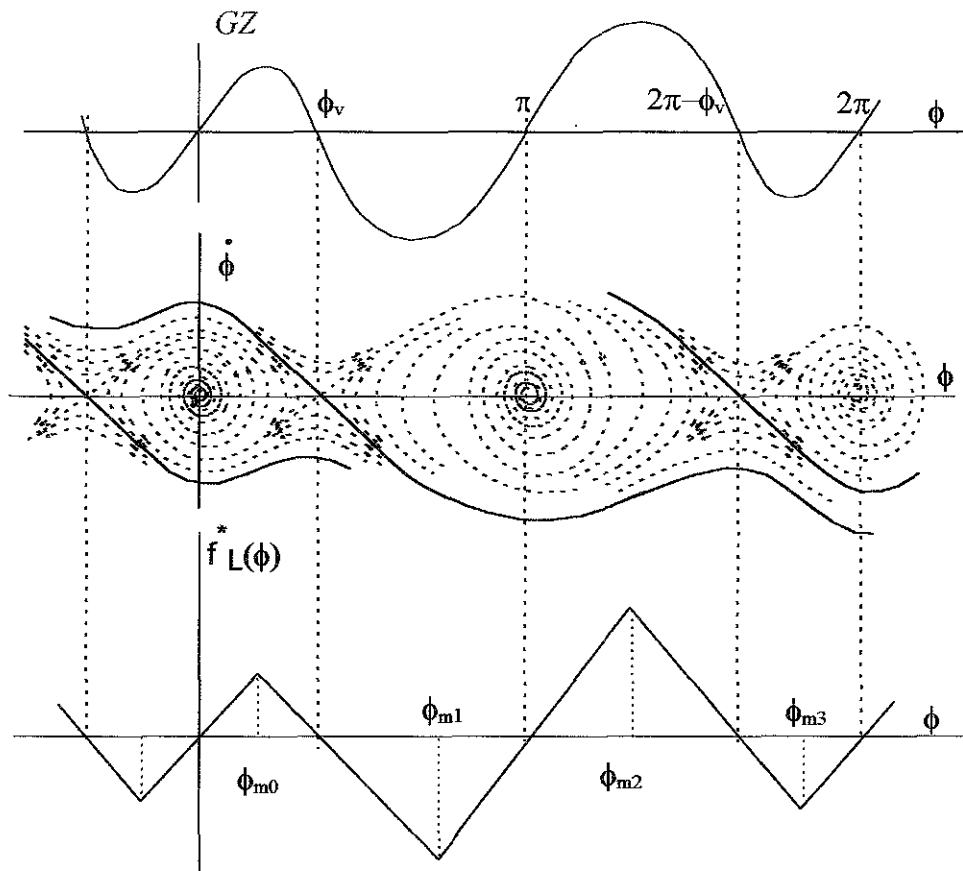
Fig. 4 GZ curve, its piecewise linear presentation and phase plane of rolling
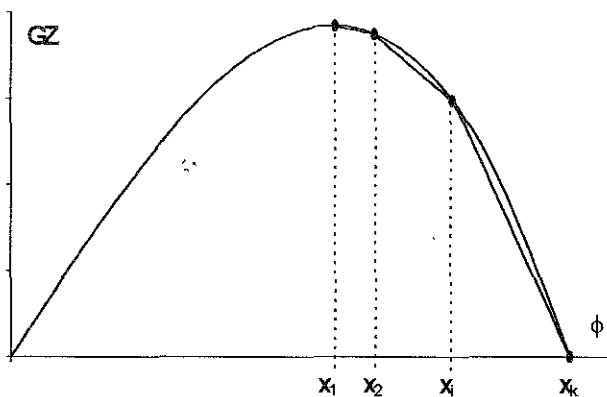
Fig. 5 Piecewise presentation of the decreasing part of GZ curve

If we focus on the vicinity of vanishing angle, ϕ_v, that is, $\phi_{m0} < \phi < \phi_{m1}$, however, the GZ curve can be approximated to be linear. Here we define this zone as the zone 1 and the zone of $-\phi_{m0} < \phi < \phi_{m0}$ as the zone 0. Ship motions are

normally observed within the zone 0 and quite rarely exceed ϕ_{m0}. In the zone 1, the uncoupled roll motion can be modelled with the following equation.

$$\ddot{\phi} + 2\delta\dot{\phi} + \omega_\phi^2 k_{f1}(\phi_V - \phi) = \alpha_E \sin(\omega\tau_1 + \varphi_1) \quad (3)$$

Here δ: roll damping coefficient, ω_ϕ: natural circular frequency in roll around an upright position, k_{f1}: angle coefficient of piecewise linear approximation, α_E: wave exciting coefficient and ω: exciting circular frequency. Since this differential equation is the second-order linear one with constant coefficients, the following solutions of it are easily found.

$$\phi(\tau_1) = Ae^{\lambda_1\tau_1} + Be^{\lambda_2\tau_1} +$$
$$+ p_a \sin(\omega\tau_1 + \beta_1 + \varphi_1) + \phi_V \quad (4)$$

Here

$$\lambda_{1,2} = -\delta \pm \sqrt{\omega_\phi^2 k_{f1} + \delta^2} \quad (5)$$

328

$$A = \frac{\left(\dot{\phi}_1 - \dot{p}_1\right) - \lambda_2\left(\phi_1 - p_1\right)}{\lambda_1 - \lambda_2} \qquad (6)$$

$$B = -\frac{\left(\dot{\phi}_1 - \dot{p}_1\right) - \lambda_1\left(\phi_1 - p_1\right)}{\lambda_1 - \lambda_2} \qquad (7)$$

$$p_a = \frac{\alpha_E}{\sqrt{\left(k_{f1}\omega_\phi^2 + \omega^2\right)^2 + 4\delta^2\omega^2}} \qquad (8)$$

$\dot{\phi}_1$ is the initial value of roll angular velocity of zone 1. Figures p_1 and $\dot{p}_1$ are the initial values of angle and angular velocity of excited roll motion, respectively. Paying attention to that $\lambda_1 > 0$ and $\lambda_2 < 0$, we can see, that.

$$A > 0 \qquad \lim_{\tau_1 \to \infty} \phi(\tau_1) = +\infty \qquad (9)$$

$$A < 0 \qquad \lim_{\tau_1 \to \infty} \phi(\tau_1) = -\infty \qquad (10)$$

$$A = 0 \qquad \left|\phi(\tau_1)\right| < p_a + \phi_v \qquad (11)$$

If $A > 0$, the ship capsizes. Because, the roll angle exceeds ϕ_{m1}. If $A < 0$, the ship returns to the zone 0. Thus, the ship does not capsize as far as this upcrossing in roll at ϕ_{m0}. Within this approach, capsizing occurs only if $\phi(t)$ exceeds ϕ_{m0} and $A > 0$.

The formula (8) for amplitude of partial solution within zone 1 has the same structure that well known formula for amplitude of forced stable state linear oscillation. The only difference is that there is sum instead of subtraction under square root. This «small» change leads to impossibility of resonance peak and to dramatic decreasing of the value of amplitude p_a in comparison with the one at zone 0, see fig. 6

This means that contribution of the external excitation decreases significantly at the zone 1. In other words, wave exciting moment need not be taken into account for the final capsizing movement while it have to been taken for the normal roll motion around the upright position. This important conclusion explains why classical definition is correct and justified the framework of the weather criteria.
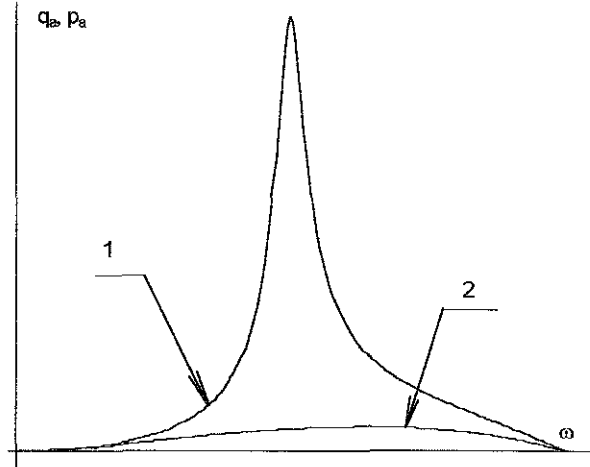
Fig. 6 Response curves of partial solutions on zone 0 (curve 1) and zone 1 (curve 2). Taken from (Belenky 1993).

In case of $A = 0$, equation (4) indicates that the ship experiences a periodic motion as an excited oscillation around ϕ_v. This periodic motion is unstable because small perturbation from $A = 0$ results in escape from the zone 1.

An example of phase trajectory when evolution when A is nearly equal to 0 is shown on figures 7 till 13, taken form (Belenky 97). All the curves shown were calculated for conditions: $\alpha_E = 0.22$, $\phi_{m0} = 0.5$, $\delta = 0.1$ s^{-1}, $k_{f0} = k_{f1} = 1$ s^{-2}, $\phi_v = 1$, $\omega = 0.72$ s^{-1}.

Origin of the 'strange' behaviour near angle of vanishing stability including small motion and 'loop' (see fig.2) becomes clear from these figures. The reason is small value of A that allows the other members of equation (4) put their contribution to the motion.
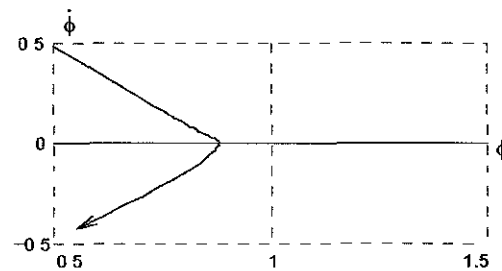
Fig. 7 $\dot{\phi}_1 = 0.48$; A = -0.003
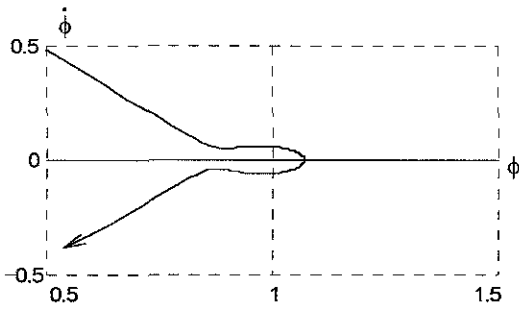
Figure 8 $\dot{\phi}_1$=0.48616; A = -2.903 10^{-6}
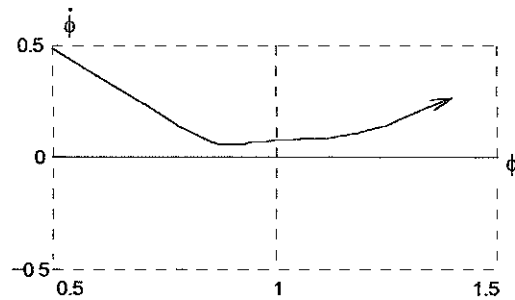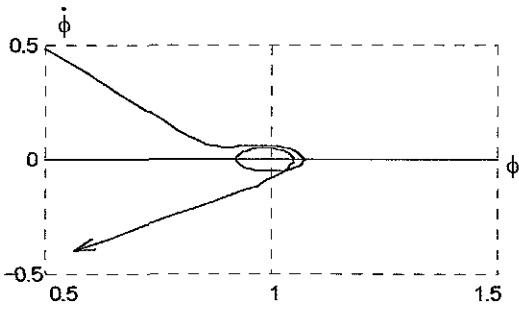
Fig. 9 $\dot{\phi}_1$=0.4861657; A = -3.870 10^{-8}
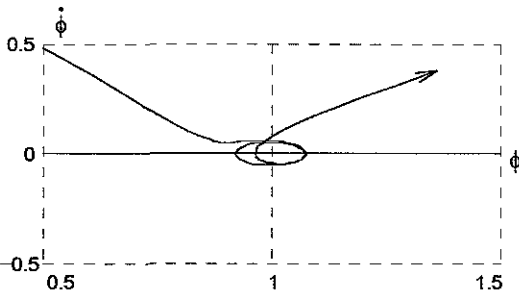
Figure 10 $\dot{\phi}_1$=0.48616578 A = 1.502 10^{-9}
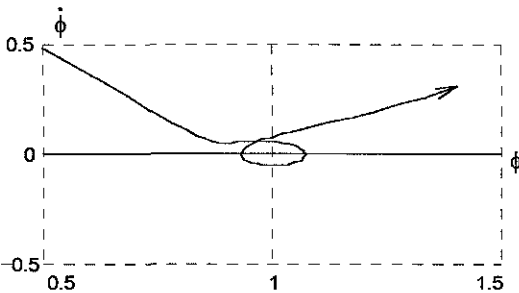
Figure 11 $\dot{\phi}_1$=0.486167 A = 6.146 10^{-7}
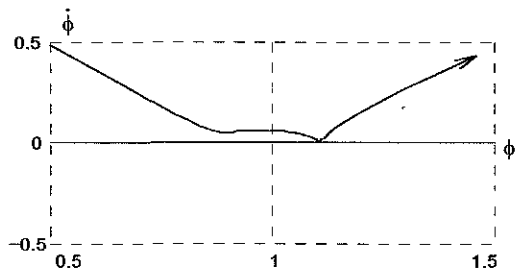
Figure 12 $\dot{\phi}_1$=0. 4863 A = 6.745 10^{-5}

Fig 13 $\dot{\phi}_1$=0. 487 A = 4.192 10^{-4}

This small motion possesses super-sensitivity to small changes of initial condition. See, for example, fig. 9 and 10: changing the value $\dot{\phi}_1$ in 7th digit leads to changing the order of the arbitrary constant A. Of course, this phenomenon could be observed in certain range of the initial condition providing small values of A.

This super-sensitivity could be considered as another aspect of chaotic behaviour. The difference with known chaotic behaviour that is yielded from the consequences of flip bifurcation is follows: flip bifurcation is a phenomenon of stable state regime of the oscillation, while the above super-sensitivity phenomenon occurs during transition process. At the same time, both cases could be reflection of one nature phenomenon: instability accompanying to the motion in vicinity of unstable equilibrium. In other words, probably we see that transition from one stable equilibrium to another one goes through chaos.

On the other hand practical needs of stability standards seems not to require such sophisticated nonlinear study - if we roughly estimate capsizing boundary from a practical view point, we do not have to pay so much attention to bifurcations and chaos. However exact understanding of capsizing nature is necessary to establish rational stability criteria and, therefore nonlinear study is important.

4. BEYOND WEATHER CRITERIA

To satisfy weather criteria, lowering KG is desirable, of course. If KG is lowered, GM is heightened and then the area «b» can increase to exceed the area «a». On the other hand, heightening KG can be another means to satisfy

weather criteria. If *KG* is heightened, *GM* is lowered and then natural roll period increases. When the natural roll period becomes very large, no resonance between existing ocean waves and roll can be expected As a result, the roll angle calculated within weather criteria becomes very small. Thus, weather criteria shall judge this ship with very large *KG* to be safe. This shortage of weather criteria had been pointed out firstly by Yamanouchi (1975). Then numerical calculation of capsizing probability in beam seas based on the one of the authors method (Umeda 1992) confirmed that this problem often occurs for existing large ships.

As far as a ship experiences only a harmonic motion in beam seas, increasing natural period beyond ocean wave periods is a theoretical solution to avoid capsizing. However, if the ship runs in following or quartering seas, the Doppler effect can make the encounter period larger and larger, even up to infinity. Therefore, operational conditions where the encounter period is equal to the natural period can exist. Under such operational conditions, harmonic roll motion in quartering seas can develop. In this case, both the reduction of restoring moment at wave crest and the above large harmonic roll may easily induce capsizing. To prevent such danger, one of the authors (Umeda 1994) proposed an operational guidance as an rational extension of weather criteria.

Furthermore, if natural roll period is very long, there is a possibility of subharmonic roll motion. As well as many theoretical works, in a model experiments in irregular waves capsizing events with subharmonic motion were observed. (Umeda et al., 1995) Here the natural roll period was twice as long as the encounter period. If the encounter period becomes extremely large, a kind of resonance with manoeuvring system can occur. Such phenomena known as broaching cannot be handled with weather criteria.

5. CONCLUSIONS

As far as capsizing through harmonic roll motion in beam seas, the classic weather criteria can be justified with contemporary ship dynamics. However, it is necessary to establish more general criterion covering harmonic motion in quartering seas, subharmonic motion and broaching. Chaos can be an important matter mainly when we intend to precisely predict capsizing boundary and for general understanding capsizing phenomenon

REFERENCES

Ananiev, D.M On stability of forced rolling of a vessel with given GZ curve, *Trans. of Kaliningrad Technical Institute*, Vol. 93, "Seakeeping of Ships", Kaliningrad, 1981, (in Russian)

Belenky, V.L. -A Capsizing Probability Computation Method, Journal of Ship Research/ SNAME, 37,(3),1993, pp.200-207.

Belenky, V.L. On the dynamics of piecewise linear system *Proc. of Int. Symp. on Ship Safety in a Seaway: Stability, Maneuverability, Nonlinear Approach (SEVASTIANOV SYMPOSIUM)*, Kaliningrad, 1995, vol.1

Belenky, V.L. Some problems of stochastic dynamics of piecewise linear and nonlinear, Report on seminar at University of Michigan, 13 March 1997

Blagoveshchensky, S.N. On a method of stability standardisation, *Trans. of Scientific Research Institute of Shipbuilding*, 1932 Vol. 12 (in Russian)

Cardo, A., Francescutto, A. and Nabergoj, R. Ultraharmonics and subharmonics in the rolling motion of ship" steady state solution., *International Shipbuilding progress*, Vol.28, No.326, 1981, pp. 234-251

Francescutto, A On the Nonlinear Motions of Ships and Structures in Narrow Band Sea-Dynamics of Marine Vehicles and Structures in Waves/ Elsevier Science Publishers, 1991, pp.291-303.

Francescutto A, Contento G., Penna R. Experimental evidence of strong nonlinear effects in the rolling motion of a destroyer in beam seas, Proc. of the 5th Int. Conf. on the Stability of Ships and Ocean Vehicles, Florida Inst. of Tech.,, Vol. 1, 1994

Hsieh S.R., Troesch A.W. Shaw S.W. A nonlinear probabilistic method for predicting vessel capsizing in random beam seas., Proc. R. Soc. London A (1994), 446, 195-211

Kan, M. et al. Model Tests on Capsizing of a Ship in Quartering Waves, Proc. of the 4th Int. Conf. on the Stability of Ships and Ocean Vehicles, Univ. of Frederico II of Naples, 1, 1990, pp.109-116.

Kan, M., Chaotic capsizing, *Proc. of ITTC.* SCR-KFR Osaka Meeting on Seakeeping performance 1992

Krylov, A.N. Selected papers, Published by Academy of Science of the USSR, Moscow, 1958 (in Russian)

Nayfeh, A.H. and Khdeir, A.A. Nonlinear rolling of ships in regular beam seas, *International shipbuilding progress* Vol. 33, 1986, pp.40

Rainey, R.C.T, Thompson, J.M.T., Tam, G.W. and Noble, P.G. The transient capsize diagram - a route to soundly-based new stability regulations *Proc. of the 4th Int. Conf. on the Stability of Ships and Ocean Vehicles*, Univ. of Frederico II of Naples, 1, 1990

Sevastianov, N.B. Mathematical experiment on ship capsizing under combined action wind and waves, Part 2 of "Investigation of Possibilities of Practical Realisation of Probabilistic Stability Standard" Report of Kaliningrad Technical Institute, No 77-2.1.6 228 p.1977 (in Russian)

Sevastianov N.B. and Pham Ngock Hoeh Boundary between the domains of stable and unstable free ship motion in drift-rolling regime, Trans. of Kaliningrad Technical Institute "Seakeeping of Fishing Vessels", Kalininrgad, 1979, Vol. 81, PP. 17-25 (in Russian)

Umeda, N. et al. -Risk Analysis Applied to the Capsizing of High-Speed Craft in Beam Seas-Proc. of the 5th Int. Symp. on the Practical Design of Ships and Mobile Units/ Elsevier Science Publishers, 2, 1992, pp.1131-1145.

Umeda, N. -Operational Stability in Following and Quartering Seas, Proc. of the 5th Int. Conf.

on the Stability of Ships and Ocean Vehicles, Florida Inst. of Tech., Vol. 2, 1994.

Umeda, N. et al. -Model Experiment of Ship Capsize in Astern Seas, Journal of the Society of Naval Architects of Japan, 177, pp. 207-217.

Virgin, L.N., The nonlinear rolling response of a vessel including chaotic motions leading to capsize in regular seas, *Applied Ocean Research* Vol.9, No.2, PP.89-95, 1987

Wellicome, J.F. An analytical study of the mechanism of capsizing, *Proc. of 1st STAB Conference*, Glasgow, 1975

Wright, J.H.G., Marshfield, W.B. Ship roll response and capsize behaviour in beam seas, *Naval Architect*, No 23, 1980 pp. 129-144

Yamagata, M. -Standard of Stability Adopted in Japan, Transaction of the Institution of Naval Architects, 1959, pp. 413-443.

Yamanouchi, Y. A Study on the Ship Stability Criteria- unpublished, 1975, (in Japanese).

TESTING THE TRANSIENT CAPSIZE DIAGRAM CONCEPT

By

Prof. D. Vassalos*, Dr. K. Spyrou[+] and Dr. N. Umeda[++]
*Director of The Ship Stability Research Centre, University of Strathclyde, UK
[+]Research Fellow, Centre for Non-Linear Dynamics, UCL, UK
[++]Head of Ship Performance Section, Nat. Research Inst. of Fisheries Eng., Japan

SUMMARY

This brief note describes an attempt to test the validity and provide corroborative evidence of the *Transient Capsize Diagram* concept, a methodology proposed by Rainey and Thompson, for developing stability criteria based on chaotic dynamics. This entails the undertaking of a series of capsizing experiments in beam seas in the manoeuvring basin of the National Research institute of Fisheries Engineering in Japan, using a 1/17.5 scale model of a purse-seiner.

1.   BACKGROUND

In simple terms, Thompson and his colleagues, [1]-[3], have studied the problem of a driven mechanical oscillator given by

$$\ddot{\phi} + \beta\dot{\phi} + \phi - \phi^2 = M \sin(\omega t + \varepsilon)$$

This equation is assumed to represent the roll motion of a ship subjected to a beam seas excitation moment M at frequency ω (ε in their studies was taken fixed at 180° with linear damping β at 0.1). The only non-linearity of parabolic restoring implies a softening spring with an underlying total potential energy that has a minimum in the upright state and a maximum at the vanishing angle beyond which the ship can capsize. In this respect, and in the relevant jargon, the problem of ship capsize is a straightforward example of an escape from a potential well.

Considering the above, the four-dimensional *phase-control space* spanned by $\{\dot{\phi}(0), \phi(0), M, \omega\}$ defines the ensuing roll motion.

In a slowly evolving sea state, implying *steady-state* behaviour, the ship motion may be summarised using a *steady-state bifurcation* diagram, Figure 1, which can be derived by tracing the steady states as one of the control parameters, say M, is slowly varied. Steady states can invariably undergo various complicated bifurcations, including jumps to resonance, subharmonic oscillations, chaotic behaviour and ultimately capsize. Repeating this procedure at different ω values, a capsizal boundary can, therefore, be

determined, Figure 2   It is conjectured that all of these can add to the overall understanding of ship behaviour and stability.

In assessing the engineering significance of such investigations the team at UCL concluded that it is too cumbersome and time consuming and, much more to the point, unnecessary and irrelevant. Instead, they rightly propose that in a noisy environment, it is more relevant and simpler to focus attention on *transient* behaviour. This would correspond to a short pulse of regular waves, such as a wave group, impinging upon the ship in otherwise relatively calm weather conditions. This is thought to be a worst-case scenario and a more realistic representation of a sea state than a long train of regular waves. In this case, a *transient safe basin* is defined, containing the set of points in the *phase-control space* referred to above that do not escape (lead to capsize) within a number of forcing cycles, typically 8. At each case, defined fully by the initial conditions in the $\{\dot{\phi}(0), \phi(0)\}$ plane under specified controls (M,ω), all interest is focused on the binary outcome of capsize-non-capsize, making no note of the steady states onto which the non-capsizing motions might settle.

In exploring *transient safe basins*, an important finding offered a platform for the team to propose what they termed a *transient capsize diagram*, Figure 3, as a possible means for developing ship stability criteria. It was observed that, for a given frequency, the erosion of the safe basin is sudden, dramatic and from the centre when a critical level of excitation (wave height) is reached, Figure 4. It was concluded, therefore, that a critical wave height could be determined through either a physical or a numerical experiment by examining transient motions from <u>any</u> initial condition and by implication non other more convenient that the upright equilibrium position   In essence, therefore, the system behaviour was studied by taking <u>all</u> possible initial conditions, in order to ensure that any sensitivity of the non-linear system to such conditions will be catered for, only to find out that ship capsizal resistance is essentially independent of which position the vessel found herself when an extreme critical wave hit her.

Such a wave, determined in turn for a range of relevant frequencies, could be used as an index of *capsizal resistance* for the vessel in question. By linking, finally, the (*steepness, wave period*) loci in the transient capsize diagram to a weather data for a given area of operation, capsizal probabilities can be established, Figure 5.

Summarising the work at UCL concerning the above, the following points are considered to be noteworthy in relation to the problem of ship capsize:

* As a concept, the *transient capsize diagram* is very simple and powerful, and could find application in addressing more practical ship stability problems. Ship stability in beam seas is a problem only for small vessels, which could simply be overturned by large breaking waves, Dahle [5]. The majority of capsizings occur in astern seas, Kan [4], as a result of pure loss of stability, parametric resonance and broaching-to, all of which require a different level of conceptual, mathematical and physical description.

334

- The reason for the above known fact derives from the favourable phasing between heave and roll motions with most ship hulls. This natural attribute of a ship hull is indeed a serious omission in the mathematical model considered and a similar claim can be made on behalf of sway. Considering a coupled non-linear three degrees of freedom model, however, would mean that a 6D phase-space would have to be considered. A crude reminder of how difficult it is to represent reality realistically!

2. VESSEL/MODEL PARTICULARS

The design condition considered in these tests corresponds to the loaded departure condition, the details for which are given in Table 1. The vessel in question is fitted with bilge keels having the following particulars:

$$d_{bk} = 0.35m; \quad l_{bk} = 14.56m$$

The bilge keels are positioned between frames 17-45 (constant frame spacing of 0.52m).

Table 1. Model/Vessel Particulars

Parameter	Vessel	Model (Scale=1/17.25)
L_{oa}	43.00m	2.493m
L_{bp}	34 50m	2.000m
B	7.60m	0.441m
D	3 07m	0.178m
d_f	2.84m	0.165m
d_a	3.14m	0.182m
θ	0.5°	-
C_b	0.652	-
Δ(fresh water)	511.2 tonnes	99.63kg
LCG	-1.741m	-0.101m
V_s	7 355m/s	1.758m/s
KG	3.42m	-
GM	0.755m	-
T_ϕ	7.47sec	-

4. MODEL EXPERIMENTS

Capsizing experiments were undertaken in beam seas for the following reasons:

- The manoeuvring basin at NRIFE is not equipped with model position tracking system which is considered to be essential for capsizing tests in astern seas to be used effectively to validate computer simulation programs

- Capsizing tests in beam seas are easier to perform (or so it was thought) and could fit within the limited period available.

As it turned out, it was necessary to change plans more than once, to produce something meaningful, even with regular wave testing in beam seas. More specifically, the following capsizing experiments were carried out.

Model with bulwark
Observation of a limited number of tests and ensuing model capsizings have led to the conclusion that the principal cause of capsize of the test model was due to the progressive accumulation of water on deck. This phenomenon is particularly difficult to model, on the one hand and, on the other, it is not taken into account in the theoretical work these model tests were aimed to corroborate.

Model without bulwark
As a consequence of the above, the bulwark was subsequently removed from the test model and sample tests performed. In this case, as a result of deck edge submergence, the roll damping of the model was increased substantially beyond the normal level for ships and no capsize was possible, even in the most extreme waves that could be generated by the manoeuvring basin, which in realistic terms were far too severe for the model in question.

Model without bulwark and reduced GM
Following the above, a number of options were discussed in order to progress further, before deciding that the most suitable option, still allowing for corroborative evidence to be produced, was to reduce the metacentric height (GM) of the model. Indeed, following a 30% reduction in GM, successful capsize experiments were undertaken and capsize boundaries in terms of wave heights established in representative wave lengths. As shown below:

<u>Capsizing Model Tests in Beam Seas</u>

- No 307 : Capsizing of model with bulwark at H / λ =1/20; f=0.968 Hz.

- No 321 : Capsizing of model without bulwark and reduced GM at H / λ =1/12; f=0.527 Hz.

5. CONCLUDING REMARKS

Deriving from the above, and taking into consideration the scarcity of experimental evidence linking chaotic dynamics with ship motion dynamics, it could be said that work in this area has not advanced to the point where material of substance could be offered to the practising Naval Architect to enhance or ensure ship safety. Some innovative concepts, however, appear to hold promise for achieving further advances in the field of ship stability but substantial development might be needed together with attempts to link these ideas to the practical ship stability problem.

7. . REFERENCES

[1]   THOMPSON, J.M.T. and SOLIMAN, M.S., "Fractal Control Boundaries of Driven Oscillators and their Relevance to Safe Engineering Design", Proc. R. Soc. Lond. A 428, 1-13, 1990.

[2]   SOLIMAN, M.S., "An Analysis of Ship Stability Based on Transient Motions", STAB'90, Naples, Italy.

[3]   RAINEY R.C.T. and THOMPSON J.M.T., "The Transient Capsize Diagram - A New Method of Quantifying Stability in Waves", JSR, Vol. 35, No 1, March 1991.

[4]   KAN, M., SARUTA, T. and TAGUCHI, H., "Capsizing of a Ship in Quartering Waves", Trans. JSNA, Vols 167-8, 1990.

[5]   DAHLE, E.A., MYRHAUG, D. and DAHL, S.J., "Probability of Capsizing in Steep and High Waves from Side in Open Sea and Coastal Waters", Ocean Engineering, Vol. 15, No 2, 1988.
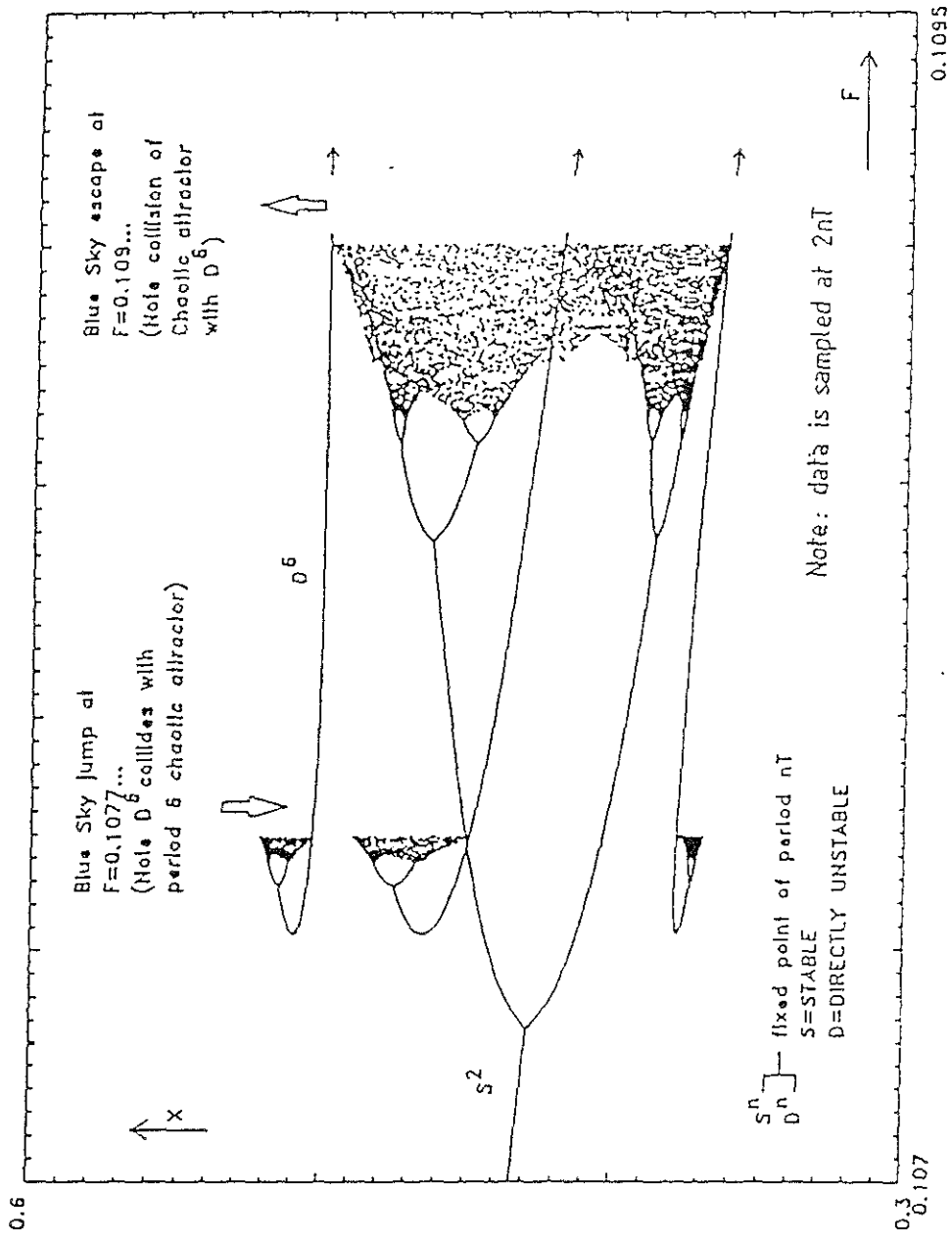
Fig 1: *Evolution of daughter attractors with increasing wave height: the horizontal axis is wave height; the vertical axis is the stroboscopically sampled horizontal coordinate of the attractors in phase space. The excitation frequency is 0.85 times the natural frequency of small roll motions, and the damping of such motions is 5 percent critical.*
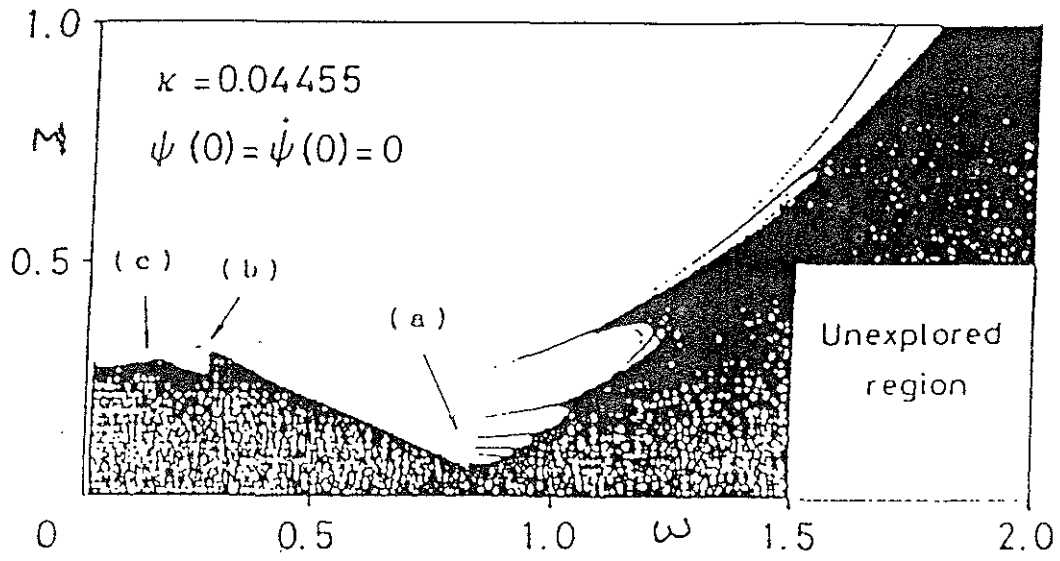
Fig 2: Fractal boundary of safe area in m-ω control space.
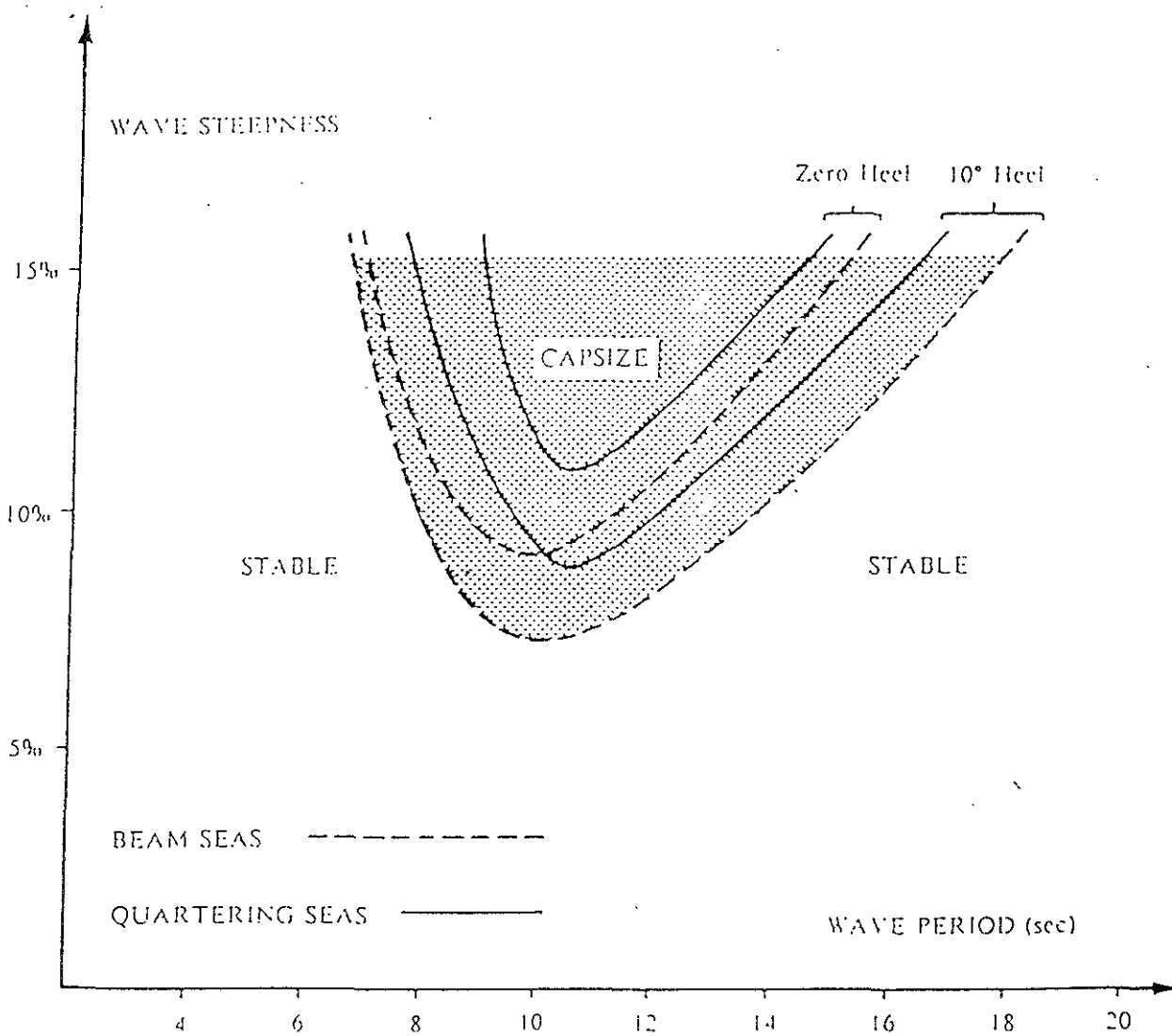
Fig 3: Typical transient capsize diagram.
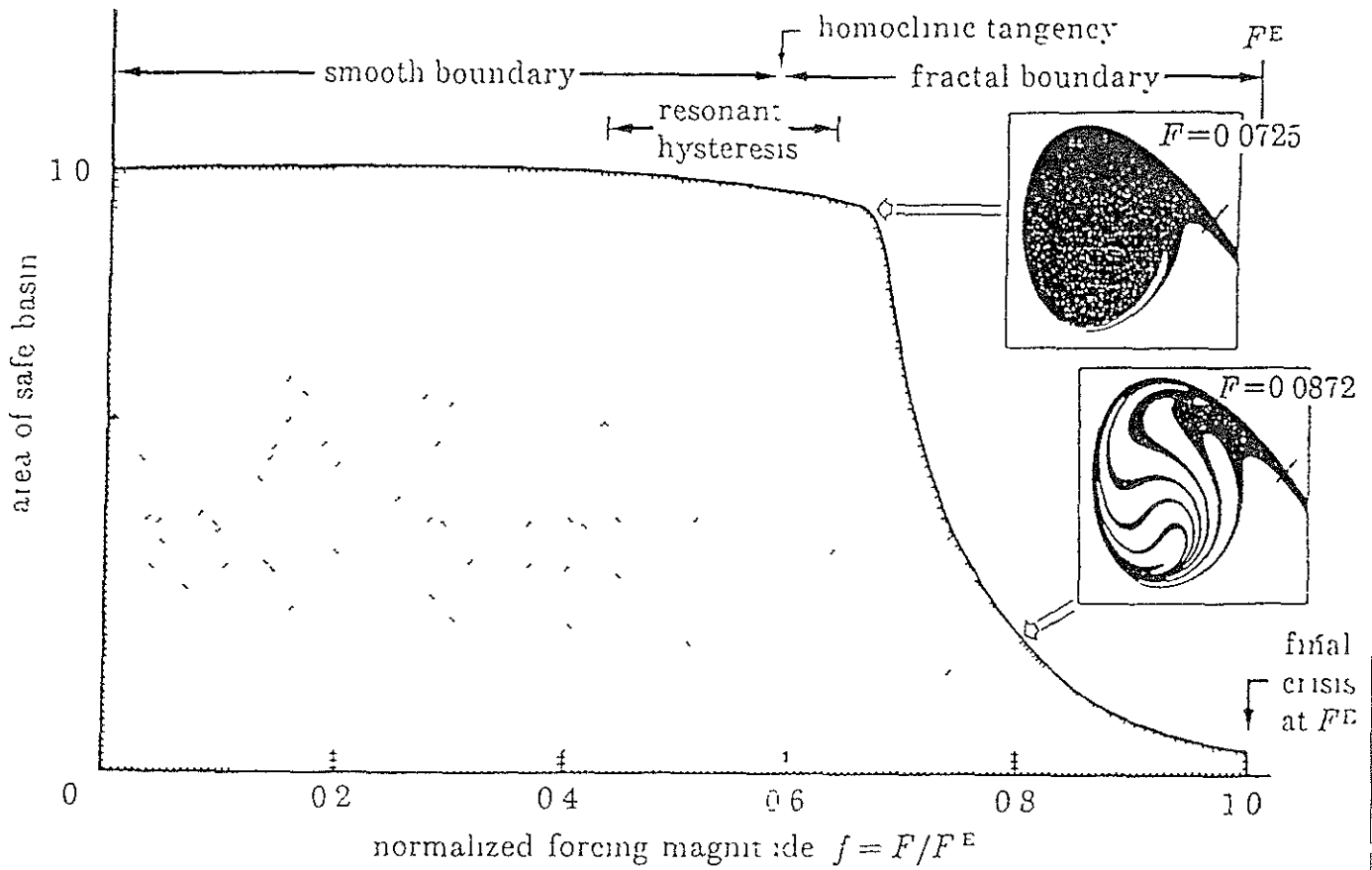
Fig 4   Loss of engineering integrity due to erosion of the safe basin of attraction   The normalized area of the safe basin, within a window, is plotted against the normalised forcing magnitude   Based on high-precision computations by Yoshisuke Ueda

| Group N buoys	All year (554945)										Total
14.75	0	0	0	0	0	0	0	0	0	1	0	1
13.75	0	0	0	0	0	0	0	0	3	0	0	3
12.75	0	0	0	0	0	0	0	2	13	2	1	18
11.75	0	0	0	0	0	0	2	18	12	2	0	34
10.75	0	0	0	0	0	2	21	58	10	2	0	92
9.75	0	0	0	0	0	6	137	79	25	5	0	252
8.75	0	0	0	0	1	152	370	113	33	6	1	675
7.75	0	0	0	0	77	828	582	178	59	10	2	1736
6.75	0	0	0	11	931	1919	845	216	49	9	2	3982
5.75	0	0	2	600	4367	3103	1127	262	43	8	5	9515
4.75	0	0	201	6204	9234	4473	1368	305	70	28	11	21893
3.75	3	28	5293	19238	12949	5283	1576	375	124	43	9	44921
2.75	37	3361	26811	27262	13581	5241	1520	413	133	26	7	78394
1.75	2094	32782	43541	25961	10896	3607	1082	332	95	16	2	120408
0.75	16740	45949	32292	12330	3505	1040	246	69	16	2	0	112188
0	1759	2577	1206	286	53	6	1	0	0	0	0	5889
Total	20634	84696	109345	91892	55592	25659	8876	2421	685	159	40	100000
Period	0	5	6	7	8	9	10	11	12	13	14	

Fig 5: Probabilistic transient capsize diagram.

DEVELOPING AN INTERFACE BETWEEN THE NONLINEAR DYNAMICS OF SHIP ROLLING IN BEAM SEAS AND SHIP DESIGN

K.J. Spyrou, B. Cotton & J.M.T. Thompson

Centre for Nonlinear Dynamics and its Applications
University College London
Gower Street, London WC1E 6BT, UK

ABSTRACT

The possibility to use in ship design certain recent results of the nonlinear analysis of beam-sea rolling in order to maximize resistance to capsize is discussed. The loci of transient and steady-state capsize are approximately located on the plane of forcing versus frequency through Melnikov analysis, harmonic balance and use of the variational equation. These loci can be parametrized with respect to the restoring and damping coefficients. The minimization of the capsize domain leads naturally to the formulation of an interesting hull optimization problem.

1. INTRODUCTION

Recent efforts to understand the mechanism of ship capsize in regular beam seas have revealed enormous complexity in large amplitude rolling response patterns, even though these investigations have relied on simple nonlinear, single-degree models [1]. Whilst the existence of bistability, jumps and subharmonic oscillations near resonance were known from earlier studies based on perturbation-like techniques (see for example [2], [3] on the forced oscillator; and [4] for a more ship-specific viewpoint) a whole range of new phenomena including global bifurcations of invariant manifolds, indeterminate jumps and chaos have been shown recently to underlie roll models with cubic or quartic potential wells. There are good reasons to believe that such phenomena are generic and their presence should be expected for a wide range of ship righting-arm and damping characteristics.

For the practising engineer this new information will be of particular value if it can be utilized effectively towards designing a safer ship. So far, rather than trying to discriminate between good and less good designs in terms of resistance to capsize in beam seas, the current analyses set their focus mainly on developing an understanding of the nature of the nonlinear responses in their various manifestations. However it seems that the time is now ripe for addressing also the design problem. Attempts to develop an interface between nonlinear analysis and ship design are by no means a novelty since they date back, at least, to the discussions about Lyapunov functions in the seventies and early eighties [5], [6]. Nonetheless, a meaningful and practical connection between nonlinear analysis and ship design is still wanting.

In our current research, the main ideas and some preliminary results of which are presented here, we are exploring the potential of two different assessment methods, based on well known approximate escape criteria of forced oscillators. The first method capitalizes upon the so-called Melnikov criterion which provides a fair estimate of the first heteroclinic tangency (homoclinic for an asymmetric system) that initiates erosion of the safe basin, Fig. 1 [7], [8], [9]. In the second method the key concept is the wedge-like boundary of steady-state escape on the *forcing* - versus - *frequency* plane [10], [11],
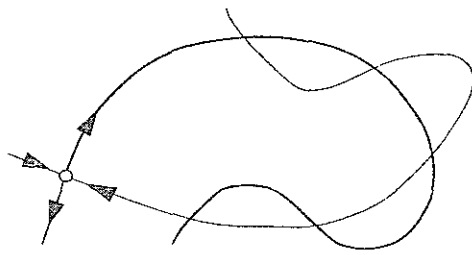
Fig. 1: Intersection of stable and unstable manifolds

[12]. The left branch of this boundary is the locus where jumps to capsize from the lower fold take place, Fig 2. As for the right branch, it is generally practical to assume as such the symmetry-breaking locus near resonance (or, the first flip for an asymmetric system).

These two criteria of transient and steady-state escape should be applied in conjunction with general-enough families of restoring and damping curves. A seventh-order polynomial is often seen as a suitable representation of restoring (see for example [13]). For damping, however, at this stage we shall confine ourselves to the equivalent linear one. Once the roll equation obtains a specific parametric form, expressions can be developed linking the coefficients of the restoring polynomial with damping, forcing and encounter frequency to the capsize loci. The obvious usefulness of these expressions is that they allow us to assess how hull modifications can affect the thresholds of transient or steady-state capsize. This leads to the setting up of an optimization process with governing objective the definition of a hull characterized by maximum resistance to capsize. The procedure offers also the interesting opportunity to evaluate the steady-state and transient criteria against each other, with the view to establishing whether they lead to similar optimum hull configurations.

2. KEY FEATURES OF THE SINGLE--WELL OSCILLATOR

Consider the following single-degree model for ship rolling, [1]:

$$\ddot{x} + D(\dot{x}) + R(x) = B + F\cos(\Omega\tau) \qquad (1)$$

where :
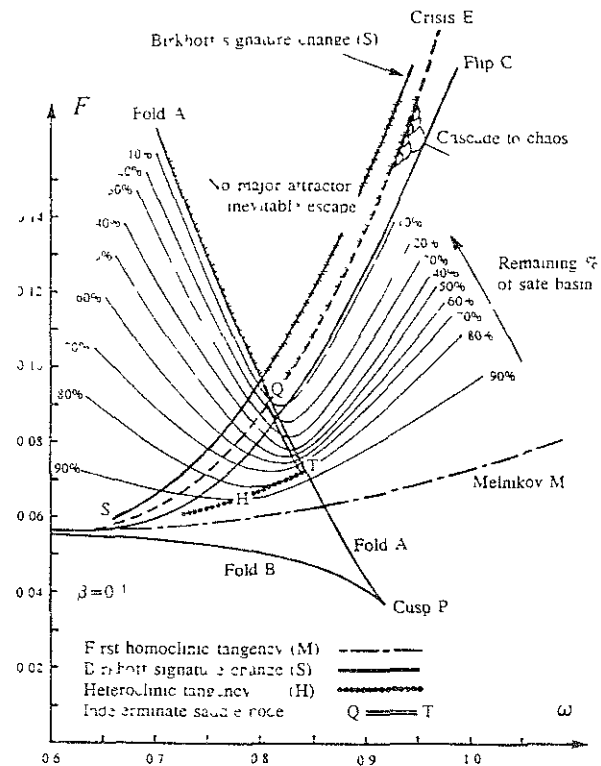
Fig. 2 : Bifurcation diagram of the escape equation, [14].

- x is the scaled roll angle, $x = \phi/\phi_v$,
- ϕ is the actual roll angle,
- ϕ_v is the angle of vanishing stability,
- $D(\dot{x})$ is the scaled damping function,
- $\Omega = \omega/\omega_0$,
- ω is the frequency of encounter between the ship and the wave (as we assume a beam-sea this is also the wave frequency),
- ω_0 is the natural frequency, $\omega_0 = [W\,(GM)/I]^{1/2}$,
- W is the weight of the ship,
- (GM) is the metacentric height,
- I is the second moment of inertia including the added moment,
- F is the amplitude of the scaled external periodic forcing, $F = Ak\Omega^2/\phi_v$,
- Ak is the wave slope,
- B is a scaled constant excitation, for example due to steady wind,
- $R(x)$ is a scaled polynomial that approximates the restoring curve with $dR(x)/dx = 1$ at $x=0$,
- τ is nondimensional time, $\tau = \omega_0 t$
- t is real time,

Let us consider for a while an asymmetric escape equation with periodic forcing, linear

344

damping and a single quadratic, "softening" type, nonlinearity in restoring :

$$D\,(\dot{x}) = 2\,\zeta\,\dot{x} \quad , \quad R\,(x) = x - x^2$$

This equation, which can be regarded as the simplest possible nonlinear equation akin to the capsize problem, has been studied to considerable depth, Figs. 2 and 3 [14]. Near resonance the response curve exhibits the well known bending-to-the-the left property that creates the lower fold A and the upper fold B. Point A is a saddle-node and a jump towards either some kind of resonant response or towards capsize will take place if the corresponding frequency threshold is exceeded. On the resonant branch different types of instability can arise. If the wave slope Ak is slowly increased, period-doublings (flips) are noticed that usually lead to chaos (a "symmetric" system with cubic instead of quadratic nonlinearity must first go through "symmetry-breaking" at a supercritical pitchfork bifurcation). Further increase in forcing leads ultimately to the so-called *final crisis*, where the chaotic attractor vanishes as it collides with a saddle forming a *heteroclinic chain*. At relatively high levels of excitation there is no alternative "safe" steady-state and subsequently escape is the only option. Long before such high levels of forcing have been attained, however, the "safe" basin has started diminishing after an homoclinic tangency (heteroclinic in the case of a symmetric system). The heteroclinic (homoclinic) tangency is usually considered as the threshold of transient escape. Melnikov analysis allows approximate analytical prediction of the relation between the oscillator's parameters on this threshold.

In a diagram of Ak versus Ω (for constant damping), the earlier discussed thresholds appear as boundary curves, Fig. 2. The locus of the first homoclinic tangency can lie at a considerable distance from the "wedge"-like boundary formed by the fold and symmetry breaking/period doubling loci. It is of course desirable that the Melnikov curve lies as high in terms of Ak as possible. It follows that a desirable hull configuration should present the minimum of its Melnikov curve at Ak as high as it can be. Alternatively, it is possible to take into account a range
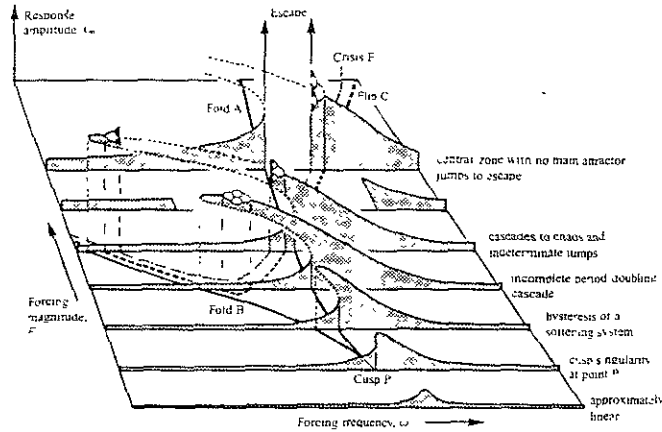

Fig. 3: Resonance response surface, [14]

rather than a single frequency, thus seeking to maximize the area below the Melnikov curve between some suitable low and high frequencies, respectively Ω_1 and Ω_2. In the ideal case where the Melnikov curve can be expressed explicitly as $Ak(\Omega)$, one will be seeking to identify the combination of restoring and damping coefficients, representing the connection with the hull, that maximizes the quantity

$$\int_{\Omega_1}^{\Omega_2} Ak(\Omega)\ d\Omega$$

More sophisticated criteria based on wave energy spectra and thus incorporating probabilistic considerations could also be considered. These are left however for later studies.

A similar type of thinking can be applied for steady-state capsize. Here one could require the lowest point of the wedge to be as high as possible in terms of forcing; or again, the area under the wedge between suitable Ω_1 and Ω_2 to be maximized. One possible way of defining Ω_1 and Ω_2 rationally could be attained by drawing the breaking-wave line on the (Ak, Ω) plane and taking its intersections with the fold and flip curves. Unfortunately for the considered range of frequencies this line may not intersect the flip curve. The rational definition of Ω_1 and Ω_2 needs further consideration.

Assume finally the following "symmetric" representation of restoring :

$$R(x) = x + a_1 x^3 - a_2 x^5 + (-1 - a_1 + a_2) x^7 \qquad (2)$$
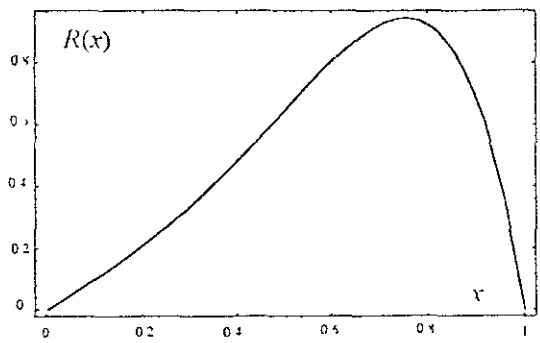
(4a)
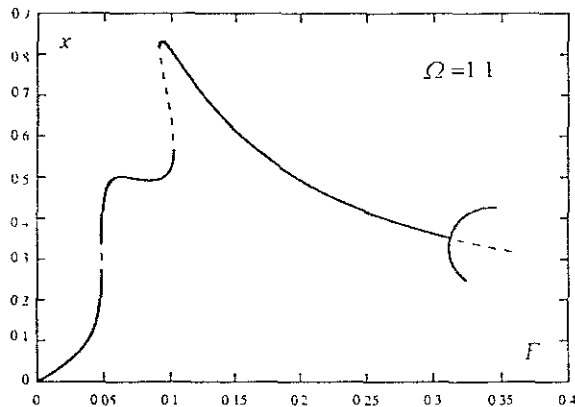
(4b)

Fig. 4 : Restoring curve, (4a), and steady response curve, (4b), for a_1=1.5 and a_2=1

The main advantage in using the seventh-order polynomial is that it provides two points of inflection, see Appendix. Here a_1, a_2 are the two free parameters of the restoring curve. The coefficient of the seventh-order term is selected so that the saddle points are always at x=1 and -1. Thus we shall be dealing from now on with the following roll equation, Fig. 4:

$$\ddot{x} + 2\zeta \dot{x} + x + a_1 x^3 - a_2 x^5 + (-1-a_1+a_2)x^7$$
$$= F\cos(\Omega \tau) \qquad (3)$$

3. MELNIKOV-BASED CRITERIA

Details about Melnikov analysis can be found in a number of texts and no attempt will be made to repeat these here, e.g. [15], [16], [17]. The method is based on the calculation of the signed distance between the stable and unstable manifolds of one or more saddle equilibrium points when this distance is small. Melnikov

analysis can also be regarded as an energy balance method where the total energy dissipated through damping should equal the energy supplied through the external forcing [14]. A more sophisticated version of the method can be applied also for highly dissipative systems [18].

Melnikov analysis includes basically the following stages. Firstly we calculate the Hamiltonian H of the unperturbed $(\zeta =F=0)$ system and from this the heteroclinic (homoclinic) orbit as $dx/d\tau=p(x)$. Then, we attempt to derive, if possible analytically, the time variation along this orbit: namely to derive expressions for x and $dx/d\tau$ that are functions of time, $x = h_1(\tau)$ and $dx/ d\tau = h_2(\tau)$. This often represents the first major difficulty in applying the method. The next step is to calculate the Melnikov function:

$$M(\tau_0) = \int_{-\infty}^{+\infty} \mathbf{f}[\mathbf{x}(\tau)] \wedge \mathbf{g}[\mathbf{x}(\tau), \tau+\tau_0]d\tau \quad (4)$$

where, $\mathbf{x} = [x, dx/d\tau]^T$; $dx/d\tau = \mathbf{f}[\mathbf{x}(\tau)]$ is the equation of the unperturbed system and the function $\mathbf{g}[\mathbf{x}, \tau]$ is periodic and represents the damping and forcing terms considered as constituting a perturbation. Also, τ_0 is phase with $0 < \tau_0 < 2\pi/\Omega$. The symbol means to take the cross product of vectors. The main objective in this method is to identify those marginal combinations of parameters where the Melnikov function admits real zeros.

Application for equation (3) :

Unperturbed system :

$$\ddot{x} + x + a_1 x^3 - a_2 x^5 + (-1-a_1+a_2)x^7 = 0 \quad (5)$$

which can be written in the form :

$$x_1 = x$$
$$\dot{x}_1 = x_2 = \partial H/\partial x_2$$

$$\dot{x}_2 = -x_1 -a_1 x_1^3 + a_2 x_1^5 - (-1-a_1+a_2)x_1^7 = -\partial H/\partial x_1$$
$$\qquad (6)$$

Hamiltonian:

$$H = 0.5 \{x_2^2 + x_1^2 + (a_1/2) x_1^4 - (a_2/3) x_1^6 +$$
$$+ [(-1-a_1+a_2)/4] x_1^8 \} \qquad (7)$$

346

Heteroclinic orbit :

$$\dot{x} = \pm \; [(\frac{3}{4} + \frac{a_1}{4} - \frac{a_2}{12}) - x^2 - \frac{a_1}{2}x^4 +$$

$$+ \frac{a_2}{3} x^6 - \frac{-1 - a_1 + a_2}{4} x^8]^{1/2} \qquad (8)$$

Let the time variation along the heteroclinic orbit be : $x = h_1(\tau)$ and $dx/d\tau = h_2(\tau)$. These can be found with appropriate variable transformations, or they can be approximated.

Melnikov function :

$$M(\tau_0) = \int_{-\infty}^{+\infty} x_2 \; \{F \cos [\Omega (\tau - \tau_0)] - 2\zeta \; x_2\} d \tau =$$

$$= F \; \cos(\Omega \tau_0) \int_{-\infty}^{+\infty} h_2(\tau) \cos(\Omega \tau) \; d\tau$$

$$- F \sin(\Omega \tau_0) \int_{-\infty}^{+\infty} h_2(\tau) \sin(\Omega \tau) \; d\tau -$$

$$- 2\zeta \int_{-\infty}^{+\infty} h_2^2(\tau) \; d\tau$$

$$(9)$$

The second integral is expected to be zero because $h_2(\tau) \sin(\Omega \tau)$ is an odd function [$h_2(\tau)$ is expected to be even, $\sin(\Omega \tau)$ is of course odd]. However if the homoclinic orbit is considered it is the first integral that can be zero.

The condition to have simple zeros for the Melnikov function written in terms of Ak is thus:

$$Ak\Omega^2/\phi_v \; > 2\zeta \; \frac{\int_{-\infty}^{+\infty} h_2^2(\tau) \; d\tau}{\int_{-\infty}^{+\infty} h_2(\tau) \cos(\Omega \tau) \; d\tau} \qquad (10)$$

The threshold Ak that gives rise to equality in (10), Ak_{min} will mean tangent manifolds and will thus define the Melnikov curve $Ak = g(\Omega)$.

Criterion 1:

$Ak_{min}(\Omega)$ to become maximum in terms of the parameters a_1, a_2, ϕ_v, ζ. It is understood of course that as $2\zeta = b/[W(GM)I]^{1/2}$, where b is the true dimensional damping, (GM) and I participate also in the optimization.

Criterion 2 :

The following objective function S should be maximized:

$$S = \int_{\Omega_1}^{\Omega_2} Ak \; d\Omega \; =$$

$$= 2 \int_{\Omega_1}^{\Omega_2} \zeta \; \frac{\int_{-\infty}^{+\infty} h_2^2(\tau) \; d\tau}{\int_{-\infty}^{+\infty} h_2(\tau) \cos(\Omega \tau) d\tau} \; d\Omega \qquad (11)$$

To make sure that the method produces meaningful alternative design solutions, additional conditions must be supplied. Current IMO or Naval GZ-curve shape criteria use as benchmarks the highest point of the curve as well as certain areas under the curve (up to 30 and 40 deg as well as between the two) see for example [19]. The search for maximum of the objective function should thus be constrained by suitable extra conditions that will guarantee that stability criteria in common use are being satisfied (see Appendix).

4. STEADY-STATE CRITERIA

These criteria require to locate the fold and symmetry breaking boundaries. Firstly, a low-order analytical solution of (3) is found with use of the method of harmonic balance. This solution is subsequently 'coupled' with suitable stability conditions. To identify the fold it is rather straightforward to request $\partial \Omega / \partial x_0 = 0$, where x_0 is the amplitude of roll motion, making sure of course that the lower fold A is the one considered. To approximate the locus of symmetry breaking we derive the variational equation and we find the relation that allows the existence of an asymmetric solution (or of a subharmonic solution in the case of an asymmetric system).

(a) Solution with harmonic balance

We rewrite (3) as follows :

$$\ddot{x} + 2\zeta \; \dot{x} + x + a_1 x^3 - a_2 x^5 + (-1 - a_1 + a_2) x^7 =$$

$$= F \cos(\Omega \tau - \theta) \qquad (12)$$

where θ is the phase difference between excitation and response that must be identified. We seek a steady-state solution $x = x_0 \cos(\Omega \tau)$. We substitute this into (12), expand the trigonometric terms, retain only the terms of harmonic frequency and equate the coefficients of $\cos(\Omega \tau)$ and

347

sin($\Omega\tau$) on both sides of the equation, obtaining finally:

$$x_0 = \frac{F}{(N^2 + 4\zeta^2 \Omega^2)^{1/2}} \qquad (13)$$

$$\theta = \arctan\left(\frac{-2\zeta\Omega}{N}\right) \qquad (14)$$

where

$$N = -\Omega^2 + M \qquad (15)$$

$$M = 1 + \frac{3a_1 x_0^2}{4} - \frac{5a_2 x_0^4}{8} + \frac{9(-1 - a_1 + a_2)x_0^6}{16} \qquad (16)$$

An alternative useful form of the above is obtained by solving for Ω :

$$\Omega = \frac{\sqrt{2}}{2} \sqrt{(2M - 4\zeta^2) \mp}$$

$$\mp \sqrt{(2M - 4\zeta^2)^2 - 4(M^2 - F^2/x_0^2)} \qquad (17)$$

With plus we obtain the high frequency branch and with the minus the low one.

(b) Approximation of the fold

With differentiation of (13) in terms of x_0, imposition of the condition $\partial\Omega/\partial x_0 = 0$ and some rearrangement, the following relation is derived:

$$\Omega^4 - (2M + x_0 M' - 4\zeta^2)\Omega^2 + (M^2 + M M' x_0) = 0 \qquad (18)$$

An alternative expression based on F can also be derived :

$$F^4 - x_0^3 M'(x_0 - 4\zeta^2)F^2 + 4M\zeta^2 = 0 \qquad (19)$$

where

$$M' = \partial M/\partial x_0 = \frac{a_1 x_0}{2} - \frac{5a_2 x_0^3}{2} +$$

$$+ \frac{27(-1 - a_1 + a_2)x_0^5}{8} \qquad (20)$$

Finally x_0 must be eliminated between (17) and

(18) and also F must be written in terms of Ak to obtain an expression, say $G(Ak,\Omega) = 0$, that defines the fold locus on the (Ak,Ω) plane.

(c) Approximation of the symmetry breaking locus

Consider again (3) and let x be increased by a very small amplitude ξ, such that ξ^2, ξ^3 etc. can be neglected. Then by substituting x with $x + \xi$ in (3) we obtain:

$$[\ddot{x} + 2\zeta\dot{x} + x + a_1 x^3 - a_2 x^5 + (-1 - a_1 + a_2)x^7 -$$

$$F\cos(\Omega\tau)] + \ddot{\xi} + 2\zeta\dot{\xi} + [\partial q(x)/\partial x]\,\xi = 0 \qquad (21)$$

where $q(x) = R(x) - F\cos(\Omega\tau)$ $\qquad (22)$

In (21) the quantity inside the first brackets is zero by definition and therefore we are left only with the so-called *variational equation* [20], [21] :

$$\ddot{\xi} + 2\zeta\,\dot{\xi} + [\partial q(x)/\partial x]\,\xi = 0 \qquad (23)$$

$$\ddot{\xi} + 2\zeta\,\dot{\xi} + [1 + 3a_1 x^2 - 5a_2 x^4 +$$

$$+ 7(-1 - a_1 + a_2)x^6]\,\xi = 0 \qquad (24)$$

where $x = x_0 \cos(\Omega\tau)$. We want to find the threshold where an asymmetric solution first appears, so we consider a perturbation ξ that includes constant term and second harmonic :

$$\xi = b_0 + b_{2c}\cos(2\Omega\tau) + b_{2s}\sin(2\Omega\tau) \qquad (25)$$

Parenthetically is mentioned that if the asymmetric equation was used we should consider a subharmonic perturbation :

$$\xi = b_{1c}\cos[(\Omega/2)\tau] + b_{1s}\sin[(\Omega/2)\tau] +$$

$$+ b_{3c}\cos[(3\Omega/2)\tau] + b_{3s}\sin[(3\Omega/2)\tau] \qquad (26)$$

With substitution of x and ξ [from (25)] in (21) and application of harmonic balance, where we retain only terms up to second harmonic, we obtain a linear system of algebraic equations in terms of b_0, b_{2c} and b_{2s} :

Coefficient of the constant term

$$[1+\frac{3}{2}a_{1}x_{0}^{2}-\frac{15}{8}a_{2}x_{0}^{4}-\frac{35}{16}(1+a_{1}-a_{2})x_{0}^{6}]b_{0}+$$

$$+[\frac{3}{4}a_{1}x_{0}^{2}-\frac{5}{4}a_{2}x_{0}^{4}-\frac{105}{64}(1+a_{1}-a_{2})x_{0}^{6}]b_{2c}+$$

$$+\quad 0\quad b_{2s}\qquad\qquad =0\qquad (27)$$

Coefficient of $\cos(2\Omega\tau)$

$$[\frac{3}{2}a_{1}x_{0}^{2}+\frac{5}{2}a_{2}x_{0}^{4}-\frac{105}{32}(1+a_{1}-a_{2})x_{0}^{6}]b_{0}+$$

$$+[1+\frac{3}{2}a_{1}x_{0}^{2}-\frac{35}{16}a_{2}x_{0}^{4}-$$

$$-\frac{91}{32}(1+a_{1}-a_{2})x_{0}^{6}-4\Omega^{2}]b_{2c}+$$

$$+(4\zeta\Omega)b_{2s}\qquad\qquad =\quad 0\qquad (28)$$

Coefficient of $\sin(2\Omega\tau)$

$$(4\zeta\Omega)b_{0}-$$

$$-(4\zeta\Omega)b_{2c}+$$

$$+[1-\frac{3}{2}a_{1}x_{0}^{2}-\frac{25}{16}a_{2}x_{0}^{4}-\frac{49}{32}(1+a_{1}-a_{2})x_{0}^{6}-$$

$$-4\Omega^{2}]b_{2s}=0\qquad (29)$$

The condition $\Delta=0$ where Δ is the determinant of (27), (28) and (29) provides the sought equation for the symmetry-breaking locus. It is interesting that the expression is analytically solvable for Ω. Again however the elimination of x_{0}, through combining with (17), is problematic.

(d) Derivation of steady-state criteria

The lowest point of the wedge corresponds obviously to the intersection of the curves $G(Ak,\Omega)$ and $\Delta(Ak, \Omega) = 0$. Let us define this point as (Ak_{0},Ω_{0}). We want to maximize Ak_{0} in terms of the coefficients a_{1}, a_{2}, ϕ_{v} and also ζ [which, it should not be forgotten, includes

(GM)]. Also in respect to the area criterion, if $Ak_{G}(\Omega)$, $Ak_{A}(\Omega)$ are explicit representations of wave slope in terms of Ω at the fold and flip loci respectively, we want:

$$\int_{\Omega_{1}}^{\Omega_{0}}Ak_{G}(\Omega)d\Omega \quad + \int_{\Omega_{0}}^{\Omega_{2}}Ak_{A}(\Omega)\,d\Omega$$

to be maximum.

5. STEADY VERSUS TRANSIENT CAPSIZE CRITERIA

Although the transient and steady-state capsize criteria are dynamically different and the basin erosion begins much earlier than the first period doubling, it is not known how they reflect on the actual optimization parameters. Do they result in similar optima or do they produce considerably different ones ? With the earlier developed tools it should be possible to infer to what extent the steady-state and capsize criteria coincide in their predictions of the optimum hull configuration. It is hoped that it will be possible to provide specific answers in a future publication.

6. REFERENCES

1. Thompson, J.M.T. Designing against capsize in beam seas: Recent advances and new insights, *Applied Mechanics Reviews*, **50**, 5, 1997, pp. 307-325.

2. Stoker, J.J. : *Nonlinear Vibrations in Mechanical and Electrical Systems*, 1950, Wiley, New York.

3. Nayfeh A.H & Mook, D.T. : *Nonlinear Oscillations*, 1979, Wiley, New York.

4. Cardo, A. Francescutto, A. & Nabergoj, R. : Ultraharmonics and subharmonics in the rolling motion of a ship: Steady-state solution. *International Shipbuilding Progress*, **28**, 326, 1981, pp. 234-251.

5. Odabashi, A.Y.: Conceptual understanding of the stability theory of ships, Schiffstechnik, **25**, 1978, pp. 1-18.

6. Caldeira-Saraiva, F.: A stability criterion for ships using Lyapounov's method, *Proceedings*, The Safeship Project, June 1986, Royal Institution of Naval Architects, London.

7. Thompson, J.M.T. , Rainey R.C.T & Soliman, M.S.: Ship stability criteria based on chaotic transients from incursive fractals. *Philosophical Transactions of the Royal Society of Lon*don A(1990) **332**, pp. 149-167.

8. Kan M.: Chaotic capsizing, *Proceedings*, ITTC SKC-KFR Meeting on Seakeeping Performance, September 1992, Osaka, pp. 155-180.

9. Falzarano, J.M., Shaw, S.W., Troesch,A: Application of global methods for analysing dynamical systems to ship rolling motion and capsizing, *International Journal of Bifurcation and Chaos*, **2**, 1, 1992 , pp. 101-115.

10. Szemplinska-Stupnicka, W.: The refined approximate criterion for chaos in a two-state mechanical oscillator, *Ingenieur-Archiv*, **58**, 1988, Springer-Verlag, pp.354-366.

11. Szemplinska-Stupnicka, W.: Cross-well chaos and escape phenomena in driven oscillators. *Nonlinear Dynamics*, **3**, 1992, pp. 225-243.

12. Virgin, L.N.: Approximative criteria for capsize based on deterministic dynamics, *Dynamics and Stability of Systems*, **4**, 1, 1989, pp. 55-70.

13. Strathclyde Stability Program, University of Strathclyde, Department of Ship & Marine Technology, 1984.

14. Thompson, J.M.T.: Global dynamics of driven oscillators: Fractal basins and indeterminate bifurcations. Chapter 1 of *Nonlinear Mathematics and its Applications*, 1996, P.J. Aston(ed.), Cambridge University Press, pp. 1-47.

15. Guckenheimer, J. & Holmes, P.J.: *Nonlinear Oscillations, Dynamical Systems and Bifurcations of Vector Fields*, 1983, Springer-Verlag, Applied Mathematical Sciences, **42**, New York.

16. Birkdash, M.U., Balachandran, B., Nayfeh, A.H.: Melnikov analysis for a ship with a general damping model, *Nonlinear Dynamics*, **6**, 1994, pp. 101-124.

17. Nayfeh, A.H. and Balachandran, B.: *Applied Nonlinear Dynamics: Analytical, Computational and Experimental Methods*, 1995, Wiley Series in Nonlinear Science, New York.

18. Salam, F.: The Melnikov technique for highly dissipative systems. *SIAM Journal of Applied Mathematics*, **47**, 1987, pp. 232-243.

19. Stability standards for surface ships, Naval Engineering Standard 109, Ministry of Defence, Sea Systems Controllerate, Issue 3, August 1989, Bath, UK.

20. Hayashi, C.: *Nonlinear Oscillations in Physical Systems*, 1964 , McGraw Hill, New York.

21. McLachlan, N.W.: *Ordinary Nonlinear Differential Equations in Engineering and Physical Sciences*, 1956, Oxford at the Clarendon Press.

APPENDIX

Consider the following polynomial for restoring:

$$R(x) = x + a_1 x^3 - a_2 x^5 + (-1 - a_1 + a_2) x^7$$

Area under the curve :

$$\int_0^1 R(x)\, dx = \frac{9 + 3a_1 - a_2}{24}$$

The 'true' area under the $GZ(\phi)$ curve is :

$$W\ (GM)\phi_v{}^2\ \frac{9 + 3a_1 - a_2}{24}$$

The area up to an angle ϕ is :

$$W \ (GM) \ [\ \frac{\phi^2}{2} + \frac{a_1 \phi^4}{4\phi_v^2} - \frac{a_2 \phi^6}{6\phi_v^4} +$$

$$+ \ \frac{(-1 - a_1 + a_2) \ \phi^8}{8\phi_v^6} \ ]$$

The maximum of the curve is found by solving for x the equation $dR(x)/dx = 0$:

$$(x^2)^3 - \frac{5 \ a_2}{7(-1-a_1+a_2)} (x^2)^2 + \frac{3 \ a_1}{7(-1-a_1+a_2)} (x^2) +$$

$$+ \ \frac{1}{7(-1-a_1+a_2)} \ = 0$$

There is one real and positive root which can be found analytically with, for example, *Mathematica* . For the equation

$$(x^2)^3 - a \ (x^2)^2 + b \ (x^2) + \ c \ x = 0$$

the real and positive root is :

$$x_{max} = \sqrt{ [\frac{a}{3} - \frac{2^{1/3} \ (-a^2 + 3b)}{3D} + \frac{D}{3 \ 2^{1/3}}]}$$

where :

$$D = \{2 \ a^3 - 9 \ a \ b + \sqrt{[4(-a^2 + 3b)^3 +}$$

$$+ \ (2a^3 - 9ab - 27c)^2] - 27c\}^{1/3}$$

Points of inflection at $d^2 R(x) / dx^2 = 0$:

$$x_{infl} = \sqrt{ \frac{10 \ a_2 \pm \sqrt{100 \ a_2^2 - 252 \ a_1(-1-a_1+a_2)}}{42 \ (-1-a_1+a_2)} }$$